

---

---

---

# 1198

TRANSPORTATION RESEARCH RECORD

---

## *Roadside Safety Features*

---

TRANSPORTATION RESEARCH BOARD  
NATIONAL RESEARCH COUNCIL  
WASHINGTON, D.C. 1988

**Transportation Research Record 1198**

Price: \$15.50

mode

1 highway transportation

subject areas

21 facilities design

40 maintenance

Transportation Research Board publications are available by ordering directly from TRB. They may also be obtained on a regular basis through organizational or individual affiliation with TRB; affiliates or library subscribers are eligible for substantial discounts. For further information, write to the Transportation Research Board, National Research Council, 2101 Constitution Avenue, N.W., Washington, D.C. 20418.

Printed in the United States of America

**Library of Congress Cataloging-in-Publication Data**

National Research Council. Transportation Research Board.

Roadside safety features.

p. cm.—(Transportation research record, 0361-1981; 1198)  
ISBN 0-309-04772-2

1. Roads—Guard fences—Testing. 2. Roads—Safety measures. I. National Research Council (U.S.). Transportation Research Board. II. Series.

TE7.H5 no. 1198

[TE228]

388 s—dc20

[625.7'95]

89-38462

CIP

**Sponsorship of Transportation Research Record 1198**

**GROUP 2—DESIGN AND CONSTRUCTION OF  
TRANSPORTATION FACILITIES**

*Chairman: David S. Gedney, Harland Bartholomew & Associates*

**General Design Section**

*Chairman: Jarvis D. Michie, Dynatech Engineering, Inc.*

**Committee on Roadside Safety Features**

*Chairman: Hayes E. Ross, Jr., Texas A&M University System  
Kenneth J. Boedecker, Jr., Maurice E. Bronstad, James E. Bryden,  
Ronald M. Canner, Jr., John F. Carney III, Duane O. Christensen,  
Harold D. Cooner, Arthur M. Dinitz, C. William Gray, James H.  
Hatton, Jr., T. Heijer, Walter P. Humble, William W. Hunter, Ivor  
B. Laker, William G. Marley, Jr., Jarvis D. Michie, Edward  
Robert Post, Robert Quincy, James F. Roberts, F. G. Schlosser,  
Louis C. Schultz, Jr., Rudolph Kenneth Shearin, Jr., Roger L.  
Stoughton, Flory J. Tamanini, Harry W. Taylor, Thomas Turbell,  
John G. Viner*

George W. Ring III, Transportation Research Board staff

Sponsorship is indicated by a footnote at the end of each paper. The organizational units, officers, and members are as of December 31, 1987.

NOTICE: The Transportation Research Board does not endorse products or manufacturers. Trade and manufacturers' names appear in this Record because they are considered essential to its object.

# Transportation Research Record 1198

---

## Contents

<b>Performance Evaluation of Breakaway-Cable-Terminal End Treatments</b>	<b>1</b>
<i>Jerry G. Pigman and Kenneth R. Agent</i>	
<b>Full-Scale Vehicle Crash Tests on Guardrail-Bridgerail Transition Designs with Special Post Spacing</b>	<b>11</b>
<i>Edward R. Post, Richard J. Ruby, Dalcyce F. Ronnau, and Milo D. Cress</i>	
<b>Full-Scale Vehicle Crash Tests on Nebraska Rural Mailbox Designs</b>	<b>31</b>
<i>Ronald K. Faller, John A. Magdaleno, Byron A. Warlick, William H. Wendling, and Edward R. Post</i>	
<b>Washington State Department of Transportation Development of a Bridgerail Retrofit Program</b>	<b>45</b>
<i>Don J. Grippe</i>	
<b>W-Beam Guiderail Transition from Light to Heavy Posts</b>	<b>55</b>
<i>Donald G. Herring and James E. Bryden</i>	
<b>Use of Guardrails on Low Fill Bridge Length Culverts</b>	<b>62</b>
<i>T. J. Hirsch and Dale Beggs</i>	
<b>Impact Attenuators: A Current Engineering Evaluation</b>	<b>76</b>
<i>John Hinch, Douglas Sawyer, Dale Stout, Martin Hargrave, and Raymond Owings</i>	
<b>Federal Outdoor Impact Laboratory—A New Facility for Evaluating Roadside Safety Hardware</b>	<b>90</b>
<i>Martin W. Hargrave and Allen G. Hansen</i>	
<b>Optimum Design of Pin and Loop Portable Concrete Barrier Connectors</b>	<b>97</b>
<i>James Loumiet, Jerry L. Graham, and James Migletz</i>	
<b>Development of a Strong Beam Guardrail-to-Bridge-Rail Transition</b>	<b>105</b>
<i>Roger P. Bligh, Dean L. Sicking, and Hayes E. Ross, Jr.</i>	

# Performance Evaluation of Breakaway-Cable-Terminal End Treatments

JERRY G. PIGMAN AND KENNETH R. AGENT

This report included an analysis of 110 accidents involving breakaway-cable-terminal (BCT) end treatments and 36 accidents involving median-breakaway-cable-terminal (MBCT) end treatments as used in Kentucky. The primary data base consisted of Kentucky accident records for the years 1980–87, with a few accidents that were identified before 1980. An attempt was made to document each accident with a police report, photographs, and a maintenance repair form. BCT end treatments evaluated included those with the terminal section installed as follows: (1) straight with no offset, (2) flared 6 feet at the end by using a 4.5-degree simple curve over 125 feet, and (3) flared 4 feet with a parabolic curve over the last 37.5 feet. Proper performance was based on a determination of whether the posts broke away as designed and/or the vehicle was redirected after impacting the guardrail. Results indicate that proper performance ranged from 60 percent for end sections with no offset to 69 percent for a “simple curve” offset, and 79 percent for a parabolic flare offset. Only 10 impacts were documented for small cars, and the BCT performed improperly in four of those accidents. Evaluation of the BCT end treatment indicates that it may be used where geometrics permit. Where those geometrics are not present, the turned-down end treatment proposed in a previous report should be used. The MBCT end treatment performed properly in 63 percent of the accidents. Problems related to stiffness of the end treatment were most apparent when impact angles were shallow. A recommendation was made to contour grade gore areas where possible and to install a crash cushion where the need for a barrier could not be eliminated. For MBCT installations at median piers and median width of 20 feet or less, crash cushions were also recommended. A turned-down end-treatment design was proposed for consideration at median piers where the median width was greater than 20 feet.

The performance of guardrail end treatments has been a subject of concern to highway engineers for many years. A concentrated effort was begun in the mid-1960s to evaluate guardrail design and recommend warrants for guardrail usage. The work was funded through the National Cooperative Highway Research Program’s (NCHRP) Project 15-1, and a review of current practices was performed by Cornell Aeronautical Laboratory (1). A second study funded by NCHRP was a compilation of recommended practices for locating, designing, and maintaining guardrails and median barriers (2). Results reported from the study were based upon a comprehensive literature review, a state-of-the-art survey, and the advice of

a selected group of experts. It was noted that ramped end treatments caused test vehicles to launch, roll, and tumble.

The next study in the series under NCHRP Project 15-1 included results of 25 full-scale crash tests and summarized the relative performance of the designs tested (3). Eight full-scale tests were performed on end terminal designs: six involved ramped designs, one was performed on a flared-end treatment, and one involved a blunt-end terminal. With the exception of one test, the vehicles were launched, rolled, and tumbled in the ramp-terminal tests. In the flared-terminal test, the vehicle penetrated the rail and decelerated in an acceptable manner. For the blunt-terminal test, the vehicle sustained major front-end damage, was launched, and landed on top of the rail. It was concluded that all designs tested were hazardous and development of a safer and treatment had the highest priority for subsequent research.

The fourth in a series of studies as a part of NCHRP Project 15-1 was a synthesis of information on warrants, service requirements, and performance criteria for all traffic-barrier systems (4). Emphasis was placed on the center section of “length of need” section rather than the terminal sections.

The last of five documents reporting on research that originated as NCHRP Project 15-1 dealt with guardrail end design and included results of full-scale tests on hydraulic-post guardrail design and concepts for improved end designs (5). Included in NCHRP Report 118 were 12 new guardrail terminal and transition concepts, one of which was the “breakaway-cable terminal” (BCT). Three full-scale crash tests were performed to evaluate the dynamic performance of the BCT. The BCT concept was an effective terminal for W-beam guardrail systems and appeared to be a significant improvement over either the turned-down or the blunt-nose terminal. It was noted that for end-on impacts the BCT performed in a manner similar to crash cushions. Maximum average vehicle deceleration permissible for crash cushions is 12 g, and average deceleration values for end-on impacts into the BCT were only 2.5 g and 3.4 g. The tests were conducted with 4,100-pound test cars, and it was noted that higher deceleration values should be experienced for smaller test vehicles. Advantages of the flared over the non-flared terminal for end-on impacts were demonstrated in the crash tests. Stabilization of the end-nose was achieved by using either steel diaphragms of vermiculite concrete to spread the beam loads over a large frontal area. As a result of tests conducted and documented in NCHRP Report 129, the BCT was recommended for immediate installation for field evaluation.

Southwest Research Institute's (SRI) work on guardrail end treatments was extended as NCHRP Project 22-2. Included were 25 full-scale crash tests to develop prototype end designs, with emphasis on the breakaway-cable terminal (6). Three tests of the BCT using subcompact cars also were performed. High rates of deceleration were measured during impacts with the small cars. Results indicated that the BCT neither eliminated nor increased the danger during small-car end-terminal collisions. Modifications to the end treatment were made to include a concrete footing and a drilled hole in the second post. Additional modifications were made to increase the size of the concrete footing that had failed in an earlier test. Overall results confirmed the recommendations for immediate trial implementation.

Development of the breakaway-cable terminal for median barriers followed research on BCTs for guardrails (7). Test results indicated the median barrier performed acceptably for the steel box-beam median barrier and the blocked-out W-beam median barrier with both steel and wooden posts. It also was noted that installation of the BCT for guardrails was encouraged by the Federal Highway Administration (FHWA) as part of the National Experimental and Evaluation Program (Notices HNG-32, December 11, 1972, and HHO-31, May 24, 1973).

Additional research conducted as part of NCHRP Project 22-2 included component testing, analytical simulation, and full-scale crash testing to further develop earlier BCT designs (8). Several modifications included the use of slip-base steel posts, a reduction in the size of wooden posts from 8 × 8 inches to 6 × 8 inches, and elimination of use of diaphragms in the nose section. It was noted that more than 12 states had installed BCTs as of March 1976.

An update on development of the BCT was reported by NCHRP in May 1978 (9). Several problems were reported, both in service and during subsequent experimental programs. Those problems included removal of the fractured wood post from the concrete footing, high costs of BCT components, and snagging of a subcompact vehicle's underside by steel-post BCTs. Modifications were made, and the BCT was judged to perform satisfactorily for most vehicle impact conditions. It was noted that 30 states had adopted the guardrail BCT as a standard, with less widespread use of the median barrier BCT.

By November 1980, it was reported by NCHRP that nearly 100,000 BCT end treatments had been installed in more than 40 states (10). Problems continued to occur with the removal of broken posts and installations where the 4-foot flare was not obtained. It was emphasized that lack of the 4-foot flare could result in spearing of vehicles during head-on impacts.

Documentation of field performance of BCT and median-breakaway-cable-terminal end treatments (MBCT) has been relatively scarce since testing by the SRI. A study by the New Jersey Department of Transportation had the objective of evaluating in-service performance of BCTs (11). Thirteen vehicular impacts into BCTs were evaluated, and results were compared with full-scale crash tests previously conducted by SRI. In-service experience was similar to the initial tests by SRI, and the BCT was recommended for flared guardrail installations. A significant problem was spearing of small cars during end-on impacts when the end had not been flared. Reinforcement of the unstiffened buffer end on straight guardrail sections was recommended. Replacement of the

two 12.5-foot sections with one 25-foot section also was recommended.

The median-breakaway-cable end treatment (MBCT) as designed and tested by SARI has had limited use. Installations are known to have been made in New Jersey and North Carolina. New Jersey has installed approximately 40 of the MBCTs, and there has been only one reported accident (letter of inquiry to E. Dayton, Assistant Chief Engineer of Roadway Design, New Jersey Department of Transportation, July 1982). A large automobile struck the device, and it performed as intended. Only one accident has been reported involving a MBCT in North Carolina (survey questionnaire from M. Bronstad, Southwest Research Institute, Feb. 1984). The terminal was impacted end-on by a full-size sedan and performed properly, even though it was damaged extensively.

A survey completed by the Kentucky Transportation Research Program (KTRP) revealed that the BCT was the most common end treatment used, with 40 states listing use of this treatment to some degree (12). In 24 states, only the BCT was used for terminating roadside steel-beam guardrail. Some form of the MBCT was used in 16 states. An investigation of 69 accidents involving BCT and MBCT end treatments was performed by the University of Kentucky, Transportation Research Program, in 1984 (13). Results indicated that the BCT performed properly in 60 percent of the accidents, and Kentucky's version of the MBCT performed properly 50 percent of the time.

According to a technical advisory distributed by FHWA in January, 1986, installation of BCTs has continued, with over 130,000 estimated to be in use (14). Reported problems with the BCT involving small cars prompted FHWA to perform additional tests on it with 1,800-pound cars. Results were satisfactory at 30 mph but caused vehicle rollover at 60 mph. Efforts to modify the BCT to accommodate 1,800-pound cars resulted in development of the Eccentric Loader BCT as detailed in the FHWA Technical Advisory (14).

## BCTS AND MBCTS USED IN KENTUCKY

Kentucky was one of the first states to install BCTs in 1974. Through 1986, the total number of installations made and included in the Kentucky Department of Highway's summaries of unit bid prices was 4,308. The weighted average cost for each BCT installation was \$509. Summaries of BCT and MBCT installations and costs for 1974–1986 are presented in Table 1. The current recommended standard in Kentucky for all fills and solid rock cut sections having an adequate recovery zone behind the guardrail is the BCT. It should be noted that there are several BCTs installed in Kentucky without the parabolic flare. Before 1982, most BCTs were installed with the last 125 feet of rail placed on a simple curve (4.5 degrees) and an offset of 6 feet. In 1982, Kentucky's Standard Drawing for BCT installations was revised to reflect a parabolic flare over the last 37.5 feet with a 4-foot offset at the end. Significant problems may occur when the end is not flared. When the BCT end treatment is installed with the designed flare and offset, impacts with the end usually result in acceptable performance. It should again be noted that the currently acceptable method of obtaining the 4-foot offset involves the use of a parabolic flare as opposed to the 4.5-degree simple curve.

TABLE 1 SUMMARY OF BCT AND "KENTUCKY" MBCT INSTALLATIONS BY YEAR

YEAR	TYPE OF END TREATMENT			
	BCT		KENTUCKY MBCT	
	NUMBER	AVERAGE UNIT PRICE (DOLLARS)	NUMBER	AVERAGE UNIT PRICE (DOLLARS)
1974	285	668	2	700
1975	443	617	98	742
1976	421	446	63	590
1977	541	423	-	-
1978	229	444	73	545
1979	350	482	101	574
1980	244	516	10	680
1981	160	519	14	657
1982	498	572	90	636
1983	462	487	122	631
1984	180	490	49	622
1985	197	484	39	585
1986	298	464	71	549
<b>TOTALS</b>	<b>4308</b>	<b>509 *</b>	<b>732</b>	<b>617 *</b>

Note: Numbers and unit prices tabulated from contracts awarded.

\*Weighted Average

Kentucky's version of the MBCT has not been installed there as extensively as the BCT. For the period 1974 through 1986, a total of 732 were installed as part of new construction or reconstruction projects, and the weighted average cost was \$617 per installation (Table 1). Kentucky's design utilizes two BCTs joined together at the end section. It was noted earlier that head-on impacts into unflared BCTs could result in spearing of the vehicle. Similar problems are associated with head-on impacts into Kentucky's MBCT design. There appears to be little uniformity nationwide in the types of designs used for MBCT end treatments. Only a few states adopted the MBCT for use as it was designed and tested by SRI. It should be noted that the BCT and MBCT evaluated in this study are the types used in Kentucky. The BCT now used in Kentucky is very similar to the design tested, evaluated, and recommended as part of the NCHRP studies (5). However, the MBCT used in Kentucky varies considerably from the MBCT design recommended as part of the NCHRP studies (7, 8).

#### DATA COLLECTION

Data were collected for this study in several phases. Initially, reports of accidents involving all types of safety barriers were collected for the years 1980-1982. The barriers included crash cushions, earth mounds, concrete median barriers, and four types of guardrail end treatments—BCT, MBCT, buried (turned down), and blunt. An inventory of all Kentucky routes having BCT and MBCT installations was used; accident reports pertaining to those routes were reviewed and appropriately selected. The next step was to make arrangements with maintenance personnel within the Kentucky Department of Highways so that the study team would be notified when accidents occurred involving BCT or MBCT treatments. The objective was to notify the study team of such accidents so that on-site investigations could be made before the guardrail was repaired. Photographs were obtained to document the performance and damage to the end treatment. In some instances, photographs of vehicles were provided by police or other agencies.

Additional accidents involving guardrails were discovered during trips or in the course of searching accident reports for other purposes. An effort was made to combine photographs with appropriate accident reports. However, some accidents involving guardrail ends went unreported. In other cases, the guardrail was repaired before photographs could be obtained.

The initial phase of data collection included a sample of 69 accidents involving BCT and "Kentucky MBCT" end treatments, results of which were reported previously (13). Data collection continued after the first research study, and the two data collection efforts have been combined. The result was a total of 146 accidents, with 77 accidents being added during the second period of data collection. Primary data collection included the period 1980 through 1987; however, 10 of the 146 accidents occurred before 1980.

## RESULTS

Data for a total of 146 BCT of "Kentucky MBCT" end-treatment accidents were obtained. It should be noted that any reference to an MBCT end treatment in the results is the Kentucky version of the MBCT. The majority of accidents (110) involved a BCT. The earliest accident date was May 1976 and the most recent was May 1987. Limited repair cost data were available. The average repair cost at eight BCT locations was approximately \$644, with a range of about \$206 to \$980. A wide range of repair costs would be expected because of differences in damage. The average cost to repair three MBCT end treatments was about \$681. Repair costs were higher than the original installation costs of \$509 for BCT's and \$617 for MBCT's.

Sources of information concerning accidents included accident reports, photographs, and repair forms. An accident report was obtained for 99 of the 146 accidents, either police photographs or site photographs were obtained for 104 accidents, and a repair form was obtained for 33 accidents. All three types of information were obtained for only 12 accidents.

### BCT End Treatment Accidents

Performance of BCT end treatments for each accident were analyzed and summarized. In addition to end treatment per-

formance, information concerning vehicle size, impact severity, impact angle, guardrail placement, end treatment configuration area, vehicle action after impact, and end treatment damage was analyzed. Subjective judgment was used to determine many of the variables.

End treatment performance, when it could be determined, was defined as either proper or improper. Proper performance resulted when the end treatment performed as intended, with the wooden posts breaking away or the guardrail redirecting the vehicle. Impact severity (which involves guardrail damage, vehicle damage, and injury severity) was not used as the criterion for assessing performances. It is possible that the end treatment could perform properly but that severe injuries could occur as a result of other factors such as vehicle size and lack of safety belt usage. Vehicle and guardrail damage may be related more to type and size of vehicle than to end-treatment performance. Therefore, the most consistent criterion to rate performance was selected to be an interpretation of the condition of whether the posts broke away as designed without causing the vehicle to overturn, or proper redirection of the vehicle after impact with the guardrail, or both. Performance was rated for 102 of the 110 BCT accidents.

Because many of the BCT end treatments were not installed with an offset of 4 feet and a parabolic flare over a distance of 37.5 feet, additional analysis was performed to document the configuration of the BCT as it was installed. End treatment configuration was categorized as one of the following:

1. Simple curve—a 4.5-degree simple curve is used to extend the standard section of guardrail to the terminal section. The last 125 feet of guardrail is installed on this 4.5-degree curve to obtain an offset of 6 feet at the end;
2. Parabolic flare—the terminal section is offset 4 feet with a parabolic flare over the last 37.5 feet (type that was tested, evaluated, and recommended as part of NCHRP studies);
3. Straight—the terminal section is placed at the end of a standard section of guardrail with very little or no offset.

Results of categorizing the end treatment configurations are presented in Table 2. Of 110 accidents, 54 involved BCTs categorized as a simple curve. BCT installations with a parabolic flare totaled 46. Five installations were determined to have very little or not offset, and five configurations were unknown due to lack of data.

An analysis of the data was made to relate performance to

TABLE 2 SUMMARY OF BCT END TREATMENT CONFIGURATIONS

END TREATMENT CONFIGURATION	NUMBER	PERCENT
Simple Curve	54	49.1
Parabolic Flare	46	41.8
Straight	5	4.5
Unknown	5	4.5
Total	110	100.0

TABLE 3 PERFORMANCE RELATED TO BCT END TREATMENT CONFIGURATION

END TREATMENT CONFIGURATION	PROPER PERFORMANCE		IMPROPER PERFORMANCE		UNKNOWN PERFORMANCE
	NUMBER	PERCENT	NUMBER	PERCENT	NUMBER
Simple Curve	35	64.8	16	29.6	3
Parabolic Flare	33	71.7	9	19.6	4
Straight	3	60.0	2	40.0	0
Unknown	3	60.0	1	20.0	1
<b>TOTAL</b>	<b>74</b>	<b>67.3</b>	<b>28</b>	<b>25.5</b>	<b>8</b>

\*Percentage include only those accidents where performance was known.

BCT end treatment configuration (Table 3). Where performance was known, it was determined that 35 of 51 (69 percent) performed properly when the end section was installed on a 4.5-degree simple curve. When the end treatment was installed on a parabolic curve, performance was rated proper in 33 of 42 (79 percent) accidents. For installations classified as straight, performance was rated proper in three of five (60 percent) accidents. When all three configurations are combined, performance was rated proper in 73 percent of the accidents.

Presented in Table 4 is a summary of impact severity cross-tabulated with end-treatment configuration and related to performance. A severe impact was one sufficient to cause heavy or extensive damage to the guardrail, disabling damage to the vehicle, or injury severity classified as fatal or incapacitating, or both. Non-severe was classified as slight or moderate damage to guardrail, functional or non-functional damage to the vehicle, or slight or no injury, or both. The data show proper performance was higher for non-severe impacts (89 percent) than for severe impacts (66 percent). For end sections installed on a simple curve, there was 61 percent proper performance in severe impacts compared with 92 percent in non-severe impacts. Severe accidents involving the parabolic flare resulted in proper performance in 72 percent of the accidents (23 of 32).

Impact angle was cross-tabulated with end treatment configuration and related to performance as shown in Table 5. The percentage of improper performance was higher for impacts at shallow angles (15 degrees or less) than for those at moderate to sharp angles (greater than 16 degrees). At shallow angles, the BCT installed on a simple curve performed properly less frequently (52 percent) than it did when impacted at moderate to sharp angles (82 percent). This could be related to the stiffness of the BCT end section when installed without the parabolic flare, a condition that would be worse when impacts were at shallow angles. For impacts into an end treatment installed on a parabolic flare, performance was proper in 9 of 14 accidents (64 percent) at shallow angles and 18 of 22 (82 percent) at moderate to sharp angles. This shows that

even when the end treatment was installed with the parabolic flare, the BCT performed properly less frequently when impacted at shallow angles than at moderate to sharp angles. In four of the eight fatal accidents involving the BCT, the approaching vehicle ran off the road before reaching the BCT and was attempting to get back onto the road when the impact occurred. This resulted in a very shallow impact angle and spearing of the vehicle. In three of these accidents, the vehicle was sliding sideways at impact, with the impact to the side of the vehicle. The BCT, in either the parabolic flare or simple curve configuration, is too stiff when impacted at a very shallow angle with the side of a vehicle. It was not designed for this type of impact.

Results of comparing damage with performance in the various end treatment configurations are presented in Table 6. End-treatment damage was classified as either slight to moderate or heavy to extensive. Generally, slight to moderate was deflection of the rail, bending both posts or breaking one, and/or movement of the concrete footing. Heavy to extensive was breaking both posts, or breaking both posts with damage to rail beyond the second post, or both. When all end treatment types were combined, performance results were nearly the same for slight to moderate and heavy to extensive end treatment damage. For BCT end treatments installed on a simple curve, performance was proper in 16 of 20 accidents (80 percent) when end treatment damage was slight to moderate and in 14 of 22 accidents (64 percent) when damage was heavy to extensive. For end treatments with the parabolic flare, performance was similar for accidents in which end treatment damage was heavy to extensive (82 percent proper performance) and slight to moderate (81 percent proper performance).

Data were summarized to show a comparison of vehicle size and impact severity. Information concerning the vehicle year, vehicle make, and vehicle style was included. Impact severity was equally severe for all vehicle sizes. Impact was judged to be severe in 72 percent of the accidents (76 of 105) where severity was known. Also, a large majority of vehicles



TABLE 4 IMPACT SEVERITY RELATED TO BCT END TREATMENT PERFORMANCE

IMPACT SEVERITY	END TREATMENT CONFIGURATION	PERFORMANCE				
		PROPER		IMPROPER		UNKNOWN
		NUMBER	PERCENT	NUMBER	PERCENT	NUMBER
Severe	Simple Curve	23	59.0	15	38.5	1
	Parabolic Flare	23	69.7	9	27.3	1
	Straight	2	100.0	0	0.0	0
	Unknown	1	50.0	1	50.0	0
	Subtotal	49	64.5	25	32.9	2
Non-Severe	Simple Curve	11	84.6	1	7.7	1
	Parabolic Flare	9	75.0	0	0.0	3
	Straight	1	33.3	2	66.7	0
	Unknown	2	100.0	0	0.0	0
	Subtotal	23	76.7	3	10.0	4
Unknown	Simple Curve	1	50.0	0	0.0	1
	Parabolic Flare	1	100.0	0	0.0	0
	Straight	0	-	0	-	0
	Unknown	0	0.0	0	0.0	1
	Subtotal	2	50.0	0	0.0	2

\*Percentages include only those accidents where performance was known.

(independent of size) received disabling damage (83 percent). There were eight fatal accidents, of which seven involved a large automobile. More than one-half of the accidents (57 percent) resulted in an injury where the severity of the accident was known. A substantial number of accidents (26 percent) resulted in either a fatality or an incapacitating injury. Vehicle size was related to end treatment damage, with accidents involving small automobiles resulting in less damage. About one-half of the accidents (47 percent) resulted in either heavy or extensive damage to the guardrail. Presented in Table 7 is a summary of performance when vehicle size was cross-tabulated with end treatment configuration. Ten impacts involved small cars, and the end treatment performed properly in four of the collisions. For impacts involving large automobiles, the end treatment performed properly in 33 of 49 accidents (67 percent) when performance was known. For accidents involving large automobiles, performance was proper for 16 of 26 (62 percent) when the BCT was installed as a

simple curve and 14 of 20 (70 percent) when the BCT included a parabolic flare. In the seven accidents involving trucks, performance was rated proper in four cases (57 percent). For all three cases of improper performance involving trucks, the vehicle overturned.

Vehicle size information was available in sufficient detail to categorize only 67 of the 110 BCT accidents. In 10 other accidents, it was determined that the vehicle was an automobile of unknown size. Performance was rated in all 10 accidents; 8 were at locations where the BCT was a simple curve, one where it was a parabolic flare, and one where the BCT was straight.

Data relating severity of injury in each accident with end treatment configuration are presented in Table 8. There were eight fatal accidents, and six of those occurred at locations where the BCT had been installed on a simple curve. Of the 42 injury accidents, 11 involved incapacitating injuries and 8 of those were the result of accidents at locations where the

TABLE 5 IMPACT ANGLE RELATED TO BCT END TREATMENT PERFORMANCE

		PERFORMANCE				
IMPACT ANGLE	END-TREATMENT CONFIGURATION	PROPER		IMPROPER		UNKNOWN
		NUMBER	PERCENT*	NUMBER	PERCENT*	NUMBER
Shallow	Simple Curve	14	51.9	13	48.1	1
	Parabolic Flare	9	64.3	5	35.7	2
	Straight	0	0.0	1	100.0	0
	Unknown	1	50.0	1	50.0	0
	Subtotal	24	54.5	20	45.5	3
Moderate	Simple Curve	14	82.4	3	17.6	0
	-Sharp Parabolic Flare	18	81.8	4	18.2	0
	Straight	0	-	0	-	0
	Unknown	1	100.0	0	0.0	0
Subtotal	33	82.5	7	17.5	0	
Unknown	Simple Curve	7	100.0	0	0.0	2
	Parabolic Flare	6	100.0	0	0.0	2
	Straight	3	75.0	1	25.0	0
	Unknown	1	100.0	0	0.0	1
	Subtotal	17	94.4	1	5.6	5

\* Percentages only include those accidents where performance was known.

BCT was a simple curve. For accidents in which injury severity was known, 8 of 74 (11 percent) resulted in a fatality. A substantial percentage of accidents (26 percent) resulted in either a fatality or an incapacitating injury. Of the eight fatal accidents, four involved spearing, two involved the vehicle breaking through, one involved overturning of the vehicle, and one involved a car breaking one post and then spinning counterclockwise 180 degrees.

Improper performance was generally associated with one of the following occurrences: (a) the vehicle hit the end treatment and was stopped when the posts did not break, (b) the vehicle overturned as it hit the end and the post did not break, or (c) a concrete footing moved and prevented the posts from breaking. There were five instances in which the BCT end-treatment speared the vehicle. Three involved a simple curve and two involved a parabolic flare installation. Other researchers have shown that the BCT has failed to perform properly when impacted head-on by small cars. Head-on crash tests performed by SRI in the study titled "Evaluation of Guardrail BCTs" showed that small cars performed satisfactorily in 30-mph tests but not in 60-mph tests (14). Spearing is usually

the result of an impact with an end treatment having no flare but may result if a vehicle travels off the road and then the driver attempts to re-enter the road at a very shallow impact angle. Such a problem may occur when impacting an MBCT end-treatment installed in a gore location.

An analysis of injury severity correlated with end treatment performance revealed performance to be proper more frequently in accidents when there were no injuries or injuries were not severe. Injury severity also was correlated with end-treatment damage, and it was noted that injuries generally were more severe when damage was greater.

#### Kentucky MBCT End Treatment Accidents

Performance was determined for 27 of the 36 accidents involving an MBCT end treatment. For those where performance could be determined, it was rated as proper in 17 (63 percent). Only 5 of 14 severe impacts (36 percent) having performance rated revealed proper performance. In contrast, performance was termed proper in 11 of 12 (92 percent) non-severe impacts.

TABLE 6 END TREATMENT DAMAGE RELATED TO BCT END TREATMENT PERFORMANCE

		PERFORMANCE				
END-TREATMENT DAMAGE	END-TREATMENT CONFIGURATION	PROPER		IMPROPER		UNKNOWN
		NUMBER	PERCENT*	NUMBER	PERCENT*	NUMBER
Slight-	Simple Curve	16	80.0	4	20.0	1
Moderate	Parabolic Flare	17	81.0	4	19.0	3
	Straight	2	66.7	1	33.3	0
	Unknown	0	-	0	-	0
	Subtotal	35	79.5	9	20.5	4
Heavy-	Simple Curve	14	63.6	8	36.4	1
Extensive	Parabolic Flare	14	82.4	3	17.6	1
	Straight	0	0.0	1	100.0	0
	Unknown	1	100.0	0	0.0	0
	Subtotal	29	70.7	12	29.3	2
Unknown	Simple Curve	5	55.6	4	44.4	1
	Parabolic Flare	2	50.0	2	50.0	0
	Straight	1	100.0	0	0.0	0
	Unknown	2	66.7	1	33.3	1
	Subtotal	10	58.8	7	41.2	2

\* Percentages only include those accidents where performance was known.

Impact angles were classified as either shallow ( or moderate) or sharp. For accidents where impact angles were known, 13 of 23 (57 percent) reflected performance. For accidents in which heavy or extensive guardrail damage resulted and in which performance was also rated, four of seven (57 percent) disclosed improper performance. Only three accidents of known vehicle size involved a small vehicle, and all showed improper performance. Two accidents involved collisions with an MBCT placed in a gore and showed improper performance, with the end spearing the vehicle. The third accident involved a small car impacting the MBCT from the back side and was non-severe.

Of the 36 accidents involving an MBCT, 31 involved an MBCT placed in the median while in five accidents the MBCT was in the gore. Of the 31 accidents in which the MBCT was in the median, 11 involved hitting the end treatment from the rear. None of the three accidents involving an MBCT in the gore reflected proper performance. Performance was rated proper in 68 percent of the accidents involving an MBCT in

the median, and proper for 60 percent when the impact was from the front and 80 percent when the impact was from the rear of the MBCT.

Of 20 accidents of known injury severity, 14 (70 percent) resulted in some type of injury and 7 (35 percent) resulted in either a fatality or an incapacitating injury. There were three fatal accidents involving an MBCT. Two fatal accidents were the result of spearing when a small vehicle impacted a MBCT in a gore area, and a third was caused by high-speed impact of a tractor trailer into an MBCT. Vehicles received disabling damage in 14 of 20 accidents (70 percent). Impact severity was classified as severe in 21 of the 34 accidents (62 percent). Collisions involving either small or large automobiles generally resulted in severe impacts. Guardrail damage was either heavy or extensive in 10 of 27 accidents (37 percent).

The MBCT end treatment has been used in medians and at least one gore location. For accidents in which performance could be rated, both gore accidents were classified as not showing proper performance, while 8 of 25 median-location

TABLE 7 VEHICLE SIZE RELATED TO BCT END TREATMENT PERFORMANCE

VEHICLE SIZE	END-TREATMENT CONFIGURATION	PERFORMANCE				
		PROPER		IMPROPER		UNKNOWN
		NUMBER	PERCENT*	NUMBER	PERCENT*	NUMBER
Small Auto	Simple Curve	2	40.0	3	60.0	0
	Parabolic Flare	2	50.0	2	50.0	0
	Straight	0	-	0	-	0
	Unknown	0	0.0	1	100.0	0
	Subtotal	4	40.0	6	60.0	0
Large Auto	Simple Curve	16	61.5	10	38.5	1
	Parabolic Flare	14	70.0	6	30.0	0
	Straight	1	100.0	0	0.0	0
	Unknown	2	100.0	0	0.0	0
	Subtotal	33	67.3	16	32.7	1
Trucks	Simple Curve	3	60.0	2	40.0	0
	Parabolic Flare	1	50.0	1	50.0	0
	Straight	0	-	0	-	0
	Unknown	0	-	0	-	0
	Subtotal	4	57.1	3	42.9	0
Auto-U	Simple Curve	8	100.0	0	0.0	0
	Parabolic Flare	1	100.0	0	0.0	0
	Straight	1	100.0	0	0.0	0
	Unknown	0	-	0	-	0
	Subtotal	10	100.0	0	0.0	0
Unknown	Simple Curve	6	85.7	1	14.3	2
	Parabolic Flare	15	100.0	0	0.0	4
	Straight	1	33.3	2	66.7	0
	Unknown	1	100.0	0	0.0	1
	Subtotal	23	88.5	3	11.5	7

\* Percentages include only those accidents where performance was known.

TABLE 8 ACCIDENT SEVERITY RELATED TO BCT END TREATMENT CONFIGURATION

END TREATMENT CONFIGURATION	ACCIDENT SEVERITY			
	FATAL	INJURY	DAMAGE	UNKNOWN
Simple Curve	6	25	11	12
Parabolic Flare	1	17	8	20
Straight	0	0	3	2
Unknown	1	0	2	2

accidents (32 percent) were classified as involving improper performance.

## SUMMARY

Analysis revealed that any accident involving collision with a guardrail end is potentially severe. Considering all configurations combined, the BCT end treatment performed properly in most accidents (73 percent); that is, the end treatment performed as it was intended, with the wooden posts breaking away or the guardrail redirecting the vehicle. This percentage of proper performance occurred even though the BCT was determined to have been installed with a parabolic flare in only 46 of the 110 accidents investigated. Results indicate that proper performance ranged from 60 percent for end sections with no offset to 69 percent for end sections with a simple curve offset and 79 percent for ends with a parabolic flare offset. Most MBCT end treatment configurations evaluated were installed on a 4.5-degree simple curve with an offset of approximately 4 to 6 feet at the end (54 installations). A few of the accidents involved a straight BCT with a very small or no offset (5 installations). Only 10 impacts involved small cars, and the BCT end treatment performed properly in 4 of them. Improper performance of the BCT was generally related either to failure of the posts and guardrail to break away as designed, causing the vehicle to stop abruptly or overturn, or to excessive movement of a concrete footing that prevented the posts from breaking. Four accidents involved spearing of the vehicle, and all were shallow-angle impacts with three involving impact with the side of the vehicles. Overall performance was not as good when the impact angle was shallow. Poor performance for shallow impact angles involving BCTs and the problem exhibited by MBCT end treatments impacted head-on show that a flare is necessary. Any installation of a BCT end treatment without proper flare creates a potential to spear a vehicle in a shallow-angle impact.

The Kentucky MBCT end treatment performed properly 63 percent of the time. A problem associated with the MBCT appears to be related to the stiffness of the end treatment. This is most apparent when the MBCT is used in a gore area where impact angles are shallow. Two fatal accidents occurred when the end treatment speared a small vehicle after a head-on collision in a gore area.

## RECOMMENDATIONS

Evaluation of the performance of Kentucky's BCT end treatment indicates that it may be used where geometrics permit, that it, when a 4-foot flare can be obtained with a 10:1 slope in advance and a sufficient recovery area, not exceeding a 3:1 slope, behind. Slopes referred to here are based on general guidelines for BCT design as noted in the survey of other states performed by the KTRP (12) and the guidance on barriers published by the AASHTO (15). Where those geometrics are not present, the turned-down end treatment proposed in the previous report should be used (12).

It is recommended that Kentucky's MBCT end treatment design be modified or eliminated because of stiffness of the MBCT and the problems associated with impacts at shallow angles. When MBCT end treatments are installed in gore areas, contour grading should be used where possible, to elim-

inate the need for a barrier system. When the need for a barrier in a gore area cannot be eliminated, a crash cushion should be installed. When the MBCT is used at median piers, it is recommended that crash cushions be used for median widths of 20 feet or less. For median widths greater than 20 feet, it is recommended that a turned-down median end treatment be used.

The question about which is the best end treatment to use for median installations has not been resolved. A continued in-field performance evaluation of the BCT, MBCT, and new turned-down end treatments through in-depth analysis of accidents is warranted. This type of performance evaluation would provide valuable information for future decisions concerning the most crashworthy end treatment to use.

## REFERENCES

1. N. J. Deleys and R. R. McHenry. *NCHRP Report 36: Highway Guardrails—A Review of Current Practices*. National Research Council, Washington, D.C., 1967.
2. J. D. Michie and L. R. Calcote. *NCHRP Report 54: Location, Selection, and Maintenance of Highway Guardrails and Median Barriers*. HRB, National Research Council, Washington, D.C., 1968.
3. J. D. Michie and L. R. Calcote. *NCHRP Report 115: Guardrail Performance and Design*. HRB, National Research Council, Washington, D.C., 1971.
4. J. D. Michie and M. E. Bronstad. *NCHRP Report 118: Location, Selection and Maintenance of Highway Traffic Barriers*. HRB, National Research Council, Washington, D.C., 1971.
5. J. D. Michie and M. E. Bronstad. *NCHRP Report 129: Guardrail Crash Test Evaluation—New Concepts and End Designs*. HRB, National Research Council, Washington, D.C., 1972.
6. *NCHRP Research Results Digest 43: Evaluation of Breakaway Cable Terminals for Guardrails*. HRB, National Research Council, Washington, D.C., Oct. 1972.
7. *NCHRP Research Results Digest 53: Development of a Breakaway Cable Terminal for Median Barrier*. HRB, National Research Council, Washington, D.C., Dec. 1973.
8. *NCHRP Research Results Digest 84: Breakaway Cable Terminals for Guardrails and Median Barriers*. TRB, National Research Council, Washington, D.C., March 1976.
9. *NCHRP Research Results Digest 102: Modified Breakaway Cable Terminals for Guardrail and Median Barriers*. TRB, National Research Council, Washington, D.C., May 1978.
10. *NCHRP Research Results Digest 124: A Modified Foundation for Breakaway Cable Terminals*. TRB, National Research Council, Washington, D.C., Nov. 1980.
11. R. F. Baker, *Breakaway Cable Terminal Evaluation*. Report FHWA/NJ-81/001. New Jersey Department of Transportation, May 1980.
12. J. G. Pigman and K. R. Agent. Survey of Guardrail End Treatment Usage. University of Kentucky, Transportation Research Program, Report UKTRP-83-23, Oct. 1983.
13. J. G. Pigman, K. R. Agent, and T. Creasey. *Analysis of Accidents Involving Breakaway-Cable-Terminal End Treatment*. Report UKTRP-84-16. University of Kentucky, Transportation Research Program, June 1984.
14. *W-Beam Guardrail End Treatments*, Federal Highway Administration Technical Advisory T5040.25, Jan. 7, 1986.
15. *Guide for Selecting, Locating, and Designing Traffic Barriers*. American Association of State Highway and Transportation Officials, 1977.
16. J. D. Michie, *NCHRP Report 230: Recommended Procedures for the Safety Performance Evaluation of Highway Appurtenances*, TRB, National Research Council, Washington, D.C., 1981.

# Full-Scale Vehicle Crash Tests on Guardrail-Bridgerail Transition Designs with Special Post Spacing

EDWARD R. POST, RICHARD J. RUBY, DALYCE F. RONNAU, AND MILO D. CRESS

Full-scale 4,500-pound vehicle impact tests at 60 mph and 25 degrees were conducted on four new guardrail-bridgerail "transition" designs for use in Nebraska in which the first wood post from the bridge end was left out. The post was left out to represent a common field problem in which a concrete footing prevents installing the post. To compensate for the missing post, a stronger beam member and heavier wood posts were used in addition to a 4:1 tapered end on the concrete bridgerail. The tapered end was used to (1) reduce the unsupported span length and (2) provide a smooth guardrail deflection curve during vehicle redirection. All of the transition designs were identical except for the transition beam member. The designs consisted of two heavy 10 inch x 10 inch posts followed by four heavy 8 inch x 8 inch posts. The remaining posts were standard 6 inch x 8 inch posts. Over a guardrail length of 18 feet 9 inches, the posts were spaced 3 feet 1½ inches on centers, whereas, over the remaining length, a standard post spacing of 6 feet 3 inches was used. The posts were installed in a "native" silty clay (type CL) soil. In terms of the evaluation guidelines in National Cooperative Highway Research Project (NCHRP) 230, the overall performance of the transition designs was as follows: single thrie beam transition—unsatisfactory, double thrie beam transition—satisfactory, tubular thrie beam transition—satisfactory, double W-beam transition—unsatisfactory.

## PROBLEM STATEMENT

The majority of the bridgerail designs in current use are rigid traffic barriers, whereas the guardrail designs on the approaches to the bridge structure are semi-rigid traffic barriers. In restraining and redirecting a large 4,500-pound automobile at 60 mph and 25 degrees, rigid and semi-rigid traffic barriers will typically undergo deflections of 0 to 6 inches and 30 inches, respectively. To provide structural stiffness compatibility between the semi-rigid guardrail and the rigid bridgerail, a guardrail consisting of reduced post spacings and larger size posts is used adjacent to the bridgerail end. A current American Association of State Highway and Transportation Offi-

cial (AASHTO) T1 (1) transition section requires that the first six wood posts back from the bridgerail end be installed on a reduced spacing of 3 feet 1½ inches, and the first three wood posts be larger, 10 inch x 10 inch posts.

Many of the bridge structures in Nebraska were constructed with concrete footings that extend back from the end of the bridgerail. The footing has created a field problem in that the first required 10 inch x 10 inch wood post located 3 feet 1½ inches from the bridgerail end connection cannot be installed in the ground. To compensate for the first post left out or installed further back, the Nebraska Department of Roads (NDR) has designed four new transition sections consisting of longer 6-foot posts and stronger guardrail beam members. Cross-section drawings of the four new beam transition sections are shown in Figure 1.

## RESEARCH STUDY OBJECTIVE

The primary objective of this study was to evaluate the performance characteristics of the four new guardrail-bridgerail transition designs by conducting full-scale vehicle crash tests. In all tests, the first 10 inch x 10 inch-wood post located 3 feet 1½ inches back from the bridgerail end connection was left out.

## DESIGN AND CONSTRUCTION OF TEST ARTICLE

### Simulated Bridge Deck and Railing

The simulated concrete bridge railing and deck were designed by the NDR Bridge Division. Design details of the bridge railing and deck are shown in Figure 2, and photographs of the bridge railing are shown in Figure 4. The bridge railing and deck were constructed by a private contractor who was qualified to bid on NDR bridge contracts. The open bridge railing is a recent design currently in use in Nebraska to help keep the roadway clear of blowing and drifting snow and to facilitate snow removal operations. The cantilevered 4:1 tapered end section was a totally new design feature that was recommended by C. F. McDevitt of the FHWA as a method to (1) provide a smooth guardrail deflection curve in redirecting the test vehicle and (2) reduce the effective unsupported span length to help compensate for the first wood post (post No. 1) that was left out.

E. R. Post, Department of Civil Engineering, University of Nebraska, Lincoln, Neb. 68588-0531. R. J. Ruby, Roadway Design Division, Nebraska Department of Roads, P.O. Box 94759, Lincoln, Neb. 68509-4759. D. F. Ronnau, Materials and Tests Division, Nebraska Department of Roads, Lincoln, Neb. 68509-4759. M. D. Cress, Structures Division, Federal Highway Administration, 100 Centennial Mall North, Lincoln, Neb. 68509-4759.

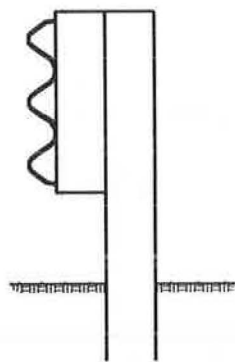


FIGURE 1a

SINGLE THRIE BEAM

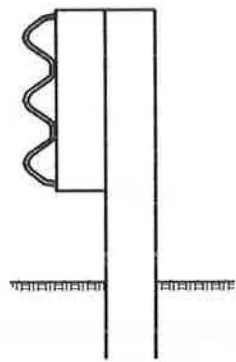


FIGURE 1b

DOUBLE THRIE BEAM

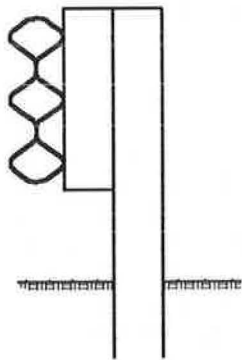


FIGURE 1c

TUBULAR THRIE BEAM

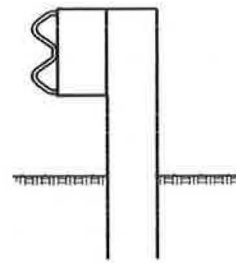


FIGURE 1d

DOUBLE W-BEAM

**FIGURE 1** Transition designs.

The concrete bridge railing and deck were designed to carry dynamic impact loads computed by the FHWA computer model, named BARRIER VII (2). The average 10 msec design impact loads were 120 kips lateral and 50 kips longitudinal. The lateral impact load is on the order of 12 times higher than the design load of 10 kips specified in the AASHTO Standard Specifications for Highway Bridges (3).

The concrete bridge railing, including the cantilevered 4:1 tapered end section, was 21.5 feet. The solid wall portion of the railing was 32 inches high, whereas the beam portion was 29 inches high. The vertical opening between the deck and railing was 17 inches. The two concrete posts were located approximately 8 feet on centers and were set back 2 inches from the traffic face of the railing to minimize vehicle snagging. The 1/8-inch diameter bolt hole pattern in the railing wall was designed to accommodate the end shoes of both the Thrie Beam and the standard W-Beam guardrail sections. The 3/4-inch recessed area adjacent to the 4:1 tapered end section was designed to accommodate the added width of the tubular thrie beam guardrail. On the other hand, a 3/4-inch-wide wood filler block was cut to fill the recessed area and to extend along the length of the tapered end section to accommodate the other non-tubular guardrail designs. The railing was reinforced with No. 7 and smaller size rebar (Grade 60) to carry the vehicle impact loads.

### Approach Guardrail

Design details of the thrie beam approach guardrail system are shown in Figure 3 and photographs of the approach guardrail system are shown in Figure 4. The overall length of the guardrail installation was 56 feet 3 inches. A 6-foot-wide strip of the concrete roadway slab was sawcut and removed to install the guardrail in native soil. The guardrail was installed at a 25 degree angle relative to the center line of the roadway.

The 12 gauge thrie beam guardrail transition section adjacent to the end of the concrete bridge railing was 12 feet 6 inches long. A 12 gauge 6 foot 3 inches Adapter section was used to transition from the thrie beam section to the upstream standard 12 gauge W-Beam section. The thrie beam was mounted 31 inches high, whereas the standard W-Beam was mounted 27 inches high. The upstream end of the W-Beam guardrail was anchored into an 18 inch (diameter) by 6 feet (deep) reinforced concrete shaft.

The first wood guardrail post (post No. 2) was installed 7 feet 7 1/2 inches from the center line of the bolt hole pattern in the concrete bridge end. The unsupported span length from the 4:1 tapered concrete bridge end to the center of post no. 2 was 4 feet 7 inches. The post spacings between post No. 2 and post No. 6 were 3 feet 1 1/2 inches on centers, whereas, the post spacings of the remaining posts were 6 feet 3 inches on centers. The posts were all 6 feet long. The size of the first 2 posts were 10 inches x 10 inches; the size of the next 4 posts were 8 inches x 8 inches, and the size of the remaining posts were 6 inches x 8 inches. The rail blockouts were all 6 inches x 8 inches.

### Soil

The guardrail wood posts were installed in a "native" silty clay topsoil. The soil was not in conformance with either the strong soil (S-1) or the weak soil (S-2) defined in NCHRP 230 (4). The decision to deviate from the recommended testing procedures in NCHRP 230 was made by NDR engineers because of the desire to evaluate the guardrail-bridgerail transition designs under typical soil conditions encountered in most of Nebraska. The properties of the native soil were

1. Unified Classification (ASTM D-2487), CL;
2. Liquid Limit (LL), 31;
3. Plastic Limit (PL), 20;
4. Plasticity Index (LL-PL), 11;
5. Optimum Moisture Content, 17.6%; and
6. Unconfined Shear Strength, 1,900 psf.

The wood posts were placed in 18- to 20-inch diameter holes. The backfill soil around the posts was compacted by hand in 6-inch layers to a density of approximately 92 percent. The field density of the soil was measured by a Troxler Nuclear Density Meter.

### TEST RESULTS

A summary and sequential photographs of the full-scale vehicle crash test on the Tubular Thrie Beam Transition are presented in Figure 5. Due to technical problems with the tow

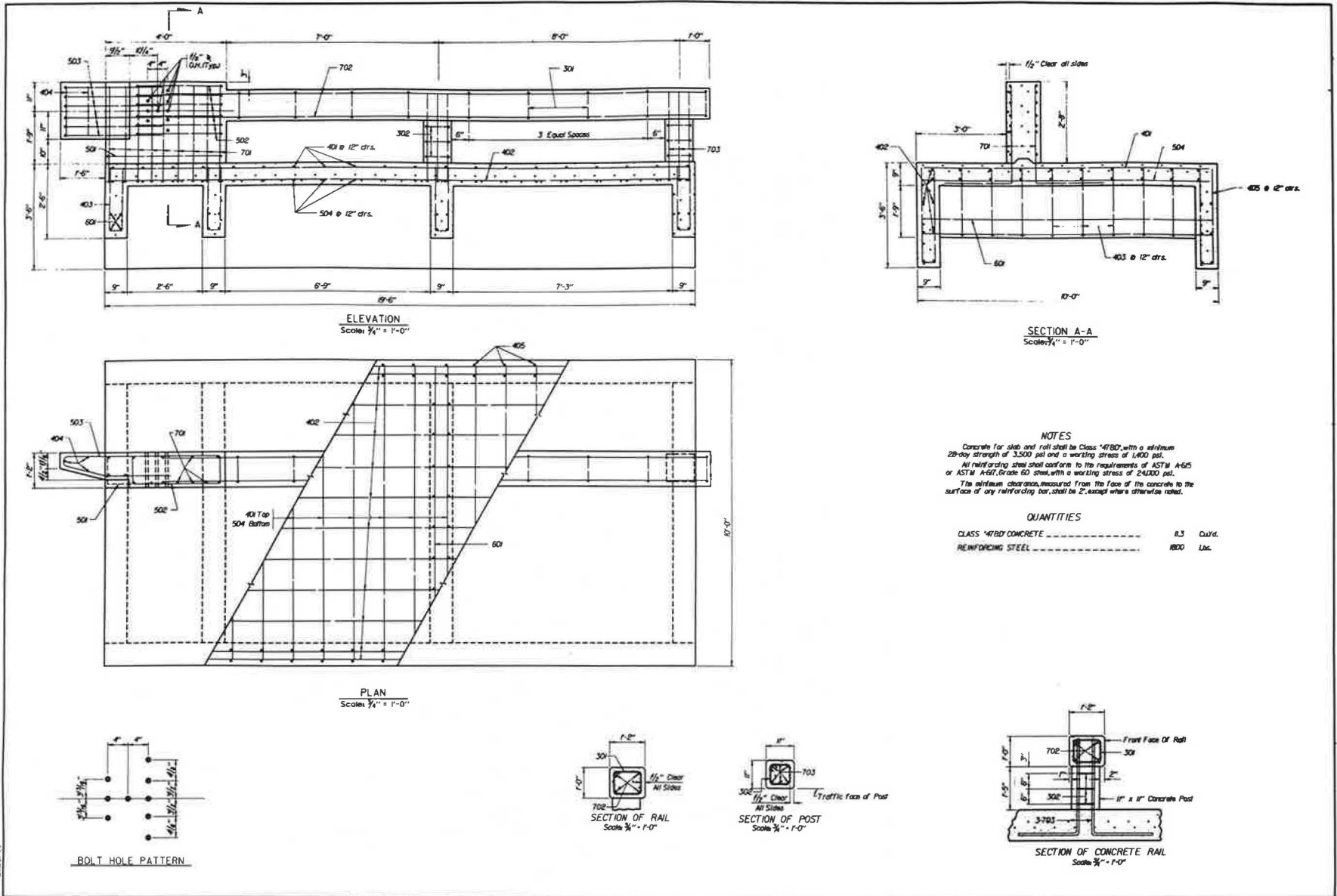


FIGURE 2 Design details of simulated bridge deck and railing.



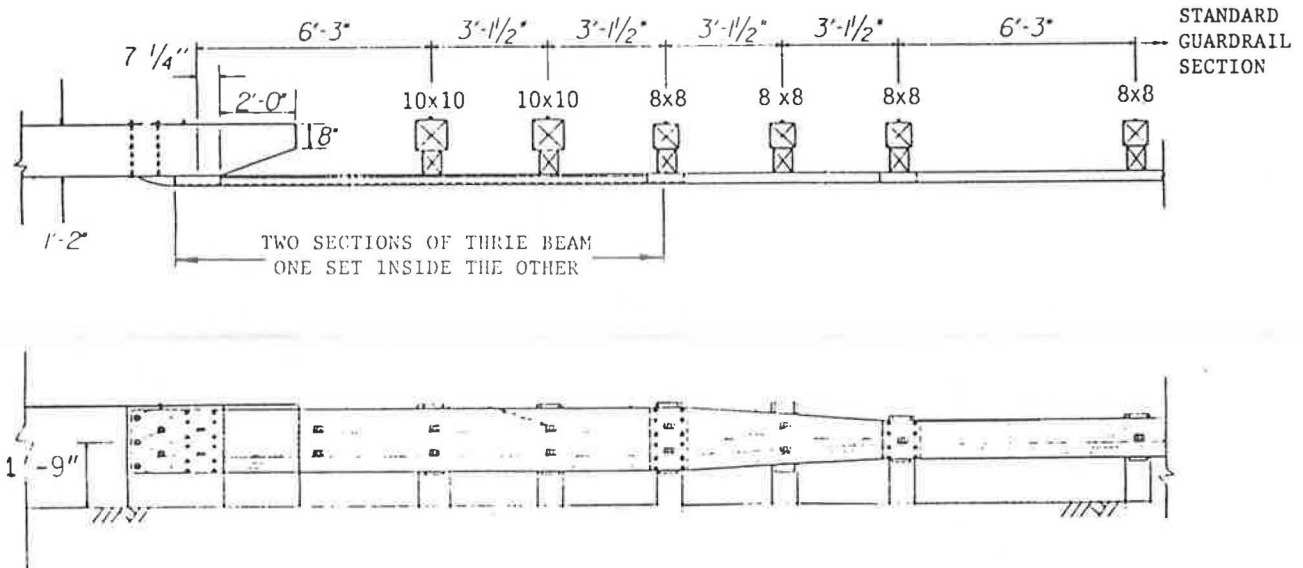


FIGURE 3 Design details of approach guardrail.

vehicle, the impact speed was 13 mph below the recommended target speed (60 mph) in NCHRP 230. The point of impact was between post Nos. 2 and 3. At 76 msec after impact, the vehicle reached its greatest depth of crushing into the guardrail. At 194 msec, the vehicle's "lateral" velocity component was zero as the vehicle became parallel to an extended center line of the traffic barrier. Somewhere between 76 and 194 msec, an occupant would have moved laterally 12 inches and struck the side of the vehicle.

Photographs of the guardrail damage are shown in Figure 6. The Tubular Thrie Beam was fabricated by a local steel manufacturer by shop welding two thrie beams back-to-back (see Figure 1c). The end shoe was welded on the outside of the tubular thrie beam. As evident, the damage to the guardrail was very minor with a maximum guardrail permanent set of only 2½ inches. Due to a technical problem with the overhead camera, the maximum guardrail dynamic deflection was not measured. Assuming a typical impact factor of 1.5, an estimate of the maximum dynamic deflection would be 4 inches.

As can be seen in Figure 6, the vehicle tire marks were relatively straight after exit from the barrier. The vehicle exit angle was 15 deg, and the vehicle travelled 270 feet before it came to a stop without braking. The tire scuff marks were caused by the deformed inward alignment of the two front wheels. The vehicle rebound distance was 72 feet.

The damage to the vehicle was moderate and repairable. The left front door was not sprung open under the lateral side impact loading of the dummy. The left front corner was crushed 15 inches and the right front corner was deformed outward 3 inches. The left rear corner was crushed 4 inches. The vehicle damage was assigned a NSC (5) TAD rating of LFQ-3. Based on the findings in NCHRP 86 (6), the damage rating indicates that injuries will occur in 18 percent of the vehicles damaged to this extent.

The vehicle impact speed was 47 mph and the exit speed was 38 mph. The change-in-speed of 9 mph was well below the 15 mph limit recommended in NCHRP 230 (4).

The results of test No. 1 were used to determine "equiv-

alent" impact conditions presented in table 1 by equating lateral kinetic energy. At an impact angle of about 20 degrees, the same guardrail damage shown in Figure 6 would have occurred under an impact speed of 60 mph. The equation to determine equivalent speeds is presented in Table 1.

In a similar manner, the results of test No. 1 were used to estimate that a dynamic deflection of 6 to 7 inches would have occurred in a 60 mph impact. This estimate is based on the assumption that the guardrail deflection is directly proportional to the vehicle lateral kinetic energy.

Based on the estimate that the guardrail dynamic deflections would have only been on the order of 6 to 7 inches under a 60 mph impact, NDR decided not to rerun the test because it would most likely be successful. It is interesting to note that the BARRIER VII computer model predicted a dynamic deflection of 9 inches. No attempt was made to fine-tune the computer model in this study.

#### Test No. 2: Single Thrie Beam Transition

A summary and sequential photographs of the full-scale vehicle crash test in the Single Thrie Beam Transition is presented in Figure 7. The point of impact was between posts Nos. 2 and 3. The vehicle impact speed was 60 mph, and the exit speed was 39 mph. During the primary (vehicle front-end) impact stage at 89 msec, the maximum guardrail deflection was 13 inches. At 108 msec, the lateral occupant displacement of 12 inches occurred nearly simultaneously to the time in which the front door sprung open under a dummy side impact loading force of 10 g. It was interesting to observe that the largest guardrail deflection of 14 inches occurred during the secondary (vehicle rear-end) impact stage at 231 msec. Vehicle exit from the barrier occurred at about 280 msec.

Photographs of the guardrail damage are shown in Figure 8. The area where the upstream end anchor was bolted to the W-Beam guardrail buckled inward under the tensile loading of about 48 kips as computed by BARRIER VII. As clearly visible in the photographs, a moderate amount of vehi-

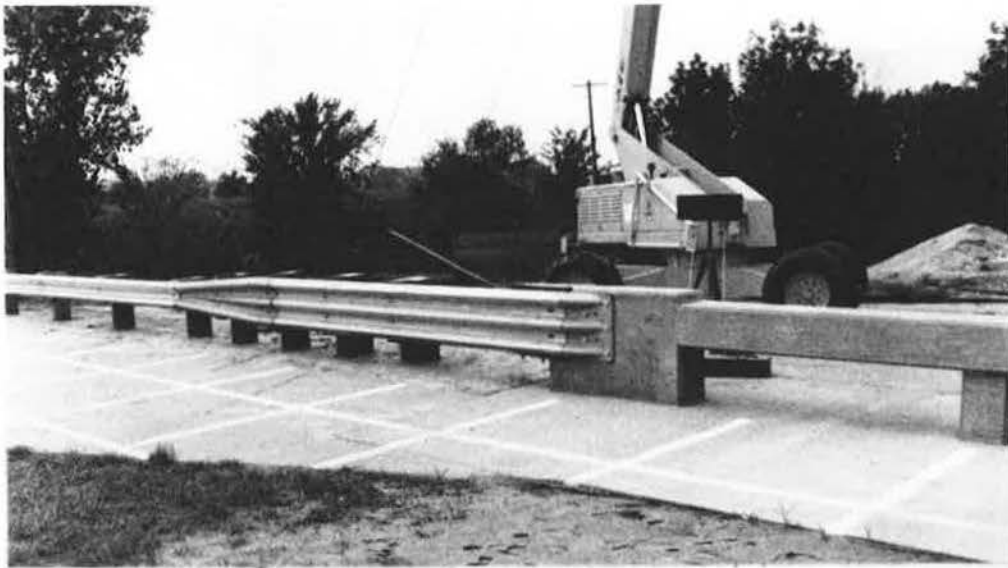


**FIGURE 4** Photographs of approach guardrail installation.



Impact



76 msec



194 msec



294 msec

TEST VEHICLE

Make . . . . . 1977 Plymouth Fury  
 Weight (excluding dummy) . . . . . 4,384 lb.

TRAFFIC BARRIER INSTALLATION

Concrete Bridgerail  
 Type . . . . . Open Rail/Post; Tapered End  
 Length . . . . . 21 ft.-6 in.

Guardrail Members  
 Transition  
 Type . . . . . Tubular Thrie Beam  
 Length . . . . . 12 ft.-6 in.

Adapter  
 Length . . . . . 6 ft.-3 in.

Approach  
 Type . . . . . Standard W-Beam  
 Length . . . . . 37 ft.-6 in.

Guardrail Wood Posts  
 Post No. 1 . . . . . Left Out  
 Post Nos. 1 and 2 . . . . . 10 x 10 x 72 in.  
 Post Nos. 3 thru 6 . . . . . 8 x 8 x 72 in.  
 Post Nos. 7 thru 12 . . . . . 6 x 6 x 72 in.

Native Soil  
 Type . . . . . Silty-Clay (CL)  
 Optimum Moisture . . . . . 18%  
 Relative Compaction . . . . . 92%  
 Test Conditions . . . . . Dry

TEST RESULTS

Vehicle Speed  
 Impact . . . . . 47 mph  
 Exit . . . . . 38 mph

Vehicle Angle  
 Impact . . . . . 25 deg.  
 Exit . . . . . 15 deg.

Vehicle Rebound Distance . . . . . 72 ft.

Vehicle Damage . . . . . TAD LFQ-3

Traffic Barrier  
 Impact Location . . . . . Bet. Post Nos.2&3  
 Max. Dynamic Deflection . . . . . 4 in. (est.)  
 Max. Permanent Set . . . . . 2 1/2 in.  
 Snagging . . . . . None

Occupant Risk (NCHRP 230)  
 Lateral Impact Velocity . . . . . Not Measured  
 Ridedown Accelerations . . . . . Not Measured

Occupant Risk (NCHRP 86)  
 Injury Accident Prob. . . . . 18%

FIGURE 5 Summary of crash test No. 1.

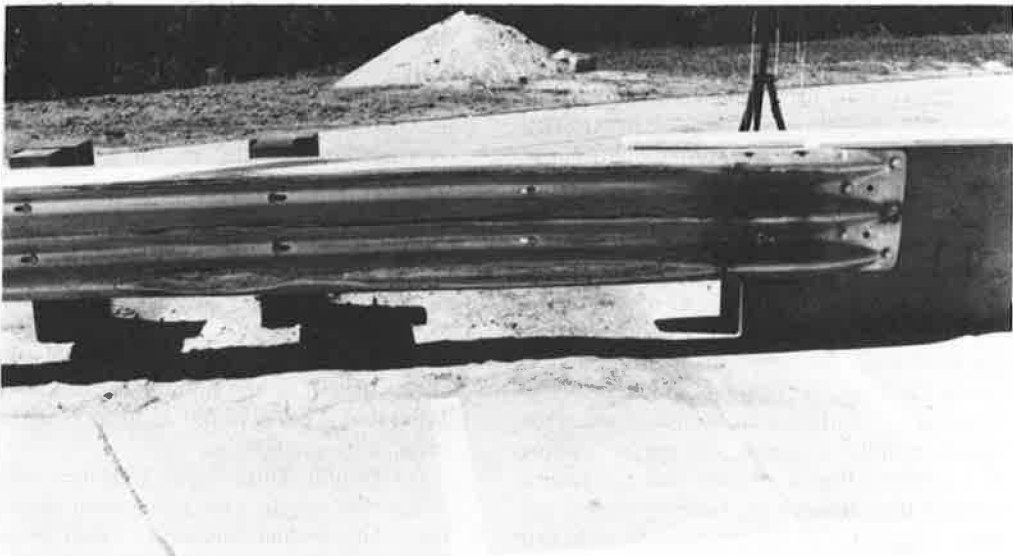


**FIGURE 6** Photographs of test No. 1 guardrail damage.

TABLE 1 EQUIVALENT TEST NO. 1 IMPACT CONDITIONS

Impact Angle (deg)	Equivalent Impact Speed (mph)
15	77
16	72
17	68
18	64
19	61
20	58

Actual Test Speed . . . 47 mph

Actual Test Angle . . . 25 deg

$$\frac{1}{2} \frac{W}{g} (V \sin \theta)^2 = \left[ \frac{1}{2} \frac{W}{g} (V \sin \theta)_{\text{test}}^2 \right]_{\text{test}}$$

$$V^2 = \frac{(V \sin \theta)_{\text{test}}^2}{\sin^2 \theta}$$

$$V^2 = \frac{394.5}{\sin^2 \theta}$$

cle snagging occurred in the lower half of the thrie beam in the area of the tapered end of the concrete bridgerail. The vehicle change-in-speed of 21 mph was also a clear indication of a moderate amount of snagging as the change-in-speed was greatly in excess of the 15 mph limit specified in NCHRP 230.

The vehicle exit angle was 11 degrees. Due to the high drag forces from the badly damaged left front wheel, the vehicle turned back in toward an extended center line of the traffic barrier after it had travelled 78 feet. The maximum rebound distance of the vehicle center of gravity (CG) was 20 feet.

Due to the snagging, the damage to the vehicle was major and not repairable. The vehicle damage was assigned a NSC TAD rating of LFQ-6½. Based on the findings in NCHRP 86 (6), the damage rating indicates that injuries will occur in 86 percent of the vehicles damaged to this extent.

A summary and sequential photographs of the full-scale vehicle crash test on the Double Thrie Beam Transition is presented in Figure 9. The point of impact was between posts Nos. 2 and 3. The vehicle impact speed was 61 mph, and the exit speed was 47 mph. During the primary (vehicle front-end) impact stage at 86 msec, the maximum guardrail deflection was 9 inches. At 114 msec, the lateral occupant displacement of 12 inches occurred nearly simultaneously to when the front door sprung open under a dummy side impact loading force of 10 g. It was interesting to observe that the largest guardrail deflection of 10 inches occurred during the secondary (vehicle rear-end) impact stage at 194 msec. Vehicle exit from the barrier occurred at about 250 msec.

Photographs of the guardrail damage are shown in Figure

10. The damaged guardrail shows no indication of vehicle snagging. The vehicle change-in-speed of 14 mph was also supportive of the fact that no snagging occurred as the change-in-speed was below the 15 mph limit specified in NCHRP 230. Overall, the guardrail "smoothly" redirected the vehicle. The maximum permanent set in the guardrail was 7½ inches.

The vehicle exit angle was 11 degrees, which is well below the 15 degree limit recommended in NCHRP 230. Due to slight damage of the left front wheel, the vehicle turned slowly back in toward an extended center line of the traffic barrier. The maximum rebound distance of the vehicle CG path was approximately 20 feet.

The vehicle damage was assigned a NSC TAD rating of LFQ-4½. Based on the findings in NCHRP 86 (6), it was predicted that injuries would occur in 41 percent of the vehicles damaged to this extent.

#### Test No. 4: Double Thrie Beam Transition

A summary and sequential photographs of the full-scale vehicle crash test on the Double Thrie Beam Transition is presented in Figure 11. The point of impact was at post No. 4; whereas, in the preceding test (No. 3) on the identical guardrail design, the impact point was between posts Nos. 2 and 3. The decision to run the second test was based on the need to determine the most critical impact location in terms of guardrail performance. The vehicle impact speed was 61 mph, and the exit speed was 48 mph. During the primary (vehicle front-end) impact stage at 90 msec, the maximum guardrail deflection was 16 inches. At 99 msec, the lateral occupant displacement of 12 inches occurred nearly simultaneously to when the front door sprung open under a dummy side impact loading force of 8 g. It was interesting to observe that the largest guardrail deflection of 17 inches occurred during the secondary (vehicle rear-end) impact stage at 201 msec. Vehicle exit from the barrier occurred at about 283 msec.

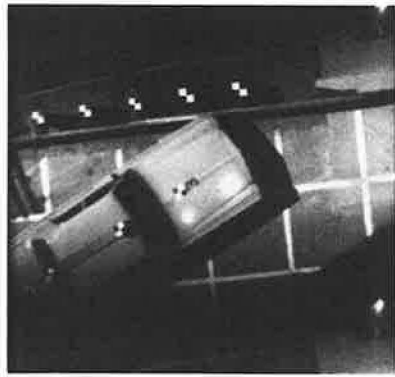
Photographs of the guardrail damage are shown in Figure 12. The soil was saturated from a heavy, two-day storm preceding the test. NDR decided to test under a saturated soil condition as this condition would be representative of the lowest possible soil shearing strength. The damaged guardrail shows no indication of vehicle snagging. The vehicle change-in-speed of 13 mph also supported the fact that no snagging occurred as the change-in-speed was below the 15 mph limit specified in NCHRP 230. Overall, the guardrail "smoothly" redirected the vehicle. The maximum permanent set in the guardrail was 11 inches.

The vehicle exit angle was 15 degrees. Due to slight damage of the left front wheel, the vehicle turned slowly back in toward an extended center line of the traffic barrier. The maximum rebound of the vehicle CG path was approximately 20 feet.

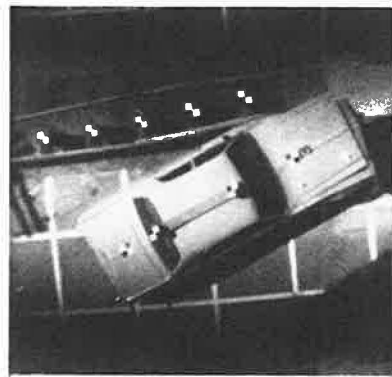
The vehicle damage was assigned a NSC TAD rating of LFQ-4. Based on the findings in NCHRP 86 (6), it was predicted that injuries would occur in 33 percent of the vehicles damaged to this extent.

The Double Thrie Beam Transition was similar to an old design that was in wide use several years ago in Nebraska. The old design had smaller (6 x 8 inch) posts spaced on longer (6 foot 3 inch) centers.

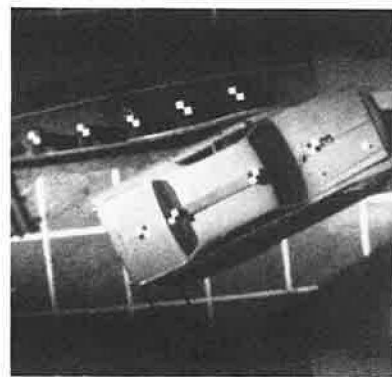
A summary and sequential photographs of the full-scale



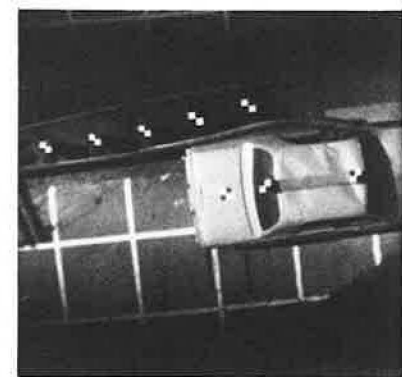
Impact



89 msec



108 msec



185 msec

TEST VEHICLE

Make . . . . . 1977 Plymouth Fury  
 Weight (excluding dummy) . . . . . 4,400 lb.

Concrete Bridgerail

Type . . . . . Open Rail/Post; Tapered End  
 Length . . . . . 21 ft.-6 in.

Guardrail Members

Transition

Type . . . . . Single Thrie Beam  
 Length . . . . . 12 ft.-6 in.

Adapter

Length . . . . . 6 ft.-3 in.

Approach

Type . . . . . Standard W-Beam  
 Length . . . . . 37 ft.-6 in.

Guardrail Wood Posts

Post No. 1 . . . . . Left Out  
 Post Nos. 1 and 2 . . . . . 10 x 10 x 72 in.  
 Post Nos. 3 thru 6 . . . . . 8 x 8 x 72 in.  
 Post Nos. 7 thru 12 . . . . . 6 x 6 x 72 in.

Native Soil

Type . . . . . Silty-Clay (CL)  
 Optimum Moisture . . . . . 18%  
 Relative Compaction . . . . . 92%  
 Test Conditions . . . . . Dry

Vehicle Speed

Impact . . . . . 60 mph  
 Exit . . . . . 39 mph

Vehicle Angle

Impact . . . . . 25 deg.  
 Exit . . . . . 11 deg.

Vehicle Rebound Distance . . . . . 20 ft.

Vehicle Damage . . . . . TAD LFQ-6½

Traffic Barrier

Impact Location . . . . . Bet. Post Nos. 2&3  
 Max. Dynamic Deflection . . . . . 14 in.  
 Max. Permanent Set . . . . . 10 in.  
 Snagging . . . . . Moderate

Occupant Risk (NCHRP 230)

Lateral Impact Velocity . . . . . 21 fps  
 Ridedown Accelerations . . . . . 10 g

Occupant Risk (NCHRP 86)

Injury Accident Prob. . . . . 86%

FIGURE 7 Summary of crash test No. 2.

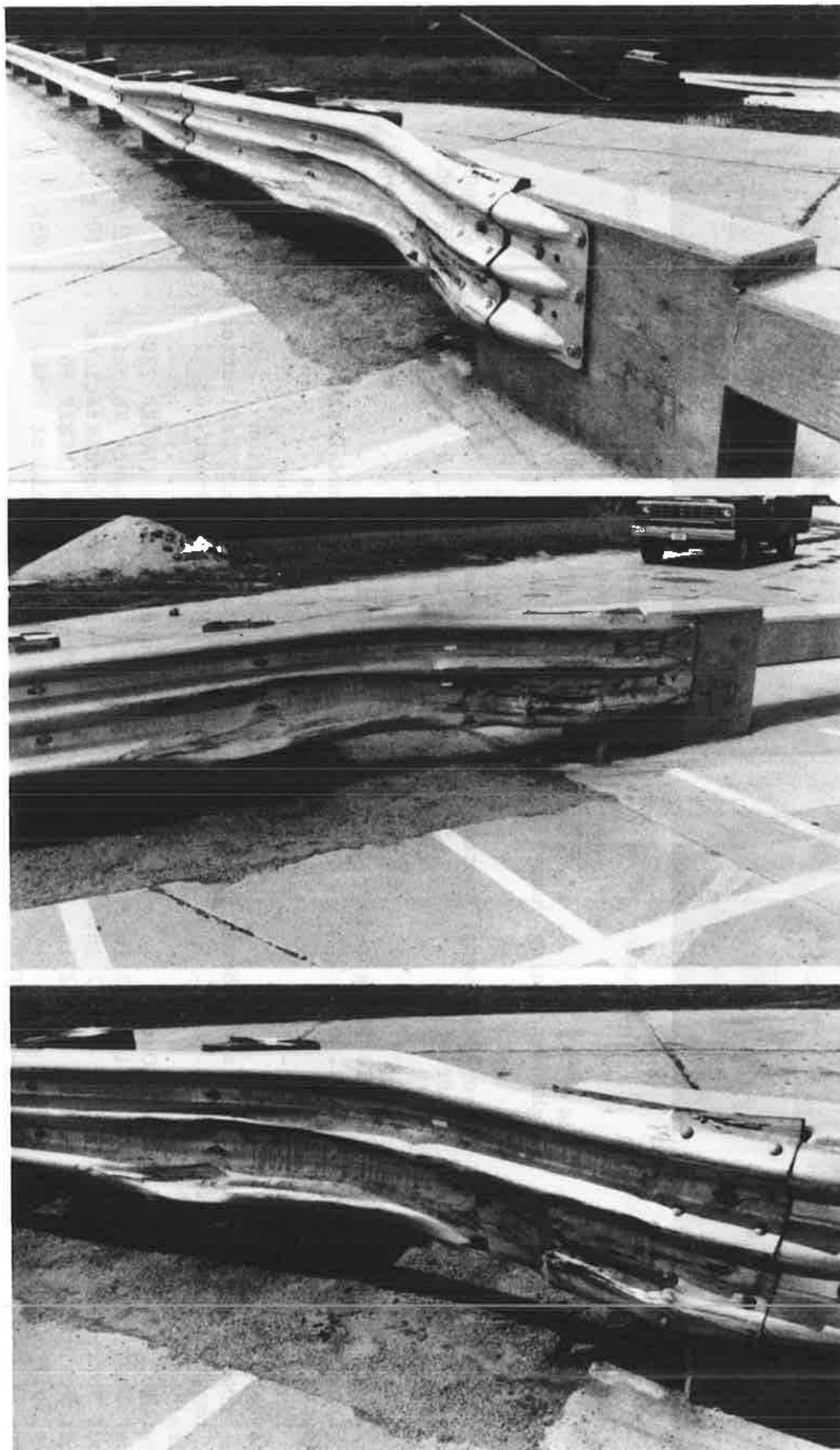
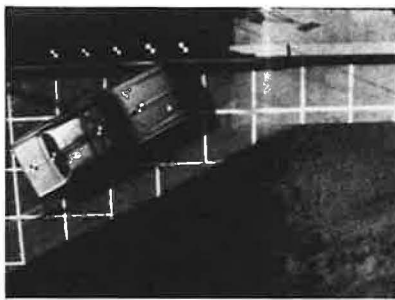
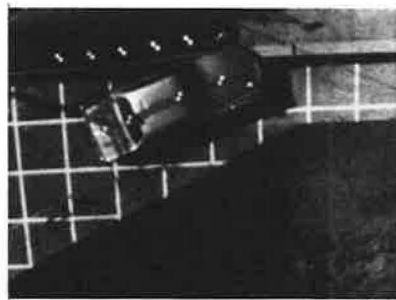


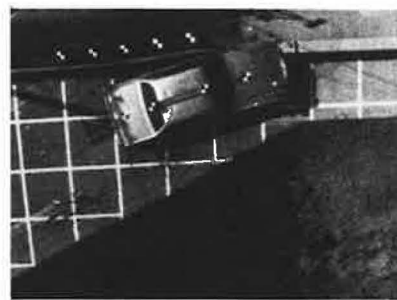
FIGURE 8 Photographs of test No. 2 guardrail damage.



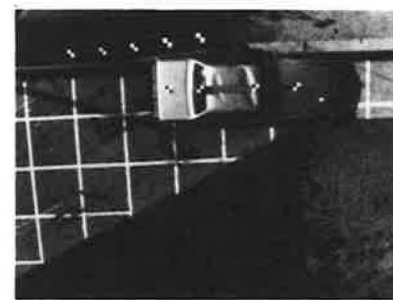
Impact



86 msec



114 msec



166 msec

TEST VEHICLE

Make . . . . . 1977 Plymouth Fury  
 Weight (excluding dummy) . . . . . 4,360 lb.

TRAFFIC BARRIER INSTALLATION

Concrete Bridgerail  
 Type . . . . . Open Rail/Post; Tapered End  
 Length . . . . . 21 ft.-6 in.  
 Guardrail Members  
 Transition  
 Type . . . . . Double Thrie Beam  
 Length . . . . . 12 ft.-6 in.  
 Adapter  
 Length . . . . . 6 ft.-3 in.  
 Approach  
 Type . . . . . Standard W-Beam  
 Length . . . . . 37 ft.-6 in.  
 Guardrail Wood Posts  
 Post No. 1 . . . . . Left Out  
 Post Nos. 1 and 2 . . . . . 10 x 10 x 72 in.  
 Post Nos. 3 thru 6 . . . . . 8 x 8 x 72 in.  
 Post Nos. 7 thru 12 . . . . . 6 x 6 x 72 in.  
 Native Soil  
 Type . . . . . Silty-Clay (CL)  
 Optimum Moisture . . . . . 18%  
 Relative Compaction . . . . . 92%  
 Test Conditions . . . . . Dry

TEST RESULTS

Vehicle Speed  
 Impact . . . . . 61 mph  
 Exit . . . . . 47 mph  
 Vehicle Angle  
 Impact . . . . . 25 deg.  
 Exit . . . . . 11 deg.  
 Vehicle Rebound Distance . . . . . 20 ft.  
 Vehicle Damage . . . . . TAD LFQ-4½  
 Traffic Barrier  
 Impact Location . . . . . Bet.Post Nos. 2&3  
 Max. Dynamic Deflection . . . . . 10 in.  
 Max. Permanent Set . . . . . 7½ in.  
 Snagging . . . . . None  
 Occupant Risk (NCHRP 230)  
 Lateral Impact Velocity . . . . . 19 fps  
 Ridedown Accelerations . . . . . 10 g  
 Occupant Risk (NCHRP 86)  
 Injury Accident Prob. . . . . 41%

FIGURE 9 Summary of crash test No. 3.



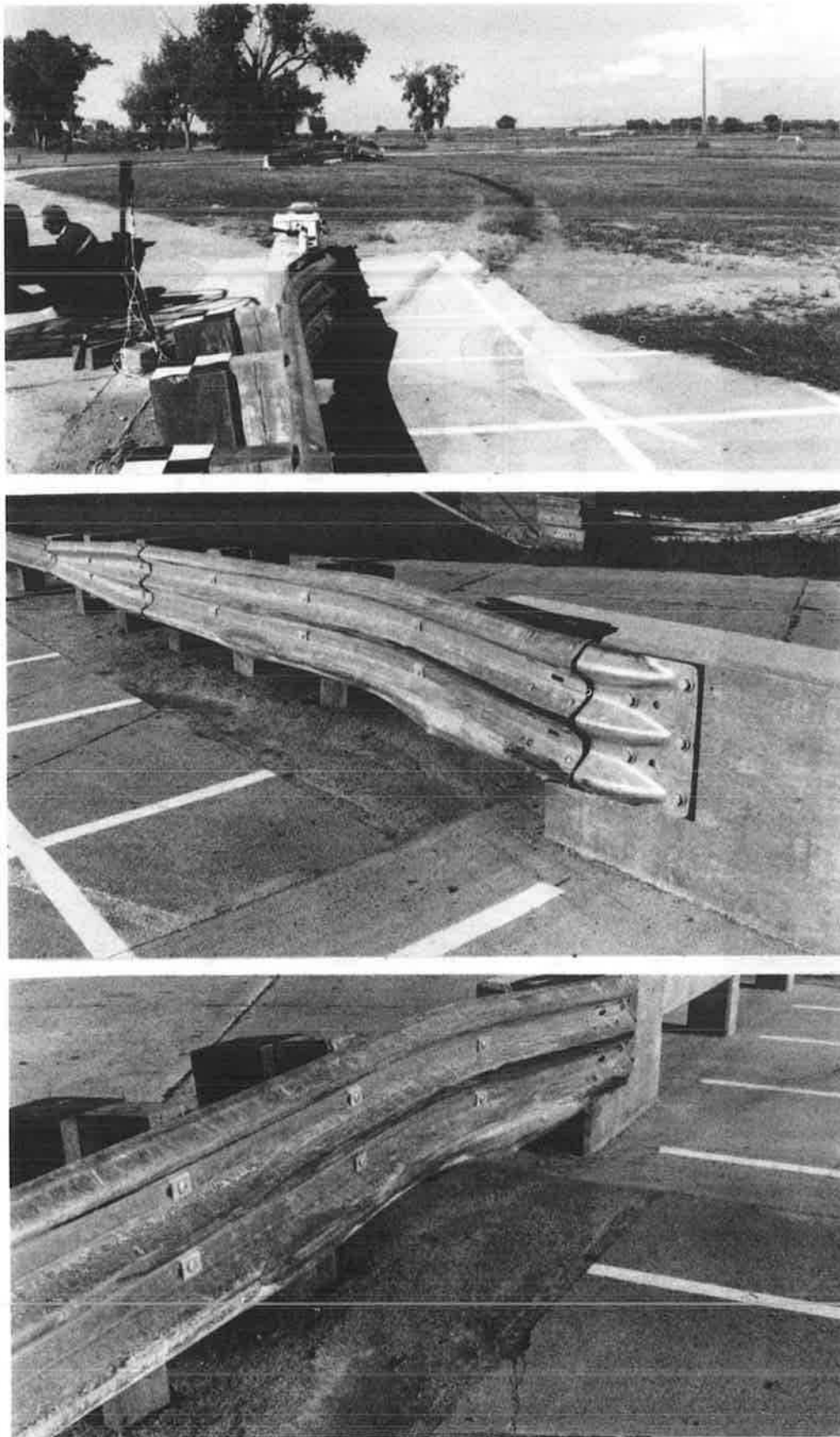


FIGURE 10 Photographs of test No. 3 guardrail damage.



Impact



90 msec



101 msec



155 msec

TEST VEHICLE

Make . . . . . 1977 Plymouth Fury  
 Weight (excluding dummy) . . . . . 4,320 lb.

TRAFFIC BARRIER INSTALLATION

Concrete Bridgerail  
 Type . . . . . Open Rail/Post; Tapered End  
 Length . . . . . 21 ft.-6 in.  
 Guardrail Members  
 Transition  
 Type . . . . . Double Thrie Beam  
 Length . . . . . 12 ft.-6 in.  
 Adapter  
 Length . . . . . 6 ft.-3 in.  
 Approach  
 Type . . . . . Standard W-Beam  
 Length . . . . . 37 ft.-6 in.  
 Guardrail Wood Posts  
 Post No. 1 . . . . . Left Out  
 Post Nos. 1 and 2 . . . . 10 x 10 x 72 in.  
 Post Nos. 3 thru 6 . . . . 8 x 8 x 72 in.  
 Post Nos. 7 thru 12 . . . . 6 x 6 x 72 in.  
 Native Soil  
 Type . . . . . Silty-Clay (CL)  
 Optimum Moisture . . . . 18%  
 Relative Compaction . . . 92%  
 Test Conditions . . . . . Wet

TEST RESULTS

Vehicle Speed  
 Impact . . . . . 61 mph  
 Exit . . . . . 48 mph  
 Vehicle Angle  
 Impact . . . . . 25 deg.  
 Exit . . . . . 15 deg.  
 Vehicle Rebound Distance . . . 20 ft.  
 Vehicle Damage . . . . . TAD LFQ-4  
 Traffic Barrier  
 Impact Location . . . . . Post No. 4  
 Max. Dynamic Deflection . . . 17 in.  
 Max. Permanent Set . . . . 11 in.  
 Snagging . . . . . None  
 Occupant Risk (NCHRP 230)  
 Lateral Impact Velocity . . . 17 fps  
 Ridedown Accelerations . . . 8 g  
 Occupant Risk (NCHRP 86)  
 Injury Accident Prob. . . . . 33%

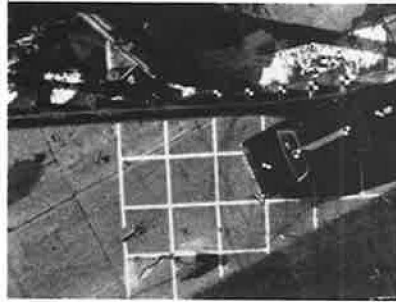
FIGURE 11 Summary of crash test No. 4.



**FIGURE 12** Photographs of test No. 4 guardrail damage.



Impact



75 msec



113 msec



182 msec

TEST VEHICLE

Make . . . . . 1977 Plymouth Fury  
 Weight (excluding dummy) . . . . . 4,560 lb.

TRAFFIC BARRIER INSTALLATION

Concrete Bridgerail  
 Type . . . . . Open Rail/Post; Tapered End  
 Length . . . . . 21 ft.-6 in.

Guardrail Members  
 Transition  
 Type . . . . . Double W-Beam  
 Length . . . . . 12 ft.-6 in.

Adapter  
 Length . . . . . 6 ft.-3 in.

Approach  
 Type . . . . . Standard W-Beam  
 Length . . . . . 37 ft.-6 in.

Guardrail Wood Posts  
 Post No. 1 . . . . . Left Out  
 Post Nos. 1 and 2 . . . . . 10 x 10 x 72 in.  
 Post Nos. 3 thru 6 . . . . . 8 x 8 x 72 in.  
 Post Nos. 7 thru 12 . . . . . 6 x 6 x 72 in.

Native Soil  
 Type . . . . . Silty-Clay (CL)  
 Optimum Moisture . . . . . 18%  
 Relative Compaction . . . . . 92%  
 Test Conditions . . . . . Ground Frozen 6 to 8 in.

TEST RESULTS

Vehicle Speed  
 Impact . . . . . 62 mph  
 Exit . . . . . 39 mph

Vehicle Angle  
 Impact . . . . . 25 deg.  
 Exit . . . . . 9 deg.

Vehicle Rebound Distance . . . . . 20 ft.

Vehicle Damage . . . . . TAD LFQ-7

Traffic Barrier  
 Impact Location . . . . . Bet.Post Nos. 2&3  
 Max. Dynamic Deflection . . . . . 10 in.  
 Max. Permanent Set . . . . . 6 in.  
 Snagging . . . . . Severe

Occupant Risk (NCHRP 230)  
 Lateral Impact Velocity . . . . . 24 fps  
 Ridedown Accelerations . . . . . 6 g

Occupant Risk (NCHRP 86)  
 Injury Accident Prob. . . . . 100%

FIGURE 13 Summary of crash test No. 5.

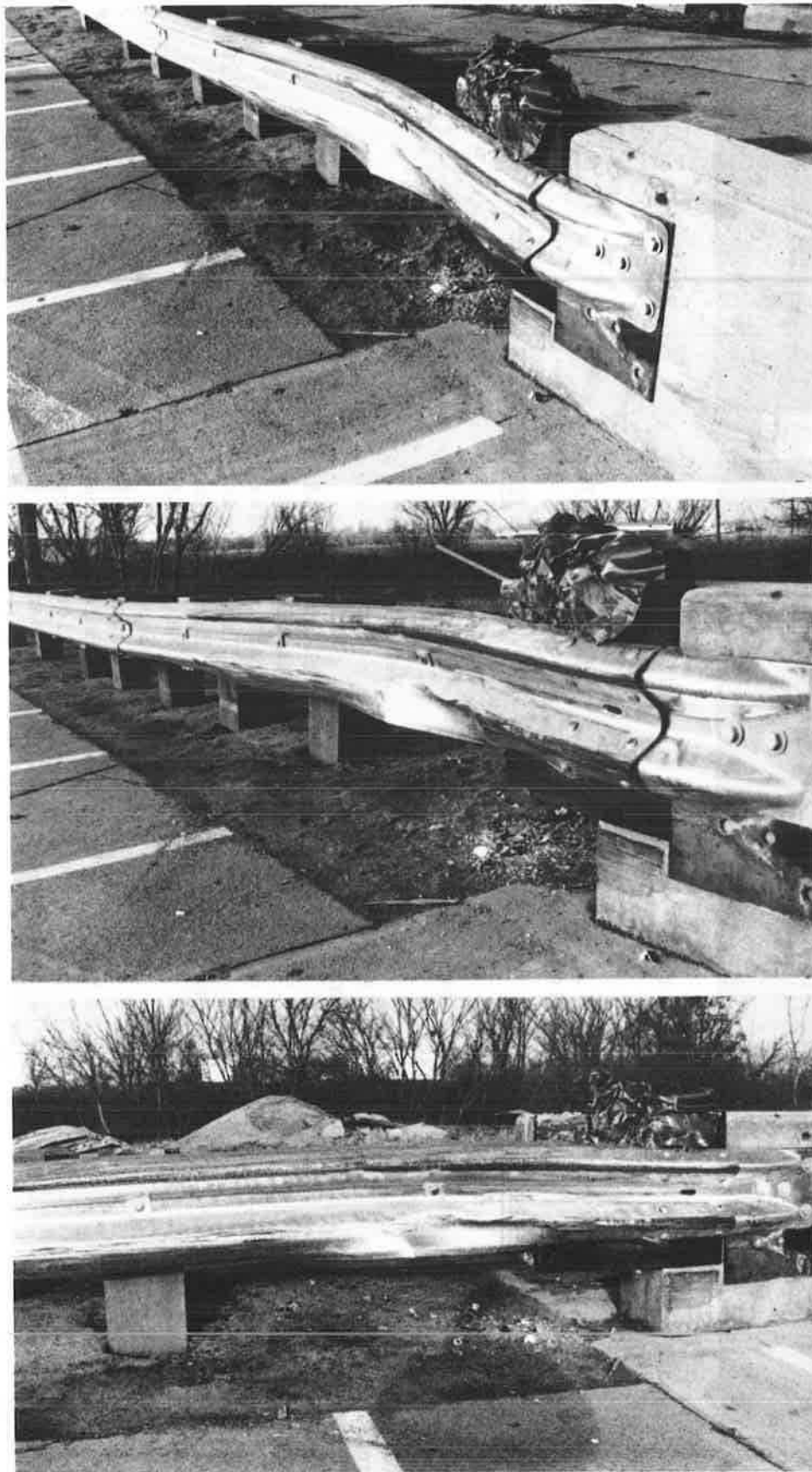


**FIGURE 14** Photographs of test No. 5 guardrail damage.

vehicle crash test on the Double W-Beam Transition is presented in Figure 13. The point of impact was between posts Nos. 2 and 3. The vehicle impact speed was 62 mph, and the exit speed was 39 mph. During the primary (vehicle front-end) impact stage at 75 msec, the maximum guardrail deflection was 9 inches. At 113 msec, the lateral displacement of an occupant was 12 inches, however, there was no sign of the front door being sprung open under the side impact loading of the dummy as had occurred in three previous tests. The largest guardrail deflection of 10 inches occurred during the secondary (vehicle rear-end) impact stage at 212 msec. Vehicle exit from the barrier occurred at 262 msec.

Photographs of the guardrail damage are shown in Figure 14. The soil was frozen 6 to 8 inches deep. The effect of the frozen soil was readily apparent by comparing the permanent set deflections in test No. 3 with this test. Aside from the fact that the strength of the Double Thrie Beam in test No. 3 was much stronger than the strength of the Double W-Beam, the permanent set deflections of the Double W-Beam were much less. The damaged guardrail in Figure 13 shows severe vehicle snagging. The vehicle change-in-speed of 23 mph also supported the fact that severe snagging occurred as the change-in-speed greatly exceeded the 15 mph limit specified in NCHRP 230. Snagging resulted when the vehicle frame and wheel assembly got under the guardrail and impacted the tapered end of the concrete bridgerail. As shown in Figure 14, sheet metal was torn from the vehicle and wedged between the guardrail and the wood filler block in the recessed area of the bridgerail tapered-end.

The vehicle exit angle was 9 degrees. Due to the badly damaged left front wheel, the vehicle turned slowly back-in toward an extended center line of the traffic barrier. The vehicle was extensively damaged due to the severe snagging. The vehicle damage was assigned a NSC TAD rating of LFQ-7. Based on the findings in NCHRP 86 (6), it was predicted that in vehicles damaged to this extent, injuries would occur in 100 percent of the accidents.

## SUMMARY AND CONCLUSIONS

A comparative summary of the crash test results is presented in Table 2, and the performance of the traffic barrier measured in terms of the NCHRP 230 safety evaluation guidelines (4) is presented in Table 3.

Due to technical problems with the tow vehicle, the impact speeds in test No. 1 were approximately 14 mph below the 60 mph target speed recommended in NCHRP 230. Test No. 1 on the Tubular Thrie Beam transition was not rerun because it was estimated that the dynamic deflection would have only been about 3 inches greater at the higher 60 mph impact speed, and hence, the 60 mph test would have most likely been satisfactory. The estimated deflections were determined on the assumption that the deflection of the guardrail was directly proportional to the lateral kinetic energy of the vehicle.

After impact with the guardrail transition, the vehicle trajectory (CG path) in each of the tests was unsatisfactory in accordance with NCHRP 230 (Item *H*), as each vehicle would have been redirected back into the adjacent lanes of traffic. To compensate for this type of situation, NCHRP 230 (Item 1) specifies that (1) the change-in-speed of the vehicle

should be less than 15 mph, and (2) the exit angle should be less than 15 degrees.

In test No. 2 on the Single Thrie Beam transition, a moderate amount of vehicle snagging occurred in the lower half of the thrie beam adjacent to the tapered end of the concrete bridgerail. As a result, the test was considered to be unsatisfactory because the vehicle change-in-speed of 21 mph was significantly higher than the limit of 15 mph specified in NCHRP 230. Due to vehicle snagging on the Single Thrie Beam transition, NDR decided to run the next test on a Double Thrie Beam transition in favor of the much stronger and costly Tubular Thrie Beam transition that was used earlier in the study.

In test No. 5 on the Double W-Beam transition, an amount of vehicle snagging occurred under the guardrail on the tapered end of the concrete bridgerail. As a result, the test was considered to be unsatisfactory because the vehicle change-in-speed of 23 mph greatly exceeded the limit of 15 mph specified in NCHRP 230. In addition, the integrity of the passenger compartment area in terms of occupant risk (Item *E*) was considered to be marginal as the engine firewall was pushed backward on the side of the driver. The last item of concern was the soil that was frozen to 6 to 8 inches deep. It is predicted that if the soil had not been frozen, the vehicle would have penetrated deeper under the flexible guardrail, and as a result, the vehicle would most likely have abruptly stopped and spun-out on the tapered end of the concrete bridgerail.

From an overall consideration, the Double Thrie Beam transition in test Nos. 3 and 4 was satisfactory in terms of the NCHRP 230 performance categories of structural adequacy (items *A* and *D*), occupant risk (Item *E*), and vehicle trajectory (Item *I*). Two tests were conducted at different points of impact to be certain that the transition design was tested under the most critical condition of impact. Also, in test No. 4 the soil was saturated from a heavy, two-day storm preceding the test. NDR decided to test under a saturated soil condition as this condition would be representative of the lowest possible soil shearing strength.

NCHRP 230 does not specify any evaluation guidelines for conducting tests on a guardrail transition in regard to the "Impact Velocity of a Hypothetical Front Seat Passenger Against the Vehicle Interior." However, data on occupant impact velocity were presented in this study because it was felt that the data provided further insight into the evaluation of the transition designs tested. To supplement the NCHRP 230 data on occupant impact velocity, data on "Injury Accident Probability" contained in NCHRP 86 (6) were also presented in this study. The two sets of data on the tests are presented in Table 2, and a graphic relationship between the two sets of data is presented in Figure 15. An occupant impact velocity of 20 feet per second (fps) is recommended in NCHRP 230 as an "acceptable" design value, whereas, a value of 30 fps is a recommended design "limit." The effects of vehicle snagging are very evident in Figure 15.

In test No. 5, severe snagging on the Double W-Beam transition would result in an injury accident probability of 100 percent; whereas, in test No. 2, moderate snagging on the Single Thrie Beam transition would result in an injury accident probability of 86 percent. In tests Nos. 3 and 4, an impact with the Double Thrie Beam transition in which no snagging occurred would result in an injury accident probability of 35 to 40 percent. Lastly, in test No. 1, at a lower impact speed

TABLE 2 COMPARATIVE SUMMARY OF CRASH TEST RESULTS

TEST NO.	1	2	3	4	5
TRANSITION BEAM DESIGN	Tubular Thrie	Single Thrie	Double Thrie	Double Thrie	Double W-Beam
SOIL (Silty-Clay)	Dry	Dry	Dry	Wet	Frozen <sup>(a)</sup>
VEHICLE WEIGHT (lb)	4,384	4,400	4,360	4,320	4,560
VEHICLE SPEED					
Impact (mph)	47	60	61	61	62
Exit (mph)	38	39	47	48	39
Change (mph)	9	21	14	13	23
VEHICLE ANGLE					
Impact (deg)	25	25	25	25	25
Exit (deg)	15	11	11	15	9
VEHICLE REBOUND DISTANCE (ft)	72	20	20	20	20
VEHICLE DAMAGE (TAD LFQ)	3 moderate	6 1/2 major	4 1/2 moderate	4 moderate	7 extensive
TRAFFIC BARRIER					
Impact Post Location	Bet. 2&3	Bet. 2&3	Bet. 2&3	4	Bet. 2&3
Max. Dynamic deflection	4	14	10	17	10
Max. Permanent Set (in)	2 1/2	10	7 1/2	11	6
Snagging	None	Moderate	None	None	Severe
OCCUPANT RISK (NCHRP 230)					
Lateral Impact Velocity (fps)	12	21	19	17	24
Ridedown Accelerations (g)	-	10	10	8	6
OCCUPANT RISK (NCHRP 86)					
Injury Accident Probability	18	86	41	33	100

Notes: (a) Soil Frozen to Depth to 6 to 8 in.

TABLE 3 PERFORMANCE OF LONGITUDINAL BARRIER, TEST NO. 30, IN TERMS OF NCHRP 230 SAFETY EVALUATION GUIDELINES

Evaluation Factor	Evaluation Criteria	TRANSITION DESIGN <sup>(1)</sup>				
		Tubular Thrie Beam (Test 1)	Single Thrie Beam (Test 2)	Double Thrie Beam (Test 3)	Double Thrie Beam (Test 4)	Double Thrie Beam (Test 5)
Impact Conditions	58 to 60 mph/25 deg	U	S	S	S	S
Structural	A. Test article shall <u>smoothly</u> redirect the vehicle.	S	U	S	S	U
	The vehicle shall not penetrate or go over the installation although controlled lateral deflection of the test article is acceptable.	S	S	S	S	S
	D. Detached elements, fragments or other debris from the test article shall not penetrate or show potential for penetrating the passenger compartment or present undue hazard to other traffic.	S	S	S	S	S
Occupant Risk	E. The vehicle shall remain upright during and after collision although moderate roll, pitching and yawing are acceptable.	S	S	S	S	S
	Integrity of the passenger compartment must be maintained with essentially no deformation or intrusion.	S	M	S	S	M
Vehicle Trajectory	H. After collision, the vehicle trajectory and final stopping position shall intrude a minimum distance, if at all, into adjacent traffic lanes.	U	U	U	U	U
	I. In test where the vehicle is judged to be re-directed into or stopped while in adjacent traffic lanes, vehicle speed change during test article collision should be less than 15 mph and the exit angle from the test article should be less than 60 percent of test impact angle, both measured at time of vehicle loss of contact with test device.	S	U	S	S	U

Notes: (1) S = Satisfactory M = Marginal U = Unsatisfactory

of 47 mph, an impact into either the Single Thrie Beam transition or the Tubular Thrie Beam transition in which no snagging occurred would result in an injury accident probability of about 20 percent.

In summary, the following conclusions were reached in regard to the overall performance of the four new guardrail-bridge-rail transition designs in restraining and smoothly redirecting a large, 4,500-pound automobile under the impact conditions of 60 mph and 25 degrees:

1. Tubular Thrie Beam Transition—Satisfactory,
2. Single Thrie Beam Transition—Unsatisfactory,
3. Double Thrie Beam Transition—Satisfactory,

4. Double W-Beam Transition—Unsatisfactory.

It is to be emphasized that the above conclusions are based on the condition that a new design in the field will be constructed to the exact design details under which the full-scale vehicle crash tests were conducted. In particular, careful attention must be given to ensure that (1) the soil has the properties of a type CL soil, (2) the wood posts are of the proper size and spacing and clear of knots, (3) the 4:1 tapered end is installed to the dimensions tested, and (4) the size and quantity of rebar in the concrete bridge end are adequate to carry a lateral impact load of 120 kips and a longitudinal load of 50 kips.



TEST NO.	TRANSITION BEAM DESIGN	IMPACT SPEED (mph)	VEHICLE SNAGGING LEVEL
1	TUBULAR THRIE	47	NONE
2	SINGLE THRIE	60	MODERATE
3	DOUBLE THRIE	61	NONE
4	DOUBLE THRIE	61	NONE
5	DOUBLE W-BEAM	62	SEVERE

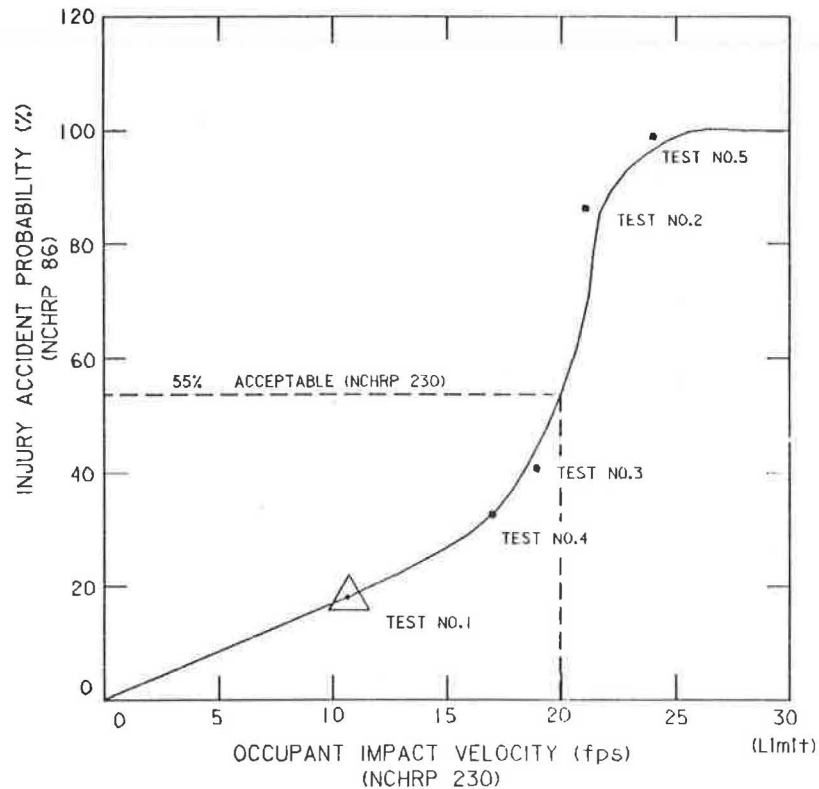


FIGURE 15 Relationship between occupant velocity and injury accident probability.

#### REFERENCES

1. *Guide for Selecting, Locating, and Designing Traffic Barriers*. American Association of State Highway and Transportation Officials, Washington, D.C., 1977.
2. G. H. Powell. *BARRIER VII: A Computer Program for Evaluation of Automobile Barrier Systems*. Report No. FHWA-RD-73-51, Final Report, FHWA, U.S. Department of Transportation, April 1973.
3. *Standard Specifications for Highway Bridges*. Sect. 1.1.8—Railings, 12th. Edition. American Association of State Highway and Transportation Officials, 1977.
4. *NCHRP Report 230: Recommended Procedures for the Safety Performance Evaluation of Highway Appurtenances*. National Cooperative Highway Research Program Report, TRB, National Research Council, Washington, D.C., March 1981.
5. *Vehicle Damage Scale for Traffic Accident Investigators*. TAD Project Technical Bulletin No. 1, National Safety Council, 1971.
6. R. M. Olson, E. R. Post, and W. F. McFarland. *Tentative Service Requirements for Bridge Rail Systems*. National Cooperative Highway Research Report HRB, National Research Council, Washington, D.C., 1970.

# Full-Scale Vehicle Crash Tests on Nebraska Rural Mailbox Designs

RONALD K. FALLER, JOHN A. MAGDALENO, BYRON A. WARLICK,  
WILLIAM H. WENDLING, AND EDWARD R. POST

The Nebraska Department of Roads, in conjunction with the Federal Highway Administration, has developed a new mailbox support system that could be used to accommodate a wide range of mailbox sizes. To be considered a safe appurtenance, the system had to be subjected to full-scale crash tests, as provided in recommended procedures published by the Transportation Research Board, March 1981. The major concern was to find whether the support system would keep the mailbox attached to the post and would not allow detached elements to penetrate the passenger compartment of a vehicle. Four full-scale crash tests were conducted with an 1,800-pound vehicle. Two tests with the post embedded in weak soil were performed at 20 mph and 60 mph, respectively. Two tests with the post embedded in strong soil were conducted at the same speeds. Three of the tests used a support system that held two mailboxes (Size 1-A). One test used a system that supported one mailbox (Size 2). After analyzing the results of the crash tests, it was evident that all of the performance criteria had been met. The major criteria evaluated were change in velocity (maximum 0.010 seconds average deceleration), whether the support system kept the mailbox attached to post, and whether the vehicle remained stable and upright during and after the impact.

Recent federal requirements have mandated that safe mailbox support systems be designed to yield or break away if struck by a vehicle. The Nebraska Department of Roads (NDOR), in cooperation with the Federal Highway Administration (FHWA), has developed a bracket for attaching the mailbox to the support post. The mounting bracket system was designed to adapt to a wide range of mailbox sizes. For the new attaching bracket to be certified as effective, it had to meet the criteria provided by the National Cooperative Highway Research Program (NCHRP) for conducting full-scale crash tests (1). If it met those criteria, it could then be considered a safe mailbox support system and become installed on the federal, state, and local highway systems.

It was decided that two mailbox support systems were to be tested. The systems were to be mounted to the Franklin Steel Eze-Erect signposts, which had been crash tested in the past (2-5). Thus, it was known that the post itself had already met the NCHRP criteria (1). The major concern now was whether the mailbox would remain attached to the post. A

second concern was whether the mailbox or detached fragments would penetrate or show potential for penetrating the passenger compartment of a vehicle or present undue hazard to other traffic.

## FULL-SCALE CRASH TEST DETAILS

### Test Description

Four full-scale crash tests were conducted on mailbox supports shown in Figures 1 and 2. Three of the tests used two mailboxes (Size 1-A) mounted side by side. The fourth test used

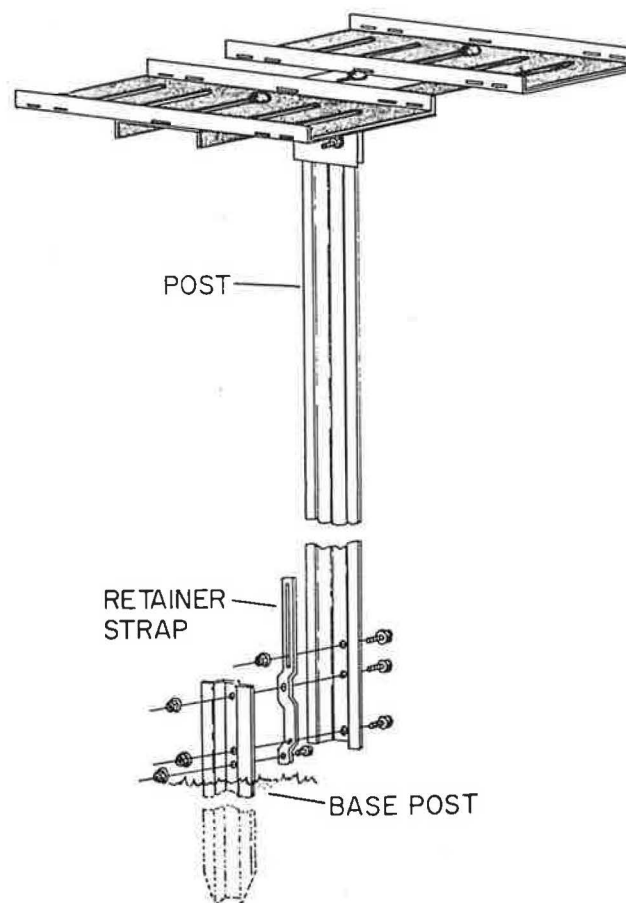
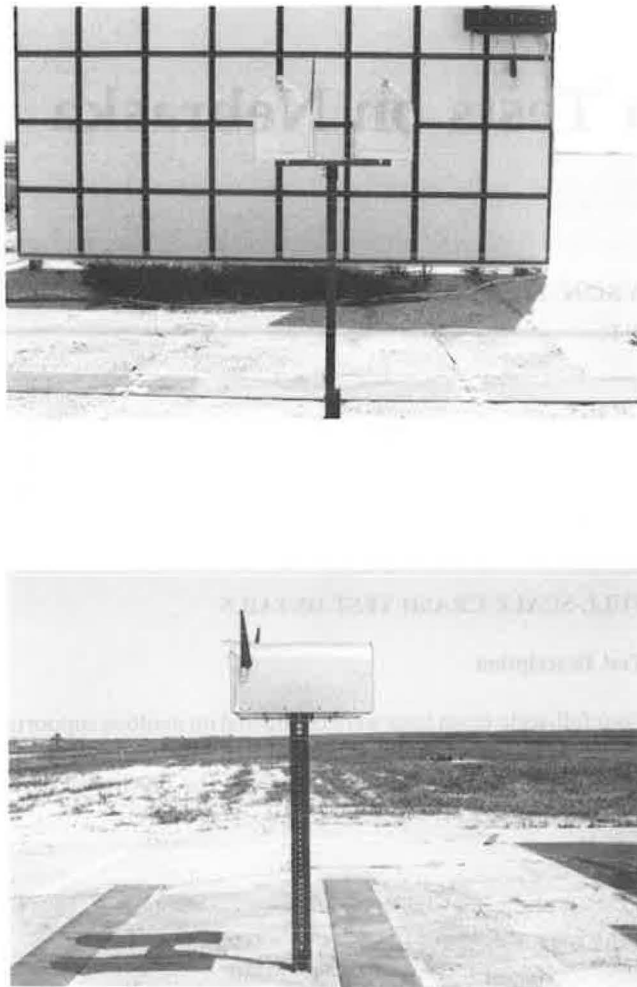


FIGURE 1 Double mailbox support system.

R. K. Faller, J. A. Magdaleno, and E. R. Post, University of Nebraska, W350 Nebraska Hall, Lincoln, Neb. 68588-0531. B. A. Warlick, Nebraska Department of Roads, P.O. Box 94759, Lincoln, Neb. 68509-4759. W. H. Wendling, Federal Highway Administration Region VII, P.O. Box 419715, Kansas City, Mo. 64141.



**FIGURE 2** Photographs of the complete double mailbox system.

one mailbox (Size 2) mounted to the post. Table 1 contains a summary of the test conditions.

Tests 1 and 2 were conducted in weak soil (S-2) and strong soil (S-1), respectively, at approximately 20 mph. Tests 3 and 4 were conducted in weak soil (S-2) and in strong soil (S-1), respectively, at approximately 60 mph. The 20-mph tests were performed with the impact at the quarter point of the bumper, in accordance with NCHRP 230 (1). The 60-mph tests were performed with the impact at the center of the bumper. For 60-mph tests, NCHRP 230 provides that a quarter point of bumper be used for the point of impact. But according to AASHTO 1985 (6), the 60-mph, off-center impact recommended by NCHRP 230 may be more stringent than current testing procedures can meet, and thus that acceptance should be based on a center of bumper, high-speed test.

According to the recommended test procedures, a weak soil (S-2) may be appropriate for breakaway/yielding supports. However, due to the variation of soil properties in Nebraska, it was decided that strong soil (S-1) also be used for the crash test. Two pits 10 feet long, 8 feet wide, and 5 feet deep were excavated and filled with strong soil (S-1) and weak soil (S-2), respectively. The soil properties and compaction procedures at the test site met the guidelines given in NCHRP 230 (1, 7).

## TEST ARTICLE DETAILS

Two mailbox support systems were tested (7). The first mailbox support system was used to support two mailboxes (size 1-A) that were 8 inches wide, 21 inches long, and 10½ inches tall. A pair of platform plates was bolted to the bottom of each mailbox. The two plates can be adjusted to fit any standard width mailbox. The two mailboxes, with the platform plates, were mounted directly onto the adapter plate or shelf. Then two L-shaped brackets were used to attach the adapter plate or shelf to the U-shaped post. The double mailbox support system is shown in Figure 1, and the complete system is shown in Figure 2.

The second mailbox support system was used to support one mailbox (Size 2), which was 11½ inches wide, 23½ inches long, and 13½ inches tall. A pair of adjustable platform plates was bolted to the bottom of the mailbox. The larger mailbox, with the platform plates, was mounted directly to the post with a pair of L-shaped brackets. The single mailbox support system is shown in Figure 3, and the complete system is shown in Figure 4.

The post system consisted of four main parts—the top post, the base post, the retainer strap, and the anti-twist plate. With the exception of the anti-twist plate, the post system is shown in Figure 1.

The top post was 42 inches long and had the cross-sectional dimensions and values as given in Table 1 (7).

The base post, which was embedded 37 inches into the soil, was also 42 inches long and had the same dimensions as the top post. Both the top and base post are fabricated from rolled rail steel.

The 17-inch long retainer strap was used to connect the two post sections together. The installation instructions for the Franklin Steel Eze-Erect sign posts are given in a report on full-scale crash tests on Nebraska rural mailbox designs produced by the University of Nebraska-Lincoln in August 1987 (7).

The anti-twist plate was made from a ⅛-inch sheet of galvanized sheet metal. It was trapezoid shaped, with the following dimensions: top horizontal length 12 inches, bottom horizontal length 6 inches, and height 6 inches. It was bolted to the base post so that it would be positioned below ground level.

## TEST VEHICLE

A 1979 Volkswagen Rabbit, weighing approximately 1,840 pounds, was used as the crash test vehicle.

## DATA ACQUISITION SYSTEMS

Two piezoresistive accelerometers (Model 7264) with a range of 200 g, were used to measure the accelerations in the longitudinal direction of the vehicle. The accelerometers were attached to metal blocks which were mounted to the front floorboards on both sides. The signals were first sent to the Metraplex FM multiplexed data acquisition system (Series 300), then to the Honeywell 101 analog tape recorder for permanent storage.

Two cameras using high-speed film recorded each test. The first camera, Locam, used a wide-angle lens and was placed approximately 80 feet perpendicular to the direction of the

TABLE 1 SUMMARY OF TEST CONDITIONS

TEST NO.	VEHICLE TYPE (lbs)	TARGET SPEED (mph)	SOIL TYPE	MAILBOX DESIGN	POST EMBEDMENT		POST SIZE (lbs/ft)	POINT OF IMPACT	TARGET IMPACT SEVERITY (ft-kips)
					DEPTH (in)	METHOD			
1	1800	20	Weak (S-2)	1-Post 2-Mailboxes (size 1-A)	37	Driven	2.0	14" to Right of Center	24 <sup>-3,+3</sup>
2	1800	20	Strong (S-1)	1-Post 2-Mailboxes (size 1-A)	37	Driven	2.0	14" to Right of Center	24 <sup>-3,+3</sup>
3	1800	60	Weak (S-2)	1-Post 2-Mailbox (size 1-A)	37	Driven	2.0	Center of Bumper	216 <sup>-21,+37</sup>
4	1800	60	Strong (S-1)	1-Post 1-Mailbox (size 2)	37	Driven	2.0	Center of Bumper	216 <sup>-21,+37</sup>

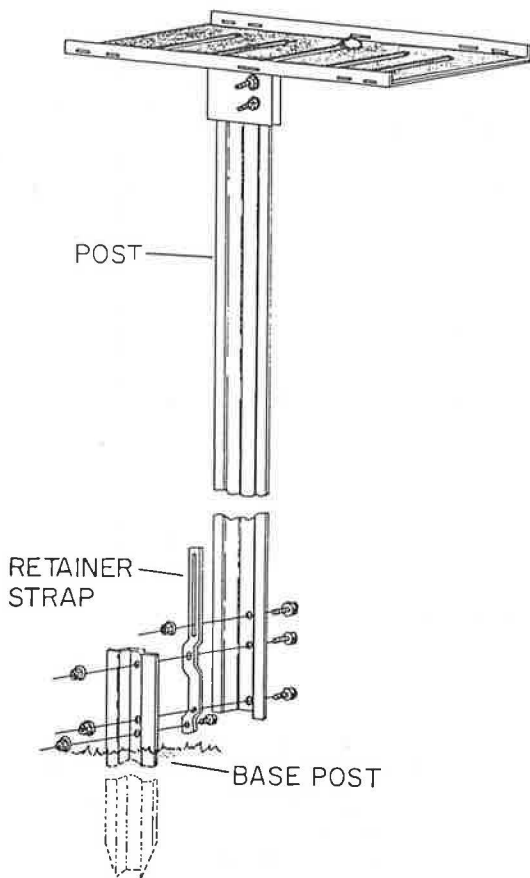


FIGURE 3 Single mailbox support system.

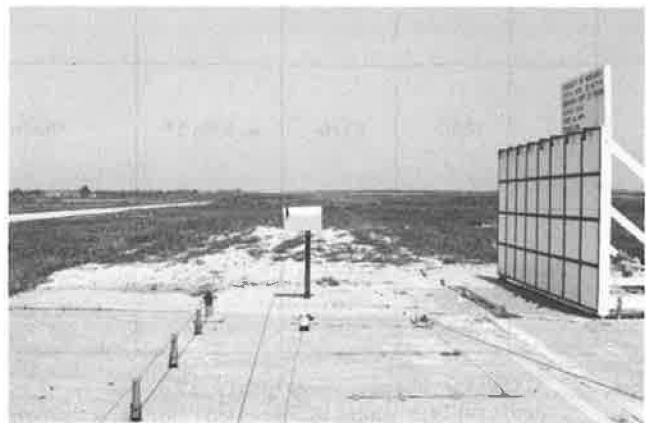
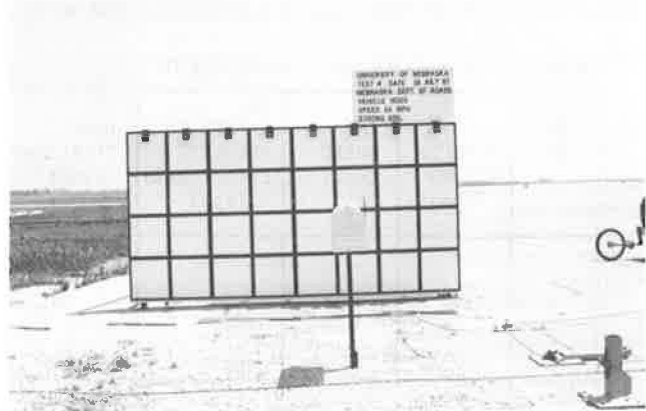


FIGURE 4 Photographs of the complete single mailbox system.

vehicle. The second camera, Photec IV, was also positioned perpendicular to the direction of the vehicle, at approximately 137 feet. After the tests, the film was analyzed using the Vanguard motion analyzer.

Tape or pressure switches positioned along the length of the impact area were activated by the vehicle to indicate the travel time over a known distance. This provided a quick check of the impact speed and also values for change in velocity.

## PERFORMANCE STANDARDS

Currently, there are no established guidelines or performance criteria that directly deal with full-scale crash tests on mailbox supports. However, an American Association of State Highway and Transportation Officials (AASHTO) procedure guide (8) provides three very useful general criteria:

1. The mailbox support details should prevent mailboxes from separating from the post if struck by a vehicle.
2. Windshield penetration from the mailbox should be minimized. Single or multiple mailbox installations should not cause vehicle ramping or rollover as a result of a mailbox collision.

In addressing safety appurtenances, AASHTO requires all new roadside signs and luminaries on high speed highways, located within the suggested clear zone width, to be placed on breakaway supports unless they are located behind a barrier or crash cushion. Therefore, it was assumed that mailbox

support systems should comply with the safety standards required for a breakaway or yielding device. Breakaway supports are all types of devices that are safely displaced under vehicle impact, whether the release mechanism is a slip plane, plastic hinges, fracture elements, or a combination of these.

According to AASHTO, "satisfactory dynamic performance is indicated when the maximum change in velocity for a standard 1800-pound (816.5 kg) vehicle, or its equivalent, striking a breakaway support at speeds from 20 mph to 60 mph (29.33 fps to 88 fps) (32 kmph to 97 kmph) does not exceed 15 fps (4.57 mps), but preferably does not exceed 10 fps (3.05 mps) or less" (6).

Other specifications require that detached elements, fragments, or other debris from the test article (mailbox assembly) shall not penetrate or show potential for penetrating the occupant compartment or provide undue hazard to other traffic. Also, the vehicle shall remain upright during and after the mailbox crash test (1).

The change in velocity, peak deceleration, maximum 10 ms average deceleration, and occupant displacement (free missile travel) were four types of data that were derived from the accelerometer readings. Change in velocity and occupant displacement are both time dependent. Due to this time dependency, guidelines have been established to determine the "duration of the event" for computation. The duration of the event is defined as the lesser of the following: (1) time between incipient contact and loss of contact between vehicle and the yielding support, or (2) the time for a free missile to travel a distance of 24 inches starting from rest with the same magnitude of vehicle decelerations (9).

TABLE 2 SUMMARY OF TEST RESULTS

TEST NO.	ACTUAL VEHICLE WEIGHT (lbs)	IMPACT SPEED (mph)	(a) CHANGE IN VELOCITY (left/right) (fps)	(b) PEAK DECELERATIONS (left/right) (g's)	(c) MAXIMUM 0.010 SEC AVERAGE DECELERATION (left/right) (g's)	(d) OCCUPANT DISPLACEMENT (left/right) (in)	ACTUAL IMPACT SEVERITY (ft-kips)
1	1840	20.5	1.9/3.2	8.2/22.6	2.74/4.60	1.30/2.10	25.8
2	1840	21.3	2.7/3.3	7.5/13.2	3.62/4.03	2.20/1.80	27.9
3	1840	63.6	4.4/4.5*	NA/NA**	NA/NA**	NA/NA**	248.6
4	1840	64.5	2.7/1.1	21.2/26.1	4.86/4.04	2.10/0.50	255.7

- (a) allowable change in velocity 15 fps  
preferable change in velocity 10 fps  
(b) allowable threshold value of deceleration 20 g's  
(c) allowable maximum 0.010 sec average deceleration 15 g's  
(d) allowable occupant displacement 24 in.

\*From high-speed film analysis  
\*\*Not available due to the breakage of the data cable

The time between incipient contact and loss of contact between vehicle and yielding support is not easily determined. By using the high-speed film, it was observed that contact between the vehicle and the support may take place over a long period of time if the vehicle moves over the mailbox. Therefore, after reevaluation of the accelerometer graphs, it was decided that the duration of the event was the time between contact and when the acceleration returned to and remained at zero. This decision was made because deceleration cannot remain at zero unless the vehicle has reached a constant velocity or has stopped.

After the test, the damage was assessed by the traffic accident data (TAD) scale (10) and the vehicle damage index (VDI) (11).

Because test conditions are sometimes difficult to control, a composite tolerance limit is presented. It is called the impact severity (IS). For structural adequacy, it is preferable for the actual impact severity to be greater than the target value rather than being below it. During low-speed tests, the goal is to determine the lower speed threshold for detaching the appurtenance. Then it is preferable to be on the low side of the target value. The IS target values for the 20 mph and 60 mph tests are  $24^{-3,+3}$  ft-kips and  $216^{-21,+37}$  ft-kips, respectively (1). Thus, the IS target values for the 20 mph tests

range from 21 ft-kips to 27 ft-kips. For the 60 mph tests, the IS target values range from 195 ft-kips to 253 ft-kips.

## TEST RESULTS

In the following section, each test will be explained along with the individual results. For all of the tests, an 1,840-pound Volkswagen Rabbit was used as the crash test vehicle. Also, the Franklin Steel Eze-Erect signpost, embedded 37 inches into the soil, was used for each test. Table 2 summarizes the results of the four tests.

The accelerometer data were used for the calculation of change in velocity, while the high-speed film was used as a backup system and check on the accelerometer results. For each test, plots of deceleration, change in velocity, and occupant displacement versus time were recorded (7).

### Test 1

Test 1 was conducted at an impact speed of 20.5 mph on the double mailbox system in the weak soil. The point of impact was 14 inches to the right of center. The results of Test 1 are shown in Table 3. A time-event summary is given in Table

TABLE 3 SUMMARY OF RESULTS, TEST 1

#### MAILBOX SUPPORT DATA

Mailbox	2 boxes (size 1-A)
Post Type	Steel U-post *
Size	2.00 lbs/ft
Embedment Method	Driven into Weak Soil (S-2)
Embedment Depth	37 in.

#### VEHICLE DATA

Make	Volkswagen
Model	Rabbit
Year	1979
Weight	1840 lbs.
Impact Point	14 in. to right of center

#### ACCELEROMETER DATA

	Left	Right
Change in Velocity (ft/sec)	1.9	3.2
Duration of Event (sec) **	0.082	
Peak Deceleration (g's)	8.2	22.6
Maximum 0.010 sec Average Deceleration (g's)	2.74	4.60
Occupant Displacement (in)	1.30	2.10

#### VEHICLE DAMAGE CLASSIFICATION

TAD	None
VDI	12FCLN1

Did test article penetrate the the passenger compartment? NO

Was windshield broken? NO

\*Franklin Steel eze-erect sign post

\*\*Time of Contact

Impact Velocity = 20.5 mph

Actual Impact Severity = 25.8 ft-kips

TABLE 4 TIME-EVENT SUMMARY FOR TEST 1

TIME (sec)	EVENT
0.000	Impact
0.006	Post begins bending
0.018	Post wrapping around bumper
0.050	Mailbox hits front end of hood
0.095	Mailbox and post being pushed over
0.147	First mailbox hits ground

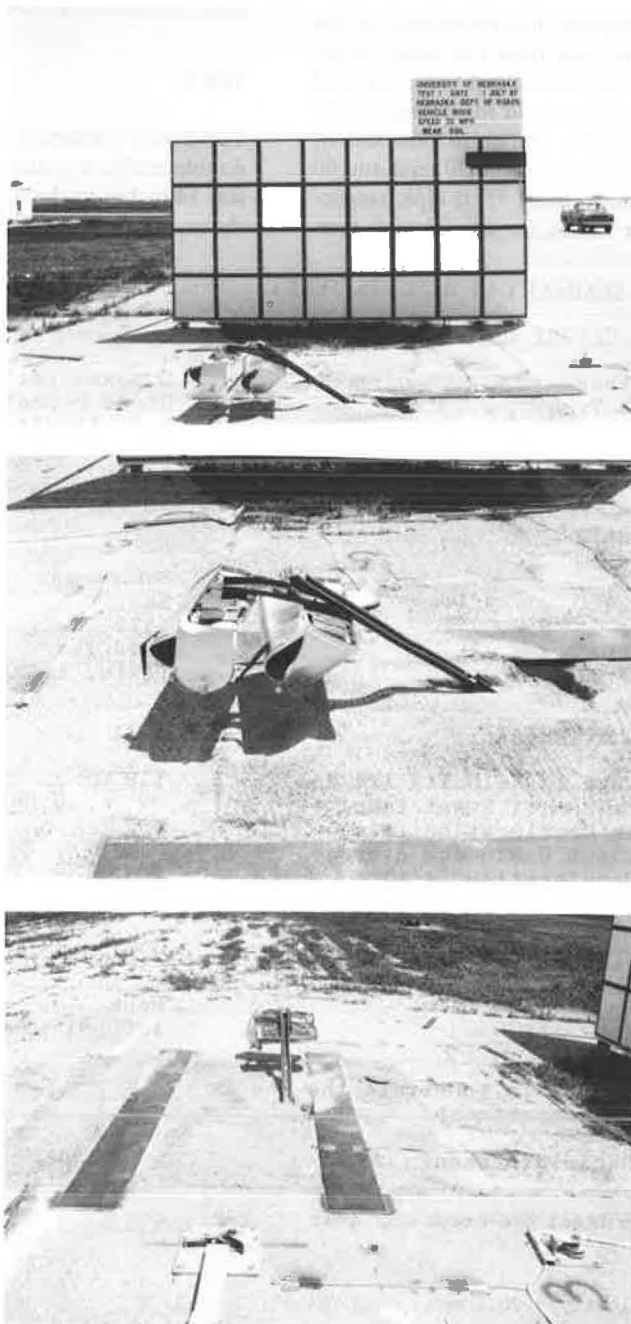


FIGURE 5 Damage to mailbox system, Test 1.

4. Upon impact, the post first wrapped around the bumper, and then the mailbox hit the front end of the hood. The car then continued to push the mailbox and post to the ground. While the car continued to move over the mailbox and post, the retainer strap held the top section of the post to the base post, which was not pulled out. Photos of the damage to the mailbox system are shown in Figure 5.

The vehicle received no damage with the exception of a small dent in the bumper. The damage was classified according to TAD and VDI scales, and the results are given in Table 3.

### Test 2

Test 2 was performed at an impact speed of 21.3 mph on the double mailbox system in the strong soil. The point of impact was 14 inches to the right of center. A summary of the results of Test 2 is given in Table 5. Table 6 gives the time-event summary. Upon impact, the post began to wrap around the bumper, and then the mailbox hit the front end of the hood. As the car continued to travel over the mailbox assembly, the

top section of the post broke away from the base post, which remained in the ground. This demonstrated the breakaway or slip feature. Photographs of the damage to the mailbox system are presented in Figure 6.

The only damage to the vehicle was a small dent in the front end of the hood and a minor dent in the bumper and front lower right fender. Table 5 gives the TAD and VDI damage ratings.

### Test 3

Test 3 was conducted at an impact speed of 63.6 mph on the double mailbox system in the weak soil. The point of impact was center of bumper. The results of Test 3 are shown in Table 7. The time-event summary is given in Table 8. After impact, the post wrapped around the bumper while the mailbox struck the hood of the car. As the car traveled forward, the mailbox remained on the hood while the post assembly was pulled from the ground. At approximately 0.090 seconds after impact, the mailbox assembly started to lose contact

TABLE 5 SUMMARY OF RESULTS, TEST 2

#### MAILBOX SUPPORT DATA

Mailbox	2 boxes (size 1-A)
Post Type	Steel U-post *
Size	2.00 lbs/ft
Embedment Method	Driven into Strong Soil (S-1)
Embedment Depth	37 in.

#### VEHICLE DATA

Make	Volkswagen
Model	Rabbit
Year	1979
Weight	1840 lbs.
Impact Point	14 in. to right of center

#### ACCELEROMETER DATA

	<u>Left</u>	<u>Right</u>
Change in Velocity (ft/sec)	2.7	3.3
Duration of Event (sec)**	0.100	
Peak Deceleration (g's)	7.5	13.2
Maximum 0.010 sec Average Deceleration (g's)	3.62	4.03
Occupant Displacement (in)	2.20	1.80

#### VEHICLE DAMAGE CLASSIFICATION

TAD	None
VDI	12FREE1

Did test article penetrate the passenger compartment?	NO
---	----

Was windshield broken?	NO
------------------------	----

\*Franklin Steel eze-erect sign post

\*\*Time of Contact

Impact Velocity = 21.3 mph

Actual Impact Severity = 27.9 ft-kips



TABLE 6 TIME-EVENT SUMMARY FOR TEST 2

TIME (sec)	EVENT
0.000	Impact
0.008	Post begins bending
0.037	Post wrapping around bumper
0.052	Mailbox hits front end of hood
0.101	Mailbox and post being pushed over
0.118	First mailbox hits ground

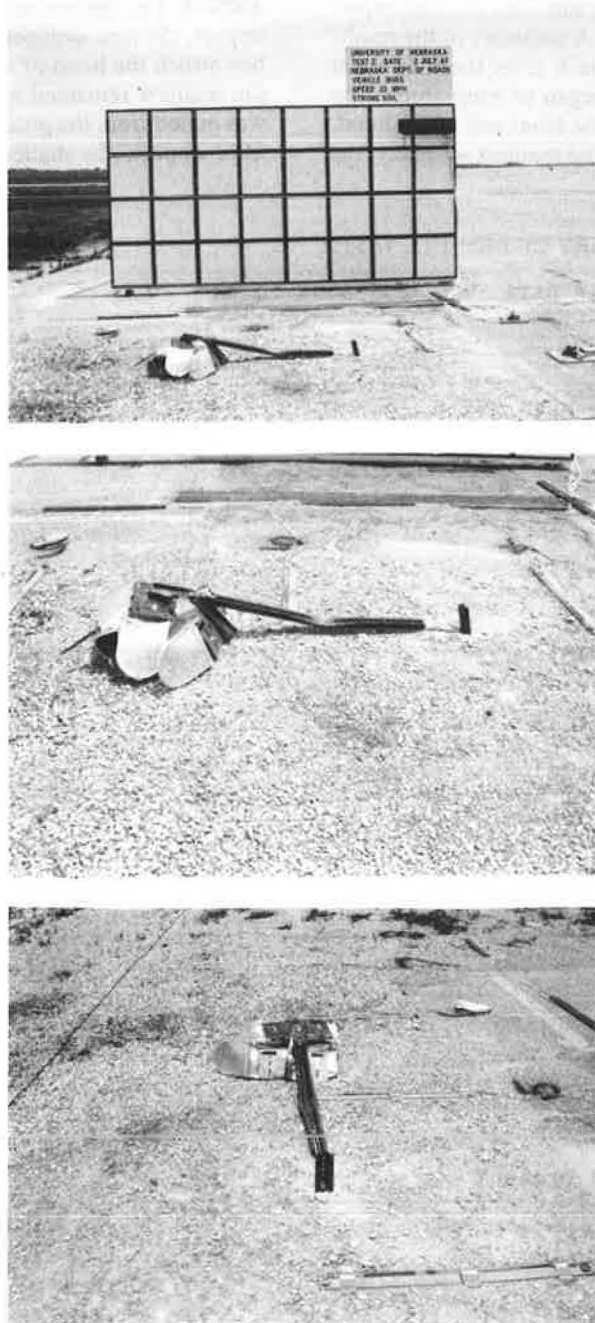


FIGURE 6 Damage to mailbox system, Test 2.

TABLE 7 SUMMARY OF RESULTS, TEST 3

MAILBOX SUPPORT DATA

Mailbox	2 boxes (size 1-A)
Post Type	Steel U-post *
Size	2.00 lbs/ft
Embedment Method	Driven into Weak Soil (S-2)
Embedment Depth	37 in.

VEHICLE DATA

Make	Volkswagen
Model	Rabbit
Year	1979
Weight	1840 lbs.
Impact Point	Center of bumper

ACCELEROMETER DATA

	<u>Left</u>	<u>Right</u>
Change in Velocity (ft/sec)**	4.4 (Photec)	4.5 (Locam)
Duration of Event (sec)***		0.090
Peak Deceleration (g's)		Not Available
Maximum 0.010 sec Average Deceleration (g's)		Not Available
Occupant Displacement (in)		Not Available

VEHICLE DAMAGE CLASSIFICATION

TAD	FC-1
VDI	12TFCN5

Did test article penetrate the passenger compartment? NO

Was windshield broken? NO

\*Franklin Steel eze-erect sign post

\*\*From high-speed film analysis

\*\*\*Time of Contact

Impact Velocity = 63.6 mph

Actual Impact Severity = 248.6 ft-kips

TABLE 8 TIME-EVENT SUMMARY FOR TEST 3

<u>TIME (sec)</u>	<u>EVENT</u>
0.000	Impact
0.002	Post begins bending
0.006	Post wrapping around bumper
0.016	Mailbox hits hood
0.040	Mailbox on hood and post being pulled out
0.080	Post dragging through sand
0.090	Mailbox loses contact with hood

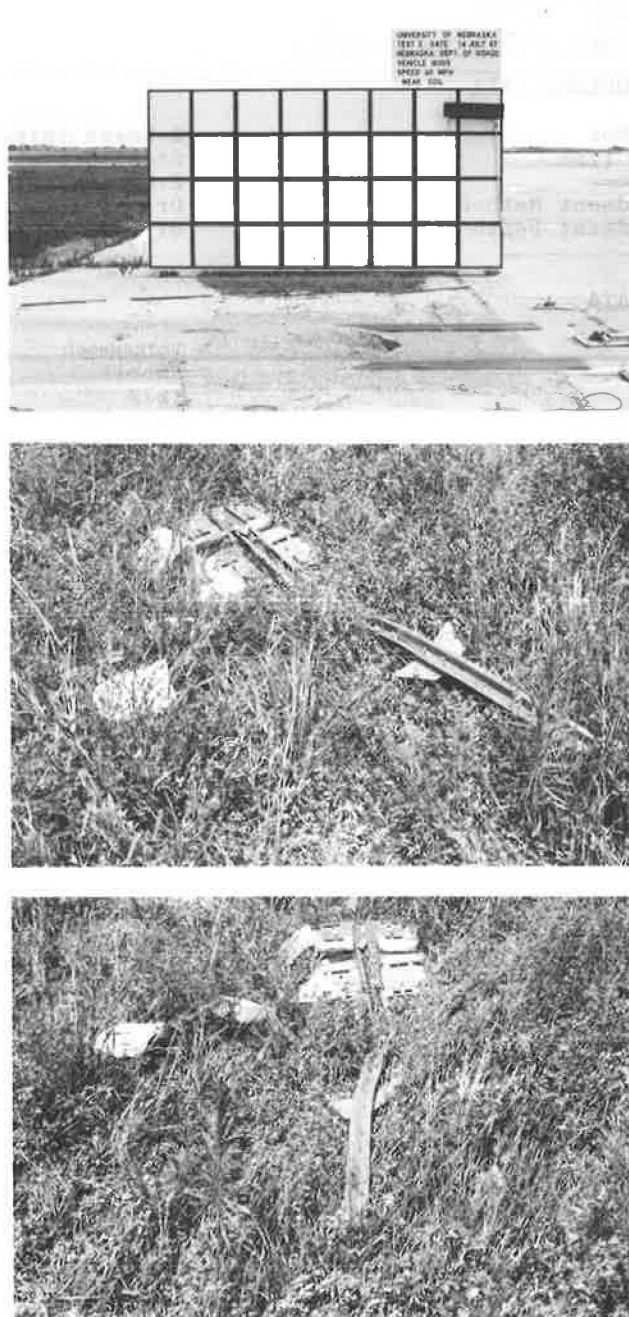


FIGURE 7 Damage to mailbox system, Test 3.

with the hood. The base post, top post, and mailbox all remained intact after they came to a rest 366 feet away, when they were run over by the vehicle. Damage to the mailbox system is shown in the photos given in Figure 7.

During Test 3, the data cable between the onboard Metra-plex unit and tape recorder became tangled with the car cable guidance system. Thus, the cable broke before the car had reached the impact point and no accelerometer data were recorded. The NDOR decided not to rerun the test because the needed information could be obtained from the high-speed film and also the vehicle had remained stable and upright during and after collision.

The most noticeable damage to the vehicle was a punctured

and dented hood and a fractured plastic grill plate. The TAD and VDI damage ratings are given in Table 7.

#### Test 4

Test 4 was performed at an impact speed of 64.5 mph on the single mailbox system in the strong soil. The point of impact was the center of bumper. A summary of the Test 4 results is given in Table 9. The sequential photos are shown in Figure 8 and a time-event summary is given in Table 10. As the vehicle moved through the impact, the mailbox post wrapped around the bumper, and then the top section of the post

TABLE 9 SUMMARY OF RESULTS, TEST 4

MAILBOX SUPPORT DATA

Mailbox	1 box (size 2)
Post Type	Steel U-post*
Size	2.00 lbs/ft
Embedment Method	Driven into Strong Soil (S-1)
Embedment Depth	37 in.

VEHICLE DATA

Make	Volkswagen
Model	Rabbit
Year	1979
Weight	1840 lbs.
Impact Point	Center of bumper

ACCELEROMETER DATA

	<u>Left</u>	<u>Right</u>
Change in Velocity (ft/sec)	2.7	1.1
Duration of Event (sec)**	, 0.048	
Peak Deceleration (g's)**	21.2	26.1
Maximum 0.010 sec Average Deceleration (g's)	4.86	4.04
Occupant Displacement (in)	2.1	0.50

VEHICLE DAMAGE CLASSIFICATION

TAD	FC-1
VDI	12TFDW5

Did test article penetrate the passenger compartment? NO

Was windshield broken? NO

\*Franklin Steel eze-erect sign post

\*\*Time of Contact

Impact Velocity = 64.5 mph

Actual Impact Severity = 255.7 ft-kips

separated from the base post. The base post remained embedded in the soil. The mailbox then struck the hood and was carried for a distance before being thrown from the car. The final resting place of the mailbox assembly was 130 feet from the point of impact. Photos of the damaged mailbox can be viewed in Figure 9.

The vehicle's hood received the most significant damage, although the center grill area received some dents. Table 9 gives the TAD and VDI damage ratings for Test 4.

**CONCLUSIONS**

Four full-scale crash tests were conducted to evaluate the impact behavior of two NDOR mailbox support systems. One design used two mailboxes (Size 1-A) mounted side by side, and the other design consisted of one mailbox (Size 2) mounted to the top of the post.

The analysis of the four crash tests revealed the following:

1. In Tests 1 and 3, the actual impact severity was within

the recommended limits. During Tests 2 and 4, the actual impact severity exceeded the recommended limits by 3.3 percent and 1.5 percent, respectively. Since the error was small, the tests were taken to be valid.

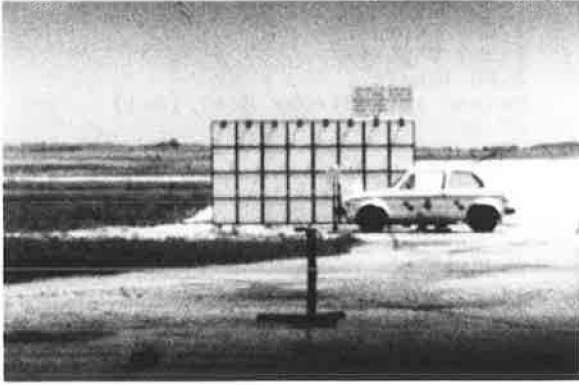
2. In each test the change in velocity of the vehicle was well below the recommended limit of 15 fps and also the preferable limit of 10 fps.

3. In each test where accelerometer data were available, the maximum 0.010-second average deceleration was well below the recommended limit of 15 g.

4. In all of the tests, the mailbox support system functioned as intended. It kept the mailbox attached to the top of the post, not allowing any detached fragments or elements to penetrate or show potential for penetration into the passenger compartment.

5. In each test the vehicle remained stable and upright during and after impact and also showed no potential for ramping or rolling over. Also, there were no severe damages assessed to the vehicle during each of the four tests.

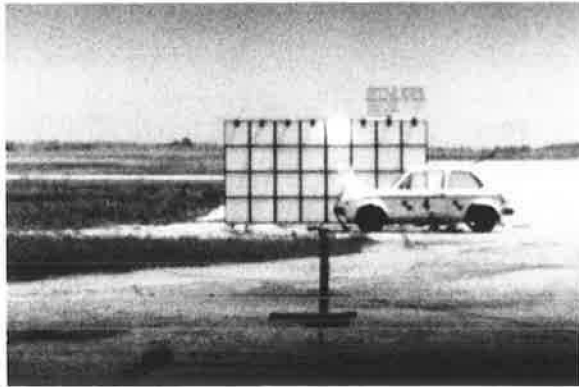
6. The breakaway device functioned as intended for Tests 2 and 4. During Tests 1 and 3, which were conducted in weak



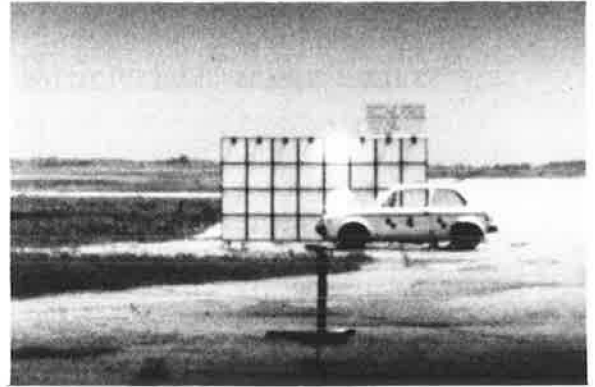
0.000 sec



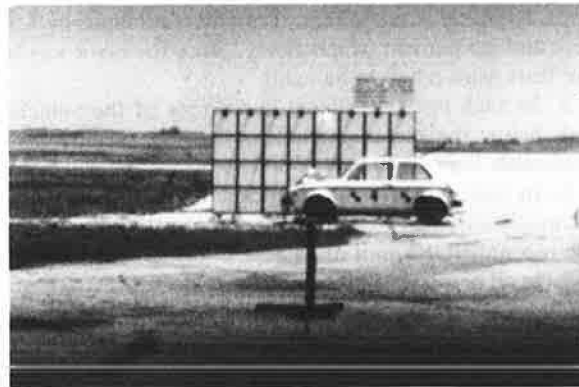
0.002 sec



0.010 sec



0.022 sec



0.040 sec



0.148 sec

**FIGURE 8** Sequential photographs, Test 4.

TABLE 10 TIME-EVENT SUMMARY FOR TEST 4

TIME (sec)	EVENT
0.000	Impact
0.002	Post begins bending
0.010	Post wrapping around bumper
0.022	Post separates from base
0.026	Mailbox hits hood
0.040	Mailbox on hood
0.148	Mailbox leaving hood

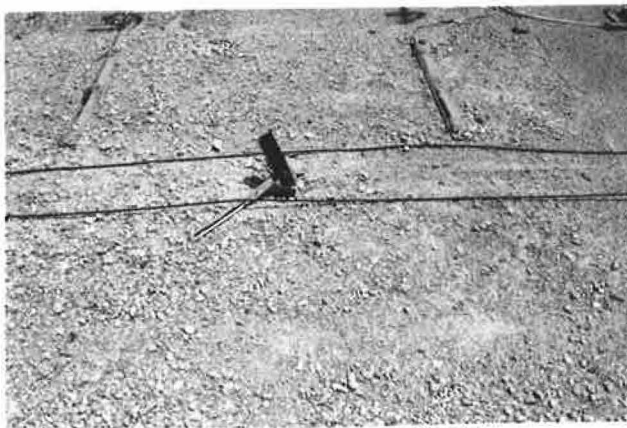
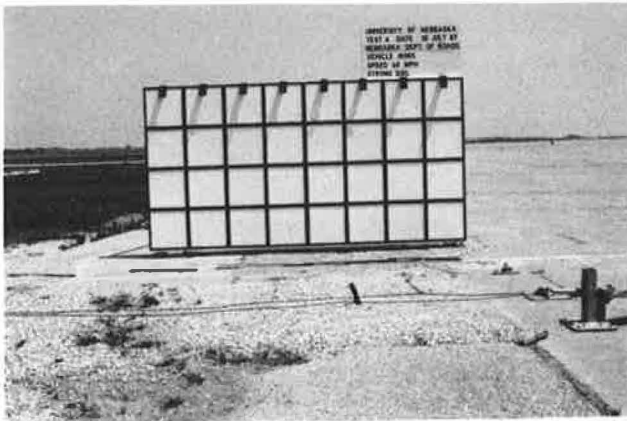


FIGURE 9 Damage to mailbox system, Test 4.

soil, the breakaway device did not function. In Test 1, the post system pushed over, allowing the vehicle to safely pass over it. In Test 3, the entire post system pulled out of the ground.

Based upon the above listed items, the results of each test are acceptable according to the NCHRP 230 guidelines, as modified by AASHTO 1985 guidelines.

#### RECOMMENDATIONS

In order to more securely tighten together the mailbox support system, it was suggested that the circular holes in the platform and L-shaped bracket be either punched to a larger size diameter or punched square so the carriage bolt shank can fit in the hole.

Also, it was suggested that the support system, consisting of the platform plates, the adapter plate, and L-shaped brackets, be treated with some type of protective surface coating such as paint or zinc plating. This would reduce the effects of rust on the system and possible mailbox detachment due to weakened steel parts.

#### REFERENCES

1. Recommended Procedures for the Safety Performance Evaluation of Highway Appurtenances. *National Cooperative Highway Research Program Report 230*, TRB, National Research Council, Washington, D.C., March 1981.
2. M. J. Effenberger, and H. E. Ross, Jr. *Report on the Static and Dynamic Testing of Franklin's U-Post and Eze-Erect Connection*. Final Report to Franklin Steel Company, Project RF 3491, Texas Transportation Institute, Texas A&M University, June 1977.
3. H. E. Ross, Jr., and W. Walker. *Static and Dynamic Testing of Franklin Steel Signposts*. Final Report to Franklin Steel Company, Project RF 3636, Texas Transportation Institute, Texas A&M University, Feb. 1978.
4. H. E. Ross, Jr., and Patrick L. O'Reilly. *Test and Evaluation of Rural Mailbox Installations*. Research Report 0982-1, Texas Transportation Institute, Texas A&M University, Aug. 1981.
5. Patricia R. Hall and H. E. Ross, Jr. *Test and Evaluation of Rural Mailbox Supports*. Research Report 2370-1F, Texas Transportation Institute, Texas A&M University, May 1983.
6. *Standard Specifications for Structural Supports for Highway Signs, Luminaires, and Traffic Signals*. American Association of State Highway and Transportation Officials, Washington, D.C., 1985.

7. R. K. Faller, et al. *Full-Scale Crash Tests on Nebraska Rural Mailbox Designs*. Final Report to Nebraska Department of Roads, RESI (0099) P415, Civil Engineering Department, University of Nebraska-Lincoln, Aug. 1987.
8. *A Guide for Erecting Mailboxes on Highways*. American Association of State Highway and Transportation Officials, Washington, D.C., 1984.
9. *Transportation Research Circular No. 191: Recommended Procedures for Vehicle Crash Testing of Highway Appurtenances*. TRB, National Research Council, Washington, D.C., Feb. 1978.
10. *Vehicle Damage Scale for Traffic Accident Investigators*. Traffic Accident Data Project Technical Bulletin No. 1, National Safety Council, Chicago, Ill., 1971.
11. Collision Deformation Classification, Recommended Practice J224 Mar 80. *SAE Handbook Vol. 4*. Society of Automotive Engineers, Warrendale, Pa., 1985.

---

*This document is disseminated in the interest of information exchange. The United States Government assumes no liability for its contents or use thereof. The contents do not necessarily reflect the official policy of the Department of Transportation. This report does not constitute a standard, specification or regulation.*

*The United States Government does not endorse products or manufacturers. Trade or manufacturers' names appear herein only because they are considered essential to the object of this document.*

# Washington State Department of Transportation Development of a Bridgerail Retrofit Program

DON J. GRIPNE

**This paper describes the development of the Washington State Department of Transportation's (WSDOT) bridgerail retrofit program. Prior to 1984, other than a program to upgrade low-base aluminum rails, the department's informal policy on replacing substandard bridgerails was to incorporate a replacement in a highway construction project to obtain a desired roadway width mandated by accident history. Otherwise, bridgerails were exempted from a project even if the approach rails were upgraded. As a result of this new retrofit policy, substandard bridgerails are being upgraded systematically, on an individual project basis, as part of WSDOT's resurfacing, restoration, and rehabilitation (3R) program. The retrofit program was developed to provide a uniform policy for upgrading substandard bridgerails. This policy is used in conjunction with our past practice of replacing substandard bridgerails with a concrete New Jersey shaped barrier. Bridgerails addressed in the development of this program included open concrete baluster, steel post rails, and wooden rails. Systems considered for the retrofit program included W-beam, 12-gauge thrie beam, and 10-gauge thrie beam. In conjunction with this program, it was also important to develop appropriate approach rails and transition sections for these systems. The application of this bridgerail retrofit policy has proven to be of real value to the state of Washington. It provides a low-cost solution to retrofitting bridgerailing.**

Prior to 1984, WSDOT did not have a formal policy for retrofitting substandard bridgerails. Historically, other than a program to upgrade low aluminum rails, bridgerails were replaced only if the bridge was widened or if accidents necessitated replacement. Thus, bridgerail replacement was not normally part of a regularly scheduled highway construction project. Even if a substandard bridgerail was not replaced, WSDOT practice was to upgrade the approach rail. Decisions concerning whether and how to improve substandard installations were made on a project-by-project basis.

The impetus for the development of this retrofit policy came from the need to address the many substandard bridgerails that were encountered when WSDOT developed a 3R project. In particular, the need to add approach guardrails to timber bridgerails brought the issue to the attention of management. Also, the Federal Highway Administration (FHWA) Washington Division asked WSDOT to consider extending approach rails across short bridges by mounting them to the

face of the bridgerail, instead of terminating them at the ends of the open concrete baluster bridge rails.

In developing the retrofit policy, the department considered numerous rail types and evaluated several rail systems developed by others. Rail height, roadway width, and the presence of curbs or sidewalks were all considered as criteria for a practical retrofit program.

The new retrofit program became effective on October 10, 1984. This program provides a consistent method with which to address all substandard bridgerails during development of 3R projects.

## BACKGROUND

Many factors were considered during the development of the retrofit program. WSDOT recognized the advantages of mounting guardrails to the face of the substandard bridgerails to improve the redirection characteristics of the existing rails. W-beam was considered first, but was rejected because of its limited flexibility. Thrie beam was selected because its 20-inch width made it flexible enough to deal with all the bridgerail configurations and heights that would be encountered. The department determined that 10-gauge thrie beam would work much better than 12-gauge thrie beam because it provided the highest quality rail at a reasonable cost.

Other applications considered in developing criteria for a practical retrofit program included rail systems developed by other agencies, such as a crash-tested system using thrie beam and steel posts mounted to the bridge deck, and the Service Level 1 (SL-1) system identified in NCHRP Report 239. Rail height, roadway width, and the presence of curbs or sidewalks were also considered.

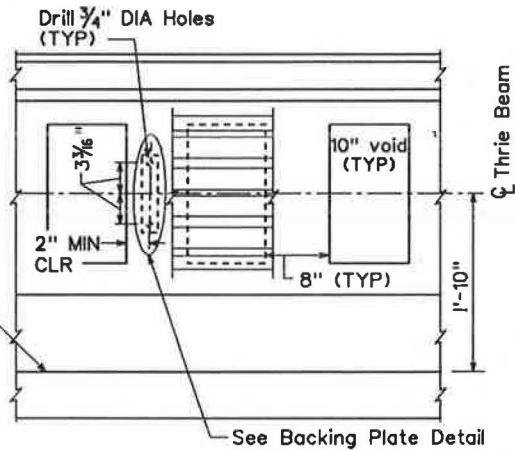
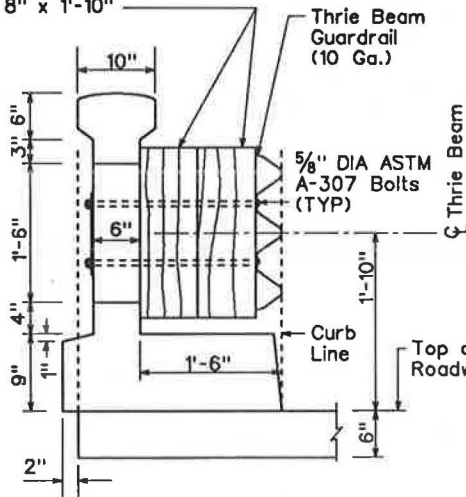
In conjunction with WSDOT's participation in FHWA's Demonstration 64 program, the department developed a rail design that utilized the SL-1 system on timber deck bridges with timber rails. This rail design was added to the retrofit program.

As the retrofit program was developed, the department evaluated the structural integrity of the thrie beam guardrail in meeting the American Association of State Highway Transportation Officials (AASHTO's) requirement of 10 kips. To determine actual performance capabilities, crash testing funded by FHWA and WSDOT was initiated to test thrie beam guardrails mounted to an open concrete baluster bridgerail. This system was tested by Southwest Research to meet the crash



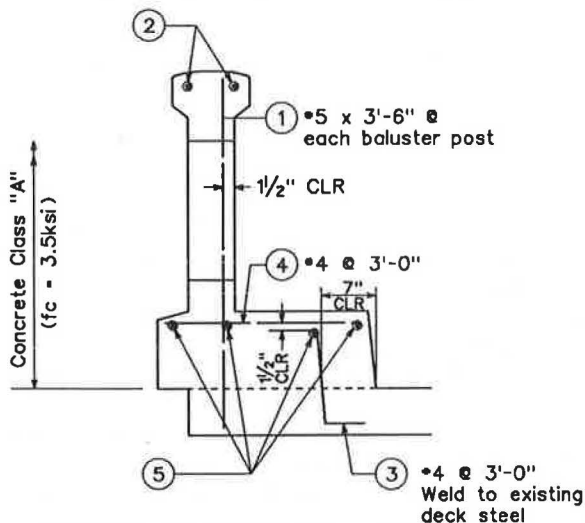
Treated timber blockout with vertical grain (Thrie Beam blocked out to curb line) nominal dimensions  
S4S 8" x 8" x 1'-10"

NOTE  
Locate holes at least 2" from edge of baluster, spacing 6'-3" MAX

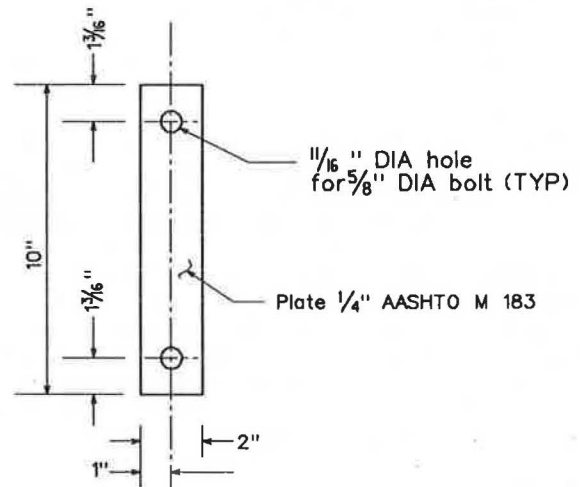


TYPICAL BALUSTER RAIL SECTION

ELEVATION OF BALUSTER



TYPICAL BALUSTER RAIL SECTION REINFORCING



BACKING PLATE DETAIL

TRAFFIC BARRIER BAR LIST				
All reinforcing shall be AASHTO M 31 (Gr. 40)				
MARK	LOCATION	SIZE	LENGTH	BENDING DIAGRAM (All dimensions are out to out)
1	Baluster Vertical	5	3'-6"	Str.
2	Baluster Top Longit.	5	(a)	Str.
3	Curb to Slab Vert.	4	1'-9"	
4	Curb Horiz.	4	2'-3 1/2"	
5	Curb Longit.	4	(a)	

(a) Continuous with 2'-0" MIN splice

FIGURE 1 Concrete baluster retrofit with thrie beam.

Test No. ....	LVWR-1
Date .....	07/27/87
Installation Length - ft (m) .....	125(38)
<b>Beam</b>	
Member .....	10 ga thrie-beam
Length .....	12.5 (3.8)
<b>Maximum Deflections - in (m)</b>	
Dynamic .....	1.3 (3.3)
<b>Barrier Description: Thrie-Beam retrofit over existing weak concrete baluster-type bridgerail</b>	
Soil type and condition .....	N/A (bridgerail)
Vehicle .....	1981 Honda Civic
<b>Mass -lb (kg)</b>	
Test Inertia .....	1675 (760)
Dummies .....	165 (75)
Gross .....	1840 (835)
Speed - mph (km/h) .....	58.8 (94.7)
<b>Angle - Deg</b>	
Impact .....	19.5
<b>Occupant Impact Velocity - fps (m/s)</b>	
Forward (film/accel) .....	6.9 (2.1)/9.8 (3.0)
Lateral (film/accel) .....	-18.6 (-5.7)/-18.4 (-5.6)
<b>Occupant Ridedown Accelerations - g's</b>	
Forward (accel) .....	-0.8
Lateral (accel) .....	6.6
<b>Maximum 50 msec Avg Accelerations - g's</b>	
Longitudinal (film/accel) .....	-3.3/-7.3
Lateral (film/accel) .....	5.8/9.8
<b>Damage</b>	
TAD .....	01-FR-5
VDI .....	01FREE7

FIGURE 2 Summary of results, Test LVWR-1.

test criteria for bridgerails (see Figure 1). Three successful tests were completed on July 27, 1987 (see Figures 2 and 3), July 29, 1987 (see Figures 4 and 5), and July 31, 1987 (see Figures 6 and 7). Because of these results, WSDOT uses the system on all open concrete baluster bridges.

## RETROFIT POLICY

The WSDOT policy begins by defining bridgerails as longitudinal barriers whose primary purpose is to redirect errant vehicles and prevent them from going over the side of a structure. Bridgerails for new bridges or replacement rails on widened bridges are based on systems which have been crash tested and meet the performance criteria in NCHRP Report 230 for structural adequacy, impact severity, and redirection.

For existing structures, the bridgerail should be evaluated to see if it meets AASHTO strength and geometric criteria or NCHRP performance criteria. If it does not, modifications to improve its redirection characteristics, and in some cases its strength, will be required. The modifications can be made using one of the retrofit methods described below.

## Modification Methods

New Jersey shape concrete rail (System MB5 in the 1977 AASHTO Barrier Guide): This treatment is preferred, if it is feasible, because of its performance characteristics and low maintenance costs when struck. A structural analysis is made to determine if the existing bridge deck and other superstructure elements are strong enough to accommodate this rail system.

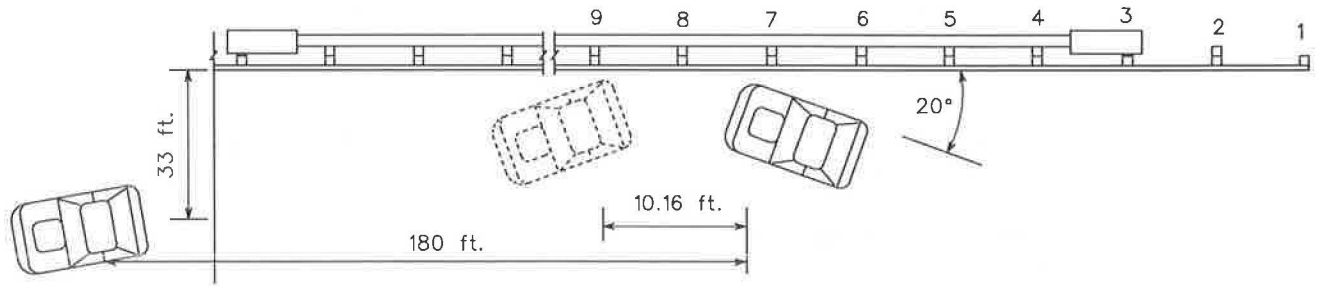


FIGURE 3 Test LVWR-1.

Test No. .... LVWR-2  
Date ..... 07/29/87  
Installation Length - ft (m) ..... 125(38)

Beam  
Member ..... 10 ga thrie-beam  
Length ..... 12.5 (3.8)

Maximum Deflections - in (m)  
Dynamic ..... 2.0 (5.1)

Barrier Description: Thrie-Beam retrofit over existing weak  
concrete baluster-type bridgerail

Soil type and condition ..... N/A (bridgerail)

Vehicle ..... 1978 Dodge

Mass -lb (kg)  
Test Inertia ..... 4395 (1993)  
Dummies ..... 330 (150)  
Gross ..... 4725 (2143)

Speed - mph (km/h) ..... 60.7 (97.7)

Angle - Deg  
Impact ..... 15.6

Occupant Impact Velocity - fps (m/s)  
Forward (film) ..... 13.9 (4.2)  
Lateral (film) ..... -18.3 (-5.6)

Occupant Ridedown Accelerations - g's  
Forward (film) ..... -5.9  
Lateral (film) ..... 5.1

Maximum 50 msec Avg Accelerations - g's  
Longitudinal (film) ..... -5.1  
Lateral (film) ..... 5.4

Damage  
TAD ..... 01-FR-5  
VDI ..... 01FREE7

FIGURE 4 Summary of results, Test LVWR-2.

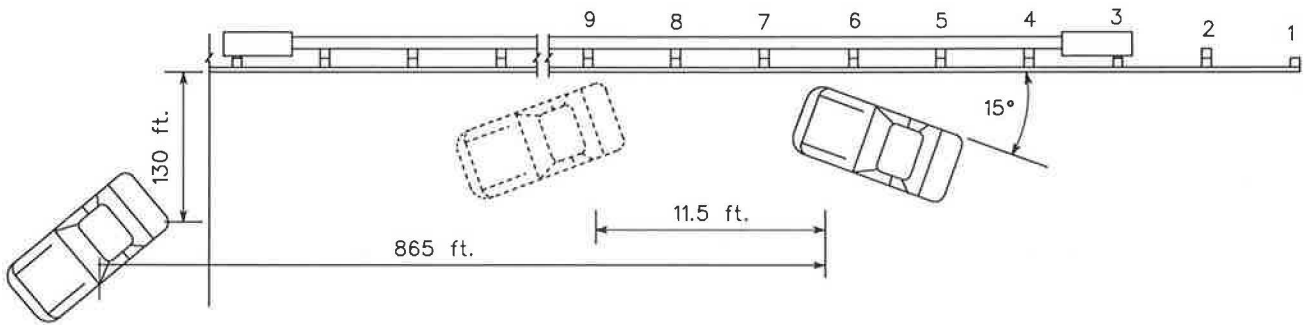


FIGURE 5 Test LVWR-2.

Test No. .... LVWR-3  
 Date ..... 07/31/87  
 Installation Length - ft (m) ..... 125(38)

Beam  
 Member ..... 10 ga thrie-beam  
 Length ..... 12.5 (3.8)

Maximum Deflections - in (m)  
 Dynamic ..... 2.6 (6.6)

Barrier Description: Thrie-Beam retrofit over existing weak  
 concrete baluster-type bridgerail

Soil type and condition ..... N/A (bridgerail)

Vehicle .....1983 Chevrolet C-10 Pickup truck

Mass -lb (kg)  
 Test Inertia ..... 5070 (2299)  
 Dummies ..... 330 (150)  
 Gross ..... 5400 (2449)

Speed - mph (km/h) ..... 66.3 (106.7)

Angle - Deg  
 Impact ..... 19.4

Occupant Impact Velocity - fps (m/s)  
 Forward (film) ..... 10.6 (3.2)  
 Lateral (film) ..... -18.4 (-5.6)

Occupant Ridedown Accelerations - g's  
 Forward (film) ..... -1.3  
 Lateral (film) ..... 5.2

Maximum 50 msec Avg Accelerations - g's  
 Longitudinal (film) ..... -4.0  
 Lateral (film) ..... 5.2

Damage  
 TAD ..... 01-FR-6  
 VDI ..... 01FREE8

FIGURE 6 Summary of results, Test LVWR-3.

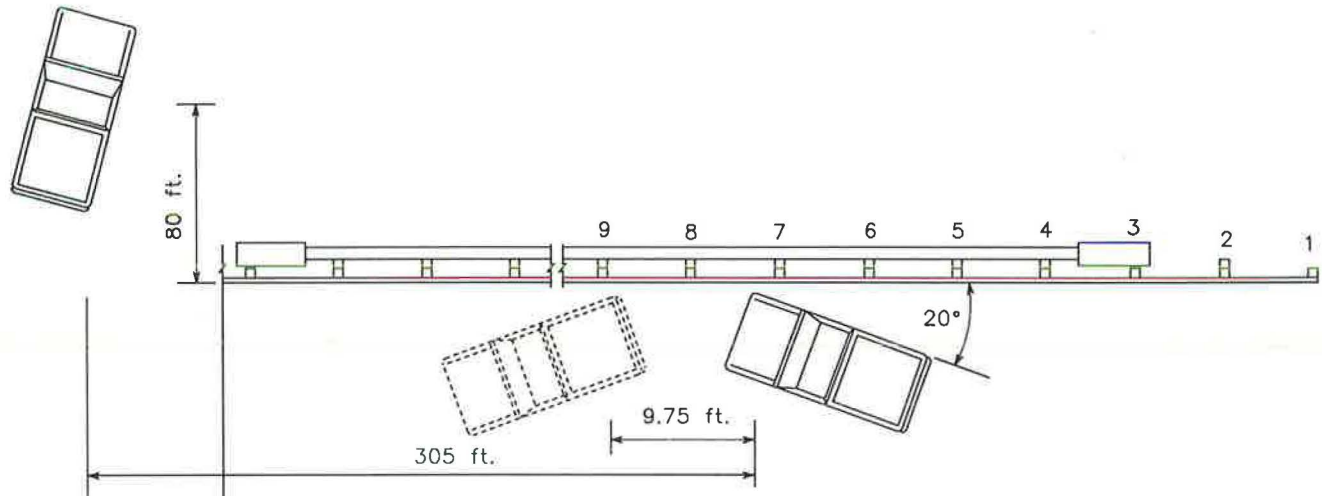


FIGURE 7 Test LVWR-3.

### Thrie Beam Mounted to Steel Posts

Placing thrie beam mounted to steel posts flush against the face of the curb is also an accepted system and is considered an appropriate treatment when New Jersey shape barriers are not feasible (see Figure 8). This is a crash-tested system and can be used under the following conditions:

- The bridge is as wide as or wider than the approach roadway, and the curb is wider than 12 inches.
- The bridge width is narrower than the approach roadway, and the curb is 12 to 18 inches wide.
- The bridge has a concrete deck and inadequate steel or wood posts for the bridgerail.
- The width of an approach bridge to a steel truss bridge is narrower than the approach roadway.

The height of the thrie beam should be 2 feet 8 inches measured from the top of the roadway.

A structural analysis is needed to determine if the existing bridge deck and other superstructure elements are strong enough to accommodate this rail system.

### Service Level 1 (SL-1)

When the existing bridge cannot accommodate either of the systems described above, an SL-1 system may be used (see

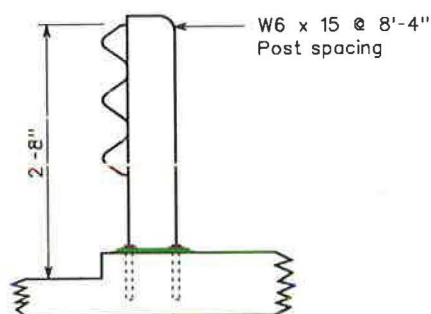


FIGURE 8 Thrie beam mounted to steel posts.

Figure 9). Examples of circumstances where this system may be used are bridges with timber decks or bridges with concrete decks in locations where an adequate stiff post transition cannot be installed. WSDOT's bridge engineer is consulted for the information required to complete the bracket design so the SL-1 system can be used.

In all cases, the curb is removed from the bridge for SL-1 type rail installations. This is necessary for proper performance of this rail system and is consistent with crash-tested systems.

Existing rigid concrete rail systems that do not meet the redirection criteria (e.g., concrete balusters, bridgerails where the face is not smooth) should also be upgraded. Based on performance history, these rails provide adequate strength for vehicle containment but can produce snagging. However, the following are recommended alternatives to improve the redirection characteristics of the bridgerail:

- Bridgerail with curb 18 inches or less: The thrie beams should be carried across the structure and blocked out flush with the face of the curb (see Figure 10). The preferred height of the top of the thrie beam is 2 feet 8 inches measured from the top of the roadway. When this height cannot be obtained, the beam should be installed so that the height of the top of the thrie beam is no lower than 2 feet 3 inches or the height of the bottom of the thrie beam is no higher than 1 foot 3 inches. These measurements are made from the top of the roadway.

• Bridgerail with a curb or sidewalk wider than 18 inches where the approach roadway shoulders are not carried across the structure: The thrie beam should be carried across the structure mounted flush to the face of the bridgerail (see Figure 11). The preferred height of the top of the thrie beam is 2 feet 8 inches measured from the top of the curb or sidewalk. When this height cannot be obtained, the beam should be installed so that the height of the top of the thrie beam is no lower than 2 feet 3 inches or the height of the bottom of the thrie beam is no higher than 1 foot 3 inches. These measurements are made from the top of the curb and sidewalk.

- Bridgerail with a curb wider than 18 inches where the approach roadway shoulders are carried across the structure:

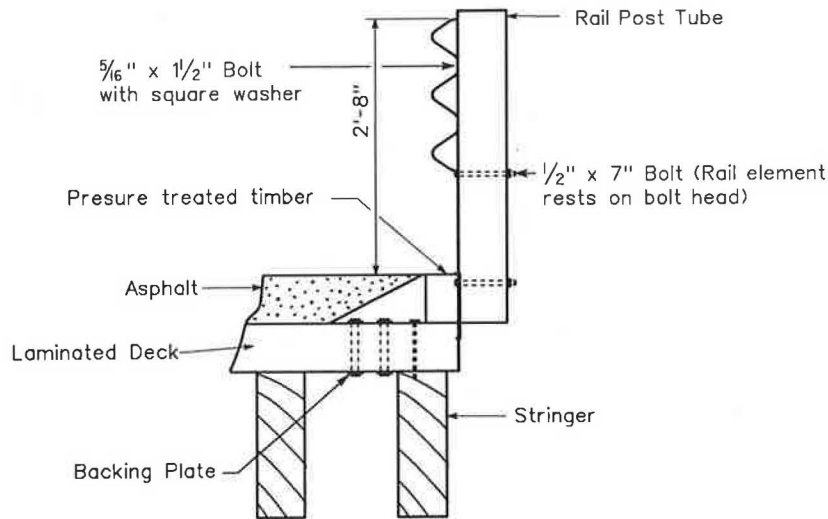


**FIGURE 9** Service Level 1 bridgerailing.

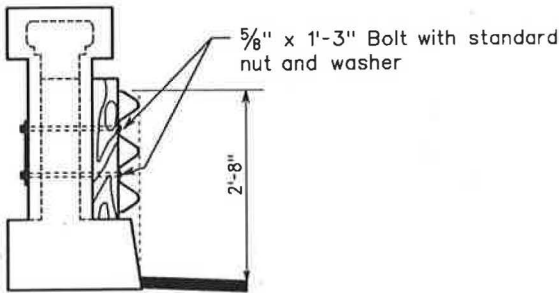


**FIGURE 10** Thrie beam mounted to concrete baluster with curb 18 inches or less.

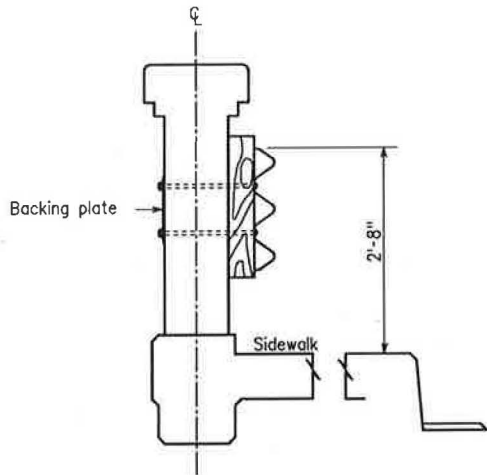


**FIGURE 11** Thrie beam mounted to concrete baluster with curb greater than 18 inches or a sidewalk.

The thrie beam should be placed flush to the face of the curb with the steel post design described above under the section on Thrie Beam Mounted to Steel Posts. The height of the top of the thrie beam should be 2 feet 8 inches measured from the top of the roadway. Any pedestrian traffic should be accommodated behind the approach rail.

**Existing Steel Most Rail Systems**

Existing steel most rail systems, which can snag vehicles when hit, should be upgraded with thrie beam mounted to the existing posts (see Figure 12). The post spacing on some of these systems may be so great that additional steel posts may be required to strengthen the rail system (see Figure 13). The posts are designed to take a 10-kip load, and the alternatives described above under the section on Existing Concrete Rail Systems are used to retrofit these types of bridgerails as to the blocking out and height placement of the thrie beam.

**Approach Rails**

Providing an appropriate approach rail and transition section to a bridge is critical in shielding a vehicle from the end of the structure. The length of the transition should not allow significant changes in the lateral stiffness to occur within a short distance. The transition length should be approximately 10 to 12 times the difference in dynamic deflections between joining barriers. The stiffness of the transition should increase smoothly and continuously from the more flexible to the less flexible system. This is usually accomplished by decreasing the post spacing and/or decreasing the post spacing and increasing the post size.

Approach rails are required on all four corners of bridges

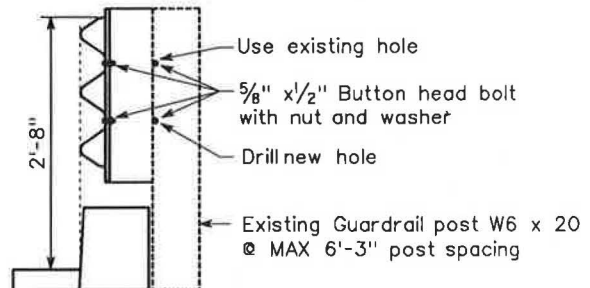


**FIGURE 12** Thrie beam mounted to existing posts.

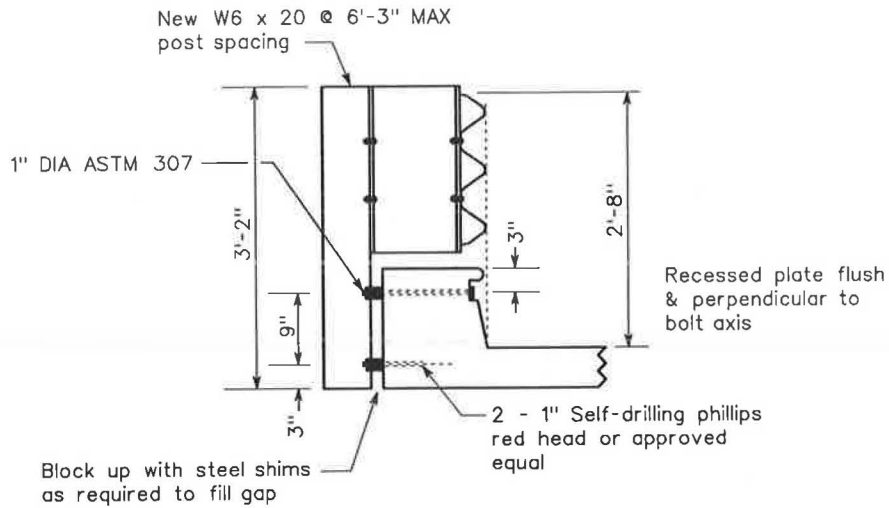


**FIGURE 13** Thrie beam mounted to existing posts with new posts placed between existing posts.

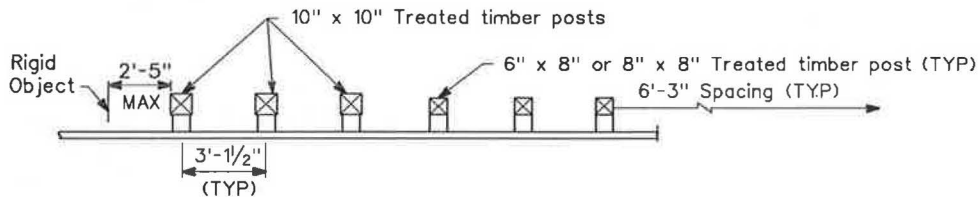


**FIGURE 14** Type 1 transition section.

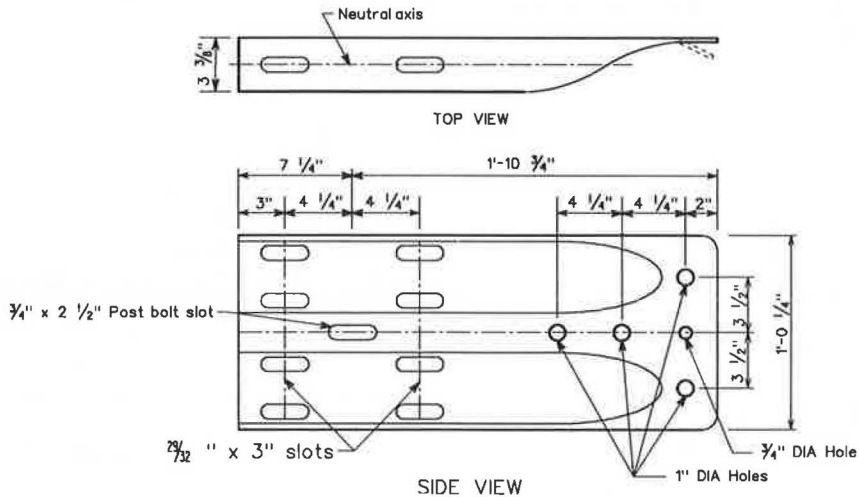


**FIGURE 15** Design F terminal section.

carrying two-way traffic and on both corners of the approach end for one-way traffic. The following criteria should be used for the bridgerails that will be encountered.

For rigid concrete bridge rail systems that meet the strength and performance criteria and do not need to be retrofitted, a Type 1 transition section (System T1 in the 1977 AASHTO Barrier Guide) is used (see Figure 14). The following is recommended for aligning and connecting a W-beam approach guardrail to the bridgerail.

- Bridgerail with no curb: The approach guardrail should be lined up with the face of the bridgerail and connected to the bridge rail with a Design F terminal section (see Figure 15).
- Bridgerail with curb 18 inches or less: The approach guardrail should be lined up with the face of the curb, blocked out from the bridgerail, and connected to the bridgerail using a Design F terminal section.
- Bridgerail with a curb or sidewalk wider than 18 inches:

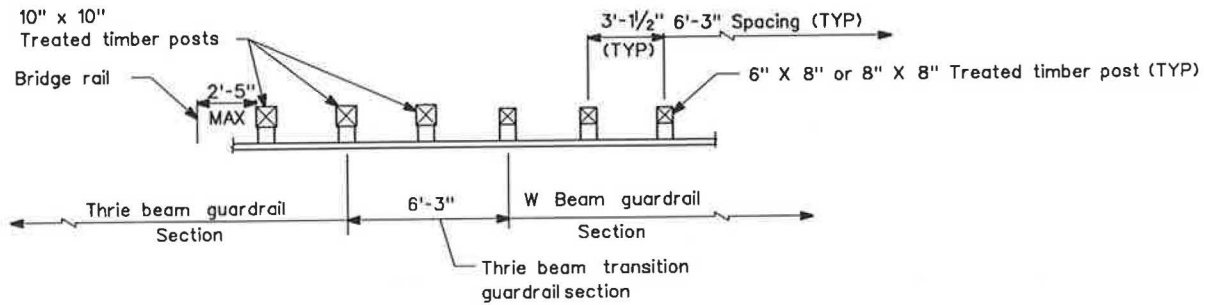


FIGURE 16 Type 4 transition section.

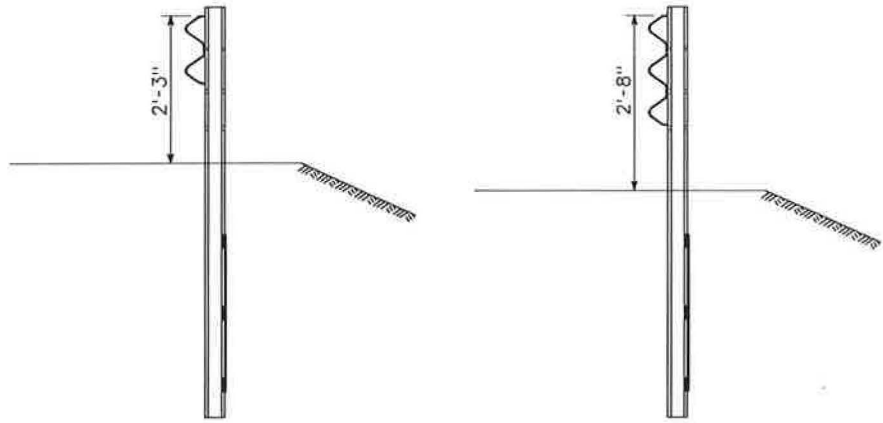
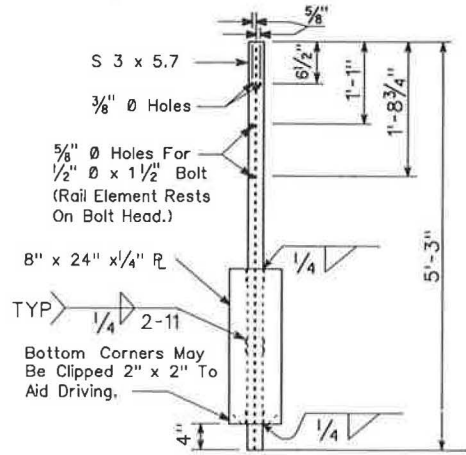


FIGURE 17 G-2 post.

The approach guardrail should be lined up with the face of the bridgerail and connected to the bridgerail using a Design F terminal section. The ends of the curb or sidewalk will be exposed, and a vehicle could snag on the blunt face. To eliminate this potential hazard, an asphalt or concrete ramp is required to shield the end of the curb or sidewalk. The slope of the ramp should be 12:1 or flatter. The ramp should be installed at all ends exposed to traffic (all four corners for two-way traffic, or the approach ends for one-way traffic).

For rigid concrete bridgerail systems modified with thrie beam and for steel post rail systems (except SL-1), the approach rail should be lined up with the face of the thrie beam and a Type 4 transition section should be used (see Figure 16). An asphalt concrete ramp, as described above, is required when the bridgerail is not lined up with the face of the curb.

For SL-1 bridgerails, no transition section is required. However, G-2 posts (see Figure 17) must be used on the approach rail to be compatible with this system.



## **COSTS**

The bids WSDOT has received for mounting thrie beams to concrete baluster bridgerails or rails with existing steel posts range from \$14 to \$42 per foot. Over 16,000 feet of thrie beam have been installed on concrete baluster bridgerails. The average cost is \$21.60. Where extra steel posts are required, the cost for adding each one is about \$100. The cost for installing a SL-1 system on a timber rail bridge is about \$80 to \$85 per foot. This includes the cost of removing the existing timber rail.

## **IMPLEMENTATION AND CONCLUSIONS**

The WSDOT retrofit applications are intended to be simple to install, requiring standard 12 feet 6 inch thrie beams to

keep costs down and repairs easy. To date, WSDOT has had 21 contracts that provided retrofits for 31 bridges, using thrie beams or W-beams. (Early WSDOT direction was to use W-beams under certain conditions.) Three bridges received the SL-1 system under the FHWA Demonstration 64 program.

On four other bridges, the SL-1 system was installed during 3R or safety projects.

The application of this bridgerail retrofit policy has proven to be of real value to the state of Washington and has received the full support of management and of the FHWA Washington Division. It provides a low-cost answer for retrofitting bridgerailing.

# W-Beam Guiderail Transition from Light to Heavy Posts

DONALD G. HERRING AND JAMES E. BRYDEN

**Two full-scale crash tests evaluated a transition between light- and heavy-post W-beam guiderail. The transition consisted of lowering the rail height from 30 to 27 inches and reducing the spacing of the light posts as the heavy-post section is approached. The crash-test impacts were just upstream of the heavy-post section using 1,800- and 4,500-pound sedans. Test results were generally acceptable in terms of National Cooperative Highway Research Program (NCHRP) criteria. Although the exit trajectory of the 4,500-pound sedan exceeded the recommended threshold limits, the vehicle was not judged to present a significant threat to other vehicles.**

The state of New York makes extensive use of corrugated-steel (W-beam) guiderail on its highway system. Two W-beam systems are used—light post and blocked-out heavy post. Cable and box-beam light-post barriers are also used. Until recently, the light-post cable, W-beam, and box-beam systems were generally not used on the same highways as the heavy-post W-beams. The heavy-post system was limited primarily to high-volume urban roadways where high accident rates make it difficult to maintain light-post barriers in functional condition. Light-post barriers were generally used elsewhere.

When using light-post barriers, system selection depends on available deflection space behind the barrier. Because cable and W-beam are more flexible and provide a more forgiving impact, as well as a lower first cost, they are used where available deflection space permits. As deflection space decreases, dynamic impact deflection can be reduced somewhat by reducing post spacing. For more severe limitations, it becomes necessary to transition from cable to W-beam or from W-beam to box-beam. However, the transition from light-post W-beam to box-beam is very expensive and, thus, not a desirable option. In addition, though performance of these guiderail systems had been documented through full-scale crash tests and in-service performance evaluations (1, 2), less is known about performance of the transition between them.

Increased use of heavy-post W-beam barrier in New York has provided an additional option for limiting dynamic impact deflections, and it was quickly recognized that a transition from light-post to heavy-post W-beam guiderail may offer advantages compared to the W-beam to box-beam transition previously used. Thus, the department's engineering staff developed the transition shown in Figure 1 and described in the Traffic and Safety Division publication *Guiderail II* (3).

Engineering Research and Development Bureau, New York State Department of Transportation, State Office Campus, Albany, N.Y. 12232.

This transition was designed to provide a gradual stiffening of the W-beam to avoid snagging vehicles that impact near it. Spacing of the light posts is decreased as they near the heavy-post section, and the rails are gradually lowered from 30 inches to match the 27-inch height on the heavy posts. While this design apparently would perform acceptably, evaluation through full-scale crash tests was desirable to ensure acceptable impact performance.

## METHODOLOGY AND BARRIER DESCRIPTION

This study consisted of two full-scale crash tests conducted to evaluate the transition section. The testing and data analysis procedures outlined in NCHRP Report 230 (4) were used. The test matrix consisted of the two tests—NCHRP Test Designations 30 and 12. Test 30 used a 4,500-pound vehicle to determine structural adequacy and is the only one specified in NCHRP 230 for transition sections. Test 12 was included to evaluate occupant risk in a small, 1,800-pound vehicle and to give a more complete picture of transition performance.

The barrier, constructed of standard 12-gauge W-beam guiderail, transitions from light post (S3 x 5.7) to heavy post (W6 x 9) with blockouts. The barrier consisted of eighteen W-beam sections totaling 225 feet in length and was terminated at both ends with standard turndowns and precast concrete anchors. A plan view of the barrier as tested is shown in Figure 2, with additional details in Figure 3.

The barrier was erected 30 inches high for the initial light-post sections. Post spacing was 6 feet 3 inches for the first two rail sections and 3 feet 1½ inches for Sections 3 and 4. In Section 4, rail height was transitioned from 30 to 27 inches. The beam was attached to every other post in Sections 3 and 4 using 5/16-inch hex-head bolts, with the quarter-point posts provided only to provide lateral support. Within the heavy-post section, the W-beam was attached to all posts using 5/8-inch hex-head bolts with rectangular washers.

## RESULTS

Results of the two full-scale crash tests are summarized in Table 1. The vehicles and barrier after the tests are shown in Figure 4, and Figures 5 and 6 provide sequential impact photographs. Vehicle trajectories are diagrammed in Figure 7.

Test 108 evaluated the transition for snagging or rollover tendencies of small cars. Excessive vehicle decelerations that might cause occupant injuries were also noted. An 1,800-pound Honda Civic impacted the barrier at 61.2 mph and 13

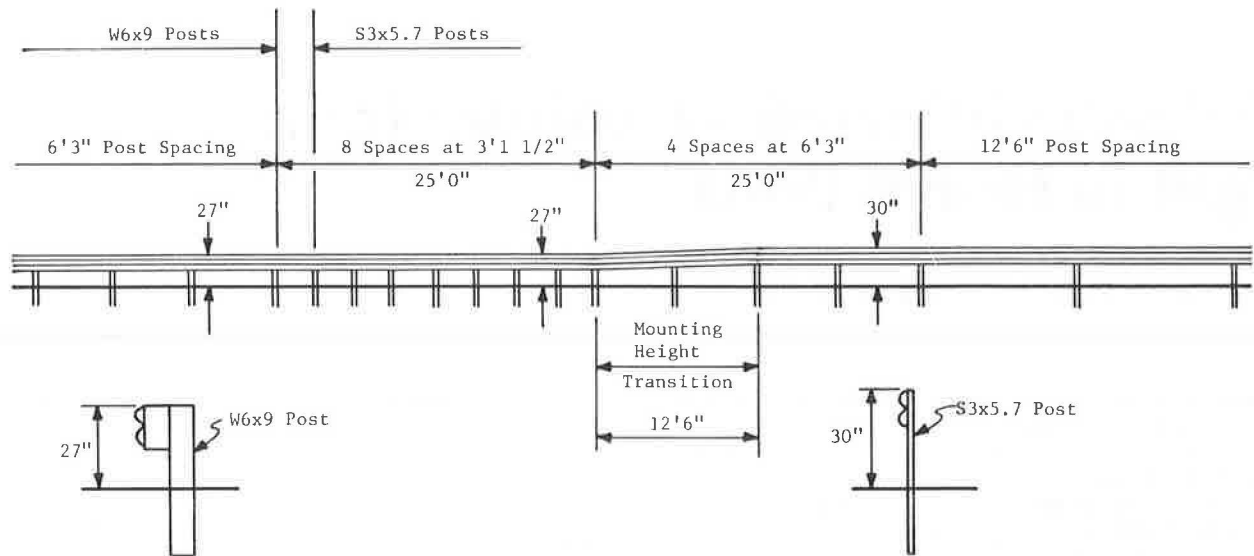


FIGURE 1 W-beam guiderail transition from light to heavy posts.

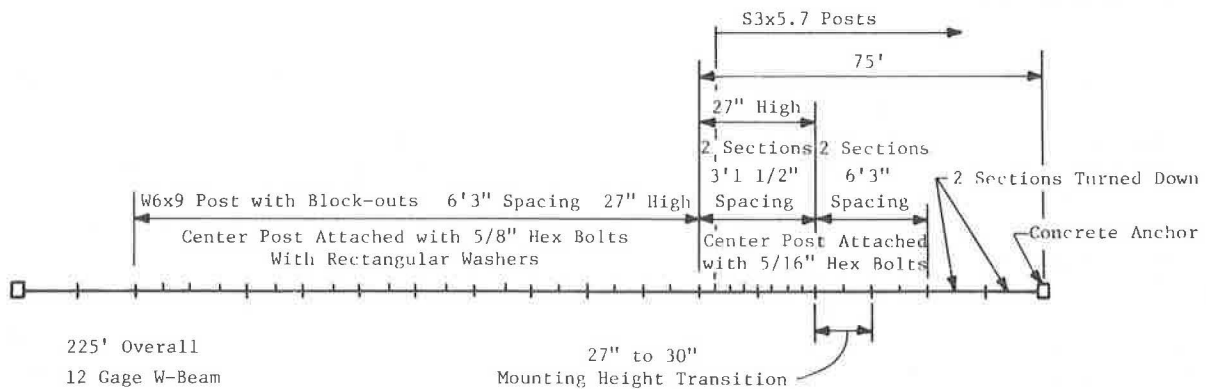


FIGURE 2 Plan view of barrier used for Tests 108 and 109.

degrees, with impact 4 feet upstream from the first heavy post. The vehicle was in contact with the barrier for only 4 feet, then exited smoothly at 8 degrees and 51.6 mph. There was no measurable barrier deflection, and the W-beam was only scuffed. Vehicle damage was light, consisting of sheet metal damage along the right side, and minor damage to the grill and bumper. Maximum vehicle roll was 3 degrees clockwise, with no measurable pitch or yaw. Peak 50-ms average decelerations were 1.2 g longitudinal and 12.2 g lateral. Thus, longitudinal critical distance was not reached, and occupant impact velocity and occupant ridedown deceleration were not computed. Lateral occupant impact velocity was 17.9 feet per second (fps), based on a measured flail distance of 0.5 feet with a ridedown deceleration of 13.5 g. Vehicle redirection was very smooth and the vehicle was operable after impact.

NCHRP Report 230 Test Designation 30 was used in Test 109 to evaluate the barrier for structural adequacy and redirection capability. A 4,600-pound Chrysler sedan impacted the barrier 17 feet upstream from the first heavy post at 58.1 mph and 27 degrees. Dynamic barrier deflection was 4 feet during the 29-foot contact distance, and the vehicle exited at

21 degrees and 33.4 mph. Maximum vehicle roll was 2 degrees clockwise, pitch was 7 degrees nose down, and no yaw was observed. Barrier and vehicle damage (Figure 4) were moderate. Three rail sections, three heavy posts, and eight light posts were bent. The vehicle sustained sheet metal damage to the right front fender, right front door, and right rear fender; there was also grill and bumper damage. Both right tires were deflated, and the right front wheel was damaged. Although not required evaluation criteria for this test, the occupant impact velocities and ridedown decelerations are reported in Table 1. The lateral values are below recommended threshold values, and the longitudinal values nearly meet those for 15 degree impacts. Redirection of the vehicle was smooth, with no excessive roll, pitch, or yaw.

## DISCUSSION AND FINDINGS

These tests were evaluated using the criteria in NCHRP 230 for structural adequacy, occupant risk, and vehicle trajectory. As mentioned previously, the only test specifically designated



FIGURE 3 Vehicles and barriers before impacts in Test 108 (top) and Test 109 (bottom).

for transitions is with a 4,500-pound vehicle impacted at 60 mph at a 25 degree angle. To provide a more complete picture of the transition's performance, a subcompact vehicle was included in this evaluation. The small-vehicle test would help point out deficiencies in redirection or occupant risk that might not affect a heavier vehicle. Measured test values and NCHRP criteria are compared in Table 2.

Structural adequacy criteria require that the barrier smoothly redirect the vehicle, without threatening the integrity of the passenger compartment by detached elements or fragmenting. The barrier showed no tendency to break apart or have loose elements fly off. As expected of a semi-rigid barrier system, the small vehicle in Test 108 caused minimal deflection, and was quickly redirected after contacting the rail for a short distance. In Test 109, the heavier vehicle caused considerable deflection, but redirection was smooth with no snagging as it traveled from the light-post to the heavy-post section. Both tests, thus, were judged to be in compliance with the structural adequacy evaluation factors.

Both tests easily met Evaluation Factor *E* that the vehicle remain upright, experiencing only mild roll, pitch, or yaw. Neither vehicle sustained passenger compartment damage. Factor *F* (occupant impact values) does not apply to the large-car test. However, those test values were provided for information, and it is seen that the longitudinal values for this 25 degree impact only slightly exceeded desirable values for 15

degree impacts, and the lateral values were below the recommended thresholds. The small-car test easily passed the longitudinal criterion, because the theoretical occupant did not travel the flail distance. Based on a measured flail distance of 0.5 feet, the lateral occupant impact velocity and ridedown acceleration were both within recommended thresholds. NCHRP Report 230 specifically provides for the use of actual measured flail distance when available, rather than the standard assumed value of 1.0 foot. Both tests thus were judged to meet the occupant risk factors.

The post-collision trajectory is required to result in no more than minimal intrusion into adjacent traffic lanes. In addition, these tests require the exit angle be less than 60 percent of the impact angle, with less than a 15-mph speed loss.

In Test 108, the speed change was less than 10 mph, and the departure angle was 62 percent of the impact angle. The vehicle departed the barrier on a straight path, and would eventually have crossed into the adjacent lane as it continued away from the barrier. However, damage to the vehicle was light, and it was fully operable after impact. Combined with the smooth redirection trajectory, risk of a secondary collision appeared low, and the test, thus, was considered satisfactory in terms of post-impact trajectory.

For Test 109, the post-impact trajectory was less favorable. Velocity change was nearly 25 mph, and the departure angle was 78 percent of the impact angle. In addition, the exit

TABLE 1 TEST RESULTS

Item	Test 108	Test 109
Point of Impact	4 ft upstream from first heavy post	17 ft upstream from first heavy post
Barrier Length, ft	225	225
Vehicle Weight, lb	1800	4600
Vehicle Speed, mph	61.2	58.1
Impact Angle, deg	13	27
Exit Angle, deg	8	21
Exit Speed, mph	51.6	33.4
Maximum Roll, deg	3 clockwise	2 clockwise
Maximum Pitch, deg	0	7 down
Maximum Yaw, deg	0	0
Contact Distance, ft	4	29
Contact Time, ms	190	750
Barrier Deflection, ft		
Dynamic	0*	4.0
Permanent	0*	2.6
Deceleration, g		
50-ms avg		
Longitudinal	1.2	8.7
Lateral	12.2	5.6
Occupant Impact Velocity, fps		
Longitudinal (2.0 ft)	**	32.1
Lateral (0.5)***	17.9	15.4
Occupant Ridedown, 10-ms avg		
Longitudinal	**	21.0
Lateral	13.5	18.7
Redirection	Smooth	Smooth
Vehicle Damage		
TAD	RFQ-3	RFQ-4
SAE	O1RDMS1	O1RFMP2

\*Deflections were too slight to permit measurement.

\*\*Critical distance not reached.

\*\*\*Measured flail distance was 0.5 ft for 1800-lb sedan; assumed distance of 1.0 ft was used for 4500-lb sedan.

trajectory carried the vehicle away from the barrier where it would have entered the adjacent lanes. Although post-impact vehicle trajectory was smooth, these test results do not comply technically with the recommended criteria. However, considering the difficulty in transitioning from a relatively flexible to a relatively stiff barrier, this comparatively abrupt redirection is not unexpected. Recently reported test results (5) show that the recommended threshold values for post-impact vehicle trajectory are not met by a number of barrier systems widely recognized as providing an acceptable level of in-service performance. It may be possible to smooth this departure trajectory somewhat by adding additional light posts to effect a more gradual stiffening of the barrier. However, these additional posts would interact with smaller cars and might adversely affect the good performance seen in Test 108. In light of the good results achieved for all other evaluation factors, vehicle trajectory in Test 109 is considered an acceptable compromise, especially since secondary collisions with other vehicles have been shown to be a rare event (6).

Based on these two full-scale crash tests, the following findings can be stated:

1. The transition from light- to heavy-post W-beam guide-rail successfully contained 1,800- and 4,500-pound sedans.

2. This transition met the occupant risk criteria of NCHRP 230 for 1,800- and 4,500-pound vehicles.

3. Both vehicles were smoothly redirected by the transition, with no danger of vehicle rollover or other adverse vehicle reactions. Although the exit trajectory of the 4,500-pound sedan exceeded the limits recommended in NCHRP 230, neither vehicle was judged a significant threat to other vehicles.

4. The design tested appears suitable for field use to transition between light- and heavy-post W-beam barrier systems.

#### ACKNOWLEDGMENTS

Research reported here was performed under the technical supervision of James E. Bryden. Full-scale tests were supervised by Donald G. Herring and Richard G. Phillips, assisted by Robert P. Murray, Wayne R. Shrome, David J. Leininger, and Robert J. Longtin. William G. Roth performed instrumentation work. Maintenance personnel from the New York State Thruway Authority helped install the barrier. Technical assistance was also provided by employees of the department's Facilities Design Division. The investigation was conducted in cooperation with the Federal Highway Administration, U.S. Department of Transportation.



**FIGURE 4** Vehicles and barriers after Test 108 (top) and Test 109 (bottom).



**FIGURE 5** Sequential photographs of Test 108.

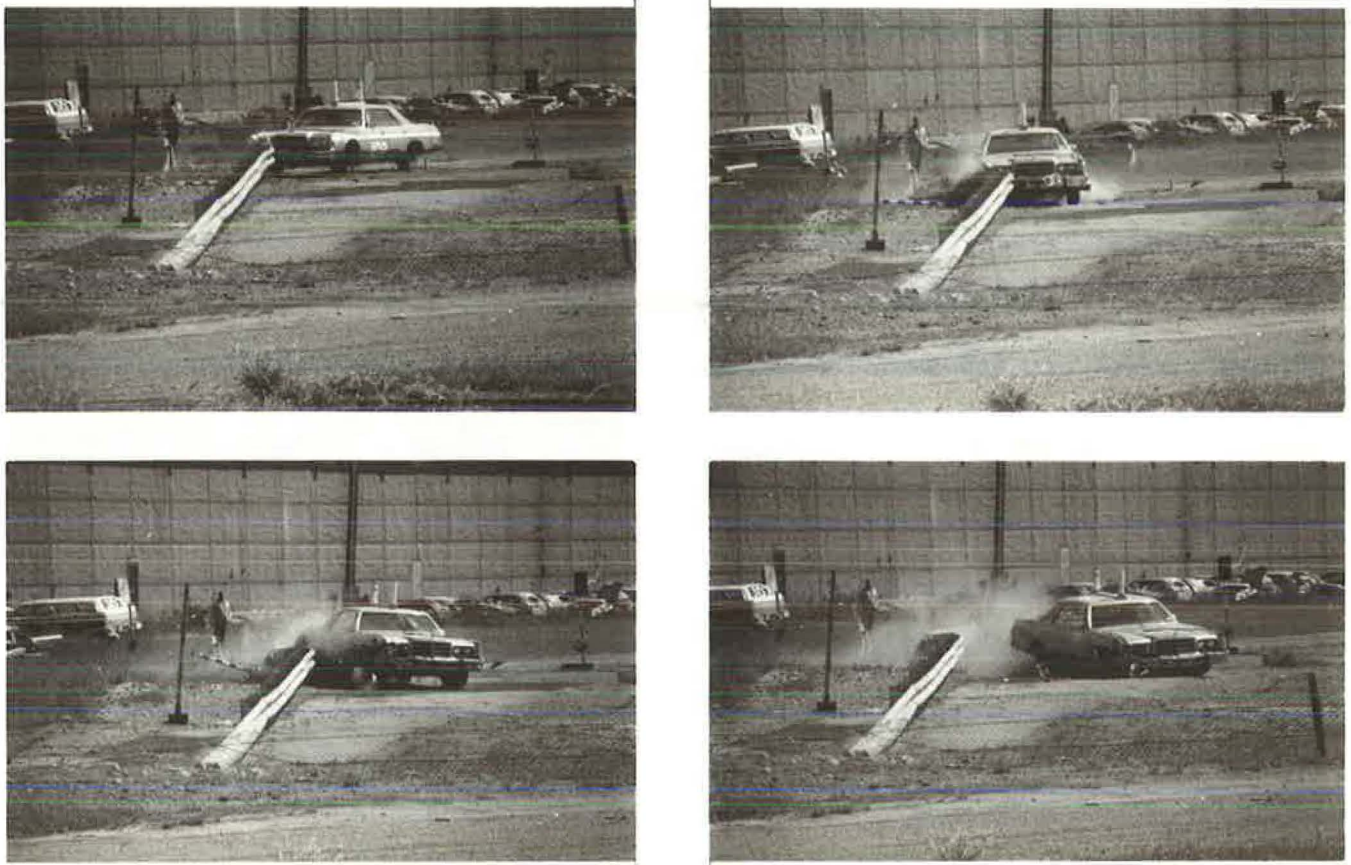


FIGURE 6 Sequential photographs of Test 109.

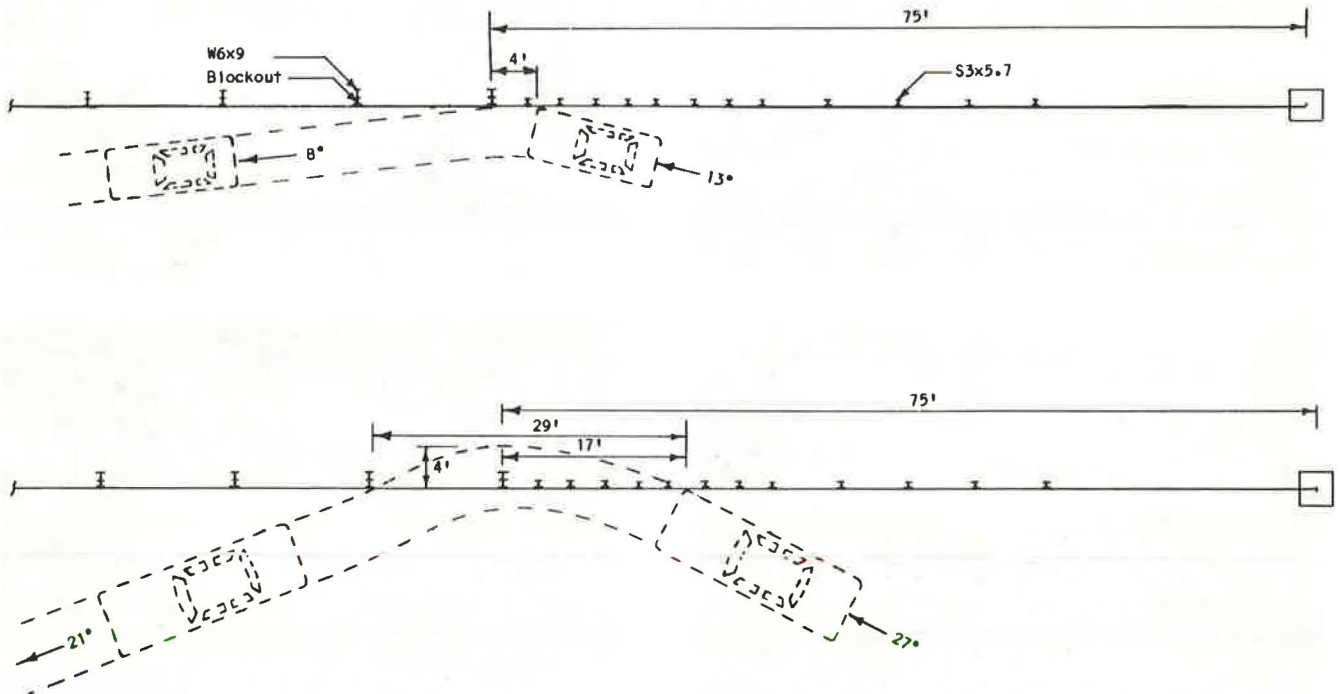


FIGURE 7 Vehicle impact trajectories in Test 108 (top) and Test 109 (bottom).

TABLE 2 TEST RESULTS COMPARED WITH NCHRP REPORT 230 EVALUATION FACTORS

NCHRP 230 Evaluation Factors	NCHRP 230 Recommended Value	Test 108 (NCHRP 12)	Test 109 (NCHRP 30)
<b>Structural Adequacy</b>			
A	Smooth redirection	OK	OK
D	No fragments, passenger compartment intact	OK	OK
<b>Occupant Risk</b>			
E	Vehicle upright, passenger compartment intact	OK	OK
F	Occupant Impact Velocity		
	30 longitudinal	*	***
	20 lateral	17.9**	***
	Ridedown Deceleration		
	15 longitudinal	*	***
	15 lateral	13.5	***
<b>Vehicle Trajectory</b>			
H	Minimum intrusion into adjacent lane	OK	Marginal
I	Speed change <15 mph	9.6	24.7
	Exit angle <0.6 impact angle	62%	78%

\*Occupant did not travel the flail distance

\*\*Based on 0.5-ft flail distance.

\*\*\*Evaluation Factor F not required for 25° impacts.

## REFERENCES

1. J. L. Whitmore, R. G. Picciocca, and W. A. Snyder. *Testing of Highway Barriers and Other Safety Accessories*. Research Report 38. Engineering Research and Development Bureau, New York State Department of Transportation, Dec. 1976.
2. J. VanZweden and J. E. Bryden. *In-Service Performance of Highway Barriers*. Research Report 51. Engineering Research and Development Bureau, New York State Department of Transportation, July 1977.
3. R. E. O'Connor and J. E. Haviland. *Guiderail II*. Traffic and Safety Division and Facilities Design Division, New York State Department of Transportation, January 1984.
4. J. D. Michie. *NCHRP Report 230: Recommended Procedures for the Safety Performance Evaluation of Highway Appurtenances*. TRB, National Research Council, Washington, D.C., March 1981.
5. M. E. Bronstad, J. D. Michie, and J. D. Mayer, Jr. *NCHRP Report 289: Performance of Longitudinal Traffic Barriers*. National Cooperative Highway Research Program, TRB, National Research Council, June 1987.
6. J. E. Bryden and J. S. Fortuniewicz. Traffic Barrier Performance Related to Vehicle Size and Type. In *Transportation Research Record 1065*, TRB, National Research Council, Washington, D.C., 1986, pp. 69-78.



# Use of Guardrails on Low Fill Bridge Length Culverts

T. J. HIRSCH AND DALE BEGGS

When multiple box culverts span more than 20 feet, the American Association of State Highway Transportation Officials (AASHTO) defines them as bridge length and, thus, normally require the use of a full-strength, rigid bridgerail. Using a rigid bridgerail creates a transition problem between the flexible metal beam guard fence, which is commonly used upstream of the bridgerail. It would be safer and more economical to continue the flexible metal beam guard fence across the culvert even when the culvert is more than 20 feet long and when the soil fill depth over the culvert is less than the standard guardrail post embedment depth (38 inches in Texas). It was believed that more posts could be used (reduced post spacing) with a shallow embedment to achieve the desired guardrail strength. A metal beam guard fence design of this type was crash tested in this study and proved to be unsatisfactory. Another concept investigated was to rigidly mount steel guard fence posts to the top of the culvert deck when full soil embedment could not be achieved. A design of this type was also crash tested in this study and proved to be satisfactory.

When multiple box culverts span more than 20 feet, the American Association of State Highway Transportation Officials (AASHTO) (1) defines them as bridge length and, thus, normally require the use of a full-strength, rigid bridgerail. Using a rigid bridgerail creates a transition problem between the flexible metal beam guard fence, which is commonly used upstream of the bridgerail. It would be safer and more economical to continue the flexible metal beam guard fence across the culvert even when the culvert is more than 20 feet long and when the soil fill depth over the culvert is less than the standard guardrail post embedment depth of 38 inches. Many of these culverts have soil fills 6 to 38 inches deep.

The objective of this research study was to develop information to promote the concept of continuing the approach flexible metal beam guard fence across bridge length (over 20 feet) multiple box culverts. This concept is believed to be safer, more economical, and more effective than using rigid bridgerails on such culverts.

Research Report 405-1, *The Effects of Embedment Depth, Soil Properties, and Post Type on the Performance of Highway Guardrail Posts* (2) presented data which could be used to modify the current metal beam guard fence for application when the full 38-inch post embedment depth could not be achieved. It was believed that more posts could be used with a shallow embedment to achieve the desired guardrail strength. A metal beam guard fence design of this type was crash tested in this study and proved to be unsatisfactory.

Another concept investigated was to rigidly mount the guard fence post to the top of the culvert deck when full soil embedment could not be achieved. A design of this type was also crash tested in this study and proved to be satisfactory.

## METAL BEAM GUARD FENCE DESIGNS AND CRASH TESTS

At the beginning of this research, it was believed that more guardrail posts could be used with a shallow embedment to achieve the necessary guard rail strength. Figure 1 shows the standard 38-inch embedment with the Texas standard 27-inch W-beam mounting height. Figure 2 shows static load test results on these posts in a cohesionless soil (3) for various embedment depths. Figure 3 summarizes the maximum force and energy absorbed for various embedment depths. These data are from figure 2 and *The Effects of Embedment Depth, Soil Properties, and Post Type on the Performance of Highway Guardrail Posts* (2) and have been modified slightly so the maximum force and energy could be presented on the same graph. The energy

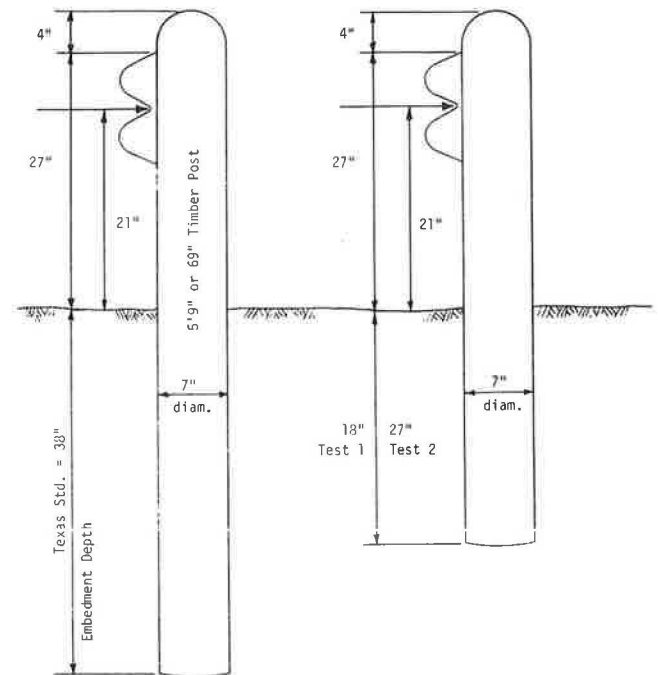
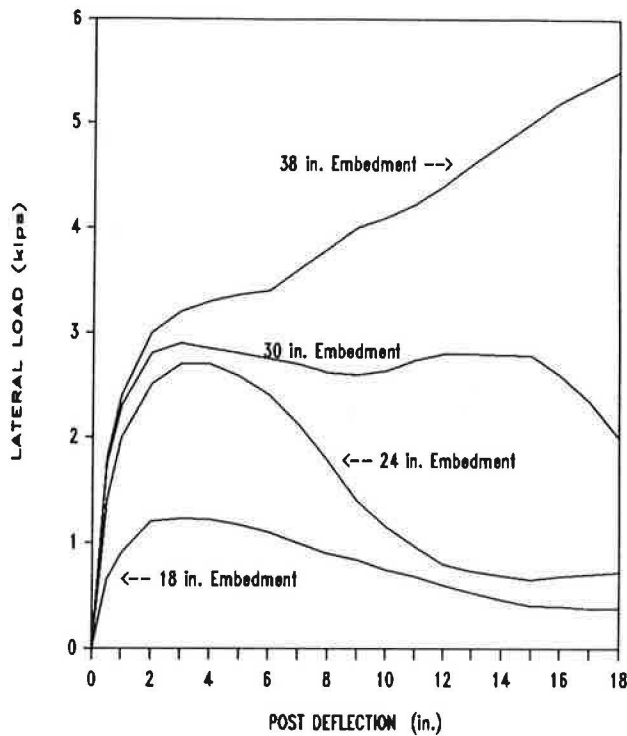


FIGURE 1 Standard Texas timber guardrail post and modified version used in Tests 1 and 2 (prior to 1984).



**FIGURE 2** Typical load vs. deflection data for 7-in. diameter timber post embedded in cohesionless soil. Load applied and deflection measured at center of W-beam (21 inches high) (5).

absorbed was computed to 18 inches of deflection. Impact tests (4) with a pendulum traveling 17 mph will yield results four to five times these values. These data were used in selecting the modified guardrail designs presented.

The plan view of the typical modified guard fence designs to be tested is shown by Figure 4. As can be seen, a 50-foot

long segment of the modified guard fence design was installed over a simulated concrete culvert. Standard guard fence with the standard turned down terminal was installed on the upstream and downstream ends of the test section. The standard turned down terminal is still used in Texas and many other states.

The single crash test conducted on each modified design was with a 4,500-pound car impacting at 60 mph and a 25 degree angle (3).

**Modified Guard Fence No. 1**

The first modification is shown by Figure 5 using 7-inch diameter timber as shown in Figure 1. Originally, it was intended to use twice as many posts with one-half the strength of a fully embedded post: for example, posts spaced at 3 feet 1½ inches and embedded 24 or 27 inches (see Figures 2 and 3). However, another hypothesis prevailed. Since a strong guard-rail and turned-down end anchor were to be used upstream and downstream of the 50-foot long simulated culvert, the post only needed to hold up the W-beam to make initial contact with the car. The hypothesis was that the W-beam firmly anchored on each end could redirect the car over this 50-foot length by itself.

This hypothesis was investigated using the BARRIER VII computer program, and a summary of the results is presented in Table 1. This table indicates the standard guard fence (6 feet-3 inch post spacing with 38-inch embedment) would deflect 20.8 inches when impacted with a 4,500 pound car at 60 mph and 25 degree angle. The modified guard fence No. 1 shown in Figure 5 (6 feet-3 inch post spacing with 18-inch embedment) would deflect 34.4 inches.

One problem with the analysis, which Crash Test 1 will demonstrate, is that BARRIER VII is a planar, two-dimensional analysis. BARRIER VII cannot indicate that the W-beam will drop vertically and the car will vault vertically over the guardrail.

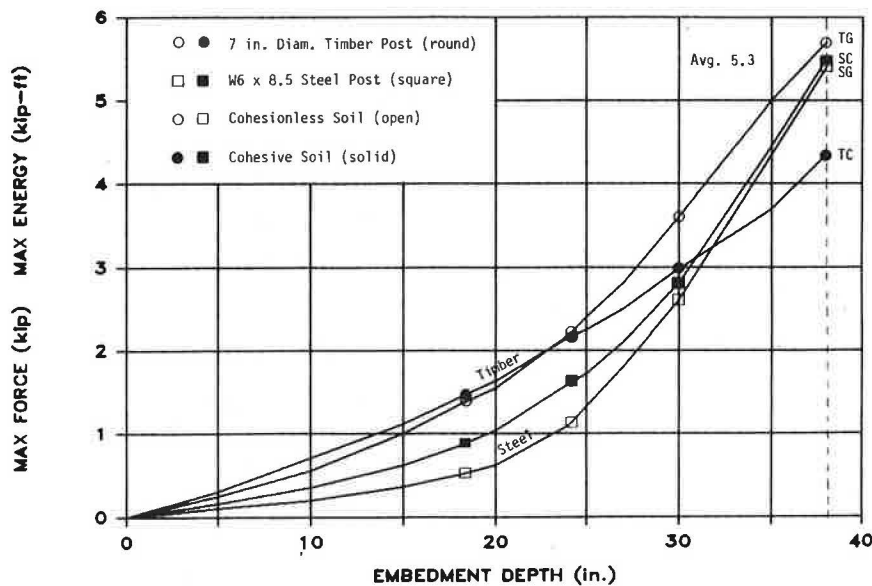


**FIGURE 3** Summary of maximum force and energy absorbed by guardrail post vs. embedment depth (5).

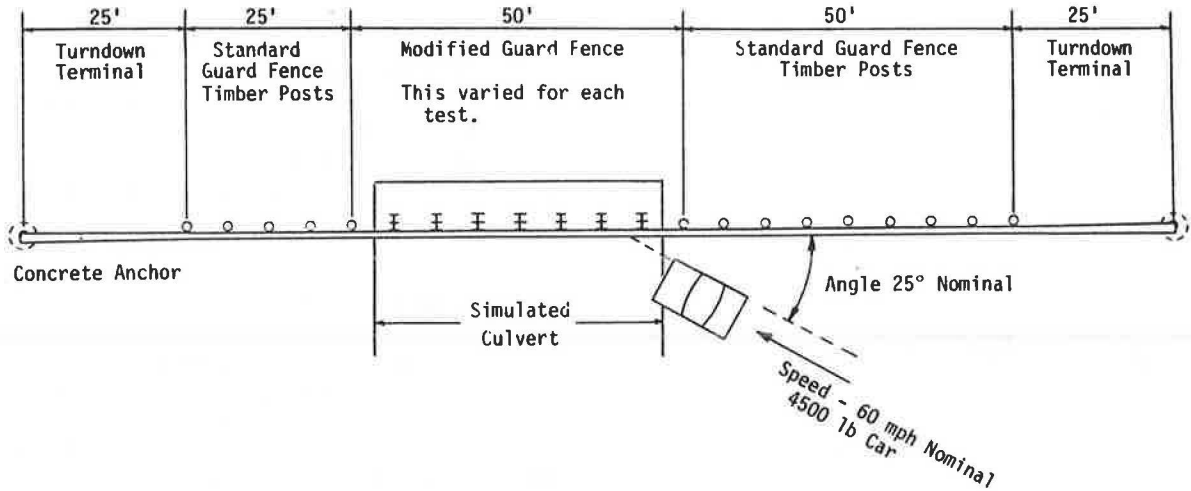


FIGURE 4 Plan view of typical crash test site for Tests 1, 2, and 3.

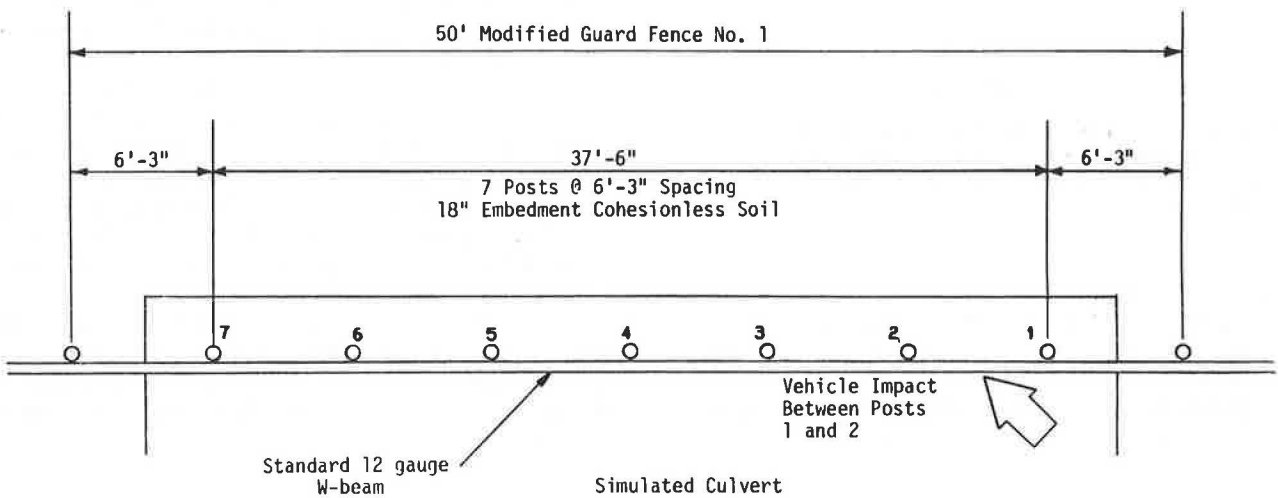


FIGURE 5 Plan view of modified guard fence No. 1 installation for Crash Test 1.

#### Crash Test 1

Figure 6 shows the modified guard fence installation and car before and after Crash Test 1. In this test, a 4,400-pound Chrysler Newport impacted modified guard fence No. 1 at 61.9 mph and 26.2 degree angle. At 0.2 seconds into the impact, the car began to parallel the deflected (about 46.8 inches) W-beam rail, the W-beam dropped, and the car ramped over it. The car penetrated behind the rail and rolled over. The test was unsuccessful.

Figure 7 presents a summary of the Crash Test 1 data.

#### Modified Guard Fence No. 2

This guard fence design was in accordance with the original hypothesis that one could use twice as many posts with one-half the strength to achieve the desired strength for vehicle redirection. Figure 3 was used to select the 7-inch diameter

timber post embedded 27 inches in cohesionless soil to obtain half the strength (both force and energy absorbed) of the standard 38-inch embedded post. This yields the design shown by Figure 8. Interpolating the data in Table 1 would indicate that this guard fence design would deflect laterally about 20 inches, which is about the same as the standard guard fence.

#### Crash Test 2

Figure 9 shows modified guard fence No. 2 and car before and after the test. In this test, a 4,500-pound Cadillac Deville impacted modified guard fence No. 2 at 61.8 mph and 23.2 degree angle. At about 0.15 seconds, the rail had deflected about 28 inches, the car was beginning to redirect (yaw about 10 degrees), and the W-beam broke into two. At 0.3 seconds, the car paralleled the guardrail and rode down it about 50 feet before coming to a stop and rolling on its side beside and behind the guardrail.

TABLE 1 SUMMARY OF BARRIER VII COMPUTER PROGRAM ANALYSIS OF MODIFIED METAL BEAM GUARD FENCE DESIGNS

POST SPACING (ft-in.)	POST EMBEDMENT (in.)	POST STATIC LOAD CAPACITY (kips)	MAX. GUARD FENCE DEFLECTION (in.)
6'-3"	38	3.0	20.8
6'-3"	24	1.5	31.0
6'-3"	18	1.0	34.4
3'-1 1/2"	24	1.5	22.0
3'-1 1/2"	18	1.0	25.6

NOTE: 50 ft length of guardrail with 25 ft turn-down terminal on each end. Elastic-plastic post-soil model which yields at 2 in. deflection.  
 $F_{dyn} = F_{static} (1 + JV)$  where  $V$  is ft/sec and  $J = 0.14$  sec/ft.  
 Impact by 4500 lb car at 60 mph and 25° angle.



Before

After

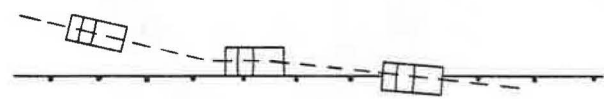
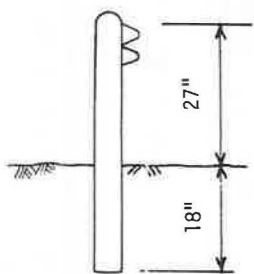
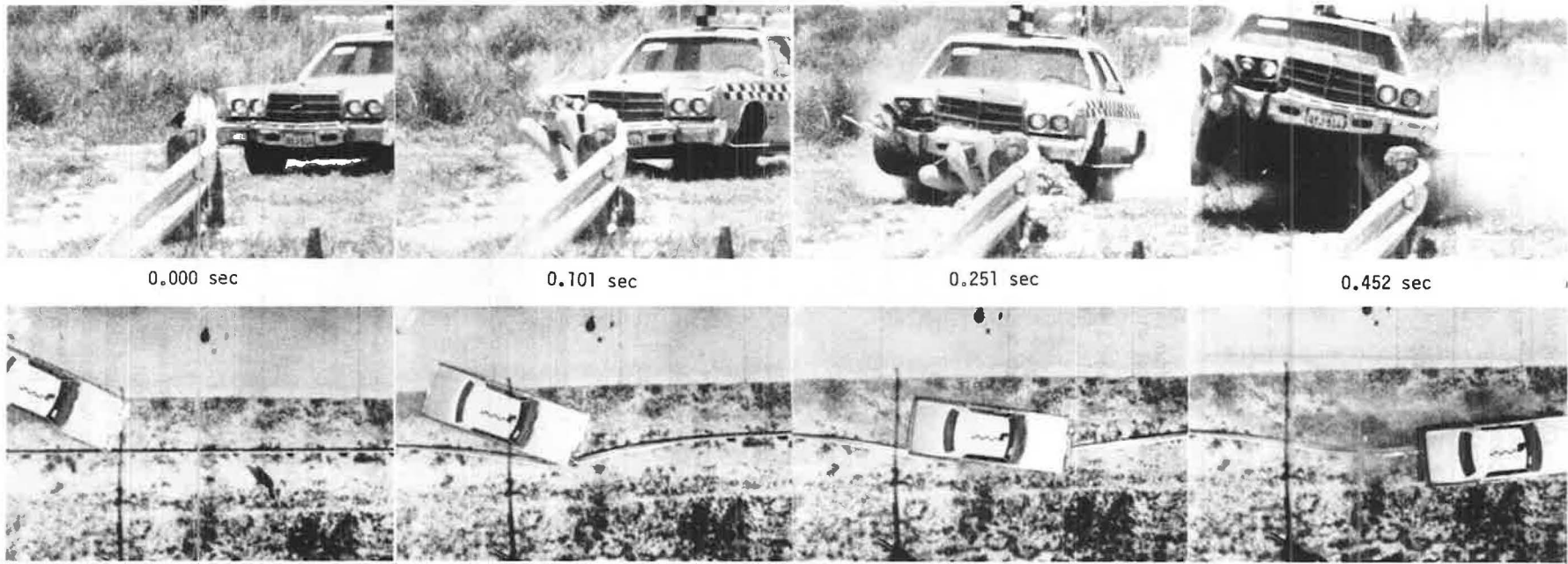


FIGURE 6 Modified guard fence No. 1 and car before and after Crash Test 1.

Tensile tests of coupons from the broken W-beam indicated its yield strength as 80 ksi, ultimate strength as 106 ksi, and ductility of 17 percent. The steel in the W-beam easily satisfied the AASHTO-required yield strength of 50 ksi (minimum), ultimate strength of 70 ksi (minimum), and 12 percent minimum ductility.

Close examination of the timber posts indicated that they

bent over and pulled out of the soil simultaneously. The car's right front tire literally rode up the inclined posts, which were spaced close together, trying to push them down. While this was happening, the car's right front bumper was firmly nestled in the groove of the W-beam and began exerting an upward force on the beam. This combination of forces—downward force from post plus tire, upward force from bumper,



Test No. . . . .	2405-1	Vehicle . . . . .	1977 Chrysler Newport
Date . . . . .	7/22/85	Vehicle Weight . . . . .	1996 kg (4400 lb)
Face Rail . . . . .	12 ga. steel W-shape	(w/instr.)	
Post . . . . .	standard timber	Impact Speed . . . . .	99.4 km/h (61.8 mph)
Post Spacing . . . . .	1.9 m (6 ft 3 in)	Impact Angle . . . . .	26.2 degrees
Length of Installation . . . . .	53.3 m (175 ft)	Exit Speed . . . . .	
Beam Rail Deflection		Exit Angle . . . . .	
Max. Dynamic . . . . .	1.19 m (3.9 ft)	Vehicle Acceleration	
Max. Permanent . . . . .	1.12 m (3.7 ft)	(Max. 0.050 sec. avg.)	
Vehicle Damage		Longitudinal . . . . .	-3.1 g
TAE . . . . .	O1RFQ4	Transverse . . . . .	2.7 g
SAE . . . . .	O1RFEK5	Vertical . . . . .	3.5 g

FIGURE 7 Summary of Crash Test 1.

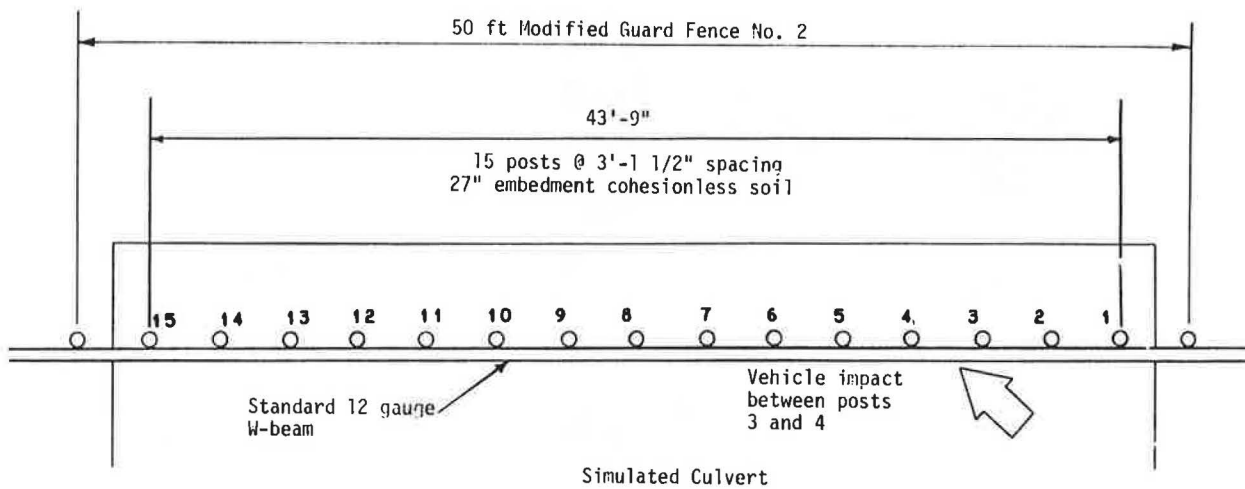


**FIGURE 8** Plan view of modified guard fence No. 2 installation for Crash Test 2.

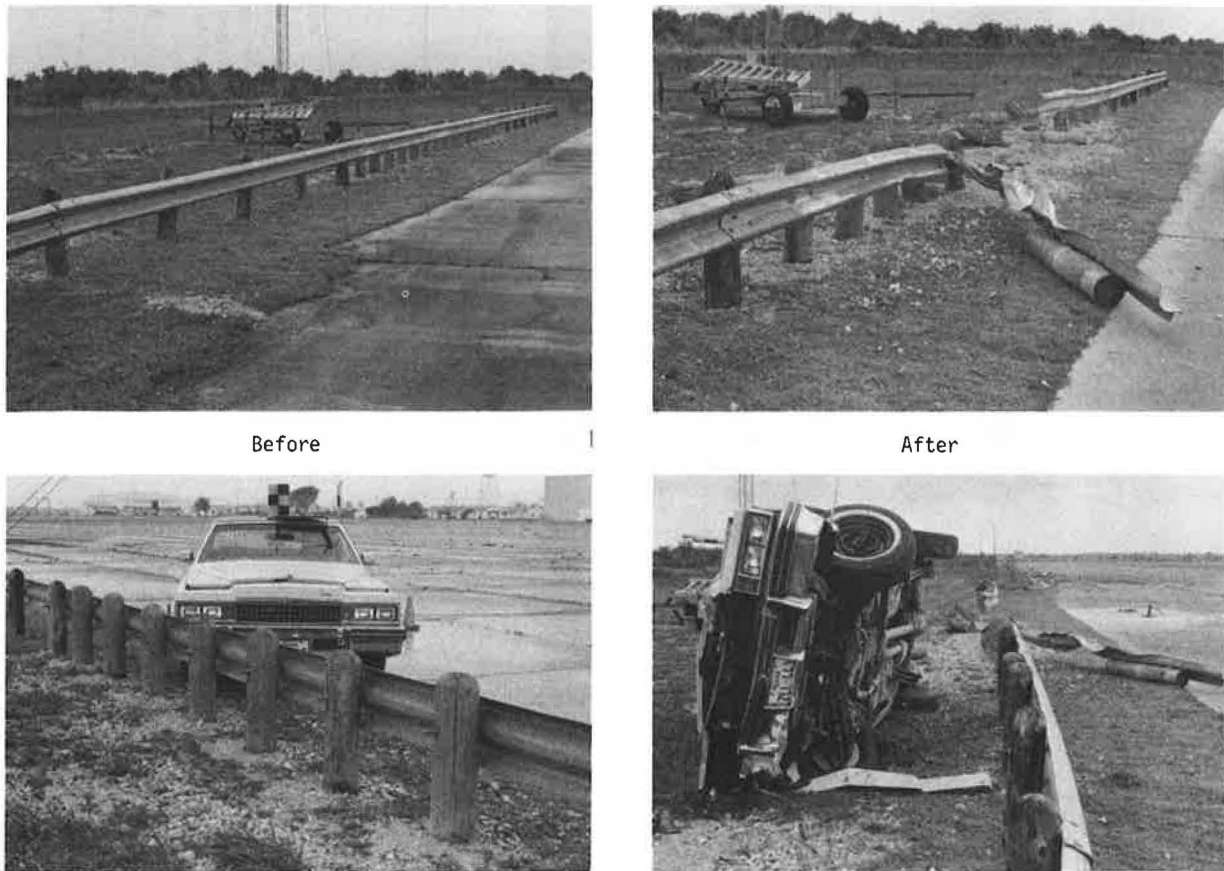


**FIGURE 9** Modified guard fence No. 2 and car before and after Crash Test 2.

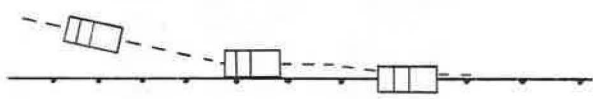
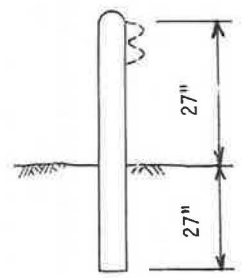
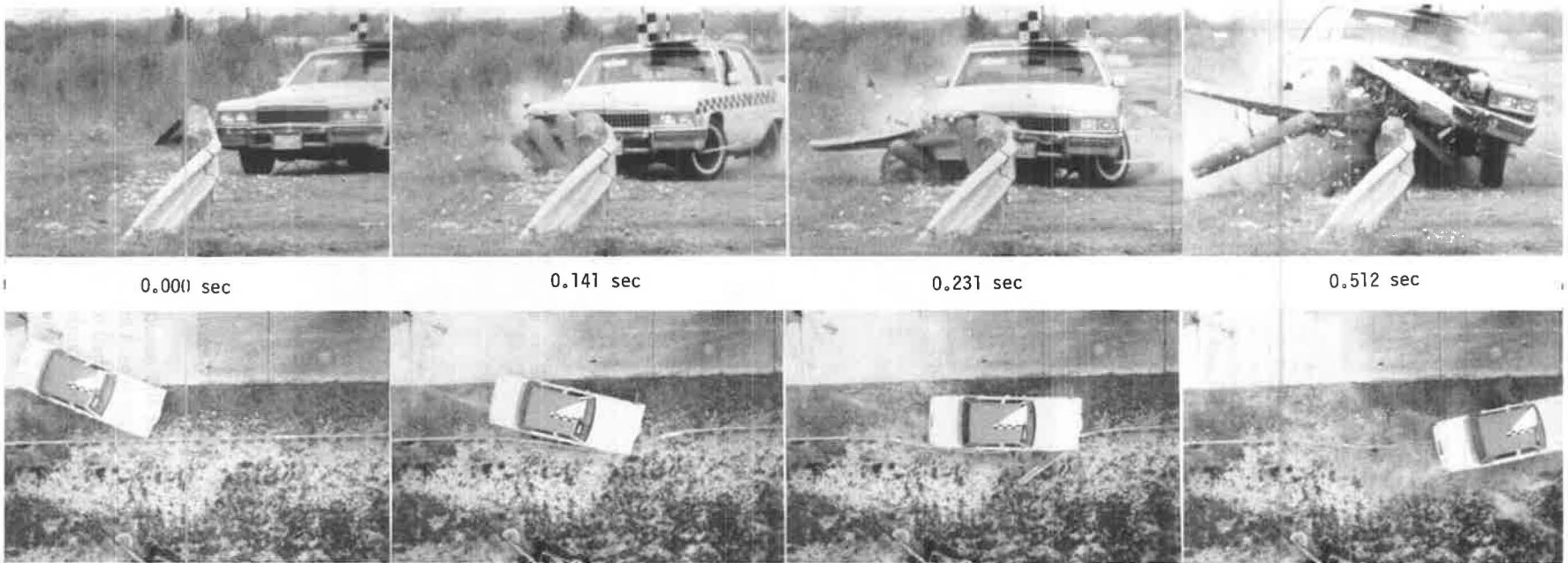
and large tensile redirection force—caused the W-beam to split longitudinally down the center of the W (about a 6.25-foot long split) then break transversely.

Tests 1 and 2 have indicated that guardrail posts need sufficient embedment to develop enough friction to keep them from pulling out of the ground. They also need sufficient embedment to develop the required bending strength or lateral load capacity. Figure 10 summarizes the test data from Crash Test 3.

**Modified Guard Fence No. 3**

After the unsuccessful crash tests on modified guard fence designs Nos. 1 and 2, it was decided that the post would have to be attached to the culvert deck when the soil fill was less than the standard 38 inches. The modified guard fence No. 3 design was as shown by Figures 11 and 12.

The W6 x 9 standard steel guardrail post with blackout was fitted with a steel base plate and bolted to the simulated



Test No. . . . .	2405-2	Vehicle . . . . .	1979 Cadillac DeVille
Date . . . . .	4/18/86	Vehicle Weight . . . . .	2041 kg (4500 lb)
Face Rail . . . . .	12 ga. steel W-shape	(w/instr.)	
Post . . . . .	standard timber	Impact Speed . . . . .	99.6 km/h (61.9 mph)
Post Spacing . . . . .	0.95 m (3 ft 1.5 in)	Impact Angle . . . . .	23.2 deg.
Length of Installation . . . . .	53.3 m (175 ft)	Exit Speed . . . . .	
Beam Rail Deflection		Exit Angle . . . . .	
Max. Dynamic . . . . .	2.56 m (8.4 ft)	Vehicle Acceleration	
Max. Permanent . . . . .	fracture	(Max. 0.050 sec. avg.)	
Vehicle Damage		Longitudinal . . . . .	-5.8 g
TAE . . . . .	O1RFQ4	Transverse . . . . .	5.3 g
SAE . . . . .	O1RFEK4	Vertical . . . . .	5.1 g

FIGURE 10 Summary of Crash Test 2.

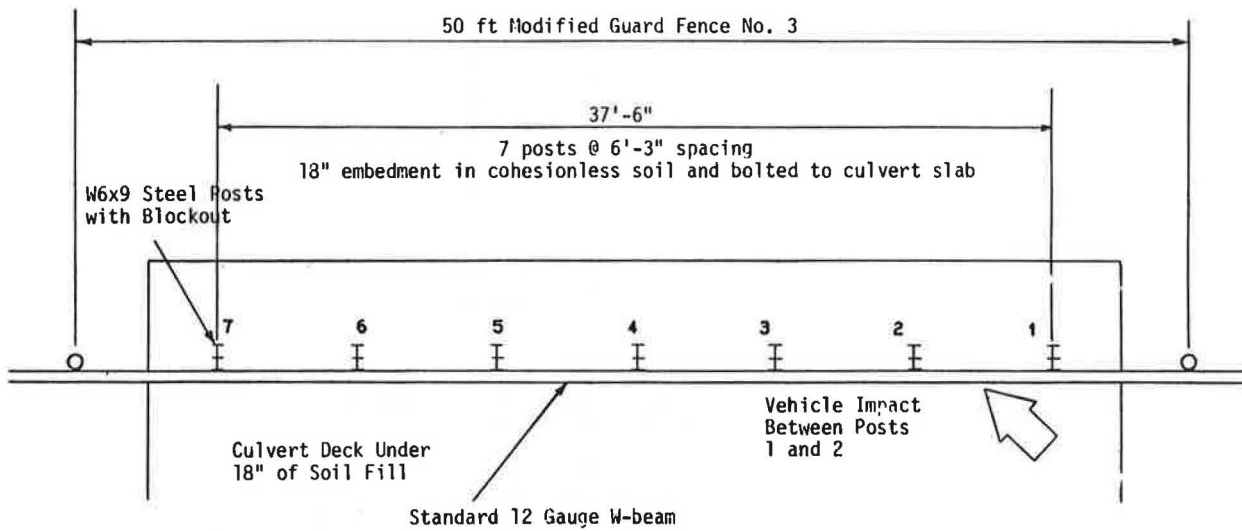


FIGURE 11 Plan view of modified guard fence No. 3 installation for Crash Test 3.

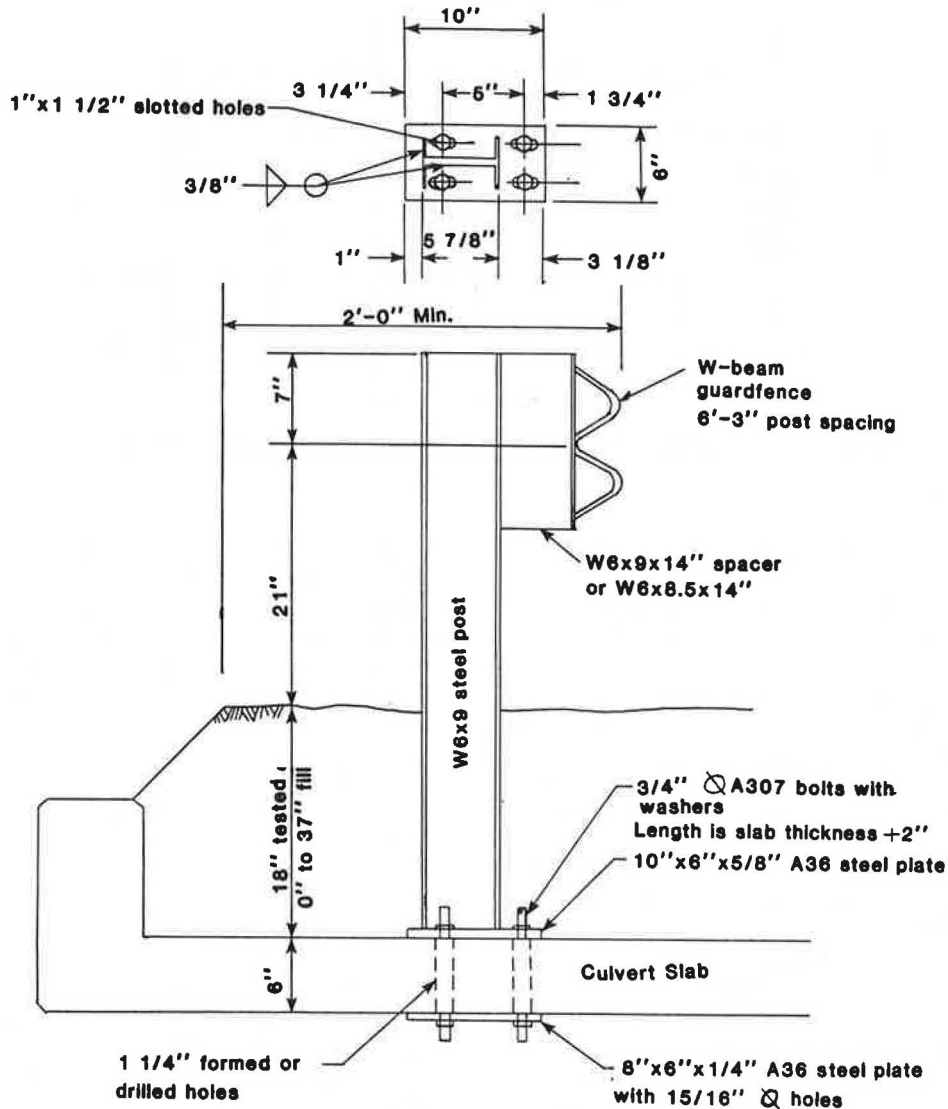
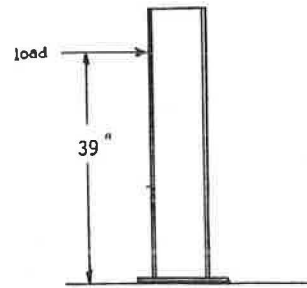


FIGURE 12 Detail of steel guard fence post and attachment to culvert slab.





Note: W6x9 steel post  
 No failure or bending of baseplates or bolts.  
 Failure due entirely to bending in post.

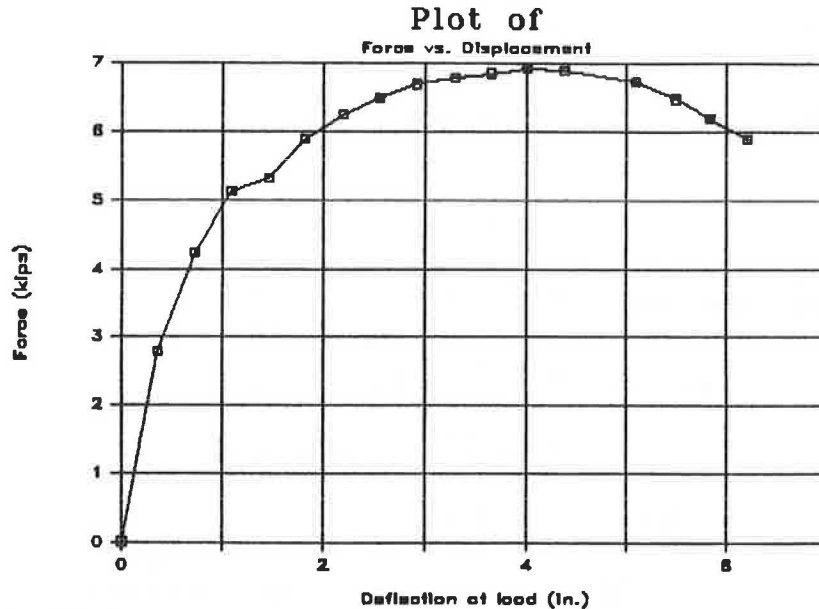


FIGURE 13 Static load test results for guard fence post used in Crash Test 3.

culvert slab as shown by Figure 12. The 6-inch thick culvert slab was reinforced as a typical Texas culvert slab. The centers of the posts were located 30 inches from the outer edge of the culvert. This design should not crack the culvert slab. Static load test results of this post (without soil fill) is shown by Figure 13. Yielding then local buckling of the compression flange caused failure. Damaged posts could be replaced relatively easily by bolting on a new post.

Figure 14 presents the results of an analysis of how the guard fence post load capacity would change with different soil fill depths. The 18-inch fill depth was chosen for this test because the load capacity is low (about 7.8 kips) and the probability of the car tire snagging a post is highest with low fill depths. At 37 inches, the post plus soil strength will be about 8 kips static load. *The Effects of Embedment Depth, Soil Properties, and Post Type on the Performance of Highway Guardrail Posts* (2) showed the dynamic load factor of such posts in soil is about 4 when impacted at 15 to 20 mph. This means the dynamic strength of this post is about 32 kips. At a 4-inch embedment, the strength of this post is about 14 kips static load. *The Effects of Embedment Depth, Soil Properties, and Post Type on the Performance of Highway Guardrail Posts*

(5) showed that the dynamic load factor of such steel posts alone is about 2. This means the dynamic strength of such posts with little to no soil embedment is about 28 kips. Therefore, the impact strengths of these posts at various soil embedment depths are close to each other (28 kips to 32 kips).

A typical guardrail post has a static strength of about 5.5 kips and a dynamic load factor of 4.5 (2). Therefore, the guardrail's dynamic impact strength is 5.5 kips times 4.5, or about 25 kips. Since all these posts have similar impact strength (25 to 32 kips) and deformation characteristics (deflect a foot or more), there should be no transition problems.

#### Crash Test 3

Figure 15 shows the modified guard fence No. 3 and car before and after Crash Test 3. The 4,450-pound Cadillac Deville impacted the guard fence at 61.8 mph and 25.3 degree angle. The car was smoothly redirected as intended. The maximum rail deflection was 2.7 feet, and four posts were severely damaged. This flexible behavior is almost identical to that of the guardrail, indicating there should be no transition problem.

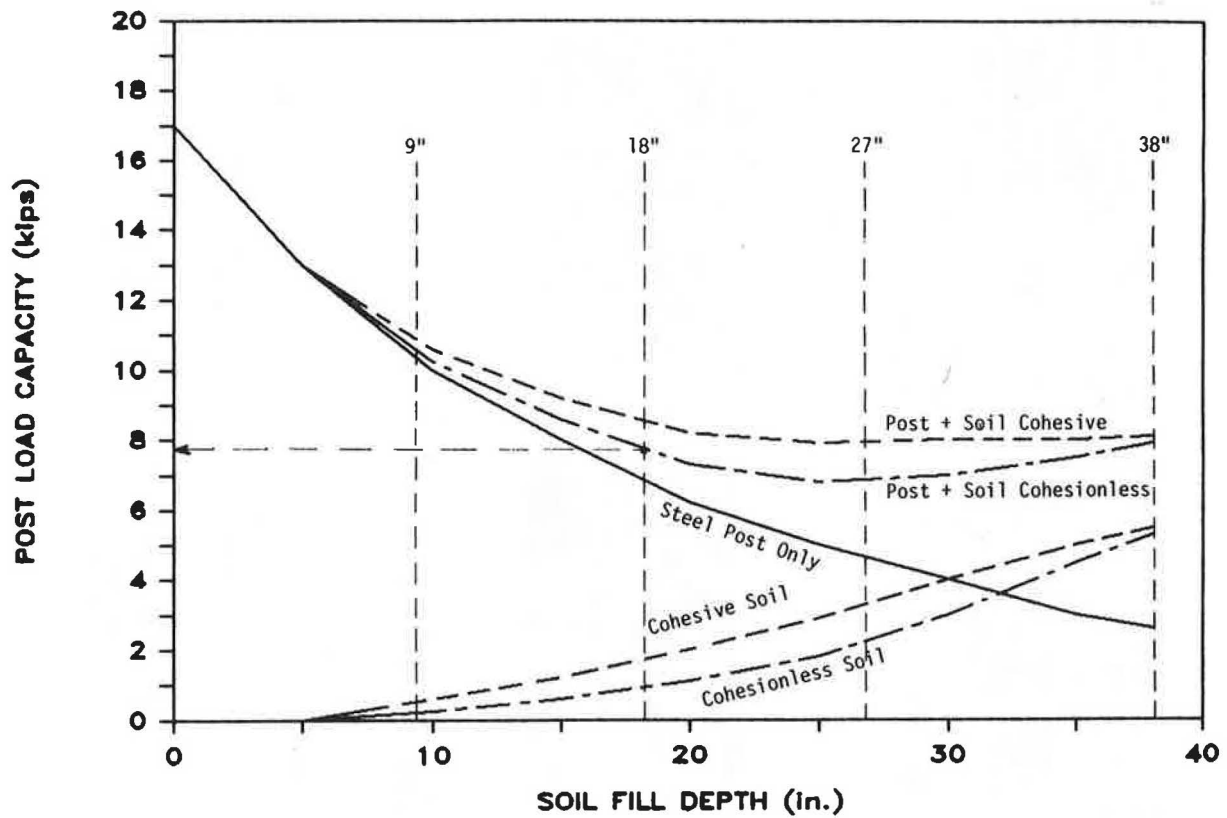


FIGURE 14 Analysis of guard fence post load capacity for various soil fill depths.



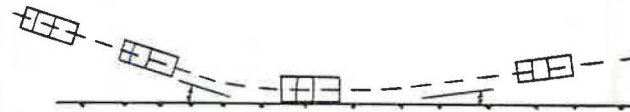
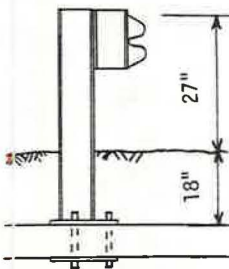
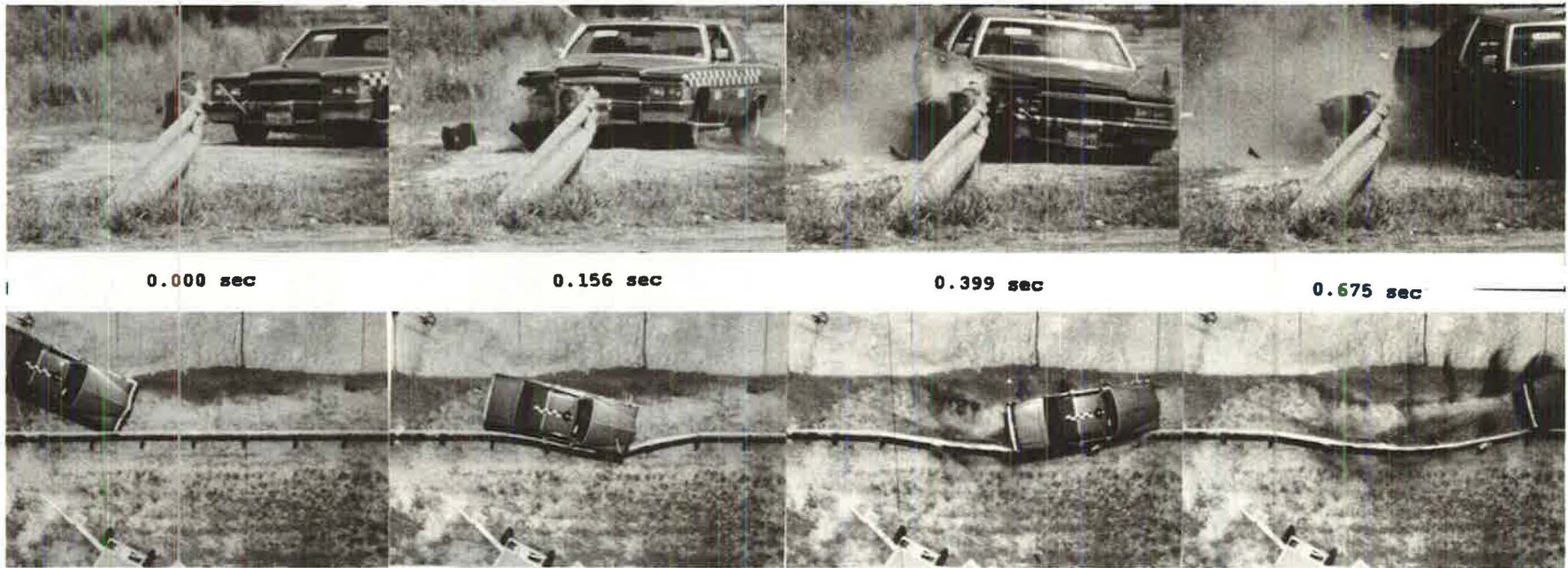
Before



After



FIGURE 15 Modified guard fence No. 3 and car before and after Crash Test 3.



Test No.	2405-3	Vehicle	1978 Cadillac DeVille
Date	7/8/86	Vehicle Weight	2019 kg (4450 lb)
Face Rail	12 ga. steel W-shape	(w/instr.)	
Post	W6x9	Impact Speed	99.4 km/h (61.8 mph)
Post Spacing	1.9 m (6 ft 3 in)	Impact Angle	25.3 deg.
Length of Installation	53.3 m (175ft)	Exit Speed	59.9 km/h (37.2 mph)
Beam Rail Deflection		Exit Angle	15.6 deg.
Max. Dynamic	0.82 m (2.7 ft)	Vehicle Acceleration	
Max. Permanent	0.67 m (2.2 ft)	(Max. 0.050 sec. avg.)	
Vehicle Damage		Longitudinal	-2.78 g
TAE	01RFQ4	Transverse	4.59 g
SAE	01RFES35	Vertical	-3.43 g

FIGURE 16 Summary of Crash Test 3.

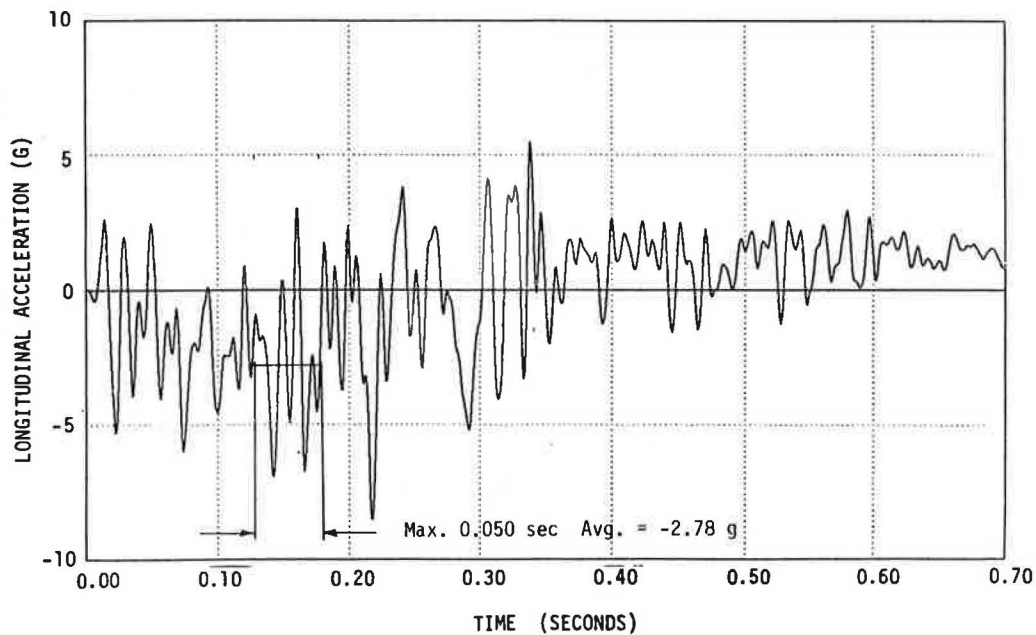


FIGURE 17 Vehicle longitudinal accelerometer trace for Test 2405-3.

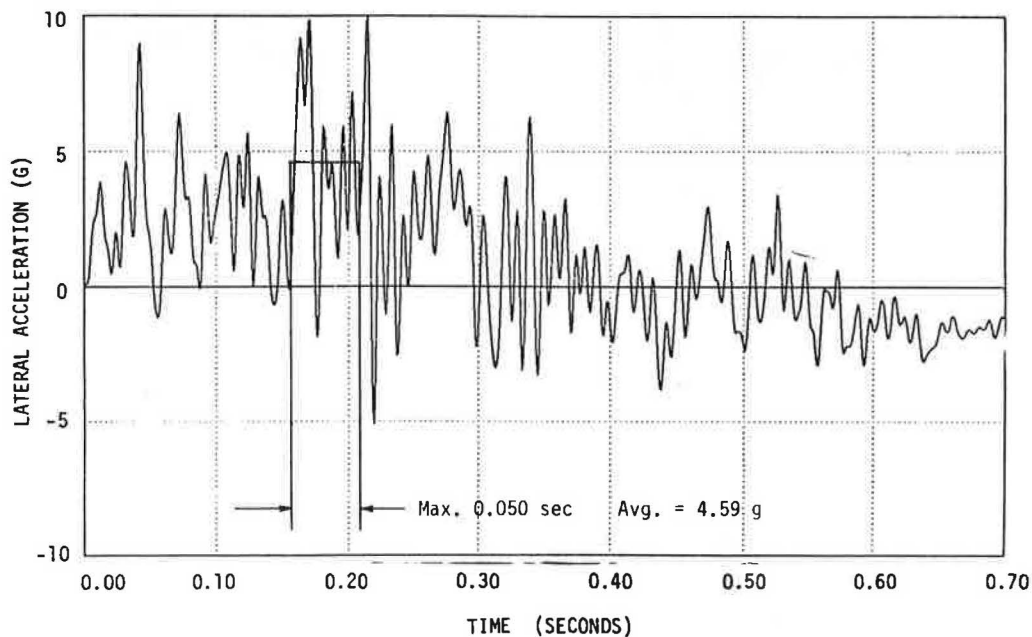


FIGURE 18 Vehicle lateral accelerometer trace for Test 2405-3.

Figure 16 summarizes the test data for Test 3. Presented in Figures 17–20 are the accelerometer and other electronic data from this successful crash test.

This test and modified guard fence No. 3 was very successful. With this design, the guard fence can now be used over culverts even when full embedment depth of the guard-rail post cannot be achieved.

#### SUMMARY AND CONCLUSIONS

The culvert-mounted modified guard fence No. 3 design should meet all crash test performance requirements. Its

strength and geometry are essentially identical to that of the typical 27-inch-high guardrail used widely. Figure 14 shows that the strength of these modified guardrail posts will be relatively constant over a wide range of soil embedment depths. The new guard fence smoothly redirected a 2,019 kg (4,450 pounds) vehicle traveling 99.4 km/hr (61.8 mph) and impacting the rail at an angle of 25.3 degrees. This guard fence system does not have the transition problem that the presently required rigid system does because it is flexible along its entire length as is the standard Texas guard fence on each end.

This new guard fence system is also cheaper than using more rigid bridge rails. The new system has an approximate

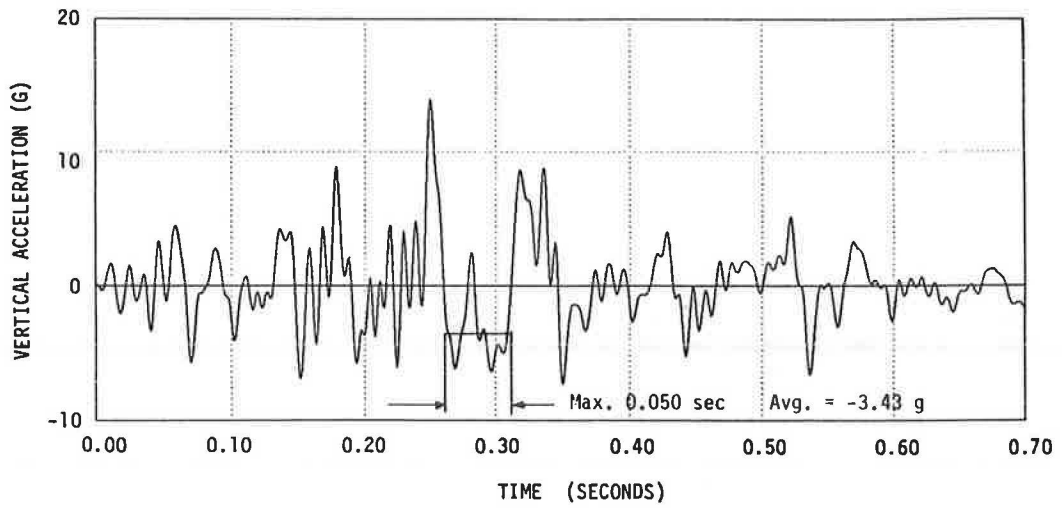
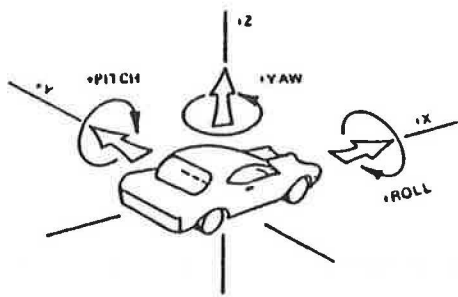


FIGURE 19 Vehicle vertical accelerometer trace for Test 2405-3.



Axes are vehicle fixed.  
 Sequence for determining orientation is:  
 1. Yaw  
 2. Pitch  
 3. Roll

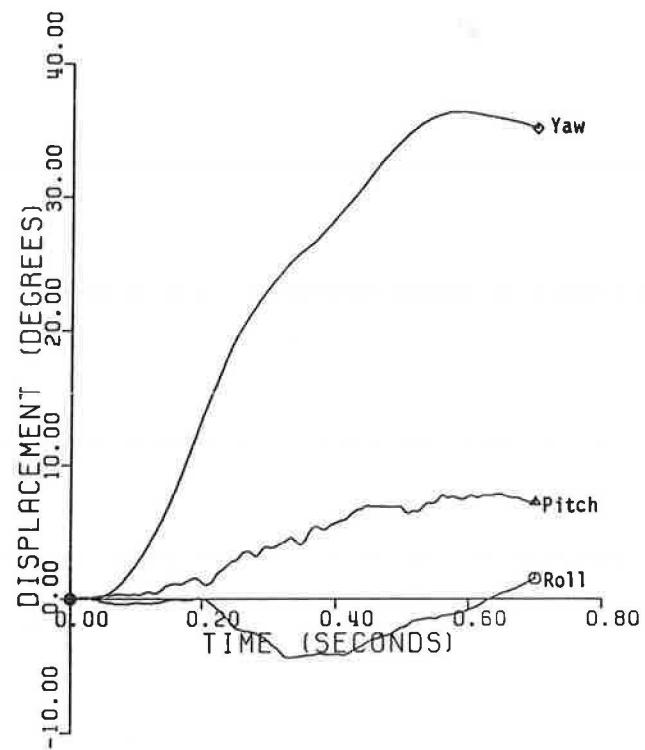


FIGURE 20 Vehicle angular displacements for Test 2405-3.

installation cost of \$17 per foot as opposed to the \$35 per foot cost of typical TI01 steel bridgerail.

#### ACKNOWLEDGMENTS

This research study was conducted under a cooperative program between the Texas Transportation Institute, the Texas State Department of Highways and Public Transportation (SDHPT), and the Federal Highway Administration. John J. Panak (Bridge Design Engineer, SDHPT) and Harold Cooner (Engineer of Geometric Design, SDHPT) were closely involved in all phases of this study.

#### REFERENCES

1. *Standard Specifications for Highway Bridges*, Thirteenth ed., American Association of State Highway and Transportation Officials, Washington, D.C., 1983.
2. D. W. Eggers and T. J. Hirsch. *The Effects of Embedment Depth, Soil Properties, and Post Type on the Performance of Highway Guardrail Posts*. Research Report 405-1, Texas Transportation Institute, Texas A&M University, College Station, Tex., Aug. 1986.
3. Jarvis D. Michie. *NCHRP Report 230: Recommended Procedures for the Safety Performance Evaluation of Highway Appurtenances*. TRB, National Research Council, Washington, D.C., March 1981.
4. J. F. Dewey, J. K. Jeyapalan, T. J. Hirsch, and H. E. Ross. *A Study of the Soil-Structure Interaction Behavior of Highway Guardrail Post*. Research Report No. 343-1, Texas Transportation Institute, Texas A&M University, College Station, Tex., July 1983.
5. Althea Arnold and T. J. Hirsch. *Bridge Deck Designs for Railing Impacts*. Research Report 295-1F, Texas Transportation Institute, Texas A&M University, College Station, Tex., Nov. 1983.

---

*The contents of this report reflect the views of the authors, who are responsible for the opinions, findings, and conclusions presented herein. The contents do not necessarily reflect the official views or policies of the Federal Highway Administration. This report does not constitute a standard, specification, or regulation.*

# Impact Attenuators: A Current Engineering Evaluation

JOHN HINCH, DOUGLAS SAWYER, DALE STOUT, MARTIN HARGRAVE, AND  
RAYMOND OWINGS

This study, sponsored by the Federal Highway Administration (FHWA) and conducted by ENSCO, Inc., used full-scale crash testing of small and large test vehicles to investigate the impact performance of inertial barrel and energy absorbing impact attenuator systems. Special emphasis was placed on impact performance of minicompact sedans. In all, 20 tests were performed: 16 with inertial barrels and 4 with an energy absorbing system. The 16 inertial barrel tests studied the effects of the following crash scenarios: large car versus small car, angled versus head-on positions, pea gravel versus sand fill material, frozen versus nonfrozen sand fill, loose sand versus bagged sand and two different brands of attenuator barrels. The four energy absorbing system tests used a six-bay Guard Rail Energy Absorption Terminal (GREAT) system and studied the effects of head-on versus angled positions and large car versus small car impacts. All tests used instrumented dummies and all tests generated a National Highway Traffic Safety Administration (NHTSA) digital data tape. Results of the program showed large and small car performance to be generally acceptable when using NCHRP 230 and dummy analysis procedures. In one test (C-04) the large car exhausted the capacity of a six-bay GREAT system.

Past testing and analysis of impact attenuators has been based on vehicles weighing 2,250 pounds (1023 kg) or greater. Because of the recent increase in sales of minicars (1,800 lb, 818 kg, range), this class is becoming a significant portion of the vehicle population. This raises new vehicle collision concerns. The small size and weight of the mini cars reduces the dimensions of the wheel base, track width, and crush space, and lowers the mass moments of inertia when compared to larger cars. These differences affect the behavior of the car in a collision.

To better understand the behavior of mini cars in impact attenuator collisions, a series of 20 full-scale crash tests were studied under a Federal Highway Administration (FHWA) contract entitled "Impact Attenuators—A Current Engineering Evaluation." For comparison, seven of the 20 tests were conducted with large cars. The major objectives of this project were as follows:

- To investigate the dynamics of mini-sized and full-sized vehicles colliding with impact attenuators currently deployed on our nation's highways.

J. Hinch, D. Sawyer, and D. Stout, ENSCO, Inc., 5400 Port Royal Road, Springfield, Va. 22151. M. Hargrave, Federal Highway Administration, U.S. Department of Transportation, Turner-Fairbank Highway Research Center, 6300 Georgetown Pike, McLean, Va. 22101. R. Owings, Rhomicon, 11840 Clara Way, Fairfax Station, Va. 22039.

- To determine the problems associated with frozen sand in inertial type impact attenuators.
- To investigate the performance of inertial type impact attenuators using alternate fill materials and techniques.

Four series of 60 mile per hour (26.8 m/s) tests were conducted using mini-sized and full-sized vehicles and different impact attenuator systems and configurations. The first series consisted of four vehicle tests using the Guard Rail Energy Absorption Terminal (GREAT) impact attenuator system configured at three different angles and positions. The second series consisted of eight vehicle tests colliding into an unfrozen inertial type impact attenuator system. Sand and pea gravel were used as fill material and two attack angle positions were used. Further, two different types of barrels (Fitch and Energite) were used, but never mixed in one array. The third test series consisted of six head-on collision tests into frozen inertial impact attenuators. For these tests, the two different types of barrels were also employed. The fourth test series consisted of two head-on collision tests into Energite III systems filled with bagged sand.

The overall matrix of the 20 full scale tests is shown in Table 1.

## TEST PROCEDURES

The tests conducted under this contract were performed using the guidelines specified in NCHRP Report 230. Test types 50, 52, 53, and 54 were conducted on the two impact attenuator models. Tests 53 and 54 were conducted with 1,800 pound vehicles to explore snagging and abrupt deceleration potential. These test types are described in Table 2.

## TEST APPURTENANCES

Test appurtenances consisted of a six-bay Guard Rail Energy Absorption Terminal (GREAT) system manufactured by Energy Absorption Systems, Inc. (EAS) and a 15-barrel inertial system composed entirely of barrels manufactured by EAS or Roadway Safety Service, Inc. The following sections describe the selection criteria, design, and configuration of the systems.

## GREAT Impact Attenuator Layout

Figure 1 shows the three configurations used to test the GREAT impact attenuator:

TABLE 1 FULL-SCALE CRASH TEST MATRIX

Series No.	Test No.	Fill Material	Condition	Impact Angle	Speed (mi/h)	Impact Point	Vehicle	Attenuator Brand
1	1625-C-01-84	-	-	0°	60	Nose	Honda Civic	EAS GREAT
	1626-C-02-84	-	-	15°	60	1' Offcenter off nose	Honda Civic	EAS GREAT
	1625-C-03-84	-	-	20°	60	Mid-terminal	Honda Civic	EAS GREAT
	1625-C-04-85	-	-	0°	60	Nose	Ford LTD II	EAS GREAT
2	1625-B-01-84	Pea Gravel	Not Frozen	0°	60	Nose	Ford LTD II	Energite III
	1625-B-02-84	Sand	Not Frozen	0°	60	Nose	Honda Civic	Energite III
	1625-B-03-84	Sand	Not Frozen	0°	60	Nose	Mercury Cougar XR7	Energite III
	1625-B-04-85	Sand	Not Frozen	15°	60	Corner of Gore	Honda Civic	Energite III
	1625-B-05-84	Sand	Not Frozen	15°	60	Corner of Gore	Honda Civic	Fitch
	1625-B-06-84	Sand	Not Frozen	0°	60	Offcenter	Honda Civic	Fitch
	1625-B-12-85	Sand	Not Frozen	0°	60	Nose	Honda Civic	Fitch
	1625-B-07-85	Sand	Not Frozen	0°	60	Nose	Mercury Cougar XR7	Fitch
3	1625-B-08-85	Sand	Frozen	0°	60	Nose	Honda Civic	Energite III
	1625-B-09-85	Sand	Frozen	0°	60	Nose	Mercury Cougar XR7	Energite III
	1625-B-10-85	Sand	Frozen	0°	60	Offcenter	Honda Civic	Fitch
	1625-B-13-85	Sand	Frozen	0°	54	Nose	Honda Civic	Fitch
	1625-B-14-85	Sand	Frozen	0°	60	Nose	Honda Civic	Fitch
	1625-B-11-85	Sand	Frozen	0°	60	Nose	Ford LTD II	Fitch
4	1625-E-01-86	Sand	Bagged	0°	60	Nose	Mercury Cougar XR7	Energite III
	1625-E-02-86	Sand	Bagged	0°	60	Nose	Honda Civic	Energite III

TABLE 2 NCHRP REPORT 230 TEST TYPES

No.	Vehicle Size	Speed (mi/h)	Angle (deg)	Location
50	4500 lb	60	0	Center of Nose
52	1800 lb	60	0	Center of Nose
53*	4500 lb	60	20	Along Mid-length
54*	4500 lb	60	15	1 ft Offset from Nose

\*Tests 53 and 54 were conducted with 1800 lb vehicles to explore snagging and abrupt deceleration potential.

- 0° Impact Angle, Vehicle Centered on Nose of Device
- 15° Impact Angle, Vehicle Offset one foot from Center of Nose of Device
- 20° Impact Angle, Vehicle Directed Toward Midpoint of the Side

The GREAT system consists of crushable Hexfoam cartridges surrounded by a framework of triple-corrugated-steel guard-rail. When hit head-on, the cartridges absorb the energy of the impact, while the steel guardrail side panels telescope. Only the cartridges are expended. When hit from the side, the steel side panels are restrained by leg pins and a center guidance cable to redirect the errant vehicle. After these tests were conducted, the Hexfoam cartridges were replaced with Hexfoam II cartridges by EAS.

Discussions were held with EAS to select the appropriate GREAT system, given the vehicle, speed, and position

requirements of the test. The GREAT system selected was a six-bay configuration 2 feet wide and 22 feet long of the "Median Barrier Protection; Bi-Directional Traffic" unit. The six-bay size was selected because it is standard on today's Interstate highway system.

#### Inertial Impact Attenuator Layout

Because of the technical requirements of this test program, all Energite or all Fitch barrels were used for crash testing in the following two configurations:

- 0° Impact Angle, Vehicle Centered on Nose of Attenuator (see figure 2),
- 15° Impact Angle, Vehicle Centered on Corner of Gore (see figure 2).



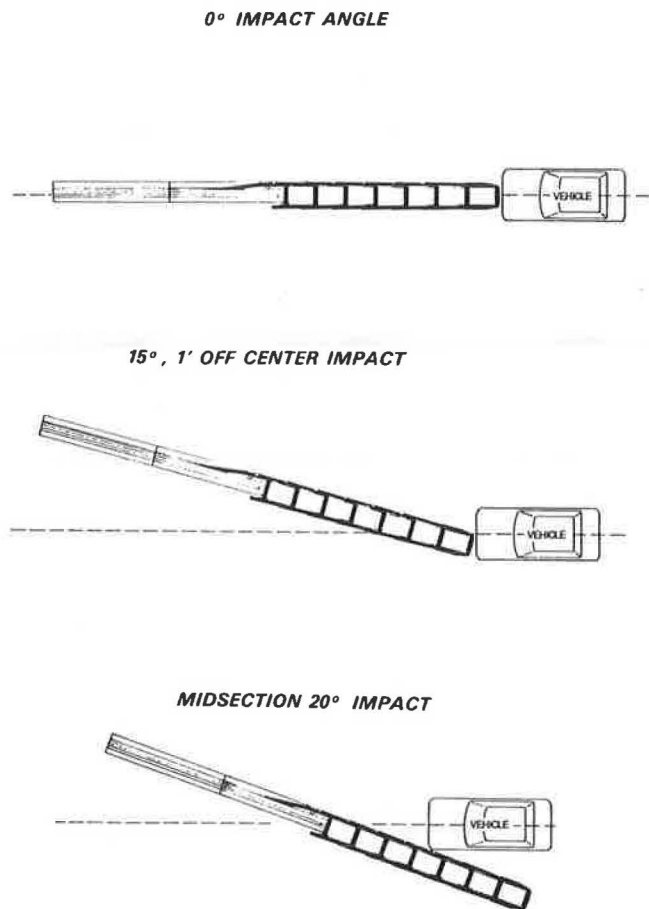


FIGURE 1 Three test configurations for the GREAT system.

Selection of the barrel configuration for the test program was based on the following requirements:

- shielding of a 5-foot wide (1.5 m) gore,
- overlapping barrels 30 inches (0.8 m) on each side of gore,
- using 7 rows of barrels or less to minimize length of installation,
- using 2,100-pound (955 kg) barrels in last row,
- leaving a 6-inch (0.2 m) longitudinal space between barrels,
- composing each test array of all Energite or all Fitch barrels, and
- using the same configuration for all tests.

The method for arriving at the configuration consisted of discussions with EAS personnel, Roadway Safety Service, Inc., personnel, FHWA personnel, and the use of a computer program to predict expected behavior. EAS and Roadway Safety Service personnel agreed on the selection of the configuration used for both the large and small car test. All barrels are approximately 3 feet in diameter and barrel weight layout is depicted in Figure 3. Figures 4 and 5 illustrate the Fitch and Energite III barrel systems.

Drainage tests were performed on Energite II, Energite

III, and Fitch barrels for the 700-pound (318 kg) and 2,100-pound (955 kg) sizes. Figure 6 provides moisture content measurements made for each of the barrel configurations for a period of 61 days.

Overall, the Energite III and Fitch barrels showed similar results when filled with sand for the 700-pound (318 kg) and 2,100-pound (955 kg) sizes with initial moisture content of 17 to 18 percent. When filled with pea gravel the Energite III 2,100-pound (955 kg) barrel drained slightly faster than the Fitch barrel because the Fitch barrel has a plastic liner. However, the moisture content for pea gravel is low enough so that freezing action is not considered important.

The key finding of the drainage test was that the 700-pound (318 kg) Energite II barrel drained much better than either the 700-pound (318 kg) Energite III barrel or the Fitch barrel. This is because of a fundamental difference in design. The Energite II barrel uses whole piece inserts with drainage holes while the Energite III barrel uses sand support cores without drainage holes. Under the sand, the cores of Energite III seal most of the water in the barrel. Thus, very high moisture contents remain. It should be pointed out that, despite the difference in the two barrels with initial moisture contents of 17.7 percent, both Fitch and Energite III barrels filled with sand could still freeze solid after 1 to 2 months of free drainage.

#### TEST VEHICLE

The test vehicles consisted of 1979 Honda Civics corresponding to the NCHRP 230 classification of 1800S and 1979 Ford LTD IIs or Mercury Cougar XR7s corresponding to the NCHRP classification of 4500S. Before testing, the vehicles were prepared by removing the gas tank, battery, and back seat (small car only). After incorporating the instrumentation and ballast necessary to meet the test inertial limits of NCHRP 230, instrumented anthropomorphic dummies (part 572) were installed. The weight limits of the vehicle with occupant(s) prior to test were  $1,950 \pm 50$  pounds ( $886 \pm 23$  kg) for the minicompact sedan and  $4,500 \pm 300$  pounds ( $2,046 \pm 136$  kg) for the large sedan.

#### TEST RESULTS

An overall summary for all tests is provided in Table 3. The table summarizes the test and impact conditions, and test results (using vehicle and dummy analysis).

#### Comparison of Force-Displacement Data

Force-displacement curves for each test were generated and documented in the technical volume of the final report. These curves are derived from the vehicle longitudinal acceleration signal. Force is derived by multiplying the acceleration signal by the mass of vehicle; displacement is derived by double integration of the acceleration signal. The major problem with this approach is that noise (e.g., ringing) in the accelerometer produces large oscillations in the force-time history. To overcome this, the data were subsequently smoothed with a 1.6-foot spacial filter (distance-based as opposed to time-based).



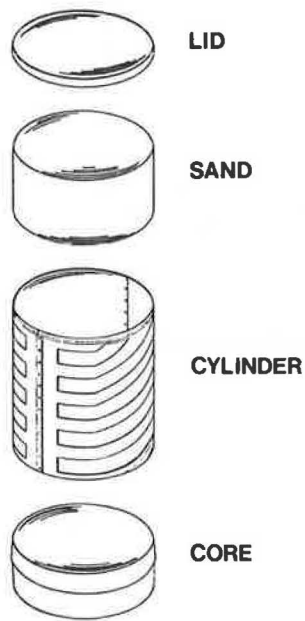


FIGURE 4 Fitch inertial barrier system.

### Comparison of Test Results

Head-to-head comparisons of all test results were performed to explore the effects of the following:

- vehicle weight,
- sand barrel attenuator type,
- attenuator configuration,
- frozen versus nonfrozen test conditions,
- sand versus pea gravel fill material,
- nonbagged versus bagged sand fill material, and
- passenger versus driver response.

Table 4 lists observations from these comparisons. Pass/fail criteria used in this paper are based on the NCHRP 230 design values of 30 feet per second for delta-V and 15 g for ridedown acceleration.

Design values were selected to better discriminate among configurations. The limit values recommended by NCHRP 230 are 40 feet per second for delta-V and 20 g for ridedown acceleration. It should be noted that the limit values were exceeded in only four tests.

### CONCLUSIONS

The following sections provide the key conclusions of this impact attenuator testing project.

#### Barrel Attenuators (Nonfrozen Sand)

The systems tested worked as designed, showing good correlation with design predictions based on momentum transfer. The 15-barrel system selected appears to provide a safe design for stopping vehicles weighing 1,800 to 4,500 pounds (818 kg to 2,045 kg) at distances of 25 feet (7.6 m) or less.

#### Barrel Attenuators (Frozen Sand)

This series of tests demonstrated that sand in barrels can freeze and produce large (400 lb, 182 kg) blocks that remain intact during an impact. These blocks were thrown up to 60 feet during the impact and could lead to additional accidents involving oncoming traffic. Complete freezing of the 15-barrel system was found to require low temperature for a period of several days. The frozen configuration showed reduced performance and safety when compared to nonfrozen tests. Reduced performance and safety resulted because freezing caused the last several rows of barrels to be pushed into the gore wall. These barrels then get squeezed between the impacting vehicle and gore wall. Instead of disintegrating, the barrels rupture. This effectively moves the

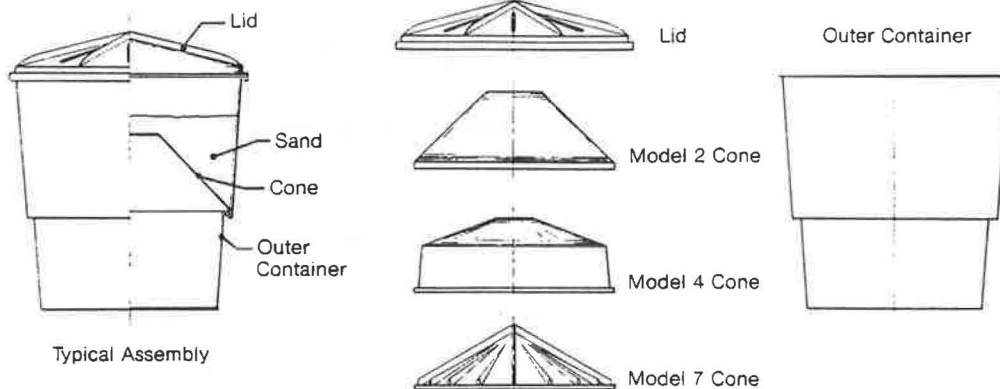
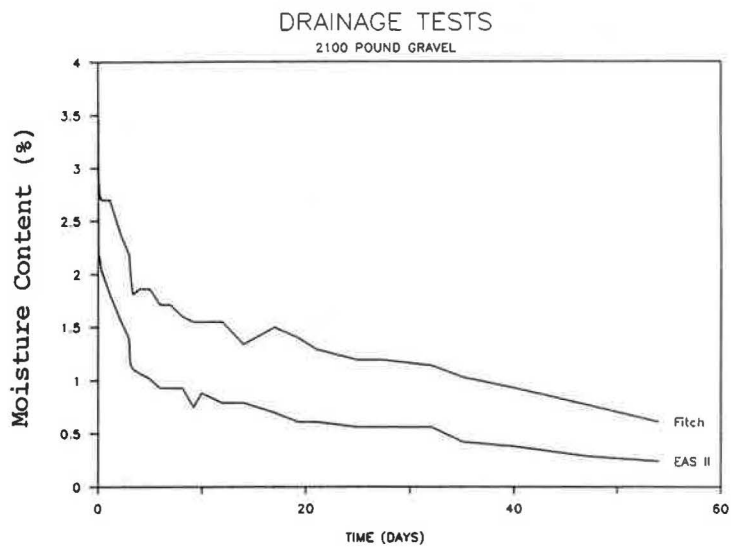
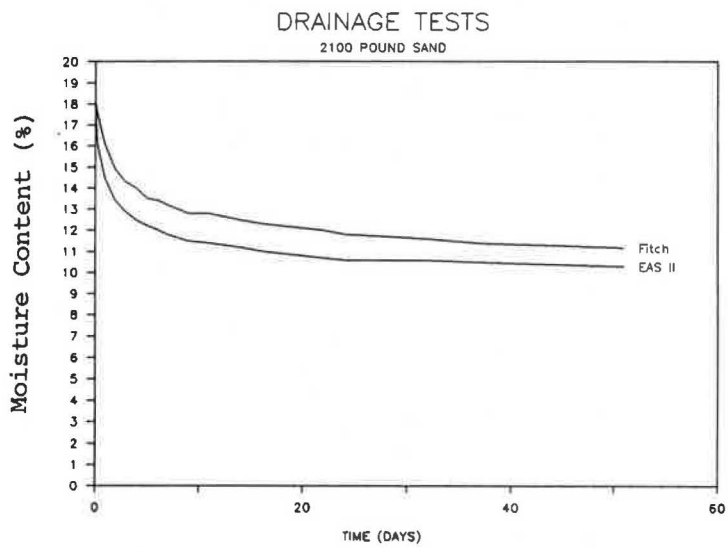
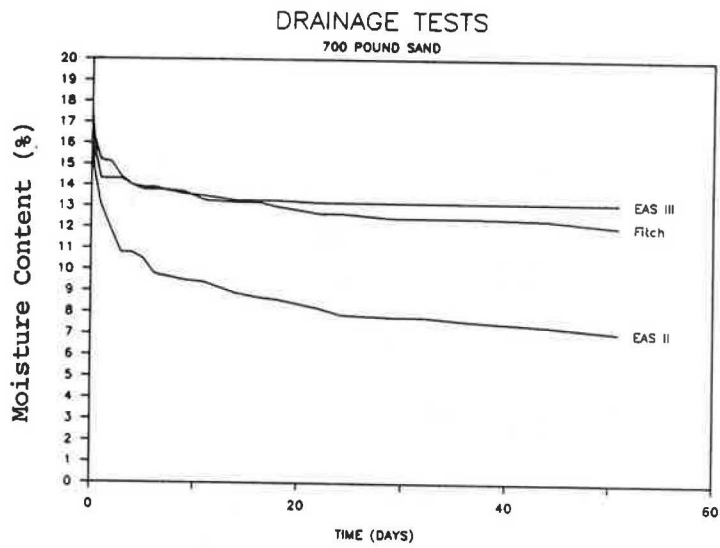


FIGURE 5 Energite barrel system.



**FIGURE 6** Moisture content measurement.

TABLE 3 TEST RESULTS

TEST NUMBER DATE	C-01 5/24/84	C-02 6/13/84	C-03 6/27/84	C-04 7/23/85	B-08 4/10/85	B-09 5/21/85	B-10 2/18/85	B-11 6/18/85	B-13 7/12/85	B-14 11/19/85
MANUFACTURER ATTENUATOR FILL MATERIAL	EAS GREAT HEXFOAM	EAS GREAT HEXFOAM	EAS GREAT HEXFOAM	EAS GREAT HEXFOAM	EAS EA III FROZEN SAND	EAS EA III FROZEN SAND	RSS FITCH FROZEN SAND	RSS FITCH FROZEN SAND	RSS FITCH FROZEN SAND	RSS FITCH FROZEN SAND
VEHICLE WEIGHT (lbs)	1794	1812	1795	4346	1798	4323	1792	4336	1795	1806
IMPACT ANGLE (deg)	0	15	20	0	0	0	7.5	0	0	0
IMPACT SPEED (mi/h)	59.9	59.5	59.7	58.4	60.4	60.9	59.4	58.8	54.6	60.8
IMPACT LOCATION	CENTER	NOSE RIGHT CORNER	MIDSPAN	CENTER	CENTER	CENTER	2.5FT RIGHT CENTER	CENTER	CENTER	CENTER
NUMBER OF DUMMIES	1	1	1	2	1	2	1	2	1	1
DUMMY WEIGHT (lbs)	155	160	155	374	146	326	158	334	154	167
TOTAL WEIGHT (lbs)	1949	1972	1950	4720	1944	4649	1950	4670	1949	1973
TOTAL KINETIC ENERGY (kip-ft)	234	233	232	538	237	576	230	539	194	244
ATTEN CRUSH ENERGY (kip-ft)	195.9	199.7	---	465.9	223.1	494.1	---	517.4	180.7	228.8
VEHICLE CRUSH ENERGY (kip-ft)	20.1	16.4	---	61.7	9.9	71.5	---	45.1	5.8	4.6
REBOUND DISTANCE (ft)	40.8	37.5	---	11.7	0.5	0.3	---	0.5	0.8	0.8
TOTAL SPEED CHANGE (ft/s)	98.0	96.7	16.1	105.2	91.4	89.8	101.0	92.1	78.2	95.1
STOPPING DISTANCE (ft)	14.7	11.8	---	18.4	17.2	22.5	25.0	22.3	16.2	16.2
AVG ACCEL OVER STOP (g's)	-8.2	-10.0	---	-6.2	-7.1	-5.5	-4.7	-5.2	-6.1	-7.6
50 MSEC PEAK (g's)	-12.3	-13.0	---	-24.1	-16.0	-14.8	-11.7	-12.1	-9.7	-14.0
DELTA V @2 FT FLAIL (ft/s)	34.7	38.5	19.7	27.0	28.3	27.7	25.8	31.1	27.9	34.8
TIME (msec)	166	119	183	155	130	160	143	162	145	125
ACTUAL FLAIL SPACE (ft)	1.35	1.92	2.05	2.08	1.75	1.75	2.0	1.83	1.58	1.67
DELTA V @ ACTUAL FLAIL (ft/s)	31.2	37.9	19.8	27.3	26.1	25.6	25.8	29.7	23.6	30.3
RIDEDOWN ACCEL (g's)	-12.7	-11.0	-0.8	-42.3	-22.3	-25.9	-16.7	-16.3	-12.1	-18.7
CLASS 60 DATA										
LONGITUDINAL (g's)	-18.3	-17.5	-9.5	-51.2	-24.0	-25.2	-17.4	-19.6	-15.8	-19.5
TIME (msec)	62	70	144	319	180	183	269	124	18	220
LATERAL (g's)	-4.4	-7.0	-17.1	17.7	-7.4	4.3	-9.3	-21.3	-7.2	-8.9
TIME (msec)	79	70	74	321	169	215	28	242	109	100
VERTICAL (g's)	-14.6	-4.6	-9.4	-25.8	-17.2	11.1	-14.7	18.5	20.6	-20.6
TIME (msec)	70	23	149	311	19	210	247	126	105	85
ROLL RATE (deg/s)	---	-142.5	-132.0	-496.6	206.9	122.3	261.4	-283.8	236.0	-334.3
TIME (msec)	---	145	187	65	87	173	149	143	118	120
YAW RATE (deg/s)	---	-82.8	-301.0	-255.0	88.4	59.8	---	258.5	179.4	-204.5
TIME (msec)	---	182	148	323	228	168	---	242	113	96
CLASS 180 DATA										
LONGITUDINAL (g's)	-21.6	-22.5	-12.0	-84.7	-25.9	-27.3	-17.9	-25.8	-23.0	-22.7
TIME (msec)	53	70	135	321	180	181	269	125	18	17
LATERAL (g's)	-10.3	-10.0	-25.5	25.8	-14.0	-9.5	-15.8	-40.9	-11.0	15.7
TIME (msec)	35	68	74	321	25	171	26	242	109	56
VERTICAL (g's)	-20.1	-10.5	-12.4	-29.5	-26.6	17.2	-17.7	-28.3	-24.6	-29.2
TIME (msec)	28	84	157	313	21	184	246	241	15	85
DRIVER R or U?	U	U	U	U	U	U	U	U	U	U
HIC	404	482	500	293	225	89	110	214	129	240
CSI	277	224	164	286	300	83	81	164	82	297
MAX CHEST (g's)	43.9	41.9	53.2	35.7	39.0	20.7	18.7	24.3	22.8	37.1
RIGHT FEMUR (lbs)	987	712	534	795	1365	141	1040	863	832	2650
LEFT FEMUR (lbs)	---	---	---	957	692	199	1635	537	524	404
PASSENGER R or U?				R		R		R		
HIC				260		---		95		
CSI				174		---		88		
MAX CHEST (g's)				30.0		---		18.4		
RIGHT FEMUR (lbs)				280		---		889		
LEFT FEMUR (lbs)				100		---		317		

TABLE 3 continued

TEST NUMBER	B-01	B-02	B-03	B-04	B-05	B-06	B-07	B-12	E-01	E-02
DATE	9/21/84	10/9/84	10/15/84	1/10/85	11/29/84	11/8/84	4/16/85	5/9/85	5/23/86	5/5/86
MANUFACTURER	EAS	EAS	EAS	EAS	RSS	RSS	RSS	RSS	EAS	EAS
ATTENUATOR	EA III	EA III	EA III	EA III	FITCH	FITCH	FITCH	FITCH	EA III	EA III
FILL MATERIAL	PEA GRAVEL	SAND	SAND	SAND	SAND	SAND	SAND	SAND	BAGGED SAND	BAGGED SAND
VEHICLE WEIGHT (lbs)	4312	1807	4306	1806	1823	1797	4317	1806	4302	1799
IMPACT ANGLE (deg)	0	0	0	15	15	0	0	0	0	0
IMPACT SPEED (mi/h)	58.8	58.0	58.6	59.4	60.0	58.4	60.6	60.1	57.7	61.1
IMPACT LOCATION	CENTER	CENTER	CENTER	CORNER OF GORE	CORNER OF GORE	5.7FT RIGHT CENTER	CENTER	CENTER	CENTER	CENTER
NUMBER OF DUMMIES	2	1	2	1	1	2	1	2	1	
DUMMY WEIGHT (lbs)	309	168	326	150	154	166	352	164	322	169
TOTAL WEIGHT (lbs)	4621	1975	4632	1956	1977	1963	4669	1970	4624	1968
TOTAL KINETIC ENERGY (kip-ft)	534	222	531	231	238	224	573	238	514	245
ATTEN CRUSH ENERGY (kip-ft)	508.7	217.4	530.0	---	---	---	525.6	221.7	475.0	225.8
VEHICLE CRUSH ENERGY (kip-ft)	11.3	5.6	12.0	---	---	---	34.5	5.9	21.1	9.1
REBOUND DISTANCE (ft)	2.0	0.5	1.0	14.0	14.0	---	1.0	1.1	2.4	0.2
TOTAL SPEED CHANGE (ft/s)	89.6	84.8	91.9	85.9	87.5	44.0	96.0	91.3	89.8	87.0
STOPPING DISTANCE (ft)	23.5	22.0	24.5	11.4	11.4	72.0	24.0	19.3	22.9	19.0
AVG ACCEL OVER STOP (g's)	-4.9	-5.1	-4.7	-10.3	-10.5	-1.6	-5.1	-6.3	-4.9	-6.6
50 MSEC PEAK (g's)	-11.2	-10.1	-11.2	-15.3	-14.3	-9.3	-9.8	-9.3	-10.9	-15.7
DELTA V @ 2 FT FLAIL (ft/s)	24.5	26.8	26.3	38.0	37.4	29.2	26.6	29.3	27.9	29.7
TIME (msec)	183	139	171	104	111	130	170	132	178	144
ACTUAL FLAIL SPACE (ft)	1.71	1.5	1.33	1.63	1.92	1.5	1.58	1.94	1.58	1.71
DELTA V @ ACTUAL FLAIL (ft/s)	22.1	24.6	24.5	37.2	36.0	25.8	24.2	29.0	22.4	26.4
RIDEDOWN ACCEL (g's)	-15.4	-18.4	-13.7	-19.2	-18.5	-15.4	-10.7	-10.2	-14.9	-22.3
CLASS 60 DATA										
LONGITUDINAL (g's)	-17.1	-21.4	-16.4	-19.9	-19.3	-20.8	-11.2	-18.5	-18.3	-24.7
TIME (msec)	243	173	242	127	112	139	214	28	263	157
LATERAL (g's)	-4.9	-2.6	-5.2	-10.0	-7.6	-8.6	3.8	4.3	-5.2	-5.2
TIME (msec)	212	183	226	28	27	31	151	3	265	165
VERTICAL (g's)	18.7	-13.0	11.7	-12.6	-10.1	9.2	6.1	-12.0	17.7	-12.5
TIME (msec)	256	37	244	49	27	89	219	23	279	24
ROLL RATE (deg/s)	118.4	68.9	-115.5	-143.0	154.7	---	77.2	-126.2	-260.0	110.2
TIME (msec)	252	141	362	130	94	---	138	80	265	190
YAW RATE (deg/s)	58.6	-28.6	44.3	---	282.5	---	41.8	50.8	-121.6	-73.9
TIME (msec)	259	265	128	---	334	---	134	61	263	185
CLASS 180 DATA										
LONGITUDINAL (g's)	-26.0	-25.3	-17.8	-21.0	-21.4	-28.2	-12.4	-25.2	-27	-26.6
TIME (msec)	255	173	242	70	112	139	201	18	263	157
LATERAL (g's)	-12.1	-5.9	-9.4	-13.9	-12.4	-11.0	8.6	11.5	-16.9	-7.7
TIME (msec)	254	173	109	29	20	173	151	3	265	165
VERTICAL (g's)	27.7	-16.2	14.6	-17.9	-12.9	13.7	-7.4	22.8	-30.8	-18.5
TIME (msec)	255	37	251	49	29	140	206	28	260	24
DRIVER R or U?	U	U	U	U	U	U	U	U	U	U
HIC	265	117	159	517	457	679	144	389	78	758
CSI	329	---	190	391	392	137	156	153	98	226
MAX CHEST (g's)	81.9	---	28.0	44.2	39.8	40.8	26.9	31.9	24.9	42.0
RIGHT FEMUR (lbs)	620	1200	959	1969	874	930	---	1813	650	841
LEFT FEMUR (lbs)	625	406	551	---	1173	800	343	351	540	500
PASSENGER R or U?	U		U				U		U	
HIC	314		424				274		299	
CSI	218		154				153		156	
MAX CHEST (g's)	47.7		28.0				32.0		27.4	
RIGHT FEMUR (lbs)	738		904				1101		720	
LEFT FEMUR (lbs)	525		544				449		500	

TABLE 4 TEST RESULTS COMPARISONS

Comparisons	Conditions	Results/Observations
Pea Gravel vs. Sand Fill	Energite/4500S/0°	No differences were observed using vehicle data. Some differences were observed in the dummy parameters.
Fitch vs. Energite	4500S/0°	Similar results
Fitch vs. Energite	1800S/15°	Similar results
Fitch vs. Energite	1800S/0°	Delta-V higher for Fitch, ridedown higher for Energite. Results were similar for dummy parameters. Energite failed ridedown.
Frozen vs. Non-Frozen	Energite/1800S/0°	Frozen test more severe. Both tests failed ridedown criteria.
Frozen vs. Non-Frozen	Fitch/1800S/0°	Frozen test more severe. Frozen test failed delta-V and ridedown.
GREAT vs. Sand	1800S/0°/Energite	GREAT test more severe for vehicle parameters. Dummy parameters show no significant difference. Stopping distance shows GREAT has a higher efficiency. GREAT failed delta-V and Energite III failed ridedown.
Head-on vs. 15°	GREAT/1800S	Similar results. Both tests failed delta-V.
Head-on vs. 20° (Redirectional)	GREAT/1800S	High maximum chest values for both; otherwise results were similar. Head-on failed delta-V.

TABLE 4 *continued*

<u>Comparisons</u>	<u>Conditions</u>	<u>Results/Observations</u>
4500S vs. 1800S	GREAT/0°	Delta-V larger for small car, higher decelerations for 4500S, maximum chest for small car higher. Small car failed delta-V and large car failed ridedown.
4500S vs. 1800S	Energite/0°	Similar results. Small car failed ridedown
4500S vs. 1800S	Fitch/0°	Similar results.
Head-on vs. 15°	Energite/1800S	15° test more severe. 15° test failed delta-V in addition to ridedown.
Head-on vs. 15°	Fitch/1800S	15° test more severe. 15° test failed delta-V in addition to ridedown.
4500S vs. 1800S	Frozen Fitch/0°	Similar results, both tests failed delta-V and ridedown.
4500S vs. 1800S	Frozen Energite/0°	Similar results, both tests failed ridedown.
Fitch vs. Energite	Frozen/4500S/0°	Similar results, both tests failed ridedown.
Fitch vs. Energite	Frozen/1800S/0°	Similar results, Energite III failed ridedown.
Frozen vs. Non-Frozen	Energite/4500S/0°	Vehicle parameters show frozen test more severe. Dummy parameters show non-frozen test more severe. Frozen test failed ridedown.
Frozen vs. Non-Frozen	Fitch/4500S/0°	Vehicle parameters show frozen test more severe. Results were similar for dummy parameters. Frozen test failed ridedown and delta-V



TABLE 4 *continued*

Comparisons	Conditions	Results/Observations
Bagged vs. Non-Bagged	Energite/1800S/0°	Bagged sand test more severe both tests failed ridedown. Occupant compartment intrusion occurred with Bagged Sand.
Bagged vs. Non Bagged	Energite/4500S/0°	Similar results.

hard point closer to the vehicle and reduces the effective stroke of the system.

#### Barrel Attenuators (Bagged Sand)

These two tests demonstrated that barrel attenuators filled with bagged sand increase occupant risk as measured by occupant compartment intrusion. During the small vehicle test, the hood, windshield, and numerous bags of sand penetrated the occupant compartment. Also, bagged sand debris resulted in potential for subsequent accidents of oncoming vehicles.

#### Barrel Attenuators (Pea Gravel)

This test was within specified values for dummy-based and vehicle-borne injury descriptors. However, the pea gravel provided potential for subsequent accidents because of the "ballbearing-like" gravel on the roadway.

#### Great System

The six-bay GREAT configuration showed good performance for an 1,800-pound (818 kg) vehicle for both redirection and arresting tests. For the 4,500-pound (2,045 kg) head-on test, the system did not have sufficient stroke. The system completely collapsed while the car was still traveling at 20 miles per hour (8.9 m/s). This resulted in a large deceleration level at the end of the impact. Thus, with a 4,500-pound (2,045 kg) vehicle impacting a six-bay GREAT at 60 miles per hour (26.8 m/s), occupant risk is considered very high. However, the system did perform well up to the point of total collapse, indicating that additional stroke (more bays) could have produced acceptable results. It should be noted that since the completion of this test program, Energy Absorption Systems, Inc., has redesigned the GREAT system with new Hexfoam II cartridges that allow the system to pass the limit criteria given in NCHRP 230.

#### Drainage Tests

Tests were conducted to observe the drainage characteristic of various sand barrel configurations. These tests indicated that drainage continues for a long period of time. Over a 60-

day period, the average moisture content of the barrels decreased from 18 percent to levels of 7 to 12 percent. These levels of moisture content can lead to frozen sand in large blocks. Based on observations from series III tests, considerable force is required to break up these blocks. It was also found that the Energite II barrels drained much better than the Energite III or Fitch barrels.

#### Safety Evaluation

The 20 impact attenuator tests of this contract provide an excellent opportunity to compare dummy-based and vehicle-borne occupant injury descriptors. In all cases except one, the dummy data were within prescribed limits. This was not true of the vehicle-borne descriptors. Thirteen of the 20 tests conducted provided results that exceeded NCHRP 230 design criteria, while only 4 of the 20 test results exceeded the NCHRP 230 limit criteria. Based on the results of this program, it appears that the design criteria may be too conservative and that a point closer to the limit values should be considered the pass/test criteria, rather than the design values.

Dummy data indicated that most injuries occur when the occupant first impacts the interior of the vehicle. This typically occurs 100 to 130 milliseconds after impact. The major exception to this is for femur loads which sometimes show peak values shortly after the initial impact.

#### Model Program for Force-Displacement

Standard design equations (momentum transfer techniques) provide good estimates of delta-V and the 50 ms acceleration but not good predictive methodology for the 10 ms acceleration (ridedown) data. For the tests conducted, the 10 ms acceleration can be calculated with good accuracy from the 50 ms acceleration using the following equation:

$$A_{10 \text{ ms}} = 1.89 \text{ accel}_{50 \text{ ms}} - 6.62$$

Force-displacement characteristics were made for all frontal head-on impacts. From these data traces, many comparisons were made. Of special interest were comparisons of the two brands of sand barrels under similar conditions (1800S, 60 mi/h, head-on), which show no difference; frozen vs. nonfrozen for similar conditions, where differences were observed; and bagged sand versus loose sand under similar conditions (1800S, 60 mi/h, head-on), where differences were observed. These comparisons are shown in Figure 7.

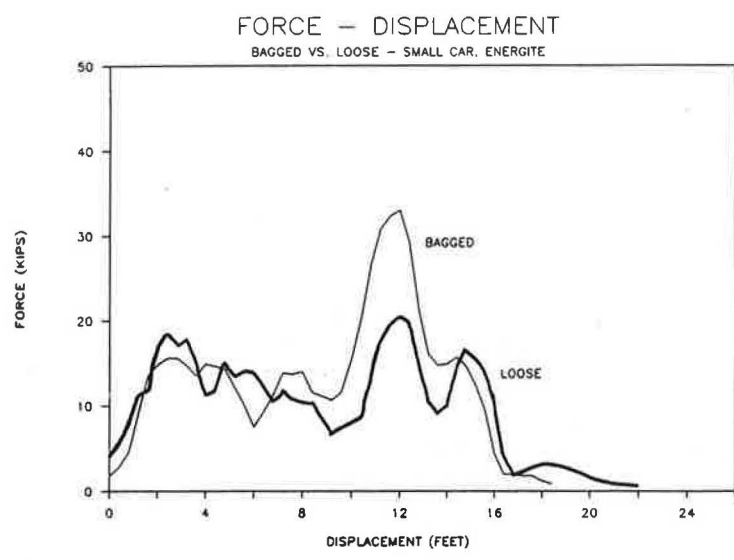
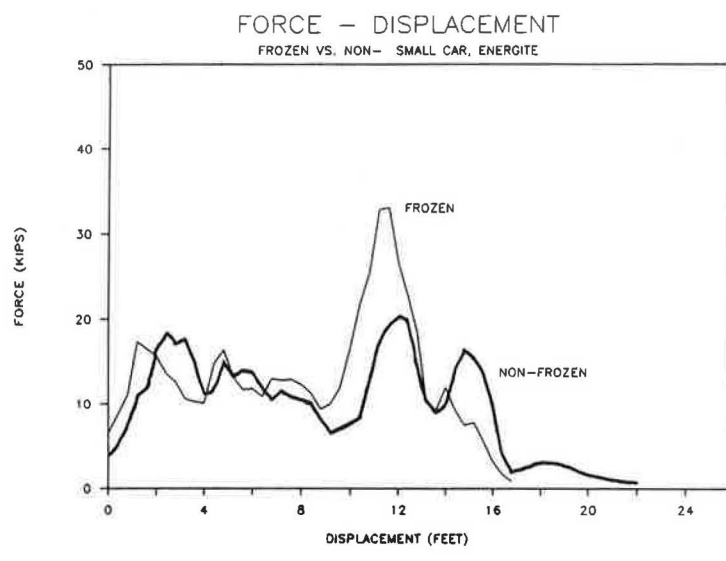
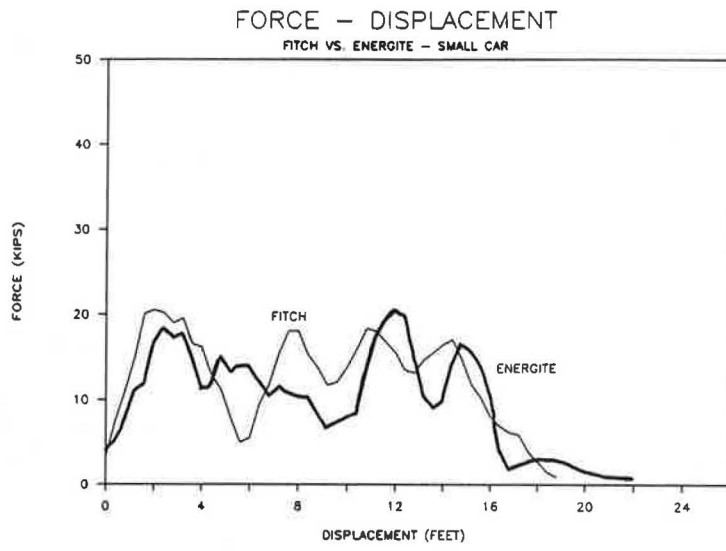


**FIGURE 7 Force-displacement comparisons.**

**Test Data Correlations**

A set of relationships between various parameters of the test data was developed. These were developed using a “least square” approach between the sets of data.

These analyses showed very good correlations (*r* greater than 0.8) between:

1. 50 ms and 10 ms (ridedown) accelerations, and
2. Delta-V based on 2-foot flail and delta-V based on actual flail.

Lower correlations were found between:

3. HIC and Delta-V based on 2-foot flail,
4. CSI and Delta-V based on 2-foot flail,
5. Maximum chest acceleration and delta-V based on 2-foot flail.

**ACKNOWLEDGMENTS**

The authors would like to acknowledge the efforts of Greg Manhard and Ta-Lun Yang of ENSCO, Inc.; Jim Hatton of

FHWA; Mike Essex and F.J. Taminini of Energy Absorption Systems, Inc.; and Scott Walters of Roadway Safety Service in supporting this successful research and development effort.

**DISCUSSION**

F.J. TAMANINI

*Energy Absorption Systems, Inc., 1104 Vassar Rd., Alexandria, Va. 22314.*

The engineering evaluation of impact attenuators, as reported in this paper, was sponsored by the Federal Highway Administration and conducted by ENSCO, Inc. It was a well planned and comprehensive program. The authors of this paper are eminently qualified researchers in vehicle crash testing and performance evaluation of highway safety appurtenances. The quality of the conducted research and of this paper attests to their prominence in the field.

However, in their comments under Results/Observations in Table 4, the authors’ use of “failed” conveys to the reader an impression that the three tested systems are unsafe and unacceptable for installation on highways. This is not the case. For approximately two decades, thousands of installations of

Impact Direction <sup>(aa)</sup> and Appurtenance Type	Occupant/Compartment Impact Velocity <sup>(b)</sup> — (fps)		Occupant Ridedown Acceleration— (g's)			
	Flail Space Recommendation		TRC 191	Flail Space Recommendation		TRC 191 <sup>(e)</sup>
	(ΔV) <sub>Limit</sub> /F <sup>(c)</sup>	(ΔV) <sub>Design</sub>		(a) <sub>Limit</sub> /F <sup>(c)</sup>	(a) <sub>Design</sub>	
<b>Longitudinal (X) Direction</b>						
Breakaway/Yielding Supports						
• Signs and luminaire	40/2.67	15	11-16 <sup>(f)</sup>	20/1.33	15	
• Timber Utility Poles	40/1.33	30	—	20/1.33	15	
Vehicle Deceleration Devices						
• Crash cushions and barrier terminals	40/1.33	30	32-39 <sup>(d)</sup>	20/1.33	15	
Redirectional Barriers						
• Longitudinal, transitions and crash cushion side impacts	40/1.33	30	25-36 <sup>(d)</sup>	20/1.33	15	
<b>Lateral (Y) Direction</b>						
Redirectional Barriers						
• Longitudinal, transitions and crash cushion side impacts	30/1.50	20	14-18 <sup>(d)</sup>	20/1.33	15	

**Notes:**

- (aa) With respect to vehicle axis.
- (b) Occupant to windshield, dash or door impact velocity with occupant propelled by vehicle deceleration pulse through 2-ft forward or 1 ft lateral flail space; multiply fps by 0.305 to convert to m/s.
- (c) F is acceptance factor to be established by highway agency.
- (d) Values calculated from TRC 191 criteria assuming that the highest 50-ms acceleration limits of TRC 191 are constant for the duration of the event and shown here for reference.
- (e) Flail space accelerations are highest 10 ms averages beginning with occupant impact to completion of pulse; TRC 191 accelerations are less severe, highest 50 ms averages or those averaged over vehicle stopping distance. These values are not comparable.
- (f) From TRC 191.

FIGURE 8 Recommended occupant risk values (I, Table 8).

these impact attenuators, approved by the Federal Highway Administration, the states, or local transportation agencies, have been most effective in saving lives and preventing serious injuries. These life-saving systems are in widespread use throughout this country and in some foreign countries.

In almost every case in the Results/Observations comments, the authors use "failed" to report a "derived" value for occupant impact velocity or ridedown acceleration when the value fell between the recommended design value and the limit value defined in NCHRP Report 230. While the lower design value is a more commendable value, highway safety appurtenances are nevertheless approved for federal aid and state construction projects when values obtained from full-scale crash tests do not exceed the limit value specified in NCHRP Report 230.

In light of the state of the art and current approval practices for highway safety appurtenances, it would have been more accurate and meaningful for the authors to have indicated where the derived occupant risk values fell with respect to the recommended design value and the limit value. The authors

are to be commended for having done such an identification in their comprehensive publication, *Impact Attenuators—A Current Engineering Evaluation* (Report FHWA/RD-86-054, August 1986).

In light of the long-term experienced effectiveness of the FITCH, ENERGITE, and GREAT attenuator systems, the information in this paper is misleading.

To enhance the value of the paper to the reader, Table 8 (Recommended Occupant Risk Values) from NCHRP Report 230 (Figure 8) (1) is included in this discussion. This table should promote a better appreciation for the authors' work, not only for this paper but also for their final research report.

#### REFERENCE

1. *NCHRP Report 230: Recommended Procedures for the Safety Performance Evaluation of Highway Appurtenances*, TRB, National Research Council, Washington, D.C., 1981.

# Federal Outdoor Impact Laboratory—A New Facility for Evaluating Roadside Safety Hardware

MARTIN W. HARGRAVE AND ALLEN G. HANSEN

---

**This paper describes the Federal Outdoor Impact Laboratory (FOIL), a new laboratory for evaluating roadside safety hardware. The FOIL has been designed and constructed to solve many of the roadside safety problems of the 1980's and beyond. As primarily a small-car crash test facility, it is used to research the higher probability of injury for small-car occupants. As a side impact test facility, it is used to develop side-impact technology and appropriate roadside solutions.**

---

Highway safety research to enhance the technology of road building as well as improve the safety of highway users has long been a priority to the Federal Highway Administration (FHWA). This is in contrast to the function of the National Highway Traffic Safety Administration, which focuses on the safety performance of vehicles.

Much of the federally funded highway research is directed from FHWA's Turner-Fairbank Highway Research Center located in McLean, Virginia, just outside of Washington, D.C. A recent addition to this center is an outdoor test facility named the Federal Outdoor Impact Laboratory (FOIL). Here, roadside safety hardware such as sign supports, light poles, crash cushions, and roadside barriers can be tested and evaluated.

Traditionally, full-scale crash testing has been the standard for the development and evaluation of roadside safety appurtenances because of its reliable, close duplication of real world collision events. However, to reduce test costs and improve the repeatability of test results, alternative test methods have been developed over the years. The latest in this evolution is the FOIL, which can operate in frontal and side impact modes. Figure 1 shows the general layout of this modern facility.

## FOIL FACILITY

### Features

The FOIL consists of a 200 foot (61 m) paved acceleration runway followed by a 200 foot wide by 350 foot (61 m by 107

m) long, grassy runout area. The runway end of the site is slightly sloped (2 percent grade) with the highest point located at the head of the runway. The area is level for 25 feet (7.6 m) immediately before and after the impact area, with gradual transitions between the sloped runway and the sloped runout area. The runout area changes gradually from a 2 percent downgrade to a 2 percent upgrade approximately 200 feet (61 m) beyond the end of the runway.

A unique feature of this test laboratory is the reusable bogie test vehicle shown in Figures 2 and 3. This vehicle is designed for frontal testing of breakaway poles, luminaires, and large sign supports and is currently configured to represent a 1979 Volkswagen Rabbit. Frontal vehicle crush is replicated using replaceable cartridges of aluminum honeycomb material. Other vehicle properties are replicated as necessary to produce realistic impact and post-impact (runout) results.

Another significant feature of this test laboratory is the use of a large weight as the propulsion system. A falling weight, connected by a cable to the test vehicle, pulls the vehicle forward, accelerating it to test speed. This propulsion method provides a reliable and low-cost drive system that can accelerate small vehicles to test velocities in a very short distance.

Side impact testing using actual automobiles, as depicted in Figure 4, is another of the FOIL's unique features. This capability is important because approximately 25 percent of all single-vehicle fatalities result from side impacts into fixed roadside objects. Unlike frontal testing, side-impact test specifications, evaluation criteria, and vehicle definition are largely undefined. Consequently, a reusable side impact bogie is not currently being developed, though it may be feasible and may later be developed.

One additional feature of the FOIL is the pendulum testing device, shown in Figure 5, which is useful for evaluating the performance of roadside hardware at low speeds. This pendulum is equipped with the same crushable frontal structure that is installed on the bogie, and the speed of impact is controlled by the drawback distance of the pendulum. The pendulum can be used only where vehicle runout and hardware trajectory after impact do not need to be determined and where the impact has a short duration, so that the curvature of the pendulum swing does not bias the test results. In addition, the pendulum cannot be used to evaluate the performance of large, multi-legged sign supports where the pendulum cables could interact with the sign blank and distort the acceleration measurements.

---

M. W. Hargrave, Federal Highway Administration, Safety Design Division, HSR-20, 6300 Georgetown Pike, McLean, Va. 22101.  
A. G. Hansen, Analysis Group, Incorporated, Engineering Systems Division, 1750 New York Ave., N.W., Washington, D.C. 20006.

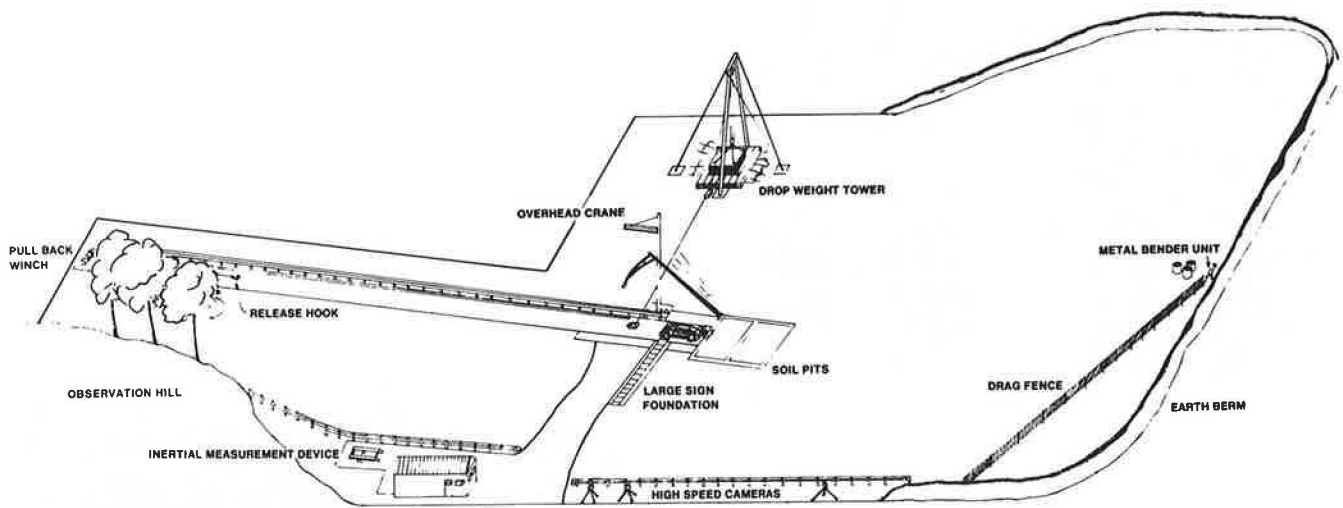


FIGURE 1 Schematic of FOIL facility.

**Acceleration and Guidance System**

The large weight that powers the FOIL's test vehicle is connected to the front of the vehicle by a cable that is released just prior to impact. Thus, at impact the test vehicle is free of all external restraints and is traveling at constant speed.

The speed of the vehicle, which can be varied between 0 and 60 mph (97 km/h) for front impacts and 0 to 45 mph (72 km/h) for side impacts, is determined by the distance of initial vehicle pullback and the size of the drop tower weight (up to 12,500 pounds or 5700 kilograms). This pullback is accomplished by a winch and second cable attached to the rear of

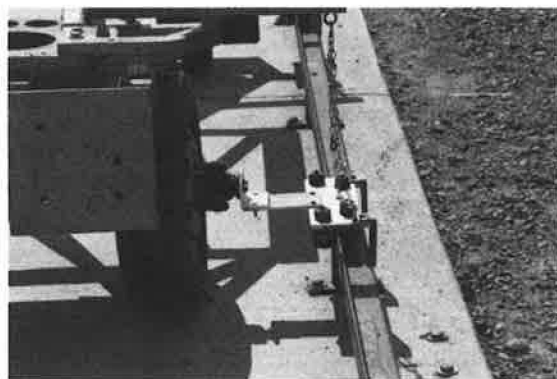
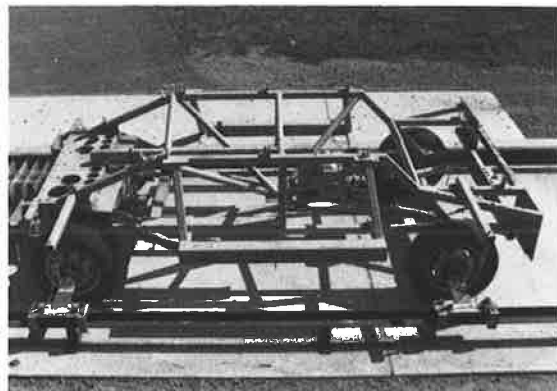
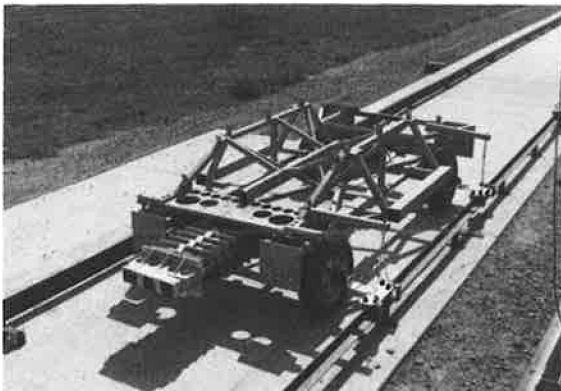


FIGURE 2 Frontal impact bogie test vehicle.

FIGURE 3 Frontal impact vehicle guidance system.



**FIGURE 4** Side impact vehicle guidance system.

the test vehicle. When the second cable is automatically released, the test sequence is initiated. For front impacts, a single fixed rail and two attachment assemblies fastened to the vehicle's front and rear spindles guide the vehicle during acceleration, as shown in figure 3. For side impacts, a second rail is used to support the bulk of the vehicle's weight, with the other rail used to support an outrigger mounted at the back of the vehicle, as shown in figure 4.

Because the entire system operates under constant acceleration caused by gravity pulling on the large drop weight, the velocity of the test vehicle at impact can be calculated. The relationship between the velocity and pullback distance can be estimated from the following equation:

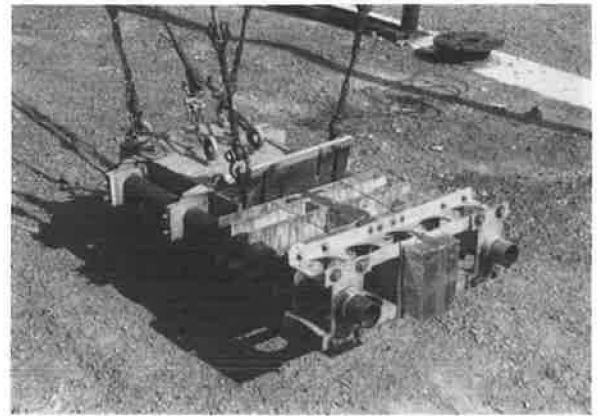
$$V^2 = \left[ \frac{2gER * (1 + 6WS)}{(1 + R^2W)} \right] L \quad (1)$$

where:

- $V$  = Impact velocity of test vehicle
- $L$  = Pullback distance
- $E$  = System efficiency (0.75 to 0.80, including losses associated with the vehicle)
- $W$  = Ratio of vehicle weight to drop weight
- $g$  = Acceleration of gravity
- $R$  = Reduction ratio of drop tower pulley system (6:1)
- $S$  = Runway slope (2 percent).



**FIGURE 5** FOIL pendulum test system.



For each test, this equation is used to estimate the pullback distance for a desired impact velocity. Since the parameters  $E$ ,  $W$ ,  $g$ ,  $R$ , and  $S$  are essentially constant for a given test, the velocity is directly proportional to the square root of the pullback distance. The system efficiency is adjusted based on environmental conditions such as ambient temperature and the presence of water on the runway.

#### Test Vehicle

The maximum vehicle weight for the full speed range is 2,250 pounds (1,020 kilograms) for front impacts and 2,500 pounds

(1,130 kilograms) for side impacts. The size of the falling weight and the corresponding strength requirements of the drop tower dictate this weight limit. Heavier vehicles can be tested but at lower maximum speeds. For example, the present system can test a 3,600 pound (1,630 kilogram) vehicle—typical of today's large size automobile—at speeds up to 50 mph (80 km/h).

The reusable bogie vehicle (Figure 2) is designed to emulate the actual impact and post-impact (the runout) performance of full-scale automobiles under real-world conditions. Any automobile weighing from 1,400 pounds (640 kilograms) to 2,250 pounds (1,020 kilograms) can be modeled by the bogie.

A principal feature of the FOIL, unlike earlier systems with reusable test devices, is the capability to observe and monitor the runout performance of the bogie after impact. Thus, in addition to analyzing injury severity criteria at impact, the tendency for a bogie to roll over after impact can also be observed and analyzed. This capability is important considering the greater likelihood of accident-related roll-overs with minisize vehicles and the higher probability of serious or fatal injury in roll-over accidents.

To emulate the crash performance of an actual automobile and to provide data for the bogie design, computer simulation runs using the Highway Vehicle Object Simulation Model were made. The results of these simulations were used to determine such properties as wheelbase, weight distribution, and suspension parameters required for a full-scale model. The computer simulations were validated by comparing the

results with a full-scale crash test. After construction, the actual performance of the bogie was validated against additional full-scale tests.

Table 1 lists the vehicle properties which are modeled on the current bogie. Also shown in this table are properties of an actual automobile and of two earlier test devices, the pendulum and a low speed bogie. This table indicates that the bogie contains all of the significant properties of an actual automobile except for a suspension system and steerable front wheels. Computer simulation results indicate that the bogie duplicates actual vehicle impact and post-impact performance up to 22 feet (6.7 m) following impact and realistically simulates runout trajectory up to 150 feet (45.7 m) beyond impact. This result is expected because suspension system responses delay impulsive force inputs and the steering system tends to self-correct the vehicle with respect to trajectory. Therefore, the lack of steerable front wheels makes the bogie a worst-case test vehicle with regard to roll-over. The lack of both steering and suspension also makes the test device rugged and lowers its initial and operating costs.

### Arrestor Systems

To stop the bogie after impact and runout, three arresting techniques are employed as shown in Figure 1: onboard four-wheel braking, an auxiliary energy absorbing arrestor system, and as a fail-safe, a large earthen berm. The onboard braking

TABLE 1 VEHICULAR DEVICES MODELED BY VARIOUS TEST DEVICES

General Category	Specific Property	Low Speed		FOIL	
		Pendulum	Bogie	Bogie	Automobile
Crush force deflection	Centered impacts	X	X	X	X
	Off-center impacts			X	X
Weight properties	Total weight	X	X	X	X
	Center of gravity			X	X
	Moments of inertia			X	X
Geometry	Wheelbase			X	X
	Track width			X	X
	Lower snag simulation	X	X	X	X
	Roof line penetration simulation		X	X	X
Suspension system	Tire stiffness		X	X	X
	Suspension stiffness damping				X
Steering system	Steerable front wheels				X
Speed capability	0 to 20 mph (32 km/h)	X	X	X	X
	0 to 60 mph (97 km/h)			X	X



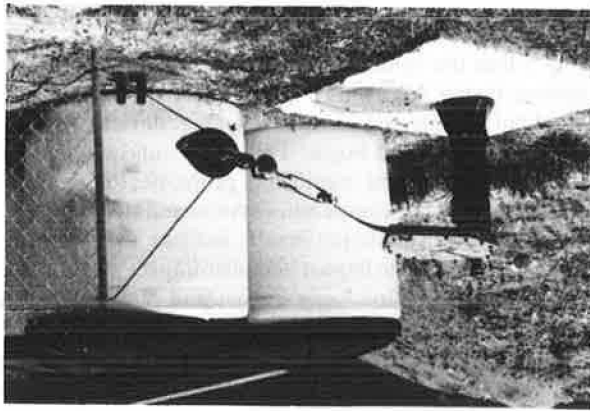


FIGURE 6 Energy absorbing arrestor system.

system is basically a pneumatic-over-hydraulic system. Under remote control, air, which is released from an onboard reservoir, acts through a piston at the interface to activate the hydraulic brakes. This braking technique is adequate for test speeds below approximately 55 mph (89 km/h) and without assistance can safely stop the test vehicle after runout.

At test speeds above approximately 55 mph (89 km/h), additional energy-absorbing devices are required. Secondary braking is achieved with two metal-bender units (see Figure 6) that absorb energy by forcing metal tape through a series of staggered rollers. The metal-bender units attach to each end of a drag fence that is stretched across the runout area. When the onrushing bogie is snagged by the fence, the kinetic energy of the vehicle is converted to strain energy as the vehicle pulls the metal tapes through and out of the metal-bender units.

Finally, as a backup to the primary and secondary braking systems, a large earthen berm surrounds the entire runout area. The berm, which is approximately 6 feet (1.8 m) high and has a sand face sloping upward at about 45 degrees, effectively contains out-of-control vehicles.

### Data Collection Systems

The current FOIL data collection system is limited to 14 channels of data (13 for data signals plus a timing signal). These signals are transferred from the vehicle to the facility control enclosure using an umbilical cable. Each signal is recorded on an analog tape system and digitized after each test using a compact digitizer coupled to a microcomputer. Two new battery-powered 32 channel digital systems are currently being developed. One system can be mounted directly on the bogie vehicle, providing a significant increase in the recording capabilities at the FOIL while eliminating both the umbilical cable and the post-test digitization. The second system can be mounted together with the first system in a full-scale vehicle to provide up to 64 channels for data acquisition, or it can be used to gather data from transducers that are not mounted on the car, such as speed traps and force gages.

The test vehicle can be instrumented with up to three accelerometers to measure the longitudinal, lateral, and vertical acceleration, and a three-axis-rate gyroscope to measure the roll, pitch, and yaw angular velocities. (Currently, two acce-

lerometers are used to provide redundancy in the measurement of the longitudinal acceleration in lieu of the vertical measurement.) These devices are located at the vehicle center of gravity and can be used to determine vehicle dynamics in addition to the following occupant injury measures:

- The velocity change (flail space velocity) of a theoretical occupant striking the interior of the vehicle just after a sudden impulsive impact (a measure of injury potential);
- The peak accelerations experienced by the vehicle averaged over 10 or 50 milliseconds (a second measure of injury potential).

A series of five contact switches both before and after impact is also used to determine the change in vehicle velocity due to impact (independent of the accelerometer data). The switches are a fixed distance apart on the runway, so that speed can be determined by measuring the time between successive pulses.

In addition to these two electronic data sources, independent film data are also recorded using a real-time documentary camera and several high speed cameras. Typically, two high-speed cameras are focused on the impact area while a third camera records the runout trajectory of the vehicle and the post-impact motion of the impacted object. The films are analyzed on a motion analysis system coupled with a microcomputer. The change in velocity of the vehicle due to impact and the motion of the impacted object are determined with this system.

The use of multiple accelerometers, speed traps, and cameras provides a high degree of redundancy in the determination of the change of velocity of the vehicle due to impact. A statistical weighted averaging technique is then used with the three independent velocity change calculations to provide a very accurate estimate of the actual velocity change of the vehicle (and the associated occupant) during a sudden impulsive impact with certain roadside safety devices such as break-away poles or luminaire and sign supports. The lower the velocity change resulting from impact, the greater the safety effectiveness of the roadside device under test.

### Other Equipment

Two additional major pieces of equipment available at the FOIL include a rigid instrumented pole (Figure 7) and an

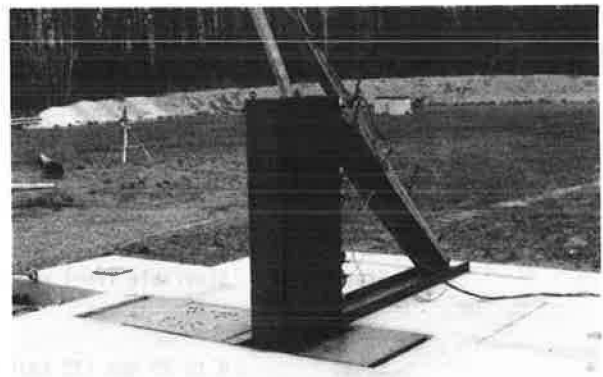
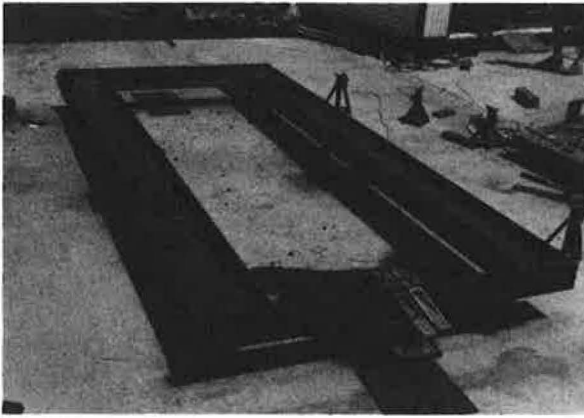


FIGURE 7 Rigid instrumented pole.



**FIGURE 8** Inertia measuring device.

inertia measuring device (IMD, as shown in Figure 8). The crush force of a vehicle's front or side structure is measured by crash testing actual vehicles into the rigid pole. The resulting force data coupled with the corresponding crush distance are required for modeling bogie vehicles or for inputs to computer simulations and bogie vehicle models.

In the frontal mode, a single pole segment and two force measuring cells measure the overall crush force of the vehicle's front end. In the side impact mode, however, three pole segments (each with two load cells attached) are used because of the differing stiffness of the door, the roof line, and the lower sill. By using two load cells per segment, the rigid instrumented pole can measure the magnitude as well as the location of the crush force—necessary parameters for modeling.

The IMD is used to determine the rotary moments of inertia (weight distribution) and the center of gravity of an actual small vehicle or the bogie. The resulting data are used to confirm that the vehicle parameters have been replicated in the bogie, as well as to provide measurements from actual vehicles for inputs to computer simulations and bogie vehicle models.

The IMD is basically a simple pendulum or seesaw device on which a vehicle can be placed. The inertia about each axis can be calculated by accurately measuring the period of each oscillation. To measure the vertical center of gravity, the IMD is tilted through a known angle until it rests on a load cell.

The center of gravity can then be determined by measuring the force at the load cell.

## RECENT TEST PROGRAMS

Several series of tests have recently been completed at the FOIL. The bogie, which was originally developed using roadside luminaire supports mounted with slip bases, has now been validated for transformer bases and couplings.

Following this validation, the bogie was used to determine the breakaway performance of luminaire support systems currently accepted for federal-aid highways when impacted with a lightweight 1,800 pound (820 kilogram) vehicle. This testing was done in accordance with the new 1985 AASHTO specifications for sign and luminaire supports. The testing program included eighteen luminaire supports mounted on transformer bases, nine anchor base supports, four progressive shear supports, three coupling mounted supports, and one slip base support. In addition, three direct burial fiberglass supports were evaluated at an independent laboratory.

These 38 devices were previously accepted for use on Federal-aid highways under older criteria which specified an impact with a heavier 2,250 pound (1,020 kilogram) vehicle. Due to the nationwide trend to lighter, more fuel efficient cars, a new rule is being proposed by the Federal Highway Administration to adopt the lighter (1,800 pound or 820 kilogram) vehicle as a test standard.

Of the 38 devices evaluated, 10 devices pass the new AASHTO change in velocity criterion. When both the change in velocity and the stub height criteria are considered, only four devices pass. It must be noted, however, that this is based upon a measurement of the remains of the breakaway device at the foundation without regard to what is considered "substantial" stub height. The substantial part of a stub is that portion that would produce significant vehicle undercarriage snagging. A review of test data is currently under way within the Federal Highway Administration to better quantify the determination of what constitutes a substantial stub.

Other test programs that have been conducted at the FOIL include the determination of significant vehicle parameters for use in modeling impacts with small base bending sign supports. The results of these tests are being used as a basis for the design of a new bogie for evaluation of the performance of small sign supports. Base bending sign supports are commonly used with stop signs, speed limit signs, and similar small roadside signs. In addition, side impact tests are being conducted to advance the state of knowledge of this important research area. Because side-impact testing is in its infancy, not only must various kinds of breakaway hardware be tested to determine acceptability under dynamic side-impact tests but the test conditions, test evaluation criteria, and test vehicle must also be defined and evaluated.

## FUTURE PLANS

### Data Collection System

The installation of the new data acquisition system mentioned earlier will allow the following data to be collected and processed:

- Anthropometric dummy data from frontal or side impact dummies (8 to 16 channels frontal, 18 to 36 channels side impact)
- Crush force of a vehicle's front or side structure measured with a rigid instrumented pole (2 channels frontal, 6 channels side impact)
- Additional vehicle and test article instrumentation to determine specific parameters of interest during a test series.

### **Bogie Development**

Currently, the bogie is designed for frontal impact testing into poles and pole-like objects. As mentioned above, a second bogie, for evaluating the performance of small sign supports, is currently being designed, and it will probably incorporate a suspension system, a windshield, and a new nose design to replicate the performance of a small car during a base bending small-sign impact.

The next step in bogie development will be to provide a full-width frontal crush capability. This will allow crash cushions and similar roadside objects to be evaluated using lower cost, reusable bogie vehicles. This could be followed by the development of a two-dimensional (longitudinal and lateral) crush bogie capable of testing roadside barriers. However, in addition to the complexity of a two-dimensional crush cartridge, a bogie capable of testing barriers would most likely require a complete suspension system and steerable front wheels for proper modeling. Although this is technically feasible, it may not be economically justifiable or prove rugged enough

for repeated testing, making the practicality of such a vehicle uncertain.

### **Test Program**

The FOIL facility is currently being upgraded to provide the capability to test large, multi-legged sign supports. When this upgrade is completed, currently accepted (for use on federal-aid roadways) large sign support systems will be evaluated using the current bogie to determine system performance with a lightweight, 1,800 pound (820 kilogram) vehicle. As with luminaire supports, these devices were previously accepted under older criteria, which specified impacts with a 2,250 pound (1,020 kilogram) vehicle.

When the new bogie for testing small sign supports is completed, it will be validated against several full-scale vehicle tests. Then a comprehensive capability program will also be conducted to evaluate the performance of small sign supports when impacted with the lighter, 1,800 pound (820 kilogram) vehicle.

### **ACKNOWLEDGMENT**

The facility development and research described in this paper were sponsored by the Safety Design Division of the Federal Highway Administration, located at the Turner-Fairbank Highway Research Center in McLean, Va.

# Optimum Design of Pin and Loop Portable Concrete Barrier Connectors

JAMES LOUMIET, JERRY L. GRAHAM, AND JAMES MIGLETZ

---

**Portable concrete barriers provide positive protection for highway work zones. Since the connection is often structurally the weakest part of the barrier system, connector design is a critical variable in barrier performance. A survey was conducted to determine which connectors are used by the states. The pin and loop connector is the most widely used, and for this reason, was singled out for analysis. This paper contains a static analysis of a pin and loop connector. The analysis, along with past crash test experience, is used to determine optimum pin and loop connector design. A table is included that lists the strengths of pin and loop connectors used by the states.**

---

Portable concrete barriers are used to provide positive protection for highway work zones and to separate work activity from traffic moving through the work zone. Originally, timber barricades were used to perform this function, but research by the Virginia Highway and Transportation Research Council in the 1970s found that 45.3 percent of the vehicles that came into contact with timber barricades penetrated the work zone (1). As a result, the timber barricade was eventually replaced by the more effective concrete barrier.

Several varieties of concrete barriers have been designed and used in the field. The most commonly used barrier is the New Jersey barrier. It is 32 inches high and has a 24-inch base width and a 6-inch top width. It also has a 55-degree batter-curb face and an upper portion that is at 84 degrees from the horizontal. The barrier is designed to both protect workers and equipment behind the work zone and to safely redirect vehicles impacting the barrier.

Originally, concrete barriers were used as permanent installations in medians to separate traffic. In some phases of highway construction, barriers were also used in work zone traffic control. While most of the concrete barrier was cast in place, some precast barriers were also used. Precast barriers led to the development of a barrier that could be moved from one location to another and could be placed in position temporarily.

Initially the segments of the portable concrete barrier (PCB) were simply butted end-to-end. It soon became evident, however, that the segments needed to be connected to be effective. While the use of PCB, especially the New Jersey barrier, spread rapidly in the 1970s, various agencies developed a wide variety of methods for connecting the barrier segments. As stated in one report, "Although the PCB is used from coast to coast, its design features vary from state to state. . . . It is in the method of joining these segments that the widest design variation takes place"(2).

---

Graham-Migletz Enterprises, Inc., P.O. Box 348, Independence, Mo. 64050.

## PRESENT USE OF PORTABLE CONCRETE BARRIER CONNECTORS

In a 1985 telephone survey, the Federal Highway Administration (FHWA) polled states through regional offices to determine what types of connectors were being used in each state. The authors sent the results of this survey to the principal construction engineer of each state highway agency, including Puerto Rico and the District of Columbia. A letter was also sent asking each engineer to verify the type of connector used in his or her state, and to send copies of the state's standard plan(s) on portable concrete barriers.

Forty-eight of the 52 agencies polled responded to the survey and confirmed the type of PCB connector used. Some states specified a number of connectors, having some as primary and others as alternates. Some states specified a number of acceptable connectors with no preference. Table 1 shows the complete survey results (3).

The most commonly used connector is the pin and loop connector. It consists of steel loops cast in each end of the barrier segment. The barriers are connected by inserting a pin through the loops of two adjacent barrier segments. Forty-six agencies use some variation of the pin and loop connector. The pin and loop category is further divided into four subdivisions: pin and rebar (27 agencies), pin and wire rope (14 agencies), pin and eyebolt (2 agencies), and pin and plate (1 agency). Two agencies did not specify the type of pin and loop connector used.

## Need for Design Analysis of PCB Connectors

For the PCB system to protect work zones and redirect vehicles, it must be capable of withstanding the kinetic energy exerted by an impacting vehicle. Since the connection is often structurally the weakest part of the barrier system, the connection design is often a critical variable in barrier performance for a given impact. The connector must not only absorb some of the impact energy, but must also be able to limit the movement and rotation of barrier segments. Past research has shown that barriers with stronger and stiffer connections will laterally deflect less than barriers with weaker and looser connections. Crash testing has shown that barrier connectors with higher torsional strength and stiffness help prevent barrier torsional rotation, and hence overturn, and prevent vehicle ramping for a vehicle impacting a barrier (3). Crash testing has also shown that loop arrangement on pin and loop connectors is a critical variable in barrier performance. Figure 1 shows the two most common types of loop arrangements—

TABLE 1 USAGE SURVEY RESULTS

State	Primary Connector	Alternate Connector	Barrier Segment Length	Confirmed By Engineer
Alabama	Pin & Rebar		10 ft ± 1/2 in	Yes
Alaska	Pin & Rebar		10 ft	Yes
Arizona	Pin & Wire Rope		12 ft 6 in, and 20 ft	Yes
Arkansas	Pin & Wire Rope		10 ft	Yes
California	Pin & Rebar		19 ft 10 in	Yes
Colorado	Pin & Rebar		10 ft	Yes
Connecticut	Pin & Rebar		20 ft	Yes
Delaware	Plate Insert		12 ft	Yes
Dist. of Columbia	Pin & Rebar	Plate Insert	12 ft	Yes
Florida	Flaring Tongue & Groove, Straight Tongue & Groove, Pin & Wire Rope, Pin & Rebar	Side Plate	12 ft min	Yes
Georgia	Pin & Rebar		10 ft	Yes
Hawaii	Pin & Rebar		19 ft 9 1/4 in	Yes
Idaho	Pin & Wire Rope		Unknown	No
Illinois	Pin & Wire Rope		10 ft	Yes
Indiana	Pin & Rebar		10 ft	Yes
Iowa	Pin & Wire Rope		10 ft	Yes
Kansas	Straight Tongue & Groove with Steel Dowels	Straight Tongue & Groove with Side Plates	10 ft	Yes
Kentucky	Straight Tongue & Groove With Side Plates, Pin & Rebar Slotted Triple Dowel		20 ft ± 1/2 in 10 ft ± 1/2 in 20 ft, 30 ft	Yes
Louisiana	Pin & Wire Rope		15 ft	Yes
Maine	Pin & Rebar		10 ft	Yes
Maryland	Plate Insert		Unknown	No
Massachusetts	Pin and Loop		Unknown	No
Michigan	Pin & Eye Bolt	Double Dowel	10 ft	Yes
Minnesota	Pin & Wire Rope		10 ft	Yes
Mississippi	Pin & Rebar		10 ft ± 1/2 in	Yes
Missouri	Straight Tongue & Groove with Continuous Cable		10 ft	Yes
Montana	Pin & Wire Rope		10 ft	Yes
Nebraska	Pin & Rebar		10 ft	Yes
Nevada	Pin & Rebar		19 ft 10 in	Yes
New Hampshire	Pin & Rebar		10 ft	Yes
New Jersey	Straight Tongue & Groove, Straight Tongue & Groove with Side Plate	Welsbach	20 ft	Yes
New Mexico	Pin & Rebar		12 ft 6 in	Yes
New York	Straight Tongue & Groove Vertical I-Beam		10 ft 8 ft, 10 ft, 12 ft, 14 ft, 16 ft, 18 ft, 20 ft	Yes
North Carolina	Pin & Rebar		10 ft	Yes
North Dakota	Pin & Wire Rope		10 ft	Yes
Ohio	Pin & Rebar	Straight Tongue & Groove Flaring Tongue & Groove	10 ft min.	Yes
Oklahoma	Pin & Rebar		10 ft	Yes
Oregon	Pin & Wire Rope		12 ft 6 in	Yes
Pennsylvania	Plate Insert Flaring Tongue & Groove		30 ft max	Yes
Puerto Rico	Pin and Loop		Unknown	No
Rhode Island	Pin & Rebar		10 ft	Yes
South Carolina	Pin & Rebar		12 ft	Yes
South Dakota	Pin & Twin Double Rebar		10 ft	Yes
Tennessee	Pin & Triple Rebar		8 ft to 12 ft	Yes
Texas	Channel Splice	Grid Slot, Lapped Joint & Bolt Flaring Tongue & Groove Triple Dowel	14 ft 11 in to 25 ft 30 ft ± 4 in	Yes
Utah	Pin & Plate	Pin & Wire Rope	10 ft, 12 ft, 12 ft 6 in, 20 ft	Yes
Vermont	Pin & Rebar		10 ft	Yes
Virginia	Flaring Tongue & Groove	Plate insert	12 ft	Yes
Washington	Pin & Wire Rope		10 ft and 12 ft 6 in	Yes
West Virginia	Flaring Tongue & Groove	Pin & Eye Bolt	12 ft and 10 ft 10 ft	Yes

TABLE 1 continued

State	Primary Connector	Alternate Connector	Barrier Segment Length	Confirmed By Engineer
Wisconsin	Pin & Rebar with Wire Rope		10 ft	Yes
Wyoming	Pin & Rebar Pin & Wire Rope		10 ft	Yes
Total:	Unspecified Pin and Loop	2 agencies		
	Pin and Rebar	27 agencies		
	Pin and Wire Rope	14 agencies		
	Pin and Eye Bolt	2 agencies		
	Pin and Plate	1 agency		
	Tongue and Groove	8 agencies		
	Plate Insert	5 agencies		
	Channel Splice	1 agency		
	Side Plates	1 agency		
	I-Beam	1 agency		
	Continuous Cable	1 agency		
	Dowel Rods	2 agencies		
	Grid Slot	1 agency		

inserted and staggered. Since limited lateral deflection and limited torsional rotation are arguably the most important feature of a PCB, it is preferable to use barriers with stronger, stiffer connectors.

Pin and loop connectors were singled out for analysis because of their widespread use. As stated earlier, analysis of these connectors is important since connector design directly influences barrier performance for a given impact. Also, there is much contradiction among previous reports for some connector static strengths. For example, one study (4) gives the tensile capacity of the Idaho pin and rebar as 61 kips, whereas another study (5) gives this same capacity as 23 kips. It was impossible to tell why these discrepancies occurred since only one report (4) showed the computations that yielded their capacities.

**Forces Involved**

Figure 2 shows the right-hand coordinate system used to define the tensile moment, shear, and torsion load capacities of a

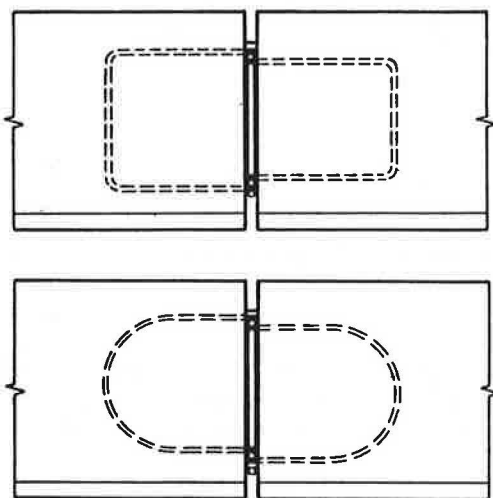


FIGURE 1 Pin and loop connectors: inserted loop arrangement (California), top; staggered loop arrangement (Arkansas), bottom.

barrier connector. The X-axis in the system is coincident with the longitudinal barrier centroidal axis. The Y-axis is vertical and forms a right angle with the X-axis. The Z-axis is orthogonal to the X and Y axes, and is in a right-hand sense.

The four capacities analyzed are the ultimate tensile capacity (P), the ultimate moment capacity (M), the ultimate shear capacity (V), and the ultimate torsion capacity (T). In general, barrier connectors will usually be subjected to moment or torsion dynamic loading because of impact. For this reason, moment and torsion capacities are the most important gauge of connector strength. Tensile capacity is important because it directly determines the moment capacity. Shear capacity is important because barrier deflection has been shown to be sensitive to this capacity. In general, a pin and loop connector under tensile loading conditions will fail because of any of the following reasons:

1. Pin fails because of transverse loading. If the pin is not anchored on both top and bottom, then failure will occur at incipient yielding of the pin, because yielding would allow the pin to bend and slip out of the loops. While the pin may not actually come out of the loops when it begins to yield, it is

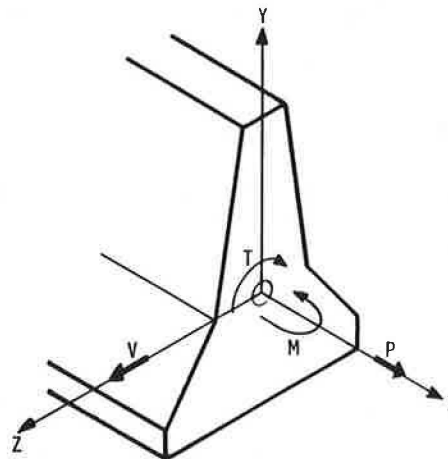


FIGURE 2 Coordinate system for portable concrete barrier.

certainly in danger of doing so. If the pin is anchored, however, then pin failure is because of rupture.

2. Loops fail in tension.
3. Loops pull out of barrier (only if top and bottom loops are not physically connected).
4. Concrete shears because of force on loops.

The tensile capacity of the connector is then the minimum force required to cause failure for any of the above-stated reasons.

A pin and loop connector under moment loading will fail for the same reason that it does for tensile loading. Moment capacity then is the distance between the pin center and the extreme fibers of the barrier crossed into the tensile capacity of the connector.

A pin and loop connector under shear loading conditions will fail for any of the following reasons:

1. Pin fails because of transverse loading.
2. Loops fail in tension.
3. Concrete shears laterally because of forces on loops (this occurs for rebar loops only).
4. For wire rope, concrete shears longitudinally because of forces on loops, since forces on wire rope always resolve into tensile forces.

The shear capacity of a pin and loop connector is then the minimum force required to cause failure for any one of the above-stated reasons.

A pin and loop connector under torsion loading conditions has the same possible modes of failure as does a pin and loop connector under shear loading conditions. The only difference is that the pin analysis will change because of the change in loading conditions on the pin itself. The torsion capacity of the connector is then the vertical distance between the loops in one barrier end crossed into the minimum force required to cause failure for any of the above-stated reasons.

### Analytical Determination of Connector Strengths

An analysis of the pin and wire rope connector used by the Arkansas State Highway Department is given in this section. The following assumptions were used for the analysis:

1. Connector strengths are analyzed using the mechanical properties of the actual materials in the connector. Mechanical properties are assumed only when actual properties are unknown.

2. Concrete is an integral part of the connector system, and is therefore taken into account in the failure analysis.

3. The ultimate shear strength ( $\nu_c$ ) of concrete is governed by the equation

$$\nu_c = 2\sqrt{f'_c} \quad (1)$$

where  $f'_c$  is the compressive strength of the concrete.

4. Barriers are pulled tight at the connectors for pin and loop connectors.

5. Anchored pins are evaluated for catastrophic failure. Unanchored pins are evaluated for incipient yielding.

6. Forces on anchor nuts that are induced by transverse

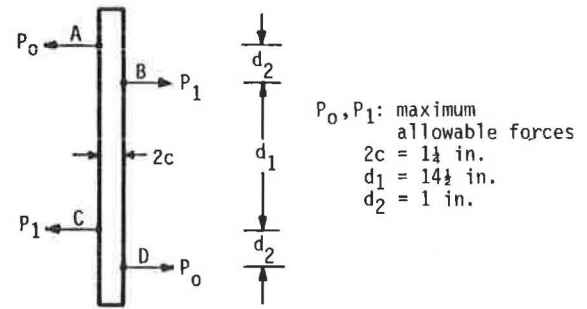


FIGURE 3 Free body diagram (FBD) of pin of Arkansas connector (tensile).

loading on the pin are assumed to be of insufficient magnitude to cause failure in the threaded portion of the pin.

7. All structural steels are considered ductile.

8. All structural hardware is the same material unless otherwise specified.

9. The masses of the various components of the connector are disregarded.

The Arkansas pin and wire rope is shown in Figure 3. It has a pin diameter of 1.25 inches and a wire rope diameter of five-eighths of an inch.

### Tensile Capacity

The possible modes of failure of this connector in tension are: (a) pin fails in transverse loading, (b) loops fail in tension, or (c) concrete shears because of forces on loops.

**Tensile Capacity of Connector for Pin Failure** The pin is under the loading condition shown in Figure 3. Letting

$$F = P_1 + P_0 \quad (2)$$

and summing forces in the  $X$  direction yields:

$$\sum F_x = P_1 + P_0 - P_1 - P_0 = 0 \quad (3)$$

Now summing moments about  $D$  yields:

$$\sum M_D = 0 \quad (4)$$

$$= d_2 P_1 - (d_2 + d_1) P_1 + (d_1 + 2d_2) P_0$$

$$P_1 = [(d_1 + 2d_2)/d_1] P_0 = 1.138 P_0 \quad (5)$$

Analysis of shear and bending moment diagrams reveals that the critical points on the pin are points  $B$  and  $C$ , where the maximum shearing force is  $P_0/A$  and the maximum moment is  $d_2 \times P_0$ .

Since the pin is anchored at both ends, it must be ruptured in order to break the connection. A conservative method to find the force ( $F$ ) required to rupture the pin is simply to calculate the shearing force required to rupture the pin. Solving for  $P_0$ :

$$P_0 (\sigma_f)(A) = (60 \text{ ksi}) \frac{\pi}{4} (1.25)^2 \quad (6)$$

$$P_0 = 73.6 \text{ kips}$$

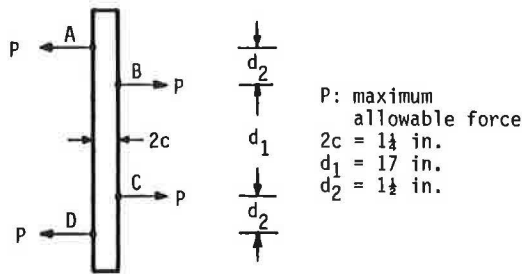


**FIGURE 4 FBD of pin of California connector (tensile).**

Now solving for the tensile capacity of the connector for pin failure:

$$F = P_0 + P_1 = 73.6 \text{ kips} + (1.138)(73.6 \text{ kips})$$

$$F = 157.8 \text{ kips}$$

The tensile capacity of the connector for pin failure is 157.4 kips.

For an unanchored pin as used by the California Department of Transportation, the pin is under the loading condition shown in Figure 4. The critical points in this member are B and C. This configuration is the same as for the pin of the Arkansas pin and wire rope in torsion loading mode except the distances  $d_1$  and  $d_2$  are different. Therefore, solving for the stresses  $\sigma_x$  produced by bending and  $\tau_{xz}$  produced by pure shear:

$$\sigma_x = \frac{Mc}{I} = \frac{4d_2P}{\pi c^3} = \frac{4(1.5)P}{\pi(0.625)^3} = 7.823 P \quad (7)$$

$$\tau_{xz} = \frac{P}{A} = \frac{P}{c^2} = \frac{P}{\pi(0.625)^2} = 0.815 P \quad (8)$$

Now using the values of  $\sigma_x$  and  $\tau_{xz}$  to solve for the principal stresses  $\sigma_1$ ,  $\sigma_2$ , and  $\sigma_3$  yields:

$$\sigma_1 = \frac{\sigma_x}{2} + \left[ \left( \frac{\sigma_x}{2} \right)^2 + (\tau_{xz})^2 \right]^{1/2} = 7.908 P \quad (9)$$

$$\sigma_2 = 0 \quad (10)$$

$$\sigma_3 = \frac{\sigma_x}{2} - \left[ \left( \frac{\sigma_x}{2} \right)^2 + (\tau_{xz})^2 \right]^{1/2} = -0.085 P \quad (11)$$

The Von Mises (Distortion Energy) Theory (6) will be used to evaluate for the strength of the pin, because this theory best agrees with experimental results. This theory states that failure will occur if:

$$(\sigma_1 - \sigma_2)^2 + (\sigma_2 - \sigma_3)^2 + (\sigma_3 - \sigma_1)^2 \geq 2 \sigma_f^2$$

Solving for  $P$ :

$$(7.908 P)^2 + (0.085 P)^2 + (9.993 P)^2 = 2 \sigma_f^2 \quad (12)$$

Because the pin is not anchored on both ends, it is evaluated for incipient yielding.

Therefore, for  $\sigma_f = 36,000$  psi,  $P = 4.5$  kips. Letting  $F = 2 P$ :

$$F = (2)(4.5 \text{ kips})$$

$$F = 9.0 \text{ kips}$$

The tensile capacity of the California connector for pin failure is 9.0 kips.

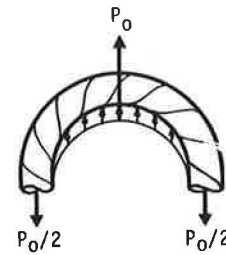


**FIGURE 5 FBD of loop of Arkansas connector (tensile).**

**Tensile Capacity of Connector for Loop Failure** For loop failure to occur, these loops loaded with  $P_0$  must fail before the connection will fail. Each loop of the barrier system loaded by  $P_0$  is shown in Figure 5.

Arkansas specifies a five-eighths of an inch diameter wire rope with a minimum breaking strength of 17.9 tons (35,800 lb).

Therefore, for  $P/2 = 35,800$  lb:

$$P_0 = (2)(35,800 \text{ lb}) = 71.6 \text{ kips}$$

$$F = 71.6 + (1.138)(71.6 \text{ kips})$$

$$F = 157.4 \text{ kips}$$

**Tensile Capacity of Connector for Concrete Shear** The concrete is in the loading condition shown in Figure 6. Therefore, for the tensile loading condition shown, the concrete is in shear, with a shear area of  $2A_c$  (for both sides of the cable). For a concrete compressive strength of 2,500 psi, the shear strength of the concrete is determined by  $v_c = 2\sqrt{f'_c}$  where  $v_c$  is the shear strength of the concrete and 2,500 psi is the compressive strength of the concrete. Therefore,

$$v_c = 2\sqrt{2,500} = 100 \text{ psi}$$

For  $A_c = 466.35$  inches,  $2 A_c = 932.7$  inches

Solving for  $F$ :

$$F = (100 \text{ psi})(932.7 \text{ inches})$$

$$F = 93.3 \text{ kips}$$

Therefore, the concrete is the failure mechanism for the connector under static loading conditions.

The tensile capacity of the Arkansas pin and wire rope connector is 93.3 kips and is determined by the capacity of the concrete in shear.

*Moment Capacity*

The moment capacity,  $M$ , of the Arkansas pin and wire rope connector is the distance,  $r$ , between the pin center and the

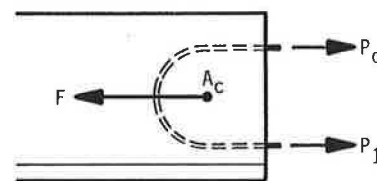


**FIGURE 6 FBD of concrete of Arkansas connector (tensile).**



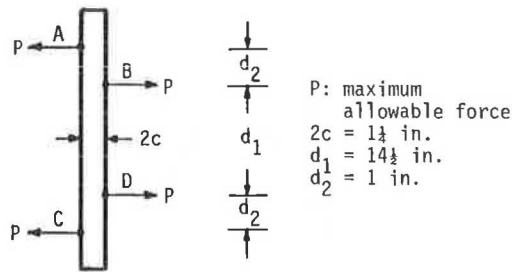


FIGURE 7 FBD of pin of Arkansas connector (torsion).

extreme fibers of the barrier crossed into the tension capacity of the connector. Therefore,

$$M = r \times F$$

$$M = (1 \text{ ft}) \times (93.3 \text{ kips})$$

$$M = 93.3 \text{ kip-ft} \quad (13)$$

The moment capacity of the connector is 93.3 kip-ft.

### Shear Capacity

The possible modes of failure of this connector in shear are: (a) pin fails in transverse loading, (b) loops fail in tension or (c) concrete shears because of forces on loops. Since these modes of failure are the same as those for tensile capacity, the shear capacity is equal to the tensile capacity. The shear capacity of the Arkansas pin and wire rope connector is 93.3 kips.

### Torsion Capacity

The failure modes for the connector in torsion are the same as the failure modes for the connector in shear. However, the pin analysis changes since the loading on the pin changes. For the torsion mode, the pin is under the loading condition shown in Figure 7. Equilibrium of moments and forces dictates that  $F = 2P$ .

TABLE 2 STRUCTURAL CAPACITIES OF PIN AND LOOP CONNECTORS

Connector Type State	Tensile (kips)	Shear (kips)	Moment (kip-ft)	Torsion (kip-ft)	Failing Component	Pin Anchored?
<u>Pin and Rebar</u>						
Alabama	3.9	3.9	3.9	5.2	pin	N
Alaska	81.8	81.8	81.8	122.7	loop	Y
California	9.1	9.1	9.1	14.0	pin	N
Colorado	2.6	2.6	2.6	3.5	pin	N
Dist. of Columbia	106.0	106.0	106.0	163.5	loop	Y
Florida	7.6	7.6	7.6	10.1	pin	N
Georgia	6.6	6.6	8.2	8.5	pin	N
Hawaii	76.6	76.6	76.6	113.5	loop	Y
Indiana	2.9	2.9	2.9	3.1	pin	N
Kentucky	88.4	88.4	88.4	132.5	loop	Y
Maine	2.6	2.6	2.6	3.5	pin	N
Mississippi	106.0	106.0	106.0	159.0	loop	Y
Nebraska	3.5	3.5	3.5	5.2	pin	N
Nevada	8.8	8.8	8.8	13.6	pin	N
New Hampshire	3.5	3.5	3.5	5.2	pin	N
New Mexico	2.6	2.6	2.6	3.5	pin	N
N. Carolina	3.9	3.9	3.9	5.2	pin	N
Ohio	6.7	6.7	6.7	8.4	pin	N
Oklahoma	3.9	3.9	3.9	5.2	pin	N
Rhode Island	3.9	3.9	3.9	6.0	pin	N
South Carolina	13.4	13.4	13.4	19.0	pin	N
Vermont	3.9	3.9	3.9	4.6	pin	N
Wisconsin	3.9	3.9	3.9	5.2	pin	N
Wyoming	2.6	2.6	2.6	3.5	pin	N
<u>Pin and Wire Rope</u>						
Arizona	3.9	3.9	3.9	4.9	pin	N
Arkansas	93.3	93.3	93.3	121.3	concrete	Y
Florida	7.6	7.6	7.6	10.1	pin	N
Illinois	2.6	2.6	2.6	3.5	pin	N
Iowa	6.5	6.5	6.5	9.2	pin	N
Louisiana	4.5	4.5	4.5	7.0	pin	N
Minnesota	7.7	7.7	7.7	9.0	pin	N
Montana	5.2	5.2	5.2	4.5	pin	N
N. Dakota	7.7	7.7	7.7	9.0	pin	N
Oregon	4.7	4.7	4.7	6.5	pin	N
Utah	3.4	3.4	3.4	3.0	pin	N
Washington	4.5	4.5	4.5	7.0	pin	N
Wyoming	2.6	2.6	2.6	3.5	pin	N
<u>Pin and Eye Bolt</u>						
West Virginia	2.6	2.6	2.6	3.1	pin	N
Michigan	1.7	1.7	2.0	1.9	pin	N

Solving for  $P$  yields:

$$P = (\sigma_f)(A) = (60 \text{ ksi}) \frac{\pi}{4} (1.25)^2 = 73.6 \text{ kips}$$

Now solving for  $F$ :

$$F = (2) (73.6 \text{ kips})$$

$$F = 147.2 \text{ kips}$$

Since this value of  $V$  (147.2 kips) is greater than the force  $V$  associated with concrete failure, concrete failure is still the failure mechanism for this connector in torsion. Therefore, the torsion capacity of this connector is given by

$$T = r_2 \times V \quad (14)$$

where  $r_2$  is the vertical distance between loops on one barrier end. Therefore,

$$T = (1.3 \text{ ft}) \times (93.3 \text{ kips})$$

$$T = 121.3 \text{ kip-ft}$$

The torsion capacity,  $T$ , of this connector is 121.3 kip-feet

### Summary of Analytical Determination of Connector Strengths

The results of the complete static analysis are shown in Table 2, which contains the structural capacities of the pin and rebar, pin and wire rope, and pin and eyebolt connectors. The structural capacities for these connectors were calculated using GME in-house software modeled after the analysis just performed.

The most interesting result of the analysis of pin and loop connectors is the large difference in the capacities of connectors with anchored pins and the capacities of connectors with unanchored pins. In general, the capacities of anchored pin connectors are an order of magnitude greater than the capacities of unanchored pin connectors. For example, the tensile capacities of unanchored pin connectors range from 3 kips to 9 kips, whereas the tensile capacities of anchored pin connectors range from 77 kips to 106 kips. This discrepancy is because the mode of failure is assumed to change from yielding to rupture when going from unanchored to anchored pins. Admittedly, these results should be viewed with some caution, since these failure modes may not be the actual failure modes of barriers under impact conditions. For example, Caltrans crash tests 291-294 showed that impacted barrier segments tend to rotate on the bottom edge opposite the impact side, rather than around the segments' longitudinal axis. Because of this, loops on inserted loop connectors interlock when a segment begins rotating, which helps to prevent segment rotation. This makes the connector much stronger in torsion than static analysis shows it to be, and much stronger in torsion than a staggered loop connector and this illustrates the importance of crash testing in determining connector acceptability. This analysis also illustrates the large difference in structural integrity between the unanchored pin connector and the structurally superior anchored pin connectors. Yet to date, only six states specify anchoring for their pins.

Invariably, the pin is the critical component of unanchored pin connectors because the pin needs only to be pulled and

bent out of the loops to destroy the integrity of the connection. One factor that compounds this problem is the distance between the two top loops or the two bottom loops of the connector. The greater this distance the greater the moment arm on the pin, and hence the lower the capacity of the pin to resist bending. The structural capacity of the pin is also very sensitive to the pin diameter since the pin diameter gets squared in strength calculations. For example, doubling the pin diameter will increase the strength of a pin by a factor of 4.

On the other hand, the structural capacity of the various components of anchored pin connectors is in the same general range, between 77 kips to 160 kips. This is because the anchored pin must now be ruptured to destroy the integrity of the connection. While unanchored pin moment capacities range from 2 kips to 13.4 kips, anchored pin moment capacities range from 76.6 kips to 106 kips.

The analysis also revealed that not all connector designs are based on standardized design practices as specified by authoritative organizations. For example, one state connector did not provide for sufficient anchoring of eyebolts in their pin and eyebolt connector to prevent the eyebolts from breaking out of the concrete as specified by American Concrete Institute (ACI) codes ACI-12.2.2 and ACI-12.5.3 and cited by Wang and Salmon (7).

As stated earlier, only one report, TTI's *Barriers in Construction Zones* (4), actually showed the computations that yielded the structural capacities for the connectors that they analyzed. Comparing GME's results to TTI's results shows that for several connectors, GME's calculated strengths are lower than TTI's calculated strengths. The main reason for these differences is that TTI generally used higher material constants or different connector specifications than GME did for analysis. For example, TTI used 60 ksi for failure strength in some calculations, whereas GME used 36 ksi for several calculations. Other differences included different analytical techniques and round-off errors.

### RECOMMENDATIONS

The following are recommendations based on the state of portable concrete barrier technology.

1. Inserted loops are preferable to staggered loops in pin and loop connector design because of the inserted loops resistance to torsional overturn of individual barrier segments.
2. Pins in pin and loop connectors should be anchored at both ends of the barrier segment. Only nut and washer anchoring will prevent pins from being bent out of the loop when the pin is loaded.
3. Because of its greater strength, wire rope is generally preferable to steel reinforcing bars for forming loops in pin and loop connectors.
4. States should use PCB connectors only if they have been structurally analyzed and successfully crash tested.
5. Connectors should be designed to match the strength of all components of the connector.

### REFERENCES

1. F. N. Lisle and B. T. Hargroves. Evaluation of Performance of Portable Precast Traffic Barriers. In *Transportation Research*

- Record 769, TRB, National Research Council, Washington, D.C., 1980, pp. 30–37.
2. J. M. Morales. *Technical Advisory for Concepts of Temporary Barriers in Work Zones*. FHWA, U.S. Department of Transportation, May 1985.
  3. J. L. Graham, J. R. Loumiet, and J. Migletz. *Portable Concrete Barrier Connectors*. Final Report, FHWA, U.S. Department of Transportation, Aug. 1987.
  4. D. L. Ivey et al. *Barriers in Construction Zones*. Volume 3: Appendices B, C, D, E, and F, Texas Transportation Institute, Texas A&M University, College Station, April 1985, pp. 163–199.
  5. D. L. Ivey et al. Portable Concrete Median Barriers: Structural Design and Dynamic Performance. In *Transportation Research Record 769*, TRB National Research Council, Washington, D.C., 1980, pp. 20–30.
  6. J. A. Collins. *Failure of Materials in Mechanical Design, Analysis, Prediction, Prevention*. Wiley-Interscience. 1981, pp. 137–141, 149.
  7. C. K. Wang and C. G. Salmon. *Reinforced Concrete Design*. 4th ed. Harper & Row, New York, 1985, pp. 209, 215–219.

# Development of a Strong Beam Guardrail-to-Bridge-Rail Transition

ROGER P. BLYGH, DEAN L. SICKING, AND HAYES E. ROSS, JR.

**This study describes the development and testing of a strong beam guardrail-to-bridge-rail transition. Barrier VII was validated and used to simulate impacts with flexible barriers attached to a rigid barrier. Design curves for selecting transition design parameters of beam strength, post size, and post spacing are presented. The selected design incorporated a tubular W-beam rail element mounted on 7-inch round posts spaced on 3-foot, 1.5-inch centers. The transition was designed to simplify retrofit operations and can be used on bridges that require bridge-end drains. Three full-scale crash tests were conducted to verify the acceptable performance of the transition when attached to either a vertical concrete parapet or a concrete safety-shaped barrier.**

A bridge rail is a longitudinal barrier to prevent errant vehicles from going over the side of a bridge. Because of their critical nature, most bridge rails are either rigid or semi-rigid so they can limit dynamic deflections and safely contain a vehicle without allowing it to extend beyond the edge of the bridge deck. Two common types of bridge rails are reinforced concrete safety-shaped barriers and vertical concrete parapets. The exposed ends of these rigid concrete barriers can pose a serious safety hazard. Safety can be increased with approach roadside barriers. Approach roadside barriers are warranted not only to shield the exposed bridge rail end but also to prevent errant vehicles from getting behind the railing and falling off the bridge. These approach barriers are typically much more flexible than the bridge rails or wingwalls to which they are attached. Flexible barriers can deflect sufficiently to allow an errant vehicle to impact or "snag" on the end of the rigid barrier, even when the two barriers are securely attached. Therefore, a transition section is required whenever there is a significant change in lateral strength from the approach barrier to the bridge rail. The transition section should provide a smooth change in lateral barrier stiffness to prevent impacting vehicles from snagging on the end of the rigid barrier.

Strong post W-beam guardrail is the most common bridge approach railing in use today. Most existing transitions involve reducing guardrail post spacing to 3 feet, 1.5 inches near the end of the bridge rail. This transition design is unable to prevent severe snagging on the end of rigid concrete barriers (1). Several acceptable guardrail-to-bridge-rail transition designs using 1-foot, 6.75-inch post spacings and rub rails near the bridge end have been developed by Bronstad (1). Although these designs exhibit good impact performance, the tight post

spacing presents a problem when used on bridges designed to drain water around the end of the railing. The maximum distance between posts in these designs is only 12 inches— inadequate for most bridge end drain designs. Drainage problems are especially acute when the new transitions are used to retrofit existing bridge sites. Other acceptable transition designs were developed by Post and presented at the meeting of TRB's Committee on Roadside Safety Features in January 1987. These systems are characterized by oversized posts, reduced post spacing near the bridge end, nested W-beam or thrie-beam rails, and flared bridge rail ends. Problems associated with implementing these designs include inventory and repair problems arising from the use of nonstandard guardrail post and the high costs of flaring bridge rail ends during retrofit operations.

In view of the general lack of acceptable guardrail-to-bridge-rail transitions that can be economically implemented in retrofit situations, this study was undertaken to develop a new transition design with the following characteristics:

1. Provide for easy retrofit of existing installations.
2. Provide sufficient post spacing to allow implementation where bridge-end drains are required.
3. Design transitions for use with either vertical concrete parapets or concrete safety shaped barriers.
4. Meet nationally recognized safety standards.

## RESEARCH APPROACH

As mentioned previously, a guardrail-to-bridge-rail transition must be designed to prevent impacting vehicles from deflecting the guardrail sufficiently to allow vehicle snagging on the end of the stiffer barrier. Standards for testing barrier transitions are presented in NCHRP Report 230 (2). This report requires that transitions be evaluated with a single test that involves a vehicle impacting the more flexible barrier upstream from its transition to the stiffer barrier. This test condition examines the propensity for the flexible barrier to deflect and allow the test vehicle to snag on the end of the rigid barrier. The size of the test vehicle and impact speed and angle vary with the level of service of the barrier system (2). Most concrete bridge rails and strong-post guardrail systems have been tested to service level 2 as described in NCHRP Report 230. For service level 2, NCHRP Report 230 requires that transitions be tested with a 4,500-pound automobile, impacting at 60 miles per hour and 25 degrees. Note that in most practical guardrail-to-bridge-rail transition designs the guardrail is first transitioned into an intermediate strength barrier that is then

TABLE 1 POST PARAMETERS FOR BARRIER VII INPUT

MATERIAL	WOOD	WOOD	STEEL
SIZE	6" X 8" (1)	7" DIAM. (7)	W8 X 8.5 (1)
$k_A$ (k/in.)	1.95	2.9	1.15
$k_B$ (k/in.)	1.56	2.9	2.46
$M_A$ (in-k)	191.1	256.	256.2
$M_B$ (in-k)	214.2	256.	107.1
$F_A$ (k)	10.2	12.2	5.1
$F_B$ (k)	9.1	12.2	12.2
$\Delta_A$ (in.)	4.7	18.	13.6
$\Delta_B$ (in.)	15.5	18.	13.2

(Effective Rail Height = 21")

A - Denotes Longitudinal or Major Axis

B - Denotes Transverse or Minor Axis

k - Stiffness of Post For Elastic Horizontal Deflections

M - Base Moment At Which Post Yields

F - Shear Force Causing Failure of Post

 $\Delta$  - Deflection Causing Failure of Post

transitioned into the rigid bridge rail. Safety performance of the design must be evaluated at both transition points.

The Barrier VII simulation model (3) is capable of accurately predicting barrier deflections for impacts involving full-size vehicles impacting at speeds up to 60 miles per hour and angles up to 25 degrees (4, 5). Further, for impacts into barriers placed on flat terrain, such as that found on the approach to a bridge, vehicle vaulting, override, and underride is of little concern. Thus the 2-D nature of the Barrier VII program was not considered to be a severe limitation and this model was chosen for use in developing the new transition design.

Although Barrier VII has been successfully used to simulate impacts with a variety of flexible barriers, its use in studying impacts near the transition from a flexible to a rigid barrier has been somewhat limited. Therefore the first step in transition development was to conduct a limited validation of

Barrier VII for analysis of impacts in the region of a transition. Two full-scale crash tests of guardrail-to-bridge-rail transitions were selected from Bronstad et al. (1) for the validation effort. Simulated guardrail beam elements were assumed to be of uniform cross section and to have bilinear elastic/perfectly plastic properties both flexurally and extensionally. Simulated beam stiffness characteristics were estimated to be approximately 1.5 times calculated static values. Table 1 shows simulated post properties collected from Bronstad et al., Calcote, and Dewey et al. (1, 6, 7).

Since barrier deflection is the primary indicator of the propensity for a vehicle to snag on the concrete barrier, this parameter was selected as the primary measure of correlation between simulation and crash testing. As shown in Table 2, Barrier VII was found to give very good predictions of maximum barrier deflections for the two tests simulated. Other measures of simulation validity, including vehicle trajectory and crush, also showed excellent correlation between Barrier VII and the two crash tests.

The critical impact point for testing guardrail-to-bridge-rail transitions is the point at which the potential for snagging on the end of the rigid barrier is maximized. Note that this critical impact point changes with the stiffness of the approach barrier. Stiff approach barriers redirect impacting vehicles more quickly and therefore have a critical impact point nearer to the rigid barrier than more flexible approach rails. Bronstad (1) determined that for double W-beam rails mounted on posts spaced 1 foot, 6.75 inches apart, the critical impact point was approximately 112 inches upstream of the rigid barrier. Barrier VII simulations indicated that the critical impact location is the same for approach barriers that deflect approximately the same as those used in the study by Bronstad (1). Therefore this impact location was used for all simulation and testing of transitions to rigid barriers. Further, Barrier VII analysis indicated that the critical impact location on standard strong post guardrails is approximately 125 inches from the end of the intermediate barrier. Therefore, analysis and testing of impacts on standard guardrails was conducted using an impact point 125 inches upstream from the start of the transition.

Barrier VII was used to conduct a parameter study of designs for transitions to rigid barriers. All simulations involved impacts with a 4,500-pound vehicle traveling 60 miles per hour and

TABLE 2 BARRIER VII CRASH TEST SIMULATIONS

TEST NO.	DESCRIPTION	CONCRETE WINGWALL	IMPACT DATA	IMPACT POINT FROM WINGWALL	MAXIMUM LATERAL DEFLECTION		
			LB/MPH/DEG		ACTUAL	SIMULATED	% DIFF
T-1 (1)	THREE BEAM BRIDGE TRANSITION	STRAIGHT	4858/61.5/25.2	96.5"	9.4"	9.92"	5.5
T-2 (1)	THREE BEAM BRIDGE TRANSITION	TAPERED w/ WOOD BLOCK OUT	4850/64.0/25.6	112.5"	14.4"	14.74"	2.4

contacting the rail 112 inches upstream of the rigid barrier end at an angle of 25 degrees. The basic transition design consisted of a standard strong-post W-beam approach rail with modified post spacing and beam strength over the last 25 feet before the bridge rail. The bridge rail was modeled as a straight vertical concrete parapet. Design parameters investigated include beam strength, post spacing, and post size. The two post sizes investigated were a standard 7-inch diameter wood post and a "double strength" post. A double strength post was defined as a post that would develop twice the dynamic lateral resistance of the standard post. This can be achieved by increasing the post section modulus and either embedment

depth or post width. Examples of double strength posts are an 8-inch  $\times$  8-inch wood post embedded approximately 48 inches and a 10-inch  $\times$  10-inch wood post embedded 40 inches. Figures 1 and 2 show predicted deflections for the two different post sizes studied. These figures were used to determine the barrier deflection that could be expected for a wide range of beam strengths and post spacings. Note that 6-inch  $\times$  8-inch wood posts and W 6  $\times$  9 steel posts have dynamic lateral capacity similar to 7-inch diameter round wood posts. Thus, although figure 1 was developed for a 7-inch round post, either of these other posts could be substituted as the deflectors.

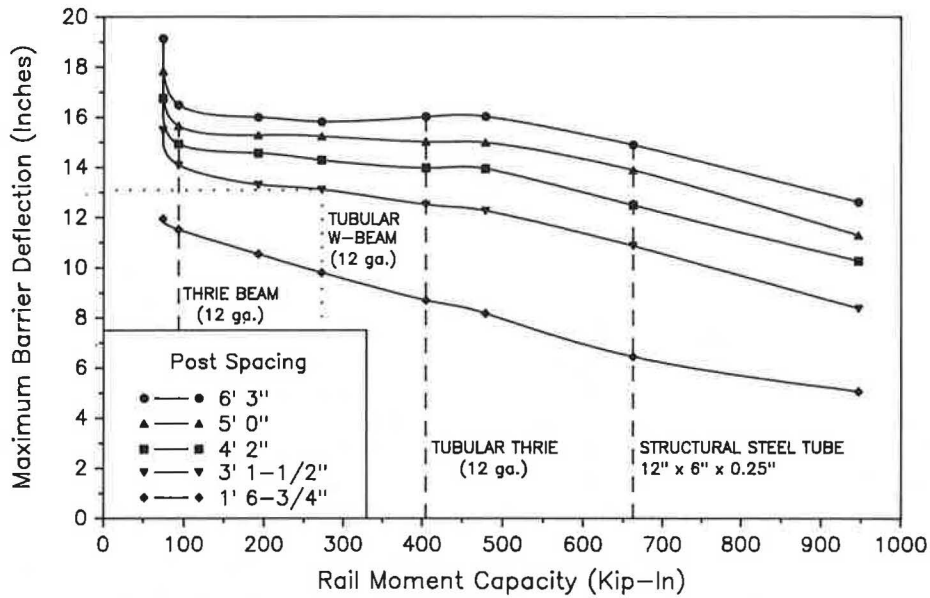


FIGURE 1 Design curves for standard post transitions.

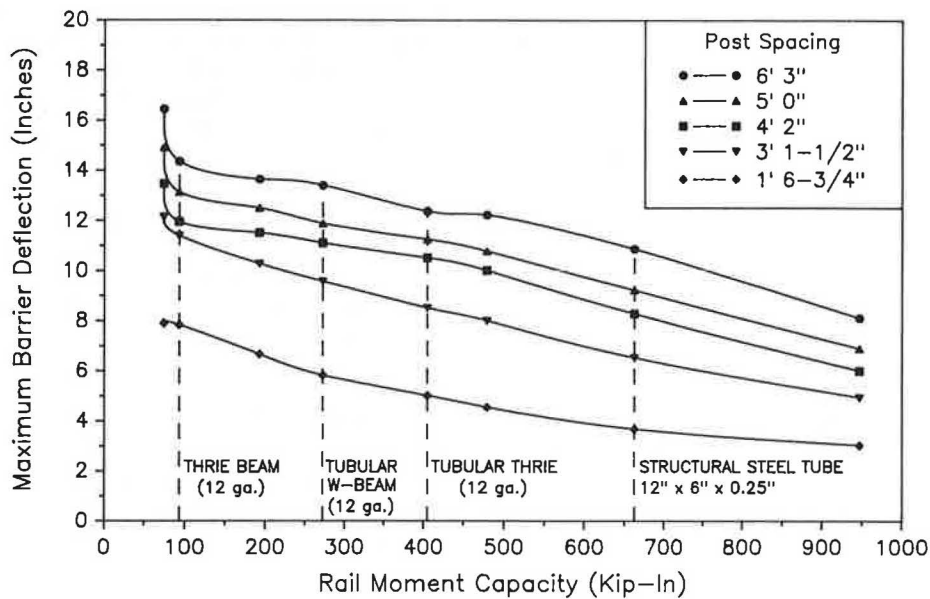


FIGURE 2 Design curves for double strength post transitions.

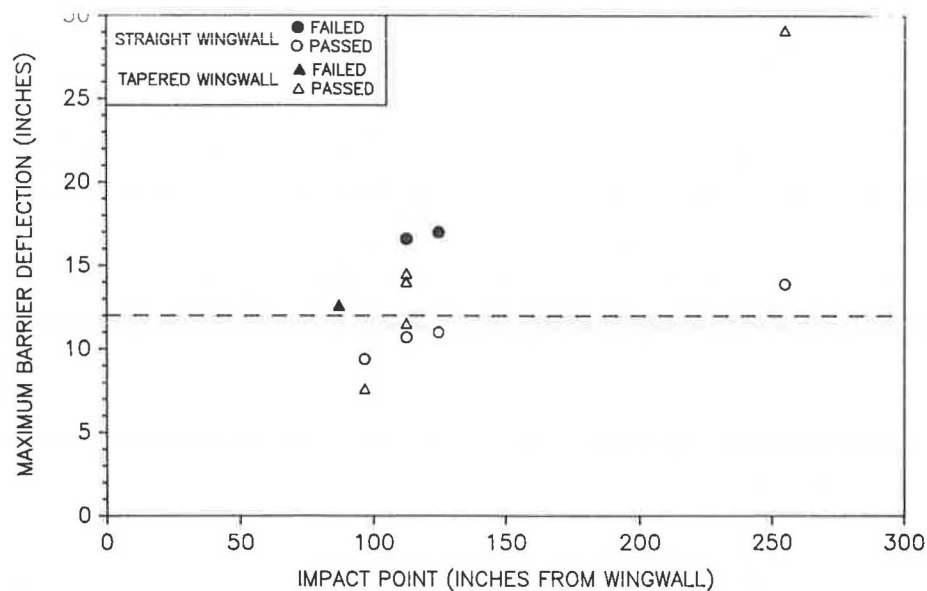


FIGURE 3 Maximum deflection from transition crash tests (I).

### DEFLECTION LIMIT DESIGN CRITERIA

As discussed above, barrier deflection is believed to be a good indicator of the probability of a vehicle snagging on the end of a rigid barrier. Twelve full-scale crash tests taken from Bronstad et al. (1) were reviewed in an effort to determine the maximum allowable barrier deflection for each of the tests conducted in the referenced study. As shown in Figure 3, for unflared bridge rail ends, the approach guardrail can be allowed to deflect no more than 12 inches before significant vehicle snagging becomes a potential problem. In support of the crash test data, a series of simulation runs were made to track wheel position past the end of the rigid barrier end. It was observed that for deflections in excess of 12 inches, the wheel followed a trajectory through the end of the concrete barrier, indicative of severe vehicle snagging and poor safety performance for the transition. However, for barrier deflections less than 12 inches the wheel followed a path safely outside of the bridge rail end. These results supported a deflection limit of 12 inches as the initial evaluation criteria in the transition design. It was concluded that all transition designs limiting maximum lateral deflections to less than 12 inches should provide acceptable performance.

### SELECTION OF TRANSITION SYSTEM

Using Figures 1 and 2, a basic design is selected by choosing the type of post to be used (i.e., standard or strong) and either the post spacing or beam type desired. The remaining parameter is then found using the 12-inch deflection limit discussed above. For example, if it is desirable to maintain a 6-foot, 3-inch post spacing, a transition design would involve a beam with a yield moment of 660-kip-inch (such as a 12-inch  $\times$  6-inch  $\times$  0.25-inch structural steel tube) mounted on strong posts. This system has a predicted maximum barrier deflection of approximately 11 inches (see Figure 2). Similarly, if it is desirable to use a nested thrie beam ( $M_y = 190$

kip-in.) in the transition zone, one alternative would be to mount it on "strong" posts spaced at 3 feet, 1.5 inches. This transition configuration has a predicted dynamic deflection of approximately 10.5 inches (see Figure 2).

As can be seen from Figures 1 and 2, numerous transition configurations were acceptable based on the 12-inch deflection limit criteria. Additional selection guidelines were established to aid in the determination of a final design. The transition should (1) be able to retrofit existing bridge rails, (2) provide sufficient post spacing to allow for adequate bridge end drainage, (3) allow for ease of transition at both approach rail and bridge rail, and (4) use standard hardware items.

Consultations with officials from the Texas State Department of Highways and Public Transportation (SDHPT) indicated that, because of inventory and maintenance problems associated with nonstandard guardrail posts, the new transition should be constructed with standard guardrail posts. Further, SDHPT engineers expressed an interest in developing a transition that used a 12 gauge tubular W-beam rail. This beam has an approximate moment capacity of 280 kip-inches. As shown in Figure 1, Barrier VII predicts a maximum deflection of 13 inches for the tubular W-beam mounted on standard posts spaced 3 feet, 1.5 inches. Although the predicted deflection for this design is slightly above the deflection limit criteria, it was believed that the added depth of tubular W-beam would act as an effective blockout. Thereby, effective deflection of the beam would be reduced to 10 inches, which is well below the deflection limit of 12 inches.

### TRANSITION DESIGN

The final transition design consisted of a 25-foot segment of 12 gauge tubular W-beam mounted on 7-inch diameter round wood posts spaced 3 feet, 1.5 inches apart with a 38 inch embedment as shown in Figure 4. In an effort to identify other potential snagging problems and to determine the necessary connection design loadings, Barrier VII was then used

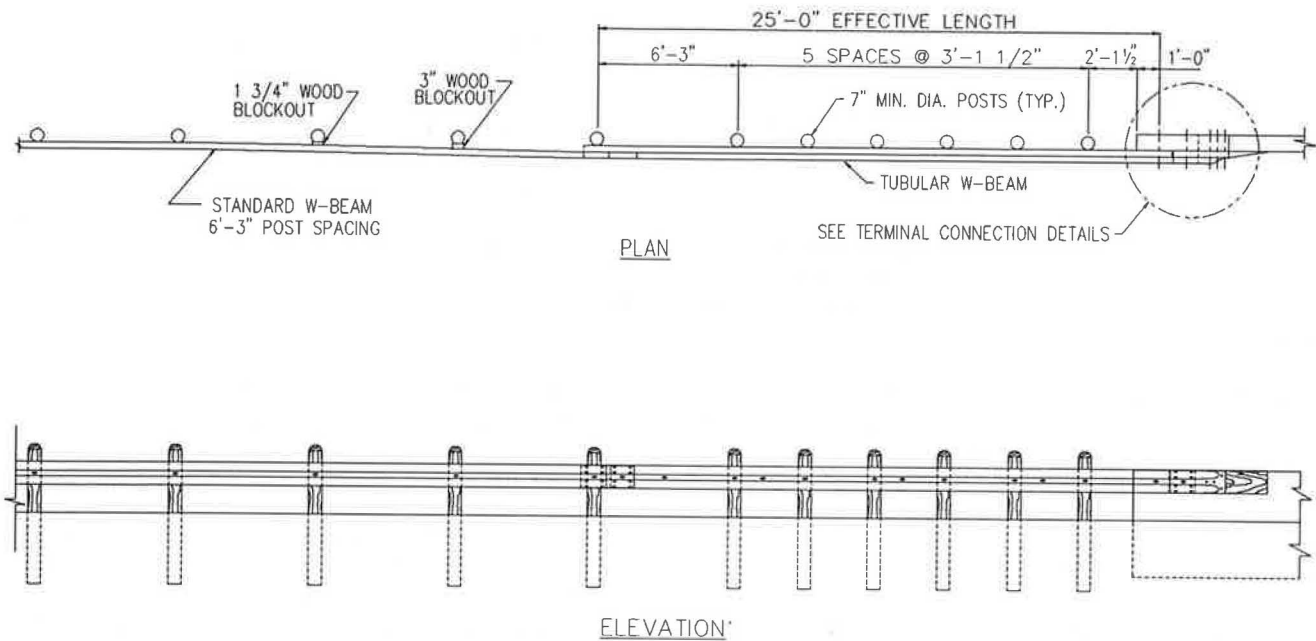


FIGURE 4 Guardrail-to-bridge-rail transition, retrofit design.

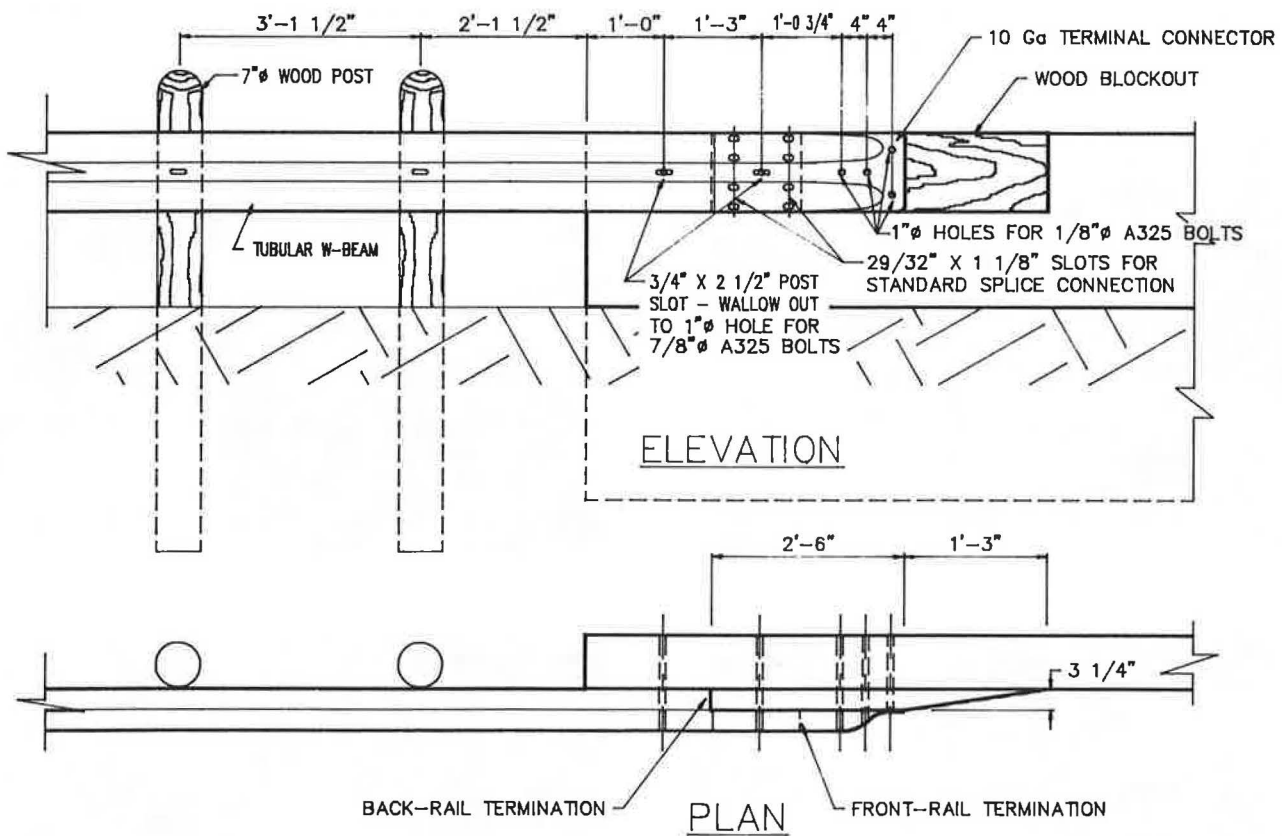


FIGURE 5 Terminal connection details.

to simulate impacts with the selected design at a number of locations. Barrier VII predicted that for impacts on the upstream transition from the single W-beam to the tubular W-beam, the possibility of wheel snagging would be reduced if the first post spacing on the tubular segment was maintained at 6-foot, 3-inch. Design loading conditions from Barrier VII for the connection between the tubular W-beam and the concrete

barrier end included a 140-kip tensile force, a 60-kip shear force, and a 280-kip-in. bending moment. This connection was accomplished with six 7/8-inch diameter high strength bolts (A325 or equivalent grade threaded rod), a steel end shoe, and a tapered wood blockout as shown in Figure 5. The connection was designed to be used with either vertical parapets or concrete safety-shaped barriers.



Note that the design shown in Figure 4 is a retrofit of the existing Texas standard transition and uses two small wood blockouts on the standard W-beam approach in order to move the rail to the outside of the tubular beam. No blocks were used in the rest of the transition to maintain compatibility with the Texas standard guardrail. Further, due to retrofit considerations, the attachment between the single W-beam barrier and the tubular W-beam rail required a small splice plate. Retrofitting an existing installation thus involves replacing a 25-foot length of W-beam railing, drilling six holes in the concrete barrier, and placing two small blockouts in the approach rail. In addition, an analysis of the bridge rail end should be made to ensure adequate strength and anchorage for carrying the increased impact forces transmitted by a strong beam transition because a strong beam barrier system is capable of transferring more shear and moment to the bridge rail end than the common flexible W-beam guardrail.

### FULL-SCALE CRASH TESTS

The tubular W-beam transition was evaluated for impact performance in accordance with Test Number 30 of NCHRP Report 230 (2). Test 30 involves a 4,500-pound vehicle impacting the transition section at 60 miles per hour at an angle of 25 degrees. The testing program consisted of three full-scale

crash tests, each of which evaluated a different aspect of the transition design. The tests conducted were as follows:

1. Evaluation of tubular W-beam transitioning into a vertical concrete parapet.
2. Evaluation of tubular W-beam transitioning into a concrete safety-shaped barrier.
3. Evaluation of the standard W-beam guardrail transitioning to the tubular W-beam.

#### Test 1

This test evaluated the tubular W-beam transition to a vertical concrete wall. The barrier transition was constructed as shown in Figure 4. Figure 6 shows the completed installation before Test 1.

A 4,570-pound Cadillac impacted the transition at 55 miles per hour and 26.4 degrees at a point 112 inches upstream from the bridge rail end. The vehicle was successfully redirected although significant wheel snagging on the bridge rail end was observed. Some sheet metal snagging occurred at the tops of the posts and minor wheel snagging occurred at the base of the posts. While the top of the tubular rail was only partially flattened, the bottom half of the rail was completely collapsed. This collapse effectively increased the maximum deflection of the rail and thus the degree of snagging. The test vehicle was

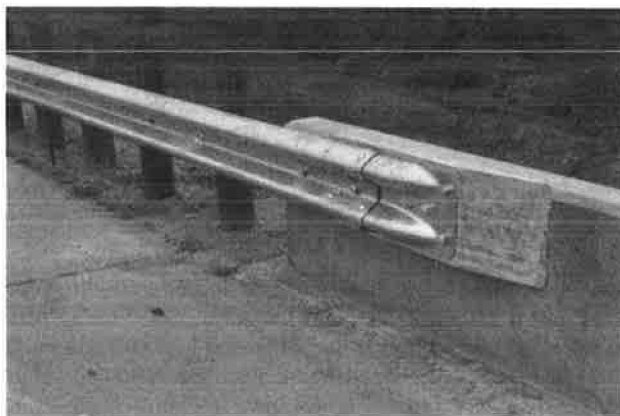
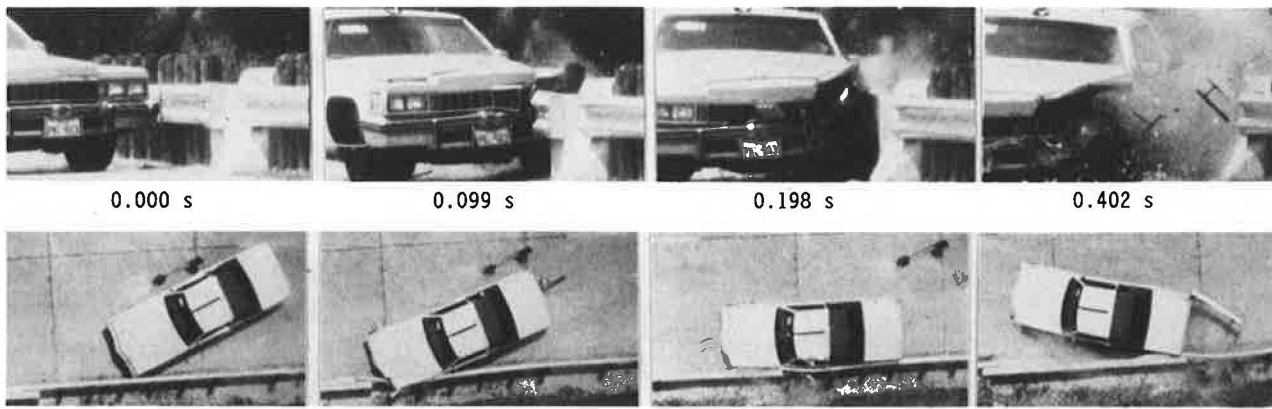


FIGURE 6 Tubular W-beam transition to vertical wall, Test 1 installation.

FIGURE 7 Vehicle and barrier damage after Test 1.



Test No . . . . .	2461-1
Date . . . . .	5/14/87
Test Installation . . . . .	Tubular W-Beam
	Transition to T201
Length of Transition . . . . .	25 ft (7.6 m)
Vehicle . . . . .	1977 Cadillac
Vehicle Weight	
Test Inertia . . . . .	4400 lb (1998 kg)
Gross Static . . . . .	4570 lb (2075 kg)
Vehicle Damage Classification	
TAD . . . . .	11LFQ6
CEC . . . . .	11LFES4
Maximum Vehicle Crush . . . . .	13.0 in (33.0 cm)
Max. Dyn. Rail Deflection . . . . .	9.6 in (24.4 cm)
Max. Perm. Rail Deformation . . . . .	4.8 in (12.2 cm)

Impact Speed . . . . .	55.0 mi/h (88.5 km/h)
Impact Angle . . . . .	26.4 deg
Exit Speed . . . . .	33.1 mi/h (53.3 km/h)
Exit Angle . . . . .	13.4 deg
Vehicle Accelerations	
(Max. 0.050-sec Avg)	
Longitudinal . . . . .	-8.0 g
Lateral . . . . .	-9.4 g
Occupant Impact Velocity	
Longitudinal . . . . .	26.7 ft/s (8.1 m/s)
Lateral . . . . .	22.0 ft/s (10.0 m/s)
Occupant Ridedown Accelerations	
Longitudinal . . . . .	-3.1 g
Lateral . . . . .	-11.5 g

FIGURE 8 Summary of results for Test 1.

only moderately damaged, considering the severity of the test. Damage to both the vehicle and barrier after Test 1 are shown in Figure 7. Note that hood snagging on the top of the wood posts and the concrete barrier was not considered to be a significant hazard since the hood rides up the post or barrier until it slips off of the top. There was no tendency for the hood to become detached from its hinges and penetrate the occupant compartment.

NCHRP Report 230 (2) does not require that a strength test such as that used for evaluation of transition designs meet occupant severity limits. However, the occupant severity measures from Test 1 were all within maximum acceptable limits. A summary of the test results is given in Figure 8.

Although the change in vehicle velocity was above the recommended value set forth in NCHRP 230 Evaluation Criteria I (2), this test was considered to be a success as presented in Discussion of Results.

**Test 2**

This test evaluated the tubular W-beam transition to the concrete safety-shaped barrier. The geometry of the safety-shaped rail increases the potential for vehicle snagging. The lower curb face of the barrier projects beyond the face of the tubular W-beam and the 32-inch wall height extends above the approaching guardrail. Some modifications were made to reduce the severity of snagging observed in Test 1. Wood inserts were added in both the top and bottom of the tubular W-beam to prevent the rail from collapsing (see Figure 9). Also, the tops

of the posts were cut at rail height with a 10-degree bevel to minimize sheet metal snagging. Figure 10 shows the modified transition before Test 2.

A 4,637 pound Cadillac impacted the transition at 60.8 miles per hour and 25.8 degrees at a point 112 inches upstream from the bridge rail end. The vehicle was smoothly redirected with



FIGURE 9 Wood inserts for tubular W-beam.

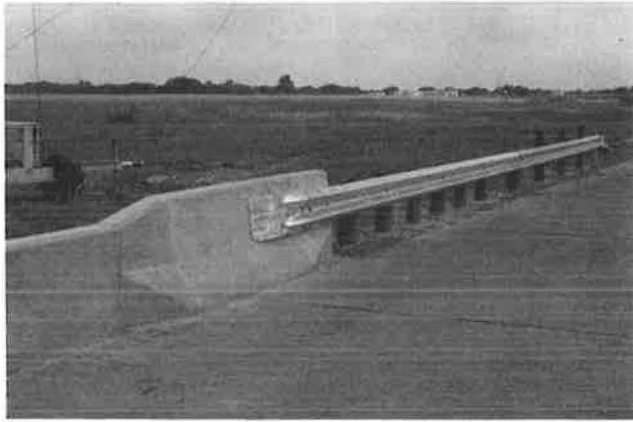


**FIGURE 10** Tubular W-beam transition to CSSB, Test 2 installation.



**FIGURE 12** Vehicle and barrier damage after Test 2.

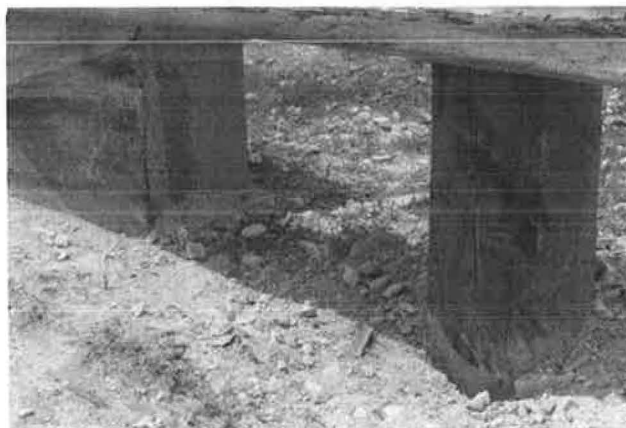
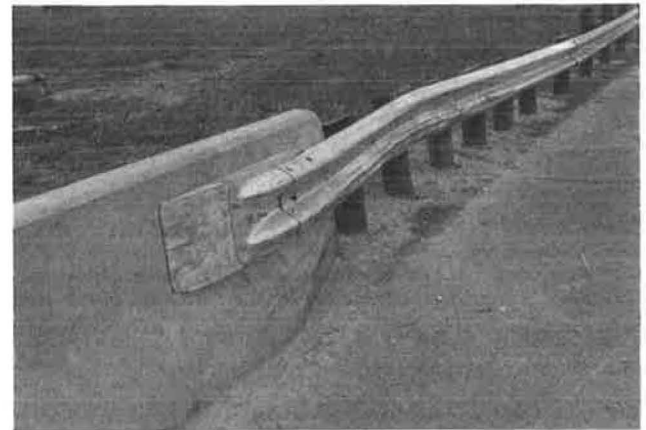


**FIGURE 11** Evidence of snagging on posts and concrete wall.



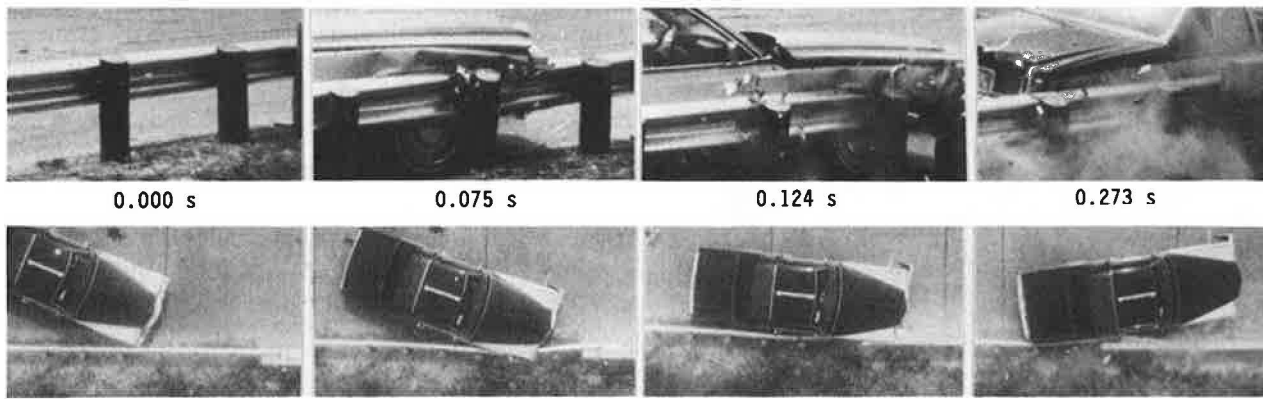
greatly improved performance over Test 1. The wood inserts prevented the tubular rail from collapsing and greatly reduced the degree of snagging. Minor wheel snagging was observed at the base of posts 1 and 2 and at the bridge rail end. Although some sheet metal snagging occurred on the top of the concrete rail, the forces involved appeared to be significantly lower than in the previous test. Evidence of the post and wingwall snagging is shown in Figure 11.

The vehicle damage sustained in Test 2 was moderate for the severity of the impact. Damage to the vehicle and barrier after Test 2 is shown in Figure 12. Although not a requirement for the transition test, the occupant impact indexes of NCHRP Report 230 (2) were all within maximum acceptable limits. A summary of Test 2 results is given in Figure 13.

### Test 3

This test evaluated the performance of the W-beam transition to the tubular W-beam. The guardrail was not blocked out for this test except for the use of two small blockouts as spacers to back up the W-beam after the tubular W-beam terminated. Figure 14 shows the installation before Test 3.

A 4,595-pound Cadillac impacted the rail at 61.8 miles per



Test No . . . . . 2461-2  
 Date . . . . . 5/28/87  
 Test Installation . . . . . Tubular W-Beam  
 Transition to T501  
 Length of Transition . . . . . 25 ft (7.6 m)  
 Vehicle . . . . . 1979 Cadillac  
 Vehicle Weight  
 Test Inertia . . . . . 4470 lb (1998 kg)  
 Gross Static . . . . . 4637 lb (2075 kg)  
 Vehicle Damage Classification  
 TAD . . . . . 11LFQ5  
 CEC . . . . . 01RYES3  
 Maximum Vehicle Crush . . . . . 7.0 in (17.8 cm)  
 Max. Dyn. Rail Deflection . . . . . 9.6 in (24.4 cm)  
 Max. Perm. Rail Deformation . . . . . 6.0 in (12.2 cm)

Impact Speed . . . . . 60.8 mi/h (97.8 km/h)  
 Impact Angle . . . . . 25.8 deg  
 Exit Speed . . . . . 41.4 mi/h (66.6 km/h)  
 Exit Angle . . . . . 15.0 deg  
 Vehicle Accelerations  
 (Max. 0.050-sec Avg)  
 Longitudinal . . . . . -7.8 g  
 Lateral . . . . . -10.6 g  
 Occupant Impact Velocity  
 Longitudinal . . . . . 24.6 ft/s (7.5 m/s)  
 Lateral . . . . . 24.1 ft/s (7.3 m/s)  
 Occupant Ridedown Accelerations  
 Longitudinal . . . . . -2.9 g  
 Lateral . . . . . -13.8 g

FIGURE 13 Summary of results for Test 2.

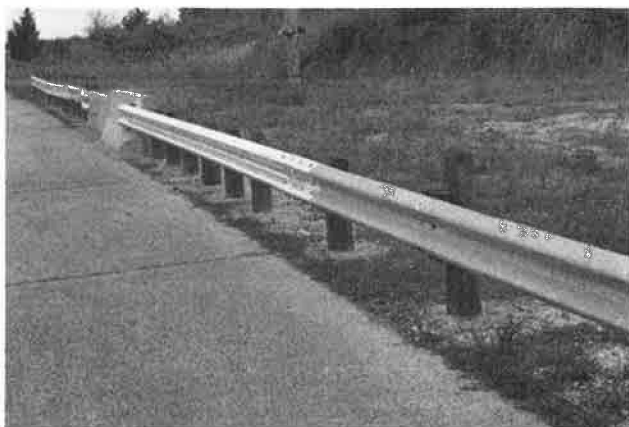


FIGURE 14 W-beam to tubular W-beam transition, Test 3 installation.



FIGURE 15 Vehicle damage after Test 3.

hour and 24.2 degree, 125 inches upstream from the end of the tubular W-beam. Although significant wheel snagging was observed at several posts, the vehicle was safely redirected. The wheel snagging caused the post at the splice connection to separate from the rail and the next post downstream to splinter. This wheel snagging can be virtually eliminated through the use of rail-to-post blockouts in the transition region.

Vehicle damage was primarily concentrated in the area of the right front wheel, which snagged on a number of posts.

Figure 15 shows vehicle damage after Test 3. Barrier damage after Test 3 is shown in Figure 16.

The exit angle and change in velocity of the test vehicle were above the recommended values of NCHRP Report 230 Evaluation Criteria I (2). Blockouts throughout the length of the transition should greatly improve overall performance and correct the deficiencies mentioned above. Although not required for evaluation of a transition, all of the occupant severity measures from Test 3 were within recommended lim-



FIGURE 16 Barrier damage after Test 3.

its set forth in NCHRP Report 230 (2). A summary of the test results is given in Figure 17.

## DISCUSSION OF RESULTS

The tubular W-beam transition was judged to have met the intent of the performance criteria set forth in NCHRP Report 230 (2). The transition test is, first and foremost, a strength test. In this regard, the tubular W-beam transition has been shown to be able to contain and redirect a 4,500-pound vehicle impacting at a high speed and angle.

It is noted that for all three tests, the change in vehicle velocity exceeded the 15 miles per hour value recommended in NCHRP 230 Evaluation Criteria I (2). Although meeting this criteria is desirable, it is believed that strict compliance to this factor is not critical. This criteria is a subjective evaluation based on whether or not the vehicle is judged to have been redirected into or stopped while in adjacent traffic lanes. In all three crash tests described herein, the test vehicle returned

to the side of the road after a short time interval and was not projected across traffic lanes. Depending on the existence and width of a shoulder, the test vehicles may or may not have briefly encroached on adjacent traffic lanes.

The primary intent of Evaluation Criteria I is to prevent the redirected vehicle from becoming a potential hazard to other traffic. It should be noted that, at this time, there is no definitive evidence that post impact trajectory is a serious problem. Further, impacting the transition at such a severe speed and angle is a low probability event. Although, as stated above, the change in vehicle velocity exceeded the recommended value of 15 miles per hour, the occupant impact velocities and ridedown accelerations were within maximum acceptable limits (2) for all three tests. This fact suggests that the severity of impact was well within tolerance limits.

## NEW CONSTRUCTION TRANSITION DESIGN

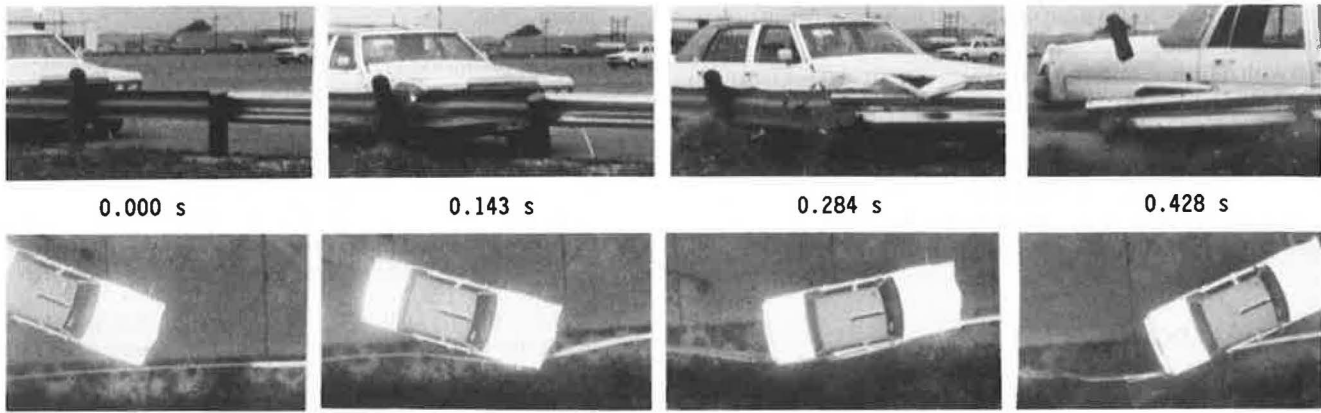
It should be emphasized that the design that was crash tested is a retrofit of the existing Texas standard transition. The basic tubular W-beam design can be adapted for new construction applications by simply moving the entire single W-beam approach barrier 15 inches closer to the end of the concrete carrier. This adjustment will eliminate the need for a splice plate and will allow the single W-beam to be spliced directly onto the front rail of the tubular W-beam. Further, the posts upstream from the tubular W-beam (i.e., the posts to which the single W-beam approach rail is attached) can be offset 3 inches closer to the roadway. This will eliminate the need for the spacer blocks at the end of the single W-beam.

The modifications described above are intended to reduce the number of details in the transition design and, thereby, aid in the ease of field installation. Further changes can be implemented to improve the impact performance of the design. The exposed end of the concrete bridge rail may be beveled or flared. This should further reduce the possibility of wheel snag and could eliminate the need for the wood inserts used in Test 2. Finally, blockouts can be provided in the transition region. Blockouts would effectively eliminate wheel snagging on guardrail posts and should improve the overall impact performance of the barrier. A conceptual transition design that uses all of the above modifications is shown in Figure 18. Any or all of these variations may be used to improve upon the retrofit transition.

## CONCLUSIONS AND RECOMMENDATIONS

A guardrail-to-bridge-rail transition from a W-beam to a rigid concrete barrier has been successfully designed and crash tested. A number of favorable characteristics have been incorporated into the design to help ensure acceptance and implementation in both retrofit and new construction applications. The tubular W-beam transition can easily retrofit existing installations, provides sufficient post spacing to allow implementation where bridge-end drains are required, and is designed for use with either a vertical concrete parapet or concrete safety-shaped barrier.

Although the change in vehicle velocity for these tests exceeded the recommended value of Evaluation Criteria I (2), it should be noted that the system that was tested is a



Test No . . . . . 2461-3  
 Date . . . . . 6/08/87  
 Test Installation . . . . . W-Beam Transition  
 to Tubular W-Beam  
 Length of Transition . . . . . 25 ft (7.6 m)  
 Vehicle . . . . . 1979 Cadillac  
 Vehicle Weight  
 Test Inertia . . . . . 4430 lb (2011 kg)  
 Gross Static . . . . . 4595 lb (2086 kg)  
 Vehicle Damage Classification  
 TAD . . . . . 11LFQ5  
 CEC . . . . . 01RYES3  
 Maximum Vehicle Crush . . . . . 12.0 in (30.5 cm)  
 Max. Dyn. Rail Deflection . . . . . 2.6 in (0.8 cm)  
 Max. Perm. Rail Deformation . . . . . 2.0 in (0.6 cm)

Impact Speed . . . . . 61.8 mi/h (99.4 km/h)  
 Impact Angle . . . . . 24.2 deg  
 Exit Speed . . . . . 33.6 mi/h (54.1 km/h)  
 Exit Angle . . . . . 18.1 deg  
 Vehicle Accelerations  
 (Max. 0.050-sec Avg)  
 Longitudinal . . . . . -6.2 g  
 Lateral . . . . . 7.9 g  
 Occupant Impact Velocity  
 Longitudinal . . . . . 25.7 ft/s (7.8 m/s)  
 Lateral . . . . . 17.4 ft/s (5.3 m/s)  
 Occupant Ridedown Accelerations  
 Longitudinal . . . . . -10.1 g  
 Lateral . . . . . 10.3 g

FIGURE 17 Summary of results for Test 3.

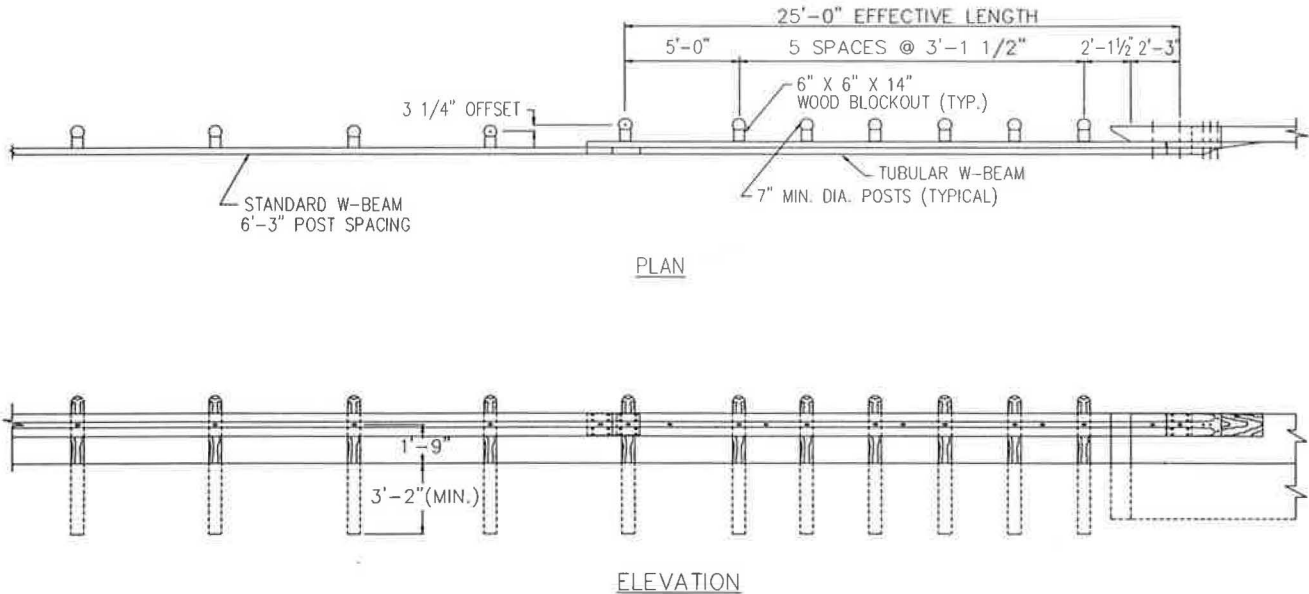


FIGURE 18 New construction transition.

retrofit design. To maintain compatibility with the standard Texas system, no blockouts were used. It is believed that the use of blockouts throughout the length of guardrail would eliminate post snagging.

Because of improved impact performance, it is recommended that the modified transition with wood inserts be used

in conjunction with both the vertical parapet and safety-shaped barriers. The wood inserts are necessary to eliminate the propensity for the tubular beam to collapse.

For new construction applications it is recommended that the end of the concrete bridge rail be beveled or flared to reduce the potential for wheel snag. These modifications will

eliminate the need for wood reinforcement of the tubular W-beam. Although this system was developed for a 7-inch diameter round wood post, it is believed that it will perform equally well with 6-inch  $\times$  8-inch wood or W 6  $\times$  9 steel posts because they have equivalent lateral strength characteristics.

The transition developed in this study greatly simplifies retrofit operations and offers designers an alternative for new construction projects. Based on the results of the full-scale testing, the tubular W-beam transition is suitable for immediate implementation for field evaluation.

#### ACKNOWLEDGMENTS

This research study was conducted under a cooperative program between the Texas Transportation Institute (TTI), the Texas State Department of Highways and Public Transportation (SDHPT), and the Federal Highway Administration (FHWA). John Panak, Harold Cooner, and Mark Marek of the SDHPT worked closely with the researchers and provided valuable input to this study. The authors are very appreciative of their comments and suggestions.

#### REFERENCES

1. M. E. Bronstad, L. R. Calcote, M. H. Ray, M. H., and J. B. Mayer. *Guardrail-Bridge Rail Transition Designs*. Report FHWA-RD-86-178, FHWA, U.S. Department of Transportation, 1986.
2. Jarvis D. Michie. *NCHRP Report 230: Recommended Procedures for the Safety Performance Evaluation of Highway Appurtenances*. TRB, National Research Council, Washington, D.C., 1981.
3. G. H. Powell. *A Computer Program for Evaluation of Automobile Barrier Systems*. Report No. FHWA-RD-73-51. FHWA, U.S. Department of Transportation, 1973.
4. H. E. Ross, Jr. Analysis and Design of Safety Appurtenances by Computer Simulation. *Proc., ASCE Specialty Conference on the Role of the Civil Engineer in Highway Safety*, New Orleans, La., 1983.
5. W. Lynn Beason et al. A Low-Maintenance, Energy-Absorbing Bridge Rail. In *Transportation Research Record 1065*, TRB, National Research Council, Washington, D.C., 1986.
6. L. R. Calcote. *Development of a Cost-Effectiveness Model for Guardrail Selection*. Southwest Research Institute Report 03-4309, FHWA contract DOT-FH-11-8827, Nov. 1977.
7. James F. Dewey, Jr., et al. *A Study of the Soil Structure Interaction Behavior of Highway Guardrail Posts*. Texas Transportation Institute Research Report 343-1, Texas A&M University, College Station, 1983.

---

*The contents of this paper reflect the views of the authors, who are responsible for the opinions, findings, and conclusions presented herein. This paper does not necessarily reflect the official views or policies of the Texas State Department of Highways and Public Transportation or the Federal Highway Administration.*

gories. This would, for example, allow for determining the incremental effects of sideslopes of 2:1 or steeper, 3:1, 4:1, 5:1, 6:1, and 7:1 or flatter. The best sideslope model of this type was as follows:

$$AS = 731.16 (0.839)^W (0.99995)^{ADT} (0.975)^{RECC} (0.909)^{SW} \\ \times (1.373)^{SS1} (1.349)^{SS2} (1.238)^{SS3} (1.164)^{SS4} (1.091)^{SS5}$$

where

- SS1 = 1 if sideslope = 2:1 or steeper, or zero otherwise,
- SS2 = 1 if sideslope = 3:1, or zero otherwise,
- SS3 = 1 if sideslope = 4:1, or zero otherwise,
- SS4 = 1 if sideslope = 5:1, or zero otherwise,
- SS5 = 1 if sideslope = 6:1, or zero otherwise.

For a sideslope of 7:1 or flatter, the last five terms of the equation would each become 1.0. For a sideslope of 2:1 or 1:1, the last four terms of the equation become 1.0 and the term  $(1.373)^{SS1} = (1.373)^1 = 1.373$ , so the remaining terms of the equation are multiplied by a factor of 1.373. Likewise, for a sideslope of 3:1, the corresponding factor would be 1.349, and so on.

This model indicates that the rate of single-vehicle accidents decreases steadily for sideslope categories of 3:1, 4:1, . . . to 7:1 or flatter, as illustrated in figure 2. Figure 2 shows a ratio of the single-vehicle accident rate for a given sideslope to the single-vehicle accident rate for a sideslope of 7:1 or flatter. These values are based on the coefficients from the predictive model and using the 7:1 or flatter category as the basis of comparison. A review of figure 2 shows, for example, that the single-vehicle accident rate is 1.24 times higher on roads with a 4:1 sideslope than on roads with a sideslope of 7:1 or flatter. Note that little difference is found for sideslopes of

3:1, compared to those of 2:1 or steeper. This indicates that flattening sideslopes from 2:1 or steeper to 3:1 would be of little, if any, value in reducing single-vehicle accidents.

Based on the model results for various sideslopes, table 5 was developed to show likely reductions in single-vehicle accidents due to various sideslope flattening projects. Table 5 indicates that flattening a sideslope of 2:1 on a two-lane rural highway would be expected to reduce single-vehicle accidents by two percent if flattened to 3:1, 10 percent if flattened to 4:1, and 27 percent if flattened to 7:1 or flatter. Similarly, flattening a 4:1 sideslope to 7:1 or flatter would be expected to yield a 19 percent reduction in single-vehicle accidents.

The  $R^2$  value for the above model was 0.19, which indicates that only 19 percent of the variation in the single-vehicle accident rate is explained by the variables in the model. While this may appear to be less than desirable, it should be remembered that high  $R^2$  values rarely result from predictive modeling of accident experience, due to random accident fluctuations, imperfect accident reporting systems, effects of driver and vehicle factors on accidents, and other reasons. Also, accident rates tend to fluctuate widely, particularly on low volume roads.

In spite of the  $R^2$  value, the model was found to be desirable in terms of reasonableness of the coefficients, significance of the model (at the 0.0001 level), inclusion of important variables (each of which had a significant effect on single-vehicle accidents), logical relationships between accidents and other variables, and reasonable predictive ability compared with real-world data.

Figure 3 shows the single-vehicle accident rate expected for six categories of sideslope and for 9-foot to 12-foot lane widths based on the predictive model. All curves are for sections with an ADT of 1,000, a shoulder width of 4 feet, and a 10-

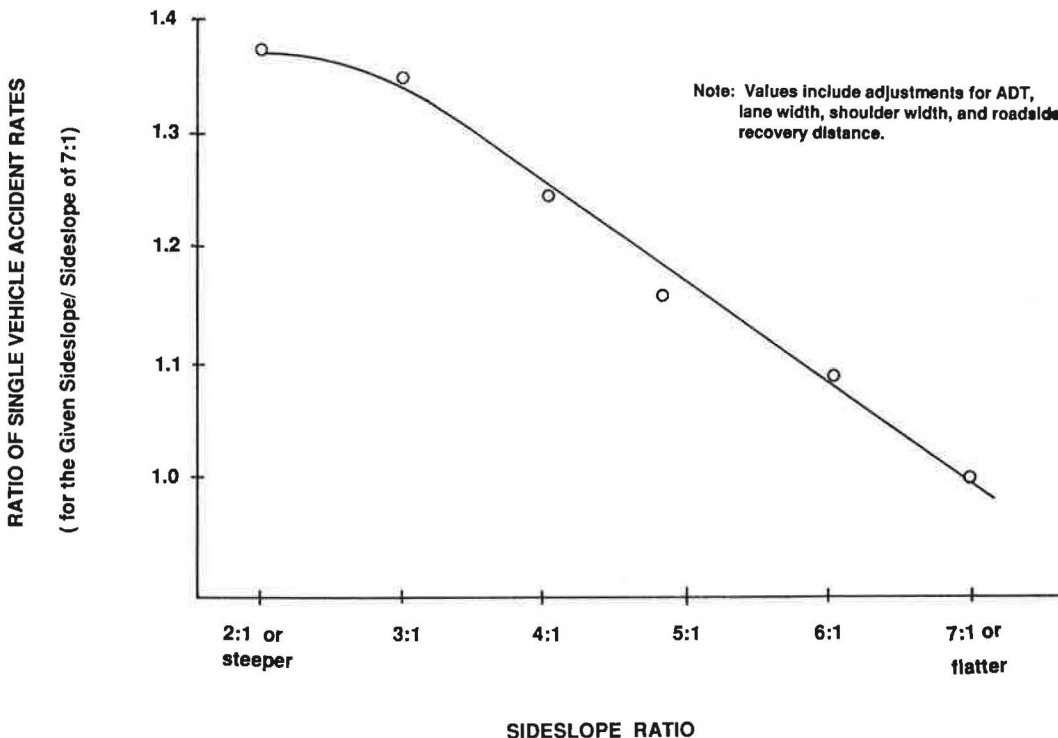


FIGURE 2 Plot of single-vehicle accident rate for a given sideslope versus single-vehicle accident rate for a sideslope of 7:1 or flatter.



TABLE 5 SUMMARY OF EXPECTED PERCENT REDUCTION IN SINGLE-VEHICLE ACCIDENTS DUE TO SIDESLOPE FLATTENING

Sideslope Ratio in Before Condition	Sideslope Ratio in After Condition				
	3:1	4:1	5:1	6:1	7:1 or Flatter
2:1	2	10	15	21	27
3:1	0	8	14	19	26
4:1	-	0	6	12	19
5:1	-	-	0	6	14
6:1	-	-	-	0	8

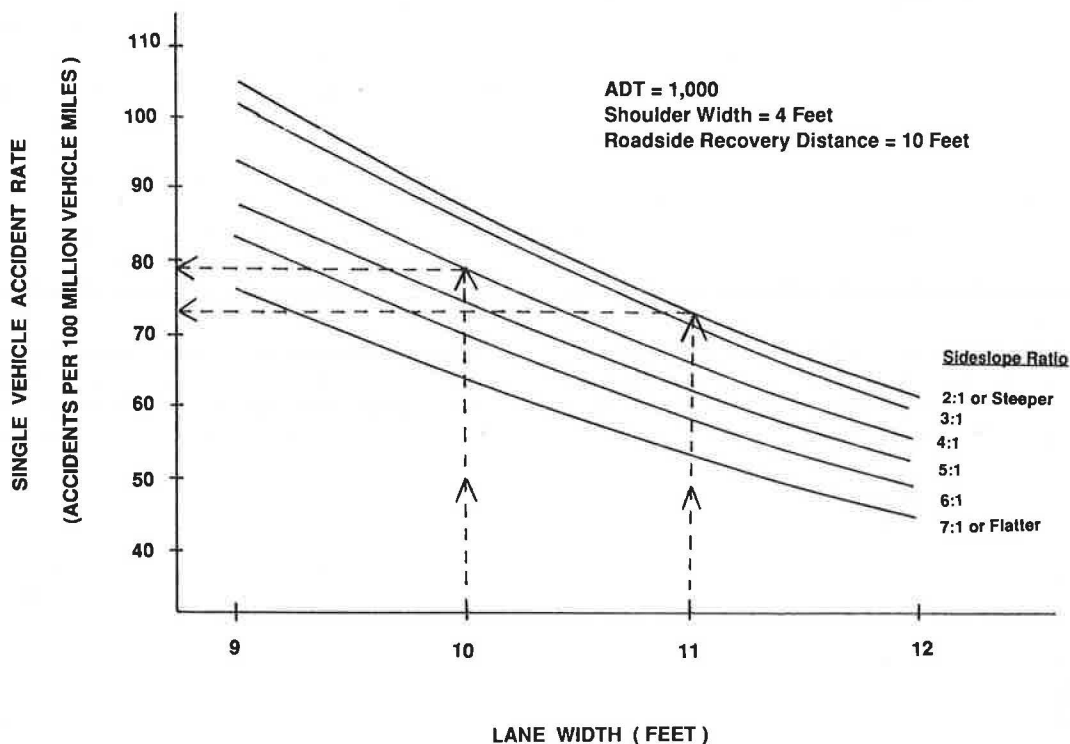


FIGURE 3 Illustration of single-vehicle accident rates for various lane widths and sideslopes.

foot roadside recovery distance beyond the shoulder edge. To illustrate the use of figure 3 for a lane width of 11 feet, sideslopes of 3:1, 4:1, and 6:1 would yield expected single-vehicle accident rates (accidents/100 mvm) of 72, 66, and 58, respectively.

The curves in figure 3 can also be used to determine tradeoffs between the effects of lane width and sideslope. For example, for a roadway section with 1,000 ADT, 4-foot shoulders, 10-foot roadside recovery distance, 10-foot lane width, and a 4:1 sideslope, the expected single-vehicle accident rate is 79 (accidents/100 mvm). Widening this roadway to 11 feet would reduce the single-vehicle accident rate to 73, even if the resulting sideslopes were 2:1. Thus, in this example, one foot of lane widening at the expense of a steeper sideslope should not adversely affect the rate of single-vehicle accidents

(although the overall accident severity may possibly be affected if, for example, more rollover accidents occur as a result of steepened sideslopes). While other types of comparisons can also be made using figure 3, the use of the predictive equation would allow for comparing the effects of sideslope changes on the single-vehicle accident rate versus lane and shoulder widening and roadside improvements.

Similar types of log-linear models were fitted using the rollover accident rate (AR) as the dependent variable. The best model for the rollover accident rate was

$$AR = 192.99 (1.319)^{SS} (0.849)^W (0.983)^{RECC} \times (0.99984)^{ADT} (0.958)^{SW}$$

$$R^2 = .25$$

where

AR = rollover accidents per 100 million vehicle miles  
 SS = 1 if sideslope is 4:1 or steeper, or zero otherwise;  
 all other terms are as previously defined.

This model has only two categories of sideslope, since no consistent trends were found in rollover rate for more defined sideslope groups. Note that in this model, a 4:1 sideslope was included with the steep (3:1 and 2:1 or steeper) group. This could indicate that sideslopes of 5:1 are more desirable than 4:1 slopes in preventing rollover accidents. Another explanation is that some vehicle types, such as mini-cars, are having a rollover accident problem on 4:1 sideslopes as well as on 3:1 and 2:1 slopes, which could partly account for the relatively high rollover accident rate for 4:1 sideslopes.

It should also be remembered that for each of the sample sections, the value of the sideslope used in the modeling was the 50th percentile (median value) of all of the field measurements for that section. A section labelled as having a 4:1 sideslope might actually consist of a range of sideslopes with 4:1 as the median value. Thus, in the database, each section labelled as 4:1 could have as much as 49 percent of the measurements steeper than 4:1 and the rest 4:1 or flatter. It is, therefore, quite possible that the 4:1 sideslope sections have rollover accident rates similar to the 3:1 and steeper category because these sections consist of a substantial portion of 3:1 and 2:1 sideslopes.

Rollover accidents represent only 23 percent of single-vehicle accidents (and only 8 percent of total accidents) in the database, so the relatively small samples of rollover accidents could have resulted in less reliable models than the models using single-vehicle accident rate. Also, the actual density of roadside fixed objects (such as trees) is generally greater on sections with steeper slopes than on sections with flat slopes. Thus, if a vehicle runs off the road onto the sideslope, it may hit an obstacle before having a chance to roll. Because of such considerations, it was believed that the rate of single-vehicle accidents was a better indication of sideslope effects than the rate of rollover accidents.

The single-vehicle accident model discussed earlier (and

corresponding accident reductions) for various sideslopes provides perhaps the most reliable results currently available of sideslope effects on accidents. However, there remains considerable uncertainty relative to the precise rollover potential of various sideslopes (in conjunction with ditch types, height of fill, shoulder dropoff, etc.) for different vehicle characteristics.

### Roadside Obstacle Types and Accidents

Another analysis involved determining the types of roadside obstacles that are most commonly struck on roads with various traffic volume conditions. The frequency of six types of fixed-object accidents for different ADT categories is summarized in table 6, based on data from six of the states in the current database. Utah accident data were not included because very few obstacle types were recorded in that state's accident file. Obstacle types other than trees, signs, utility poles, mailboxes, bridge ends, and guardrails were defined or recorded differently in different states, making tabulation of those types impossible.

Overall, the most frequently struck obstacles listed on table 6 were trees (14.8 percent) and utility poles (14.1 percent). This finding agrees with Jones and Baum (10) who cited these two obstacle types as among the most frequently struck fixed objects. Guardrail (9.6 percent), signs (6.5 percent), mailboxes (4.7 percent), and bridge ends (1.1 percent) were hit less frequently. The "other obstacle" category in table 6 includes all other obstacle types (including earth embankments) in addition to obstacles that were not specifically coded by the police officers.

For roads with ADTs of 4,000 or less, trees are the single most common type of obstacle struck. This may simply be the result of the fact that trees are generally the most common type of obstacle along low-volume rural roads. For roads with ADTs over 4,000, utility poles are the single most frequent type of fixed object struck, which is logical in view of the fact that higher volume roads are generally in the urban and suburban areas where utility poles are frequently placed near the roadway. Guardrail accidents accounted for less than seven

TABLE 6 FIXED-OBJECT ACCIDENTS BY ADT GROUP AND TYPE OF OBSTACLE STRUCK ON URBAN AND RURAL HIGHWAYS

ADT Group	Number of Accidents (Percent of accidents by ADT class)							
	Trees	Signs	Utility Poles	Mail Boxes	Bridge Ends	Guard Rail	Other Obstacles	Total FO Accs.
50-400	31(24.0)	6(4.7)	2(1.6)	2(1.6)	1(0.8)	5(3.9)	82(63.6)	129(100.0)
401-750	92(23.7)	20(5.2)	24(6.2)	10(2.6)	5(1.3)	20(5.2)	217(55.9)	388(100.0)
751-1,000	107(22.4)	9(1.9)	26(5.4)	6(1.3)	2(0.4)	33(6.9)	295(61.7)	478(100.0)
1,001-2,000	278(15.8)	95(5.4)	118(6.7)	46(2.6)	33(1.9)	192(10.9)	997(56.7)	1,759(100.0)
2,001-4,000	467(15.8)	200(6.8)	319(10.8)	144(4.9)	29(1.0)	319(10.8)	1,475(49.9)	2,953(100.0)
4,001-7,500	483(13.8)	235(6.7)	611(17.5)	198(5.7)	31(0.9)	323(9.3)	1,609(46.1)	3,490(100.0)
> 7,500	275(10.9)	198(7.9)	556(22.1)	145(5.8)	31(1.2)	239(9.5)	1,070(42.6)	2,514(100.0)
Total	1,733(14.8)	763(6.5)	1,656(14.1)	551(4.7)	132(1.1)	1,131(9.6)	5,745(49.1)	11,711(100.0)

Note: The data base includes 1,741 urban and rural sections in six states (excludes Utah).

percent of all fixed-object accidents on roads with ADTs of 1,000 or less, but they account for 9.3 to 10.9 percent of fixed-object hits for roads with ADTs of 1,001 or greater. The values in table 6 represent only the frequency of accidents and do not account for the placement or frequency (exposure) of these roadside objects.

It was impossible to determine the relative severity of accident types from the seven-state database, since data were aggregated by sections. However, accident data from the states of Michigan, Utah, and Washington were available for this analysis. These data include the rural two-lane roads, urban two-lane roads, and/or multi-lane roads. Nonetheless, the analysis afforded a reasonable look at the relative severity of different fixed-object (FO) accident types.

The severity of run-off-road fixed-object accidents relative to other common accident types was investigated, and the results are summarized in table 7. The percentage of FO accidents resulting in injury were 35, 36, and 44 for Michigan, Utah, and Washington, respectively. These percentages were lower than the percentages for rollover, head-on, and pedestrian/bicycle accidents; higher than the percentages for sides-

wipe opposite direction and sideswipe same direction; and about the same as the percentages for rear-end and angle accidents. The percentages of FO accidents resulting in a fatality were 0.8, 2.0, and 1.5 for Michigan, Utah, and Washington, respectively. These percentages again ranked FO accidents in the middle of the eight accident types shown in table 7. In terms of absolute numbers of injury accidents, however, FO accidents were the most frequent of the eight accident types in Michigan, the second most frequent in Washington, and the fourth most frequent in Utah. FO accidents were also the accident type most frequently associated with fatalities in Michigan and in Washington (fifth in Utah). In summary, FO accidents are both frequent and severe compared to other accident types.

The relative severity of the different types of fixed-object accidents is summarized by state in table 8. Fixed-object accidents which resulted in injuries generally ranged from 24 to 64 percent, depending on the type of object struck. Fatalities generally ranged from 0.2 to 6.1 percent. Among the objects associated with the highest percentage of injury and fatality were trees, culverts, bridges (bridge columns and bridge ends),

TABLE 7 SEVERITY OF COMMON ACCIDENT TYPES IN SEVERAL DATABASES

Accident Type	Percent of accidents within type resulting in injury or fatality			
	Accident Severity	State		
		Michigan	Utah	Washington
Run-off-road fixed object	Injury	35 (10137)	36 (827)	44 (15902)
	Fatal	0.8 (228)	2.0 (46)	1.5 (532)
Run-off-road rollover	Injury	55 (6587)	55 (1076)	56 (6488)
	Fatal	1.1 (73)	3.2 (63)	2.1 (245)
Head on	Injury	41 (1922)	50 (237)	60 (803)
	Fatal	2.7 (127)	11.9 (56)	20.4 (272)
Sideswipe Opposite dir.	Injury	21 (27)	30 (162)	41 (1118)
	Fatal	2.4 (3)	1.9 (10)	2.0 (54)
Sideswipe Same dir.	Injury	13 (42)	11 (87)	20 (2012)
	Fatal	1.6 (5)	0.2 (2)	0.2 (20)
Rear end	Injury	27 (2228)	33 (2320)	43 (21239)
	Fatal	0.3 (27)	0.2 (11)	0.2 (96)
Pedestrian or bicycle	Injury	86 (1769)	84 (654)	90 (2007)
	Fatal	7.0 (144)	7.8 (61)	9.8 (218)
Angle	Injury	46 (3145)	31 (2768)	37 (13272)
	Fatal	1.1 (78)	0.1 (55)	0.5 (174)

Note: The Michigan data base consisted of all reported accidents on rural roads in 1983. The Utah data base consisted of accidents reported from mid-1980 to mid-1985 on routes which had portions chosen as sections for the seven-state data base (and thus, included limited amounts of urban and multi-lane road accidents). The Washington data base consisted of all accidents reported in the State from 1980 through 1984.

( ) = The total numbers of accidents of the given type are in parenthesis.

TABLE 8 SEVERITY OF COMMON RUN-OFF-ROAD FIXED-OBJECT ACCIDENT TYPES IN SEVERAL DATA BASES

Accident Type	Accident Severity	Percent of total accidents resulting in injury or fatality		
		Data Base		
		Michigan	Utah	Washington
Utility/Light Pole	Injury	45 (3385)	39 (163)	47 (2282)
	Fatal	0.8 (58)	1.2 (5)	1.6 (75)
Guardrail	Injury	35 (1392)	42 (130)	41 (3403)
	Fatal	0.7 (28)	4.2 (13)	1.7 (144)
Sign	Injury	25 (1397)	24 (74)	40 (700)
	Fatal	0.4 (22)	1.3 (4)	1.4 (25)
Fence	Injury	28 (851)	35 (139)	40 (594)
	Fatal	0.2 (7)	1.0 (4)	1.7 (26)
Tree	Injury	47 (4419)		53 (984)
	Fatal	1.8 (171)		3.4 (64)
Culvert	Injury	49 (250)		64 (277)
	Fatal	3.3 (17)		2.1 (9)
Bridge Rail	Injury	41 (178)		41 (1060)
	Fatal	0.7 (3)		1.6 (42)
Bridge Column	Injury			54 (53)
	Fatal			6.1 (6)
Bridge End	Injury			53 (72)
	Fatal			5.2 (7)
Barrier Wall	Injury			41 (908)
	Fatal			0.5 (10)
Earth Embankment	Injury			53 (1793)
	Fatal			1.6 (55)
Rock	Injury			49 (891)
	Fatal			1.1 (21)
Mailbox	Injury			40 (132)
	Fatal			0.0 (0)
Fire Hydrant	Injury			30 (44)
	Fatal			0.7 (1)

Note: The Michigan data base consisted of all reported accidents on rural roads in 1983. The Utah data base consisted of accidents reported from mid-1980 to mid-1985 on routes which had portions chosen as sections for the seven-state data base (and thus, included limited amounts of urban and multi-lane road accidents). The Washington data base consisted of all accidents reported in the State from 1980 through 1984.

( ) = The total numbers of accidents of the given type are in parenthesis.

rocks, utility poles, and earth embankments. Objects associated with the lowest percentages of injury and fatality were signs, mailboxes, fire hydrants, barrier walls, and fences. Trees, utility and light poles, guardrails, and earth embankments are the objects involved in the most FO injury and fatal accidents.

## SUMMARY AND CONCLUSIONS

The purpose of this study was to determine the effects of various roadside features on accident experience. Detailed

traffic, accident, roadway, and roadside data were collected on 4,951 miles of two-lane rural roads in seven states. Statistical analyses and log-linear modeling were used to determine the effects of various roadside and roadway features on single-vehicle and other related accident types. Roadside measures used in the analysis included a roadside hazard scale (a seven-point pictorial scale), the roadside recovery distance (clear zone distance), and field measurements of roadside side slope.

A reduction of one rating value on the seven-point roadside hazard scale (such as a five hazard rating to a four rating) due to a roadside improvement is estimated to result in a 19 percent reduction in related (AO) accidents. A 34 percent reduc-

tion in related accidents may be expected for a two-point reduction in hazard rating, a 47 percent reduction for a three-point decrease in roadside hazard rating, and a 52 percent accident reduction for a four-point decrease in hazard rating. Similar effects on accidents were found using a different predictive model when roadside recovery distance was increased. Reductions in related accidents were found to be 13 percent, 25 percent, 35 percent, and 44 percent, when the roadside recovery distance (as measured from the outside edge of shoulder to the nearest roadside obstacles or hazards) was increased on a section by an additional five feet, 10 feet, 15 feet, and 20 feet, respectively. These results were based on log-linear models that controlled for the effects of lane width, width of paved and unpaved shoulders, traffic volume, and terrain.

The effects of sideslope on accident experience were determined using a sample of 595 rural roadway sections (1,776 miles) in Alabama, Michigan, and Washington where field sideslope measurements were taken. Based on log-linear modeling that controlled for the effects of ADT, lane width, shoulder width, and roadside recovery distance, increased rates of single-vehicle accidents and rollover accidents were found for steeper sideslopes. The rate of single-vehicle accidents decreased steadily for sideslopes of 3:1 to 7:1 or flatter. However, only a slight reduction (2 percent) in single-vehicle accidents was found for a 3:1 sideslope compared to a sideslope of 2:1 or steeper. Expected reductions in single-vehicle accidents due to sideslope flattening ranged from 2 to 27 percent, depending on the sideslope in the before and after condition. For example, flattening sideslopes of 2:1 or steeper to 3:1, 4:1, 5:1, 6:1, or 7:1 or flatter would be expected to result in reductions in single-vehicle accidents of two percent, 10 percent, 15 percent, 21 percent, and 27 percent, respectively. Improvements to existing 3:1 sideslopes would reduce single-vehicle accidents by 8 percent, 19 percent, and 26 percent due to flattening them to 4:1, 6:1, and 7:1 or flatter, respectively.

Overall, trees and utility poles are the roadside fixed obstacles most often struck, while guardrails, signs, mailboxes, and bridge ends are less frequently struck. On roads with traffic volumes of 4,000 vehicles per day or less, trees are the obstacles most often struck, while utility poles are the obstacles most frequently struck on roadways with higher volumes. Roadside objects associated with the highest percentages of severe (injury plus fatal) accidents include culverts, trees, utility and light poles, bridges, rocks, and earth embankments, while signs, mailboxes, fire hydrants, barrier walls and fences were associated with lower percentages of severe accidents.

## RECOMMENDATIONS

The results of this study clearly show the importance of roadside conditions on accidents for two-lane roads, and the safety effects of improving roadside conditions were quantified. It is recommended that highway agency officials use this information to determine where roadside improvements are justified. For example, on future 3R projects and highway reconstruction projects, the benefits of various roadside improvements should be determined using the information described in this paper. By estimating the costs for such road-

side improvements such as sideslope flattening, removing trees, and relocating utility poles, the cost effectiveness may be determined.

Agencies could also consider the safety impacts of various roadside conditions when designing new highway segments, in order to minimize roadside hazards. Highway agencies should also be sensitive to highway sections where roadside improvements are feasible. In addition, when locations are identified which have an unusually high incidence of single-vehicle accidents, the accident reduction factors contained in this paper may be useful for computing expected accident benefits from roadside improvements and thus for weighing various project alternatives.

## ACKNOWLEDGMENTS

This paper was based on joint study for the Federal Highway Administration and Transportation Research Board by Goodell-Grivas, Inc. The Highway Safety Research Center of the University of North Carolina served as a Subcontractor for the study. Appreciation is given to Justin True, the FHWA Contract Manager and John Deacon and Robert Skinner, who served as the TRB contract managers. Special thanks are also given to numerous state representatives in Alabama, Michigan, Montana, North Carolina, Utah, Washington, and West Virginia, who cooperated with the project team and provided necessary data and information. The field sideslope measurements used in the analysis were collected by Analysis Group, Inc., under a separate contract for FHWA. The authors assume responsibility for the accuracy of the information contained herein.

## REFERENCES

1. S. A. Smith, J. Purdy, H. W. McGee, D. W. Harwood, A. D. St. John, and J. C. Glennon. *Identification, Quantification, and Structuring of Two-Lane Rural Highway Safety Problems and Solutions*. Volumes I and II, Report Nos. FHWA/RD/83/021 and 83/022, Federal Highway Administration, Washington, D.C., 1983.
2. C. V. Zegeer, J. G. Mayes, and R. C. Deen. *Cost-Effectiveness of Lane and Shoulder Widening of Rural, Two-Lane Roads in Kentucky*. Bureau of Highways, Kentucky Department of Transportation, 1979. Also in *Transportation Research Record 806*, TRB, National Research Council, Washington, D.C., 1981.
3. C. V. Zegeer, J. Hummer, L. Herf, D. Reinfurt, and W. Hunter. *Safety Effects of Cross-Section Design for Two-Lane Roads*. FHWA/RD/87/008, Federal Highway Administration, Washington, D.C., 1986.
4. F. D. Newcomb, and D. B. Negri. *Motor Vehicle Accidents Involving Collision with Fixed Objects*. New York State Department of Motor Vehicles, 1971.
5. E. A. Rinde. *Conventional Road Safety: Phase I—A Study of Fixed Objects*. California Department of Transportation, 1979.
6. T. J. Foody and M. D. Long. *The Specification of Relationships Between Safety and Roadway Obstructions*. Report No. OHIO-DOT-06-74, Ohio Department of Transportation, 1974.
7. J. W. Hall, C. J. Burton, D. G. Coppage, and L. V. Dickinson. *Roadside Hazards on Non-Freeway Facilities*. In *Transportation Research Record 601*, TRB, National Research Council, Washington, D.C., 1976.
8. C. V. Zegeer and M. R. Parker. *Cost-Effectiveness of Coun-*

- termeasures for Utility Pole Accidents. Report No. FHWA/RD/87/008, Federal Highway Administration, Washington, D.C., January 1983.
9. K. K. Mak and R. L. Mason. *Accident Analysis—Breakaway and Non-breakaway Poles Including Sign and Light Standards Along Highways*. Federal Highway Administration, Washington, D.C., 1980.
  10. I. S. Jones and A. S. Baum. *An Analysis of the Urban Utility Pole Problem*. Federal Highway Administration, Washington, D.C., 1980.
  11. J. L. Graham and D. W. Harwood. *NCHRP Report 247: Effectiveness of Clear Recovery Zones*. TRB, National Research Council, Washington, D.C., 1982.
  12. J. D. Weaver and E. L. Marquis. *Roadside Slope Design for Safety*. *Transportation Engineering Journal*, American Society of Civil Engineers, 1976.
  13. K. Perchonok, T. A. Ranney, S. Baum, D. F. Morrison, and J. D. Eppick. *Hazardous Effects of Highway Features and Roadside Objects*. Calspan Field Service, Inc., Federal Highway Administration, Washington, D.C., 1978.
  14. L. Graf, J. U. Boos, and J. A. Wentworth. *Single-Vehicle Accidents Involving Utility Poles*. In *Transportation Research Record 571*, TRB, National Research Council, Washington, D.C., 1976, pp. 36–43.
  15. T. C. Edwards, J. E. Martinez, W. F. McFarland, and H. E. Ross. *NCHRP Report 77: Development of Design Criteria for Safer Luminaire Supports*. HRB, National Research Council, Washington, D.C., 1968.
  16. J. C. Glennon and C. J. Wilton. *A Methodology for Determining the Safety Effectiveness of Improvements on All Classes of Highways. Volume I: Effectiveness of Roadside Safety Improvements*. Report No. FHWA/RD/75/23, Federal Highway Administration, Washington, D.C., 1974.
  17. D. E. Cleveland and R. Kitamura. *Macroscopic Modeling of Two-Lane Rural Roadside Accidents*. In *Transportation Research Record 681*, TRB, National Research Council, Washington, D.C., 1978.
- 
- Publication of this paper sponsored by Committee on Methodology for Evaluating Highway Improvements.*

# Intersection Channelization Guidelines for Longer and Wider Trucks

DANIEL B. FAMBRO, JOHN M. MASON, JR., AND NANCY STRAUB CLINE

Turning characteristics of large trucks, such as offtracking (the difference in paths of the front-most and rear-most inside wheels of a vehicle as it negotiates a turn) and swept-path width (the amount of offtracking plus the width of the truck), require special consideration in the design of at-grade intersections. Five large truck combinations, representative of the longer and wider trucks permitted by the Surface Transportation Assistance Act of 1982, were selected and their paths computer-simulated traversing different turning radii at several angles of turn. The findings were tabulated as guidelines for intersection channelization designed to accommodate these longer and wider trucks. The results include several specific truck turning templates; tables containing cross-street width occupied and swept-path width for various combinations of design vehicle, curb radii, and degree of turn; and recommended guidelines that illustrate conditions where channelization is feasible when designing for larger trucks. These guidelines include the minimum required curb radii to eliminate encroachment into either opposing or adjacent traffic lanes on the cross-street, the minimum required width of turning roadway, and the approximate size of the space available for channelizing islands.

The introduction of larger and heavier trucks into the traffic stream by recent federal and state legislation has prompted research by the Texas State Department of Highways and Public Transportation (SDHPT) on how to accommodate these vehicles on their highway system. Consequently, the Texas Transportation Institute (TTI) and the Center for Transportation Research (CTR) studied the impact of these larger vehicles on geometric design, traffic operations, and highway safety. The first objective of this study, an annotated bibliography summarizing research concerning operational characteristics and geometric design implications of longer and wider trucks, has been completed and published as TTI Research Report 397-1 (1). Another objective, involving the development of channelization guidelines to accommodate longer and wider trucks at at-grade intersections, is the subject of this paper. Related research results are documented in other reports (2-4).

Turning characteristics of large trucks, such as offtracking and sweptpath width, require special consideration when designing at-grade intersections. If the curb radius is large enough for trucks to make right turns without encroaching on adjacent lanes, the paved area at the intersection can become

so large that through drivers may not understand where to position their vehicles. In such instances, it becomes necessary to construct a channelizing island to properly control traffic. If the curb radius is so small that trucks cannot make right turns without encroaching on adjacent lanes, the truck either encroaches and interferes with adjacent traffic, or its rear wheels run over and possibly damage the curb and/or shoulder. In addition, the front overhand of the truck may strike traffic control devices located near the outside of its turning path, or the right rear trailer tire may strike devices located near the inside of its turning path when offtracking. Turning characteristics of large trucks in a left-turn maneuver must also be considered in the design process; this paper, however, presents the findings of an investigation regarding only right-turn maneuvers.

The objective of the study was to establish a set of guidelines for channelization that would accommodate selective longer and wider trucks at at-grade intersections. To accomplish this objective, the following tasks were performed:

- Reviewed literature concerning truck turning characteristics and intersection channelization;
- Determined truck turning characteristics for various combinations of large design vehicle and intersection geometry; and
- Developed guidelines for design, operation, and channelization of at-grade intersections to accommodate these larger vehicles.

## TRUCK TURNING CHARACTERISTICS

Because of a truck's long wheelbase, its rear wheels do not follow the same path as its front wheels when making a turn. The differences in these paths is defined by the terms offtracking and swept path. Offtracking is generally defined as the difference in paths of the front-most inside wheel and rear-most inside wheel of a vehicle as it negotiates a turn (5). The distance may also be measured between the tracking of the front and rear outside wheels, or the center of the front and rear axles, but its value will be the same. Offtracking is known to vary directly with the wheelbase of a unit and inversely with the radius of turn. Its magnitude "is affected in combination by the number and location of articulation points, by the length of the arc and the type of curve, and by the speed and turnability of the wheels" (6, p. 73).

Swept-path width may be defined as the amount of offtracking plus the width of the truck. It can also be defined as the difference in paths of the front-most outside wheel and

D. B. Fambro, Texas Transportation Institute, Texas A&M University, College Station, Tex. 77843. J. M. Mason, Jr., Department of Civil Engineering, The Pennsylvania State University, 212 Sackett Building, University Park, Pa. 16802. N. S. Cline, City of Dallas, 320 East Jefferson, Dallas, Tex. 75203.

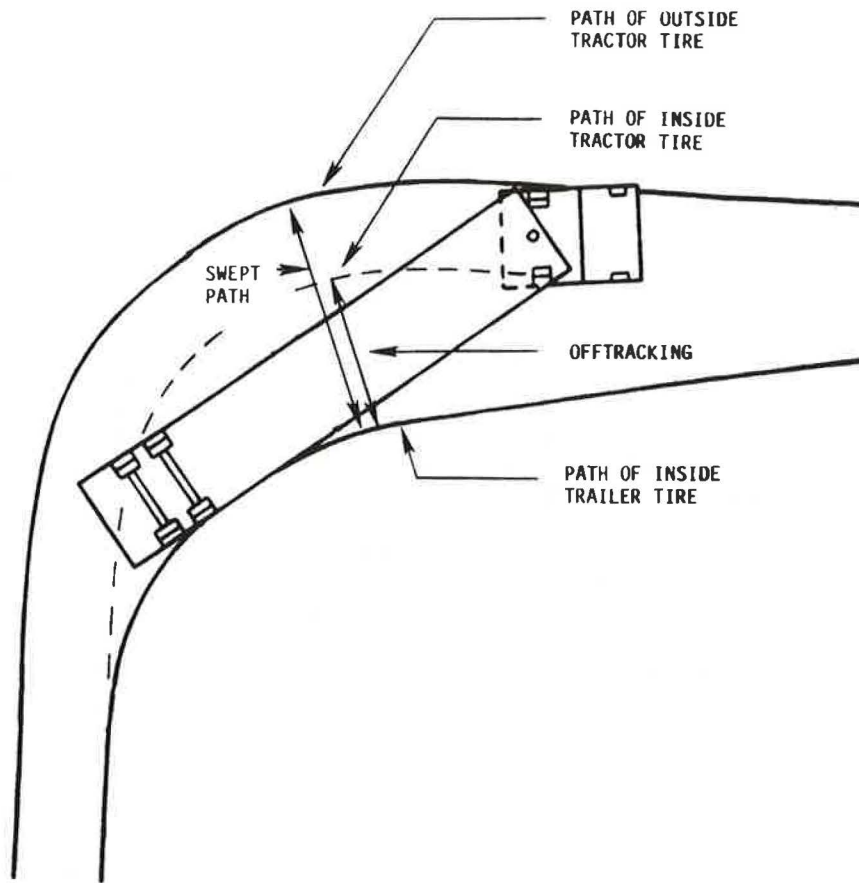


FIGURE 1 Swept-path width and offtracking of a truck negotiating a 90-degree turn.

the rear-most inside wheel of the vehicle as it negotiates low-speed turns. At higher speeds, negative offtracking may occur; that is, the rear-most wheels may actually travel outside the path of the front-most wheels because of side slippage. In this case, swept path would be defined as the difference in paths of the front-most inside wheel and rear-most outside wheel of the vehicle as it negotiates the turn. With the exception of negative offtracking, these terms are illustrated in figure 1 (7).

#### Full-Scale Tests and Formulas

Full-scale tests done on test-track curves of known radius were one of the first methods used to determine offtracking. The tests were extremely accurate because they involved professional drivers and an actual vehicle traversing a measured turn. These tests, however, were based on the assumption that other drivers could repeat this optimum performance in the real world. Also, this method of testing was expensive, and the number of truck-turn combinations that would have to be tested made it necessary to develop less expensive, yet equally reliable methods.

#### Scale Modeling

Scale modeling was found to be more efficient than working with the actual vehicles. The Tractix Integrator, an instrument

used to simulate actual vehicle offtracking characteristics, has been used to develop turning templates for a number of different design vehicles (5). The Tractix Integrator provides an immediate plot of the truck path and is especially well-suited for many roadway design situations. Its use, however, is relatively slow and tedious, and special points of interest must be manually added to the centerline paths.

#### Computer Models

The first computer model that simulated vehicle offtracking was developed by the University of Michigan Transportation Research Center (UMTRI). This modeling package was quite an advancement in working with vehicle offtracking when compared to the previously described methods for studying turning characteristics. The program was developed for a microcomputer environment and designed to be user-friendly. The program output was a scaled plot of the paths followed by the vehicle tires in a format that could be overlaid on drawings of intersections or other situations involving restrictive geometry.

The Truck Offtracking Model (TOM), developed by the California Department of Transportation (Caltrans), is most frequently used for trucks, although it also simulates the offtracking characteristics of any vehicle combination when making a turn (8). TOM evolved from the Apple II personal computer offtracking model developed by UMTRI, and the simulation portion of the Apple program was adopted by



Caltrans' Division of Transportation Planning and placed on the state's IBM mainframe computer. TOM was not as user-friendly as the Apple version, but its plotting capacity was much greater, resulting in plots of larger scale and higher quality.

### INTERSECTION CHANNELIZATION

At-grade intersection channelization is defined as the separation or regulation of conflicting traffic movements into definite paths of travel by the use of pavement markings, raised islands, or other suitable means to facilitate the safe and orderly movements of both vehicles and pedestrians (9). Proper channelization increases capacity, improves safety, provides maximum convenience, and instills driver confidence. Improper and/or over-channelization often have the opposite effect and should be avoided because of the confusion they can cause (10). Currently, there are no guidelines for intersection channelization when larger trucks are the design vehicles. The following literature review highlights several references that address channelization at at-grade intersections.

The Highway Research Board (HRB) sponsored two publications on intersection channelization containing examples and critical analyses so that highway and traffic engineers might benefit from a review of other works. Special Report 5 (10) provided fifty-nine examples of channelized intersections as of 1952. A revision by the same title was published in 1962 as Special Report 74 (11) and provided more examples of channelization to illustrate design practice as of that date. This report also defined the special objectives of intersection channelization, which are to assure orderly movement, increase capacity, improve safety, and provide maximum convenience.

The most recent publication dealing with channelization is a 1986 version of Special Report 74 (12), which includes illustrative examples of channelization designs and more detailed guidelines than were provided in the earlier reports. In addition, the report covers channelization of both new and reconstructed intersections in urban and rural environments. Its contents include typical intersection types such as four-way, Y, T, oblique, and multi-leg intersections, as well as freeway ramp intersections with surface streets.

The American Association of State Highway and Transportation Officials' (AASHTO's) Policy on the Geometric Design of Highways and Streets—1984 ("Green Book") contains discussions of both offtracking and channelization. The book specifies that larger semitrailer combinations should be used as design vehicles where truck combinations approximating this size will turn repeatedly. Such designs, particularly when used in two or more quadrants of an at-grade intersection, produce large paved areas that may be difficult to control. It is usually desirable to channelize such intersections, requiring larger radii (7).

### DESIGN VEHICLES

The design vehicles selected for this study were two singles, two doubles, and one triple. They are typical of the larger vehicles currently being operated on the nation's highways. One of the vehicles, the WB 50, was the same as one of the design vehicle configurations defined in the "Green Book"

(7) and was used to check the study results for accuracy and consistency. The tractor used in each combination had a 16-foot wheelbase with the cab placed behind the engine. This particular tractor was selected because of its longer wheelbase, typical of cab-behind-engine tractors. The five design vehicles are described below, and their dimensions are shown in table 1.

#### Singles

The first design vehicle, the WB-50, represents the design vehicle with the worst turning characteristics of those contained in the "Green Book." As of 1984, the WB-50 was nearly all-inclusive of the tractor-semitrailer combinations in use. The tractor and trailer in the WB-50 have wheelbases of 16 and 34 feet respectively, with an overall combination length of 50 feet from the front-most axle to the rear-most axle. The WB-55, a larger single, was the second design vehicle selected for the study. Its tractor has a 16-ft wheelbase, and its 48-ft trailer has a 38.5-ft effective wheelbase, for an overall wheelbase of 56 feet from the front-most to rear-most axles. The WB-55 represents the longest single trailer vehicle allowed by the Surface Transportation Assistance Act (STAA) of 1982.

#### Doubles

The third design vehicle was the WB-70 with a 16-ft tractor, two 28-ft trailers, and an overall wheelbase spacing of 70 feet. It is sometimes referred to as the "western double" and is slightly larger than the WB-60 design vehicle used in the "Green Book." The fourth design vehicle, the WB-105, is frequently referred to as the "turnpike double" and represents, in some western states, the maximum allowable trailer lengths for combination vehicles. It consists of a 16-ft tractor towing two 48-ft trailers, for an overall length of 105 feet. The WB-105 is the most critical of the five design vehicles because, as is discussed later, it has the worst turning characteristics of the vehicles studied.

#### Triple

The fifth design vehicle, the WB-100, was a tractor-trailer combination with three 28-ft trailers behind a 16-ft tractor, resulting in an overall length from front-most axle to rear-most axle of 100 feet. Because of these relatively short wheelbases, the WB-100 can turn much sharper radii than the WB-105 without encroaching; because of its numerous articulation points, however, its swept path is much greater.

### INTERSECTION GEOMETRICS

In addition to the design vehicle, the other parameters investigated in this study were curb return radius and degree of turn. The values for curb return were as specified in table II-19 in the "Green Book." A radius of 25 feet was included in addition to the values in the table of 50, 75, 100, 150, and 200 feet. These radii were drawn to a scale of 1 inch equals 20 feet on sheets of clear mylar so that turning paths of the

TABLE 1 DESIGN VEHICLE DIMENSIONS

Design Vehicle Type	Symbol	Dimensions (ft)													
		Overall			Overhang		WB <sub>1</sub>	WB <sub>2</sub>	S	T	WB <sub>3</sub>	S	T	WB <sub>4</sub>	
		Ht.	Width	Length	Front	Rear									
<b>Combination Trucks:</b>															
Semitrailer	WB-50	13.5	8.5	55	3	2	16	34.0	---	---	---	---	---	---	---
Large Semitrailer	WB-55	13.5	8.5	60	3	2	16	39.1	---	---	---	---	---	---	---
Semitrailer-trailer	WB-70	13.5	8.5	75	3	2	16	20	2.5	7.5	23.0	---	---	---	---
Large Semitrailer-trailer	WB-105	13.5	8.5	110	3	2	16	37.3	6.7	6.3	37.8	---	---	---	---
Semitrailer-trailer-trailer	WB-100	13.5	8.5	105	3	2	16	21.9	3.0	6.2	22.3	3.0	6.2	22.3	---

WB<sub>1</sub>, WB<sub>2</sub>, WB<sub>3</sub>, WB<sub>4</sub> are effective vehicle wheelbases.

S is the distance from the rear effective axle to the hitch point.

T is the distance from the hitch point to the lead effective axle of the following unit.

design vehicle could be superimposed on an intersection layout.

A 2-ft clearance was desirable between the curb radius and the vehicle travel path. Therefore, the actual radii were drawn at 27, 52, 77, 102, 152, and 202 feet, respectively. Another result of the 2-foot clearance was that the lane lines (normally 12 feet) were drawn at 10 feet to show the effective lane width. Sets of the various radii were drawn for turning angles of 60, 75, 90, 105, and 120 degrees, as they were considered to be representative of typical intersection geometry. In addition to the typical angles of turn, a 180-degree turn was simulated for completeness and to define the minimum possible turning radius for each design vehicle.

### SIMULATION MODEL

The California Truck Offtracking Model (TOM) (13) originally written for an IBM mainframe computer, was modified to run on a VAX 11/750 computer. A brief discussion of required input and resulting output follows.

#### Inputs

There are five input cards or lines of data that supply the necessary information to the offtracking program. The critical path geometry, described below, is input on card 1. The data on card 2 is the vehicle configuration, that is, the number of

units and axle spacing. The simulation parameters, initial x- and y-coordinates and distance increments for simulation calculations, are input on card 3. Card 4 includes all the plotting data necessary to specify the number of paths and additional reference points to be plotted and to define the area in which the paths are to be plotted. The title information is given on card 5.

The critical path geometry in the computer input data stream is the radius of curvature for the turning vehicle and the angle of turn. Computer runs were made for each design vehicle making turns of 60, 75, 90, 105, and 120 degrees. These turns were made at the minimum radius possible (to within 5 feet) and increased at intervals of 10 to 15 feet depending on the minimum turning radius of the design vehicle. The minimum radius was determined by the method described by AASHTO in 1965 (14), which states that "the minimum turning radii for the design vehicles (WB-40 and WB-50) was largely determined by the paths of the inner rear wheels." The turning path chosen was one that would result in a minimum radius of the inner rear wheel track of approximately 19 feet when negotiating turns of 90 to 180 degrees.

#### Outputs

The outputs of TOM were printouts detailing the input values, a table listing offtracking at the beginning of curve (BC), end of curve (EC), the point of maximum offtracking (MOT), and

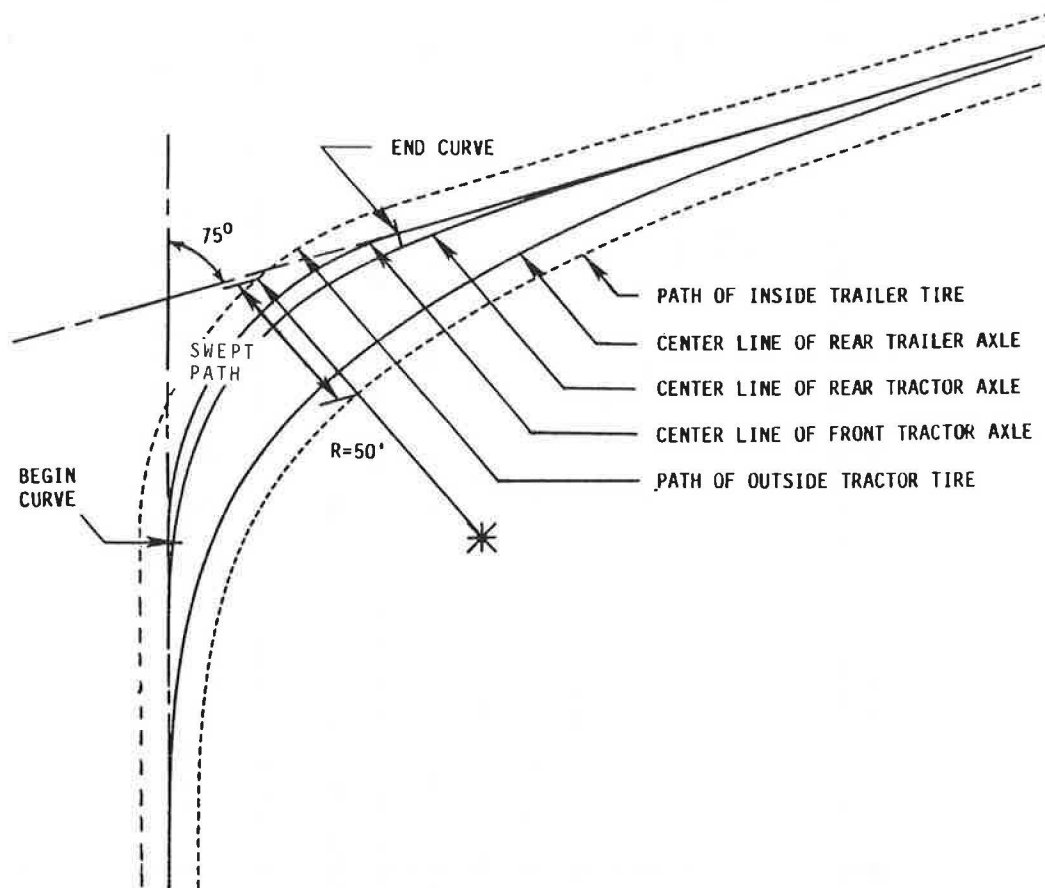


FIGURE 2 Example plot from truck offtracking model (WB-55, 75-degree turn, 50-foot radius).

the plot of the vehicle turning path (see figure 2). It was necessary to modify the plot routine to work with the HP plotter connected to the VAX 11/750 computer used in this study. For convenience as well as comparative purposes, plots were made at a scale of 1 inch equals 20 feet.

The output of the Truck Offtracking Model was verified by preparing a turning template for a vehicle configuration that closely matched that of the WB-50 design vehicle shown in the Leisch turning templates (15). A second template was made and compared to a vehicle modeled using the Tractix Integrator (16). Both templates drawn by the model closely matched the Leisch and Tractix Integrator templates.

## DATA ANALYSIS

The optimum turning radius for each curb return was defined as the smallest turning radius that the design vehicle could negotiate without running over the inside curb, while at the same time minimizing cross street encroachment; that is, the design vehicle's minimum turning radius until the curb return became large enough to allow the vehicle to turn on a longer radius. For each vehicle-geometric combination, the following design parameters were determined:

## Cross Street Width Occupied

The cross street width occupied was defined as the amount of encroachment plus a 12-ft lane width (see figure 3). Encroachment was defined as the distance that the vehicle trespassed beyond the 12-ft lane stripe in order to complete its turn. It was assumed that the vehicle positioned itself to the far left of the right-most lane on the approach street and only swung wide when on the cross-street; in other words, the vehicle remained within the 12-ft lane lines when approaching the turn.

## Swept-Path Width

Swept-path width was defined earlier as the difference in paths of the front-most outside wheel and rear-most inside wheel of a vehicle as it negotiated a turn (see figure 3). Swept-path width could also be defined as the offtracking plus the width of the vehicle, and it is important in determining the minimum width of turning roadways. The maximum swept-path widths measured from the plots generally agreed with the offtracking values from the computer printouts.

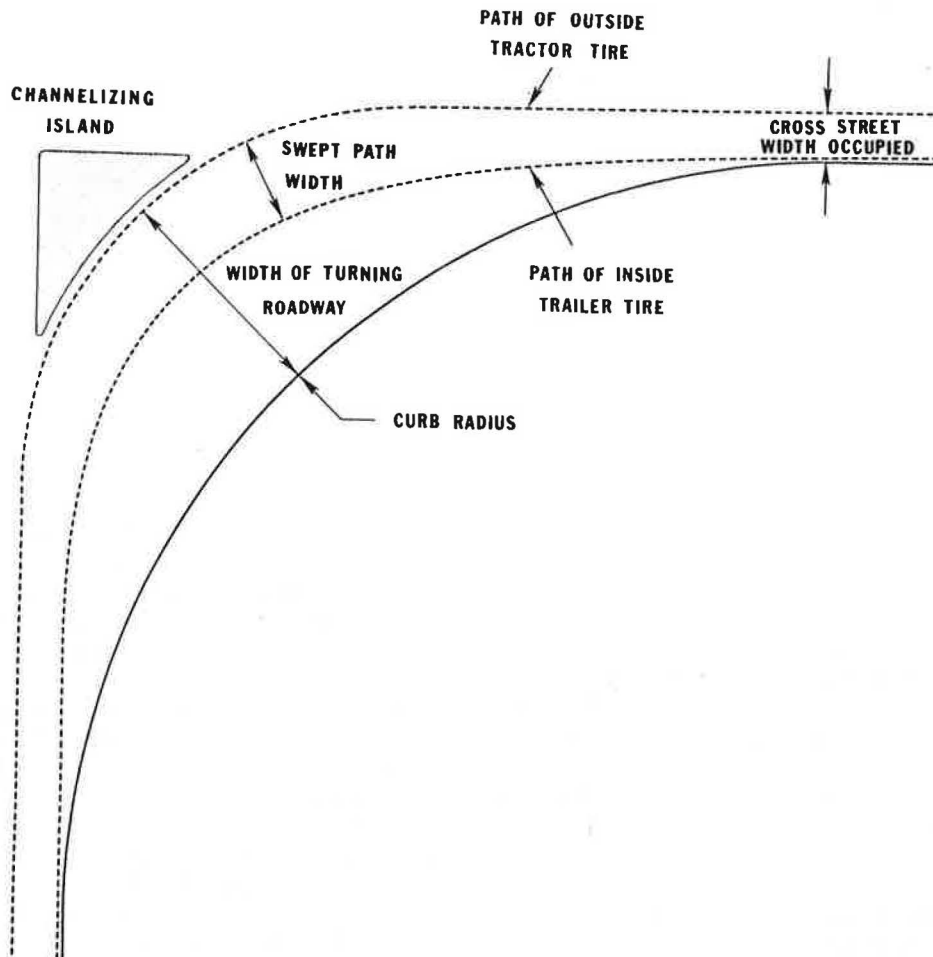


FIGURE 3 Cross street, swept path, and turning roadway width for a truck negotiating a 90-degree intersection turn.

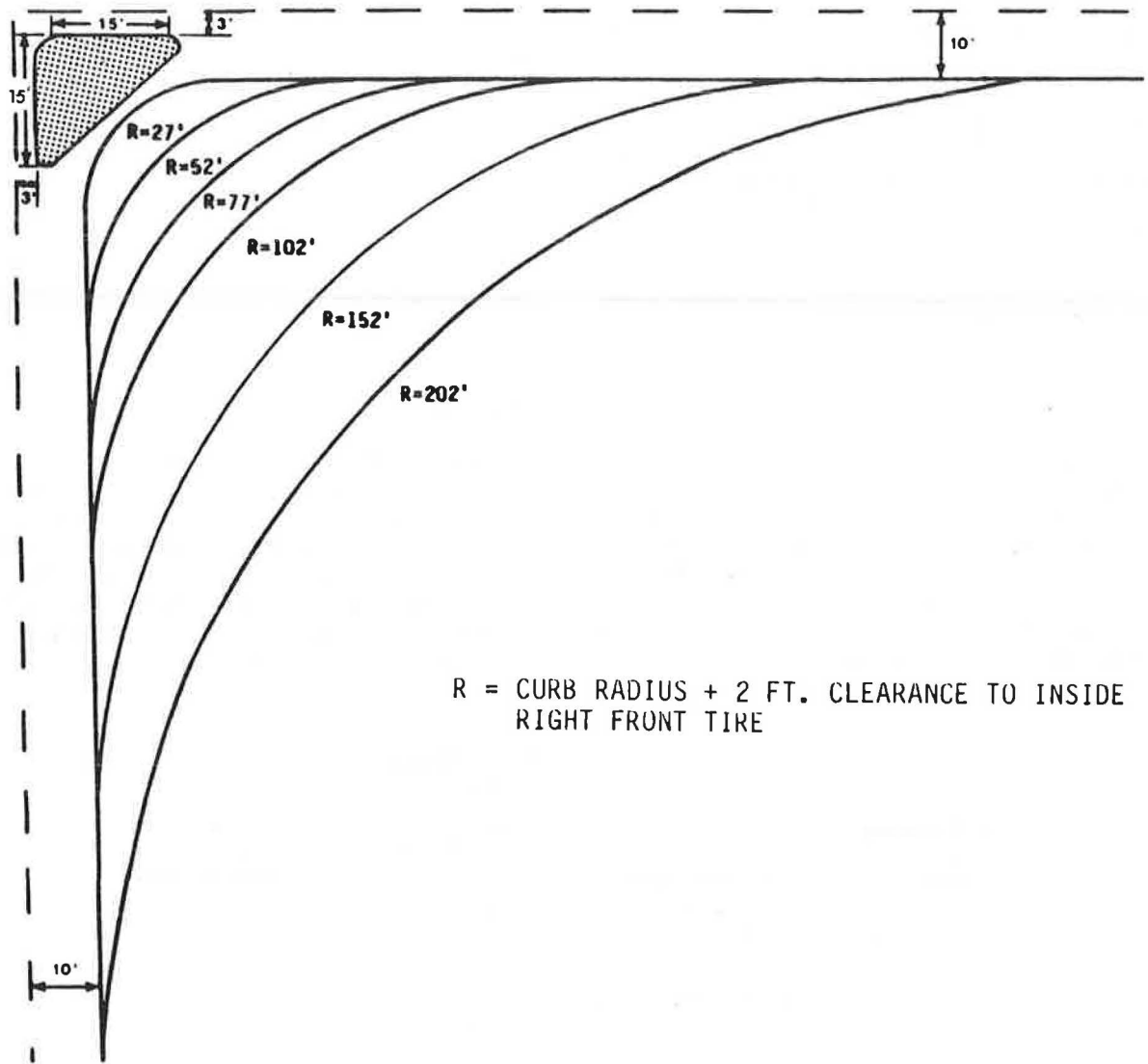


FIGURE 4 Curb radii and minimum island size for a 90-degree intersection turn.

### Channelization

The critical design consideration in deciding whether or not to use channelization was the curb return radius of the intersection. It was not the same as the turning radius of the vehicle. In order to determine where there was enough pavement area to justify channelization, the 12-ft lane lines on each street were extended until they intersected. An island was then drawn with the curb radii that would satisfy the preferred criteria in the "Green Book"—3-ft offset from through traffic, 3-ft corner radii, and minimum leg lengths of 15 feet (7) (figure 4).

In order to determine the values for each vehicle-geometric combination, the turning templates were grouped first according to the design vehicle and then according to the angle of turn. For each design vehicle at each angle of turn, the minimum turning path (determined from the 180-degree turns) was placed over the 27-ft curb radius at the same angle of

turn. Wheel paths of the vehicles could lie on the line, offset two feet from the curb, because of the allowances previously described. The amount of encroachment beyond the 12-ft lane line was measured at the end of the turning curve, EC, as this was the point where the truck began moving back into its lane. The assumption was made that the vehicle turned from the proper lane of the approach street, and, therefore, all of the encroachment occurred in the cross-street lane. No allowances were made in the simulation for shoulders for the truck to encroach upon.

As the curb radius was increased, the minimum turning path became too tight, and it was necessary to go to a larger turning path. Preferably, the turning path that encroached the least or not at all was the one chosen. If, for example, both the 60-ft turning radius and the 75-ft turning radius could each turn a 150-ft curb radius without encroaching, then the 75-ft turning path would be selected because it had a smaller swept width.

## STUDY RESULTS

Computer simulation runs were made for each of the different scenarios, and the resultant output was converted to a more comprehensive format. The study results were broken down into the following five topic areas:

### Minimum Turning Radii

The boundaries of the turning paths for a design vehicle making its sharpest possible turn were established by the paths followed by its outer front wheel and inner rear wheel as it made the turn. The minimum turning radii of the outside and inside wheel paths for each of the five design vehicles are given in table 2. The values for the WB-50 vary slightly from those in the "Green Book" due to shorter tractor and longer trailer axle spacings. The minimum turning radii and the transition lengths shown here and in the "Green Book" are for turns made at less than 10 mph. This assumption minimizes the effects of driver characteristics (such as the rate at which the driver approaches centripetal acceleration) and the slip angles of wheels.

### Turning Templates

Turning templates for each of the five design vehicles were developed using their minimum turning paths for various angles of turn: 60, 90, 120, and 180 degrees (figures 5-9). For each of the four angles of turn, templates were prepared by drawing each design vehicle on a sheet of mylar and then tracing its turning path onto the same sheet. They were originally drawn at a scale of one inch equals 20 feet, and three of them, figures 4 through 6, were reduced for inclusion in this paper.

### Cross Street Width Occupied

Table 3 illustrates the effect of the angle of intersection on turning paths of various design vehicles on streets without parking lanes. It was structured similarly to table IX-3 in the

"Green Book." Dimensions  $d_1$  and  $d_2$  were defined as the widths occupied by the turning vehicle on the main street and cross street, respectively, while negotiating turns through various angles. Both dimensions are measured from the right-hand curb to the point of maximum encroachment on either adjacent or opposing lanes (figure 10). These widths generally increase with increasing angle of turn and decrease with increasing curb radii. The right-turn maneuver modeled in this study assumed that the vehicle positioned itself to the far left of the right-most lane on the approach street and only swung wide when on the cross-street. This assumption results in the worst case scenario on the cross-street. Therefore, the dimension  $d_1$  equals 12 feet, and  $d_2$  is the value shown in table 3.

The values for the WB-50 design vehicle in table IX-3 of the "Green Book" should have closely resembled values for the WB-50 vehicle used in this study. The values from table IX-3 in the "Green Book" indicate that AASHTO WB-50 has less severe turning characteristics than the WB-50 with a slightly shorter tractor wheelbase that was used in this study. It should be remembered, however, that a longer semitrailer wheelbase is associated with a shorter tractor wheelbase. Since offtracking is a function of the sum of the squares of the different wheelbase lengths, a decrease in a short wheelbase will be more than offset by a corresponding increase in a long wheelbase. Thus, the larger values of cross-street width occupied are consistent with the theory.

Assuming a road with two 12-ft lanes in either direction, a truck must be able to turn without occupying more than 24 feet of the cross street width. Referring to table 3, none of the vehicles can negotiate any of the turning angles (60 to 120 degrees) at either a 25-ft or a 50-ft curb radius without occupying more than 24 feet of cross street width. At a 75-ft curb radius, however, all of the vehicles except the WB-100 (triple) and the WB-105 (turnpike double) can make the turns and stay within 24 feet of cross-street width. These two larger vehicles can make the turn within the stated constraints at radii of 100 and 150 feet, respectively.

If the example were modified and there were a 10-ft shoulder or parking lane provided on the cross street, the available cross street width would be 34 feet. Under these circumstances, the less critical design vehicles (WB-50, WB-55, and WB-70) could turn at 50-ft curb radii, and the WB-100 could turn

TABLE 2 MINIMUM TURNING RADII OF DESIGN VEHICLES

Design Vehicle Type	Semitrailer Combination	Semitrailer Combination (Large)	Semitrailer-Full Trailer Combination	Semitrailer-Full Trailer Combination (Large)	Semitrailer Full Trailer-Full Trailer Combination
Symbol	WB-50	WB-55	WB-70	WB-105	WB-100
Configuration	3-S2	3-S2	3-S1-2	3-S2-4	2-S1-2-2
Minimum Turning radius (ft.)	45	50	50	65	55
Minimum Inside radius (ft.)	20.5	19	24.3	25.8	25.6

## WB-50

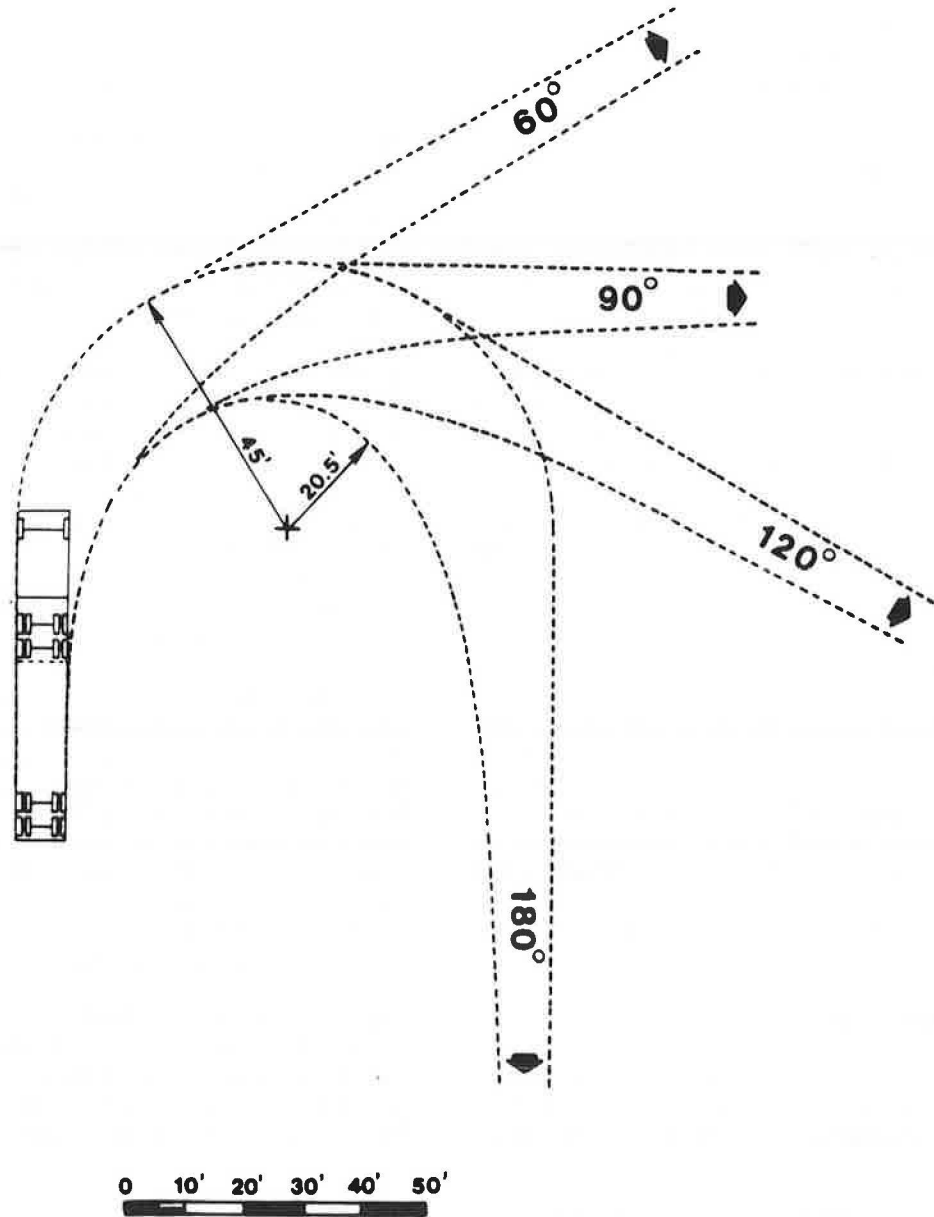


FIGURE 5 Minimum turning paths for WB-50 design vehicle.

the smaller angle turns at a 75-ft radius and all angles at the 100-ft curb radii. The most critical design vehicle (WB-105), however, can still only turn 150-ft and 200-ft curb radius turns. As the angle of turn increases past 90 degrees, the turning problems of the WB-105 become much more pronounced, especially at a 105-degree, 150-ft curb radius where the other four vehicles maneuver well.

#### Turning Roadway Width

Table 4 contains the values for the swept width of the various design vehicles shown for various angles of turn and curb radii. The swept width is a function of the optimum turning radius

of the vehicle at a certain angle and curb return. By close inspection of table 3, it was possible to determine the point at which the minimum turning radius of each design vehicle reached the point where it was no longer the optimum, and a larger turning radius (with a smaller swept width) could negotiate the curb radius equally well, if not better, than the minimum. This point was identified by the decrease in the swept width for a particular design vehicle at a certain degree of turn as the radius increases. The 65-ft minimum radius of the turnpike double was never replaced by a greater radius as the curb radii increased up to 200 feet.

The greater the swept width of a vehicle negotiating a turn, the greater the width of turning pavement necessary. Although the "Green Book" classifies pavement widths for turning

WB-55

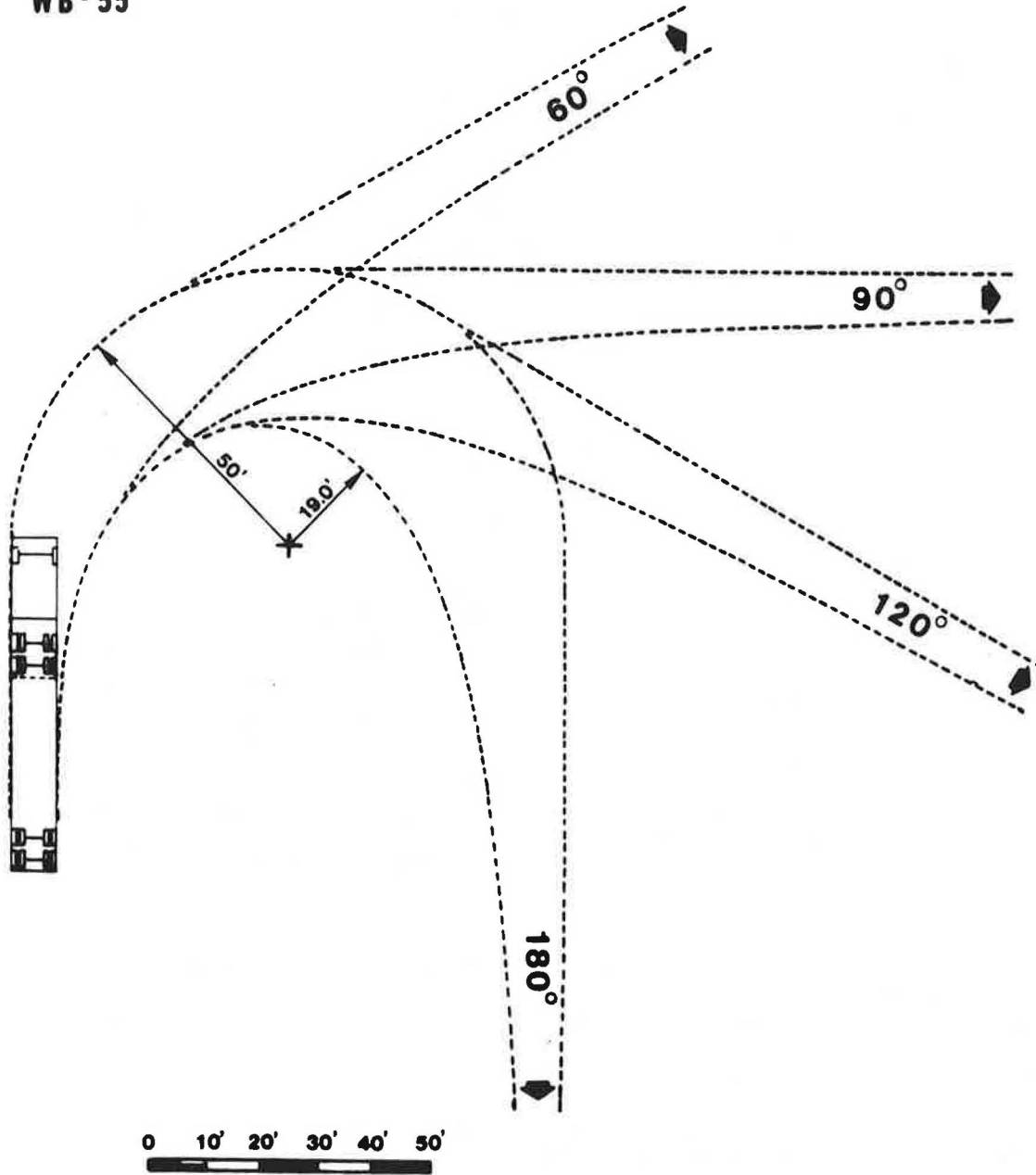


FIGURE 6 Minimum turning paths for WB-55 design vehicle.

roadways for several types of operations, Case 1—one-lane, one-way operation with no provision for passing a stalled vehicle—is the type of operation that was considered in this study.

The WB-105 (turnpike double) had a wheelbase just slightly longer than the WB-100 (triple); its swept path width, however, was much greater due to its greater axle spacings. The sum of the squares of axle spacings and the number of points of articulation govern the way a vehicle will offtrack around a curve. The number of articulations will affect the shape of the curve, while the sum of the squares will determine the magnitude of offtracking (5). Because of this, the two 48-ft trailers of the turnpike double cause more severe offtracking than the 28-foot trailers of the triple.

**Channelization Guidelines**

The boxed-in area in both tables 3 and 4 are the conditions where the curb radius combines with the optimum turning radius in such a way as to leave room for an island of at least 100 square feet in size, the minimum size of channelized island recommended by the "Green Book" (7). Conditions where channelization is feasible are the larger curb radii and frequently the larger degrees of turn. Channelization is recommended at a 200-ft curb radius for all of the vehicles except the turnpike double at 60- and 70-degree turns. As the curb radius decreases, the angle of turn, in combination with the design vehicle, influences whether channelization is feasible. Overall, as the angle of turn increases beyond 90 degrees, the



TABLE 3 CROSS STREET WIDTH OCCUPIED BY TURNING VEHICLE FOR VARIOUS INTERSECTION ANGLES AND CURB RADII

Angle of Turn (Degrees)	Design Vehicle	Curb Radius					
		25 ft.	50 ft.	75 ft.	100 ft.	150 ft.	200 ft.
60	WB-50	33.5	24.0	17.0	14.0	12.0	12.0
	WB-55	40.0	29.8	21.5	17.3	13.0	12.0
	WB-70	38.8	23.7	19.5	15.0	12.0	12.0
	WB-100	46.5	36.2	27.0	18.0	12.0	12.0
	WB-105	56.0	46.5	37.0	29.0	18.0	12.0
75	WB-50	37.0	26.0	16.5	13.5	12.0	12.0
	WB-55	44.0	34.7	21.5	16.8	12.0	12.0
	WB-70	43.0	34.0	20.0	14.5	12.0	12.0
	WB-100	52.0	41.0	28.5	17.0	12.0	12.0
	WB-105	65.0	36.0	42.5	30.0	17.0	12.0
90	WB-50	43.0	26.0	17.0	13.0	12.0	12.0
	WB-55	53.0	37.0	21.8	17.0	13.0	12.0
	WB-70	53.0	36.0	21.0	14.0	12.0	12.0
	WB-100	66.0	46.5	31.0	17.5	12.0	12.0
	WB-105	81.0	63.0	48.0	33.0	17.3	12.0
105	WB-50	52.0	32.0	18.0	13.0	12.0	12.0
	WB-55	62.0	42.0	23.5	18.0	12.0	12.0
	WB-70	61.5	42.0	23.0	14.0	12.0	12.0
	WB-100	74.0	52.0	32.5	19.0	12.0	12.0
	WB-105	95.0	75.0	55.0	39.0	18.0	12.0
120	WB-50	59.0	40.0	23.0	14.5	12.0	12.0
	WB-55	80.0	51.0	35.0	21.0	13.5	12.0
	WB-70	72.0	52.0	34.0	17.0	12.0	12.0
	WB-100	84.5	63.0	47.0	29.0	13.0	12.0
	WB-105	106.0	85.0	68.5	49.0	21.0	12.0

Note: Boxed-in areas are conditions with enough room for an island of at least 100 square feet in size, i.e., they may require channelization.

skewed intersection angle leaves an open pavement area that, when combined with curb radii of 75 to 200 feet and a fairly narrow swept width, results in a good-size island area to channelize the right turns. At the 60-degree and 75-degree turns, the geometry is such that few of the combinations warrant channelization.

Table 5, similar to table IX-4 in the "Green Book," contains minimum designs and channelization guidelines for turning roadways. The parameters that govern the design are angle of turn, design vehicle, curb radius, width of lane, and approximate island size. For each design vehicle, table 5 lists a suggested island size and width of turning lane at each angle of turn that might need channelization, that is, those conditions that were boxed-in in tables 3 and 4. As the curb return radius increases towards 200 feet, the area of the island becomes larger and the width of the turning lane decreases. The size of islands for the larger turning angles indicates the otherwise unused and uncontrolled areas of pavement that were eliminated by the use of islands. Turning roadways for flat-angle turns, less than 75 degrees, involve relatively large radii and require designs to fit site controls and traffic conditions.

Because the truck configurations spiral into a curve, it would be desirable to fit the edge of the pavement closely to the minimum path of the design vehicle by using three-centered compound curves or simple curves with tapers to minimize

the amount of unused pavement. The unnecessarily wide turn-lane widths in table 5 (see figure 3) are an indication that simple radius curves are not well suited to the turning paths of large trucks.

## CONCLUSIONS

The selection of a design vehicle is a critical decision in intersection design. It is generally based on the largest standard or typical vehicle type that would regularly use the intersection. Where reliable vehicle classification counts are available, they can be used to select a design vehicle. More often, selection is based on the area type and functional classification of the intersecting highways (12).

The adoption of the Truck Offtracking Model that was developed by Caltrans for use in this study was advantageous for studying truck turning characteristics because it was capable of simulating various truck paths in a relatively short time period as compared to other methods. It is a powerful program once the user is familiar with all of the items which may be varied. The procedure used herein could be used for intersection design where there are high volumes of large or unique trucks. The results are of particular value at truck terminals, major ramp terminal intersections, and commercial and industrial developments.

WB-100

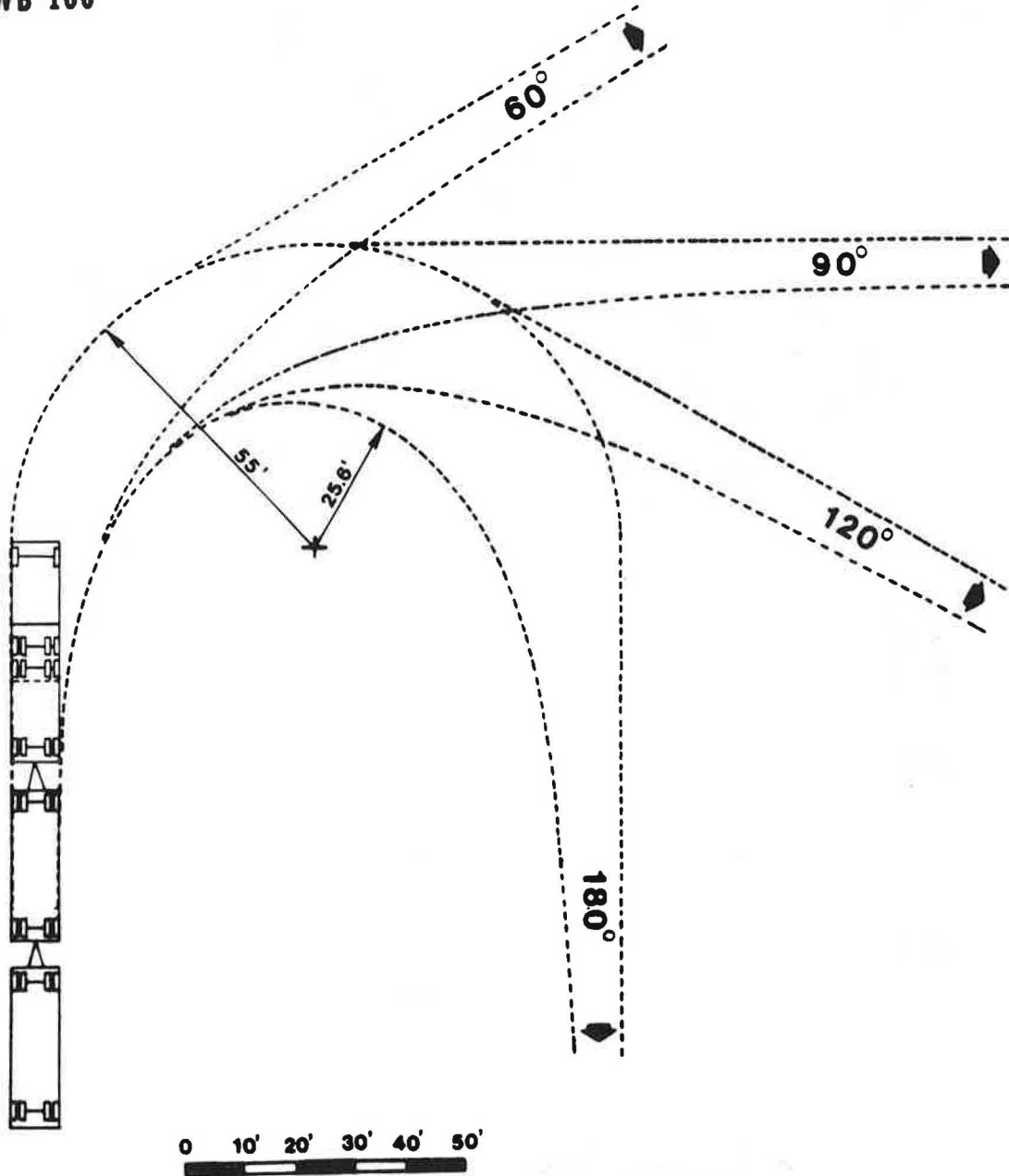


FIGURE 8 Minimum turning paths for WB-100 design vehicle.

WB-70

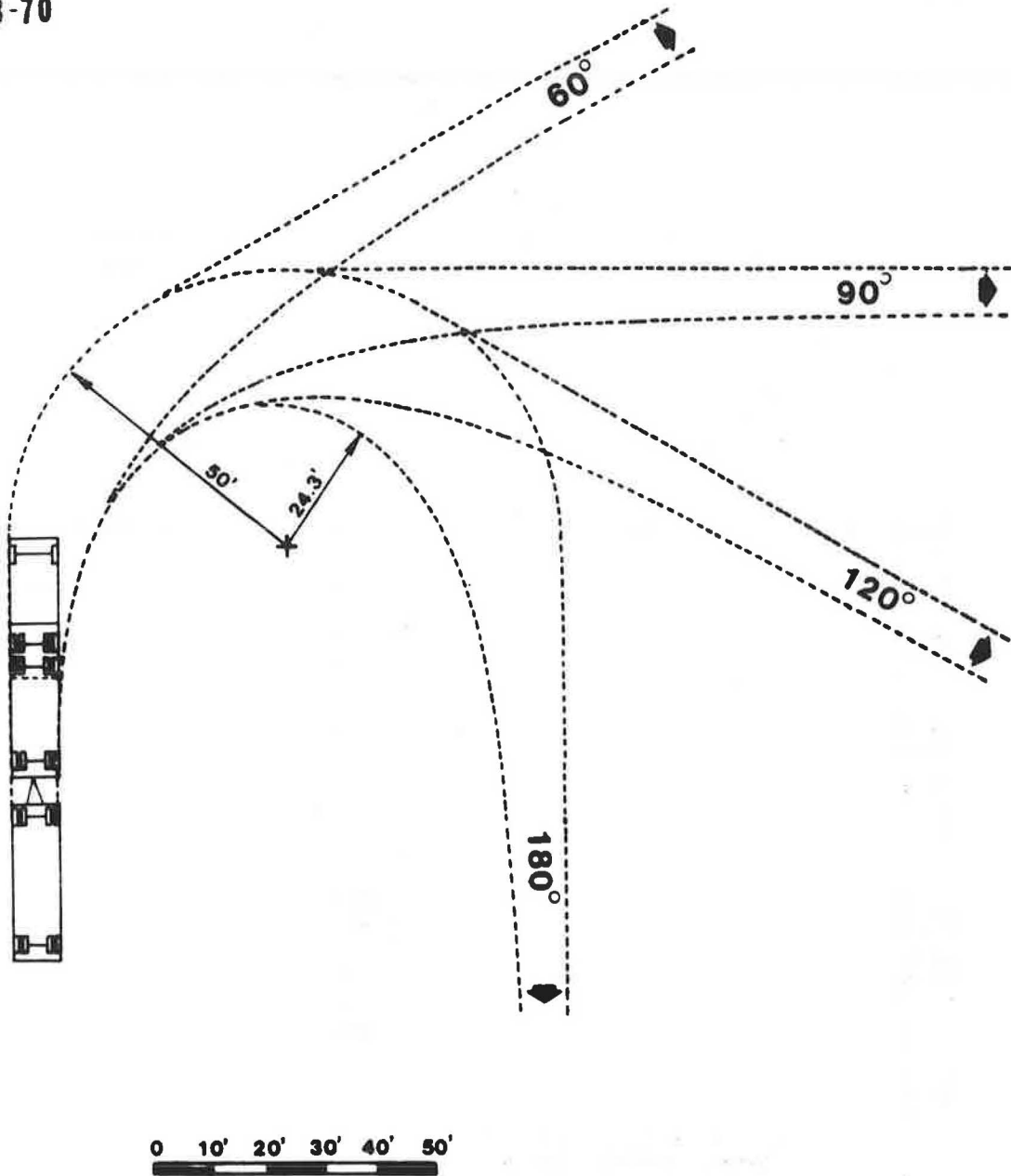


FIGURE 7 Minimum turning paths for WB-70 design vehicle.

WB-105

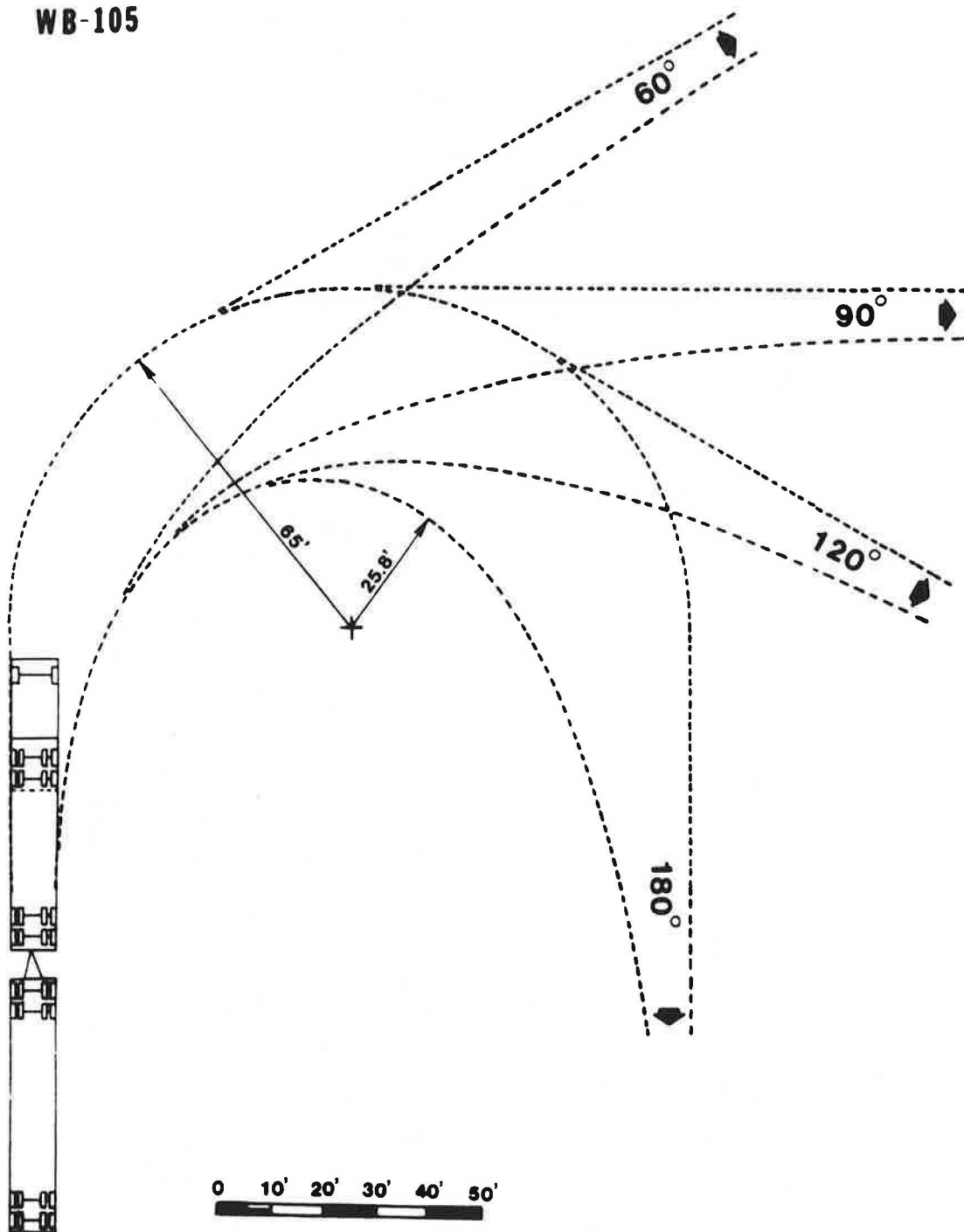
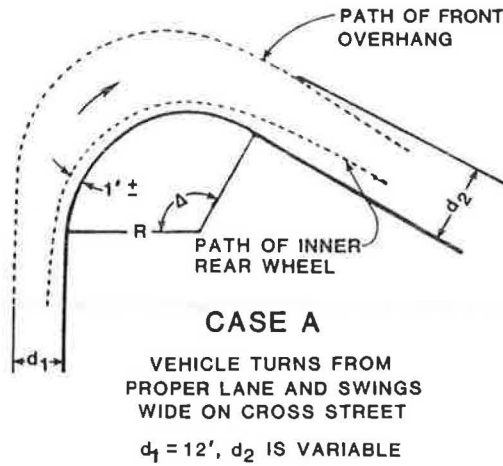


FIGURE 9 Minimum turning paths for WB-105 design vehicle.



**FIGURE 10** Cross street width occupied by turning vehicle.

**TABLE 4** SWEPT-PATH WIDTH OCCUPIED BY TURNING VEHICLE FOR VARIOUS INTERSECTION ANGLES AND CURB RADII

Angle of Turn (Degrees)	Design Vehicle	Curb Radius					
		25 ft.	50 ft.	75 ft.	100 ft.	150 ft.	200 ft.
60	WB-50	18.0	18.0	18.0	18.0	16.5	15.0
	WB-55	20.5	20.5	20.5	20.5	18.8	17.0
	WB-70	19.0	19.0	19.0	19.0	16.5	15.5
	WB-100	20.7	20.7	20.7	20.7	20.0	17.8
	WB-105	24.9	24.9	24.9	24.9	24.9	24.9
75	WB-50	19.5	19.5	19.5	19.5	16.0	15.0
	WB-55	22.5	22.5	22.5	22.5	20.0	18.0
	WB-70	20.0	20.0	20.0	20.5	17.5	16.5
	WB-100	22.5	22.5	22.5	22.5	21.8	17.5
	WB-105	27.7	27.7	27.7	27.7	27.7	27.7
90	WB-50	20.5	20.5	20.5	20.5	16.5	15.0
	WB-55	24.0	24.0	24.0	24.0	22.2	18.5
	WB-70	21.5	21.5	21.5	21.5	18.0	16.5
	WB-100	24.2	24.2	24.2	24.2	23.1	19.0
	WB-105	30.0	30.0	30.0	30.0	30.0	30.0
105	WB-50	21.3	21.3	21.3	21.3	16.5	15.0
	WB-55	25.5	25.5	25.5	25.5	23.3	19.0
	WB-70	22.5	22.5	22.5	22.5	18.5	16.5
	WB-100	25.5	25.5	25.5	25.5	24.4	19.5
	WB-105	32.1	32.1	32.1	32.1	32.1	32.1
120	WB-50	22.0	22.0	22.0	22.0	19.0	15.0
	WB-55	26.8	26.8	26.8	26.8	26.8	22.0
	WB-70	23.5	23.5	23.5	23.5	21.0	18.5
	WB-100	26.5	26.5	26.5	26.5	26.5	22.0
	WB-105	33.8	33.8	33.8	33.8	33.8	22.0

Note: Boxed-in areas are conditions with enough room for an island of at least 100 square feet in size, i.e., they may require channelization.

**ACKNOWLEDGMENTS**

The research reported herein was performed as a part of a study entitled "Longer and Wider Trucks on the Texas Highway System" by the Texas Transportation Institute and sponsored by the Texas State Department of Highways and Public Transportation in cooperation with the U.S. Department

of Transportation, Federal Highway Administration. The contents of this paper reflect the views of the authors, who are responsible for the facts and accuracy of the data presented herein. The contents do not necessarily reflect the official views or policies of the Federal Highway Administration or the State Department of Highways and Public Transportation.

TABLE 5 MINIMUM DESIGNS AND CHANNELIZATION GUIDELINES FOR TURNING ROADWAYS

Angle of Turn (degrees)	Design Vehicle	Curb Radius (ft.)	Width of Turning Lane (ft.)	Approximate Island Size (sq. ft.)
60	WB-50	200	27	250
	WB-55	200	22	160
	WB-70	200	22	160
	WB-100	200	27	160
	WB-105	-	-	-
75	WB-50	150	28	320
	WB-55	150	30	160
	WB-70	150	23	200
	WB-100	200	34	300
	WB-105	-	-	-
90	WB-50	150	30	670
	WB-55	200	38	900
	WB-70	150	22	560
	WB-100	200	40	900
	WB-105	200	54	260
105	WB-50	150	32	980
	WB-55	150	41	740
	WB-70	150	31	1320
	WB-100	200	41	1940
	WB-105	200	57	940
120	WB-50	150	40	1640
	WB-55	200	45	3400
	WB-70	150	39	1600
	WB-100	200	48	2580
	WB-105	200	60	1740

## REFERENCES

1. J. M. Mason, Jr., L. Griffin, N. Straub, C. J. Molina, Jr., and D. B. Fambro. *Annotated Bibliography of Research on Operational Characteristics and Geometric Implications of Longer and Wider Trucks*. Texas Transportation Institute Research Report 397-1, February 1986.
2. C. J. Molina, Jr., C. J. Messer, and D. B. Fambro. *Passenger Car Equivalencies for Large Trucks at Signalized Intersections*. Texas Transportation Institute Research Report 397-2, November 1986.
3. T. Chira-Chavala. *An Analysis of Truck Accident Involvement and Truck Accident Severity on the Texas Highway System*. Texas Transportation Institute Research Report 397-4, November 1986.
4. D. Burke. *Larger Trucks on Texas Highways*. Texas Transportation Institute Research Report 397-5F, November 1986.
5. D. S. Millar and C. M. Walton. Offtracking of the Larger, Longer Combination Commercial Vehicles. In *Transportation Research Record 1026*, TRB, National Research Council, Washington, D.C., 1985, pp. 62-65.
6. *NCHRP Report 141: Changes in Legal Vehicle Weights and Dimensions*. TRB, National Research Council, Washington, D.C., 1973.
7. *A Policy On the Geometric Design of Highways and Streets—1984*. American Association of State Highway and Transportation Officials, Washington, D.C., 1984.
8. K. T. Fong and D. C. Chenu. Simulation of Truck Turns With a Computer Model. In *Transportation Research Record 1100*, TRB, National Research Council, Washington, D.C., 1986, pp. 20-28.
9. *Manual on Uniform Traffic Control Devices for Streets and Highways*. Federal Highway Administration, Washington, D.C., 1978.
10. *Special Report No. 5: Channelization—The Design of Intersections at Grade*. HRB, National Research Council, Washington, D.C., 1952.
11. *Special Report No. 74: Channelization—The Design of Highway Intersections at Grade*. HRB, National Research Council, Washington, D.C. 1962.
12. T. R. Neuman. *Intersection Channelization Design Guide. National Cooperative Highway Research Program Report 279*, TRB, National Research Council, Washington, D.C., November 1985.
13. *Truck Offtracking Model (TOM), Program Documentation and User's Guide*. Draft Report, Division of Transportation Planning, California Department of Transportation, Sacramento, 1985.
14. *A Policy on Geometric Design of Highways and Streets—1965*. American Association of State Highway Officials, Washington, D.C., 1965.
15. J. E. Leisch and Associates. *Turning Vehicle Templates: A Transportation Design Aid*. Transportation Design Techniques, Inc., Evanston, Illinois, 1977.
16. *Highway Design Division Operations and Procedures Manual*. Texas Department of Highways and Public Transportation, Austin, Texas, 1986.

Publication of this paper sponsored by Committee on Operational Effects of Geometrics.

# Effects of Turns by Larger Trucks at Urban Intersections

JOSEPH E. HUMMER, CHARLES V. ZEGER, AND FRED R. HANSCOM

**This paper gives results and conclusions from part of a study done for the Federal Highway Administration on the safety and operational effects of large truck operations. Computer simulation and manual observations at six intersections in California and New Jersey were used to investigate turns by large trucks at urban intersections. The encroachment of a truck into adjacent lanes during a turn was studied using the computer simulation. The field data examined on a particular truck turn included the encroachment, the time to complete the turn, and the conflicts with other vehicles in the traffic stream caused by the truck. Field observations were made of turning trucks in the traffic stream and also of a control truck of known size driven repeatedly through a study intersection by a professional driver who knew the purpose of the experiment. The results showed that small curb radii, narrow lane widths, and narrow total street widths were among the geometric features associated with increased operational problems. The results also showed that large trucks will have little impact (compared with smaller trucks) at most urban intersections of the types tested, but some adverse operational effects should be expected at some intersections. Trailer length was found to be a more critical element to smooth operations than trailer width for the trucks tested. Many site, driver, and equipment factors should be considered before the decision is made to regulate truck traffic in a certain manner.**

The Surface Transportation Assistance Act of 1982 (1982 STAA) required some states to change their restrictions on the sizes of trucks operating on their portions of the national truck network of interstate and other designated Federal-aid highways. Due to the 1982 STAA, states may not impose trailer width limits of less than 102 inches. A 96-inch maximum trailer width had been in effect in most states prior to the 1982 STAA. The 1982 STAA also provided that states allow tractor-semitrailer combinations with semitrailer lengths of up to 48 feet and tractor-semitrailer-trailer combinations with semitrailer and trailer lengths of up to 28 feet on the national network. Previously, states had the freedom to impose maximum semitrailer lengths and in some cases had prohibited tractor-semitrailer-trailer combinations.

The interstate and turnpike systems have generally been built to very high geometric standards. However, other Federal-aid systems often contain lower standard design features, which may impact safety and necessitate limiting operations of the large trucks specified in the 1982 STAA. It was, there-

fore, timely to evaluate the impacts of large truck operation on roads and streets with restrictive geometry and to provide insights relative to the selection of routes for the national network.

This paper gives results and conclusions from part of a study done for the Federal Highway Administration (FHWA) on the safety and operational effects of large truck operations (1). Two particular situations were identified for study: truck negotiation of winding rural roads and truck turns at urban intersections. This paper details only the urban intersection portion of the study.

A review of previous research revealed that some operational problems are expected when large trucks make turns at urban intersections, but many questions on the issue remain unanswered. An analysis in Texas of the impact of different truck sizes on a variety of geometric conditions concluded that increases in allowed truck size may warrant highway design standard changes (2). A 1982 study conducted in Ontario, Canada, showed that large trucks, including tractor-semitrailer-trailer combinations, offtrack (swing wide during turns) farther than smaller trucks (3). A study by the Western Highway Institute showed that longer combinations required extra lanes or overlapped into adjacent lanes to negotiate right-angle turns at intersections (4). Tractor-semitrailer-trailer combinations were observed in California to use extra lanes, traverse curbs and channels, and use excessive time during turns at intersection (5). A 1981 field study that attempted to correlate increase in truck size with operational problems at several sites, including intersections, concluded that increased truck lengths were associated with only negligible operational traffic effects, however (6).

Two investigation methods were employed during the study of larger truck turns at urban intersections. A computer simulation technique was used to analyze the offtracking of different sizes of trucks during different turning maneuvers. The simulation provided information that may be useful in selecting routes for the national network. In addition, turning trucks were observed at actual intersections during the study. The field observations allowed comparisons between different truck sizes for particular intersections, which may be useful in predicting the impact of large truck operations.

## COMPUTER SIMULATION OF TRUCK TURNS

The turning characteristics of larger trucks were investigated using the Vehicle Offtracking Model and Computer Simulation developed by FHWA and the University of Michigan Transportation Research Institute. The software package

J. E. Hummer, School of Civil Engineering, Purdue University, West Lafayette, Ind. 47907. C. V. Zegeer, Highway Safety Research Center, University of North Carolina, Chapel Hill, N.C. 27514. F. R. Hanscom, Transportation Research Corporation, Haymarket, Va. 22069.

allowed plotting of the positions of the outside edges of the tractor and trailer(s) and the positions of the tires as a given type of truck completed a turn at an intersection with a given configuration. From such a plot, a more useful plot of the area covered by the truck during the turn was made and analyzed.

The simulation was run for eight types of larger trucks: a tractor-semitrailer combination with a 48-foot semitrailer that was 96 inches wide (semi 48), a semi 48 that was 102 inches wide (semi 48 wide), a tractor-semitrailer combination with a 55-foot semitrailer that was 96 inches wide (semi 55), a semi 55 which was 102 inches wide (semi 55 wide), a tractor-semi-trailer-trailer combination with 28-foot trailers that were 96 inches wide (double 28) a double 28 that was 102 inches wide (double 28 wide), a tractor-semitrailer-trailer-trailer combination with 28-foot trailers that were 96 inches wide (triple 28), and a triple 28 that was 102 inches wide (triple 28 wide). Each of the eight truck types was run over many combinations of angle and radius of turn which are representative of intersections in the United States.

Two measures were used to analyze the offtracking plots produced from the simulation runs. The maximum offtracking distance was recorded for each plot. This distance represents the widest swing of a truck during a turn, as shown in figure 1. The other measure employed was the lane encroachment of the truck during the turn. The lane encroachment was defined as the distance between the curb and the farthest edge of the truck's path measured at the end of the curvature of the curb (at the stop bar of the street onto which the truck is turning). The lane encroachment was measured from the simulation plot by aligning the point of maximum offtracking and the center of the curve of the curb as shown in figure 2. The significance of the lane encroachment is seen, for example, by a truck turning onto a four-lane street with 12-foot wide lanes. If the lane encroachment of the truck for the angle and radius of turn at the intersection is greater than 24 feet, the truck cannot complete the turn without crossing the centerline of the street onto which it is turning. If there is a vehicle

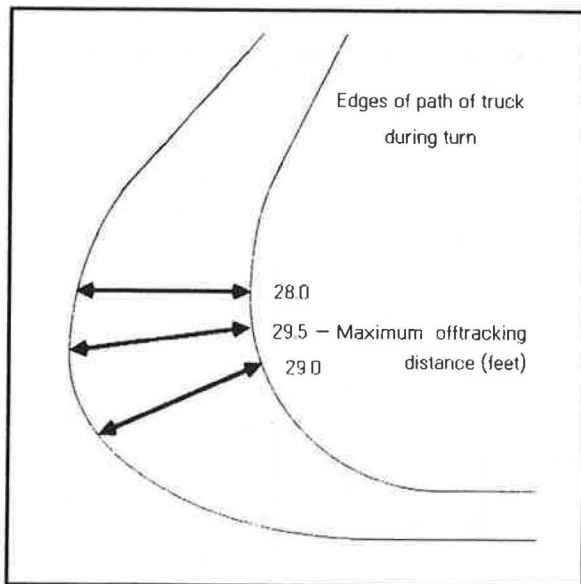


FIGURE 1 Illustration of measurement of maximum offtracking distance.

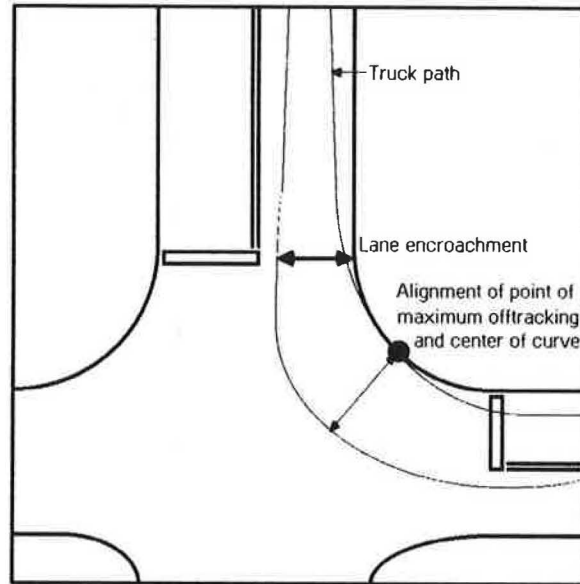


FIGURE 2 Illustration of measurement of lane encroachment.

idling next to the centerline at the stop bar of that street, the truck cannot complete the turn.

A summary of the simulation results is given in tables 1 and 2 for the maximum offtracking distance and the lane encroachment measures, respectively. From tables 1 and 2, it can be seen that the most serious operational problems at intersections can be expected (of the eight large truck types examined) from the semi 55 wide. Other truck types, in descending order of space required, are the semi 55, the semi 48 wide, and semi 48, the triple 28 wide, the triple 28, the double 28 wide, and the double 28.

Tables 1 and 2 also show that, for a given trailer configuration and length, 102-inch wide trucks generally exhibited greater maximum offtracking distances and greater lane encroachments than 96-inch wide trucks, but the difference was usually only 0.5 or 1.0 feet. Thus, for the field observations reported later, the issue of the width of the turning trucks was ignored, and the effort was directed at examining the effects of different trailer lengths and configurations.

Table 2 also provides guidance for the selection of truck routes. In general, lane encroachment magnitudes were large (that is, the truck would cross the centerline on a four-lane street) for most larger angles of turn for radii of 22 and 40 feet. Greater intersection angles did not necessarily mean greater lane encroachment values for most truck types, however. Only the semi 55 and semi 55 wide displayed generally greater lane encroachments with greater intersection angles.

The results shown in tables 1 and 2 should be used judiciously, since the simulation was limited in a number of ways. Differences between individual truck drivers may be great enough to overcome the effects of different-size vehicles, but such variability was not included in the simulation. The reactions of the drivers of other vehicles in the traffic stream and the volume of such other vehicles were also omitted from the simulation. Finally, the speed of a turn was not an output of the simulation. This is a serious limitation since a truck driver who slows a great deal in order to complete a turn without encroaching on the centerline or curb may cause as great a



TABLE 1 MAXIMUM OFFTRACKING DISTANCES USING SIMULATION

Truck type	Maximum offtracking distances, in feet, for given angles of intersection in degrees and curb radii in feet														
	angle=60			angle=70			angle=90			angle=105			angle=120		
	R=20	R=40	R=60	R=20	R=40	R=60	R=20	R=40	R=60	R=20	R=40	R=60	R=20	R=40	R=60
Semi 48	23.5	21.0	*	*	*	*	31.0	25.5	22.0	35.0	28.0	*	39.0	29.0	*
Semi 48 Wide	24.0	22.0	*	*	*	*	31.0	26.0	22.5	35.0	28.0	*	39.5	29.5	*
Semi 55	*	23.0	21.0	28.0	25.0	22.5	33.5	28.5	*	38.0	31.0	*	43.0	33.5	*
Semi 55 Wide	*	23.5	22.0	29.0	26.0	23.0	34.0	29.0	25.5	38.5	31.5	*	43.0	34.0	27.5
Double 28	20.0	17.5	16.0	21.5	18.5	16.5	25.0	20.0	*	28.0	21.0	17.0	30.0	22.0	17.5
Double 28 Wide	*	18.0	16.0	22.0	18.5	16.5	25.5	21.0	18.0	26.0	21.5	*	30.5	22.5	18.0
Triple 28	*	20.5	18.0	25.0	22.0	19.0	30.0	25.0	*	33.0	26.0	*	37.0	28.0	*
Triple 28 Wide	*	21.0	19.0	26.0	22.5	20.0	31.0	25.5	21.5	34.0	27.0	*	39.0	28.0	*

\* - No data were recorded.

TABLE 2 LANE ENCROACHMENT DISTANCES USING SIMULATION

Truck type	Lane encroachment distances, in feet, for given angles of intersection in degrees and curb radii in feet														
	angle=60			angle=70			angle=90			angle=105			angle=120		
	R=20	R=40	R=60	R=20	R=40	R=60	R=20	R=40	R=60	R=20	R=40	R=60	R=20	R=40	R=60
Semi 48	22.0	21.0	*	*	*	*	27.0	22.0	19.0	27.0	22.5	*	28.0	21.5	*
Semi 48 Wide	23.5	21.5	*	*	*	*	26.0	22.0	20.0	27.5	22.5	*	27.5	22.0	*
Semi 55	*	22.5	19.0	27.0	24.0	20.5	30.0	26.0	*	32.0	27.0	*	33.5	26.0	*
Semi 55 Wide	*	22.5	19.0	27.5	25.0	21.0	29.5	26.0	23.0	31.0	26.0	*	33.0	25.0	21.0
Double 28	18.5	16.5	14.0	20.0	17.0	15.0	20.0	17.0	*	21.5	17.0	*	20.5	15.5	12.5
Double 28 Wide	*	17.0	15.0	20.5	17.0	15.0	21.0	17.0	15.0	22.0	18.0	*	21.5	17.0	14.0
Triple 28	*	18.5	16.5	22.5	20.0	16.5	25.0	20.5	*	26.5	21.5	*	24.5	19.5	*
Triple 28 Wide	*	19.0	17.0	24.0	20.5	16.5	25.0	21.0	18.0	27.0	22.0	*	24.5	20.0	*

\* - No data were recorded.

traffic operation or safety problem as a truck driver who does encroach on the centerline or curb.

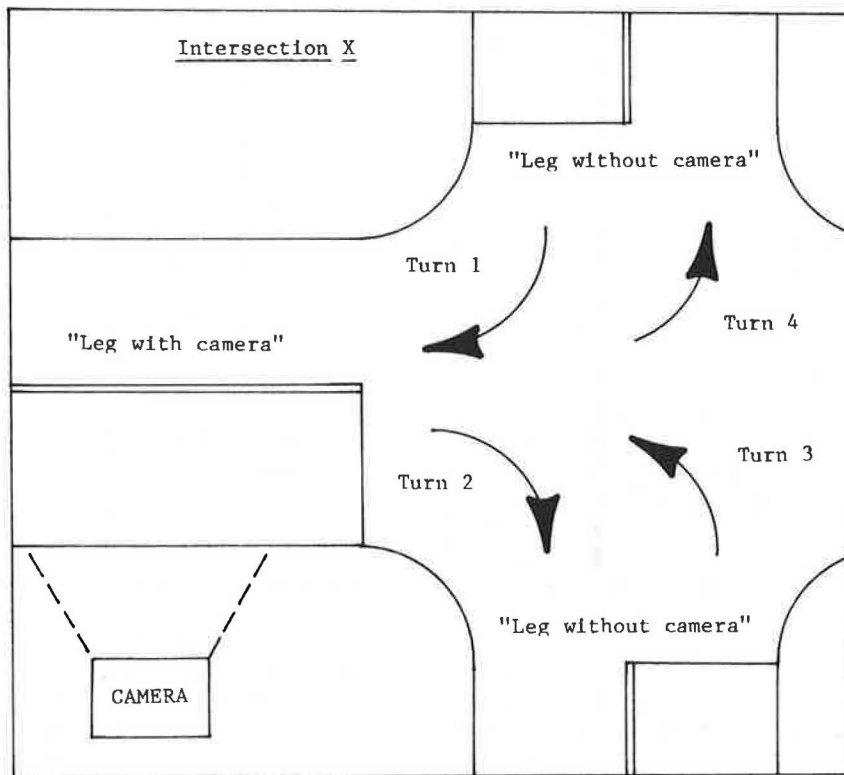
**FIELD OBSERVATION METHODOLOGY**

The discussion of the field observation methodology and data in the following sections is given in terms of a specific turn at an intersection, or site. Each site was assigned a two-digit number for identification as shown in figure 3. The first digit of the site number represents the intersection number (for example, 1 through 6, since data were collected at six intersections). The second digit of the site number represents the specific turn at the intersection. A "1" in the second digit represents a right turn onto the leg of the intersection where the data collection camera was stationed, a "2" represents a right turn from the leg with the camera, a "3" represents a left turn onto the leg with the camera, and a "4" represents a left turn from the leg with the camera.

Intersections for the field observation of turning trucks were chosen on the basis of a number of criteria. It was desired

that the study should include at least two states in different regions of the United States, and New Jersey and California were chosen. Those states had relatively large samples of large trucks operating on non-freeway routes, and officials in those states were willing to cooperate with the study. Intersections within those states were sought that had large volumes of turning truck traffic as well as certain geometric and traffic features, such as available observer positions, no channels or median barriers, no protected signal phases, no recessed stop bars, 90-degree turns, and minimal pedestrian volumes. It was desired that other geometric features such as lane widths, numbers of lanes, and curb radii vary between the observed intersections. Six intersections that were considered to best fit these criteria were selected. Some of the geometric features that varied among intersections are shown in table 3. The intersections range from a major intersection of seven-lane and five-lane arteries to a three-legged unsignalized intersection between four-lane and two-lane collector streets.

Both left and right turns by trucks were observed in the field. The measures of effectiveness (MOEs) examined during observations of truck turns included encroachments into adja-



"Site X1" refers to intersection X, turn 1.

"Site X2" refers to intersection X, turn 2.

"Site X3" refers to intersection X, turn 3.

"Site X4" refers to intersection X, turn 4.

**FIGURE 3** Field observation site numbering system.

TABLE 3 FIELD OBSERVATION SITE CHARACTERISTICS

Intersection Characteristic	1	2	3	4	5	6
State	NJ	NJ	Calif.	Calif.	Calif.	Calif.
Number of legs	4	4	4	4	3	3
Number of lanes, leg with camera	3	2	7	5	2	4
Number of lanes, legs without camera	4	4	5	4	4	4
Avg. lane width (ft.), leg with camera	16	11	12	10.5	12	10
Avg. lane width (ft.), legs without camera	12	10.5	12	10	10	11
Width of lane from which turn 1 was made (ft.)	No Turn	11	13	11	10	12
Width of lane from which turn 2 was made (ft.)	17	11	14	13	12	10
Avg. curb radius (ft.), turn 1	No Turn	45	55	32	12	40
Avg. curb radius (ft.), turn 2	21	55	55	35	12	32
Signalized?	Yes	Yes	Yes	Yes	No	Yes
Protected turn phases?	For turn 3 only	No	No	No	Not appli- cable	No

cent lanes, over the centerline, and over the curb; traffic conflict events such as weaving, stopping, and backing by vehicles into the traffic stream and by the truck; and the clearance time of the truck through the intersection. The clearance time was defined for trucks making right turns and trucks making rolling left turns (in other words, no impeding traffic forced the truck to stop beyond the stop line) as the difference between the time the front tires of the truck crossed the stop bar of the origin street into the intersection and the time the rear tires of the truck crossed the stop bar of the destination street. For left-turning trucks delayed by impeding traffic when they were beyond the stop bar of the origin street, the clearance time was defined as the difference between the time the truck began rolling forward and the time the rear tires crossed the stop bar on the destination street. Since there were very few rolling left turns completed by the trucks at most sites, the analyses were not biased by the use of the two definitions.

The hypotheses tested using the field observations were that larger trucks did not degrade operations at particular turns as measured by the MOEs in comparison to pre-STAA trucks. Larger trucks of interest were the semi 48 and the double 28. The semi 55, triple 28 and other larger trucks were not in common use at the times and locations of testing so adequate samples were not available for observation. Pre-STAA trucks of interest were the tractor-semitrailer combinations with semitrailer lengths of 40 feet (semi 40) and 45 feet (semi 45).

Manual observation was used to collect MOE data on turning trucks. A team of three observers stationed on different corners of the intersection examined turning trucks selected for study, with each observer recording only those MOEs for which he/she had the best view (each observer looked for different MOEs, depending on the turn the truck was making). A fourth observer recorded clearance time, using a stopwatch. A fifth observer photographed each truck selected for study. The slides of the photographs, taken from a known

distance at ground level, were later projected onto a screen, scaled off, and used to obtain the truck dimensions. Other clues, such as the number of 4-foot wide panels on the side of the trailer and the trailer size printed on the side of the trailer, were used to corroborate the scaled estimates of the truck dimensions.

Up to four different turns were observed at each intersection—each turn originating from or destined for the leg of the intersection on which the camera was stationed. Trucks approaching the intersection apparently ready to make one of the four turns were assigned an identification number and communication between the observers via walkie-talkie ensured that all observers were viewing the same truck. Observations were made only during daylight hours with dry pavement conditions.

The manual data collection method proved sensitive and accurate. Pretests with several people recording conflict and encroachment data at one observer position simultaneously and independently showed a high degree of correlation among observers. The photographic method of estimating truck size, when checked with trucks of known dimensions, proved sufficiently accurate to obtain trailer lengths within one foot of the actual length.

During the test period at the two New Jersey intersections (intersection numbers 1 and 2), control trucks were used to ensure adequate samples of certain types of trucks. These control trucks (a semi 40, a semi 48, and a double 28) were driven through the intersections repeatedly by a professional driver who knew the purpose of the testing.

#### FIELD OBSERVATION DATA

Data were collected on a total of 1,151 turning trucks, as shown in table 4. The sample included 412 semi 40s (108 control trucks and 304 trucks in the traffic stream), 443 semi

45s (all traffic stream), 177 semi 48s (90 control and 87 traffic stream), and 119 double 28s (61 control and 58 traffic stream). The samples per intersection ranged from 132 trucks at intersection 3 to 308 at intersection 1. Small samples of semi 48s and double 28s were collected at some intersections. It is not assumed that the sample of turning trucks observed is representative of the states of California and New Jersey or of the United States. Summary data from the field tests are given in tables 5, 6, and 7 for turn time, the proportion of trucks committing at least one encroachment, and the proportion of trucks causing at least one vehicle conflict, respectively.

#### COMPARISONS AMONG SITES

During the analysis of the field observation data, comparisons were made among sites to see where the most operational problems from large trucks can be expected and to see whether the sites were similar enough to warrant pooling the data. Pooling the data for different sites would allow larger sample sizes of semi 48 and double 28 observations to be formed which would allow more powerful testing among truck types.

Turn times for the traffic stream semi 45 (for which observations were plentiful at most sites) were compared for each pair of right turns at signalized intersections using the *t*-test. The tests revealed that the right turns from the leg with the camera at intersections 1 and 3 (sites 12 and 32) had significantly faster turn times (at the 0.05 level) than several other sites. These differences were not surprising, since table 3 shows that those sites had a relatively wide turn lane and a relatively long curb radius, respectively. Thus, the data from the remaining signalized right turn sites were pooled for comparisons of turn times between different truck types. In a similar series of *t*-tests using semi 45 turn times on signalized left turn sites, the left turn to the leg with the camera at intersection 1 and both left turns at intersection 4 (sites 13, 43, and 44, respectively)

TABLE 4 SAMPLE SIZES OF TRUCK TYPES AT INTERSECTIONS

Truck type	Number of trucks observed at Intersection						
	1	2	3	4	5	6	All inter- sections
Control - Semi 40	48	60	0	0	0	0	108
Control - Semi 48	60	30	0	0	0	0	90
Control - Double 28	29	32	0	0	0	0	61
Traffic - Semi 40	63	30	44	42	67	58	304
Traffic - Semi 45	94	67	42	65	121	54	443
Traffic - Semi 48	14	9	17	21	6	20	87
Traffic - Double 28	0	0	29	17	2	10	58
All truck types	308	228	132	145	196	142	1151

TABLE 5 FIELD OBSERVATIONS OF TURN TIME

Truck type	Inter-section number	Mean turn time (seconds) with sample size in parentheses			
		Right Turn		Left Turn	
		Turn 1	Turn 2	Turn 3	Turn 4
Control - Semi 40	1	(0)	7.56 (24)	7.21 (24)	(0)
	2	(0)	6.52 (30)	7.80 (30)	(0)
Control - Semi 48	1	(0)	7.98 (31)	9.15 (27)	(0)
	2	(0)	8.41 (15)	8.23 (14)	(0)
Control - Double 28	1	(0)	8.58 (16)	7.95 (16)	(0)
	2	(0)	8.22 (16)	9.16 (16)	(0)
Traffic - Semi 40	1	(0)	7.93 (26)	7.48 (16)	8.16 (21)
	2	7.76 (15)	8.35 (5)	6.85 (6)	10.95 (4)
	3	8.42 (4)	6.27 (14)	8.51 (13)	7.70 (13)
	4	12.63 (16)	11.88 (6)	11.70 (10)	10.32 (10)
	5	8.87 (5)	8.82 (23)	9.36 (36)	9.54 (2)
	6	8.22 (24)	7.79 (1)	8.85 (11)	9.80 (22)
Traffic - Semi 45	1	(0)	8.75 (42)	7.91 (34)	8.76 (18)
	2	10.17 (19)	8.66 (13)	9.06 (23)	10.31 (12)
	3	7.79 (9)	7.38 (15)	9.73 (12)	7.62 (6)
	4	10.40 (22)	11.96 (10)	10.51 (18)	10.76 (15)
	5	10.40 (6)	10.30 (49)	8.76 (63)	9.60 (3)
	6	8.62 (20)	6.73 (1)	9.39 (5)	9.13 (28)
Traffic - Semi 48	1	(0)	8.14 (8)	7.65 (5)	11.18 (1)
	2	6.77 (4)	7.87 (2)	8.93 (1)	13.19 (2)
	3	9.36 (3)	7.14 (4)	7.44 (4)	7.07 (6)
	4	12.42 (8)	15.71 (1)	9.03 (6)	11.72 (6)
	5	(0)	9.67 (4)	7.68 (2)	(0)
	6	7.31 (4)	5.95 (1)	9.86 (1)	9.46 (14)
Traffic - Double 28	3	6.66 (4)	6.34 (1)	9.66 (12)	11.62 (12)
	4	9.22 (8)	8.45 (1)	(0)	12.09 (8)
	5	(0)	(0)	9.24 (2)	(0)
	6	6.67 (3)	17.69 (1)	(0)	9.18 (6)

exhibited significantly different turn times (at the 0.05 level) than other sites. Site 13 had lower turn times, probably due to the protected turn signal phase for that turn. Sites 43 and 44 had higher turn times, due perhaps to the combination of narrow turn lanes and narrow destination streets. Data from the remaining signalized left turn sites were pooled in comparisons between truck types using turn times.

The proportion of semi 40s, semi 45s, and double 28s that committed at least one encroachment was compared for each pair of sites using the Kruskal-Wallis One-Way Analysis of Variance test. Significant differences were found to exist (at the 0.05 level) between each site and at least three other sites. Individual site characteristics apparently play a large role in the incidence of encroachments by turning trucks. A similar statistical analysis using vehicle conflict MOEs was not possible due to small numbers of conflicts at most sites, but inspection of the data does suggest variations in rates of con-

flict between sites. Thus, the conflict and encroachment data from different sites were not pooled.

A combination of several site characteristics appear to affect the encroachment rates, including lane widths, curb radii, stop bar location, and the number of lanes. Encroachment rates were relatively high at the right turn onto the leg with the camera at intersections 4 and 6 (sites 41 and 61, respectively) which has narrower turn lanes and narrower widths on the destination street than some other sites. Conversely, there was a relatively low proportion of encroachments at the right turn onto the leg with the camera at intersection 3 (site 31) where there was a wide turn lane and a long curb radius. Encroachment rates were relatively high at the left turn onto the leg with the camera at intersections 1 and 5 (sites 13 and 53, respectively), with only one lane on the target streets and stop bars set close to the intersection, and at the left turn from the leg with the camera at intersection 4 (site 44) with

TABLE 6 ENCROACHMENT DATA FROM FIELD OBSERVATIONS

Site number	Number of trucks with one or more encroachments/Observed total of trucks						
	Truck type						
	Control Semi 40	Control Semi 48	Control Db1. 28	Traffic Semi 40	Traffic Semi 45	Traffic Semi 48	Traffic Db1. 28
12	7/24	31/31	5/14	19/26	29/42	7/8	
13	3/24	25/29	5/15	14/16	28/34	5/5	
14				7/21	7/17	0/1	
21				13/15	19/19	4/4	
22	0/30	15/15	15/16	5/5	13/13	2/2	
23	0/30	11/15	2/16	1/6	8/23	0/1	
24				2/4	11/12	2/2	
31				0/4	4/9	1/3	2/4
32				6/14	8/15	4/4	0/1
33				0/13	0/12	0/4	0/12
34				1/13	4/6	0/6	3/12
41				15/15	22/22	8/8	8/8
42				6/6	10/10	1/1	1/1
43				5/10	9/18	4/6	
44				7/10	13/15	6/6	4/8
51				6/6	6/6		
52				22/23	48/49	3/4	
53				16/36	41/63	2/2	1/2
54				2/2	3/3		
61				23/24	19/20	4/4	3/3
62				1/1	1/1	1/1	1/1
63				0/11	0/5	0/1	
64				8/22	13/28	6/14	1/6
Total encroachments	10	85	27	179	316	60	24
Total number of trucks	108	90	62	303	442	87	58

a very narrow turn lane. Both left turns at intersection 3 sites (33 and 34), however, with relatively wide left turn lanes and wide destination streets, had virtually no encroachments.

#### COMPARISONS AMONG TRUCK TYPES

Comparisons were made among the data for control and for traffic-stream trucks of a given size at a given site, with a view toward pooling those observations. In general, *t*-tests on turn times for sites with sufficient sample sizes showed few differences between control and traffic-stream trucks. However, *Z*-tests on proportions of conflicts and encroachments for sites with sufficient samples showed many differences between control and traffic-stream trucks. This is reasonable, since the drivers of the control trucks were aware of the experiment and repeated the same turns many times. These drivers were familiar with each site and were likely to exercise special care

in making turns, particularly trying to avoid encroaching curbs or centerlines. Thus, in the comparisons among different truck types, the control and traffic-stream observations for a particular truck size at a particular site were not pooled.

The turn-time data were analyzed statistically using the *t*-test to compare two truck types for a particular site or pool of sites whenever there were at least five observations for each truck type. The *t*-test results, summarized in table 8, show that there were insufficient samples of turning trucks at many sites to conduct *t*-tests. For sites with sufficient samples, the test most often supported the hypothesis that there was no difference between truck types. The hypothesis was rejected for two important cases, however. First, in comparisons between semi 40 and semi 48 control trucks at two different sites, one right turn and one left turn, the semi 40 completed turns significantly faster. In both of those comparisons, the mean time for the semi 40 turn was about seven seconds while the mean time for the semi 48 was about nine seconds. It is not

TABLE 7 VEHICLE CONFLICT DATA FROM FIELD OBSERVATIONS

Site number	Number of trucks which caused one or more vehicle conflicts/ Observed total of trucks						
	Truck type						
	Control Semi 40	Control Semi 48	Control Db1. 28	Traffic Semi 40	Traffic Semi 45	Traffic Semi 48	Traffic Db1. 28
12	0/24	9/31	0/14	2/26	1/42	1/8	
13	7/24	9/29	3/15	2/16	11/34	1/5	
14				3/21	0/18	0/1	
21				2/15	7/19	2/4	
22	0/30	0/15	0/16	0/5	0/13	0/2	
23	4/30	5/15	6/16	1/6	6/23	1/1	
24				0/4	0/12	0/2	
31				1/4	1/9	1/3	0/4
32				2/14	0/15	0/4	0/1
33				1/13	0/12	1/4	0/12
34				1/13	0/6	1/6	0/12
41				3/16	4/22	4/8	0/8
42				1/6	2/10	0/1	1/1
43				0/10	1/18	1/6	
44				2/10	7/15	2/6	3/8
51				0/6	3/6		
52				1/23	5/49	1/4	
53				8/36	10/63	0/2	1/2
54				0/2	1/3		
61				1/24	3/20	0/4	0/3
62				0/1	0/1	0/1	1/1
63				0/11	0/5	0/1	
64				1/22	3/28	0/14	0/6
Total conflicts	11	23	9	32	65	16	6
Total number of trucks	108	90	62	304	443	87	58

clear why two sites showed differences while at two other sites the comparison of control truck turn times for the semi 40 and semi 48 had no differences. Second, the double 28 proved significantly slower in one comparison of right turn time (a control truck comparison with the semi 40 at site 22) and in four comparisons of left turn time (a control truck comparison with the semi 40 at site 23 and traffic stream comparisons for the pooled data with the semi 40, semi 45, and semi 48). The differences in mean turn times for these comparisons were usually 1.5 to 2.5 seconds. It appears that the double 28 generally had longer turn times where the intersection characteristics were less restrictive, since site 22 had a long curb radius, site 23 had a recessed stop bar, and the pooled data were heavily influenced by data from intersection 3 with less restrictive geometry.

The data in table 6 show that there were differences in the proportions of trucks committing at least one encroachment between truck types at some sites. The differences for the

control trucks are large. The semi 48 committed encroachments significantly more often (at the 0.05 level) than the semi 40 at all four sites observed and significantly more often (at the 0.05 level) than the double 28 at sites 12, 13, and 23. The control double 28 committed encroachments at a significantly greater rate (at the 0.05 level) than the semi 40 at site 22 and marginally more often (not statistically significant at the 0.05 level) at sites 13 and 23. The differences between truck types were less apparent for the traffic-stream trucks than for the control trucks, due to smaller samples of the semi 48 and double 28 or to the effects of differences among individual truck drivers who were unaware of the purposes of the observers. Statistical tests were inappropriate for most possible comparisons due to the small samples of semi 48s and double 28s.

Table 7 shows that the proportions of trucks causing a conflict did not vary much at particular intersections between truck types. For control trucks, the semi 48 caused conflicts

TABLE 8 SUMMARY OF *t*-TESTS ON TURN TIME DATA

Truck type comparison		Right turn sites							Left turn sites					
		12	22	32	41	52	61	Site* Group A	13	14	23	53	64	Site* Group B
Control trucks	Semi 40 vs. Semi 48	●	↑	▨	▨	▨	▨	▨	↑	▨	●	▨	▨	▨
	Semi 40 vs. Double 28	●	↑	▨	▨	▨	▨	▨	●	▨	↑	▨	▨	▨
	Semi 48 vs. Double 28	●	●	▨	▨	▨	▨	▨	●	▨	●	▨	▨	▨
Traffic trucks	Semi 40 vs. Semi 45	●		●	●	●	●	●	●	●		●	●	●
	Semi 40 vs. Semi 48	●			●			●	●				●	●
	Semi 40 vs. Double 28				●			●					●	↑
	Semi 45 vs. Semi 48	●			●			●	●				●	●
	Semi 45 vs. Double 28				●			●					●	↑
	Semi 48 vs. Double 28				●			●					●	↑

Note: Sites not shown had insufficient samples for t-test or no data collected for all comparisons.

\* - Site Group A includes sites 21, 22, 31, 41, and 42; B includes sites 14, 23, 33, 34, 63, and 64.

□ - Insufficient sample size for t-test.

▨ - No data collected.

● - No significant (0.05 level) difference in average turn time.

↑ - Significant (0.05 level) increase in mean turn time for second truck type.

marginally more often than the semi 40 and the double 28 at site 12, and the semi 48 and double 28 caused conflicts marginally more often than the semi 40 at site 23. Among traffic-stream trucks, a marginal difference among truck types was apparent only at site 41 between the semi 48 and the other truck types. Statistical tests again were generally inappropriate due to the small samples.

Until this point in the report, the fact that many semi 48s have moveable rear axles has not been mentioned. The computer simulation was performed with the rear axles of the semi 48 and semi 55 placed as far to the rear of the semitrailer as possible, and the control truck was also set up in this way. However, for the sample of semi 48s observed in the field, there was a noticeable variety in the position of the rear axles. The photographs of the turning semi 48s were thus examined for rear axle position. Of the 87 traffic-stream semi 48s, 43 had axles placed forward (six to nine feet from the center of the rear set of wheels to the rear of the semitrailer), 36 had axles placed back (three to six feet from the center of the rear set of wheels to the rear of the semitrailer), and eight had axle placements that could not be measured from the photographs. Since the rear axle placement affects offtracking and could affect truck performance on turns in terms of the MOEs studied in the field, the data for semi 48s were examined for the effects of different axle placements. The turn times for the pooled right turns and the pooled left turns were used to compare the semi 48 with axles forward to axles back. For the right turns, the trucks with axles back had a mean time of 11.3 seconds, compared to a mean of 7.3 seconds for the trucks with axles forward. This difference was statistically

significant at the 0.05 level using the *t*-test with 16 degrees of freedom. For left turns, the difference in mean turn times was negligible and statistically insignificant. Insufficient samples were available to analyze encroachments or conflicts for the axle positions.

The final step of the data analysis involved a look at the effect of the presence of a vehicle near the turning truck. There was concern that a given truck turned differently depending on whether there was a vehicle beside the truck before the turn or waiting at the stop bar in the center lane of the destination street (in other words, the truck was not free to swing wide during the turn) and that this bias was reflected in the turn time and encroachment results given previously. In addition, there was concern that analysis of the conflict data was biased against high-volume intersections, since low-volume intersections would have a greater proportion of turning trucks with no chance of conflicts (no other vehicles present to conflict with the truck). However, a duplication of the analyses described above using only the data recorded when there were other vehicles present (approximately four-fifths of all observations) showed that no important changes in the results already reported were necessary.

**CONCLUSIONS**

In reviewing the study results, the limitations of the study methods must be kept in mind. The simulation was limited because the differences among individual truck drivers, the reactions of the drivers of other vehicles in the traffic stream,



and the speed of the turn were not modeled. The field observations were limited because they were based partially on a control truck with a professional driver knowledgeable of the purpose of the observations and because of the small samples of traffic-stream truck data gathered at some sites. The results and conclusions should not be generalized to cover truck types or types of intersections that were not specifically tested.

No blanket regulations on truck routes should be based on this study. Many site, driver, and equipment variables must be examined before the decision to regulate truck traffic in a certain manner can be made. The computer simulation and field observation results showed that different types of trucks perform differently at different intersections and that small curb radii, narrow lane widths, and narrow destination roadways were among the geometric factors associated with increased operational problems.

Semi 48s and double 28s will have little impact on traffic operations at most intersections like those tested, but limited operational problems should be expected at some intersections. The simulation demonstrated that trailer width is not as critical to smooth operations as trailer length, over the ranges of trucks and intersections simulated. Among the larger trucks simulated, the semi 55 would be expected to cause the most operational problems at a given intersection, followed by the semi 48, the triple 28, and the double 28. In field tests, the semi 48 sometimes turned slower, committed more encroachments, and caused more conflicts than the semi 40. The double 28 sometimes turned slower, committed more encroachments, and caused more conflicts than the semi 40, but committed fewer encroachments and caused fewer conflicts than the semi 48. The axle position of the semi 48 made a difference in right turn time, with the larger offtracking of the truck when the axles are back causing a longer turning time, but did not make a difference in left turn time.

Tests in this research were conducted under ideal conditions. Many of the important field test results were based on an experienced driver operating a truck in good condition through a familiar intersection with dry pavement during the day. There remains a need for study of large truck operations under less-than-ideal conditions. Future examinations of large truck operation should include problems associated with inex-

perienced or impaired drivers, faulty equipment, and wet pavement, for instance.

#### ACKNOWLEDGMENT

This paper is based on work performed by the authors at Goodell-Grivas, Inc., of Southfield, Michigan, for the Office of Safety and Traffic Operations Research and Development of the Federal Highway Administration. The views and opinions expressed in this paper are those of the authors and do not necessarily reflect the views of the Federal Highway Administration. The authors assume sole responsibility for the accuracy of the data and conclusions presented in this paper.

#### REFERENCES

1. C. V. Zegeer, J. E. Hummer, and F. Hanscom. *The Operation of Larger Trucks on Roads With Restrictive Geometry*. FHWA/RD-86/157 and FHWA/RD-86/158 (two volumes), FHWA, U.S. Department of Transportation, July 1986.
2. O. F. Gericke and M. Walton. Effect of Truck Size and Weight on Rural Roadway Geometric Design (and Redesign) Principles and Practices. In *Transportation Research Record 806*, TRB, National Research Council, Washington, D.C., 1981, pp. 13-21.
3. *Test and Demonstration of Double and Triple Trailer Combinations*. Ontario Ministry of Transportation and Communications, Aug. 1982.
4. *Offtracking Characteristics of Trucks and Truck Combinations*. Research Committee Report Number 3, Western Highway Institute, San Francisco, California, September 1970.
5. *Triple Trailer Study in California*. California Department of Public Works in cooperation with the California Highway Patrol, March 1972.
6. F. R. Hanscom. *The Effect of Truck Size and Weight on Accident Experience and Traffic Operations*, Volume II, *Traffic Operations*. FHWA/RD-80/136. FHWA, U.S. Department of Transportation, July 1981.

---

*Publication of this paper sponsored by Committee on Operational Effects of Geometrics.*

*Abridgment*

# Magnitude and Severity of Drainage-Structure-Related Highway Accidents

H. DOUGLAS ROBERTSON

The Federal Highway Administration sponsored a study to determine the nature and magnitude of accidents related to roadside drainage structures. Accident data from national and state databases for the years 1981–1984 were analyzed with respect to their relationship to drainage structures. The findings revealed that drainage structures were involved in approximately 9 percent of all accidents on Federal-aid roads and were the first object struck in approximately 4.5 percent of all accidents. A high incidence of fatalities and serious injuries were associated with these accidents. Most of the accidents involved a single vehicle that struck a curb, ditch, embankment, or culvert. Drainage-structure-related accidents predominantly involved a single vehicle and occurred in a higher proportion at night and in adverse weather compared to the same characteristics for all accidents. Based on the findings related to roadway characteristics, drainage-structure accidents were over-represented on Federal-aid secondary roads, at non-junctions, in curves and on grades, and on wet surfaces. This paper contains a brief summary of the study results. A complete documentation of the methodology and findings may be found in FHWA Report DTFH61-85-C-00065.

Safety enhancement is a high priority on federally funded 3R and 4R (resurfacing, restoration, rehabilitation, and reconstruction) programs. Much effort has been directed at reducing roadside hazards through removing, relocating, or protecting fixed objects from errant vehicles. In spite of these improvements, fixed objects were the most harmful event in 47.1 percent of the fatal single-vehicle accidents in 1983.

Research to date has focused largely on improvements to utility poles, sign supports, guardrails, median barriers, and bridge rails. Concern has been expressed that drainage structures may also pose significant safety hazards in run-off-road accidents. Thus the Federal Highway Administration (FHWA) sponsored a study to determine the nature and magnitude of accidents in which drainage structures were involved.

To identify the nature and magnitude of hazardous conditions that are associated with drainage structures is neither a straightforward nor an easy task. While there is a tremendous amount of data available on highway accidents, there are no known accident databases that either uniformly or directly code accidents involving vehicles that strike the various types of drainage structures. The information contained in those databases that code drainage structures is limited and generic in nature.

University of North Carolina at Charlotte, Civil Engineering Department, Charlotte, N.C. 28223.

## FINDINGS

The following discussion is based on the results of an analysis of the 1982, 1983, and 1984 National Accident Sampling System (NASS) raw data files and the 1983 NASS weighted data file, which contains an estimate of total accidents and their characteristics. The NASS data are for Federal-aid roads only and represent police-reported accidents where the first harmful event was coded as a collision with a drainage structure. In addition, the NASS raw data files contain information on situations where one or more of the first four objects contacted by any vehicle involved in the accident was a drainage structure.

Computer printouts of one-way and two-way variable tables were obtained from the 1983 NASS weighted data file for both drainage-structure-related accidents and for all accidents on Federal-aid roads. The following discussion summarizes the key findings from an analysis of those tables.

The first question addressed was, "What is the magnitude of drainage-structure-related accidents?" The answer is summarized in table 1. Drainage-structure-related accidents, as defined by first harmful event, constitute approximately 4.5 percent of annual accidents on Federal-aid roads in the United States, or 176,120 of the 3,934,006 police-reported accidents. Accidents involving curbs are the most frequently occurring, representing 31.5 percent of drainage-structure-related accidents and 1.4 percent of all accidents.

The question that came to mind, however, was just how well did the first-harmful-event criterion serve as an indicator of drainage-structure-related accidents? To answer that question, further analyses were performed, using first the 1983 NASS raw data file.

A search of the vehicle file revealed 664 cases in which one or more of the up to four objects struck was either a culvert, ditch, curb, or soft embankment. A cross check of these same cases in the accident file revealed that in 333 of the 664 cases (50 percent) the first harmful event was either a culvert, ditch, curb, or soft embankment. The immediate conclusion, then, was that first harmful event underestimated the number of drainage-structure-related accidents by a factor of two.

To ensure that this was not an anomaly in the 1983 data, a similar analysis was performed on the 1982 and the just-completed 1984 NASS data files. In both cases, drainage structure first harmful events occurred in 51 percent of the cases where a drainage structure was coded as one or more of the objects struck in the vehicle file. Thus, it was concluded

TABLE 1 DRAINAGE STRUCTURE ACCIDENTS BY FIRST HARMFUL EVENT

Object Struck	Frequency	Percent	% of Total Accidents*
Curb	55,440	31.5	1.41
Ditch	37,282	21.2	0.95
Embankment (soft)	33,313	18.9	0.85
Culvert	24,885	14.1	0.63
Wall	20,790	11.8	0.53
Embankment (hard)	4,410	2.5	0.11
Total	176,120	100.0	4.48

\* 1983 NASS estimate of 3,934,006 police-reported accidents on Federal-aid roads.

TABLE 2 SEVERITY OF DRAINAGE STRUCTURE ACCIDENTS

Injury-Severity	Frequency	Percent	% Of Total Accidents*	% Of Total Accidents w/ Same Severity
Fatal	2,136	1.2	0.06	9.3
Incapacitating	18,152	10.5	0.47	7.2
Non-incapacitating	26,327	15.3	0.69	5.0
Possible	39,470	23.0	1.03	6.8
None	85,753	50.0	2.24	3.5

\*1983 NASS weighted estimate of 3,831,841 accidents on Federal-aid roads with known accident severity.

TABLE 3 COMPARISON OF THE SEVERITY OF DRAINAGE-STRUCTURE ACCIDENTS TO THE SEVERITY OF ALL ACCIDENTS (IN PERCENT)

Injury Severity	Drainage Structure	All Accidents
Fatal	1.2	0.6
Incapacitating	10.5	6.6
Non-incapacitating	15.3	13.8
Possible	23.0	15.0
None	50.0	64.0
Total	100.0	100.0

that drainage-structure-related accidents are involved in approximately 8 to 9 percent of all police-reported accidents on Federal-aid roads.

In addition to occurrence, it is important to assess the severity of these accidents. Table 2 shows that one or more fatalities occurred in 1.2 percent of and incapacitating injuries occurred in 10.5 percent of the drainage-structure-related accidents based on the first-harmful-event criterion from the 1983 NASS weighted data file. In terms of all accidents, fatal accidents represented 0.06 percent and incapacitating injuries represented 0.47 percent. The last column of table 2 indicates that

drainage-structure-related accidents represent 9.3 percent of all fatal accidents and 7.2 percent of all incapacitating injury accidents on Federal-aid roads. On the other hand, they represent only 3.5 percent of the accidents with no injuries.

To provide yet another perspective and a basis of comparison, table 3 shows the distribution of all accidents and reveals that drainage accidents are almost twice as severe, in terms of fatalities and incapacitating injuries, as all accidents. One-half of all drainage-structure accidents involve injuries compared to 38 percent of all accidents.

Table 4 characterizes the relative severity of the accidents

TABLE 4 SEVERE (FATAL OR INCAPACITATING INJURY)  
ACCIDENTS BY TYPE OF DRAINAGE OBJECT STRUCK

Object Struck	Frequency	Percent of Type Object
Embankment (hard)	1,349	30.6
Embankment (soft)	4,425	13.3
Curb	7,324	13.2
Ditch	3,694	9.9
Wall	1,805	8.7
Culvert	1,691	6.8

TABLE 5 COMPARISON OF LIGHT CONDITIONS (IN PERCENT)

Light Condition	Drainage Structure Accidents	All Accidents
Daylight	44.5	62.2
Dark	28.1	11.0
Dark, Lighted	22.8	22.4
Dawn	1.8	1.0
Dusk	2.8	3.4
Total	100.0	100.0

TABLE 6 COMPARISON OF WEATHER CONDITIONS (IN PERCENT)

Weather	Drainage Structure Accidents	All Accidents
No Adverse	69.3	78.4
Rain	18.2	14.8
Sleet	1.6	0.3
Snow	3.7	5.7
Fog	6.6	0.6
Other	0.6	0.2
Total	100.0	100.0

involving each of the drainage-structure types. It shows the number of fatal or incapacitating-injury accidents for each object type and the percent they represent of the total accidents of that type. For example, 30.6 percent (1,349) of the total hard embankment accidents (4,410 from table 1) involve fatalities or incapacitating injuries. While hard embankments exhibit the highest proportion of severe accidents, they occur with the lowest frequency.

It must be remembered that this analysis does not account for exposure. For example, there are more miles of soft embankment than hard ones; therefore, the rate of occurrence (per vehicle miles traveled) might not be the lowest. From table 4, it appears that curb-related accidents are severe and occur with the greatest frequency of all the drainage structure categories.

The remaining findings are based on selected general accident characteristics of drainage accidents compared and contrasted to the same characteristics of all accidents from the 1983 NASS weighted data file. These findings in part describe the nature of drainage-structure-related accidents.

Drainage structure accidents occur at a higher proportion in the dark than all accidents, 28 percent compared to 11 percent (table 5). Table 6 indicates that a higher proportion of drainage-structure accidents occurs in adverse weather than is the case for all accidents.

The incidence of drainage-structure accidents in curves and on grades is twice that of all accidents (tables 7 and 8). Finally, table 9 shows that a higher proportion of drainage structure accidents occurs on a wet road surface than is the case for all accidents.

TABLE 7 COMPARISON OF ROADWAY ALIGNMENT (IN PERCENT)

Alignment	Drainage Structure Accidents	All Accidents
Straight	62.1	83.0
Curved	37.0	17.0
Total	100.0	100.0

TABLE 8 COMPARISON OF ROADWAY PROFILE (IN PERCENT)

Grade	Drainage Structure Accidents	All Accidents
Level	57.7	75.1
Grade (-2%)	40.3	23.0
Hillcrest	0.8	1.0
Sag	1.2	0.9
Total	100.0	100.0

TABLE 9 COMPARISON OF ROADWAY SURFACE CONDITION (IN PERCENT)

Surface Condition	Drainage Structure Accidents	All Accidents
Dry	64.8	70.2
Wet	27.8	21.5
Snow or Slush	3.0	4.5
Ice	4.4	3.8
Total	100.0	100.0

## CONCLUSIONS

Based on the findings of the NASS accident data analysis, drainage-structure-related accidents represent eight to nine percent of the total highway safety problem on Federal-aid roadways. These accidents are quite severe. In terms of all accidents, those involving curbs occur most frequently, while in terms of accident severity, hard embankments are the most dangerous. The review of scene photographs suggests that curb design improvements and, in some cases, curb removal would have reduced the severity, if not the occurrence, of many of the curb accidents reviewed.

Drainage-structure-related accidents occur in a higher proportion at night and in adverse weather compared to the same characteristics for all accidents. Based on the findings related

to roadway characteristics, drainage-structure accidents are overrepresented in curves, on grades, and on wet surfaces.

## REFERENCES

1. *Fatal Accident Reporting System*. National Highway Traffic Safety Administration, Washington, D.C., 1983.
2. H. D. Robertson, S. Basu, K. Colpitts, S. Stein, F. Johnson, and G. K. Young. *Safer Drainage Systems*. Report DTFH61-85-C-00065, Federal Highway Administration, Washington, D.C., July 1986.

*Publication of this paper sponsored by Committee on Operational Effects of Geometrics.*

# Effective Use of Passing Lanes on Two-Lane Highways

DOUGLAS W. HARWOOD, CHRIS J. HOBAN, AND DAVEY L. WARREN

---

Passing lanes have been found to be effective in improving overall traffic operations on two-lane highways. Many of the traffic operation problems on rural two-lane highways result from the lack of passing opportunities due to limited sight distance and heavy oncoming traffic volumes. Passing lanes can provide an effective method for improving traffic operations on two-lane highways at a lower cost than required for constructing a four-lane highway. The paper presents guidelines for effectively locating, designing, signing, and marking passing lanes to improve traffic operations. A procedure for estimating the operational effectiveness of passing lanes in terms of improved service is presented. The paper also presents an evaluation of the effectiveness of passing lanes in reducing accidents on two-lane highways.

---

A passing lane is an added lane provided in one or both directions of travel on a conventional two-lane highway to improve passing opportunities. This definition includes passing lanes in level or rolling terrain, climbing lanes on grades, and short four-lane sections. The length of the added lane can vary from 1,000 feet to as much as three miles. Figure 1 illustrates a plan view of a typical passing lane section.

Many of the traffic operational problems on rural two-lane highways result from the lack of passing opportunities due to limited sight distance and heavy oncoming traffic volumes. Passing lanes provide an effective method for improving traffic operations on two-lane highways by providing additional passing opportunities at a lower cost than required for constructing a four-lane highway. This lower-cost approach is appropriate because there is a growing backlog of rural roads requiring improvement, and the funds are simply not available to four-lane every two-lane highway that experiences poor levels of service.

## FUNCTIONS OF PASSING LANES

Passing lanes have two important functions on two-lane rural roads:

- To reduce delays at specific bottleneck locations, such as steep upgrades where slow-moving vehicles are present and
- To improve overall traffic operations on two-lane high-

ways by breaking up traffic platoons and reducing delays caused by inadequate passing opportunities over substantial lengths of highway

The first function, to reduce delays at bottleneck locations, has been recognized for some time, and guidelines for the provision of climbing lanes on grades have been established. The second function, to improve overall traffic operations, has evolved more recently, particularly as a result of the lack of funds for major road improvements. In practice, many passing lanes perform both functions, and it is often difficult to make a clear operational distinction between the two. The distinction is important, however, in planning and design. The evaluation of a climbing lane considers only the bottleneck location, with the objective of improving traffic operations at the bottleneck to at least the same quality of service as adjacent road sections. For passing improvements, on the other hand, the evaluation should consider traffic operations for an extended road length, typically 5 to 50 miles. Furthermore, the location of the passing improvement can be varied and selecting an appropriate location is an important design decision.

## LOCATION AND CONFIGURATION

When passing lanes are provided at an isolated location, their function is generally to reduce delays at a specific bottleneck, and the location of the passing lane is dictated by the needs of the specific traffic problem encountered. Climbing lane design guidelines, for example, usually call for the added lane to begin before speeds are reduced to unacceptable levels and, where possible, to continue over the crest of the grade so that slower vehicles can regain some speed before merging. Requirements for sight distance and taper lengths further define the location of such lanes. In some cases, construction of a climbing lane over the full length of a grade may be too expensive, and the use of shorter lanes over part of the grade may be considered. Recent research at the University of California (1) suggests that single short climbing lanes of approximately 1,500 feet near the midpoint of the grade, or two such lanes at the one-third and two-thirds points, are cost-effective methods for providing passing opportunities on long sustained grades. The location of a climbing lane drop on an upgrade section has been found to produce no adverse safety problems, provided sight distance is adequate (2).

When passing lanes are provided to improve overall traffic operations over a length of road, they are often constructed at regular intervals. The designer can choose from a number of alternative configurations (3), as illustrated in figure 2.

---

D. W. Harwood, Midwest Research Institute, 425 Volker Boulevard, Kansas City, Mo. 64110. C. J. Hoban, Australian Road Research Board, 500 Burwood Highway, Vermont South 3133, Victoria, Australia. D. L. Warren, Federal Highway Administration, 6300 Georgetown Pike, McLean, Va. 22101.

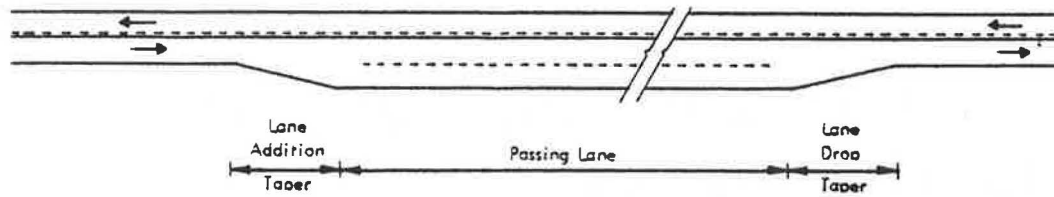


FIGURE 1 Plan view of typical passing lane section.

Factors that should be considered in choosing the location and configuration for passing lanes are discussed below.

### Location

A primary objective in choosing the location for a passing lane should be to minimize construction costs, subject to other constraints. Data from several states indicate that the cost of constructing a passing lane can vary from \$200,000 to \$750,000 per mile, depending on terrain. Climbing lanes in mountainous areas can cost as much as \$1,800,000 per mile. Thus, the choice of a suitable location for a passing lane may be critical to its cost-effectiveness. A construction cost profile indicating the longitudinal variation of construction cost per mile along the road can be a useful tool in selecting passing lane locations.

The passing lane location should appear logical to the driver. The value of passing lanes is more apparent to drivers at locations where passing sight distance is restricted than on long tangent sections that already provide good passing opportunities. In some cases, a passing lane on a long tangent may encourage slow drivers to speed up, thus reducing the passing lane effectiveness. At the other extreme, highway sections with low-speed curves are not appropriate for passing lanes, since passing may be unsafe.

The passing lane location may be on a sustained grade or on a relatively level section. If delay problems on a grade are severe, the grade will usually be the preferred location for a passing lane. However, if platooning delays exist for some distance along a road, locations other than upgrades should also be considered for passing lanes. While speed differences between vehicle types are often greater on upgrades than on level or rolling sections, particularly if heavily loaded trucks are present, construction costs and constraints may be greater at such locations. Some types of slow vehicles, such as recreational vehicles, are not slowed by upgrades as dramatically as heavy trucks; passing lanes in rolling terrain may provide opportunities to pass such vehicles that are just as good as the opportunities provided by passing or climbing lanes on upgrades. Passing lanes are also effective on level terrain where the demand for passing opportunities exceeds supply.

The passing lane location should provide adequate sight distance at the lane-addition and lane-drop tapers.

The location of major intersections and high-volume driveways should be considered in selecting passing lane locations, to minimize the volume of turning movements on a road section where passing is encouraged. Low-volume intersections and driveways do not usually create problems in passing lanes. Where the presence of higher-volume intersections and driveways cannot be avoided, special provisions for turning

vehicles should be considered. The prohibition of passing by vehicles travelling in the opposing direction should also be considered on passing lane sections with high-volume intersections and driveways.

Locations with other physical constraints, such as bridges and culverts, should be avoided if they restrict the provision of a continuous shoulder.

Passing lanes can also be constructed as part of realigning a road segment that has safety problems.

### Configuration

Separated or adjoining passing lanes (shown as (c) through (f) in figure 2) are often used in pairs, one in each direction, at regular intervals along a two-lane highway.

Where pairs of adjoining passing lanes are used and passing by opposing direction vehicles is prohibited, the use of configuration (e) in figure 2 has the advantage of building platoons before the passing lane, whereas the reverse configuration tends to rebuild platoons more quickly after the passing lane. This configuration is also preferred because the lane-drop areas of the opposing passing lanes are not located adjacent to each other.

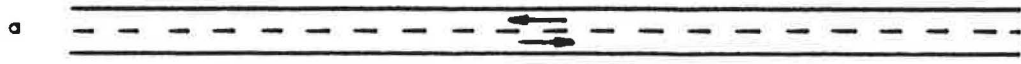
Transitions between passing lanes in opposing directions should be carefully designed; intersections, bridges, two-way left-turn lanes, or painted medians can often be used effectively to provide a buffer area between opposing passing lanes.

Alternating passing lanes (shown as (g) and (h) in figure 2) are sometimes appropriate where a wide pavement is already available. However, the provision of passing lanes over 50 percent of the road length is probably excessive. Drivers may also feel unduly constrained when passing is prohibited on the other 50 percent of the road length if sight distance is good and traffic volumes are low.

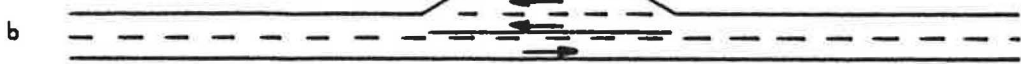
Short, four-lane sections, both divided and undivided, are particularly appropriate where the ultimate design is for the highway to have four lanes. Construction of short, four-lane sections at the least expensive locations can provide a substantial proportion of the benefits of the ultimate design for a relatively small proportion of the total cost, particularly if major bridge work or right-of-way acquisition can be avoided. This staged four-laning will generally return a high benefit-cost ratio, while economic justification for the remaining stages will increase with increasing traffic volumes in future years. Where the ultimate design is uncertain or the need for it is many years away, however, the use of lower cost options should be considered.

Overlapping passing lanes (shown as (i) and (j) in figure 2) are often used at crests where a climbing lane is provided on each upgrade.

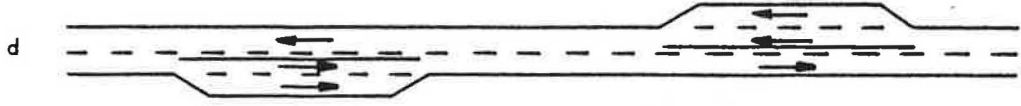
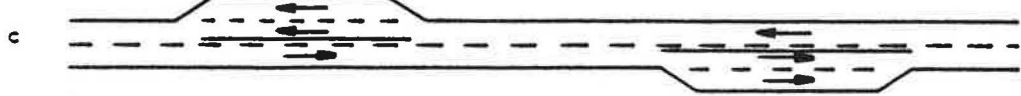
Conventional Two-lane Highway



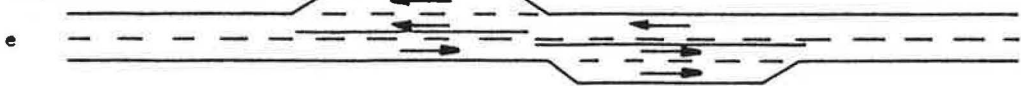
Isolated Passing Lane



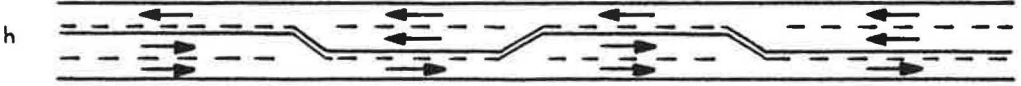
Separated Passing Lanes



Adjoining Passing Lanes



Alternating Passing Lanes



Overlapping Passing Lanes



Side-by-side Passing Lanes



FIGURE 2 Alternative configurations for passing lanes.



## GEOMETRIC DESIGN

The length of the passing lane, the lane and shoulder widths, and the lane-addition and lane-drop taper designs should be considered in the geometric design of passing lanes. The following guidelines for geometric design were developed by Harwood and Hoban (5).

Passing lanes should generally be from 0.5- to 1.0-mile long, excluding tapers. Passing lanes less than 0.5-mile long are usually not effective in creating additional passing opportunities, and passing lanes over 1.0-mile long are usually not cost-effective (5, 6). The choice of an optimal design length for passing lanes on two-lane highways should be a function of the traffic flow rate and is addressed in a later section of this paper.

The lane widths in a passing lane section usually should not be narrower than the lane widths on the adjacent sections of two-lane highway; 12-foot lane widths are desirable. It is also desirable for passing lane sections to have a minimum four-foot shoulder width on either side of the highway. Wherever possible, the shoulder width in a passing lane section should not be narrower than the shoulder width on the adjacent sections of two-lane highway.

The lane-addition and lane-drop transition areas at the beginning and end of a passing lane should be designed to encourage safe and efficient traffic operations. Many highway agencies have used relatively short lane-addition and lane-drop tapers at passing lanes. However, the use of longer tapers should be encouraged to minimize traffic conflicts and to get the greatest operational benefit from the investment in passing lanes.

The lane-drop taper at the downstream end of a passing lane should be designed in accordance with the requirements for lane reduction transitions set by the FHWA Manual on Uniform Traffic Control Devices for Streets and Highways (MUTCD), Section 3B-8. The recommended geometric configuration is to terminate the right lane with a lane-drop taper and merge the traffic from both lanes into a single lane. In a few cases, such as alternating passing lanes on a three-lane pavement of constant width, dropping the left lane is appropriate. The lane-drop taper length should be computed from the formula  $L = WS$ , where  $L$  is the taper length in feet,  $W$  is the width of the dropped lane in feet, and  $S$  is the prevailing off-peak 85th percentile speed in miles per hour (mph). At the termination of a 12-foot lane, the required taper length for a 60-mph prevailing speed is 720 feet. A wide shoulder is desirable at the lane-drop taper to provide a recovery area in case drivers encounter a merging conflict.

There is no MUTCD requirement for the length of the lane-addition taper at the upstream end of a passing lane. The diverge maneuver does not require as much length as the merge maneuver, but a good lane-addition transition design is needed for effective passing lane operations. The recommended length for a lane-addition taper is half to two-thirds of the length of a lane-drop taper, or 360 to 480 ft in the example of the 60-mph design speed presented above.

Passing lanes are most effective if the majority of drivers enter the right lane at the lane-addition transition and use the left lane only when passing a slower vehicle. Little or no operational benefit is gained from passing lanes if most drivers continue in the left lane. The geometric design of the lane-addition transition area, together with appropriate signing and

marking (discussed below) should encourage drivers to enter the right lane of the passing lane section.

Safe and effective passing lane operations require adequate sight distance on the approach to both the lane-addition and lane-drop tapers. Inadequate sight distance in advance of the lane-addition taper may result in lack of readiness by vehicles wishing to pass, so that some of the length of the passing lane is wasted. When sight distance approaching the lane-drop taper is limited, vehicles may merge too early or too late, resulting in erratic behavior and poor use of the passing lane. Therefore, passing sight distance appropriate for the speed of the highway on the approach to each taper is recommended. Above-minimum passing sight distance in the taper areas is desirable.

## TRAFFIC CONTROL DEVICES

The signing and marking of passing lanes is partially addressed in the MUTCD (4), which indicates the appropriate centerline markings for passing lanes and the signing and marking of lane-drop transition areas. The following discussion extends the MUTCD criteria to provide a consistent set of traffic control devices for use at passing lanes, as illustrated in figure 3. The recommended signing and marking practice presented here were developed by Harwood and Hoban (5) from review of the practices of 13 states (6) and the practices used in Australia and Canada (3). The recommended practice is presented here not to suggest that it should be adopted in precisely this form by every highway agency, but to illustrate the types of signs and markings that are needed for effective operation of passing lanes.

### Signing

Signing is needed to convey information to drivers at three locations at passing lane sites:

- In advance of the passing lane,
- At the lane addition, and
- In advance of the lane drop.

#### *Advance Signing*

A sign with the legend **PASSING LANE ½ MILE** should be placed 0.5 mile in advance of each passing lane. This sign provides advance notice of the passing lane to the drivers of both slow-moving vehicles and following vehicles so that they can prepare to make effective use of the passing lane. Additional advance signs are desirable two to five miles in advance of a passing lane. Such advance signing may reduce the frustration and impatience of drivers following a slow-moving vehicle because they know they will soon have an opportunity to pass. Driver frustration and impatience when following slow-moving vehicles has been shown to be a potential safety problem on two-lane highways. Hostetter and Seguin (7) found, for example, that when forced to follow a slow-moving vehicle for up to 5 miles, almost 25 percent of drivers passed illegally in a no-passing zone.

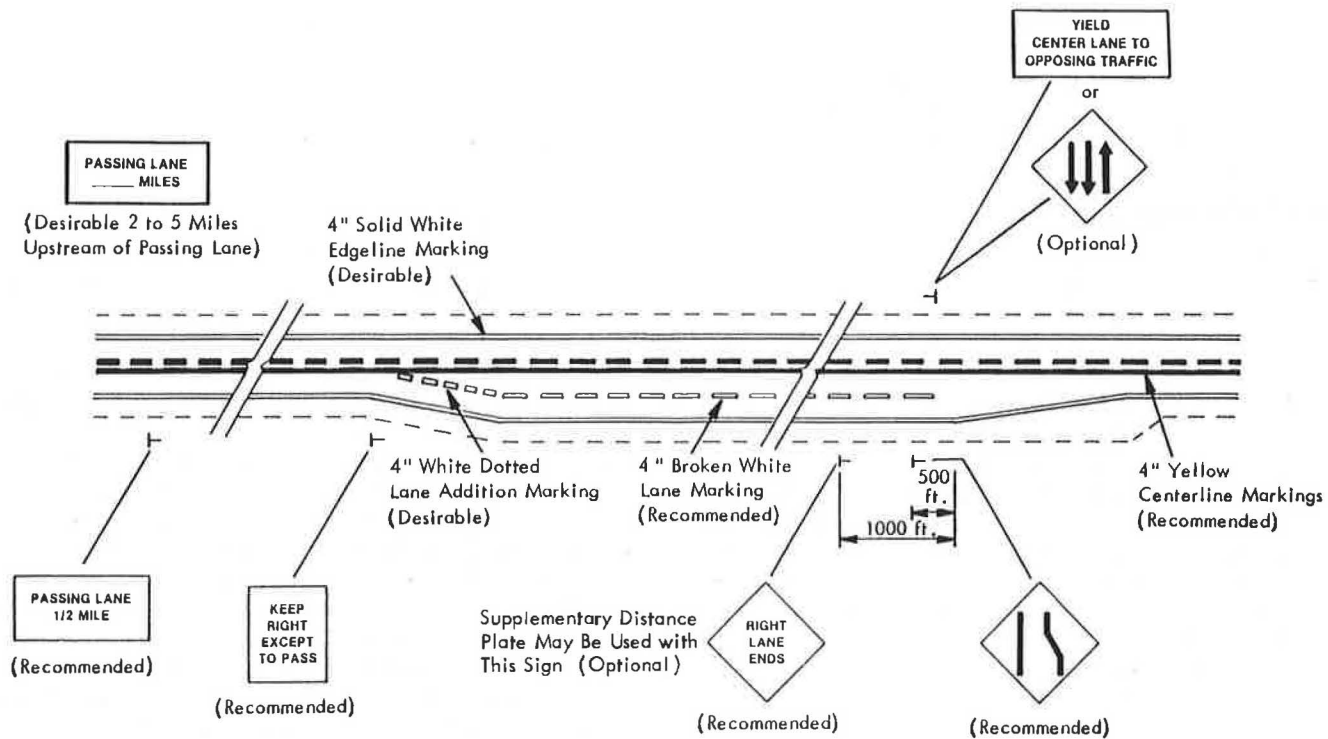


**FIGURE 3** Recommended signing and marking practices for passing lanes.

*Lane-Addition Signing*

A black-on-white regulatory sign with the legend **KEEP RIGHT EXCEPT TO PASS** should be placed at the beginning of the lane-addition taper. This sign, in conjunction with the geometrics and pavement markings at the lane-addition taper, informs drivers of the beginning of the passing lane and encourages them to enter the right lane unless they are immediately behind a vehicle they wish to pass. An acceptable alternative legend for this sign is **SLOWER TRAFFIC KEEP RIGHT**, although this legend is not preferred because it provides less definite instructions to drivers. Sign legends that refer specifically to trucks, such as **TRUCKS USE RIGHT LANE**, are not recommended because they appear to exclude other vehicle types, such as slow-moving recreational vehicles and passenger cars, which should also be encouraged to use the right lane.

*Lane-Drop Signing*

The MUTCD requires a black-on-yellow warning sign, either a symbol sign or a text sign, in advance of a lane drop. According to MUTCD table II-1, for a prevailing speed of 60 mph, a single warning sign should be placed 775 feet in advance of a decision point that requires a high degree of judgment, such as a lane-drop merging maneuver. Many highway agencies use two warning signs in advance of the lane-drop transition areas of passing lanes, and this practice is recommended. The first advance warning sign with the legend **RIGHT LANE ENDS**, should be located 1,000 feet in advance of the lane-drop taper. This sign may carry a supplemental distance plate (for example, 1,000 FEET) below the sign. The second advance warning sign should be the lane reduction transition symbol

sign and should be located 500 feet in advance of the lane-drop taper.

*Signing for Opposing Traffic*

Highway agencies that generally provide signing for passing and no-passing zones on conventional two-lane highways, including the **DO NOT PASS** sign, the **PASS WITH CARE** sign, and the pennant-shaped **NO PASSING ZONE** sign, usually continue this practice in the opposing direction of travel at passing lane sites. Where passing by vehicles travelling in the opposing direction is permitted, some agencies use a regulatory sign specifically appropriate to passing lanes, such as **YIELD CENTER LANE TO OPPOSING TRAFFIC**, in place of the **PASS WITH CARE** sign. An alternative sign for use in the opposing direction to a passing lane is the three-arrow sign used in Australia, which is illustrated in figure 3. This sign does not identify whether passing by vehicles travelling in the opposing direction is permitted or prohibited, but it does inform drivers that there are two lanes of oncoming traffic.

**Marking**

A passing lane section with two lanes in one direction of travel and one lane in the opposite direction of travel should be marked in accordance with MUTCD figure 3-2. A yellow centerline marking should be used to separate the lanes normally used by traffic moving in opposite directions. A broken white lane line is used to separate traffic in lanes normally moving in the same direction. Pavement edge lines are desirable on both sides of the highway in passing-lane sections to

guide drivers and to delineate the boundary between the pavement and shoulder.

Passing by vehicles travelling in the opposing direction to a passing lane may be either permitted or prohibited, as illustrated in MUTCD figure 3-2. A study by Harwood and St. John (6) found no difference in cross-centerline accident rates between passing lane sections where passing in the opposing direction was prohibited and passing lane sections where passing in the opposing direction was permitted where adequate sight distance was available. Therefore, passing by opposing-direction vehicles may be allowed where sight distance is adequate. This finding indicates that passing lanes where passing by opposing direction vehicles is permitted do not have safety problems of the type that occurred many years ago on three-lane highways with center lanes available for unrestricted use by vehicles travelling in either direction. Passing zones should be marked for the opposing direction of travel in passing lanes where warranted by the same criteria used in marking normal two-lane highways, specified in MUTCD Section 3B-5. For a 60-mph prevailing speed, a no-passing zone is warranted in the opposing direction of travel where sight distance is less than 1,000 feet.

It is not a desirable practice to prohibit passing by vehicles travelling in the opposing direction at all passing lane sites, because this unnecessarily reduces the level of service in that direction of travel. Prohibition of passing in the opposing direction at all passing lanes, regardless of sight distance, may be counterproductive to improved safety, since some drivers travelling in the opposing direction may be tempted to pass despite the prohibition in areas of good sight distance. Some agencies may choose to institute a site-by-site review of passing lanes and prohibit opposing direction passing at particular sites on the basis of unusual geometrics, roadside development, high traffic volumes, or similar factors, in addition to limited sight distance. The prohibition of passing by vehicles travelling in the opposing direction is particularly appropriate at sites with roadside development that generates frequent left-turn movements from the left lane of the treated direction in the passing lane section.

#### *Lane-Addition Markings*

The MUTCD does not provide any specific guidance for marking a lane-addition transition area. The recommended pavement marking scheme is illustrated in figure 3. The use of a pavement edge marking in the lane-addition transition area is recommended. A white dotted marking tapering across the left lane immediately prior to the beginning of the lane line is recommended. Several highway agencies have found this marking to be effective in guiding most drivers into the right lane. Drivers who desire to pass immediately upon entering the passing lane are permitted to cross the dotted marking.

#### *Lane-Drop Markings*

Pavement markings in the lane-drop transition area should be provided in accordance with MUTCD Section 3B-8, as illustrated in MUTCD figure 3-10. For a 60-mph prevailing speed, the broken white lane line should be discontinued 580 feet prior to the beginning of the lane-drop taper. The use of

a pavement edge marking in the lane-drop transition area is recommended.

### OPERATIONAL EFFECTIVENESS

The operational effectiveness of passing lanes on two-lane highways has been evaluated extensively in Australia, Canada, and the United States. The results of the recent evaluation of passing lanes in the United States are summarized in the following discussion to provide guidance on where passing lanes should be used and what operational benefits should be expected. International research has also demonstrated the effectiveness of passing lanes. Australian research has resulted in the development of minimum-volume warrants for passing lanes based on average daily traffic (ADT) volumes and percent of highway length providing passing opportunities over the previous 2 to 6 miles (8). Canadian research has developed a concept based on the percentage of highway length with "assured" passing opportunities to determine where passing lanes are needed (9, 10). Summaries of these results have also been presented by Harwood and Hoban (5).

The research approach used in the United States has focused on tying the operational effectiveness of passing lanes to the levels of service for two-lane highways used in Chapter 8 of the 1985 Highway Capacity Manual (HCM) (11). These levels of service, illustrated in table 1, are defined in terms of the percentage of travel time spent delayed, such as travelling in platoons behind other vehicles. The percent of time delay was chosen as the measure of service for the 1985 HCM because it is more sensitive to variation in flow rate than other candidate measures, such as vehicle speeds (12). On steep grades, the average upgrade speed serves as an additional criterion to define the levels of service.

The operational effectiveness of passing lanes in the United States was previously evaluated based on field data by Harwood and St. John (6) and Harwood, St. John, and Warren (13). This field evaluation compared the quality of traffic operations (level of service) upstream and downstream of passing lanes. Field evaluations cannot compare the quality of traffic operations on a highway section with and without passing lanes, but comparisons of this type can be made with a computer simulation model. Therefore, simulation modeling of passing lanes was recently conducted with a computer model known as TWOPAS (14).

TWOPAS is a microcomputer simulation model of traffic operations on two-lane, two-way highways. TWOPAS is a

TABLE 1 LEVEL OF SERVICE CRITERIA FOR TWO-LANE HIGHWAYS

Level of Service	Percent Time Delay on General Segments	Average Upgrade Speed (mi/hr) on Specific Grades
A	≤ 30	≥ 55
B	≤ 45	≥ 50
C	≤ 60	≥ 45
D	≤ 75	≥ 40
E	> 75	≥ 25-40
F	100	< 25-40

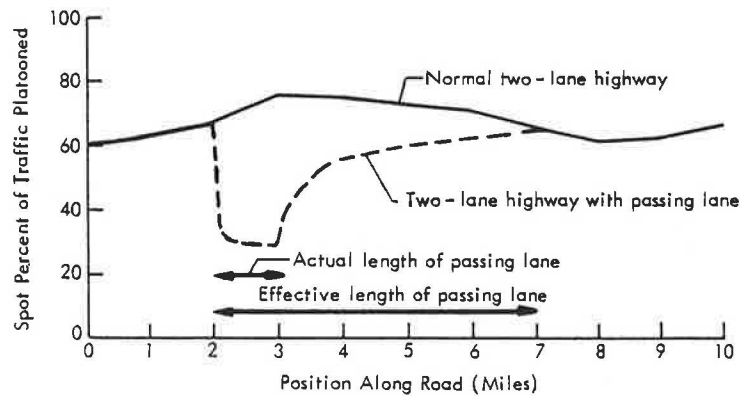


**FIGURE 4** Example of the effect of a passing lane on two-lane highway traffic operations.

modified version of the TWOWAF model used in the development of Chapter 8 of the 1985 HCM. TWOPAS has the added capability to simulate the operational effects of passing and climbing lanes. The TWOWAF model was validated from field data for conventional two-lane highways by St. John and Kobett (15) and by Messer (12), and the added capability to simulate passing and climbing lanes was validated from field data by Harwood and St. John (14). The latter effort found good agreement between model results and field data for traffic platooning and traffic speeds upstream and downstream of passing lanes.

Figure 4 presents a conceptual illustration of the effect of a passing lane on traffic operations on a two-lane highway. The solid line in this figure shows the normal fluctuation of platooning on a two-lane highway with the availability of passing sight distance. When a passing lane is added, the percentage of vehicles following in platoons falls dramatically and stabilizes at about half the value for the two-lane road. Because platoons are broken up in the passing lane, its effective length extends for a considerable distance downstream of the passing lane. Thus, the installation of passing lanes on parts of a two-lane highway can improve traffic operations on the entire highway. The next section of the paper illustrates the determination of the effective length of passing lanes for different lengths and traffic flow rates, based on computer simulation results.

#### Effective Length of a Passing Lane Used for Analysis

Figure 5 illustrates the effects of passing lanes of various lengths on traffic platooning within a passing lane and downstream of a passing lane for flow rates of 400 and 700 vehicles per hour (vph) in one direction of travel. Figure 5 is based on the percentage of vehicles delayed in platoons at specific spot locations on the highway. It can be seen in figure 5 that the level of traffic platooning within a passing lane is less than half of the level observed upstream of the passing lane. Traffic platooning remains at a reduced level downstream of a passing lane. For a flow rate of 400 vph, the effects of passing lanes can still be substantial seven miles downstream of the beginning of the passing lane, especially for longer passing lanes. At the higher flow rate of 700 vph, nearly all of the operational

benefits of the passing lane are gone within five miles, although there is a small residual effect even at seven miles downstream. The length of the passing lane has a strong influence on the improvement in traffic operations immediately downstream of the passing lane, but this differential between passing lane lengths largely disappears farther downstream.

The results in figure 5 indicate that the effective length of a passing lane can vary from three to eight miles, depending on passing lane length, traffic flow and composition, and downstream passing opportunities.

The concept of effective length is needed for analysis purposes to determine the overall effect of a passing lane on level of service over an extended highway section. For most cases, effective length can be estimated from figure 5, with adjustments for factors that might hasten or slow the downstream overtaking or catch-up process. If the two-lane highway downstream of the passing lane has few passing opportunities, for example, the effective length determined from figure 5 should be reduced.

In some cases, the effective length of a passing lane is constrained by other road features, such as small towns, four-lane sections, or additional passing lanes a few miles downstream. In these situations, the distance to the downstream constraint should be used as the effective length for analysis purposes, if this is less than that estimated from figure 5.

#### Effectiveness Over an Extended Road Section

Figure 6 illustrates the effectiveness of passing lanes of various lengths in improving traffic operations on two-lane highways, based on results obtained with the TWOPAS simulation model. The curves presented in figure 6, for passing lanes of varying lengths, represent their effectiveness in increasing traffic speeds and decreasing the percent of time vehicles spend delayed in platoons on a two-lane highway in moderately rolling terrain. The vehicle speed and platooning measures in figure 6 are averages over an eight-mile highway section with the passing lane located at the beginning; thus, these curves represent the combined effects of improved traffic operations in the passing lane and downstream of the passing lane. Figure 6 illustrates that passing lanes produce relatively small increases in vehicle speeds, but can dramatically decrease vehicle platooning.

An eight-mile highway section is used in figure 6 because

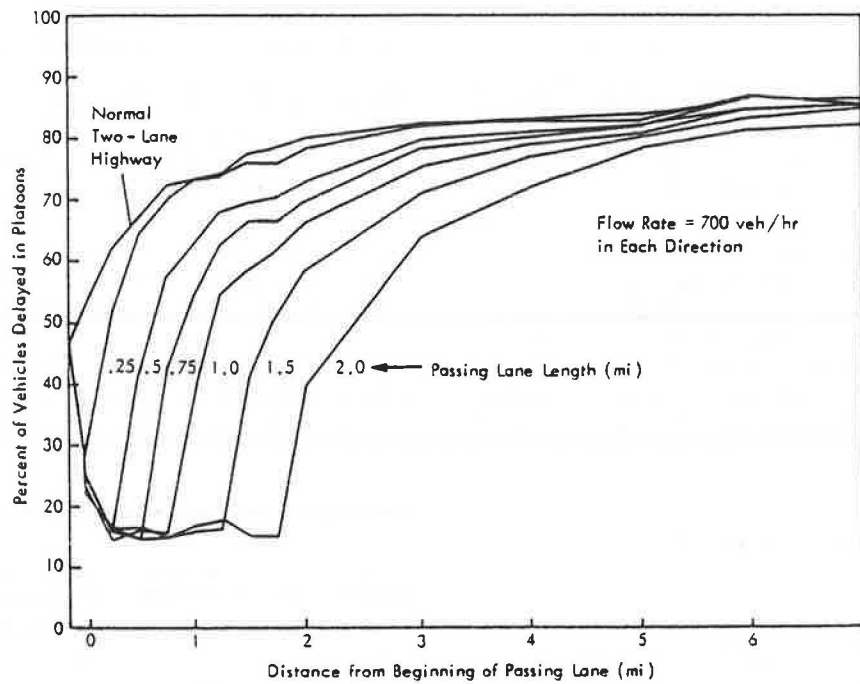
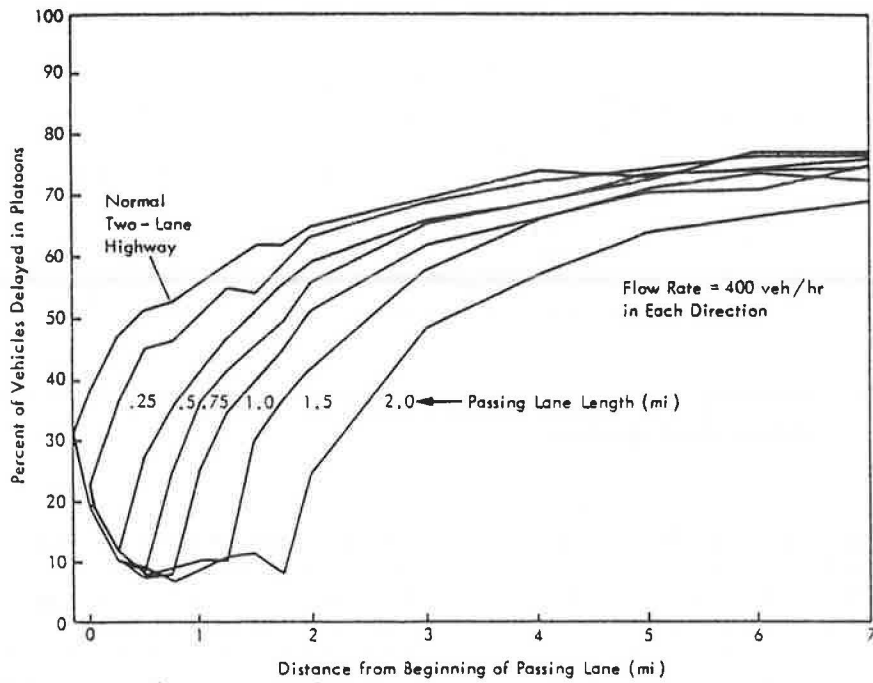


**FIGURE 5** Gradual increase in percentage of vehicles delayed in platoons downstream of passing lanes.

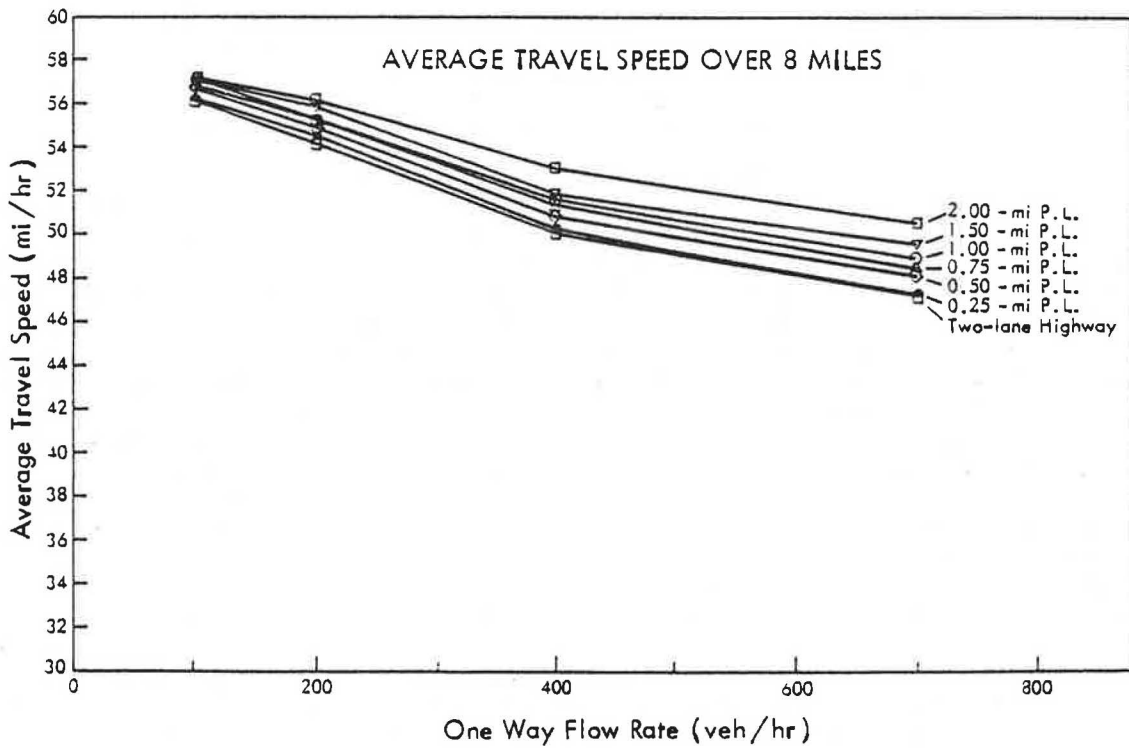
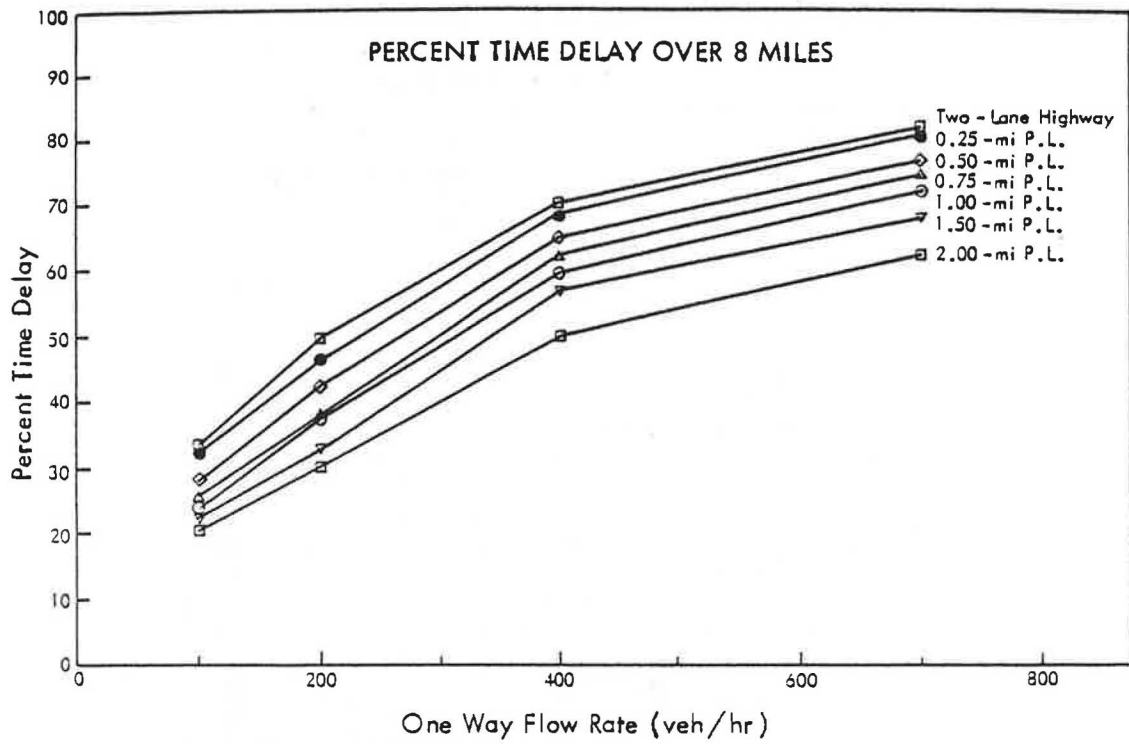


FIGURE 6 Computer simulation results for operational effectiveness of passing lanes.

TABLE 2 EFFECT OF PASSING LANES ON PERCENT TIME DELAY OVER AN EXTENDED ROAD LENGTH

Effective Length (mi)	PERCENT TIME DELAY						
	Passing Lane Length (mi)						
	0	0.25	0.50	0.75	1.00	1.50	2.00
One-way Flow Rate = 100 veh/hr							
3	33	30	20	17	17	17	17
5	33	31	25	22	19	17	17
8	33	32	28	26	24	22	20
One-way Flow Rate = 200 veh/hr							
3	50	39	29	25	25	25	25
5	50	44	37	31	29	25	25
8	50	46	42	38	37	33	30
One-way Flow Rate = 400 veh/hr							
3	70	67	57	49	43	35	35
5	70	68	62	57	54	49	38
8	70	69	65	62	60	57	50
One-way Flow Rate = 700 veh/hr							
3	82	79	69	63	55	45	41
5	82	80	74	71	66	60	52
8	82	81	77	75	72	68	63

the effective length of a passing lane includes both the passing lane itself and the downstream section of two-lane highway where platooning is lower than it would be without the passing lane. Table 2 presents the estimated reductions in percent time delay for three different effective lengths—3, 5, and 8 miles—as well as for different lengths of passing lane.

The selection of the design length of a passing lane is discussed in the following sections. Once the design length and the effective length used for analysis are determined, table 2 can be used to predict the percent time delay and, hence, the level of service on a highway section which includes a passing lane.

It should be noted that the base values of percent time delay for a normal two-lane highway in table 2 are higher than those specified in the HCM (see table 1) for ideal conditions. This is because the simulated results were derived for non-ideal conditions of terrain, no-passing zones, and traffic composition. Since these conditions can vary from one case to another, it is recommended that table 2 be entered using a given base value of percent time delay, rather than the traffic flow. In other words, the estimated two-lane highway percent time delay should be used to select the appropriate row of table 2, regardless of traffic flow. Linear interpolation in table 2 is acceptable.

#### Optimum Design Length for Passing Lanes

The optimum design length for a passing lane can be determined through a cost-effectiveness analysis. This can be illus-

trated by the data in table 3, which presents the percent time delay over an effective length of eight miles for passing lanes of various design lengths, the difference between the percent time delay for each design length and a conventional two-lane highway, and the ratio of this difference to the design length. This effectiveness ratio, the effectiveness in reducing vehicle platooning per unit length of passing lane, represents the relative cost-effectiveness of passing lanes, if one assumes that the cost of constructing a passing lane is proportional to its length. This assumption is reasonable for most situations, although the cost of constructing passing lanes can vary widely as a function of terrain. The passing lane lengths shown in table 3 were increased by 600 feet, half of the combined length

TABLE 3 REDUCTION IN PERCENT TIME DELAY PER UNIT LENGTH OF PASSING LANE

One-Way Flow Rate (veh/hr)	Passing Lane Length (mi) <sup>a/</sup>					
	0.25	0.50	0.75	1.00	1.50	2.00
100	2.8	8.2	8.1	8.1	6.8	6.2
200	11.1	13.1	14.0	11.7	10.6	9.5
400	2.8	8.2	13.1	9.0	8.1	9.5
700	2.8	8.2	8.1	9.0	8.7	9.0

<sup>a/</sup> Unit length of passing lanes increased by 600 ft to account for cost of constructing lane addition and lane drop tapers.

TABLE 4 OPTIMAL DESIGN LENGTHS FOR PASSING LANES

One-Way Flow Rate (veh/hr)	Optimal Passing Lane Length (mi)
100	0.50
200	0.50-0.75
400	0.75-1.00
700	1.00-2.00

of typical lane-addition and lane-drop tapers, in the computation of the effectiveness ratios to account for the cost of constructing these transition areas.

The optimum design lengths for passing lanes, based on the data in table 3, are tabulated in table 4. For flow rates of 200 vph or less in one direction of travel, the highest effectiveness per unit length is obtained for passing lanes with design lengths between 0.5 and 0.75 of a mile. Passing lanes shorter than 0.5 mile or longer than 0.75 mile are not as desirable at this flow rate because they provide less operational benefit per unit length. As flow rate increases above 200 vph, the optimum design length for a passing lane also increases. At a flow rate of 400 vph in one direction of travel, the optimum design length for a passing lane is 0.75 to 1.0 mile. At very high flow rates, such as 700 vph in one direction of travel, the optimum design length of passing lanes ranges from 1.0 to 2.0 miles. However, passing lanes longer than 1.0 mile may not be desirable, even for highways with peak flow rates of 700 vph in one direction of travel, because longer passing lanes would be suboptimal throughout the remainder of the day when traffic volumes are lower.

The effectiveness analysis indicates that short passing lanes are usually more effective per unit length and, therefore, per dollar spent on construction than long passing lanes. Thus, the overall level of service on a highway can often be improved more by constructing three 0.5-mile passing lanes spaced at intervals than by constructing one two-mile passing lane. The optimum design length for passing lanes on a specific section

of two-lane highway could be based on the highest hourly flow rate that occurs frequently (for example, on a daily basis) on that specific highway section. The design hour volume, which occurs in only a few hours out of each year, may be too high to serve as the basis for the choice of a cost-effective passing lane length. It may be useful to evaluate traffic operations for several design hours, especially when the composition of traffic differs between weekdays and weekends.

#### SAFETY EFFECTIVENESS

Safety evaluations have shown that passing lanes and short four-lane sections reduce accident rates below the levels found on conventional two-lane highways.

Table 5 compares the results of two before-and-after evaluations of passing lane installation. These studies include accidents of all types for both directions of travel within the portion of the two-lane highway where the passing lanes were installed. A California study by Rinde (16) at 23 sites in level, rolling, and mountainous terrain found accident rate reductions due to passing lane installation of 11 to 27 percent, depending on road width. The accident rate reduction effectiveness at the 13 sites in level or rolling terrain was 42 percent. In data from 22 sites in four states, Harwood and St. John (6) found the accident rate reduction effectiveness of passing lanes to be 9 percent for all accidents and 17 percent for fatal and injury accidents. The combined data from both studies indicates that passing lane installation reduces accident rate by 25 percent. No difference was found between the accident rates of passing lanes of level and rolling terrain.

Harwood and St. John (6) found no indication in the accident data of any marked safety problem in either the lane-addition or lane-drop transition areas of passing lanes. In field studies of traffic conflicts and erratic maneuvers at the lane-drop transition areas of 10 passing lanes, lane-drop transition areas were found to operate smoothly. Overall, 1.3 percent of the vehicles passing through the lane-drop transition area created a traffic conflict, while erratic maneuver rates of 0.4 and 0.3 percent were observed for centerline and shoulder encroachments, respectively. The traffic conflict and

TABLE 5 ACCIDENT REDUCTION EFFECTIVENESS OF PASSING LANES

Source	Type of Terrain	Total Roadway Width (ft) <sup>a</sup>	No. of Passing Lane Sites	Percent Reduction	
				All Accidents	Fatal and Injury Accidents
Rinde <sup>16</sup>	Level, rolling, and mountainous	36	4	11	-
		40	14	25	-
		42-44	5	27	-
	Level and rolling sites only	36-44	13	42	-
Harwood and St. John <sup>6</sup>	Level and rolling	40-48	22	9	17
Combined Totals for Level and Rolling Terrain			35	25	-

<sup>a</sup> Total roadway width includes both traveled way and shoulders.



TABLE 6 RELATIVE ACCIDENT RATES FOR IMPROVEMENT ALTERNATIVES

Alternative	All Accidents	Fatal and Injury Accidents
Conventional two-lane highway	1.00	1.00
Passing lane section	0.75	0.70
Four-lane section	0.65	0.60

encroachment rates observed at lane-drop transition areas in passing lanes were much smaller than the rates found in lane-drop transition areas at other locations on the highway system, such as work zones.

An evaluation of cross-centerline accidents involving vehicles travelling in opposite directions on the highway found no safety differences between passing lanes with passing prohibited in the opposing direction and passing lanes with passing permitted in the opposing direction where adequate sight distance was available (6). The provision for passing by vehicles travelling in the opposing direction does not appear to lead to safety problems at the types of sites and flow rate levels (up to 400 vph in one direction of travel) where it has been permitted by the highway agencies that participated in the Harwood and St. John study. Both types of passing lanes had cross-centerline accident rates lower than those of comparable sections of conventional two-lane highway.

Reviewing a small number of climbing-lane sites in the United States, Jorgensen (17) found no change in accident experience. In the United Kingdom, Voorhees (18) found a 13 percent reduction in accidents where a climbing lane was provided.

A safety evaluation of nine short, four-lane sections in three states found a 34 percent lower total accident rate and a 43 percent lower fatal and injury accident rate on the short, four-lane sections than rates on comparable sections of conventional two-lane highways (5). These differences, although substantial, were not statistically significant because of the limited number of sites available. The cross-centerline accident rates for the short, four-lane sections were generally less than half the rates for the comparable two-lane sections.

Table 6 summarizes the relative accident rates found in recent research for passing lane sections and short, four-lane sections, expressed as ratios between the expected accident rate for each and the expected accident rate of a conventional two-lane highway.

## SUMMARY

Passing lanes have been found to be effective in improving overall traffic operations on two-lane highways, and they provide a lower cost alternative to four-laning extended sections of highway. Passing opportunities on two-lane highways can be increased by the installation of passing lanes in level and rolling terrain, of climbing lanes on sustained grades, and of short sections of four-lane highway. The traffic operational effectiveness of passing lanes can be predicted as a function of flow rate, passing-lane length, and the percentage of traffic travelling in platoons, using the procedure presented above. The installation of a passing lane on a two-lane highway reduces accident rate by approximately 25 percent. Recommended

geometric design, signing, and marking practices for passing lanes have also been developed. Further guidance on the use of passing lanes and other low-cost methods of improving traffic operations on two-lane highways (such as turnouts, shoulder driving sections, intersection turn lanes, and center two-way left-turn lanes) is provided by Harwood and Hoban (5).

## ACKNOWLEDGMENTS

The work reported in this paper was conducted under sponsorship of the Federal Highway Administration. However, the findings and conclusions in the paper are those of the authors and do not necessarily represent the views of the Federal Highway Administration.

## REFERENCES

1. J. Botha et al. *A Decision-Making Framework for the Evaluation of Climbing Lanes on Two-lane Two-way Rural Roads: Research Summary*. Report No. FHWA/CA/T0-80, University of California, California Department of Transportation, July 1980.
2. W. S. Homburger. *An Analysis of Safety at the Terminals of Climbing Lanes on Two-Lane Highways*. Report No. FHWA-CA-UCB-ITS-RR-86-3, University of California, Berkeley, May 1986.
3. C. J. Hoban and J. F. Morrall. *Overtaking Lane Practice in Canada and Australia*. Research Report No. ARR 144, Australian Road Research Board, 1985.
4. *Manual on Uniform Traffic Control Devices for Streets and Highways*, Federal Highway Administration, Washington, D.C., 1978 and subsequent revisions.
5. D. W. Harwood and C. J. Hoban. *Low-Cost Methods for Improving Traffic Operations on Two-Lane Highways—Informational Guide*. Report No. FHWA-IP-87-2, Federal Highway Administration, Washington, D.C., January 1987.
6. D. W. Harwood and A. D. St. John. *Passing Lanes and Other Operational Improvements on Two-lane Highways*. Report No. FHWA/RD-85/028, Federal Highway Administration, Washington, D.C., July 1984.
7. R. S. Hostetter and E. L. Seguin. The Effects of Sight Distance and Controlled Impedance on Passing Behavior. *Highway Research Board Bulletin 92*, HRB, National Research Council, Washington, D.C., 1965.
8. *Guide to Geometric Design of Rural Roads*. National Association of Australian State Road Authorities, Sydney, Australia, 1985.
9. *Design Procedure for Passing Lanes*. Ontario Ministry of Transportation and Communications, Downsview, Ontario, 1975.
10. A. Werner and J. F. Morrall. A Unified Traffic Flow Theory Model for Two-lane Rural Highways. *Transportation Forum*, Vol. 1, No. 3, 1985, pp. 79-87.
11. *Highway Capacity Manual*. Transportation Research Board

- Special Report 209, TRB, National Research Council, Washington, D.C., 1985.
12. C. J. Messer. *NCHRP Project 3-28A Report: Two-Lane, Two-Way Rural Highway Capacity*. TRB, National Research Council, Washington, D.C., February 1983.
  13. D. W. Harwood, A. D. St. John, and D. L. Warren. Operational and Safety Effectiveness of Passing Lanes on Two-Lane Highways. In *Transportation Research Record 1026*, TRB, National Research Council, Washington, D.C., 1985.
  14. D. W. Harwood and A. D. St. John. *Operational Effectiveness of Passing Lanes on Two-lane Highways*. Report No. FHWA/RD-86/196, Federal Highway Administration, Washington, D.C., 1986.
  15. A. D. St. John and D. R. Kobett. *NCHRP Report 185: Grade Effects on Traffic Flow Stability and Capacity*. TRB, National Research Council, Washington, D.C., 1978.
  16. E. A. Rinde. *Accident Rates vs. Shoulder Widths: Two-lane Roads, Two-lane Roads with Passing Lanes*. Report No. CA-DOT-TR-3147-1-77-01, California Department of Transportation, September 1977.
  17. Roy Jorgensen and Associates. *Evaluation of Criteria for Safety Improvements on the Highway*. U.S. Department of Commerce, Bureau of Public Roads, 1966.
  18. Martin Voorhees Associates. *Crawler Lane Study: An Economic Evaluation*. Department of the Environment, Great Britain, 1978.

---

*Publication of this paper sponsored by Committee on Operational Effects of Geometrics.*

# Design Guide for Auxiliary Passing Lanes on Rural Two-Lane Highways

ALAN R. KAUB AND WILLIAM D. BERG

The objective of this research was to determine the conditions under which the construction of an auxiliary passing lane on two-lane rural highways is economically justified. A conflict-opportunity model was developed which estimates the number of potential passing conflicts with an opposing vehicle that a given traffic volume will generate. By assigning a cost-per-conflict opportunity and adjusting for the length of passing zones available, the passing-accident costs for a given roadway segment were estimated. Based on prior research, a deterministic reduction of this cost was used to estimate the savings that would result from an auxiliary passing lane. The TWOWAF model was then used to simulate delay and travel speeds for trucks and passenger vehicles for typical highway sections both without and with an auxiliary passing lane. Benefit-cost analysis was applied to determine the average daily traffic (ADT) levels at which an auxiliary passing lane would be economically justified as a function of section length, percent passing zones available, cost per conflict, construction cost, and discount rate.

Rural, two-lane highways constitute over 80 percent of the national highway system mileage but carry only approximately 35 percent of the total annual vehicle-miles of travel (1). Yet this system is responsible for over 48 percent of all fatal motor vehicle accidents and 30 percent of all injury accidents each year (2). On this rural two-lane system, the head-on collision is the second most common type of rural fatal accident, responsible for approximately 5,100 fatalities annually (3). One of the most common and complex rural, two-lane operational maneuvers, and one which has the potential to cause head-on or severe accidents is the passing maneuver. But it is also the passing maneuver which has the capability to substantially reduce rural, two-lane travel time and delay. Thus, on the rural two-lane system there exists a need to improve safety performance by reducing severe accidents while maintaining or improving traffic operational performance.

Prior research has suggested that one alternative for improving rural roadway passing performance is to design for passing opportunities such that the following driver will generally not become intolerant to delay by having to seek too diligently for an acceptable passing gap in opposing traffic (4). If passing opportunities were provided either by the absence of opposing traffic or by the placement of passing lanes at appropriate locations, much of the accident cost of the passing maneuver might be eliminated. On many rural highways this minimized probability of accident and minimized delay occur

frequently where the volumes of traffic are light, and thus the probability of meeting an opposing vehicle while performing the passing maneuver is small. However, where the volume of traffic increases and the percent passing decreases such that delay and the probability of an accident become high, the construction of auxiliary passing lanes or various types of four-lane highways may be justified to provide for additional safe passing opportunities.

Because of the expense associated with freeway construction, auxiliary passing lanes have begun to receive greater attention. Past research on the operational aspects of passing lanes by Franklin Research Institute (5) concluded that road widening, shoulder widening, and added lane construction would have marginal benefit-cost ratios less than 1.0. However, delay benefits were not included in the study because of insufficient data relating delay savings to improvements in operating speed. In another study, Harwood, St. John, and Warren (6) performed an operational evaluation of auxiliary passing lane (non-truck climbing) performance and concluded that passing lanes decrease the percentage of vehicles platooned, increase the rate of passing maneuvers, and have a small effect on mean travel speeds. A concurrent safety evaluation of passing lanes indicated that a passing lane can reduce the total accident rate by 38 percent with an approximate 29 percent reduction of fatal and injury accident rates.

Past research on the economic desirability of auxiliary lanes has concentrated on identifying those geometric and traffic conditions under which a truck climbing lane is warranted (5, 7, 8). Little consideration has been given to the need for passing lanes where truck climbing lanes are not warranted. The objective of the research reported herein was, therefore, to establish general guidelines for the construction of auxiliary passing lanes on two-lane rural highways based on an economic analysis of road-user benefits versus construction and maintenance costs (9). The scope of the research was confined to conditions found on those State Primary Highway System roads having pavement widths of 20 feet or greater. These roads represent approximately 78 percent of the entire State Primary Highway System (10).

## PASSING CONFLICT MODEL

Models for accident occurrence are generally difficult to develop and calibrate due to the rare nature of an accident. However, in research by Stockton, Mounce, and Walton (11), a conflict analysis of the passing maneuver for low-volume, rural, two-lane roadways was performed using the Poisson distribution as the assumed empirical accident model. This analysis con-

A. R. Kaub, Department of Civil Engineering and Mechanics, University of South Florida, Tampa, Fla. 33620. W. D. Berg, 2206 Engineering Building, University of Wisconsin-Madison, Madison, Wis. 53706.

sidered the probability of simultaneous arrivals of two vehicles of different speeds in one direction and the probability of opposition to the resultant passing maneuver from the opposing vehicle. This methodology was used to develop an expected number of annual conflicts. Although developed for low-volume, rural roadways, the above procedure was judged to offer a reasonable basis for estimating the number of passing conflict opportunities on the higher volume State Primary Highway System. It was further assumed that any passing conflict that occurs with an opposing vehicle can be assigned a proportional share of the total passing-accident costs on two-lane roadways.

In adapting the above passing conflict opportunity model to this research, it was assumed that

1. A conflict opportunity is defined as that maneuver of vehicle A (following), B (lead), or C (opposing), such that the driver of the following vehicle will have less than the AASHTO time exposed to traffic in the left lane ( $t_2$ ) plus the clearance time ( $t_3$ ), which is assumed to be a minimum of 16 seconds when the pass is completed (12).

2. Average speed is 55 mph, which is the average of all three speeds of the lead vehicle (50 mph), following vehicle (60 mph) and opposing vehicle (assumed 55 mph).

3. Passing sight distance is at least 1,000 feet, which is the minimum operational (distance considered acceptable for passing operations at 60 mph speeds). Where this sight distance is not available, it is assumed the pass will not be completed. This minimum sight distance conforms to the requirements of the Manual on Uniform Traffic Control Devices for Streets and Highways (MUTCD) for the marking of no-passing zones at 60 mph (13).

4. The probabilities of passing and arrival of opposition assume that all vehicles arrive during a 1-hour analysis period.

5. A passing situation occurs when a pair of vehicles arrive following a Poisson distribution within an assumed constant headway of 2 seconds or less.

6. The average directional distribution is assumed to be 50/50.

The probability of a passing conflict opportunity occurring can be calculated as follows for a highway with an assumed traffic volume of 250 vehicles per hour (vph) and a 50/50 directional distribution. From the Poisson distribution

$$P(X) = e^{-m} m^x / x! \quad (1)$$

The probability that any two vehicles will be close enough for the following driver to desire to pass in any one hour is

$$P(h_i < 2 \text{ sec}) = 1 - P(0) - P(1) = 0.002302 \quad (2)$$

and the number of such passing opportunities per hour, per direction is

$$[P(h_i < 2 \text{ sec})] \times 1800 = 4.15 \quad (3)$$

In the passing maneuver, vehicle A will be exposed to traffic in the left lane for an assumed 16-second time interval. If an opposing vehicle appears within this 16-second interval, then by definition a conflict with the opposing vehicle is assumed to have occurred. The probability of arrival of the opposing vehicle in the 16-second interval is given by

$$P(1 \text{ or more}) = 1 - P(0) = 0.426 \quad (4)$$

The number of such conflicts is given by the product of the number of passing opportunities per hour and the probability of the arrival of an opposing vehicle during the passing maneuver, or 1.77 passing-conflict opportunities per hour, per direction.

The above conflict situation occurs over an 18-second interval (including the two-second headway for vehicle A) during which time vehicle A is traveling at 60 mph and traverses a distance of 0.3 miles. Placing the conflict rate on a vehicle-mile basis

$$\begin{aligned} \text{Conflict opportunities/veh-mi/hr} &= 1.77/0.3/250 \\ &= 0.0236 \end{aligned} \quad (5)$$

Thus, over a 1-mile segment under the above traffic conditions and assumptions, there will develop approximately 5.91 (1.77/0.3) conflict opportunities with opposing vehicles during the hour the 250 vph volume level exists, or each vehicle will experience 2.36 conflict opportunities in every 100 miles of travel regardless of the direction of travel. Utilizing the above methodology, probable conflict opportunities per mile, per hour were developed over two-way volume levels ranging from 0 to 1,800 vph as shown in table 1. It was further assumed that these values would be reduced in direct proportion to the amount of available passing sight distance on the highway segment. Thus, where 50 percent passing sight distance is available, the conflict opportunities would be reduced from 5.91 to 2.95 conflicts per mile, per hour. This assumption is a conservative approach because where passing is severely restricted, passing conflicts may actually increase to compensate for the reduced opportunity to pass.

## PASSING-ACCIDENT COSTS

The presence of an auxiliary passing lane is intended to reduce the number of catastrophic passing accidents that occur due to the presence of an opposing vehicle in the passing maneuver. Such accidents normally involve high-speed head-on, or run-off-the-road accident types. To identify the value of aggregate passing-accident costs, and, ultimately, the pro rata individual conflict costs, it was necessary to quantify the cost of passing-related accidents caused by the presence of an opposing vehicle. However, the lack of detailed data on passing accidents required that an approximate accident cost framework be developed using summary statistics from available data bases. Using data published by the Federal Highway Administration and the National Safety Council (10, 14), the distribution of accidents per year by severity on two-lane rural highways was estimated as

Fatal Accidents: 7,469

Injury Accidents: 148,591

PDO Accidents: 1,578,800

Total: 1,734,839

In a study conducted by the Franklin Institute Research Laboratories (5), it was concluded that approximately 10 percent of the accidents on the two-lane system are passing related. Therefore, the total number of passing-related accidents was estimated as 10 percent of the above value, or 173,484 per

TABLE 1 NUMBER OF ANNUAL PASSING CONFLICTS IN THE PRESENCE OF AN OPPOSING VEHICLE

	AVERAGE	HOURLY	PASSING	ANNUAL
HOURLY	VOLUME	MILES*	CONFLICT	PASSING
VOLUME	(VPH)	(MILLIONS)	RATE	CONFLICTS
			(#/MI/HR)	(MILLIONS)
0 - 100	50	2041.1	.0605	123.5
100 - 200	150	333.7	1.437	479.5
200 - 300	250	130.2	5.91	765.8
300 - 400	350	16.7	14.37	239.9
400 - 500	450	19.3	27.27	526.3
500 - 600	550	5.4	44.60	240.8
600 - 700	650	2.1	66.29	139.2
700 - 800	750	3.2	92.03	294.5
800 - 900	850	1.1	122.0	133.7
900 - 1000	950	2.4	154.3	370.3
1000 - 1100	1050	0	190.1	0
1100 - 1200	1150	0.4	228.9	91.6
1200 - 1300	1250	0.5	270.1	135.0
1300 - 1400	1350	0	313.5	0
1400 - 1500	1450	0	358.9	0
1500 - 1600	1550	0.3	406.2	121.9
1600 - 1700	1650	0	455.1	0
1700 - 1800	1750	0.1	505.5	50.5
TOTAL				3712.5

\*Ref. 10

year. This aggregate number of passing-related accidents is consistent with NSC statistics, which indicate that 3.2 percent of all rural accidents (5,188,500), or 166,032 rural passing accidents, are caused by improper overtaking (14). Other research has estimated that 3.5 percent of all passing accidents involve a fatality, and 42 percent of all non-fatal accidents involve personal injury (10).

Not all of the above-mentioned accidents can be attributed to the presence of opposing vehicles because passing accidents on two-way rural roads may also occur at intersections (driveways), railroad crossings, narrow bridges, roadside developments, or other such sites. The results of other research indicate that 20 percent, 58 percent, and three percent of all

passing-related accidents occurred at "special situation" locations in the states of North Carolina, Texas, and Utah respectively (15). These particular states were selected to permit a representation of geographical distributions to approximate the effects of flat, rolling, and mountainous terrains. The remaining non-special situation passing-related accidents, which constitute 80 percent, 42 percent, and 97 percent, respectively, of all rural, two-lane passing accidents, were therefore assumed to be high-speed passing maneuvers that could result in catastrophic accidents.

For this research, it was assumed that these remaining non-special situation passing accidents are passing accidents that occur in the presence of an opposing vehicle such that the

TABLE 2 ESTIMATES OF THE COST OF EACH CONFLICTING PASS DUE TO THE PRESENCE OF AN OPPOSING VEHICLE

	Low	Average	High
Estimated Total Passing	\$1616.1	\$2424.2	\$3232.3
Accident Costs per Year (Millions)			
Estimated Total Conflicts Per Year (Millions)	3712	3712	3712
Estimated Cost per Conflict (two-way)	\$ 0.44	\$ 0.66	\$ 0.88

presence of the opposition vehicle contributed to the occurrence of the accident. Because the Utah data were reportedly inaccurate, due to underreporting, only the Texas and North Carolina data were used to establish boundary conditions for opposing vehicle-related passing accidents. Values of 40 percent, 60 percent, and 80 percent were therefore used as estimates of low, average, and high opposing-vehicle passing-related accidents. The actual value will depend upon the general terrain, roadway characteristics, and other factors appropriate to a particular state or region within a state.

Using 1978 data, passing-accident costs were assumed to be \$300,700 for a fatal accident, \$15,800 for a personal-injury accident, and \$750 for a property-damage accident (16). Combining these values with the estimated opposing vehicle-related, passing-accident frequency data, total nationwide passing-accident costs were estimated to range from \$1.6 to \$3.2 billion per year. These accident costs were divided by the number of annual passing conflicts in the presence of an opposing vehicle for volumes ranging from 0 to 1,800 vph, as listed in table 1. The resulting estimated proportional cost associated with each passing conflict opportunity is shown in table 2. A comparison of the estimated passing conflict cost over various average daily traffic (ADT) volumes is presented in figure 1. It may be noted that the 2,000 to 5,000 and the 5,000 to 10,000 ADT ranges appear to be generating costs far in excess of other ADT levels. This, in general, suggests that a substantial number of miles of rural two-way, two-lane mileage in the 2,000 to 10,000 ADT range should receive consideration for upgrading to freeway standards or being provided with auxiliary passing lanes to reduce conflict and accident costs.

**PASSING LANE EFFECTIVENESS**

A study by the California DOT reported on the accident reduction potential attributable to the construction of passing lanes on two-lane rural highways (17). This study examined 19 projects that reconstructed over 48 miles of rural roadway from their original two-lane cross-section to a three-lane cross-section composed of the original roadway plus a third lane

for passing. It was found that auxiliary passing lanes can be expected to reduce fatal accidents by approximately 60 percent, personal injury accidents by approximately 20 percent, and property damage accidents by approximately 20 percent. Applying these effectiveness measures to the previously estimated nationwide passing-accident data, the estimated annual dollar savings that could be expected if auxiliary passing lanes

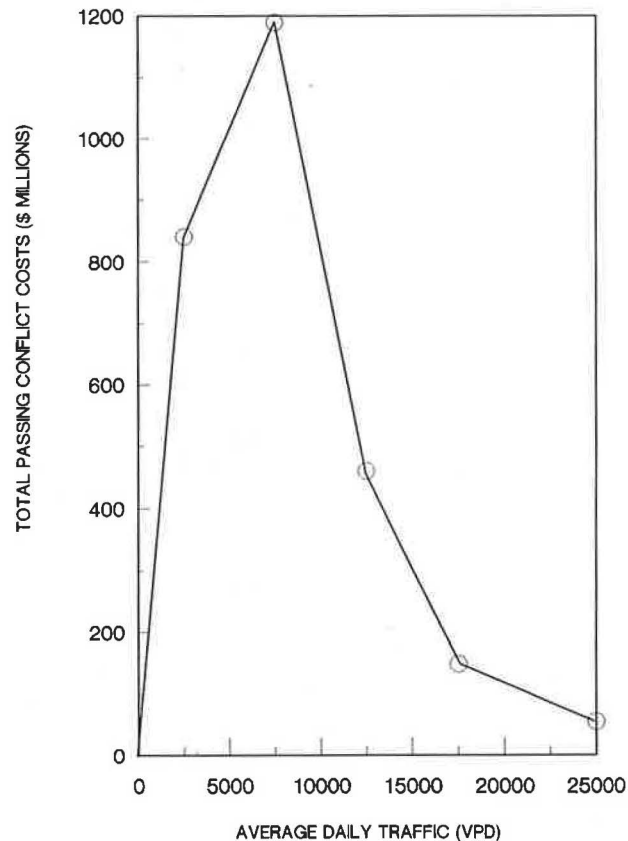


FIGURE 1 Comparison of passing conflict costs over various average daily traffic volumes.

TABLE 3 ESTIMATED PASSING ACCIDENT COST SAVINGS PRODUCED BY AUXILIARY PASSING LANES ANNUALLY

Accident Type	Cost Per Occurrence	Estimated Total Savings (\$x10 <sup>6</sup> )			% of Total
		Low	Average	High	
Fatality	\$300,700	438.1	657.3	876.2	71
Injury	\$ 15,800	171.3	256.9	324.6	28
PDO	\$ 750	5.9	8.7	11.7	1
Total		615.3	922.9	1230.5	100

were constructed on all two-lane state primary highways are shown in table 3. A comparison of the total cost savings to the total passing-related accident costs indicated that the construction of auxiliary passing lanes may reduce by approximately 38 percent the total cost of passing-related accidents. Thus, for purposes of this research, it was assumed that an auxiliary passing lane would be 38 percent effective in reducing opposing vehicle-related passing accident costs.

To examine the benefits of reduced vehicle operating cost and travel time savings, it was necessary to simulate traffic flow conditions both with and without the presence of an auxiliary passing lane. The TWOWAF model was used for this purpose (10, 19). An experimental design was developed to generate simulation data that could be used to estimate the travel-time and vehicle-operating-cost savings associated with auxiliary passing lanes. Parameters that were assumed to be randomized and held constant include

1. Alignment. A flat, tangent alignment was assumed for the simulation modeling. The influence of horizontal and vertical curves was introduced by varying the percent of roadway with no-passing zones.

2. Sight Distance. A minimum of 1,000 feet was defined as available except where limited by no-passing zones.

3. Desired Speeds. A speed of 55 mph was assumed for autos with a standard deviation of 5.3 mph. However, because average truck speeds in the 10-year period preceding the imposition of the 55 mph speed limit were 6 mph below passenger speeds, it was assumed that trucks operate at speeds 7.5 mph below passenger car speeds (20). An examination of this speed reduction for trucks indicated that this 7.5 mph assumption reduced the speed of all vehicles approximately 3 mph and caused an increase in delay to all vehicles of approximately 10 percent compared to all vehicles operating at identical speeds. These overall reductions were judged to be consistent with the general effect of trucks on rural two-lane roadways. The assumed standard deviation for trucks speeds was also 5.3 mph.

4. Directional Distribution. For the purpose of developing average speed and delay models, A 50/50 split was assumed as the most common directional distribution on two-lane rural roads.

5. Traffic Composition. A traffic stream composed by 10 percent trucks was assumed.

Independent variables used in the simulation modeling were ADT volume, percent of the highway with permitted passing, and length of highway section being considered for auxiliary passing-lane treatment. ADT was varied from 2,000 to 9,500 vehicles per day. The percent passing was varied from zero to 100 percent with no-passing zones introduced in 528-foot segments. Section length was defined in terms of a replicated standard passing lane module consisting of one passing lane in each direction within a two-mile module, and varied from two miles to ten miles in total length. The selection of these lengths corresponds to the California study, which recommended alternating the direction of the passing lane each mile (17). Based on this recommendation, the assumed passing lane plan view is shown in figure 2.

The full experimental design would have required 880 cells to be tested. To reduce the computational requirements, the statistical technique of response surface methodology was applied (22). The TWOWAF simulation model was then used to develop the speed and delay values for both passenger cars and trucks. For the without-passing-lane configuration, data were generated for each flow direction and then averaged. Because the passing lane configuration could not be explicitly simulated by the TWOWAF model, an auxiliary passing lane was approximated by removing traffic volumes from the opposite direction, thus permitting passing only at specified one-mile intervals in one direction.

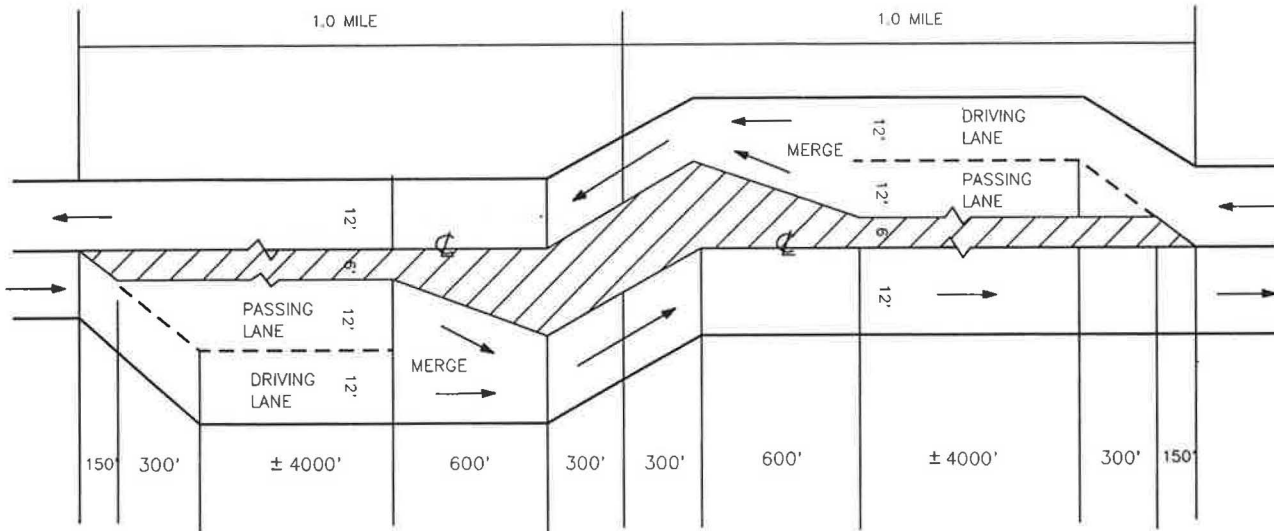
Stepwise regression analysis was used to develop the speed and delay relationships from the TWOWAF simulation data. The resulting delay models are listed below, where  $X_1$  = one way volume (100 to 580 vph range),  $X_2$  = section length (10,560 to 52,800 ft range), and  $X_3$  = percent passing (0 to 100 percent range).

1. Without auxiliary passing lane:

Average passenger car delay (sec/mi)

$$= -0.475 + 0.020X_1 + 0.000139X_2 - 0.020X_3 \quad (6)$$

This model provided an  $R^2$  of 96 percent with normal plots of residuals.



(NOT TO SCALE)

**FIGURE 2 Typical passing lane horizontal alignment.**

Average truck delay (sec/mi)

$$= -1.82 + 0.0095X_1 + 0.0001X_2 - 0.0078X_3 \quad (7)$$

This model provided an  $R^2$  of 89 percent with normal plots of residuals.

2. With auxiliary passing lane:

Average passenger car delay (sec/mi)

$$= 0.250 + 0.017X_1 \quad (8)$$

This model provided an  $R^2$  of 88 percent with normal plots of residuals.

Average truck delay (sec/mi)

$$= 0.0038 + 0.0083X_1 + 0.000029X_2 \quad (9)$$

This model provided an  $R^2$  of 63 percent with normal plots of residuals.

Examination of the above delay models indicates that the traffic volume, percent passing, and section lengths are all significant variables for a two-lane roadway. However, with an auxiliary passing lane in place, delay is primarily dependent upon the traffic volume. These delay relationships may be expected, since delay should be a function of all three independent variables when an auxiliary lane does not exist. However, with the addition of an auxiliary passing lane, the effect of percent passing becomes insignificant because passing is normalized at 50 percent.

Vehicle operating costs vary as a function of travel speed and longitudinal grade. Because longitudinal grade was constrained to 0 percent, the only parameter assumed to affect running cost was the speed of the various vehicles with and without the presence of an auxiliary passing lane. Regression analysis was again used to develop the following speed models from the TWOWAF simulation data. The independent variables are as defined above.

1. Without auxiliary passing lane:

Average passenger car speed (ft/sec)

$$= 79.8 - 0.0189X_1 - 0.00013X_2 + 0.018X_3 \quad (10)$$

This model provided an  $R^2$  of 96 percent with normal plots of residuals.

Average truck speed (ft/sec)

$$= 70.3 - 0.00798X_1 - 0.000088X_2 + 0.006X_3 \quad (11)$$

This model provided an  $R^2$  of 96 percent with normal plots of residuals.

2. With auxiliary passing lane:

Average passenger car speed (ft/sec)

$$= 79.1 - 0.0174X_1 \quad (12)$$

This model provided an  $R^2$  of 87 percent with normal plots of residuals.

Average truck speed (ft/sec) =  $68.3 - 0.0077X_1$  (13)

This model provided an  $R^2$  of 66 percent with normal plots of residuals.

An examination of the speed models indicates that volume, percent passing, and section length are significant variables in the case of a two-lane roadway, while traffic volume is the only significant variable when an auxiliary passing lane is added. The models were used in conjunction with 1977 running-cost data (22) to estimate vehicle operating costs.

### PASSING-LANE COSTS

To determine typical passing lane quantities and construction cost, it was assumed that most passing lanes would require some minor earthwork, 6 inches of aggregate base course, and 6 inches of asphalt surface course for the addition to the existing two lanes, and 1.5 inches of asphalt resurface over the entire length of the passing lane project. With this esti-



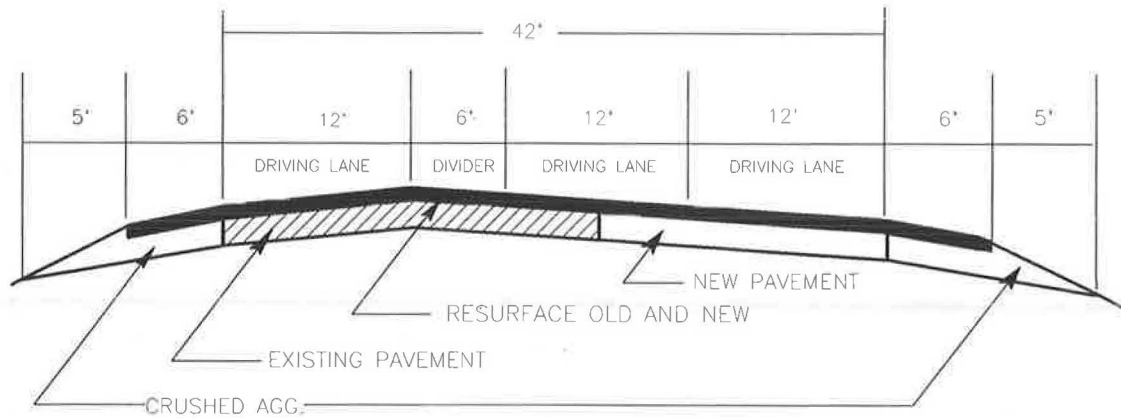


FIGURE 3 Typical APL cross section.

mate, figure 3 presents a typical cross-section of an auxiliary passing lane added to the outside of an existing two-lane roadway. It should be noted that the passing lane will vary from one side of the centerline to the other after each mile (thus the centerline location remains constant), and that, assuming a 42-foot surface width and 12-foot lanes, a six-foot median exists between opposing lanes. Using 1978 cost data, the initial cost of the typical auxiliary passing lane was estimated to range from \$250,000 to \$400,000 per mile. Maintenance cost savings attributable to the construction of an auxiliary passing lane plus overlay surface on the existing pavement was estimated at \$2,000 per mile, per year. The salvage value at the end of an assumed 20-year service life was estimated at \$35,000 per mile, which consists of the cost of right-of-way and one-half the cost of earthwork from the original estimate as suggested by AASHTO (22).

### ECONOMIC ANALYSIS

The final task of the research was to incorporate the conflict, speed, delay, and cost relationship in an economic analysis model that would reveal the relative attractiveness of an auxiliary passing lane as traffic volumes vary over peak, off-peak, weekday, weekend, and monthly levels for highway sections of a given length and percent passing. By subtracting annual without-passing lane road-user costs from the with-passing lane user costs, an estimate of the total benefits of an auxiliary passing lane were determined. These benefits were then compared to the cost to construct and maintain an auxiliary passing lane after all costs and benefits were discounted to net present value. All cost data were adjusted to reflect 1978 conditions. The methodology used corresponds to that outlined in the 1977 AASHTO guidelines on economic analysis (22).

The results of the benefit-cost analyses were used to develop a break-even model that used two discount rates (four and eight percent), two construction costs (\$250,000 and \$400,000 per mile), and three conflict costs (\$0.22, \$0.33, and \$0.44 per conflict). Regression analysis was used to develop a break-even model which, for a given set of conditions, would indicate the minimum ADT at which an auxiliary passing lane would be economically justified. This would be that ADT associated with a benefit-cost ratio of 1.0. The resulting model

is expressed as

$$\text{ADT} = \exp[(17.0 - 0.369X_1 - 0.386 \ln X_2 + 0.138X_3 - 1.84X_4 + 0.00232X_5)/1.82] \quad (14)$$

where:

- $X_1$  = section length
- $X_2$  = length of roadway with permitted passing (%),
- $X_3$  = discount rate (%),
- $X_4$  = conflict cost (\$), and
- $X_5$  = construction cost (\$1,000's).

An examination of the structure of the break-even model indicates that as the section length (number of replicated passing lanes constructed) increases, the ADT required to economically justify construction of the auxiliary passing lane section decreases, as it does when the percent passing and conflict cost are increased. However, when the discount rate or the cost of construction increases, the ADT at which the auxiliary passing lane is justified increases. Both of these observations conform to general expectations because more passing lanes (length), high percent passing available on the old road, and higher conflict costs should lower the ADT required to economically justify an auxiliary passing lane.

To simplify use of the break-even model, a nomograph was developed and is presented in figure 4. The nomograph is based on a 4 percent discount rate which has been recommended for safety projects (16) and includes values for passenger and truck delay costs (\$3.50 and \$10.00 per hour, respectively). To use the nomograph:

1. Estimate the per-mile construction cost of the auxiliary passing lane for the site as well as the cost of conflicts for the region or state. These estimates may be updated to current year dollar costs if it is assumed that any cost increases since 1978 are constant over all costs and all benefits. However, a better approach is to reduce current cost to 1978 cost levels.
2. Connect these estimated values to turn line 1.
3. Determine the extent to which passing is permitted on the existing road by comparing the directionally averaged length of no-passing zones to the total roadway length.
4. Connect turn line 1 and the percent passing to turn line 2.
5. Determine the length of roadway section that is to receive

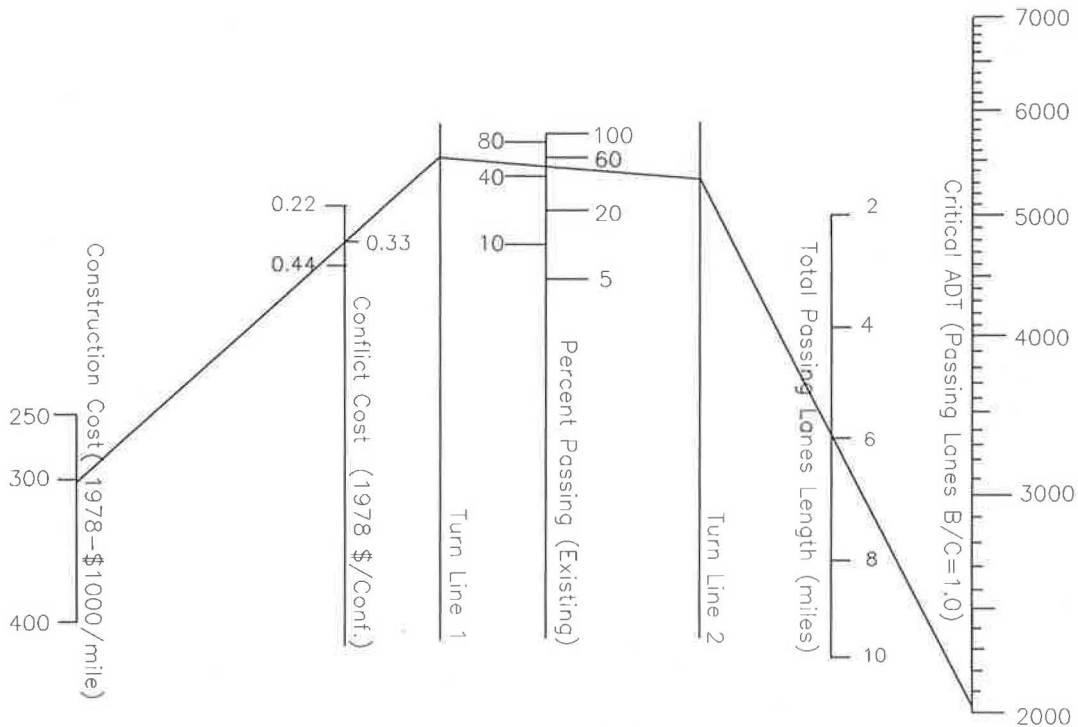


FIGURE 4 Economic analysis nomograph.

new passing lane construction, and connect the point on turn line 2 to the length to establish the ADT that must be exceeded to economically justify construction of the auxiliary passing lane. Conversely, the existing ADT at the site may be connected to the point on turn line 2 to determine the length of section for which the construction of auxiliary passing lanes is justified.

**CONCLUSIONS**

The auxiliary passing lane benefit-cost model and the nomograph for the critical ADT are based on a number of assumptions that constrain their general applicability.

The conflict-probability model estimates the number of passing conflicts that will occur on a two-lane roadway. The assumption of linear reduction to conflicts as the percent passing is reduced should be considered a limitation because, for some sites, a reduction in the percent passing may in fact stimulate the presence of conflict rather than reduce conflicts. However, since no research exists regarding an increase in accidents or conflicts as the percent passing is varied, the assumption of direct linearity appears reasonable. When figuring the cost per conflict, the relationship of intersection (special situation) passing accidents to all passing accidents was a determinant to the use of low, average, or high cost-per-conflict values, depending on the number of intersection-related passing accidents compared with all passing accidents. Care needs to be exercised in selecting an appropriate value for any case study application of the design warrant.

Similarly, with regard to the cost per conflict and the benefit to be derived from the construction of an auxiliary passing lane, the assumption of the accident reduction value of 38

percent of the original condition was based solely on California data. With further study of the safety benefits of other auxiliary passing lanes, this estimate of accident reduction potential may also vary, and may be increased to reflect the passing lane safety savings due to reduced passing accidents at special situation sites such as intersections and driveways.

The two-way traffic simulation model (TWOAF) used to estimate speed and delay was capable of modeling a passing lane within the test section length only by eliminating traffic in the opposite direction. Thus, for a 6-mile segment, passing lanes were artificially introduced into alternating 1-mile lengths (1 mile in each direction) for the total 6-mile length. This was accomplished by restricting traffic flow in the opposing direction and permitting passing only at 1-mile intervals where passing is permitted. Future research should use a newer version of TWOAF, which contains a passing-lane model capable of placing a specific size passing lane anywhere, and in either or both directions within the test section, and then developing several other general warrants where only one such lane, and not successive passing lanes, are used over varying length test sections.

Further limitations of the break-even model arise from the use of many assumed average values that were input to the TWOAF traffic simulation model to generate travel speeds and delays for passenger and truck vehicles. Some of these parameters include vehicle composition, desired travel speeds and standard deviations of speed, available passing-sight distance and passing zone locations, as well as an assumed tangent roadway with a flat terrain, which inhibited truck speeds to 7.5 mph below passenger vehicle speeds. While it was necessary to normalize these and other roadway characteristics due to financial limitations placed on this research, a major revision of one or more of these assumed average con-

ditions might cause the break-even model to overestimate or underestimate benefit-cost ratios and critical ADTs.

In summary, the model developed in this research was designed to assist engineers in evaluating the need for auxiliary passing lanes on two-lane highways. Where the critical ADT is determined to be substantially larger or substantially smaller than the ADT that exists at a site, many of the above limitations are expected to have only minor impact and may not affect the benefit-cost ratio or the critical ADT significantly. Where the critical ADT is reasonably close to the ADT that exists at the site in question, a detailed economic analysis should be undertaken using site-specific, TWOWAF-generated speed and delay data. A microcomputer program is available to provide detailed economic analysis of specific sites with specific input parameters.

## REFERENCES

1. U.S. Department of Transportation, *Highway Statistics*, 1984.
2. U.S. Department of Transportation, *Fatal & Injury Accident Rates*, 1984.
3. U.S. Department of Transportation, *Fatal Accident Reporting System*, 1984.
4. R. S. Hostetter and E. L. Sequin. The Effects of Sight Distance and Controlled Impedance Distance on Passing Behavior. In *Highway Research Record 292*, HRB, National Research Council, Washington, D.C., 1969.
5. M. S. Janoff and A. Cassel. *Identification and Evaluation of Remedial Aid Systems for Passing Maneuvers on Two-Lane Rural Roads*, Volumes II, III and V. The Franklin Institute Research Laboratories, Washington, D.C., 1970.
6. Hardwood, St. John, and Warren. Operational and Safety-effectiveness of Passing Lanes on Two-lane Highways. In *Transportation Research Record 1026*, TRB, National Research Council, Washington, D.C., 1985.
7. E. G. Evans and T. B. Treadway. Economic Analysis of Truck Climbing Lanes on Two-lane Highways. In *Highway Research Record 245*, HRB, National Research Council, Washington, D.C., 1968.
8. D. G. McCallum. *The Economic Evaluation of Crawler Lanes*. Geometric Road Design Standards, Organization for Economic Cooperation and Development, Paris, 1977.
9. A. R. Kaub. A Design Warrant for Auxiliary Passing Lanes on Rural Two-lane Highways. Ph.D. thesis, University of Wisconsin-Madison, 1987.
10. Weaver, D. Graeme, and D. L. Woods. *Passing and No Passing Zones; Signs, Markings and Warrants*. Report FHWA-RD-79-5, Federal Highway Administration, Washington, D.C., September 1978.
11. W. R. Stockton, J. M. Mounce, and N. E. Walton. Guidelines for the Application of Selected Signs and Markings to Low Volume Rural Roads. In *Transportation Research Record 597*, TRB, National Research Council, Washington, D.C., 1976.
12. *Policy on Geometric Design of Highways and Streets*. AASHTO, 1984.
13. *Manual of Uniform Traffic Control Devices*, U.S. Department of Transportation, Washington, D.C., 1978.
14. *Accident Facts of 1978*. National Safety Council, Washington, D.C., 1979.
15. G. D. Weaver and D. L. Woods. *No Passing Zone Treatments for Special Geometrics and Traffic Operational Situations*. Report FHWA-RD-81-093, Federal Highway Administration, Washington, D.C., September 1981.
16. W. F. McFarland, et al. *Assessment of Techniques for Cost Effectiveness of Highway Accident Countermeasures*. Report FHWA-RD-79-53, Federal Highway Administration, Washington, D.C., January 1979.
17. E. A. Rinde. *Accident Rates vs. Shoulder Widths*. CALTRANS Report #Ca-DOT-TR-3147-1-77-01, 1977.
18. R. Goldblatt and E. Lieberman. *Review of Existing Two-Lane, Two-Way Rural Road Computer Simulation Models*. NCHRP Project 3-28-A, unpublished report, TRB, National Research Council, Washington, D.C., 1981.
19. R. Goldblatt and E. B. Lieberman. *Calibration and Validation of TWOWAF, Two-Lane, Two-Way Rural Road Computer Simulation Model*. NCHRP Project 3-28A, unpublished paper. TRB, National Research Council, Washington, D.C., December 1981.
20. *Highway Statistics, Summary to 1985*. U.S. Department of Transportation, Washington, D.C., 1986.
21. G. E. P. Box, W. G. Hunter, and J. S. Hunter. *Statistics for Experimenters*, J. Wiley & Sons, 1978.
22. *A Manual on User Benefit Analysis of Highway and Bus Transit Improvements*. AASHTO, Washington, D.C., 1977.

---

Publication of this paper sponsored by Committee on Operational Effects of Geometrics.

# Uniform Delay Approach to Warrants for Climbing Lanes

K. M. WOLHUTER AND A. POLUS

**Current warrants for climbing lanes are discussed, and the consequences of their usage are explored. Data were obtained and analyzed to derive relationships among flow, gradient, and speed on South African roads. These relationships were used to calibrate TRARR, a simulation program developed by the Australian Road Research Board, and this, in turn, was used to establish relationships between delay and flow for various gradients. Actual delay is offered as an alternative warrant, it being pointed out that the Highway Capacity Manual offers delay as a criterion of Level of Service. The paper postulates that delay suffered would not be a function of the gradient on which it occurs if the climbing lane were the subject of economic analysis. Various isochronistic warrants are offered for consideration with the consequences of adoption of this approach being pointed out.**

Most vehicles can maintain relatively high speeds on level terrain; consequently, the flow on these grades is characterized by low speed differentials and minimal turbulence, and high flow levels may occur. As soon as a gradient of any consequence is encountered, (in excess of about 3 percent) the situation changes dramatically. Speed differentials increase, leading to an increase in platooning of vehicles and reduction in the level of service. This phenomenon has long been recognized, and auxiliary lanes (variously known as climbing lanes, crawler lanes, truck lanes and, confusingly, passing lanes) have been provided to overcome this problem. In this paper, reference will be made throughout to climbing lanes. Passing lanes are generally found on flat gradients and are intended to increase the overall capacity of a road above that of a normal two-lane road, whereas climbing lanes, found on gradients, serve to match the capacity of the grade to that of the flatter sections of the road and eliminate excessive delay due to the low speeds of trucks.

The first problem confronting the designer in the provision of climbing lanes along a route is to determine at which points along the route climbing lanes can be installed to best advantage. This problem is invariably resolved by the use of warrants. Warrants may be described as surrogates for economic analysis and are often based on fairly arbitrary but easily measured parameters. A general economic analysis procedure is proposed by the British Department of Transport (1). Other than this, economic analysis has seldom, as far as can be established, been seriously attempted by practitioners.

The form and value of these warrants are legion. Warrants can be subdivided into five broad groups: truck speed reduc-

tion, speed differential between trucks and passenger cars, either of the above in association with a traffic volume, and, lastly, reduction in level of service. Reference to the literature reveals that, in each group, a range of values is encountered.

AASHTO (2) recommends the inclusion of climbing lanes where the critical length of grade, that distance which causes a reduction of 10 mph in the speed of a loaded truck, is exceeded. AASHO (3) used a truck speed reduction of 15 mph, whereas Glennon and Joyner (4) recommend the criterion of 10 mph, quoting increased accident risk in support of their contention. Polus et al. (5) proposed a truck speed reduction of 12 mph (20 km/h) as the speed warrant for climbing lanes, using the truck speed/gradient relationship quoted in the 1965 edition of "A Policy on Geometric Design of Rural Highways," and this suggests that the entry speed to a gradient be accepted as 40 mph (64 km/h). South Africa (6) also uses a truck speed reduction of 20 km/h, but assumes a truck speed of 80 km/h on level grades. Canada (7) considers that a truck speed reduction of 15 km/h warrants a climbing lane but measures the speed reduction from the 85th percentile or running speed. It is not clear whether this is the 85th percentile speed of trucks or of the whole traffic stream. Botswana (8) uses a truck speed reduction of 25 km/h.

The use of truck speed reduction as a warrant implies that passenger car speed is totally unaffected by gradient. Some authorities take cognizance of the fact that passenger car speed is, in fact, influenced by gradient and refer to the speed differential between cars and trucks as a warrant. For example, the *Transportation and Traffic Engineering Handbook* (9) refers to a speed differential of 10 mph between trucks and the mainline flow.

Very often, the speed reduction warrant is associated with a volume warrant. *The Highway Capacity Manual* (10) considers climbing lanes as an alleviating treatment when the following warrants are met:

- upgrade volumes exceed 200 vph,
- upgrade truck volumes exceed 20 vph, and
- a speed reduction of 10 mph or more is expected for the average truck.

Wolhuter also provides a volume warrant, based on the catch-up rate on various grades and with various percentages of trucks in the traffic stream, as illustrated in table 1.

The above warrants are intended for application to individual grades. The philosophy adopted by Australia (11), on the other hand, considers the need for climbing lanes based on examination of a considerable length of the road in question. The justification for climbing lanes is based on traffic

K. M. Wolhuter, National Institute for Transport and Road Research, Pretoria 0001, Republic of South Africa. A. Polus, Technion-Israel Institute of Technology, Haifa, Israel.

TABLE 1 VOLUME WARRANTS FOR CLIMBING LANES

Gradient (%)	Traffic volume in design hour	
	5 % trucks	10 % trucks
4	632	486
6	468	316
8	383	243
10	324	198

volume, the percentage of trucks in the traffic stream, and the availability of overtaking opportunities on the route. The speed reduction criterion is reduction to 40 km/h. Climbing lanes should span the full length of the grade, but partial climbing lanes may be considered when truck speeds fall below 40 km/h and a full lane is not justified because of low traffic volumes or high construction cost. On extreme grades, where truck speeds are reduced to 20 km/h or less, passing bays, typically less than 100 m long, can be considered when all the following conditions are met:

- long grades over 8 percent,
- high percentage of heavy vehicles,
- low overall traffic volumes, and
- high construction costs.

A separate class of warrants refers to level of service. Level of service is a descriptor of operational characteristics in a traffic stream, measured in terms of delay, speed, and ratio of volume to capacity. An important feature of this descriptor is that it is a representation of driver perception of the traffic environment and bears little or no relation to the cost of creating that environment or the cost of operating in it. The warrants suggested by the *Highway Capacity Manual* are—

- a reduction of two or more levels of service in moving from the approach segment to the grade and
- Level of Service E (LoS E) exists on the grade.

Polus et al. suggest that a climbing lane is warranted if the design hourly volume exceeds the specific grade service volume for a level of service one lower than that adopted for the design of a level section of the road.

Typically, the motivation given for selection of a particular warrant is based on qualitative arguments. An alternative approach to warrants for climbing lanes is presented in this paper.

## BACKGROUND TO STUDY

Whereas estimation of the construction and maintenance costs of a climbing lane usually does not present any problem, derivation of the benefit accruing from this investment is more intractable. Economic analyses have often indicated that the benefit derived from time savings alone overshadows other benefits. However, to achieve a correct perspective, the overall benefit is briefly discussed below.

The benefit subdivides into benefit to the road user and

benefit to the community as a whole as represented by the road authority. Benefit to the road user involves changes in—

- extent of delay, a time benefit;
- operating cost, an economic benefit;
- accident exposure, a safety benefit; and
- level of stress, a comfort benefit.

Benefit to the community derives from—

- higher levels of service, hence postponement of the obsolescence of a facility and
- reduced need to provide additional passing sight distance elsewhere, hence a potential reduction in construction cost.

Although sometimes described differently, it is clear that all these benefits have strong economic overtones, but, as stated above, the value accrued from time savings alone tends to overshadow the economic benefits derived by other means. For this reason, the attention of this paper is focused on the calculation of delay. The contention is that a specific climbing lane, warranted by time savings alone, could show a “profit” if the other factors were also taken into account; that is, such a warrant tends to be conservative.

Delay does not lend itself readily to direct measurement in the field, hence the use of alternative criteria, such as the percentage of time spent following. Seeing, however, that delay is simply the time added to a trip by travelling at a speed lower than desired, simulation offers a convenient technique for its determination.

## MODUS OPERANDI EMPLOYED

Time mean speeds were measured at various sites, covering a range of gradients and under widely varying traffic flows, and classified according to vehicle type. These were used to calibrate a simulation model, TRARR, developed by the Australian Road Research Board, to local prevailing conditions.

Delay is a function of space mean speed. The simulation model was used to derive space mean speeds achieved by passenger cars on a range of gradients across a range of traffic flow. Gradients varied between 3.6% and 8.4%, and flow from 30 vehicles per hour (vph) to 1,500 vph. Space mean speeds achieved by vehicles traveling at headways of 10 s or longer are considered to be desired speeds, in other words, dictated by the hill-climbing capability of the individual vehicle or by the preference of the driver when the gradient is not sufficiently steep to govern vehicle performance. Increasing flow levels inevitably lead to a drop in space mean speed below that desired, and this reduction in speed is the basis for calculation of delay.

Data collection, calibration and calculation of delay are described in more detail in the following sections.

## DATA COLLECTION

### Data Acquisition System

The data were acquired for this analysis using the Traffic Engineering Logger (TEL) developed by the National Insti-

TABLE 2 DESCRIPTION OF VEHICLE CLASSES

Class	Length (m)	Description
Light	Short	<5.9
	Long	5.91 - 10.0
Heavy	Short	<10.0
	Medium	10.1 - 16.8
	Long	>16.8

tute for Transport and Road Research, South Africa. The TEL is a microprocessor-based system capable of collecting traffic data in one of three modes of operation. These are—

- roadside installation,
- vehicle mounted installation, and
- hand-held operation.

For this study, the roadside installation was employed, in which traffic data are collected from successive induction loops buried in the road surface.

The TEL differentiates among classes of vehicles on two bases. Cars, in spite of their lesser mass, show a greater disturbance of the magnetic field than do trucks because of their lower center of gravity. The length of vehicles is measured on the basis of their speed and corresponding time of occupation of the loops. Data acquired by this system include time of arrival (to nearest 0.1s), speed (to nearest 1 km/h), vehicle length (to nearest 0.1m), and class of vehicle, for each vehicle.

Table 2 lists the classes of vehicles among which the TEL can differentiate. For the purpose of this study, vehicles in the light category were grouped together as it was found that the percentage of cars in the traffic stream that were towing caravans (trailers) was very low. It was also found, as discussed later, that further aggregations could also be employed with advantage.

**Data Acquired**

Two sets of data were collected and subdivided as shown in table 3. The observation points were located sufficiently far

along the grade for vehicle speeds to have stabilized to the gradient.

**PRELIMINARY ANALYSIS OF DATA**

Speed distributions for uninterrupted flow conditions were derived by considering only those speeds associated with headways of 10 s and longer and by aggregating them into 5 km/h intervals. Typical distributions for the various classes of vehicles are illustrated in figure 1 for the Ben Schoeman site.

The means and the standard deviations of the speed distributions were calculated for each of the sites as shown in table 4. The means are plotted as shown in figure 2, which illustrates what appears to be an inconsistency with expectations, as speeds at the four-lane sites are lower than those at the two-lane sites. These lower speeds are attributed principally to the fact that the speeds recorded on the freeway sections refer only to the slow lane. There is also a difference between the occurrence of headways longer than 10 s on two-lane roads and freeways, as illustrated in figure 3, and it is presumed that this would also account, even if only in part, for the difference. Further analysis established that the difference in speeds between two) and four-lane roads is statistically insignificant at the 5 percent confidence level. It is thus possible to ignore differences in cross-section in the study that follows.

It was also found that the difference in speeds between medium-heavy and long-heavy vehicles is statistically insignificant. Operators match the mass hauled to the capacity of the tractor, and the additional trailer serves to accommodate high-volume, low-mass loads. It is thus not surprising that there should be relatively little difference in performance

TABLE 3 DESCRIPTION OF DATA SETS

Site	Lanes	Gradient (%)	Distance along grade (m)	Sample size (veh)
Cornelia	2	3.62	1 600	9 232
Colenso	2	5.21	3 000	17 196
Long Tom	2	8.38	2 000	15 980
Rigel North	4	3.54	3 100	16 132
Rigel South	4	4.45	4 000	4 651
Ben Schoeman	4	4.97	1 400	20 945
Krugersdorp	4	6.44	1 800	21 254

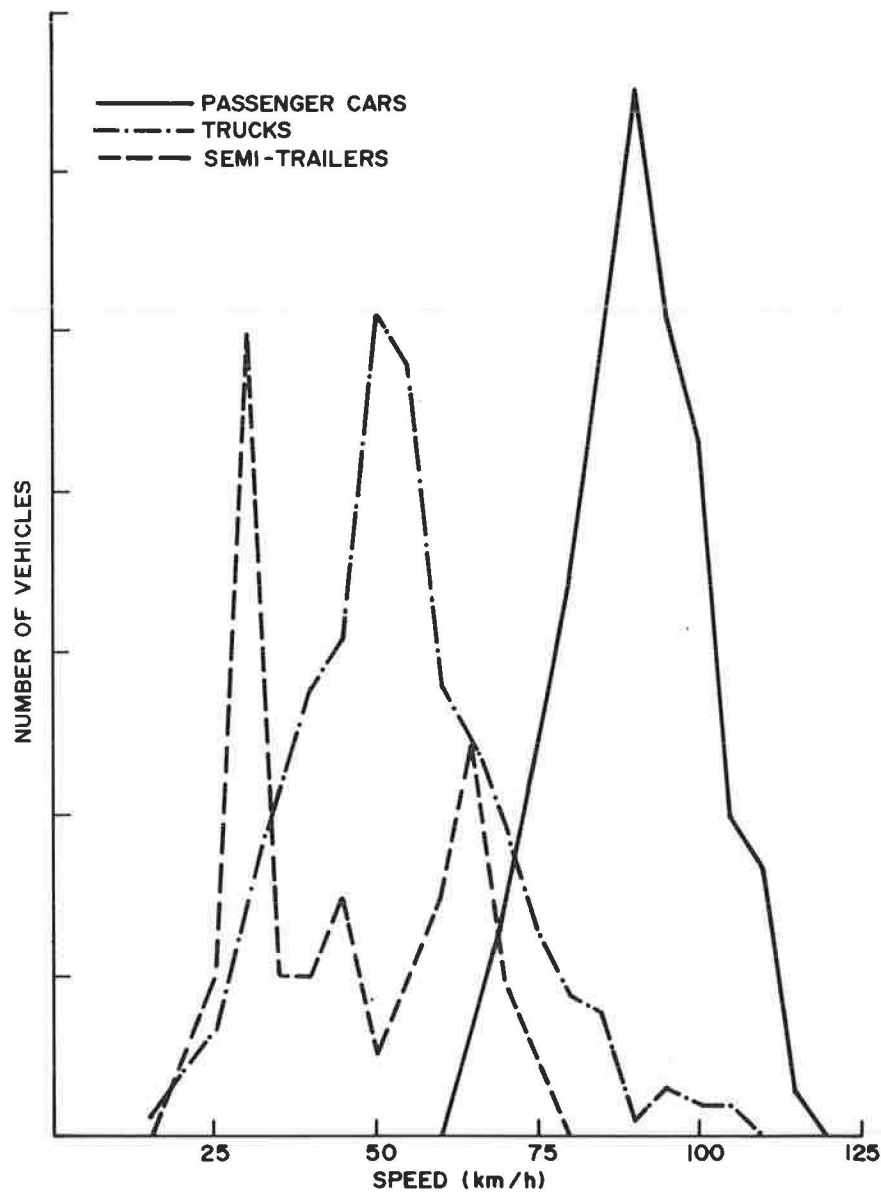


FIGURE 1 Distribution of speed on a gradient of 4.97% by class of vehicle.

between the two vehicle configurations. Consequently, only three classes of vehicles, passenger cars, single unit trucks, and semitrailers, are considered in this study. Average speeds derived for the semi-trailers are shown in table 5.

#### RELATIONSHIP BETWEEN GRADIENT AND SPEED

The speeds shown for the various vehicles on the observed gradients (as reflected in table 4) and the aggregated speeds for the semitrailers (as listed in table 5) represent what can be considered desired speeds for the purposes of this study. In short, they represent the limiting performance of the vehicle class in question or, alternatively, the speed preferences of the drivers where the performance of the vehicle does not dictate the selection of speed.

The following relationships between gradient and desired speed (or limit of vehicle performance) were derived by means of regression:

$$V_c = 123.32 - 6.99 G \quad (R^2 = 0.986)$$

$$V_t = 76.89 - 4.79 G \quad (R^2 = 0.994)$$

$$V_s = 69.13 - 5.33 G \quad (R^2 = 0.946)$$

where

$V_c$  = passenger car speed (km/h)

$V_t$  = truck speed (km/h)

$V_s$  = semi-trailer speed (km/h)

$G$  = gradient (%)

These relationships are plotted in figures 4 and 5 as dotted lines and represent actual performances by the various classes of vehicles as measured on South African roads. These are

TABLE 4 SPEED VERSUS GRADIENT FOR VARIOUS VEHICLE CLASSES

Num. of Lanes	Grade (%)	Vehicle class							
		Light		Heavy					
				Short		Medium		Long	
		Mean	S.D.	Mean	S.D.	Mean	S.D.	Mean	S.D.
2	3.62	100.6	15.6	60.6	15.6	51.8	14.3	49.8	15.4
2	5.21	89.2	16.0	52.3	18.4	37.6	13.8	34.6	12.9
2	8.38	64.5	12.9	37.7	11.8	32.4	15.9	19.0	10.2
4	3.54	95.7	14.3	60.2	16.1	52.1	16.8	50.9	16.8
4	4.45	92.5	14.4	55.1	14.4	47.4	16.2	48.2	15.9
4	4.97	86.7	15.8	52.2	16.7	40.4	15.3	42.3	16.8
4	6.44	78.2	15.1	44.9	17.3	32.7	12.3	26.4	9.3

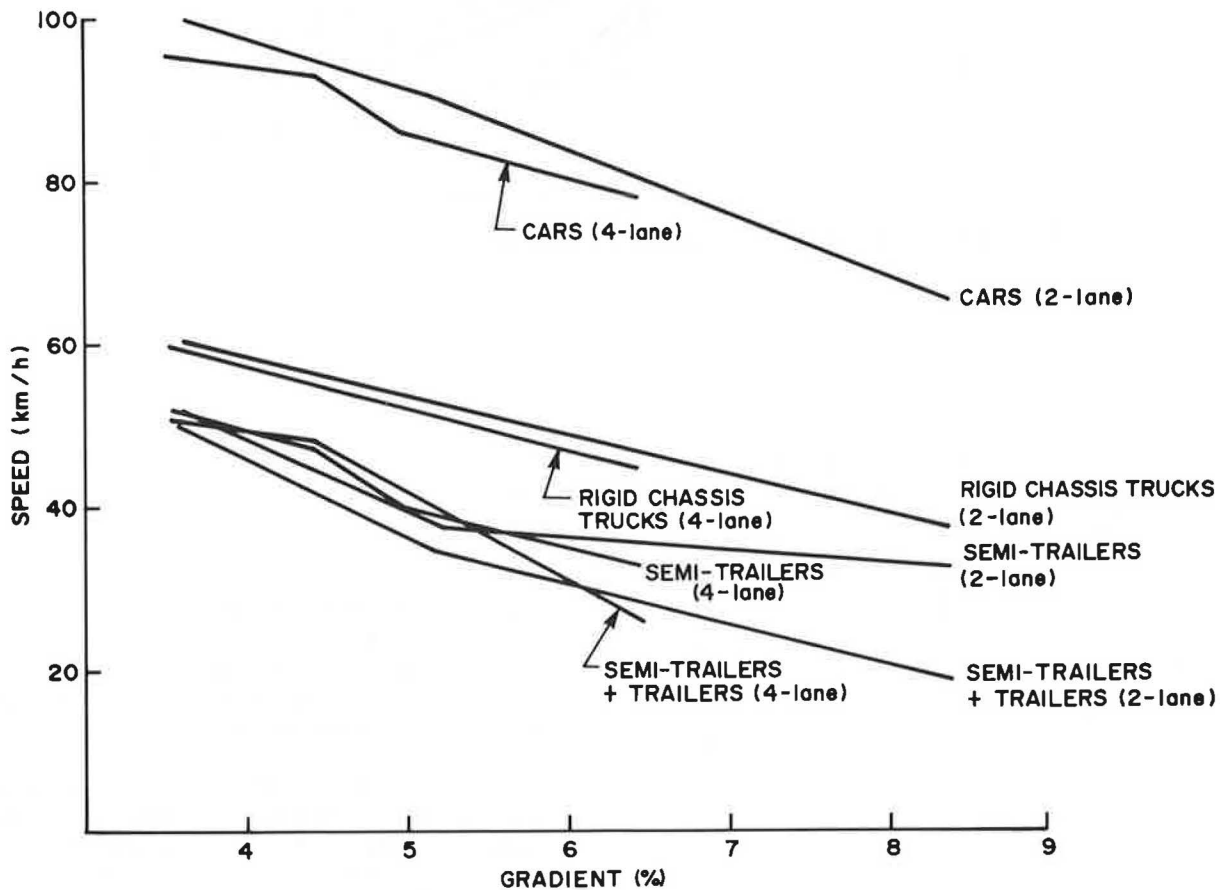


FIGURE 2 Observed mean speeds on gradients by class of vehicle.



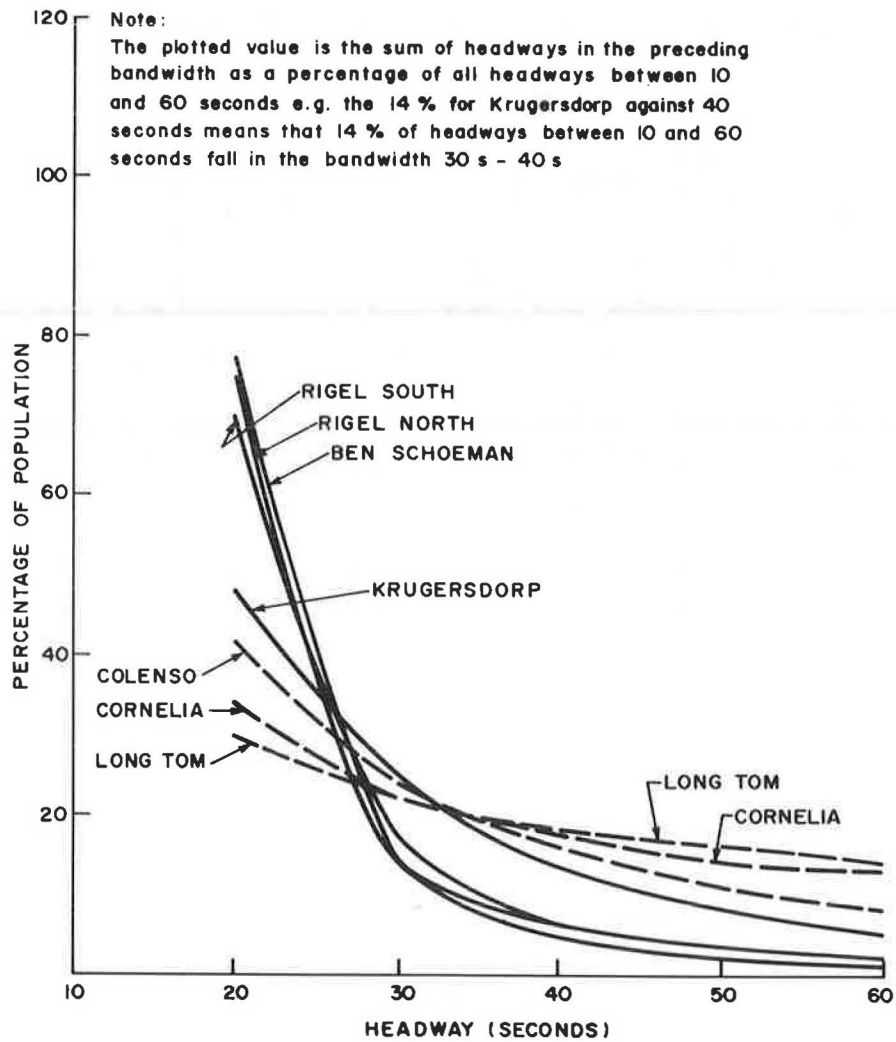


FIGURE 3 Distribution of observed headways greater than 20 s.

TABLE 5 AGGREGATED SPEED ON GRADIENTS FOR SEMITRAILERS

Gradient (%)	Speed (km/h)
3.54	52.60
3.62	51.44
4.45	47.49
4.97	40.83
5.21	36.66
6.44	31.93
8.38	28.00

speeds measured at a point, or spot speeds, whereas, for the purposes of study of delay, reference to speed will imply space mean speed.

**RELATIONSHIP BETWEEN FLOW AND SPEED**

The relationship between flow and speed on each grade was derived by a laborious process consisting of a number of computational steps, as described below:

1. The entire period of observation at each site, typically with a duration of 72 hours, was divided into successive 2-minute intervals, and the volume of vehicles in each class for each 2-minute interval was derived. A volume of between 1 and 50 vehicles is thus equivalent to a flow of between 30 and 1,500 vph.
2. The range of speeds, between 0 km/h intervals, and the

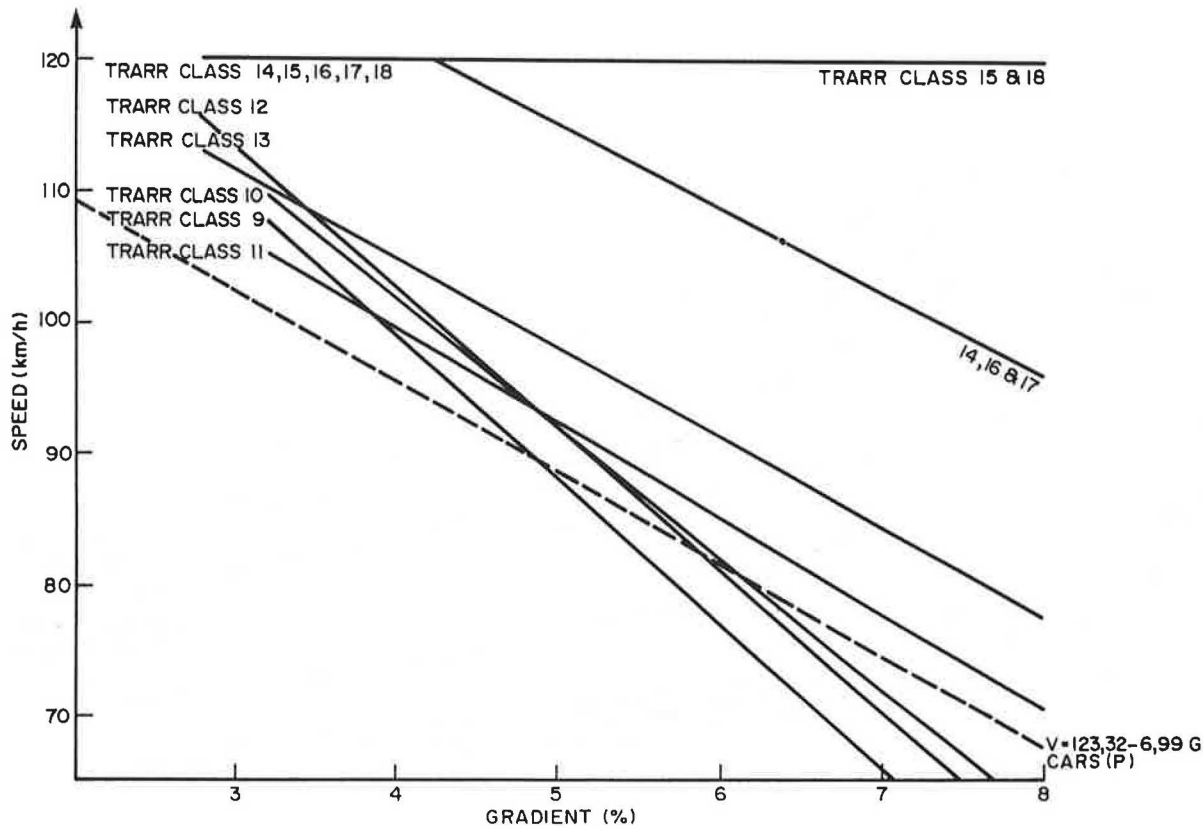


FIGURE 4 Comparison of observed mean speeds of passenger cars and TRARR Vehicle Classes 9 to 18.

number of vehicles of each class falling into each individual speed range calculated.

3. The histogram of speed so derived was then aggregated with the histograms of other two-minute intervals with the same flow.

4. Step 3 thus leads to the creation of a three-dimensional surface, with speed and flow as its base and number of vehicles as the vertical coordinate.

5. For convenience, and to apply a degree of smoothing, five successive flow levels were aggregated, representing steps of 150 vph between the various flow levels, or a total of ten points between zero and 1,500 vph.

6. Finally, the mean speed for each class of vehicle and for each aggregated flow level was calculated.

7. The process described above was repeated for each of the seven sites.

It was found that the relationship can be expressed as

$$V_{ca} = 128.38 - 6.89 G - 0.008 Q \quad (R^2 = 0.87)$$

where

- $V_{ca}$  = actual speed for passenger cars (km/h)
- $G$  = gradient (%)
- $Q$  = flow along upgrade (vph)

**Calibration of Model**

The simulation model, TRARR (Traffic on Rural Roads), was obtained from the Australian Road Research Board and calibrated in two stages.

This model employs eighteen different classes of vehicles, and, as a first step, runs were carried out with each of the eighteen classes of vehicles on each of the seven gradients. The conditions of the runs were that the position of the observation points in the simulation corresponded with the points at which data were actually gathered on the various gradients, and that flows were selected to represent headways of 10 s or longer.

The desired speeds for each of the classes of vehicle on the various gradients as derived from the simulation were also regressed to secure relationships between speed and gradient, and these are shown as solid lines in figures 4 and 5. Visual inspection suggested that the best correspondence could be obtained by using—

- for cars TRARR Class 11
- for trucks TRARR Class 7
- semi-trailers TRARR Class 6

The next stage involved running traffic streams containing these classes of vehicles, in the percentages observed in the field, on the various gradients. The delays of particular interest in this study are those suffered by passenger vehicles. Further analysis was carried out to derive a relationship between average passenger car speed versus gradient and flow for the chosen classes of vehicles in the simulation model. The relationship found is—

$$V_{cs} = 131.660 - 6.538 G - 0.017 Q \quad (R^2 = 0.95)$$

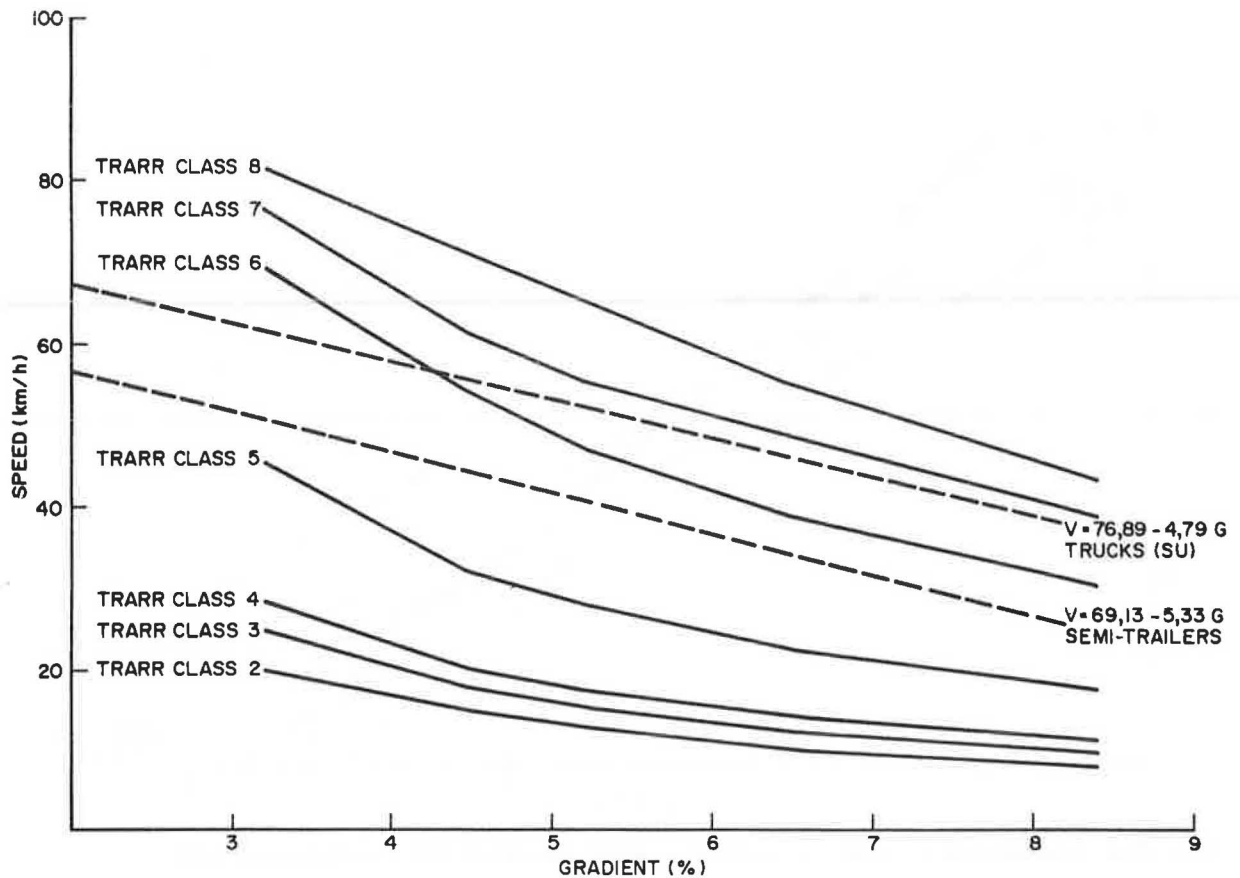


FIGURE 5 Comparison of observed mean speeds of trucks and semitrailers and TRARR Vehicle Classes 2 to 8.

where

- $V_{cs}$  = simulated speed for passenger cars (km/h)  
 $G$  = gradient (%)  
 $Q$  = flow along upgrade (vph)

This relationship compares reasonably well with that found for the field data.

#### DELAY

As suggested earlier, delay is that period of time added to a trip by a reduction of space mean speed to a value less than the desired. Space mean speed is calculated as the quotient of distance and mean journey time, and the speeds compared are those attained on the various grades at various flow levels against speeds attained on the same grades at very low flow levels.

Delay is thus calculated as:

$$T_d = 3600 (1/V_a - 1/V_d)$$

where

- $T_d$  = delay/km/passenger car(s)  
 $V_a$  = speed achieved by passenger cars at varying flow levels (km/h) =  $131.660 - 6.538 G - 0.017 Q$   
 $V_d$  = speed achieved by passenger cars at headways of 10 s or longer (km/h) =  $131.660 - 6.538 G$

$G$  and  $Q$  have the same meaning as before.

Ultimately, the product of delay per passenger car and the passenger car flow provides the total delay per kilometer experienced per hour, assuming that the flow rate remains constant for the entire hour.

There could be fluctuations in flow within the hour, which would introduce an underestimation in the calculated delay. For example, a flow of 750 vph could either be absolutely uniform or a volume of 749 vehicles in 30 minutes followed by a vehicle with a headway of 30 minutes. Using the above relationships, the total delay to passenger cars (on a 5 percent gradient with an assumed 15 percent trucks in the traffic stream) would amount to 57.15 min/km in the case of the uniform flow; whereas, in the second case, the total delay would be 134.14 min/km. It is suggested that the likelihood of such an extreme fluctuation is remote. However, if a flow of 750 vph represents a flow of 600 vph for 30 minutes followed by a flow of 900 vph for a further 30 minutes, there is still an underestimation of delay, although the error reduces from 76.99 min/km (134.14 - 57.15) to 3.01 min/km, an error of 5.27 percent. Clearly, further research is required to establish typical ranges of variation and to introduce appropriate corrections into the calculation of delay.

Using the relationships derived above, delay, suffered per kilometer by an individual passenger car, was calculated for a range of gradients, 3 to 9 percent, and flows along the upgrade varying from zero to 1,500 vph. These are plotted as shown in figure 6.

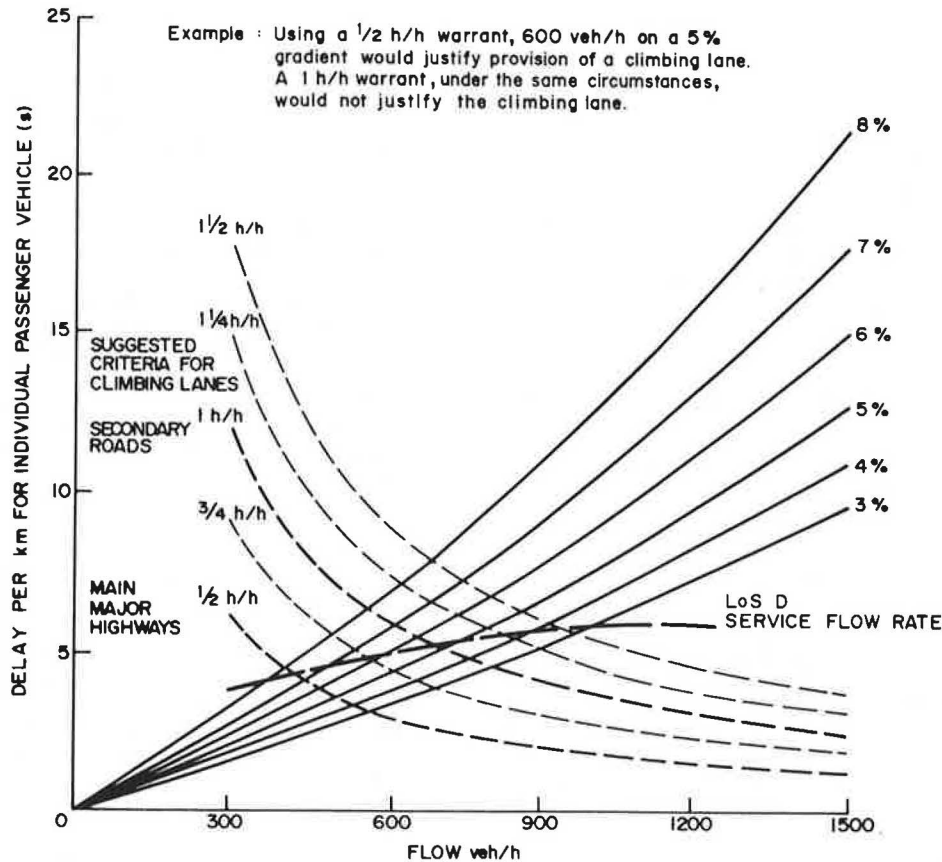


FIGURE 6 Relationship between flow, gradient, and delay.

**DELAY CONSEQUENCES OF EXISTING WARRANTS**

On level sections, rural roads typically operate in the range of LoS A or LoS B, except when close to urban areas. Seasonal fluctuations on recreational routes could produce the same result. *The Highway Capacity Manual* suggests, as one of the warrants for climbing lanes, a reduction by two levels of service, such as from LoS B to LoS D. The contention is that most drivers would be prepared to accept that operating conditions on a steep upgrade need not be comparable to those on level sections, suggesting that a reduction would be acceptable. However, a reduction through two levels, such as from LoS B to LoS E, would not be acceptable, and could thus lead to a reduction in safety being generated by impatience and ill-considered overtaking maneuvers. Such a reduction could also lead to a considerable increase in delay.

By way of illustration, a curve representing service flow rates for LoS D for various gradients is also shown on figure 6. The plotted values are based on the assumption of 15 percent trucks in the traffic stream and a grade 2.5-km (1.5-mi) long. This distance allows for a substantial length of gradient over which vehicle speeds are no longer influenced by preceding gradients.

It can be observed that the level of service warrant indicates a reasonably constant delay per vehicle regardless of the gradient. Because of the higher flows that can be accommodated on the flatter slopes before LoS D occurs, the overall delay to the traffic stream required to warrant a climbing lane is considerable.

**AN ALTERNATIVE WARRANT FOR CLIMBING LANES**

Also presented in figure 6 are five lines that represent isochronistic warrants for climbing lanes. These lines are based on the assumption that the total hourly delay for a given section, 1 km in this example, should remain constant regardless of the gradient. Thus, lines for 1/2, 3/4, 1, 1 1/4, and 1 1/2 hours of total delay per hour are presented. These are simply hyperbolae of the form:

$$W = Q * D * Pp / 3600$$

where

- W = constant, equal to selected warranting total delay = 1/2, 3/4, 1, 1 1/4 or 1 1/2 (h/h/km)
- Q = flow (vph)
- D = delay per individual passenger car(s)
- Pp = percentage passenger cars in stream

A climbing lane will be justified to the right of each line and not justified to its left.

The selection of a particular criterion (1/2, 3/4, etc.) is left to the individual agency and ought to be determined beforehand, based on general and economic design policies. It is suggested, for example, that on major highways an agency may prefer a higher standard by opting for the 1/2 h/h criterion and on secondary roads accept the 1 h/h criterion.

A decision to adopt delay as a warrant in preference to those currently in use has consequences that may not be over-

looked. The most obvious of these is that the flow at which a climbing lane is warranted shows a dramatic decrease on the flatter grades and a similar increase on steeper grades. The  $\frac{3}{4}$  h/h warrant demonstrates a break-even point with the current LoS warrant at 600 pcp/h and a 5 percent gradient. Experience indicates that the majority of gradients on any route are likely to be less steep than 5 percent, and flows in excess of 600 pcp/h are not uncommon. It is therefore reasonable to expect that, if the values in the above example are adopted, delay would illustrate a need for more climbing lanes than current warrants would suggest. At low volumes there would be some reduction in the number of climbing lanes called for on steeper grades. Construction costs, in the more rugged terrain that these gradients imply, could be substantially reduced.

A further consequence of delay as a warrant is that levels of service on steeper gradients may decrease, theoretically to beyond capacity. There is thus a logical cut-off point, in terms of flow and gradient, beyond which delay becomes meaningless and, therefore, a level of service criterion may have to be employed. This cut-off point, as well as the exact criterion of total delay, is still to be established. The basic concept, however, of a diminishing level of service with increasing gradient is seen as matching driver expectations which anticipate worsening of conditions with increasing steepness of grades. This expectation can be used to advantage to provide climbing lanes where drivers do not expect unnecessary delay.

#### ACKNOWLEDGMENTS

This paper is presented with the permission of the Divisional Director, Division of Road and Transport Technology, Council for Scientific and Industrial Research, Pretoria.

#### REFERENCES

1. *Highway Link Design*. TD 9/81. U.K. Department of Transport, 1981.
2. *A Policy on Geometric Design of Highways and Streets*. AASHTO, Washington, D.C., 1984.
3. *A Policy on the Geometric Design of Rural Highways*. AASHTO, Washington, D.C., 1965.
4. J. C. Glennon and C. A. Joyner. Re-evaluation of Truck Climbing Characteristics for use in Geometric Design. *Journal of Texas Transportation Institute*, 1969.
5. A. Polus, J. Craus, and I. Greenberg. Applying the Level-of-Service Concept to Climbing Lanes. In *Transportation Research Record 806*, TRB, National Research Council, Washington, D.C., 1981.
6. K. M. Wolluter. *Geometric Design of Rural Roads*. Technical Recommendations for Highways 17. National Institute for Transport and Road Research, CSIR, Pretoria, South Africa, 1985.
7. *Geometric Design Standards for Canadian Roads and Streets*. Roads and Transportation Association of Canada, Ottawa, Ontario, 1976.
8. *Botswana Road Design Manual*. Botswana Ministry of Works, Gaborone, 1982.
9. *Transportation and Traffic Engineering Handbook*. Institute of Transportation Engineers; Prentice-Hall, N.J. 1976.
10. *Special Report 209: Highway Capacity Manual*. TRB, National Research Council, Washington, D.C., 1985.
11. *Guide to the Geometric Design of Rural Roads*. National Association of Australian State Road Authorities, Canberra, 1985.

---

*Publication of this paper sponsored by Committee on Geometric Design.*

# Possible Design Procedure To Promote Design Consistency in Highway Geometric Design on Two-Lane Rural Roads

RUEDIGER LAMM, ELIAS M. CHOUERI, JOHN C. HAYWARD, AND ANAND PALURI

European design guidelines explicitly address horizontal design consistency for two-lane, rural roads in an attempt to promote smooth operating speed profiles and, in turn, safe operation. U.S. practice qualitatively advocates consistent alignment but provides little objective guidance to assure that consistency is achieved. This paper presents a procedure for measuring the consistency of horizontal design as defined by operating speed and accidents expected. Operating speeds and accident rates can be predicted for various lane widths based on degree of curve and posted recommended speeds, as derived from measurement of 261 sites in New York state. Guidelines for changes in operating speeds and acceptable accident rates for good, fair, and poor designs are suggested, and various nomographs are developed to evaluate roadway sections based on design parameters. In addition, an example application is provided to illustrate the case of fair design practices. It is concluded that such a procedure could readily be adapted by the design community in prescribing improvements to existing facilities or in fine tuning new highway design.

Abrupt changes in operating speed because of horizontal alignment are a leading cause of accidents on two-lane, rural roads, according to many experts (1-6). State and Federal agencies spend approximately 2 billion dollars annually to resurface, restore, and rehabilitate these roadways, exclusive of major reconstruction required to refine roadway geometrics (7). It seems that in an improvement program of this magnitude a convenient method for locating alignment inconsistencies, which may cause abrupt operating speed changes, would be beneficial. Such a mechanism would enable the engineering agency to provide cost-effective horizontal alignment modifications consistent with the resurfacing, restoration, and rehabilitation (RRR) program and thereby enhance traffic safety on two-lane, rural highways. An objective method of identifying hazardous elements that require abrupt operating speed changes would enable the agency to make geometric revisions at the same time that other deficiencies are being remedied.

## REVIEW

An international review of existing design guidelines (8-14) has shown that European countries directly or indirectly address

R. Lamm, and A. Paluri, Clarkson University, Potsdam, N.Y. 13676. E. M. Choueiri, N. Country Community College, Saranac Lake, N.Y. 12982. J. C. Hayward, Michael Baker Jr., Inc., Beaver, Pa. 15009.

three design issues in their guidelines much more explicitly than U.S. agencies (2, 15-19). French, German, Swedish, and Swiss designers are provided with geometric criteria which direct them toward—

- achieving consistency in horizontal alignment,
- harmonizing design speed and operating speed, and
- providing adequate driving dynamic safety.

The objective of this research was to explore whether these guidelines could be adopted for U.S. practice in new design, major reconstruction, and, especially, RRR projects.

Prior studies by the authors (15-21) were relied on to develop the proposed methodology. Research that evaluated the impact of design parameters (degree of curve, length of curve, super-elevation rate, lane width, shoulder width, sight distance, gradient, and posted recommended speed) and traffic volume on 261 two-lane, rural highway sections in New York state demonstrated that the most successful parameters in explaining the variability in operating speeds and accident rates were degree of curve and posted recommended speed limits. The relationship of operating speed and degree of curve is quantified by the following regression model (15-18) between operating speed and various design and traffic volume parameters:

$$V_{85} = 34.700 - 1.005DC + 2.081LW + 0.174SW + 0.0004AADT \quad R^2 = 0.842$$

$$SEE = 2.814$$

where

$V_{85}$  = Estimate of operating speed, expressed by the 85th-percentile speed (mph) of passenger cars under free-flow conditions,

$DC$  = Degree of curve (deg./100 ft.) (range: 0° to 27° for investigations on operating speeds, and 1° to 27° for investigations on accident rates, since the accident situation on tangents is clearly affected by variables other than those on curves),

$LW$  = Lane width (ft.),

$SW$  = Shoulder width (ft.),

$AADT$  = Average Annual Daily Traffic [range: 400 to 5,000 vehicles per day (vpd)],

$R^2$  = Coefficient of determination, and

$SEE$  = Standard error of estimate (mph).

The independent variables in the above equation were selected by the step-wise regression technique in the order: *DC*, *LW*, *AADT*, and *SW*. For instance, *DC* had the highest correlation with the dependent variable (*V85*); thus, it was the first variable included in the equation, and so forth.

Design parameters, sight distance, length of curve, and gradient (up to 5 percent) were not included in the regression model because the regression coefficients associated with these parameters were not significantly different from zero at the 95 percent level of confidence. Superelevation rate and posted recommended speed were withheld from the regression analysis because they are highly correlated with degree of curve.

However, in comparing the above equation with the following equation, which only includes the design parameter degree of curve, note from the coefficients of determination ( $R^2$ ) that the influence of *LW*, *SW* and *AADT* in the above equation explains only an additional of about 5.5 percent of the variation in the expected operating speeds.

$$V85 = 58.656 - 1.135 DC \quad R^2 = 0.787 \quad (1)$$

$$SEE = 3.259$$

Note that this regression equation has an  $R^2$  value of 0.787 and its standard error for estimating the observed operating speed is 3.259 mph. It is clear including the additional design and traffic volume parameters adds little to the predictive capability of the model.

Similar relationships were established between operating speeds and posted recommended speeds, and accident rates and degrees of curve; table 1 shows some of the results. Note that (1) the models are valid for road sections with grades up to 5 percent, and low and intermediate traffic volumes (between 400 and 5,000 vpd); and (2) a cross-validation of the models on a new sample of 61 rural, two-lane, curved sections determined that they can be used, with a marked degree of confidence, for prediction purposes. It is likely that grades over 5 percent and *AADT* volumes greater than 5,000 vpd will measurably influence operating speeds and accident rates on two-lane, rural highways; however, because of a lack of data (less than 20 percent of the two-lane, rural highway network in New York is made up of sections where grades are greater than 5 percent and traffic volume exceeds 5,000 vehicles per day), these effects were not analyzed.

TABLE 1 PREDICTIVE REGRESSION EQUATIONS OF OPERATING SPEEDS AND ACCIDENT RATES FOR DIFFERENT LANE WIDTHS (16-18)

All lanes

$$V85 = 58.656 - 1.135DC; R^2 = 0.787 \quad (1)$$

$$V85 = 25.314 + 0.554RS; R^2 = 0.719 \quad (2)$$

$$ACCR = -0.880 + 1.410DC; R^2 = 0.434 \quad (3)$$

10-ft lanes

$$V85 = 55.646 - 1.019DC; R^2 = 0.753 \quad (1a)$$

$$V85 = 27.173 + 0.459RS; R^2 = 0.556 \quad (2a)$$

$$ACCR = -1.023 + 1.513DC; R^2 = 0.300 \quad (3a)$$

11-ft lanes

$$V85 = 58.310 - 1.052DC; R^2 = 0.746 \quad (1b)$$

$$V85 = 29.190 + 0.479RS; R^2 = 0.744 \quad (2b)$$

$$ACCR = -0.257 + 1.375DC; R^2 = 0.462 \quad (3b)$$

12-ft lanes

$$V85 = 59.746 - 0.998DC; R^2 = 0.824 \quad (1c)$$

$$V85 = 26.544 + 0.562RS; R^2 = 0.835 \quad (2c)$$

$$ACCR = -0.546 + 1.075DC; R^2 = 0.726 \quad (3c)$$

where

*V85* = Estimate of the operating speed, expressed by the 85th-percentile speed for passenger cars (mph),

*DC* = Degree of curve (degree/100 ft), range: 0° to 27°,

$R^2$  = Coefficient of determination,

*ACCR* = Estimate of accident rate for all vehicle types (acc./10<sup>6</sup> vehicle-miles), range: 1° to 27°,

*RS* = Posted recommended speed in the curve or curved section (mph).

TABLE 2 T-TEST RESULTS OF ACCIDENT RATES FOR DIFFERENT DEGREE OF CURVE CLASSES (16-18)

Degree of Curve Classes	Mean Accident Rate	t calc.	t crit.	Significance	Remarks
tangent (0°)	1.87	4.00	> 1.96	Yes	Considered as
1° - 5°	3.66	7.03	> 1.96	Yes	---- Good Design
> 5° - 10°	8.05	6.06	> 1.99	Yes	---- Fair Design
> 10° - 15°	17.55	3.44	> 1.99	Yes	---- Poor Design
> 15° - 26.9°	26.41				---- Poor Design

In addition, the research studies (15-21) determined that

1. No statistically significant difference exists between operating speeds on dry and wet pavements, as long as visibility is not affected decisively.

2. The gap between operating speeds of passenger cars and trucks increases with increasing degree of curve, but not in a manner that could create critical driving maneuvers on gradients up to 5 percent.

3. Accident rates increase with increasing degree of curve, despite the presence of stringent traffic warning devices at curved sites.

4. Vehicle acceleration and deceleration end or begin about 700 to 750 feet from the end of an observed curved road section.

5. Consistency in horizontal alignment, as reflected by a smooth operating speed profiles, can be achieved by examining the degree of curve.

6. For evaluating horizontal design consistency or inconsistency, the following changes in degrees of curve and their subsequent impact on changes in operating speeds, based largely on mean accident rates (see table 2), provide a reasonable (and quantifiable) classification system for differentiating good design and poor design:

*Case 1 (good design):*

Range of change in degree of curve:  $\Delta DC \leq 5^\circ$ .

Range of change in operating speed:  $\Delta V_{85} \leq 6$  mph (10 km/h).

For these road sections, consistency in horizontal alignment exists, and the horizontal alignment does not create inconsistencies in vehicle operating speeds.

*Case 2 (fair design):*

Range of change in degree of curve:  $5^\circ < \Delta DC \leq 10^\circ$ .

Range of change in operating speed:  $6 \text{ mph} < \Delta V_{85} \leq 12$  mph (20 km/h).

These road sections have at least minor inconsistencies in geometric design.

*Case 3 (poor design):*

Range of change in degree of curve:  $\Delta DC > 10^\circ$ .

Range of change in operating speed:  $\Delta V_{85} > 12$  mph (20 km/h).

These road sections have strong inconsistencies in horizontal geometric design combined with breaks in the speed profile that may lead to critical driving maneuvers.

As shown in table 2, the results indicate significant increases (at the 95 percent level of confidence) in the mean accident rates among the different degree of curve classes compare. In other words, higher accident rates can be expected with higher degree of curve classes, despite stringent traffic warning devices often installed at the curve sites.

The results of table 2 indicate that gentle curvilinear horizontal alignments consisting of tangents or transition curves combined with curves up to 5° showed the lowest average accident risk. These observations agree well with the findings of some European guidelines (8, 10, 11) and the statements of AASHTO 1984 (14, pp. 248f) concerning "General Controls for Horizontal Alignment."

For horizontal alignments with changes in degrees of curve between 5° and 10° between successive design elements (defined as fair designs), the average accident rate in table 2 is twice as high as for those between 1° and 5°. For changes between 10° and 15° of curve (defined as poor designs), the accident rate is four times the rate associated with degrees of curve between 1° and 5°. For greater changes in degree of curve, the average accident rate is even higher. This confirms that changes in degree of curve between successive design elements that exceed 10° should be interpreted as poor designs while those in the range between 5° and 10° can still be judged as fair designs.

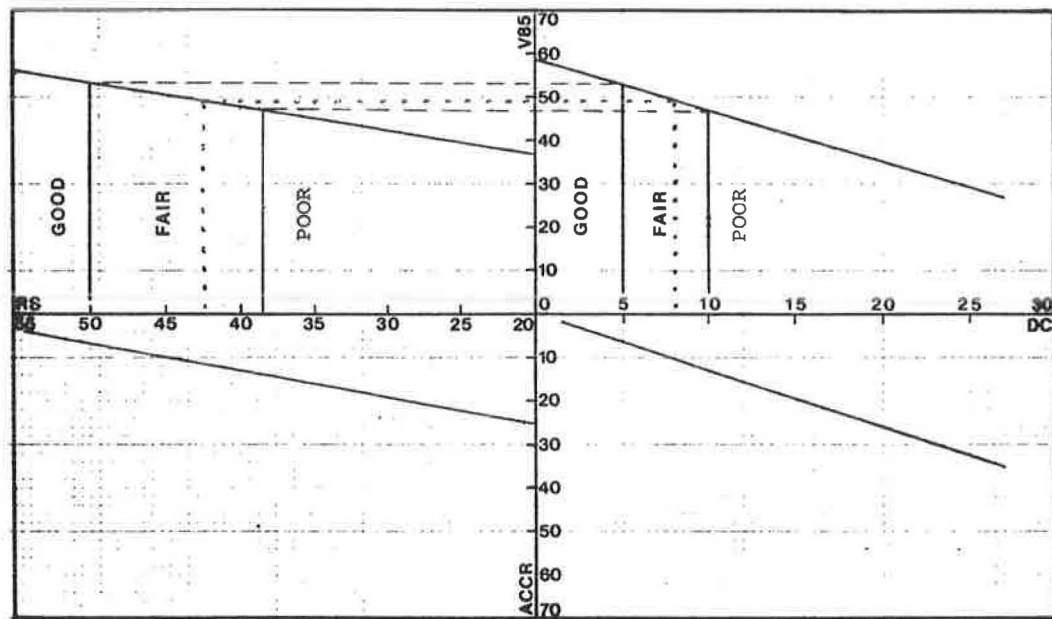
## NOMOGRAMS FOR EVALUATING OPERATING SPEEDS AND ACCIDENT RATES

The regression models for all lanes combined, formulated in table 1, are depicted in figure 1. From the resulting nomogram, the designer is able to roughly predict operating speeds (85th-percentile speeds) and accident rates on curves or curved sections of two-lane, rural highways from beforehand knowledge of the degree-of-curve or posted-recommended-speed parameters.

On the other hand, the regression models for the individual lane widths formulated in table 1 are depicted in figure 2. As the figure shows, operating speeds decrease with increasing degree of curve, for different lane widths, in a nearly parallel manner.

With respect to the relationship "accident rate vs. degree of curve" figures 1 and 2 reveal that accident rates increase





DC = Degree of curve (degree/100 feet),  
 V85 = Estimate of operating speed, expressed by the 85th-percentile speed (mph)  
 (range up to 27°),  
 ACCR = Estimate of accident rate (acc./10<sup>6</sup> vehicle-miles)(range: 1° - 27°),  
 RS = Estimate of recommended speed (mph).

**FIGURE 1** Nomogram for evaluating operating speeds and accident rates in curves or curved sections as related to degree of curve and posted recommended speed for all lane widths (17).

with increasing degree of curve, despite the presence of posted advisory speeds at curved sites (see figure 1). Furthermore, as figure 2 reveals, for degrees of curve  $\leq 5^\circ$ , there appear to be non-significant differences in accident rates between the individual lane widths. For higher degrees of curve, the gap between accident rates on 12-foot and 11/10-foot lanes becomes wider and wider.

For all lanes combined, one can expect, as figure 1 reveals, an accident rate of about six accidents per million vehicle miles (mvm) for a  $5^\circ$  of curve, and an accident rate of about thirteen accidents per mvm for a  $10^\circ$  curve. That means that the accident risk on sections with a change in degree of curve of  $\Delta DC > 10^\circ$ , as compared to sections with a change in degree of curve of  $\Delta DC > 5^\circ$  is at least twice as high. For higher degrees of curve, these comparisons are even more unfavorable. Similar results are obvious from figure 2, too, when comparing the accident rates for individual lane widths. Note that the differences between 12-foot and 11-foot lane widths are, more or less, more pronounced than those between 11-foot and 10-foot lane widths.

These relationships between roadway geometry, operating speeds and accidents in conjunction with the classification system form the basis for a design methodology. From geometric definition, the designer may predict operating speeds. Wide variations in operating speeds are shown to be further indicators of accidents. Reasonable judgments can then be applied to discriminate good, fair, and poor design on the basis of safety indicators but using only design information.

### TUNING OF RADII-SEQUENCES

For an easy illustration of the following design procedure, the recommended boundaries for good, fair, and poor designs, as related to degree of curve, were converted to radii of curve. For instance, figure 3 shows the tuning of radii-sequences for succeeding curves, in the same or in the opposite direction, for different design cases. As figure 3 demonstrates, a radius of  $R = 500$  feet can be combined, for example, in the case of—

- good designs: with a range of radii between  $\sim 350 < 500 < 900$  feet and
- fair designs: with a range of radii between  $\sim 270 < 500 < 3,500$  feet.

Regarding a sequence tangent-to-curve, the boundaries of good designs ( $DC \leq 5^\circ$ ) correspond to radii of curve ( $R \geq 1,200$  ft); thus, curves with radii  $R \geq 1,200$  feet should follow an "Independent Tangent" in order to not create inconsistencies in vehicle operating speeds. The boundaries of fair designs ( $5^\circ < DC \leq 10^\circ$ ) correspond to radii of curve ( $1,200 \text{ ft} > R \geq 600 \text{ ft}$ ); radii within this range should follow an "Independent Tangent" in the sequence tangent-to-curve for fair design practices. These values agree well with the minimum radii for design speeds of 60 mph (good design) and of about 45 mph (fair design) for a superelevation rate of 8 percent in table III-6 (14).

By applying figure 3, the designer could immediately decide

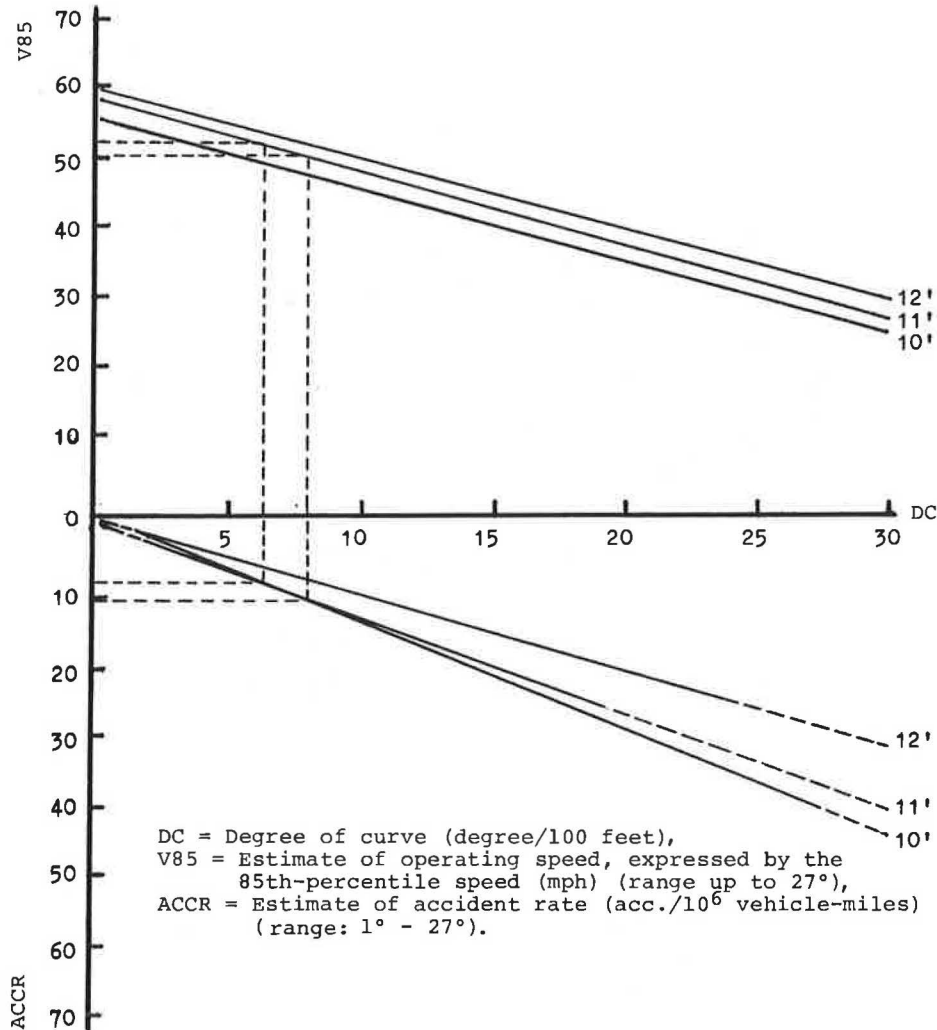


FIGURE 2 Nomogram for evaluating operating speeds and accident rates as related to degree of curve for individual lane widths.

whether or not certain radii of succeeding curves fall into the range of good, fair or poor design practices. For example, combining a radius of 1,000 feet—

- with 300-foot radius would be a poor design,
- with a 500-foot radius would be a fair design, and
- with a 700-foot radius would be a good design.

### EVALUATION OF TANGENTS IN THE DESIGN PROCESS

Lamm et al. (companion paper in this Record) have established boundaries for tangent-lengths that are to be regarded as “independent” or “non-independent” design elements. For independent tangents, the sequence “tangent-to-curve” controls the design process, while for non-independent tangents, it is the sequence “curve-to-curve” that controls the design process.

Table 3 shows maximum allowable lengths of tangents that are regarded as non-independent design elements. The values with an asterisk represent lengths of tangents on which 85th-

percentile speeds of 58 mph can be reached, as determined by Lamm et al. in a companion paper in this Record.

When dealing with tangent lengths, the following three cases must be distinguished.

#### Case 1

The existing tangent length is smaller than the maximum allowable one in table 3 that corresponds to the nearest 85th-percentile speed of the curve with the higher degree of curve. From this it follows that the tangent is to be regarded as non-independent (companion paper in this Record by Lamm et al.). Changes in degree of curve and operating speeds must be related to any two successive curves since the tangent in-between can be assumed to be negligible in the design process; that is, the sequence curve-to-curve controls the design process in this case.

#### Case 2

The existing tangent length is at least twice as long as the values listed in the last column of table 3, again related to the

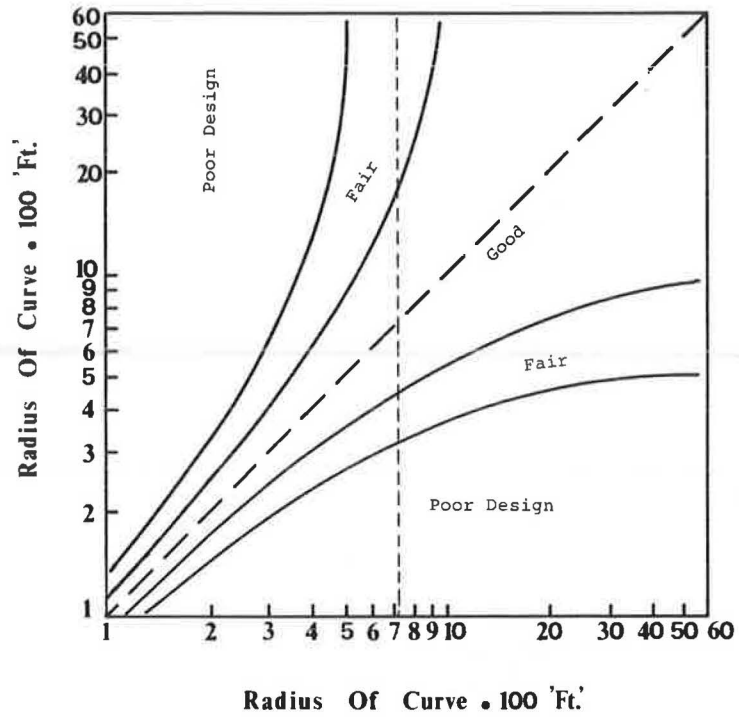


FIGURE 3 Tuning of radii-sequences of succeeding curves for good and fair design practices.

TABLE 3 RELATIONSHIP BETWEEN TANGENT LENGTHS AND 85TH-PERCENTILE SPEED CHANGES FOR SEQUENCES: TANGENTS TO CURVES

V85 in Curve	V85 in Tangent				
	34	40	46	52	58
22	250	425	625	850	1100*
28		325	500	725	1000*
34			375	600	850*
40				425	675*
>46					475*

Maximum allowable Lengths of Tangents, regarded as "Non-Independent Design Elements", (ft)

V85 = 85th-Percentile speed in curve or tangent (mph)

\* For these values the highest operating speed in tangents V85 = 58 mph can be expected.

nearest 85th-percentile speed of the curve with the higher degree of curve. In this case, it can be assumed, without any calculations, that the tangent is independent (Lamm et al.), and that operating speeds of 56 to 60 mph are good estimates, depending on the individual lane widths (see equations (1a) through (1c) of table 1). In other words, the sequence tangent-to-curve controls the design process.

### Case 3

The existing tangent length lies somewhere between Case 1 and Case 2. The operating speed in the independent tangent can be estimated from figure 4 and equations (2) through (4), as derived by Lamm et al.; in other words, the sequence tangent-to-curve controls the design process for both directions of travel.

## PROCESS FOR EVALUATING HORIZONTAL DESIGN CONSISTENCY WITH EXAMPLE APPLICATIONS

Primarily at lower design speeds, the changing alignment may cause variations in operating speeds, which may, in turn, increase the accident risk by substantial amounts. Therefore, one of the important tasks in modern rehabilitation of the two-lane, rural road network in the United States is to ensure design consistency and to detect critical inconsistencies in horizontal alignment, especially with regard to RRR projects.

In what follows, the various steps of the design procedure are presented:

(a) Assess the road section where new designs, major reconstructions, or redesigns, such as in the case of RRR projects, may be considered.

(b) Determine for this road section the degree of curve of each curve within the section and the existing tangent length.

(c) Determine the expected 85th-percentile speed for each curve, in accordance with degree of curve, by applying figure 1 for a rough estimate or figure 2 for a more accurate estimate depending on the lane width. Compare equations (1a) through (1c) also.

(d) Conclude whether or not each tangent is an independent design element. For independent tangents, the tangent-to-curve sequence is of prime importance in the design process. For non-independent tangents, it is the sequence curve-to-curve. For independent tangents, determine the corresponding operating speeds according to Case 2 or Case 3 of the previous section.

(e) In accordance with the results of step (c) and step (d), calculate the change in degree of curve ( $\Delta DC$ ), and the change in operating speeds ( $\Delta V_{85}$ ) for the independent tangent-to-curve or curve-to-curve sequence.

### Good Design Practices

( $f_1$ ) Determine all road sections where changes in degree of curve and changes in operating speeds correspond to the boundaries of good design practices:

Range of change in degree of curve:  $\Delta DC \leq 5^\circ$ .

Range of change in operating speed:  $\Delta V_{85} \leq 6$  mph (10 km/h).

### Result

For these road sections, consistency in horizontal alignment exists and the horizontal alignment does not adversely detract from the expected operating speed profiles. Thus, RRR improvements can be made in most cases without considering traffic warning devices or horizontal alignment redesign. The majority of existing state routes in the United States exhibit these characteristics.

### Note

The radii of successive curves should fall into the range of good design practices as shown in figure 3. For a tangent-to-curve sequence, at least curves with radii ( $R \geq 1,200$  ft) should follow an independent tangent.

Rough estimates of expected accident rates may be made possible from figures 1 and 2 or equations (3a) through (3c) in table 1, depending on the lane width.

### Fair Design Practices

( $f_2$ ) Determine all road sections where changes in degree of curve and changes in operating speeds correspond to the boundaries of fair design practices:

Range of change in degree of curve:  $5^\circ < \Delta DC \leq 10^\circ$ .

Range of change in operating speed:  $6 \text{ mph} \leq \Delta V_{85} \leq 12$  mph.

### Result

These road sections exhibit at least minor inconsistencies in geometric design. Normally, correcting the existing alignment is not necessary since low cost projects such as traffic warning devices may, to a certain extent, be successful in correcting these defects. For instance, RRR improvements can be installed which consider appropriate recommended speeds (see figure 1), unless a safety problem has been documented. One should note that despite traffic warning devices, road sections with changes in degree of curve that fall into the range ( $5^\circ$  to  $10^\circ$ ) have average accident rates that are about twice as high as those falling into the range of good design (see table 2).

### Note

The radii of successive curves should fall into the range of fair design practices, as shown in figure 3. For a tangent-to-curve sequence at least curves with radii ( $1,200 \text{ ft} > R \geq 600$  ft), equipped with posted recommended speeds (see figure 1) and arrow designations, should follow an independent tangent.

Rough estimates of expected accident rates may be made from figures 1 and 2 or equations (3a) through (3c) in table 1, depending on the lane width.

To achieve a high level of driving safety, superelevation rates and stopping-sight distances should be related to the expected operating speeds wherever possible.

**Example Related to Figure 5**

*Step (a)*

State of New York,  
County No. 3604,  
Route Number SR34 (mile markers 3094–3115),  
Lane Width 11 feet.

*Step (b)*

Section	Design Element	Degree of	
		Curve	Length
A–B	Tangent	0	0.2 mi ~ 1,060 ft
B–C	Curve	6.4	0.2 mi ~ 1,060 ft
C–D	Tangent	0	0.1 mi ~ 530 ft
D–E	Curve	8.0	0.1 mi ~ 530 ft
E–F	Tangent	0	1.5 mi ~ 7,920 ft

*Step (c)*

Expected 85th-Percentile Speed	From Figure or Equation	Measured 85th-Percentile Speed
Curve BC	52 mph	Figure 2 or Eqn. (1b)
Curve DE	50 mph	53 mph

*Step (d)*

**Tangent AB (1,060 feet)** In accordance with Case 2, see the section on “Evaluation of Tangents.” The expected operating speed in the following curve is 52 mph; the nearest value in table 3 is 46 mph; two times the value of the last column of table 3 is 950 feet < 1060 feet. That means that tangent AB is independent. It follows that  $V_{85} = 58$  mph, according to figure 2 or equation (1b) for a lane width of 11 feet.

**Tangent CD (530 feet)** In accordance with Case 3, see the section on “Evaluation of Tangents.” The expected operating speed in the curve with the higher degree of curve is 50 mph; the nearest value in table 3 is 46 mph; the maximum length of tangent regarded as non-independent is 475 feet < 530 feet. That means that tangent CD is independent. Thus, the operating speed in the tangent can be estimated, according to Figure 4 (from the companion paper in this Record), as follows:

$$X = \frac{(52 + 50) \cdot (52 - 50)}{2 \cdot 1.302} \approx 80 \text{ ft} \quad (2)$$

$$TL - X = 530 - 80 = 450 \text{ ft}$$

$$\Delta V_{85T} = \frac{-2 \cdot (52) \pm \sqrt{4 \cdot (52)^2 + 5.208 \cdot (450)}}{2} \quad (3)$$

This implies the operating speed in Tangent CD is

$$V_{85T} = 52 + 5 = 57 \text{ mph} \quad (4)$$

**Tangent EF (7,920 feet)** Independent,  $V_{85} = 58$  mph.

*Step (e)*

Sequence	Change in Degree of Curve $\Delta DC$	Change in Operating Speed $\Delta V_{85}$
Tangent AB to Curve BC	$ 0-6.4  = 6.4$	$ 58-52  = 6$ mph
Curve BC to Tangent CD	$ 6.4-0  = 6.4$	$ 52-57  = 5$ mph
Tangent CD to Curve DE	$ 0-8.0  = 8.0$	$ 57-50  = 7$ mph
Curve DE to Tangent EF	$ 8.0-0  = 8.0$	$ 50-58  = 8$ mph

*Step (f<sub>2</sub>)*

For the existing alignment of figure 5, step (e) reveals that changes in degree of curve, and changes in operating speeds between tangent AB and curve BC in the direction AF, between tangent CD and curve DE in the direction AF, and between tangent EF and curve DE in the direction FA fall into the range of fair design.

Note that the degrees of curve of 6.4° and 8.0° correspond to radii of 900 feet and 720 feet. Since these radii lie between 600 feet and 1,200 feet, curve BC and curve DE, combined with independent tangents, fall into the range of fair design. This can be determined from figure 3, too, when radii of 720 feet and 900 feet are combined with a tangent ( $R$  is greater than or equal to 6,000 feet), according to the scale. The existing recommended speed of 45 mph combined with arrow designations, see figure 5, agrees well with the value of about 45 mph that can be determined from figure 1 for curve DE with a degree of curve of 8°. The expected accident rate can be determined from figure 2 or calculated from equation (3b). The observed accident rate was calculated from the following equation:

$$ACCR = \frac{(\text{No. Acc.}) \cdot (10^6)}{(365) \cdot (\text{No. Years}) \cdot (L) \cdot (AADT)} \quad (5)$$

where

$ACCR$  = number of accidents per 1 million vehicle miles,

No. Acc. = number of accidents per years investigated,

No. Years = number of years investigated,

$L$  = length of curve or curved section in miles, and

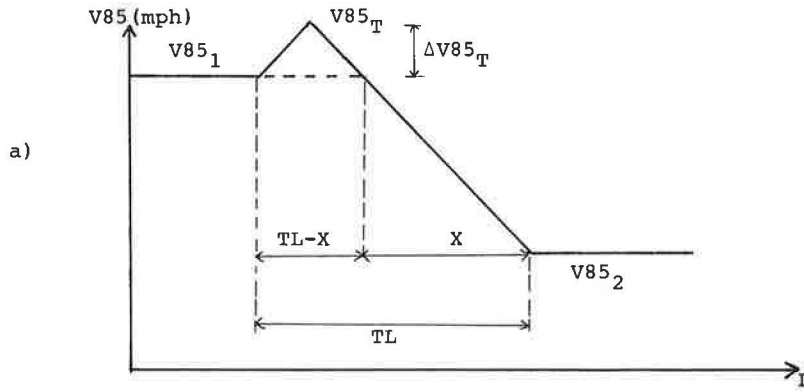
$AADT$  = Average Annual Daily Traffic (vehicles in both directions).

This implies that

	Expected Accident Rate	Observed Accident Rate
Curve BC	8.5	6.9
Curve DE	10.7	9.1

The expected accident rates agree, relatively well, with the observed ones and the mean accident rate for fair design of table 2.

Thus, one can conclude that the horizontal alignment of figure 5 corresponds to fair design practices and does not necessarily need improvements in geometric design. But it should not be forgotten that at least minor inconsistencies in



Legend:

TL = Tangent length, greater than the maximum allowable lengths for "Non-Independent Tangents" of Table 3 (ft),

X = Acceleration or deceleration distance between curve 1 and curve 2 (ft),

V85<sub>1</sub>, V85<sub>2</sub> = Operating speeds in curves (mph),

V85<sub>T</sub> = Operation speed in tangent (mph),

ΔV85<sub>T</sub> = Difference between the operating speed in the curve with the lower degree of curve and the operating speed in the tangent (mph).

$$X = \frac{(V85_1 + V85_2) \cdot (V85_1 - V85_2)}{2.604} \quad (4)$$

$$V85_T^* = V85_1 + \Delta V85_T \quad (5)$$

$$\Delta V85_T = \frac{-2 \cdot (V85_1) \pm \sqrt{4(V85_1)^2 + 5.208(TL-X)}}{2} \quad (6)$$

\* Note that for determining V85<sub>T</sub> always the operating speed of the curve with the lower degree of curve has to be selected.

FIGURE 4 Example for estimating the operating speed in an independent tangent.

horizontal alignment do exist. For instance, despite the presence of traffic warning devices (recommended speeds of 45 mph and arrow signs), the accident rates on the observed curved sites are about twice as high as the mean accident rate for good design, as shown in table 2.

To achieve a high level of driving dynamic safety, it is recommended to increase the existing superelevation rates from six percent to nine percent during the next resurfacing project, as shown for curve DE by the following calculation:

$$e_{max} = \frac{DC \cdot V85^2}{85,660} - f_R$$

$$e_{max} = \frac{8 \cdot 50^2}{85,660} - 0.14 = 0.09$$

where  $f_R$  = side friction factor obtained from table III-6 (14);  $f_R = 0.14$  (estimated for an operating speed of 50 mph).

Similar calculations have to be performed if stopping sight distances are insufficient.

### Poor Design Practices

(f3) Determine all road sections where changes in degree of curve and changes in operating speeds correspond to the boundaries of poor design practices:

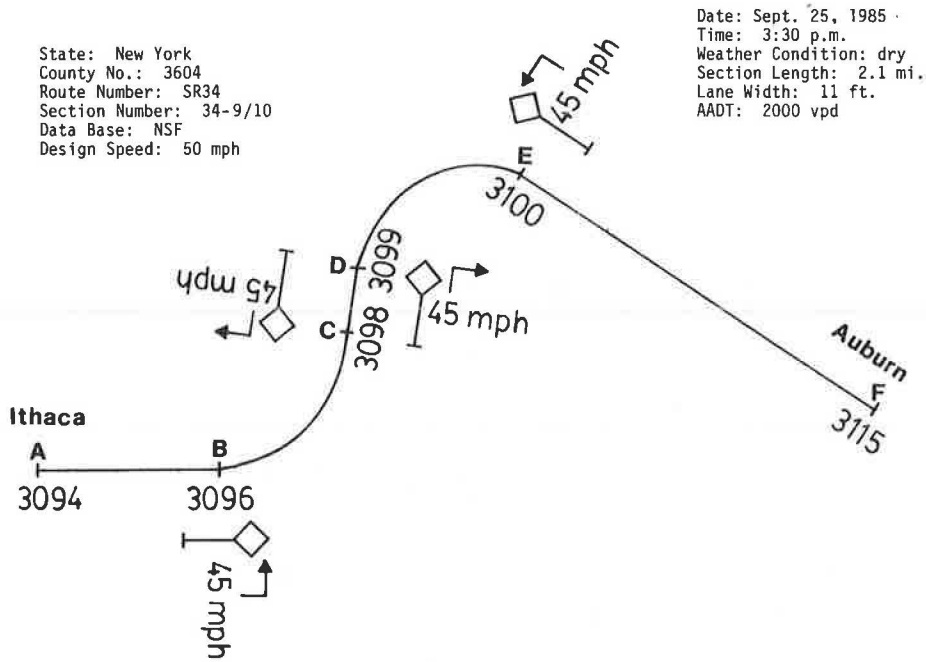
Range of change in degree of curve:  $\Delta DC > 10^\circ$ .

Range of change in operating speed:  $\Delta V85 > 12$  mph (20 km/h).

### Result

These road sections represent strong inconsistencies in horizontal geometric design, combined with those breaks in the speed profile that may lead to critical driving maneuvers.

Despite stringent recommended speeds combined with arrow designations and chevrons (see figure 1), road sections with changes in degree of curve that fall into this range (10° to 15°) have about four times an average accident rate as those that



	Curve BC	Curve DE
Degree of Curve	6.4°	8.0°
Superelevation Rate	6%	6%
Measured 85th-percentile Speed* (Average for both directions)	--	53 mph
Stopping Sight Distance	0.1 mi.	0.1 mi.
Grade	0%	±0.5%
Recommended Speed	45 mph (Arrow Signs)	45 mph (Arrow Signs)
Number of Accidents**	3	2

\* Not required for the design procedure, here only presented for comparison reasons.  
 \*\* For an investigated period of three years (Jan. 1982 to Dec. 1984).

FIGURE 5 Case study of State Route 34 in the State of New York.

fall into the range of good design, and about twice as high as those that fall into the range of fair design (see table 2). Normally, for example, for RRR projects, high cost projects such as redesigns of at least hazardous road sections should be recommended, unless there was no documented safety problem.

Note

- Ranges of radii of successive curves that would represent poor design practices are shown in figure 3. For a tangent-to-curve sequence, curves with radii ( $R < 600$  feet) should not be allowed to follow an independent tangent.
- Rough estimates of expected accident rates may be made possible from figures 1 and 2 or equations (3a) through (3c) in table 1, depending on the lane width.

PROCESS FOR EVALUATING DESIGN SPEED AND OPERATING SPEED DIFFERENCES

All reviewed highway geometric design guidelines (8-14) indicate that the design speed should be constant along longer roadway sections. Furthermore, the design speed ( $V_d$ ) and

the 85th-percentile speed ( $V_{85}$ ) must be well balanced to insure a fine tuning between road characteristic, driving behavior, and driving dynamics. Experiences (1, 5, 6) have shown that the design speed is sometimes lower than driver expectations and judgement of what the logical speed should be, especially on independent tangents. Therefore, harmonizing design speed and operating speed is another important goal that should be considered in rehabilitation of two-lane, rural highways.

To achieve this goal, it is recommended that the designer refer to step (c) and step (d) of the previous section and determine the expected 85th-percentile speed of every independent tangent or curve in the observed road section.

The 85th-percentile speed ( $V_{85}$ ) of every independent tangent, curve, or curved section must be tuned with the existing or selected design speed ( $V_d$ ) in the following manner:

1.  $V_{85} - V_d \leq 6$  mph (10 km/h) (good designs); no adaptations or corrections are necessary.
2.  $6 \text{ mph} < V_{85} - V_d \leq 12$  mph (fair design); superelevation rates in curves or curved sections and stopping sight distances must be related to the expected 85th-percentile speed. Thus, it is inferred that the driving dynamic safety demand will not exceed the driving dynamic safety supply under wet pavement conditions, compare step ( $f_2$ ).
3.  $V_{85} - V_d > 12$  mph (20 km/h) (poor design). The 85th-

percentile speed should not be allowed to exceed the design speed by more than 12 mph (20 km/h). If such a difference occurs, normally the design speed should be increased. For example, redesigns of hazardous road sections are recommended, unless there was no documented safety problem.

With regard to a well-balanced design one should strive for a uniform design speed within an observed road section of substantial length, especially between independent tangents and curves. This conclusion is well expressed in the AASHTO Design Guide (14), as follows:

In horizontal alignment, predicted on a given design speed, consistent alignment always should be sought. Sharp curves should not be introduced at the end of long tangents. Sudden changes from areas of flat curvature to areas of sharp curvature should be avoided. Where sharp curvature must be introduced it should be approached, where possible, by successively sharper curves from the generally flat curvature.

This can be done by applying the ranges of good designs, or, if necessary, of fair designs in figure 3.

In an example related to figure 5, where the design speed is 50 mph,

Design Speed: 50 mph

Section	$V_{85} - V_d$ (mph)	$\Delta V$ (mph)
Tangent AB	58 - 50	8
Curve BC	52 - 50	2
Tangent CD	57 - 50	7
Curve DE	50 - 50	0
Tangent EF	58 - 50	8

The results are inconsistent. At least for three design elements the differences between operating speeds and design speeds correspond to fair design practices  $6 \text{ mph} < V_{85} - V_d \leq 12 \text{ mph}$ . That means that minor inconsistencies in horizontal alignment do exist. However, correcting the existing alignment is not necessary since a documented safety problem related to fair designs does not exist (compare step ( $f_2$ )). Superelevation rates on curves have to be adjusted to the expected operating speeds to achieve a high level of driving dynamic safety, as it was shown in step ( $f_2$ ).

## CONCLUSION

By applying this procedure, the highway engineer can easily control good and fair designs and can detect poor horizontal designs during RRR project planning. The procedure has been illustrated using existing alignments to verify its validity, but such a technique could be applied as well for new designs, major reconstructions, or redesigns. From knowledge of degree of curve of each curve, and the existing transition length (length of transition curves or length of tangent) between two curves, the highway engineer can evaluate the horizontal alignment during the design stages according to the discussed design procedure.

For example, where the design analysis reveals road sections of fair or even poor designs, these sections can be corrected by changing the design element sequences in question. Such changes may be an independent tangent-to-curve sequence, or a curve-to-curve sequence, according to design-

element sequences for good design practices shown in figure 3.

The impact of tuning the alignment in this way would result, in general, in more curvilinear alignments. Furthermore, the designer can predict expected operating speeds and accident rates on curved sections by applying the nomograms of figures 1 and 2. However, because of the low coefficients of determination for the accident rate related regression equations, caution should be exercised when using the equations for prediction purposes. In addition, the designer can predict appropriate recommended speeds by using figure 1 in cases where fair designs have to be maintained, or even newly introduced, such as when poor designs can only be improved to fair designs because of terrain or other constraints.

Finally, the design speed concept can be applied in the future in a more appropriate way by harmonizing design speeds and expected operating speeds for the selected design element sequences, already during the design stages.

It is felt that routine use of a procedure such as this by design agencies could lead to more cost effective and safe geometry for new designs, major reconstruction, and, especially, RRR projects. It is hoped that such procedures will be adopted and will ultimately become a part of national and state guidelines.

Note, the prediction equations formulated and cross-validated in this study are based on data from a limited geographic area of the state of New York and may only be appropriate for investigations within that state or region. Some caution should be exercised in extrapolating the design procedure to other areas with differing laws, law enforcement, driver behavior, terrain, weather, and traffic control devices. The models are quite possibly applicable in wider areas (and that is certainly desirable), but testing will be required to determine their suitability in other geographical areas.

## ACKNOWLEDGMENT

This study was sponsored by the New York State Governor's Traffic Safety Committee, Albany, New York and by the National Science Foundation. The senior author wishes to thank the members of the TRB Geometric Design Committee for their encouragement and their valuable discussions while the research on consistency of highway geometric design was being conducted. Special thanks go to Prem Goyal for his assistance in preparing the example applications.

## REFERENCES

References with an asterisk (\*) have been translated from their original language into English for easy reference in the United States. The authors apologize for any inaccuracies that may have resulted as a consequence of the process of translation.

1. J. E. Leisch and J. P. Leisch. New Concepts in Design Speed Application. In *Transportation Research Record 631*, TRB, National Research Council, Wash., D.C., 1977.
2. J. Hayward, R. Lamm, and A. Lyng. *Survey of Current Geometric and Pavement Design Practices in Europe: Geometric Design*. International Road Federation, July, 1985.
3. E. U. Hiersche, R. Lamm, K. Dieterle, and A. Nikpour.



- Effects of Highway Improvement Measures Designed in Conformity with the RAL-L on Traffic Safety on Two-Lane Highways. *Forschung Strassenbau und Strassenverkehrstechnik*, Vol. 431, 1984.
4. J. C. Hayward. Highway Alignment and Superelevation: Some Design-Speed Misconceptions. In *Transportation Research Report 757*, TRB, National Research Council, Wash., D.C., 1980.
  5. G. Kocppel and H. Bock. Operating Speed as a Function of Curvature Change Rate. *Forschung Strassenbau und Strassenverkehrstechnik*, Vol. 269, 1979.
  6. R. Lamm. *Driving Dynamics and Design Characteristics—A Contribution for Highway Design under Special Consideration of Operating Speeds*. Publications of the Institute of Highway and Railroad Design and Construction, University of Karlsruhe, Vol. 11, Federal Republic of Germany, 1973.
  7. J. A. Cirillo. Safety Aspects of RRR Projects. *Public Roads*, Vol. 48, No. 3, 1984, pp. 103–107.
  8. *Guidelines for the Design of Roads (RAS-L-1)*. German Road and Transportation Research Association, Committee 2.3, Geometric Design Standards, Edition 1984.
  9. R. Lamm and J. Cargin. Translation of the *Guidelines for the Design of Roads (RAS-L-1)*. Federal Republic of Germany, and the Swiss Norm SN 640080a, *Highway Design, Fundamentals, Speed as a Design Element*, 1981, as discussed by K. Dietrich, M. Rotach, and E. Boppert, in *Road Design*, ETH Zuerich, Institute for Traffic Planning and Transport and Technique, Edition 1983, prepared at Clarkson University for the Safety and Design Division, Federal Highway Administration, U.S. Department of Transportation, May 1985.
  10. *Highway Design, Fundamentals, Speed as a Design Element*. Swiss Association of Road Specialists (VSS), Swiss Norm SN 640080a, Edition 1981.
  11. *Standard Specifications for Geometric Design of Rural Roads*. National Swedish Road Administration, Sweden, Edition 1982.
  12. *Instruction sur les Conditions Techniques D'Aménagement de Routes Nationales*. Ministère de l'Équipement et du Logement, France, Edition 1975.
  13. *Highway Link Design, Geometric Alignment Standards*. Departmental Standard TD9/81, Department of Transport, Great Britain, 1981.
  14. *A Policy on Geometric Design of Highways and Streets*. AASHTO, Washington, D.C., 1984.
  15. R. Lamm and E. M. Choueiri. Recommendations for Evaluating Horizontal Design Consistency Based on Investigations in the State of New York. In *Transportation Research Record 1122*, TRB, National Research Council, Washington, D.C., 1987.
  16. E. M. Choueiri. *Statistical Analysis of Operating Speeds and Accident Rates on Two-Lane Rural State Routes*. Ph.D. Dissertation, Clarkson University, January 1987.
  17. R. Lamm and E. M. Choueiri. *A Design Procedure to Determine Critical Dissimilarities in Horizontal Alignment and Enhance Traffic Safety by Appropriate Low-Cost or High-Cost Projects*. Final Report for the National Science Foundation, Washington, D.C., March 1987.
  18. E. M. Choueiri and R. Lamm. *Operating Speeds and Accident Rates on Two-Lane Rural Highway Curved Sections—Investigations about Consistency and Inconsistency in Horizontal Alignment*. Part I of the Research Contract "Rural Roads Speed Inconsistencies Design Methods," State University of New York Research Foundation, Albany, New York, July 1987.
  19. R. Lamm, J. C. Hayward, and J. Cargin. Comparison of Different Procedures for Evaluating Speed Consistency. In *Transportation Research Record 1100*, TRB, National Research Council, Washington, D.C., 1986.
  20. R. Lamm and E. M. Choueiri. Relationship Between Design, Driving Behavior and Accident Risk on Curves. *Proceedings of the Fortieth Annual Ohio Transportation Engineering Conference*, Ohio State University, in Cooperation with the Ohio Department of Transportation, December 1982, pp. 87–100.
  21. R. Lamm and J. Cargin. Identifying Operating Speed Inconsistencies on Two-Lane Rural Roads. *Proceedings of the Thirty-Ninth Annual Ohio Transportation Engineering Conference*, Ohio State University, in Cooperation with the Ohio Department of Transportation, December 1985, pp. 13–22.

---

Publication of this paper sponsored by Committee on Geometric Design.

# Tangent as an Independent Design Element

RUEDIGER LAMM, ELIAS M. CHOUERI, AND JOHN C. HAYWARD

Reviews of design guidelines for rural roads in Germany, France, and Switzerland reveal that highway designers adhere to controls on maximum and minimum lengths of tangents between successive curves. Minimum tangent lengths are prescribed to promote operating speed consistency, and maximum lengths are suggested to combat driver fatigue. Current U.S. practice does not set maximum or minimum lengths of tangents; instead current AASHTO policy favors long tangent sections for passing purposes on two-lane, rural roads. This paper presents a recommended strategy for U.S. highway designers to consider tangent lengths explicitly in rural highway design. The proposed approach uses recommended operating speed differences between successive horizontal geometric elements (curves and tangents) and acceleration or deceleration profiles derived from car-following tests to establish limits. Recommendations are also provided for transition lengths (tangent length) between successive curved roadway sections for (a) tangents that should be regarded as "non-independent" design elements; that is, the sequence "curve-to-curve" is the most important element of the design process and (b) tangents that should be regarded as "independent" design elements; that is, the sequence "tangent-to-curve" is the most important element of the design process.

In the highway geometric design process, tangents and horizontal curves with or without transition curves are regarded as design elements. Most of the reviewed highway geometric design guidelines (1-7) give recommendations for maximum or minimum tangent lengths.

For example, in the Federal Republic of Germany (2, 3) tangent lengths between curves are limited by the design speed. The maximum length in meters of tangent sections between two curves may not exceed twenty times the design speed of that roadway. In this way long tangents are controlled and a curvilinear environment is encouraged.

Minimum tangent lengths must be at least six times the design speed. For a typical design speed of 100 km/h (~60 mph) this would correspond to a maximum tangent length of 2,000 meters (6,500 feet) and a minimum tangent length of 600 meters (2,000 feet).

To avoid driver fatigue, it is recommended in France (6) that tangent sections be limited to a maximum of 40 to 60 percent of long roadway sections with maximum single tangent lengths between 2,000 and 3,000 meters (6,500 to 10,000 feet).

Swiss highway officials (3, 4) also limit tangent lengths to limit driver fatigue. Designs that permit more than one minute

of driving on a straight section are not permitted. Minimum tangent lengths are related to "project speeds," which roughly translate to American practice as "theoretical operating speeds." For example, for a project speed of 100 km/h (~60 mph) a minimum tangent length of 150 meters (500 feet) would be permitted.

In the 1984 AASHTO Policy on Geometric Design of Highways and Streets (1), specific values for maximum or minimum tangent lengths are not specified. But the following statement is listed under General Controls for Horizontal Alignment: "Although the aesthetic qualities of curving alignment are important, passing necessitates long tangents on two-lane highways with passing sight distance on as great a percentage of the length of highway as feasible." This statement clearly supports the application of long tangents, especially for the design of two-lane, rural highways.

The only method developed to evaluate acceleration or deceleration movements between sequences of curve-to-curve or tangent-to-curve was found in the geometric design guidelines of Switzerland (3, 4). The Swiss have developed a formula for calculating transition lengths (tangent length), that is, the distance required for acceleration or deceleration of a vehicle as it approaches or leaves a curve based on the project speed difference between two curves or between a tangent and a curve. Unallowable ranges, or those that should be avoided for these transition lengths, are also tabulated (8).

## BACKGROUND AND OBJECTIVE

In several publications and research reports (8-15) the authors recommend the following boundaries for changes in degree of curve and operating speed between successive design elements for good, fair and poor design practices. With the exception of some very good designs, the existing American design for low-volume, two-lane rural roads consists of sequences of curves and tangents where the transitions are rarely equipped with transition curves.

- Good design is present where successive changes in degree of curve are limited to 5°, and changes in operating speeds are limited to 6 mph (10 km/h) between successive design elements. The horizontal alignment operates well.

- Fair designs exist where changes of 5-10° in degree of curve are present, and changes of 6 mph to 12 mph (20 km/h) in operating speeds between successive design elements are permitted. Normally, low-cost projects such as traffic warning devices are warranted unless there is a documented safety problem.

- Poor designs show changes of more than 10° in degree

of curve and differences of more than 12 mph (20 km/h) in operating speeds. Normally, high-cost projects such as redesign of at least hazardous road sections are recommended, unless there is no documented safety problem.

Furthermore, the following prediction equation was developed in references (13–15) for the relationship between expected operating speed and degree of curve, including all investigated lane widths from 10 feet to 12 feet.

$$V_{85} = 58.656 - 1.135DC; R^2 = 0.787 \quad (1)$$

where

- $V_{85}$  = Estimate of operating speed, expressed by the 85th-percentile speed for passenger cars (mph),
- $DC$  = Degree of curve (degree/100 ft), range:  $0^\circ$  to  $27^\circ$ , and
- $R^2$  = Coefficient of determination.

(The above equation is valid for road sections with grades less than or equal to 5 percent and annual average daily traffic (ADT) values between 400 and 5,000 vehicles per day.)

To illustrate the application of equation (1), the following operating speeds could be expected in a sequence from a tangent to a curve with a degree of curve of  $15^\circ$  or vice versa:

Tangent:  $DC = 0^\circ \rightarrow \rightarrow V_{85} \sim 58$  mph

Curve:  $DC = 15^\circ \rightarrow \rightarrow V_{85} \sim 41$  mph

The speed change from the tangent to the curve is  $\Delta V_{85} = 17$  mph. This value is far beyond the maximum allowable change in operating speeds, even for fair design practices defined above where  $\Delta V_{85} \leq 12$  mph.

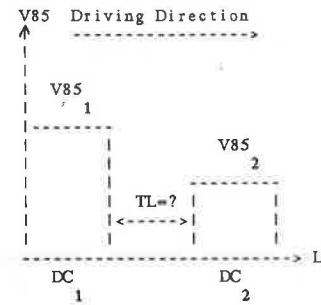
However, this statement would be true only for a relatively long tangent. The tangent must be long enough that a driver can reach the top 85th-percentile speed of 58 mph expressed by equation (1) for  $DC = 0^\circ$ . For shorter tangents between succeeding curves, it would be expected that the average driver in a typical vehicle would not be able to accelerate or decelerate in such a way that the boundaries for good design practices ( $\Delta V_{85} \leq 6$  mph) or even for fair design practices ( $\Delta V_{85} \leq 12$  mph) may be exceeded. In those cases, operating speed changes would be related to the two successive curves, and the relatively short tangent between could be neglected in the design process for evaluating horizontal design consistency or inconsistency and for harmonizing design speed and operating speed. Therefore, the task of this research is to provide recommendations for transition lengths (tangent lengths) between successive curves for

- Tangents that should be regarded as non-independent design elements and the sequence curve-to-curve controls the design process, and
- Tangents that should be regarded as independent design elements and the sequence tangent-to-curve controls the design process.

#### ACCELERATION AND DECELERATION RATES

The transition length ( $TL$ ) is that road section where the operating speed is changing between two design elements with the operating speeds  $V_{85_1}$  and  $V_{85_2}$  as assumed in the fol-

lowing sketch (3, 4). The transition length is given by



$$TL = \frac{v_1^2 - v_2^2}{2a}$$

$$= \frac{v_1 + v_2}{2} \cdot \frac{v_1 - v_2}{a}$$

$$= \frac{\overline{V_{85}} \cdot \Delta V_{85}}{0.465a} \quad (2)$$

where

- $\overline{V_{85}}$  = average 85th-percentile speed between successive curves (mph),
- $\Delta V_{85}$  = difference between the 85th-percentile speeds (mph),
- $TL$  = transition length (tangent length) (ft), and
- $a$  = acceleration/deceleration rate (ft/sec<sup>2</sup>).

When the degrees of curve of two successive design elements are known, the expected 85th-percentile speeds can be determined by equation (1). To evaluate the transition lengths from equation (2), acceleration or deceleration rates between successive design elements must be known.

To determine an estimate of the coefficient  $a$  in equation (2), typical accelerations and decelerations were studied between tangents and specific curved sections of two-lane rural highways (13–15). Because of financial and time constraints, acceleration and deceleration movements from tangents-to-curves or curves-to-tangents were made at curves where speeds of 30 mph (three sections), 35 mph (two sections), and 40 mph (one section) were recommended. The study sites were located in St. Lawrence County in New York.

The optimal procedure required that the speeds of individual vehicles be recorded. To accomplish this, an investigation car (the “follow car”), a car observed in the field (the “test car”), and a tape recorder on which to place any relevant information were used. Note that two persons, a driver and an observer, were required in the “follow car” to allow observation of the situation while speed data were being recorded.

Measurements of travel speeds were made at particular points along the routes. The measurement points were uniform in characteristics:

- Sections were horizontal (longitudinal grades less than 1.5%).
- Intersections and places where an influence on traffic flow might be expected through changes in the highway surroundings were not present in the sections.
- Cross sections were representative with regard to the width of the roadway. Three sections with 10-ft lane width and three sections 11-ft lane width were selected.
- Sight conditions at measuring points were adequate.
- Points of measurements were equipped so as not to be recognizable as such by drivers but obvious enough to be seen by the observers in the follow car.

In all cases, eleven spots (from the beginning of the curve into the tangent section) marked with driveway reflectors were

set up along the routes investigated on both sides of the roadway. The distance between two spots was 250 feet; thus, the measurement sections were about 1/2-mi long. On the average, the recommended speed plates were located about 500 feet (0.1 mile) from the curves in the deceleration direction, while in the acceleration direction at this spot the normal speed limit of 55 mph was posted.

The car speeds were measured during off-peak periods of the week, during dry conditions, and in daylight. The traffic flows were light, and cars were capable of attaining the speeds they desired under the conditions of the site; in other words, a car was selected for speed survey if it had sufficient headway to be considered travelling at its own free speed.

With regard to the analysis process, the observer in the follow car observing the cars crossing his field of view had to select the cars to be sampled. Once a car was spotted under free-flow conditions, an initial acceleration by the driver of the follow car was made in order to catch up and adjust his speed to that of the test vehicle. Then, at each of the study spots along the highway, the observer in the follow vehicle would record the speed of the test vehicle by reading the speed from the speedometer of the follow car. Other relevant information, such as the sex and approximate age of the driver of the test vehicle and the type and mark of the test vehicle, were also recorded, but their effect was not considered in this study. A distance of at least one mile was necessary for the follow car to accelerate and adjust its speed to that of the test car.

All conflicts in which evasive action was taken, such as turning maneuvers into driveways before the end of the speed measurements, were recorded, but those measurements were not considered in the analysis.

Normally the speeds of at least twenty passenger cars (test cars) were recorded on the tape recorder at each of the eleven test points along the routes investigated from the tangent to the curve (deceleration) and from the curve to the tangent

(acceleration). The data on the tape recorder was later analyzed, and the 85th-percentile speed at each of the set-up test spots was determined.

Regression equations relating the 85th-percentile speeds to distances travelled are as follows:

Acceleration:  
 Recommended Speed in Curve: 30 mph  
 $V_{85} = 37.0 + 0.05DT - 0.00002DT^2$  (3a)

Recommended Speed in Curve: 35 mph  
 $V_{85} = 42.0 + 0.04DT - 0.00002DT^2$  (3b)

Recommended Speed in Curve: 40 mph  
 $V_{85} = 47.0 + 0.04DT - 0.00002DT^2$  (3c)

Deceleration:  
 Recommended Speed in Curve: 30 mph  
 $V_{85} = 33.0 + 0.05DT - 0.00002DT^2$  (4a)

Recommended Speed in Curve: 35 mph  
 $V_{85} = 38.0 + 0.04DT - 0.00002DT^2$  (4b)

Recommended Speed in Curve: 40 mph  
 $V_{85} = 43.0 + 0.04DT - 0.00002DT^2$  (4c)

where

$V_{85}$  = estimate of 85th-percentile speed (mph), and  
 $DT$  = distance travelled (feet).

The above equations are plotted in figures 1 and 2. The acceleration and deceleration processes are clearly indicated to end or begin at about 700 to 750 feet from the end of the observed curved sections. This means that any reaction from

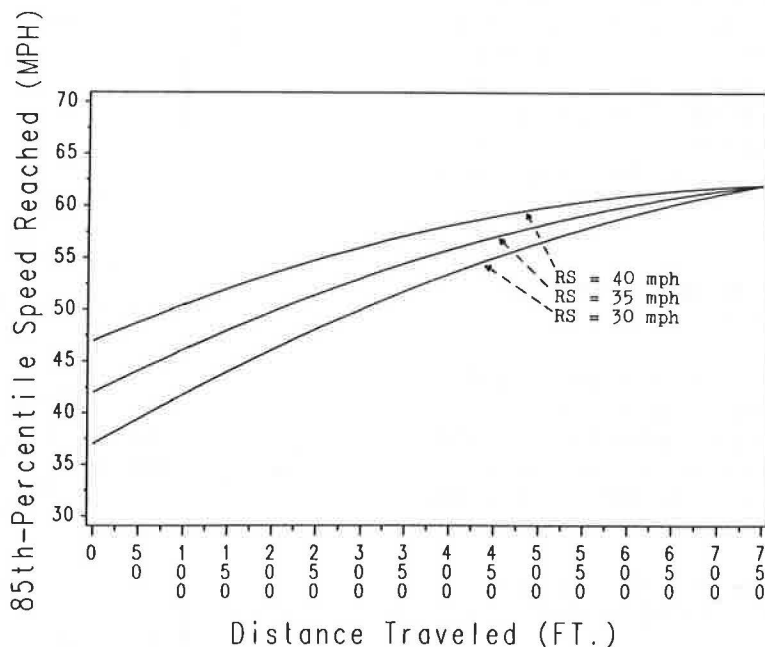
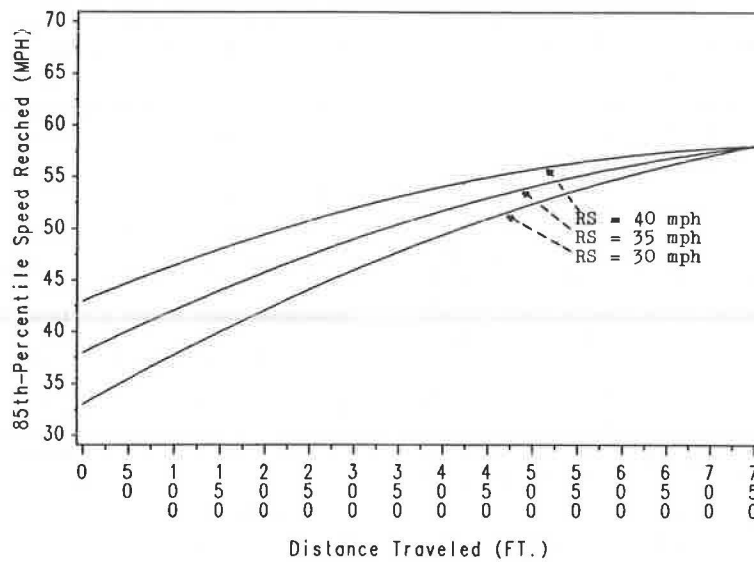


FIGURE 1 85th-Percentile speed vs. distance traveled; passenger cars (acceleration).



**FIGURE 2** 85th-Percentile speed vs. distance traveled; passenger cars (deceleration).

the driver in the deceleration direction begins nearly 200 to 250 feet from the recommended speed plates, which are normally posted 500 feet in front of a curve or a curved section. Another finding is that the operating speeds at the beginning of a curve in the deceleration direction are nearly 4 to 5 mph lower (figure 2), than those at the end of the curve in the acceleration direction (figure 1).

Related to the distance of 750 feet, the average deceleration and acceleration rates ranged between 2.8 and 2.9 ft/sec<sup>2</sup> for the tested six road sections consisting of tangents (length of at least 1/2 mile) followed by curves with recommended speeds between 30 and 40 mph. Since the differences between deceleration and acceleration rates are more or less negligible, an average acceleration or deceleration rate of 2.8 ft/sec<sup>2</sup> was selected for the following analysis. This value agrees well with the deceleration and acceleration rate of 0.8 m/sec<sup>2</sup> (2.64 ft/sec<sup>2</sup>) on which the design of transition lengths in the Swiss Standard (3, 4) is based. Furthermore, this value agrees well with the values in the AASHTO design guide (1), table III-4, where average acceleration rates of about 2.1 ft/sec<sup>2</sup> for passing maneuvers in the speed groups 30 to 40 mph and 40 to 50 mph are tabulated.

**DETERMINATION OF NECESSARY TRANSITION LENGTHS (TANGENT LENGTHS)**

For traffic safety reasons driving behavior during the deceleration process is a particularly important factor.

As previously outlined, operating speed differences ΔV85 between two successive design elements greater than 6 mph should be avoided for good designs and greater than 12 mph for fair designs. An illustration of the above conclusion is given in figure 3.

With an average acceleration or deceleration rate of a = 2.8 ft/sec<sup>2</sup> the transition length in equation (2) now reads:

$$TL = \frac{\overline{V85} \cdot \Delta V85}{1.302} \tag{5}$$

where

- $\overline{V85}$  = average 85th-percentile speed between successive curves (mph),
- $\Delta V85$  = difference between the 85th-percentile speeds (mph), and
- $TL$  = transition length (tangent length)(in feet).

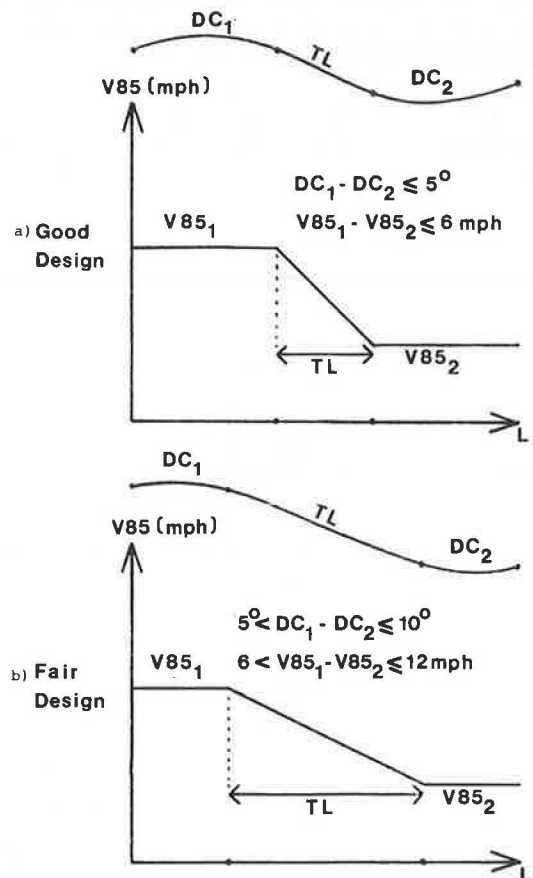


**FIGURE 3** Transition length between successive design elements.

TABLE 1 NECESSARY TRANSITION LENGTHS (TANGENT LENGTHS) FOR GOOD AND FAIR DESIGN PRACTICES

V	22								
8									
5	28	115*							
1									
r	34	260	145*						
e	40	430	315	170*					
s									
p	46	625	510	370	200*				
.									
V	52	850	735	595	425	225*			
8	58	1105	990	850	675	480	255*		
5									
2		22	28	34	40	46	52	58	
		V85 (mph) resp. V85							
		2				1			

\* good designs  
 | | fair designs

Based on the above equation, necessary transition lengths for good and fair design practices are shown in table 1. The values with an asterisk represent good design practices, meaning a driver is able to decelerate or accelerate within the range of operating speed changes of up to 6 mph. The values within boxes represent fair design practices, meaning a driver is able to decelerate or accelerate within the range of operating speed changes of up to 12 mph (see figure 3).

Thus, from the viewpoint of reasonable changes in degree of curve and the corresponding changes in operating speeds, the transition lengths (mostly expressed by tangents) in table 1 should represent maximum boundaries for good and for fair design practices.

In all the other cases (see, for example, the unmarked values in table 1), a driver is able to exceed the recommended operating speed changes, which may result in critical driving maneuvers, especially during the deceleration process.

An illustration of the above statement is given in figure 4 for a sequence of two curves ( $DC = 16.5^\circ$ ) joined by a relatively long tangent ( $DC = 0^\circ$ ,  $L = 1,500$  ft). The 85th-percentile speeds can be determined from equation 1. As can be seen from figure 4, a driver is able to accelerate within the tangent from an operating speed of 40 mph in the curve to the highest operating speed of 58 mph in the tangent, for which, according to table 1, a transition length of 675 ft is needed. In this example the maximum allowable operating speed change even for fair designs of  $\Delta V_{85} \leq 12$  mph has thus been exceeded, a clear indication of poor design practices.

**RECOMMENDATIONS FOR TANGENTS**

The majority of transitions between curves on the two-lane, rural highway network in the United States consist of tangents, with the exception of very good designs where transition curves are applied and operating speed changes exceed-

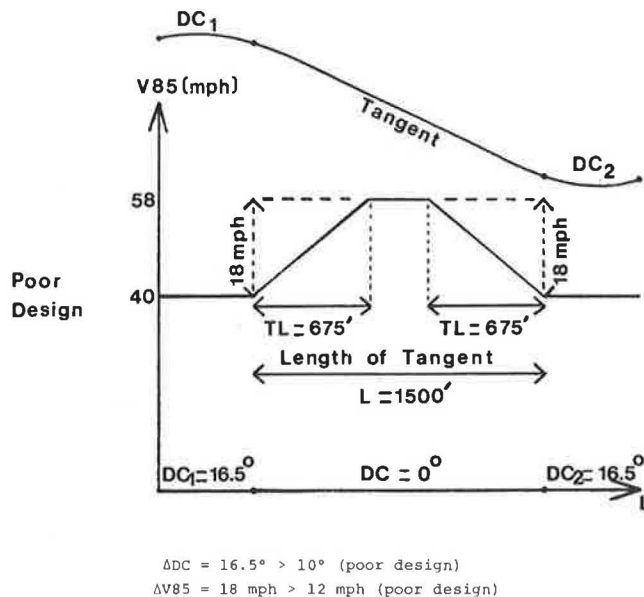


FIGURE 4 Example of poor design practices.

ing the boundaries for good design or even fair design normally do not exist.

With regard to tangents between succeeding curves the following criteria must be distinguished:

1. The transition lengths (tangent lengths) given in table 1 represent maximum boundaries to allow non-critical deceleration or acceleration movements between successive curves for good or fair designs. In order not to be too conservative, tangent lengths between two successive curves, which fall in the range of fair design practices (table 1) may be considered as non-independent design elements. That means, changes in degrees of curve and operating speeds between two successive curves may be calculated directly without regarding the tan-

gent in-between as an independent design element. By this assumption the most critical case for fair design practices, especially during a deceleration process ( $\Delta V_{85} = 12$  mph, see figure 3b) is covered. In all the other cases ( $\Delta V_{85} < 12$  mph) the tangent lengths are not sufficient for the average driver to decelerate or accelerate in such a way that the assumed boundaries of operating speed changes for fair or even good designs are exceeded.

Note that the values of the transition lengths for fair design practices (table 1) agree well with the lengths of superelevation runoffs provided in table III-14 (I) in case of a reversal in alignment, for example, for a maximum superelevation rate of 8 percent.

2. Tangent lengths between successive curves that exceed the values of fair design (table 1) should be regarded as independent design elements. In these cases a driver is able to accelerate or decelerate in such a way that even the maximum allowable operating speed changes for fair designs ( $\Delta V_{85} \leq 12$  mph) may be exceeded; that means, critical driving maneuvers already have originated. Therefore, in case of a relatively long tangent between two successive curves, changes in degrees of curve and operating speeds on this section must be calculated by regarding the tangent in between as an independent design element (see, for example, figure 4).

**DESIGN PROCEDURE WITH EXAMPLE APPLICATIONS**

The results of table 1 are rounded in table 2, where the values within boxes represent the maximum allowable lengths of

tangents regarded as non-independent design elements, as outlined in the previous section. The values with an asterisk represent lengths of tangents for which, related to the speed changes of table 2, 85th-percentile speeds of 58 mph can be reached. As the research of the authors (11, 15) has revealed, on long tangents an 85th-percentile speed value of 58 mph is a good estimate for a degree of curve  $DC = 0^\circ$ , see equation (1). Thus, the maximum operating speed in tangents will be confined in what follows to this value.

To evaluate a tangent between two successive curves as independent and to estimate the expected operating speed in the tangent ( $V_{85_T}$ ), the following procedure is recommended:

(1) Assess the tangent length ( $TL$ ) between the two successive curves (these may be in the field, as in the case of RRR projects, or in the design stages for new designs, major reconstructions, or redesigns).

(2) Determine for the degree of curve 1 ( $DC_1$ ) and the degree of curve 2 ( $DC_2$ ) the corresponding 85th-percentile speeds ( $V_{85_1}$  and  $V_{85_2}$ ) by applying equation (1).

(3) Compare the existing tangent length between the two successive curves with the maximum allowable tangent length (from table 2) that corresponds to the nearest 85th-percentile speed of the curve with the higher degree of curve.

(4) Conclude that if the existing tangent length is smaller than the maximum allowable one, then the tangent is to be regarded as non-independent. That means changes in degree of curve and operating speed will be especially related to the two successive curves since the tangent can be assumed to be negligible. Note that the requirements for sufficient lengths of superelevation runoffs should be fulfilled.

TABLE 2 RELATIONSHIP BETWEEN TANGENT LENGTHS AND 85TH-PERCENTILE SPEED CHANGES FOR SEQUENCES: TANGENTS TO CURVES

V85 in Curve	V85 in Tangent				
	34	40	46	52	58
22	250	425	625	850	1100*
28		325	500	725	1000*
34			375	600	850*
40				425	675*
>46					475*

Maximum allowable Lengths of Tangents, regarded as "Non-Independent Design Elements", (ft)

V85 = 85th-Percentile speed in curve or tangent (mph)

\* For these values the highest operating speed in tangents  $V_{85} = 58$  mph can be expected.

**Example**

$TL = 300$  ft,  
 $DC_1 = 3^\circ \rightarrow \rightarrow \rightarrow V_{85_1} = 55$  mph,  
 $DC_2 = 9^\circ \rightarrow \rightarrow \rightarrow V_{85_2} = 48$  mph, see equation (1).

The 85th-percentile speed in table 2 that is closest to 48 mph in the curve with the higher degree of curve is 46 mph. (This simplification was done for an easier application of table 2.) For 46 mph the maximum length of tangents regarded as non-independent is 475 feet. Since  $TL = 300$  feet  $<$  475 feet, the tangent has to be evaluated as non-independent design element, and no individual operating speed ( $V_{85_T}$ ) is to be assigned to the tangent.

Thus, only the sequence curve-to-curve with the corresponding operating speeds ( $V_{85_1}$  and  $V_{85_2}$ ) plays an important role in the design process for evaluating horizontal design consistency or inconsistency, since the tangent in between can be assumed to be negligible. For the example discussed a change in degree of curve and operating speed

$\Delta DC = |3^\circ - 9^\circ| = 6^\circ$ , and  
 $\Delta V_{85} = |55 - 48 \text{ mph}| = 7$  mph

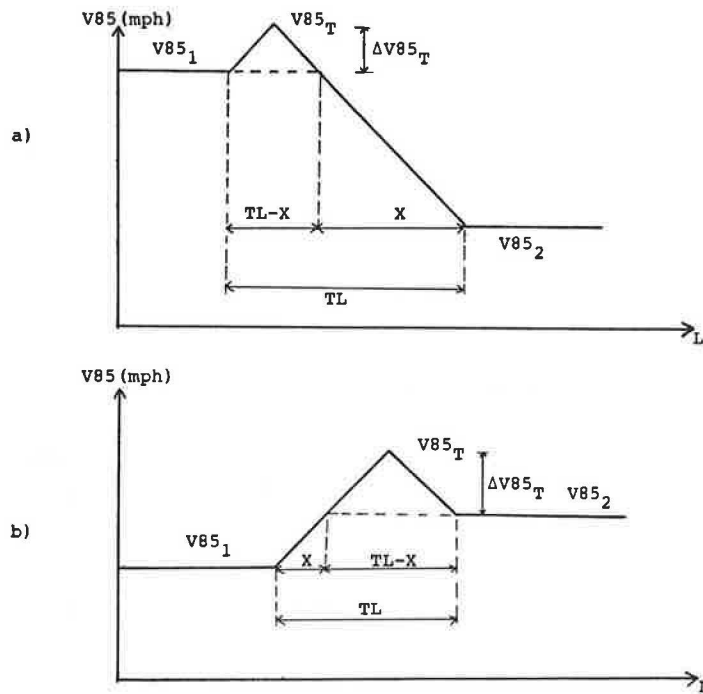
can be expected on the above road section. In conformity with the recommended boundaries for good, fair, and poor design practices, the existing horizontal alignment thus corresponds to fair designs ( $\Delta V_{85} > 6$  mph).

(5) Conclude that if the existing tangent length between successive curves is greater than the maximum allowable (table 2), then the tangent is to be regarded as an independent design element. That means, changes in degree of curve and operating speed are to be especially related to the sequence tangent-to-curve. The 85th-percentile speed in the tangent ( $V_{85_T}$ ) can be estimated as outlined in the following examples, see figure 5.

**Example Related to Figure 5a**

$TL = 0.20$  mi  $\sim$  1,050 ft,  
 $DC_1 = 6^\circ \rightarrow \rightarrow \rightarrow V_{85_1} = 52$  mph,  
 $DC_2 = 22.4^\circ \rightarrow \rightarrow \rightarrow V_{85_2} = 33$  mph, see equation (1).

The 85th-percentile speed in table 2 that is closest to 33 mph in the curve with the higher degree of curve is 34 mph. For 34 mph the maximum length of tangents regarded as non-independent is 375 feet.



**Legend:**

- TL = Tangent length, greater than the maximum allowable lengths for "Non-Independent Tangents" of Table 2 (ft),
- X = Acceleration or deceleration distance between curve 1 and curve 2 (ft),
- $V_{85_1}, V_{85_2}$  = Operating speeds in curves (mph),
- $V_{85_T}$  = Operation speed in tangent (mph),
- $\Delta V_{85_T}$  = Difference between the operating speed in the curve with the lower degree of curve and the operating speed in the tangent (mph).

**FIGURE 5** Typical examples for estimating operating speed in independent tangents.



Since  $TL = 1050$  feet  $> 375$  feet the tangent has to be evaluated as an independent design element. Thus, the sequence tangent-to-curve plays an important role in the design process for evaluating horizontal design consistency or inconsistency for both directions of travel on this road section. The 85th-percentile speed in the tangent ( $V_{85T}$ ) can be estimated as shown below (see figure 5a).

Equation (5) is used to calculate the acceleration or deceleration distance ( $X$ ) between curve 1 and curve 2. This implies

$$X = \frac{\sqrt{V_{85}} \cdot \Delta V_{85}}{1.302} \quad (5a)$$

$$X = \frac{42.5 \cdot 19}{1.302} = 620 \text{ ft}$$

Then, the remaining tangent length is

$$TL - X = 1050 - 620 = 430 \text{ feet}$$

along which a driver is able to perform additional acceleration or deceleration maneuvers. (Exceptional case:  $DC_1 = DC_2 \rightarrow \rightarrow \rightarrow V_{85_1} = V_{85_2}$   $X = 0$ ; perform the calculations in the same way with  $X = 0$ ). By transforming equation (5), in order to calculate the difference  $\Delta V_{85_T}$  between the operating speed in the curve with the lower degree of curve ( $V_{85_1}$ ) and the estimated operating speed in the tangent ( $V_{85_T}$ ), the formula now becomes (see figure 5a):

$$\frac{[V_{85_1} + (V_{85_1} + \Delta V_{85_T})] \cdot \Delta V_{85_T}}{2 \cdot 1.302} = \frac{(TL - X)}{2}$$

or

$$\Delta V_{85_T} = \frac{-2 \cdot (V_{85_1}) \pm \sqrt{4(V_{85_1})^2 + 5.208(TL - X)}}{2} \quad (6)$$

It follows that

$$\Delta V_{85_T} = \frac{-2 \cdot (52) \pm \sqrt{4(52)^2 + 5.208(430)}}{2} \approx 5 \text{ mph}$$

Thus, the operating speed in the independent tangent for evaluating the sequences tangent-to-curve in both directions of travel becomes  $V_{85_T} = V_{85_1} + \%V_{85_T} = 52 + 5 = 57$  mph.

For the discussed example the following changes in degrees of curve and operating speeds can be expected between

tangent to curve 1:

$$\Delta DC = |0^\circ - 6^\circ| = 6^\circ,$$

$$\Delta V_{85} = |57 - 52 \text{ mph}| = 5 \text{ mph, and}$$

tangent to curve 2:

$$\Delta DC = |0^\circ - 22.4^\circ| = 22.4^\circ,$$

$$\Delta V_{85} = |57 - 33 \text{ mph}| = 24 \text{ mph.}$$

The changes in operating speeds reveal that the sequence independent tangent-to-curve 1 corresponds to good design practices ( $\Delta V_{85} < 6$  mph), while the sequence independent tangent-to-curve 2 corresponds to poor design practices ( $\Delta V_{85} > 12$  mph). In the event the calculated 85th-percentile speed in the independent tangent exceeds the value of 58 mph, it is recommended that the 85th-percentile speed in the examined tangent be confined to this value. As previously mentioned, 58 mph is a good estimate for the 85th-percentile speed in

long tangents for the nationwide speed limit of 55 mph on two-lane, rural roads.

### Example Related to Figure 5b

$$TL = 0.15 \text{ mi} = 790 \text{ ft,}$$

$$DC_1 = 27^\circ \rightarrow \rightarrow \rightarrow V_{85} = 28 \text{ mph,}$$

$$DC_2 = 22.4^\circ \rightarrow \rightarrow \rightarrow V_{85} = 33 \text{ mph, see equation (1).}$$

The 85th-percentile speed in table 2 that is closest to 28 mph in the curve with the higher degree of curve corresponds exactly to 28 mph. For 28 mph the maximum length of tangents that is regarded as non-independent is 325 feet. Since  $TL = 790$  feet  $< 325$  feet, the tangent has to be evaluated as an independent design element.

The 85th-percentile speed in the tangent, related to figure 5b, can be estimated in the same way as discussed in the previous example.

According to equation (5a), the acceleration or deceleration distance between curve 1 and curve 2 is as follows:

$$X = \frac{30.5 \cdot 5}{1.302} = 117 \text{ ft.}$$

Therefore, the remaining tangent length becomes

$$TL - X = 790 - 117 = 673 \text{ feet}$$

According to equation (6), the difference between the operating speed in the curve with the lower degree of curve and the operating speed in the tangent now becomes

$$\Delta V_{85_T} = \frac{-2(33) \pm \sqrt{4(33)^2 + 5.208(673)}}{2} \approx 11 \text{ mph}$$

Note that for the example of figure 5b curve 2 is the curve with the lower degree of curve.

It follows that the operating speed in the independent tangent is

$$V_{85_T} = V_{85_2} + \Delta V_{85_T} = 33 + 11 = 44 \text{ mph.}$$

For the discussed example the following changes in degrees of curve and operating speeds can be expected between

tangent to curve 1:

$$\Delta DC = |0^\circ - 27^\circ| = 27^\circ,$$

$$\Delta V_{85} = |44 - 28 \text{ mph}| = 16 \text{ mph, and}$$

tangent to curve 2:

$$\Delta DC = |0^\circ - 22.4^\circ| = 22.4^\circ,$$

$$\Delta V_{85} = |44 - 33 \text{ mph}| = 11 \text{ mph.}$$

The changes in operating speeds reveal that the sequence independent tangent-to-curve 1 corresponds to poor design practices ( $\Delta V_{85} > 12$  mph), while the sequence independent tangent to curve 2 can be still evaluated as fair design ( $\Delta V_{85} < 12$  mph).

(6) The calculations of step (5) must not be performed on long tangents between two successive curves. The length of those tangents must be at least twice as high as the values listed in the last column of table 2, related to the nearest 85th-percentile speed of the curve with the higher degree

of curve. In these cases, it can be assumed without any further calculation that the tangents are independent, and that an operating speed of 58 mph is a good estimate on those long tangents.

A typical example for such a case is shown in figure 4.

#### Example Related to Figure 4

$$TL = 1500 \text{ ft,}$$

$$DC_1 = 16.5^\circ \rightarrow \rightarrow \rightarrow V85_1 = 40 \text{ mph,}$$

$$DC_2 = 16.5^\circ \rightarrow \rightarrow \rightarrow V85_2 = 40 \text{ mph, see equation 1.}$$

The 85th-percentile speed in table 2 that is closest to 40 mph is exactly 40 mph. To accelerate or decelerate from 40 mph to the highest operating speed of 58 mph in the tangent a distance of 675 feet is needed (compare corresponding value in the last column of table 2):  $2 \cdot 675 = 1,350$  feet  $< 1,500$  feet. Thus, it can be concluded that the tangent is independent and an operating speed of  $V85_T = 58$  mph is a good estimate in the long tangent. For the example the following change in degree of curve and operating speed can be expected for this road section:

$$\Delta DC = |0^\circ - 16.5^\circ| = 16.5^\circ,$$

$$\Delta V85 = |58 - 40 \text{ mph}| = 18 \text{ mph.}$$

It follows that the existing horizontal alignment corresponds to poor design practices since  $\Delta V85 > 12$  mph.

#### CONCLUSION

Several countries have limitations on maximum and minimum tangent lengths between curves. The procedure presented above is a rational method to set tangent guidelines for U.S. practice and to provide recommendations for transition lengths (tangent lengths) between successive curved roadway sections for

- tangents that should be regarded as non-independent design elements; that is, the sequence curve-to-curve is the most important element of the design process, and
- tangents that should be regarded as independent design elements; that is, the sequence tangent-to-curve is the most important element of the design process.

The method can be used for new design as well as evaluating in-place roadways in need of safety upgrades.

#### ACKNOWLEDGMENTS

This study was sponsored by the New York State Governor's Traffic Safety Committee, Albany, New York and by the National Science Foundation. The senior author wishes to thank the members of the TRB Geometric Design Committee for their encouragement and their valuable discussions. Special thanks go to Anand Paluri for his support in elaborating this publication.

#### REFERENCES

1. *A Policy on Geometric Design of Highways and Streets*. AASHTO, Washington, D.C., 1984.
2. *Guidelines for the Design of Roads*, (RAS-L-1). Committee on Geometric Design Standards, German Road and Transportation Research Association, Edition 1984.
3. R. Lamm and J. G. Cargin. *Translation of the Guidelines for the Design of Roads* (RAS-L-1), Federal Republic of Germany, and the Swiss Norm SN 640080a, *Highway Design, Fundamentals, Speed as a Design Element*, 1981, as discussed by K. Dietrich, M. Rotach, and E. Boppert in *Road Design*, ETH Zuerich, Institute for Traffic Planning and Transport and Technique, Edition 1983, Federal Highway Administration, Washington, D.C., May 1985.
4. *Highway Design, Fundamentals, Speed as a Design Element*. Swiss Association of Road Specialists (VSS), Swiss Norm SN 640080a, Edition 1981.
5. *Standard Specifications for Geometric Design of Rural Roads*. National Swedish Road Administration, Sweden, Edition 1982.
6. *Instruction sur les Conditions Techniques D'Aménagement de Routes Nationales*. Ministère de l'Équipement et du Logement, France, Edition 1975.
7. *Highway Link Design, Geometric Alignment Standards*. Departmental Standard TD9/81, Department of Transport, Great Britain, 1981.
8. R. Lamm, J. C. Hayward, and J. G. Cargin. Comparison of Different Procedures for Evaluating Speed Consistency. In *Transportation Research Record 1100*, TRB, National Research Council, Washington, D.C., 1986.
9. R. Lamm and J. G. Cargin. Identifying Operating Speed Inconsistencies on Two-Lane Rural Roads. *Proceedings of the Thirty-Ninth Annual Ohio Transportation Engineering Conference*, conducted by the Department of Civil Engineering, The Ohio State University in Cooperation with The Ohio Department of Transportation, December 1985, pp. 13-22.
10. J. Hayward, R. Lamm, and A. Lyng. *Survey of Current Geometric and Pavement Design Practices in Europe, Part: Geometric Practices*, International Road Federation, Washington, D.C., July 1985.
11. R. Lamm and E. M. Choueiri. Relationship Between Design, Driving Behavior, and Accident Risk on Curves. *Proceedings of the Fortieth Annual Ohio Transportation Engineering Conference*, conducted by the Department of Civil Engineering, The Ohio State University in Cooperation with the Ohio Department of Transportation, December 1986, pp. 87-100.
12. R. Lamm and E. M. Choueiri. Recommendations for Evaluating Horizontal Design Consistency Based on Investigations in the State of New York. In *Transportation Research Record 1122*, TRB, National Research Council, Washington, D.C., 1987, pp. 68-78.
13. E. M. Choueiri. *Statistical Analysis of Operating Speeds and Accident Rates on Two-Lane Rural State Routes*. Ph.D. Dissertation, Clarkson University, January, 1987.
14. R. Lamm, R. and E. M. Choueiri. *A Design Procedure to Determine Critical Dissimilarities in Horizontal Alignment and Enhance Traffic Safety by Appropriate Low-Cost or High-Cost Projects*. Report for the National Science Foundation, Washington, D.C., March 1987.
15. E. M. Choueiri and R. Lamm. *Operating Speeds and Accident Rates on Two-Lane Rural Highway Curved Sections—Investigations about Consistency and Inconsistency in Horizontal Alignment*. Part I of the Research Contract "Rural Roads Speed Inconsistencies Design Methods," State University of New York Research Foundation, Albany, New York, July 1987.

# New and Improved Model of Passing Sight Distance on Two-Lane Highways

JOHN C. GLENNON

**A mathematical model is derived for describing the critical nature of the passing maneuver on two-lane highways. This model is based on the hypothesis that a critical position exists during the passing maneuver where the passing sight distance requirements to either complete or abort the pass are equal. At this point, the decision to complete the pass will provide the same head-on clearance to an opposing vehicle as will the decision to abort the pass. Current highway practice in both designing and marking for passing sight distance uses a model that assumes that once a driver starts a pass, he must continue until the pass is completed. In other words, the model assumes that the driver has no opportunity to abort the pass. Because this hypothesis is unrealistic, the model derived here is recommended for determining new passing sight distance requirements for both designing and marking passing zones. Suggested values are given for these requirements. A brief analysis is also presented of the sensitivity of passing sight distance requirements to vehicle length. This analysis shows that the effect of truck length is not as dramatic as previously reported in the literature.**

Although significant advances have been made since 1971 in understanding the critical aspects of the passing maneuver on two-lane highways, the highway community still clings to false and archaic principles. Actually in the current practice for both the design and the marking of passing zones, these zones are neither designed nor marked directly. Current marking practice in the 1978 *Manual of Uniform Traffic Control Devices (MUTCD)* (1), for example, is concerned with no-passing zones, and passing zones merely happen where no-passing zones are not warranted. In highway design, the current practice is stated in the 1984 *Policy on Geometric Design of Streets and Highways* (2) by the American Association of State Highway and Transportation Officials (AASHTO). In AASHTO policy, which has remained unchanged since 1954, the design of passing sight distance (PSD) only considers the percentage of highway that has PSD, regardless of whether that PSD forms passing zones of adequate length.

Another inconsistency exists in that, although the AASHTO design and MUTCD marking practices are based on the same hypothetical model, they use completely different criteria to exercise that model. Whereas the current AASHTO practice assumes a 10-mph speed differential between passing and impeding cars for all design speeds, the MUTCD practice comes from the 1940 AASHO policy (3), which used speed differentials ranging from 10 mph at a 30-mph design speed to 25 mph at a 70-mph design speed.

Besides the inconsistencies already discussed, the basic hypothesis underlying both current PSD design and PSD marking practices is flawed. Although this hypothesis correctly considers the opposing vehicle and the final head-on separation distance as integral components of the critical passing maneuver, it determines overly long PSD requirements by assuming that the passing driver has no opportunity to abort the maneuver.

This paper first addresses the development of a more appropriate model for PSD requirements. With this model developed, the paper then focuses both on the application of the model to proper highway design and marking practices and also on the sensitivities of PSD requirements to vehicle length.

## RESEARCH SINCE 1971

In 1971, Weaver and Glennon (4) and Van Valkenberg and Michael (5) independently recognized that the AASHTO model (2-3, 6-7) for PSD fails to address the critical nature of the passing maneuver. These studies also both recognized that a safe passing maneuver not only requires continuously varying amounts of PSD (depending on the lesser of the needs for completing or aborting the maneuver), but also has a relative position between the passing and impeding vehicles where the ability to complete the pass is equal to the ability to abort the pass. Weaver and Glennon called this the critical position, and Van Valkenberg and Michael called it the point of no return. Neither study, however, attempted to mathematically define this critical position.

In 1976, Harwood and Glennon (8) attempted to better explain the state-of-the-art concerning PSD requirements. This paper contributed further definition of the critical position as that point where the PSD needed to complete the pass is equal to the PSD needed to abort the pass. As shown in figure 1, the pass starts with a minimal PSD needed to abort, the PSD increases through the maneuver until the PSD needed for either completing or aborting the maneuver is equal, and then the PSD decreases through the remainder of the maneuver based on the temporal needs for pass completion.

Lieberman (9), in 1982, added further insight by developing a mathematical time-distance model that identified the critical position and the critical PSD as a function of design speed. However, he incorrectly concluded that AASHTO requirements for PSD were inadequate by calculating his PSD requirements as the sum of both the critical PSD and the distance needed for the passing vehicle to get from the initial trailing position to the critical position. His model also ignored the direct effects of vehicle length and the elapsed time for

John C. Glennon, Chartered, 8340 Mission Road, Suite B-12, Prairie Village, Kans. 66206.

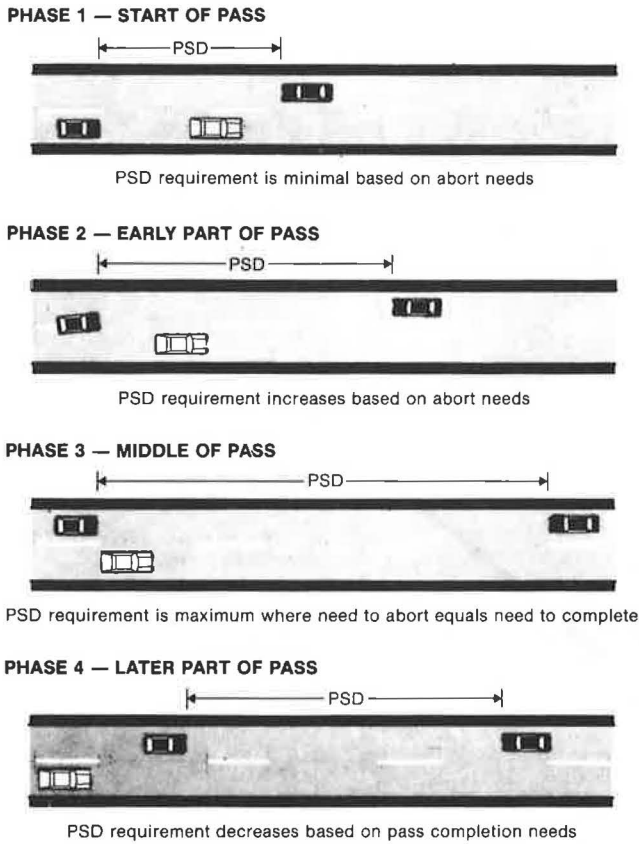


FIGURE 1 Four phases of a passing maneuver.

perception-reaction in the abort maneuver. Regardless of these shortcomings, the Lieberman formulation was conceptually correct and, as such, provided the inspiration for the model developed in this paper.

Saito (10), in 1983, re-emphasized the importance of the abort maneuver in determining PSD requirements. To that date, his modeling came closest to determining true PSD needs. However, he looked only at the needs of the abort maneuver and ignored the trade-offs between the completed and abort maneuvers. In other words, rather than calculating the critical position, he assumed that position was where the passing vehicle is immediately behind the impeding vehicle. As indicated later, this assumption gives PSD requirements that are not too different from those found by using a critical position calculated as a function of design speed.

**DERIVATION OF A CRITICAL PASSING MODEL**

Figure 2 shows time-space diagrams for both the completed passing maneuver and the aborted passing maneuver from the critical position where the PSD needed for safe completion equals the PSD needed for safe abortion. If an opposing vehicle appears before the passing vehicle reaches the critical position, the PSD needed to abort the pass is less than the PSD needed at the critical position. Likewise, if an opposing vehicle appears after the passing vehicle reaches the critical position, the PSD needed to complete the pass is less than the PSD needed at the critical position. Therefore, the maximum or critical PSD is that needed at the critical position.

The proposed model assumes that the opposing vehicle travels at the design speed, that the passing vehicle accelerates to the design speed at or before the critical position and continues at that speed unless the pass is aborted, and that the impeding vehicle travels at a constant speed at some increment less than the design speed.

Since the initial part of the pass is of no consequence in determining the critical sight distance,  $S_c$ , figure 2 starts the passing vehicle at the critical position and equates the two possible maneuvers in time and space. The sub-model for the completed pass assumes that each vehicle maintains a constant speed and that at the end of the pass there is an acceptable clearance,  $C$ , between passing and opposing vehicles and an acceptable gap,  $G$ , between passing and impeding vehicles. For the aborted pass, the impeding and opposing vehicles maintain their constant speeds, but the passing vehicle after a one-second driver perception-reaction time decelerates at rate,  $d$ , until it achieves an acceptable gap,  $G$ , behind the impeding vehicle and an acceptable head-on clearance,  $C$ . [Note that the one-second perception-reaction time is also a part of the completed pass time, but can be ignored in this part of the analysis because it does not affect any of the key time-distance parameters.]

To develop a usable model for the critical PSD requires simultaneous solutions of equations for both the completed and aborted passes, knowing by definition that their critical positions and critical sight distances are equal. The following sections illustrate the development of this model.

**Equate Critical Positions**

The critical position for the completed pass is shown on figure 2A as:

$$\Delta_c + vt_1 = L_p + G + (v - m)t_1$$

or

$$\Delta_c = L_p + G - mt_1 \tag{1}$$

The critical position for the aborted pass is shown on figure 2B as:

$$\Delta'_c + v + vt_2 - \frac{dt_2^2}{2} = (v - m) + (v - m)t_2 - G - L_i$$

or

$$\Delta'_c \frac{dt_2^2}{2} - m(t_2 + 1) - G - L_i \tag{2}$$

Since by definition  $\Delta_c = \Delta'_c$ , Equations 1 and 2 can be solved simultaneously for  $t_1$ , as follows:

$$t_1 = t_2 + 1 - \frac{dt_2^2}{2m} + \frac{(2G + L_i + L_p)}{m} \tag{3}$$

**Equate Critical Sight Distances**

The critical PSD for each maneuver is taken directly from figure 2 as the total distance between passing and opposing vehicles when the passing vehicle is in the critical position.

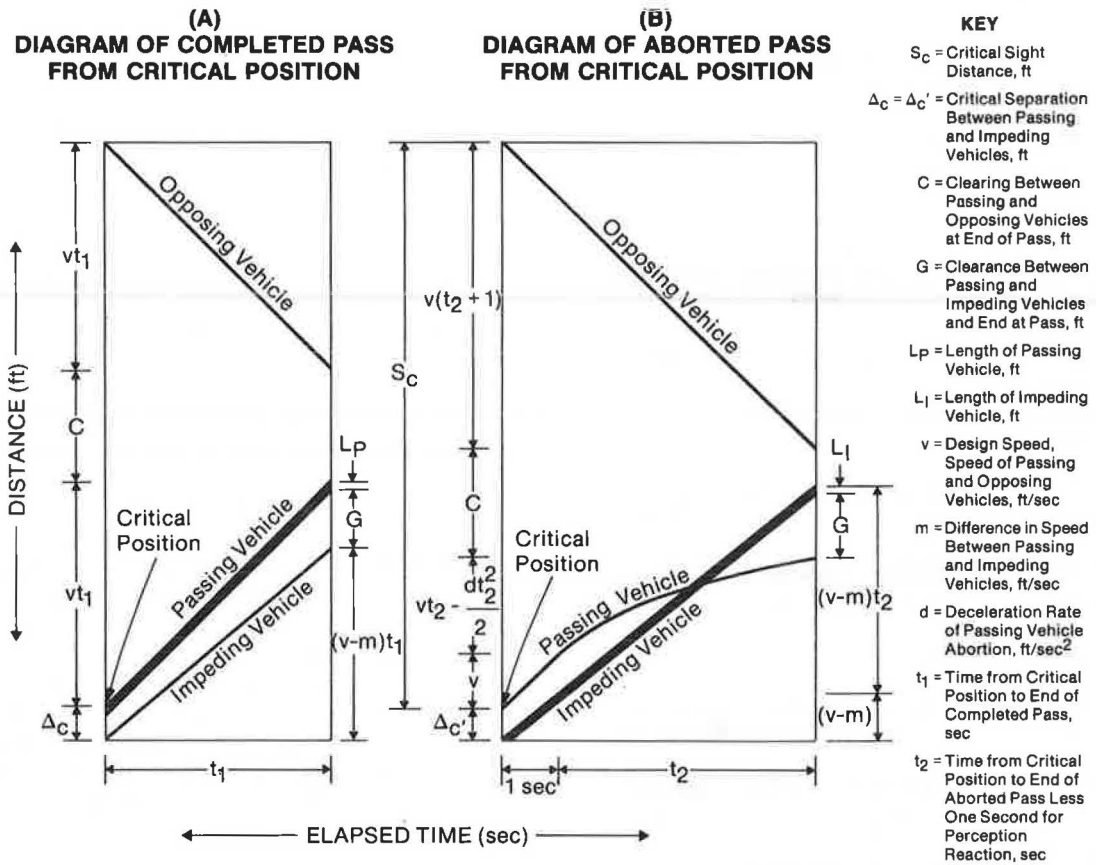


FIGURE 2 Time-space diagrams for the critical passing maneuver.

Equating these distances and solving for  $t_1$  gives:

$$2vt_1 + C = v + vt_2 - \frac{dt_2^2}{2} + C + v(t_2 + 1)$$

$$t_1 = t_2 + 1 - \frac{dt_2^2}{4v} \tag{4}$$

**Solve Time Relationships**

By simultaneous solution of Equations 3 and 4,  $t_2$  can be isolated as a function of definable parameters as follows:

$$t_2 + 1 - \frac{dt_2^2}{4v} = t_2 + 1 - \frac{dt_2^2}{2m} + \frac{(2G + L_l + L_p)}{m}$$

or

$$t_2 = \sqrt{\frac{4v(2G + L_l + L_p)}{d(2v - m)}} \tag{5}$$

since

$$t_1 = t_2 + 1 - \frac{dt_2^2}{4v}$$

then

$$t_1 = 1 + \sqrt{\frac{4v(2G + L_l + L_p)}{d(2v - m)}} - \frac{(2G + L_l + L_p)}{2v - m} \tag{6}$$

**Solve the Critical Position**

Equations 1 and 6 can be solved simultaneously to derive an expression for the critical position as a function of design speed,  $v$ , speed difference,  $m$ , desired gap,  $G$ , deceleration rate,  $d$ , and lengths of vehicles,  $L_l$  and  $L_p$ , as follows:

$$\Delta_c = L_p + G - mt_1$$

or

$$\Delta_c = L_p + G - m + m \left[ \frac{(2G + L_l + L_p)}{2v - m} - \sqrt{\frac{4v(2G + L_l + L_p)}{d(2v - m)}} \right] \tag{7}$$

Assuming a minimum acceptable headway of one second for  $G$ , then  $G = m$  and Equation 7 is revised as follows:

$$\Delta_c = L_p + m \left[ \frac{(2m + L_l + L_p)}{2v - m} - \sqrt{\frac{4v(2m + L_l + L_p)}{d(2v - m)}} \right] \tag{8}$$

[Note that the same relationship is found if, in Figure 2, the passing vehicle is assumed to be behind the impeding vehicle at the critical position.]

**Solve the Critical Passing Sight Distance**

Using Figure 2 and Equation 1, the passing sight distance,  $S_c$ , can be solved for any design speed as a function of the critical position,  $\Delta_c$ , speed differential,  $m$ , and length of passing vehicle,  $L_p$ , as follows:

$$S_c = 2vt_1 + C$$

and

$$t_1 = \frac{L_p + G - \Delta_c}{m}$$

therefore

$$S_c = \frac{C + 2v(L_p + G - \Delta_c)}{m}$$

Having already assumed  $G = m$  and also assuming a minimum acceptable head-on clearance of one second, then  $C = 2v$ . Therefore:

$$S_c = 2v + \frac{2v(L_p + m - \Delta_c)}{m}$$

or

$$S_c = 2v \left[ 2 + \frac{L_p - \Delta_c}{m} \right] \tag{9}$$

**PASSING SIGHT DISTANCE REQUIREMENTS**

Now that a usable model has been developed for the critical PSD, the question remains how to apply it to the design and marking of a passing zone. Obviously,  $S_c$  defines the minimum PSD required for any part of the passing zone where a passing vehicle can reach the critical position. As a worst-case scenario, it seems appropriate to provide  $S_c$  at the end of a passing zone, assuming that it is reasonable to expect the critical situation at this point. It is not reasonable, however, to expect that the passing vehicle will be in the critical position at the beginning of a passing zone. Actually the PSD requirement at the beginning of the zone is something less than  $S_c$ ; however, because passing operations vary widely by speed differentials, opposing vehicle speeds, and vehicle lengths, an added safety factor would be incorporated by starting the passing zone where  $S_c$  first becomes available.

Recognizing that the assumptions used to develop the critical passing model may be subject to some interpretation and adjustment, this section provides recommendations for PSD requirements based on the following additional assumptions:

1. The AASHTO use of passenger cars for the passing and impeding vehicles are appropriate criteria.
2. The length of the average passenger car is 16 feet.
3. A reasonably safe deceleration rate in the abort maneuver is 8 ft/sec<sup>2</sup>.
4. Based on the Weaver and Glennon study (4), the following table of critical (15th percentile) speed differentials is appropriate:

Design Speed (mph)	Speed Differential (mph)
30	12
40	11
50	10
60	9
70	8

Substituting Assumptions 1 through 3 into Equations 8 and 9, the critical passing model is reduced to relationships that are a function of the design speed and the speed differential as follows:

$$S_c = 2v \left[ 2 + \frac{16 - \Delta_c}{m} \right]$$

where

$$\Delta_c = 16 + m \left[ \frac{(2m + 32)}{2v - m} - \sqrt{\frac{v(2m + 32)}{2(2v - m)}} \right]$$

Using these equations and solving for the design relationships found under Assumption 4 above, table 1 shows the derived PSD requirements. In comparing these recommendations with current AASHTO and MUTCD requirements, they are found to be considerably less than the AASHTO requirements, but very close to the MUTCD requirements (even though the MUTCD requirements were derived with a completely different set of models and criteria.)

Although this paper does not analyze the requirements for passing zone length, previous studies (4, 11) have shown that very short zones, such as the 400-ft default length allowed by the MUTCD, are not appropriate for safe highway operations. Therefore, the recommendations of Weaver and Glennon (4) for minimum passing zone length, based on 85th percentile passing vehicle distances, should be implemented unless another rationale is shown to be more appropriate. These passing zone lengths are also shown in table 1.

**TRUCK LENGTH CONSIDERATIONS**

Several authors (9, 12-14) have expressed alarm at the supposed inadequacy of PSD requirements (most particular AASHTO requirements) for passes involving trucks in general and longer trucks, in particular. These studies were dramatized by Donaldson (15) as follows:

The recent research of Lieberman demonstrates the thorough inadequacy of the AASHTO sight distance formulae for the successful execution of the passing maneuver . . . Lieberman has shown that significantly longer sight distances are needed when the impeding vehicle is a truck . . . The research of Gericke and Walton demonstrates that the AASHTO sight distance formulae for geometric design are inadequate for any vehicle and especially inadequate for cars passing trucks . . . Saito shows that successful aborts are impossible under most high-speed conditions on the basis of current MUTCD standards . . . If one extrapolates his kinematic model, it shows substantial increases in the lengths of time and distances for successful aborts of cars attempting to pass longer trucks . . . The passenger car/truck relationship in the passing maneuver is highly dangerous on many thousands of our rural arterial and collector routes that have inadequate sight distance but which are marked to permit passing maneuvers that cannot be accomplished by most of the vehicles making the attempts.

The flaw in the remarks quoted above is that none of the studies cited by Donaldson were based on a correct analysis of passing sight distance requirements. Of the sources cited, Lieberman (9) failed to correctly apply his own insights on the definition of the critical sight distance, Saito (10) ignored the trade-offs between completed and aborted passes, and Gericke and Walton (12) used the [incorrect] AASHTO

model to derive their results, as did Fancher (13) and Khasnabis (14).

Table 2 shows the sensitivity of the derived PSD requirements to vehicle length. As can be seen, the PSD requirements increase as a function of vehicle length but not as dramatically as previously stated in the literature.

Whether a truck should be considered as a design vehicle

TABLE 1 DERIVED PASSING SIGHT DISTANCE REQUIREMENTS

Design Speed (mph)	Critical Position Front of passing vehicle relative to front of imped- ing vehicle (ft)	Maximum Abort Position Front of passing vehicle relative to front of imped- ing vehicle (ft)	Minimum Length of Passing Zone (Ref. 4)	PSD Requirement (ft)
40	-43	-10	600	670
50	-38	-10	900	830
60	-32	-8	1200	990
70	-25	-5	1500	1140

TABLE 2 DERIVED PASSING SIGHT DISTANCE REQUIREMENTS AS A FUNCTION OF PASSED VEHICLE LENGTH

Design Speed (mph)	Rounded PSD Requirements for Various Passed Vehicle Lengths (ft)*			
	Passenger Car	55-ft. Truck	65-ft. Truck	110-ft. Truck
40	670	760	780	850
50	830	960	980	1080
60	990	1150	1180	1320
70	1140	1320	1380	1550

\* Uses passenger car for passing vehicle

for PSD is a moot point, considering, first, that the vehicle length is really only critical for an end-zone pass and, second, that passing drivers have adaptive behavior that considers not only their position in the zone but the vehicle length to be passed.

## CONCLUSIONS

The current AASHTO (2) model for passing sight distance requirements ignores the possibility of an aborted maneuver and thereby determines overly long distances. This paper derives a more appropriate model that considers the trade-offs between aborted and completed passes. The passing sight distance requirements derived with this model are considerably less than the AASHTO requirements but are surprisingly close to those presented in the MUTCD (1). Application of the derived model also shows that the effect of truck length is not as dramatic as previously reported in the literature.

The derived model should be used to revise both the AASHTO and MUTCD practices so that a correct and consistent basis is used for both the design and marking of passing zones. In doing so, the assumption of a one-second, head-on clearance; a one-second gap; an 8-ft/sec<sup>2</sup> deceleration; and a 15th-percentile speed differential should all be questioned. However, because the critical condition addresses only the infrequent pass at the end of a zone, care should be exercised in being overly conservative in selecting these values. For example, the one-second, head-on clearance and one-second gap seem short but may be reasonable considering the rarity of a [small] 15th-percentile speed differential and a [relatively low] 8-ft/sec<sup>2</sup> abort deceleration.

## REFERENCES

1. *Manual on Uniform Traffic Control Devices*. Federal Highway Administration, Washington, D.C., 1978.
2. *A Policy on Geometric Design of Highways and Streets*. AASHTO, Washington, D.C., 1984.
3. *A Policy on Criteria for Marking and Signing No-Passing Zones on Two and Three Lane Roads*. AASHTO, Washington, D.C., 1940.
4. G. D. Weaver and J. C. Glennon. *Passing Performance Measurements Related to Sight Distance Design*. Research Report 134-6, Texas Transportation Institute, July 1971.
5. G. W. Van Valkenberg and H. L. Michael. Criteria for No-Passing Zones. *Highway Research Record 366*, HRB, National Research Council, Washington, D.C., 1971.
6. *A Policy on Geometric Design of Rural Highways*. AASHTO, Washington, D.C., 1954.
7. *A Policy on Geometric Design of Rural Highways*. AASHTO, Washington, D.C., 1965.
8. D. W. Harwood and J. C. Glennon. Framework for Design and Operation of Passing Zones on Two-Lane Highways. In *Transportation Research Record 601*, TRB, National Research Council, Washington, D.C., 1977.
9. E. B. Lieberman. Model for Calculating Safe Passing Distances on Two-Lane Rural Roads. In *Transportation Research Record 869*, TRB, National Research Council, Washington, D.C., 1982.
10. M. Saito. Evaluation of the Adequacy of the MUTCD Minimum Passing Sight Distance Requirement for Aborting the Passing Maneuver. *ITE Journal*, January 1984.
11. J. R. Jones. *An Evaluation of the Safety and Utilization of Short Passing Sections*. Master's thesis, Texas A & M University, 1970.
12. O. F. Gericke and C. M. Walton. Effect of Truck Size and Weight on Rural Roadway Geometric Design (and Redesign) Principles and Practices. In *Transportation Research Record 806*, TRB, National Research Council, Washington, D.C., 1981.
13. P. S. Fancher. Sight Distance Problems Related to Large Trucks. In *Transportation Research Record 1052*, TRB, National Research Council, Washington, D.C., 1986.
14. S. Khasnabis. Operational and Safety Problems of Trucks in No-Passing Zones on Two-Lane Highways, In *Transportation Research Record 1052*, TRB, National Research Council, Washington, D.C., 1986.
15. G. A. Donaldson. Large Truck Safety and the Geometric Design of Two-Lane, Two-Way Roads. *ITE Journal*, September 1985.

---

*Publication of this paper sponsored by the Committee on Geometric Design.*



Abridgment

# Development of Limiting Velocity Models for the Highway Performance Monitoring System

GARY E. ELKINS AND JEREMY SEMRAU

A study was performed for the Federal Highway Administration to increase the efficiency of vehicle speed models for the Highway Performance Monitoring System analytical process. Probabilistic and deterministic models developed by the World Bank were adapted for conditions in the United States. These models estimate vehicle average travel speed as a function of relevant road and traffic characteristics. This is done by evaluating a set of constraining speed models that consider the influence of vertical grades, horizontal curves, roughness, traffic congestion, and highway type. These models were adapted to conditions in the United States using engineering judgment and limited available data. Although further research is needed to refine these models, the models produce reasonable results and are recommended for use in planning models as a basis for computation of road user costs. More research is needed in this general area from the engineering community. Input from experts in vehicle mechanics, dynamics, and human factors would be particularly helpful in determining driver reactions and behavior and further developing speed prediction models as a function of road characteristics and vehicle class.

The Federal Highway Administration (FHWA) uses a set of approximately 92,000 annually monitored sample pavement sections across the United States to assess the condition of the nation's highways and road network. This system is called the Highway Performance Monitoring System (HPMS). One part of the HPMS analysis package is used for planning purposes to study the impacts of different funding scenarios on highway users. A complex, time-consuming, computer algorithm is presently used to estimate vehicle speeds on each sample section from which travel time, fuel consumption, and vehicle operating cost impacts are computed. This paper summarizes the development of an efficient speed prediction model for use in the HPMS analytical process (1) and discusses problems encountered in development of the model.

## LIMITING VELOCITY MODELS

Limiting velocity models developed by the World Bank were chosen for adaptation to United States conditions (2). Using the results of past studies and engineering judgement, the following limiting velocity models were formulated. One model

relates a vehicle speed to the minimum of five constraining speeds:

$$V_{ss} = \text{Min} (V_{DRIVE}, V_{BRAKE}, V_{CURVE}, V_{ROUGH}, V_{DESIR}) \quad (1)$$

where:

- $V_{ss}$  = steady state speed,
- $V_{DRIVE}$  = maximum possible driving speed,
- $V_{BRAKE}$  = maximum allowable braking speed on downgrades,
- $V_{CURVE}$  = maximum allowable speed on horizontal curves,
- $V_{ROUGH}$  = maximum allowable ride severity speed
- $V_{DESIR}$  = desired speed.

This model is called the Minimum Limiting Velocity Model (MLVM).

The second model treats each constraining speed as a random variable. This model, called the Probabilistic Limiting Velocity Model (PLVM), is:

$$V_{ss} = \exp(S^2/2) / [(1/V_{DRIVE})^{1/B} + (1/V_{CURVE})^{1/B} + (1/V_{BRAKE})^{1/B} + (1/V_{ROUGH})^{1/B} + (1/V_{DESIR})^{1/B}]^B \quad (2)$$

where:

- $S^2$  = variance associated with unmeasured vehicle, road, and speed measurement characteristics,
- $B$  = a constant parameter for each vehicle class.

The PLVM has several interesting features. When two or more speeds become equally dominant, the probabilistic speed drops below the deterministic speed by a larger amount. Also, as more speeds begin to lower the probabilistic speed, they do so at a diminishing rate. Thus, the stochastic nature of driver perception is modeled such that as the driver reacts to a greater number of speed constraints, he or she will drive slower than the minimum of the constraining speeds.

## MODEL PARAMETERS FOR UNITED STATES CONDITIONS

The parameters of the limiting velocity models that were examined for adjustment to U.S. conditions are:

G. E. Elkins, Texas Research and Development Foundation, 2602 Dellana Lane, Austin, Tex. 78746. J. Semrau, Department of Civil Engineering, University of Texas at Austin, Austin, Tex. 78712.

- The constraining speeds for each class, including *VDRIVE*, *VBRAKE*, *VCURVE*, *VROUGH*, and *VDESIR*;
- The exponential parameter *B* for each vehicle class;
- The variance term *S*<sup>2</sup>, which represents the errors associated with speed predictions for each vehicle class.

Ideally, calibration of these models for United States conditions should be based on direct field measurements. To best model the effects of various road characteristics, actual sites that have only one dominating characteristic must be selected. Vehicle spot speeds should be measured and the model fitted to the data. Unfortunately, no suitable data representative of conditions in the United States could be found.

**Maximum Possible Driving Speed (*VDRIVE*)**

The maximum possible driving speed is the speed a vehicle travels when all the available driving power is used. *VDRIVE*

becomes a constraint on the speeds of vehicles on positive vertical grades. The force balance and power relationship used to find *VDRIVE* is

$$Av(VDRIVE)^3 + mg(GR + CR)VDRIVE = 375 HPDRIVE \quad (3)$$

where

- VDRIVE* = maximum possible driving speed, mph;
- HPDRIVE* = maximum available driving power, horsepower;
- m* = vehicle mass;
- g* = acceleration due to gravity;
- CD* = aerodynamic drag coefficient;
- Av* = frontal area of vehicle;
- GR* = vertical gradient;
- CR* = rolling resistance coefficient

The terms *HPDRIVE*, *m*, *CD*, *Av*, and *CR* are vehicle

TABLE 1 1985 U.S. VEHICLE FLEET MODELING PARAMETERS

Vehicle Class	Frontal Area Sq. Ft.	Vehicle Weight lb.	Drag Coef.	Rolling Resistance <sup>(1)</sup>		HPDRIVE Hp
				CR - RC1 + RC2 (v) <sup>n</sup>		
				RC1	RC2	
<b>Small</b>						
Auto	22.8	2,720	0.42	.0125	6.5E-07	93
<b>Medium</b>						
Auto	25.9	3,780	0.45	.0125	6.5E-07	140
<b>Large</b>						
Auto	28.7	4,560	0.49	.0125	6.5E-07	200
Pickup	30.8	5,000	0.59	.016	6.5E-07	175
<b>2A-SU</b>						
Truck	36.9	12,000	0.70	.0076	9.0E-05	230
<b>3A-SU</b>						
Truck	55	35,000	0.70	.0076	9.0E-05	275
<b>2S-2</b>						
Semi	90	50,000	0.80	.0076	2.0E-05	325
<b>3S-2</b>						
Semi	90	62,500	0.80	.0076	2.0E-05	325

(1) NOTE: v = speed, mph  
 n = 2 for autos and pickups  
 n = 1 for trucks and semi

dependent. The values of these parameters developed for the U.S. vehicle fleet are shown in table 1. All terms but *HPDRIVE* are from automotive industry literature. *HPDRIVE* is the available horsepower after accounting for internal power losses. To find this parameter, *HPDRIVE* was back-calculated from Equation 3 by inserting the observed top speeds of various vehicles on 0-% grades. For automobiles it was found that the calculated *HPDRIVE* approximated the SAE net braking horsepower, which includes the effects of internal power losses. This quantity is recommended as *HPDRIVE* for automobiles.

A different approach to the estimate of *HPDRIVE* was required for trucks with diesel engines. The best source of information found for U.S. trucks was a 1970 study by the Western Highway Institute (WHI) (3). The WHI recommended multiplying the rated horsepower of a diesel engine by a factor varying from .78 to .85, depending on the number of axles, gear range, and engine size. This equation is suspect since the truck population has changed significantly since 1970. Although the relationship is used in this study, these results should be reviewed in future studies to determine its suitability.

#### Maximum Allowable Braking Speed (*VBRAKE*)

On steep downgrades, a maximum constraining speed, or braking crawl speed, has been observed (4, 5). The braking crawl speed is believed to be related to vehicle braking capability resulting through use of the retardation power of the engine (downshifting) and the brakes. In general, only large vehicles have been observed to slow down on steep downgrades. Limiting crawl speeds on downgrades are not generally found on grades less than 4% or shorter than 3,000 feet.

Although large trucks may have braking speeds, little information examining this effect was found. *The 1985 Highway Capacity Manual* (6) indicates that very few studies have been performed to analyze the impact of heavy vehicles on traffic flow on downgrades. Due to the lack of information on this behavior, this term is not included in this model.

#### Maximum Allowable Curve Speed (*VCURVE*)

Most drivers decrease their speed to negotiate sharp horizontal curves. The effect of curves on vehicle speed has been widely studied. The World Bank model (2) related vehicle speed on a horizontal curve to the "maximum perceived friction ratio," called *FRATIO*. *FRATIO* is defined as the ratio of lateral forces on a vehicle to the normal force on the vehicle. The vehicle speed on the curves, with simplifying assumptions can be written as

$$VCURVE = [(FRATIO + SP) g RC]^{0.5} \quad (4)$$

where:

- VCURVE* = maximum allowable speed on curves,
- FRATIO* = maximum perceived friction ratio,
- SP* = superelevation of curve,
- RC* = radius of curvature.

The *FRATIO* value is used to characterize different vehicle classes. A *FRATIO* value of 0.155 was found to provide a

good fit to the speed-curve model used in the present HPMS for automobiles, pickups and single unit trucks. For large trucks and semitrailer units, a value of .103 was used, based on the relationship between cars and trucks determined from the World Bank study.

Other forms of this model could be used; however, the PLVM requires that this model predict high speeds on curves with large radii to avoid interaction with other terms in the PLVM that would falsely decrease the predicted speeds. Field studies of the performance of trucks on curves and the suitability of this model for U.S. conditions appear warranted.

#### Maximum Allowable Ride Severity Speed (*VROUGH*)

It is a common observation that road roughness influences vehicle speed. Few studies, however, relate vehicle speed to the roughness measures used in the United States or in the HPMS. A model is needed that explains differences in vehicle type and road type and accounts for limiting roughness thresholds and minimum speeds at maximum roughness levels.

Based on the information developed in Brazil and the speed-roughness model used in the current HPMS analytical process, the following equations were developed:

$$VROUGH = 1.0 / (.0250 - .00275(PSR)) \text{ automobiles} \quad (5)$$

$$VROUGH = 0.9 / (.0255 - .00333(PSR)) \text{ large trucks} \quad (6)$$

where

- VROUGH* = ride severity speed, mph;
- PSR* = present serviceability rating, (0-5).

More work is needed on speed-roughness relationships. The above equations are primarily based on engineering judgment. Relationships derived from direct measurements and based on common roughness measures used in the U.S. are needed to extend the accuracy and usefulness of these speed prediction models.

#### Desired Speed of Travel (*VDESIR*)

The desired travel speed is the speed at which drivers travel when they are not constrained, typically less than the maximum possible speed a vehicle can attain. This speed is governed by subjective considerations of safety, speed law enforcement, fuel cost, and vehicle wear. For the purposes of the HPMS, the term should also be sensitive to the effects of traffic congestion and traffic control devices.

A limited nationwide source of information on *VDESIR* is the annual free flow speed tables published by the FHWA (7). Average, median, and 85th-percentile speeds on highways on which the 55-mph speed limit is the primary speed constraint are published.

To incorporate the effects of traffic congestion and traffic control devices into the model, tables of average speed as a function of highway type, traffic control, number of lanes, and speed limit were developed (1). These tables were devel-

oped from tables of initial running speed contained in the current HPMS model and are based on and extrapolated from the general speed-volume capacity relationships shown in the 1965 and 1985 Highway Capacity Manuals.

Due to the generalized information from which these speeds were developed, more work is needed to relate the desired speed constraint to physical road characteristics. A separate speed constraint term related to a simple measure of traffic congestion such as volume capacity ratio should also needs be developed, particularly for signalized urban streets.

### ***B* and *S*<sup>2</sup> Parameters**

The exponential *B* parameter and variance parameter *S*<sup>2</sup> are part of the probabilistic limiting velocity model (PLVM). They are included to account for the stochastic nature of observed vehicle speeds. *B* and *S*<sup>2</sup> are primarily used to reduce the predicted speed when two or more constraining speeds become dominant. The *B* parameter acts similarly to the coefficient of the standard deviation of a normal distribution typically used to determine confidence levels. The smaller the value of *B*, the closer the probabilistic speed is to the minimum constraining speed. Meanwhile, the *S*<sup>2</sup> parameter is associated with errors in speed prediction, due to variations in vehicle and road characteristics, and other errors, due to speed measurements and quantification of road attributes.

These parameters are properly determined using a nonlinear least-squares regression analysis between observed speeds and speed constraint terms. Because there is no U.S. data base from which to develop these parameters, the values of *B* = 0.1 and *S*<sup>2</sup> = 0.01 were selected to cause the model to predict speeds that are less than the minimum speed constraint. The choice of these values causes the MLVM and PLVM models discussed in this paper to produce essentially the same results.

### **SUMMARY**

The minimum and probabilistic forms of the limiting velocity model offer an excellent method to predict vehicle speeds as a function of relevant constraining speeds due to curvature, gradient, road roughness, braking capability, and other road features. The models presented here can be implemented into planning models for use in predicting user impacts. As discussed, further development of these models is required in order to better define the interrelations between road characteristics and vehicle speed.

The recommended method of further refinement of these models is through a structured nationwide study of vehicle speeds. This study would consist of spot speed studies on sections selected to study a particular speed constraint term.

A full statistical analysis similar to that performed by the World Bank should be performed on this data base. In the face of a more limited study, the authors feel that the speed models presented here could best be improved by studies into the following topics in the following order:

1. Effects of signalization and traffic control
2. Effects of traffic congestion
3. Effect of roughness
4. Large truck performance on downgrades and horizontal curves

Input from experts in vehicle mechanics, dynamics, and human factors is also important in better defining the needed speed estimation models.

### **ACKNOWLEDGMENT**

This work was performed under the sponsorship of the U.S. Department of Transportation, Federal Highway Administration, Office of Highway Planning.

### **REFERENCES**

1. G. E. Elkins, B. C. Butler, R. High, and R. Harrison. *Estimating Vehicle Performance Measures: Volume I*. Technical Report, Federal Highway Administration, Washington, D.C., July 1987.
2. Watanatada, P. R. S. Rezende-Lima, and A. Dhahreshwar. *Models for Predicting Vehicle Speed and Operating Costs Based on Principles of Vehicle Mechanics and Driver Behavior: Theory and Qualification*. Highway Design and Maintenance Standards Study, Volume II, World Bank, March 1985.
3. *Horsepower Considerations for Trucks and Truck Combinations, 1969, Acceleration Tests*. Supplement No. 1, Research Committee Report No. 2, Western Highway Institute, 1970.
4. H. Hide, S. W. Abayanayaka, I. Sayer, and R. I. Wyatt. *The Kenya Road Transport Cost Study: Research on Vehicle Operating Costs*. TRRL Laboratory Report 672, Transport and Road Research Laboratory, Crowthorne, Berkshire, U. K., 1975.
5. A. D. St. John and D. R. Kobett. *Grade Effects on Traffic Flow Stability and Capacity*. National Cooperative Highway Research Program Report 185, TRB, National Research Council, Washington, D.C., 1978.
6. *Highway Capacity Manual*. Special Report 209, TRB, National Research Council, Washington, D.C., 1985.
7. *Highway Statistics*, Federal Highway Administration, Washington, D.C., annual publication.

---

*Publication of this paper sponsored by Committee on Geometric Design.*